A STUDY OF THE SOMATOSENSORY EVOKED POTENTIAL IN MAN USING BRAIN MAPPING TECHNIQUES

PAUL LAWRENCE FURLONG
MASTER OF PHILOSOPHY

THE UNIVERSITY OF ASTON IN BIRMINGHAM
APRIL 1990

THE UNIVERSITY OF ASTON IN BIRMINGHAM

A STUDY OF THE SOMATOSENSORY EVOKED POTENTIAL IN MAN USING BRAIN MAPPING TECHNIQUES

PAUL LAWRENCE FURLONG
MASTER OF PHILOSOPHY
1990

SUMMARY

Despite studies on the scalp distribution of upper limb SEP components in normal man (Goff et al 1977) and descriptions of the effect on SEP components of discrete cortical lesions (Mauguière et al 1983), there have been few descriptions of the clinical application of an SEP control population database using 'brain mapping' systems.

The purposes of this study were to analyze the morphology and topography of the first 56ms of scalp recorded SEP activity from a broad age range of normal control volunteers and to collate a normative database to investigate its effectiveness in the detection of pathology. The control database was used to study patients with discrete cortical lesions to discover whether topographical techniques contributed to knowledge on the origin of the scalp recorded SEP components. Finally to discover whether the use of an SEP topographical mapping database and statistical mapping methods was useful in the detection of abnormalities associated with such lesions.

Data from this thesis showed that the perirolandic P22 and N31 SEP components were important measures to examine in cases of lesions affecting the primary somatosensory cortex. The differential affect of such lesions provided important evidence that there are discrete and separate generators for these components.

Interpretation of standard deviation maps created by the univariate Z transform software of the Brain Atlas III™ system were of limited value in the detection of SEP abnormalities associated with cortical lesions.

A new sagittal polar projection system of local electrode placement was employed to investigate the SEP in a control group. This system was both easy to employ and points could easily and effectively be communicated.

A final study investigating the lateralisation of the SEP in schizophrenia could not confirm previous reports of this measure being of value in the diagnosis and classification of this condition.

KEY WORDS: SOMATOSENSORY EVOKED POTENTIAL BRAIN MAPPING TOPOGRAPHY CORTICAL LESIONS CORTICAL GENERATORS

ACKNOWLEDGEMENTS

I would like to thank Professor Graham Harding and Dr Lesley Jones for their support, advice and encouragement without which this study would not have been possible.

Thanks to Neville Drasdo for his inspiration and support.

Sincere thanks are also due to staff and students of the Department of Vision Sciences who offered both advice and practical assistance.
Particular thanks are due to Andrea Edson, Anne Hughes and Vivica Van der Vliet - my technical colleagues who have supported my endeavours and lightened my workload and without whom the project would not have been practical.

A final thanks to my wife Diane who has always had a greater belief in my abilities than I frankly merit or deserve.
I could not have done without your devoted support and encouragement .

DEDICATION

TO MUM & DAD

INDEX

CHAPTER 1. THE ANATOMY AND PHYSIOLOGY OF THE SOMATOSENSORY PATHWAYS

CHAPTER 2. THE SOMATOSENSORY EVOKED POTENTIAL

CHAPTER 3 CORTICAL GENERATORS - IDENTIFICATION/ METHODOLOGY.

CHAPTER 3 (CONTD)

CHAPTER 4 **STUDY OF THE TOPOGRAPHY OF THE UPPER LIMB SOMATOSENSORY EVOKED POTENTIAL IN THE HEALTHY HUMAN ADULT.**

CHAPTER 5 SOMATOSENSORY EVOKED POTENTIALS IN PATIENTS WITH KNOWN CORTICAL LESIONS.

CHAPTER 5 (CONTD)

CHAPTER 6 **THE USE OF A NEW COORDINATE SYSTEM IN THE MEASUREMENT OF THE SOMATOSENSORY EVOKED POTENTIAL IN THE HEALTHY HUMAN ADULT.**

CHAPTER 5 (CONTD)

CHAPTER 7 SOMATOSENSORY EVOKED POTENTIALS IN SCHIZOPHRENIA. A LATERALIZATION STUDY.

CHAPTER 8 SUMMARY AND CONCLUSIONS ON THE VALUE OF THE SEP USING BRAINMAPPING TECHNIQUES

APPENDIX 1 (CONTD)

INDEX OF FIGURES

FIGURES OF CHAPTER 1

FIGURES OF CHAPTER 2

FIGURES OF CHAPTER 3

FIGURES OF CHAPTER 4

FIGURES OF CHAPTER 4 (CONTD)

FIGURES FOR CHAPTER 5

FIGURES OF CHAPTER 5(CONTD)

FIGURES OF CHAPTER 5(CONTD)

FIGURES FOR CHAPTER 6

FIGURES FOR CHAPTER 7

CHAPTER 1.

THE ANATOMY AND PHYSIOLOGY OF THE SOMATOSENSORY PATHWAYS

1.1.0. The receptors

There is still much debate as to the anatomical sources of the somatosensory derived potentials, particularly at the cortical level. It seems wise therefore to detail the anatomical pathways that are considered to be involved in somesthesis and to outline the 'grey' areas of knowledge.

Since this study is involved primarily with upper limb pathways only these will be examined in detail.

The skin contains several forms of sense organs as well as free nerve endings. These receptors are classified in a number of ways. Three main divisions are Exteroceptors, Proprioceptors and Interoceptors. The latter constitute the receptor end organs of the visceral afferent components and detect internal events such as changes in blood pressure; we will not consider these further. Exteroceptors respond to stimuli from the external environment and are therefore found at or close to the surface of the body. These include the encapsulated and non-encapsulated terminals in the skin and around hairs; examples of the encapsulated terminals are i) Tactile Corpuscles of Meissner - found in papillae of skin of all parts of the hand and foot. ii) Lamellated Corpuscles of Pacini - subcutaneous tissue of the palmer aspects of the hand and planter aspects of the digits, generally accepted as pressure receptors and probably sensitive to vibration. iii) Bulbous corpuscles of Krause. iv) Ruffini endings (Figure 1.1)

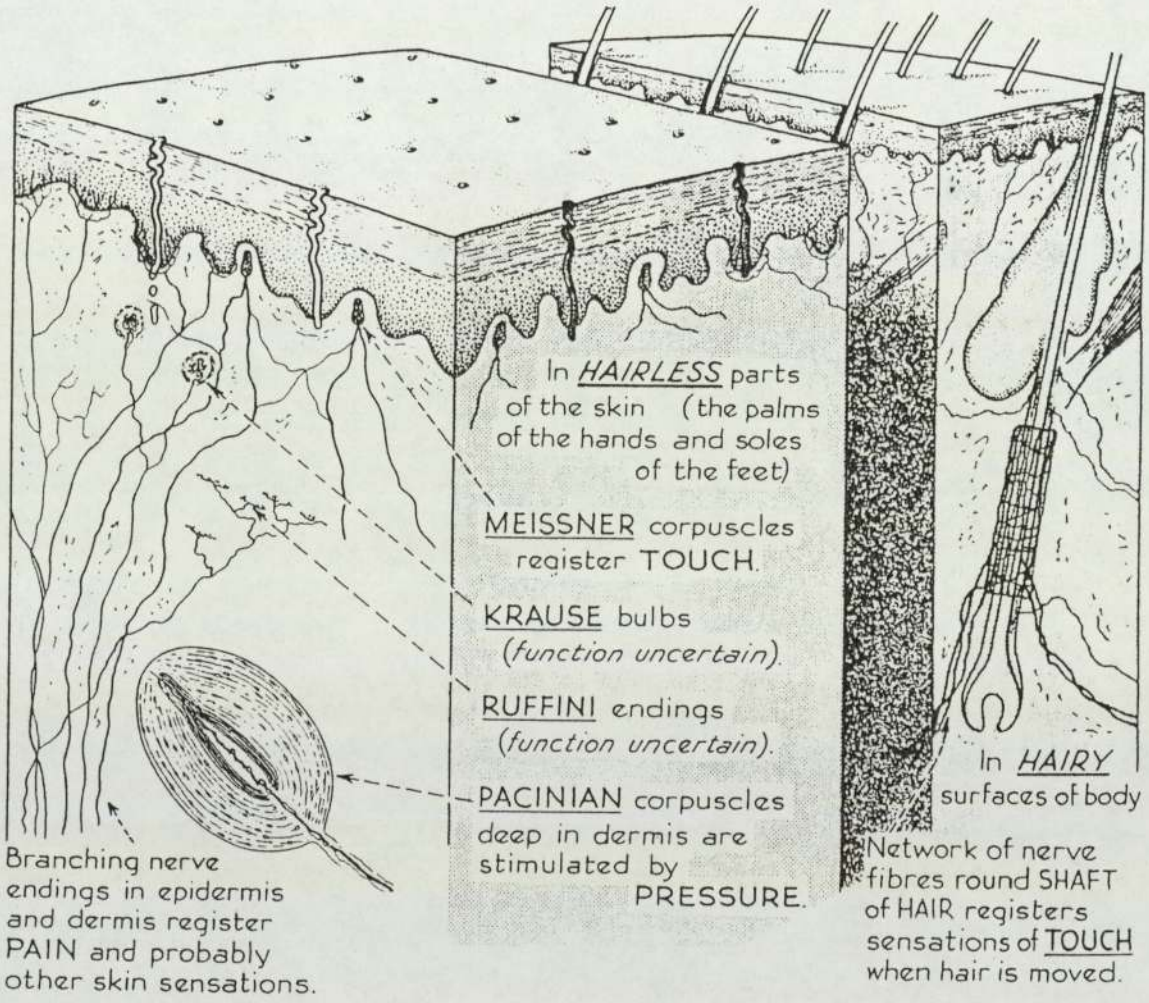

Figure 1.1. Cross section of the skin indicating the variety of sensory receptors.

From McNaught and Callander (1983).

Proprioceptors respond to stimuli arising in deeper tissues. They are concerned with movement, position and pressure and include the neurotendinous organs of Golgi, the neuromuscular spindles and deeply placed Pacinian corpuscles. They are stimulated by the activity of the muscles, movements of the joints and changes in the position of the body as a whole or in part. They are essential to the co-ordination of muscles, the grading of muscular contraction and the maintenance of equilibrium.

Free nerve endings occur in may different sites in the body. In the skin they are generally regarded as 'pain receptors' or '*nociceptors* ' since they have a high sensory threshold and only potentially traumatic stimuli will cause a high level of activity in these fibres. Many nociceptors may be specialised chemoreceptors that are excited by tissue substances released in response to noxious stimuli; such substances include histamine, bradykinin, serotonin, acetylcholine, substance P and high concentrations of K^+.

The other receptors may also be classified on the basis of their properties as afferent units, such as *mechanoreceptors* that fire maximally following mechanical deformation or *thermoreceptors* , firing maximally following temperature change.

Mechanoreceptors can be further subdivided into Rapid adapting and Slow adapting types based on their type of response and distribution. Rapid adaption indicates that the unit is firing only as long as the stimulus is moving or active whereas slow adaption indicates that the unit also fires when the stimulus is held constant. It has been suggested that tactile corpuscles (Meissners) and the nerve endings around hair follicles respond to touch (Rapid adaption), the bulbous corpuscles to cold, the Ruffini type of receptor organ to warmth (Slow adaption) and the free nerve endings in the epidermis and dermis to pain. The lamellated corpuscles are sensitive to deformation. However, it is suggested that the appreciation of the different modalities of cutaneous sensation depends more on the pattern of the impulses arriving at the sensory cortex, including their number and spatial and temporal arrangements. For example, touch, heat, cold and pain can be appreciated in the cornea where only free nerve endings exist.

All cutaneous sensors and many proprioceptors are thought to be of one structural type. This is where the neuronal receptor is itself a primary sensory neuron with a perikaryon situated in a craniospinal ganglion and a long peripheral process, the ending of which constitutes the actual sensory terminal.

1.1.1 Receptors of proprioception

The problem of which receptors are responsible for mediating proprioception is still debated in the literature. Joint receptors, once thought entirely dominant in this role, are losing ground to both muscle and cutaneous receptors. Moberg (1983) made many observations on patients during four decades of reconstructive limb surgery, together with the results of some simple experiments, also on man, and mainly by blocking the afferent input from different parts of the forearm and hand, have suggested that the role of cutaneous receptors in position sense and kinaesthesia has been greatly underestimated. The following contribution is from a review by Matthews (1988) who examines a number of these factors.

Table 1.1 (overleaf) lists the numerous receptors that transmit signals whenever we move. The question is which of them contribute significantly to position sense.

The standard neurological test of position sense, namely waggling the patients passive finger, does not correspond to any commonly occurring natural stimulus. The detection of such essentially external stimuli cannot be the prime function of the internally placed proprioceptors. A priori, this would seem to fall equally within the sphere of action of the cutaneous receptors.

1.1.1.1. Cutaneous receptors

Recent observations, shown by recording from single fibres in man, is that for the hand virtually all of the receptors are excited whenever we move it. It is reasonable to suppose that the sensation during movement bears no relation to that elicited by an external stimulus.

TABLE 1.1 RECEPTORS THAT TRANSMIT SIGNALS DURING MOVEMENT (MATTHEWS 1988)

POSITION SENSE	POSSIBLE NEURAL INPUTS
1. Joint	In capsule
	In ligaments
2. Skin	Fast adapting I and II
	Slow adapting I and II
3. Muscle	Spindle: primary and secondary
	Tendon organ
4. Motor centres	Corollary discharges.

1.1.1.2. Joint Receptors

As mentioned earlier, these are now out of favour as producing a significant contribution to position sense. This is largely due to work in animals on studies of the knee that intimates that they are only effectively excited by moving the joint to one or other of its extremes. In the middle of the range most, if not all, are normally quite silent, including while the joint is being moved (Burgess and Clark 1969; Grigg and Greenspan 1977).

1.1.1.3. Muscle receptors

Their sensory contribution would be expected to be in the genesis of sensations of force and effort rather than position. Of undoubted importance however are the muscle spindle afferents that lie in parallel with the main muscle and so signal its length; in addition they can be specifically excited by the fusimotor system or gamma efferents.

1.2.0. The Peripheral Nerve

There are pure sensory nerves, pure motor nerves and mixed nerves. The skin is innervated by cutaneous nerves; most but not all of them are branches from mixed sensory-motor nerves. In cutaneous nerves about 50% of the sensory fibres originate from nociceptors.

Mixed peripheral nerves have been classified according to total fibre diameter and conduction velocity. The three main classifications are A,B and C. Class B comprises the myelinated preganglionic fibres of the autonomic nervous system and we will consider these no further.

Class A fibres can be further subdivided and we will consider the afferent sensory fibres within this classification.

Group I The thickest myelinated A fibres (type A alpha) vary from 1μm to 20μm in diameter. Their excitability threshold is low and their conduction velocity is high - as much as 100 m/sec. They include the primary sensory fibres from muscle spindles (subgroup Ia) and from tendon organs (Ib).

Group II The diameters of group II fibres range from 5 to 15μm, and their conduction velocities from 20 to 90 m/sec. Includes cutaneous afferent fibres from various mechanoreceptors such as touch and Pacinian corpuscles, receptors associated with larger, 'guard' hair follicles and fibres of the secondary endings on the intrafusal muscle fibres of muscle spindles.

Group III (A delta fibres) Their diameters range from 1 to 7μm and their conduction speeds from 12 to 30 m/sec. Fibres innervate follicle receptors associated with finer hair, sensory endings in the walls of some blood vessels, and a variety of nociceptors.

Group IV (type C fibres)

These are non-myelinated nerve fibres with diameters ranging from 0.2μm to about 1.5μm and conduction velocities of 0.3-1.6 m/sec. Such fibres include autonomic efferents which are postganglionic in position, and both visceral and somatic sensory fibres, many of which are 'pain' fibres serving all the tissues of the body except the interior of the central nervous system.

Each sensory neurone works on the 'all or none' principle; all impulses in a given neuron are identical to one another, and the only variables will be the number of impulses transmitted along the neurone per second, and the pattern of this discharge. Since neurones do not vary the amplitude or size of the nerve impulse, an increase in a sensory stimulus is transmitted to the CNS as more impulses per second.

1.2.1. Somatosensory activity in peripheral nerve.

With electrical skin stimuli in the glabrous skin of the hand and the microelectrode positioned in the appropriate median nerve fascicle, the response in A-alpha fibres can be recorded at the threshold for perception of the stimulus (Valbo et al 1979). At this weak stimulus strength the subjects report tactile sensations, described as tapping, flutter or vibration, dependent on the stimulation frequency. At 5-10 times threshold, A-delta fibres are recruited. Single stimuli are felt to be sharp and pricking, and repetitive stimulation at 50 hz causes severe pain. Further increase in stimulus intensity up to 15-20 times thrshold recruits C fibre deflections. Single shocks are described as heavy sharp pain followed by an aching "afterpain". In the radial nerve some A delta and C fibre deflections may be activated by non-painful skin stimuli just above threshold for perception (Hallin et al 1974), indicating that impulses in thin fibres need not necessarily be associated with pain.

1.2.2. Proprioceptive activity in peripheral nerve

Most units encountered in muscle nerve fascicles are mechanoreceptive afferents of muscular origin. They do not respond to skin stimuli or local joint pressure, but they do respond to mechanical stimulation of the receptor bearing muscle by passive stretch and local pressure and to an isometric voluntary contraction of this muscle. Muscle receptors responding in this way are likely to be either primary spindle endings, secondary spindle endings, or Golgi tendon organs. Sudden light taps on the muscle belly or tendon are usually sufficient to induce a spindle discharge.

Some characteristics of proprioceptive receptor stimulation are;

1) Primary muscle spindle endings

a) High dynamic sensitivity to passive muscle stretch, the firing rate increasing with speed of movement.

b) Silence during the rising phase and discharge during the falling phase of an electrically induced twitch contraction of the receptor bearing muscle.

2) Secondary muscle spindle endings

a) Have a position sensitivity similar to that of the primary endings but a much smaller dynamic sensitivity to sudden stretches or relaxations.

b). Silence during the rising phase of an electrically induced twitch contraction of the receptor bearing muscle.

3). Golgi tendon organs

a). No resting discharge at intermediate muscle length and relatively low dynamic sensitivity to passive stretch.

b). Close relation between discharge rate and contraction force.

c). Discharge during the rising phase of an electrically induced muscle twitch.

1.3.0. Dorsal Nerve Roots

Sensory and motor nerves run for the greater part of their route as a mixed nerve with motor and sensory fibres in adjacent bundles, although they have separate spinal cord roots. Motor nerves have their cells of origin in the anterior horn of grey matter of the spinal cord. These nerves leave via the ventral nerve roots. Sensory nerves have their cells of origin outside the spinal cord in the spinal ganglia, entering the cord via the dorsal nerve roots.

Each ganglion cell possesses a single nerve process that divides in the form of a "T", with a central branch running to the spinal cord and a peripheral branch coming from a receptor organ or organs. There are no synapses in a spinal ganglion.

The area in which the dorsal root fibres enter the spinal cord, in the region of the dorsolateral sulcus, is called the dorsal root zone. The largest and most heavily myelinated fibers generally occupy the most medial position in this zone, and the small myelinated and unmyelinated fibers the most lateral.

The subsequent pathways after dorsal root entry, now depend on the type of sensation.

1.4.0. Pathways mediating sensation.

Tactile sensations are complex in nature because they involve a blending of light cutaneous contact and variable degrees of pressure, depending upon the intensity of the stimuli. Two different forms of touch sensibility are recognised: simple touch and tactile discrimination. Simple touch involves a sense of light contact with the skin associated with light pressure and a crude sense of tactile localisation. Tickling and itching sensations are related to pain sense. Tactile discrimination conveys the sense of spatial localisation and perception of the size and shape of objects.

At least three different spinal cord pathways mediate tactile sensation:

The LEMNISCAL PATHWAYS are concerned with the discriminative aspects of touch, including place, contour and quality of the stimulus, and identification of objects and numbers on the hand. This latter sensory capacity is stereognosis.

The ANTEROLATERAL SYSTEM, comprising the lateral and ventral spinothalamic tracts subserves simple touch sensation. The other component of the anterolateral system, the spinoreticular projections, is concerned with responses to noxious stimuli.

Finally the LATERAL CERVICAL SYSTEM (Spincervicothalamic pathway) is thought to mediate touch sensation as well as vibratory and proprioceptive senses.

We will now consider these pathways individually:

1.4.1. Lemniscal System.

This pathway comprises two large ascending tracts, the fasciculi gracilis and cuneatus, which are separated from each other by the postero-intermediate septum. The fasciculus gracilis receives fibres from the lower thoracic, lumbar, saccral and coccygeal segments and we will consider this no further.

The fasciculus cuneatus commences in the mid thoracic region and derives its fibres from the dorsal roots of the upper thoracic and cervical nerves and in consequence is situated laterally to the fasciculus gracilis. The fasciculus is heavily myelinated and contain the central processes from cells in the spinal ganglia, and these pass without interruption or decussation to the medulla oblongata, where they terminate in the cuneate nuclei.

The dorsal column nuclei are not simple 'relay nuclei' as was long supposed - afferent information is separated in channels which are discrete both for spatial origin and stimulus specificity (Uddenberg1968) - in the cat, those fibres conducting impulses from hair receptors being most superficial,followed by fibres mediating tactile and vibratory sensibility in successively deeper layers.

All the large calibred fibres of the dorsal funiculus (excepting some of the medially placed ones), have collaterals which pass through the medial two thirds of laminae I,II and III.

The internal structure of the spinal cord changes gradually to that of the **medulla oblongata.** The posterior region is divisable into caudal and cranial levels. The caudal part, consists of the upward continuation of the fasciculi gracilis and cuneatus of the spinal cord. These two fasciculi are at first vertical but at the caudal end of the fourth ventricle they diverge from the median plane, and each presents an elongated swelling; that on the fasciculus cuneatus is termed the cuneate tubercle and is caused by a nucleus of grey matter termed the nucleus cuneatus. Most of the fibres of the fasciculus end by forming synapses in this nucleus. The somatotopic arrangements in the tracts is also evident in the nuclei, within which there is also a specific distribution of terminals on the basis of sensory modalities, including hair displacement, light touch, pressure, vibration and joint movement.

New fibres arise in the nucleus and constitute the second neurons on the pathway of tactile and proprioceptive sensibilities. These internal arcuate fibres emerge from the ventral aspects of the nuclei and, curving forwards and laterally at first round the central grey matter, they bend medially to reach the median plane, where they decussate with the corresponding fibres of the opposite side.

The fibres of the medial lemniscus, after emerging from the lemniscal decussation, turn upwards on each side in the form of a flattened tract. In this position they ascend to the pons, increasing in number as additional fibres join them from the upper levels of the decussation.

The spinocerebellar, spinotectal, vestibulospinal, rubrospinal and lateral spinothalamic tracts (spinal lemniscus), are all in the anterolateral area.

Inferiorly **the pons** is continuous with the medulla oblongata. Here the medial lemniscus is joined by the second neuron fibres from the principal sensory nucleus of the trigeminal nerve, which convey proprioceptive, tactile and pressure impulses from the receptive field covered by it.

The somatotopic lamination is maintained throughout the passage of the tracts through the medulla oblongata and the pons. In **the midbrain** however, the fibres from the lower limbs extend dorsally, and in this part of their course it is possible for the surgeon to divide the pain and temperature fibres of the upper limb and trunk without injury to the corresponding fibres of the lower limb.

The ascending somatosensory fibres terminate in the VENTRAL GROUP OF THALAMIC NUCLEI.

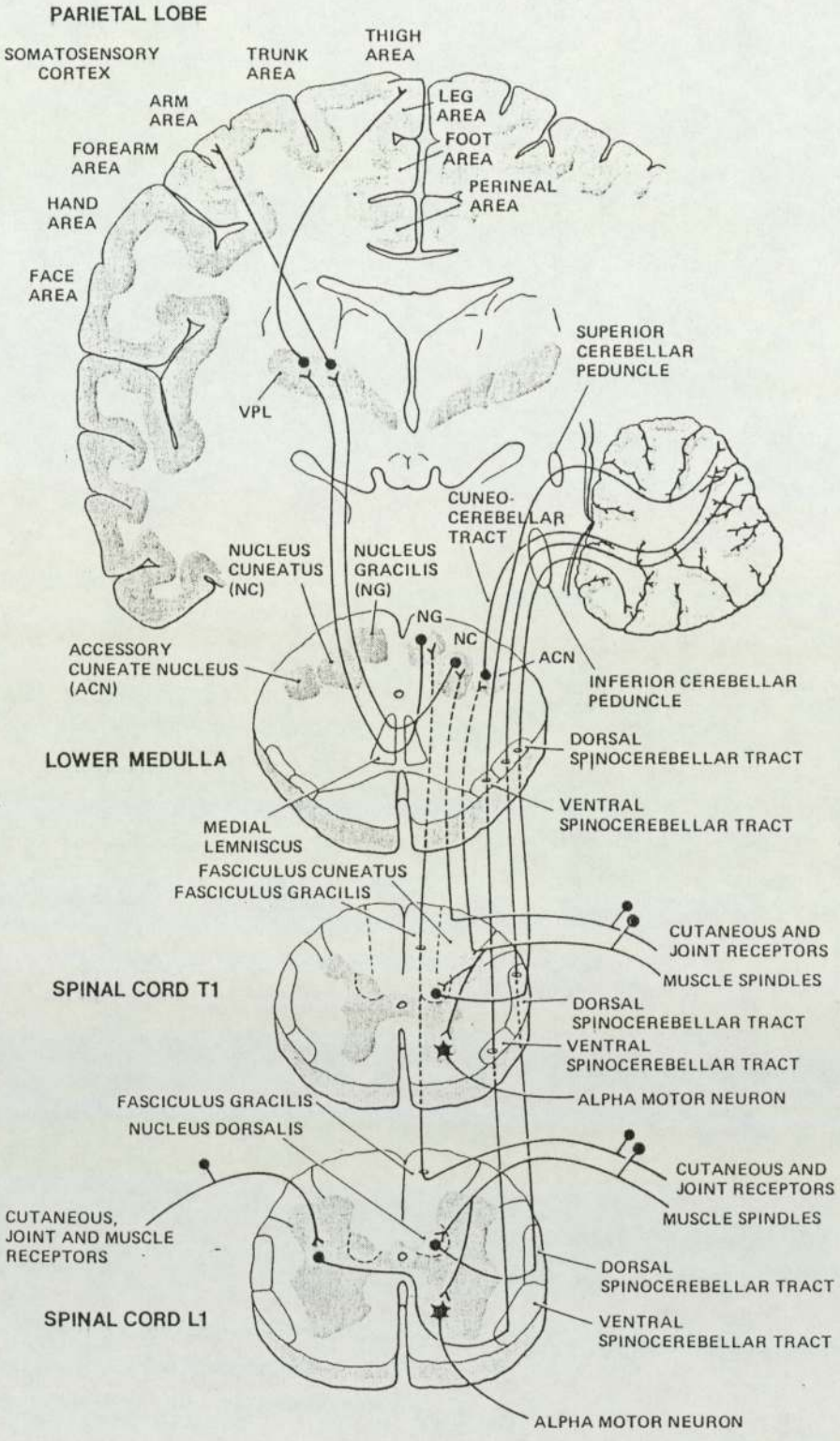

Figure 1.2. The central nervous system pathways mediating proprioception and stereognosis.

NG= nucleus gracilis; NC= nucleus cuneatus; ACN= accessory cuneate nucleus; VPL= thalamic nucleus ventralis posterolateralis.

Adapted from Gilman and Newman (1987).

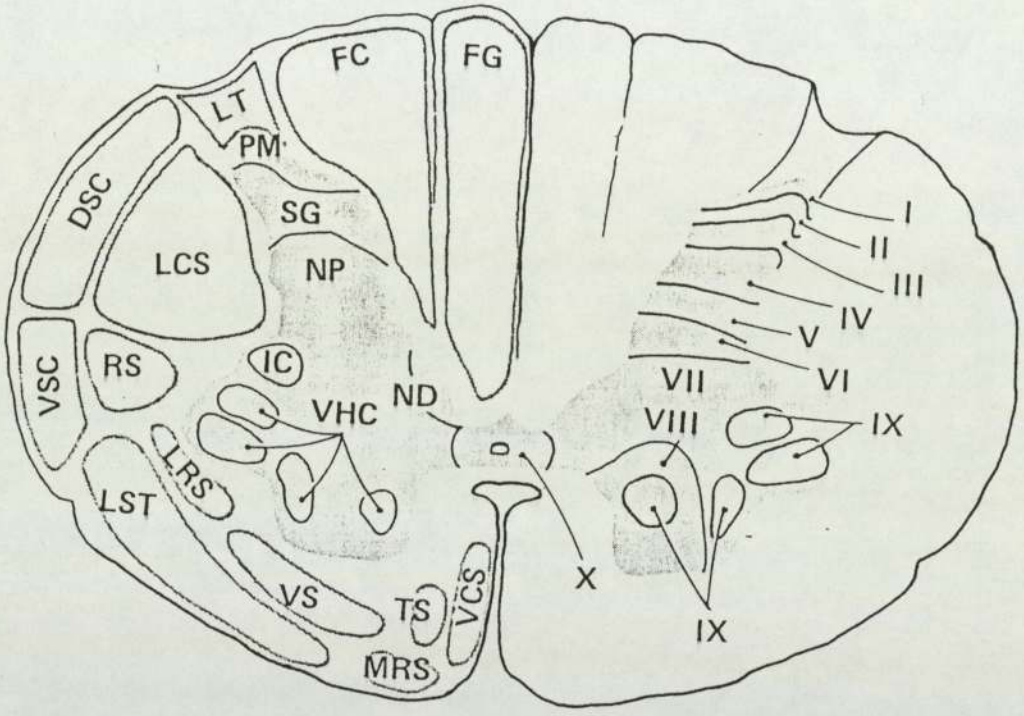

Figure 1.3 Cross section of spinal cord at approximately the C8/T1 segmental level. Tracts and nuclei of the cord are illustrated on the left; Rexed's laminar organisation of the grey matter are illustrated on the right.
DSC= dorsal spinocerebellar tract; FC= fasciculus cuneatus; FG= fasciculus gracilis; IC=intermediolateral cell column; LCS= lateral corticospinal tract; LRS= lateral reticulospinal tract; LST= lateral spinothalamic tract; LT= Lissauer's tract; MRS= medial reticulospinal tract; ND= nucleus dorsalis; NP= nucleus proprius; PM= posteromarginal nucleus; RS= rubrospinal tract; SG= substantia gelatinosa; TS= tectospinal tract; VCS= ventral corticospinal tract; VHC= ventral horn cell columns; VS= vestibulospinal tract; VSC= ventral spinocerebellar tract.
Adapted from Gilman and Newman (1987)

1.4.2. Anterolateral System

The sensations of pain, temperature and crude touch are mediated by the anterolateral system. The system contains pathways that include the lateral and ventral spinothalamic tracts. Other components of the anterolateral pathway, mainly spinoreticular, do not reach the thalamus and thus cannot be termed "spinothalamic".

Portions of the anterolateral system are phylogenetically old. The system consists of the "paleospinothalmic tract" which projects to the medial portions of the thalamus (the intralaminar nuclei), and the "neospinothalamic tract" which projects to the ventral posterolateral region of the thalamus.

The anterolateral system is predominantly a slowly conducting, polysynaptic system. In humans, a small percentage of fibres go directly to the thalamus, but most synapse in the medial aspect of the reticular formation throughout its length in the brain stem.

Neural responses to noxious stimuli mediated by Aδ and C peripheral nerve fibres enter the spinal cord through the lateral part of the dorsal root zone and divide at once into short ascending and descending branches that run longitudinally in the Tract of Lissauer (posterolateral fasciculus). Within a segment or two, these fibres leave this tract to make synaptic connections with neurons in the dorsal horn, including interneurons in laminae I, II and III (substantia gelatinosa), IV and V. The interneurons project to neurons in laminae V through VIII and there make synaptic connection upon the cells of origin of the anterolateral system, including the lateral and ventral spinothalamic tracts and the spinoreticular projections.

The axons of the spinothalamic tract cells cross anterior to the central canal in the ventral white commissure and then rostrally in the antero-lateral funiculus.

The subsequent projection of the anterolateral system to the thalamus is organised somatotopically so that the upper body is located medial to that from the lower body (see Figure 1.4).

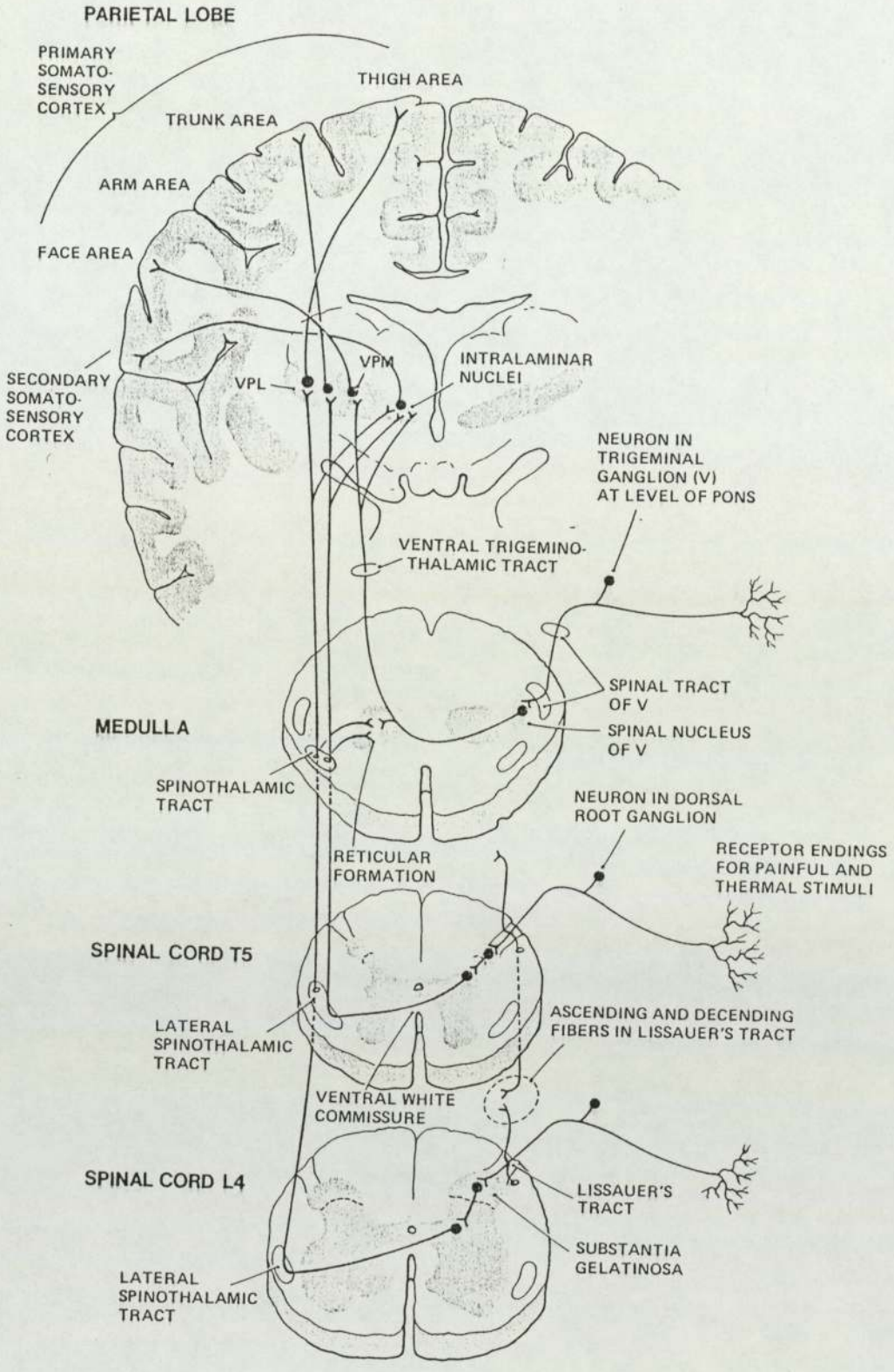

Figure 1.4. The central nervous system pathways that mediate the sensations of pain and temperature.

Adapted from Gilman and Newman (1987).

The lateral spinothalamic tract extends through the spinal cord and brain stem, supplying inputs to the reticular formation, the superior coliculus and several thalamic nuclei, including the intralaminar nuclei, the posterior nuclear complex (PO), and the ventral posterolateral nucleus (VPL) (See section 1.5.0).

Previously, the lateral and ventral components of the spinothalamic tract were thought to subserve different functions, with the lateral spinothalamic tract mediating nociceptive information and the ventral spinothalamic tract mediating tactile sensation. Recent evidence indicates no functional difference between the lateral and ventral components of the spinothalamic tract. Both are capable of mediating nociceptive and tactile sensation.

1.4.3. Lateral Cervical System

Almost all of the cells of the lateral cervical system are sensitive to light mechanical stimulation of the skin of the ipsilateral side of the body, but a few are activated by noxious stimuli. Peripheral nerve fibres entering this system make synaptic connections in the dorsal horn (laminae III, IV and V) throughout the length of the spinal cord. Heavily myelinated second-order neurons arise in these laminae and ascend ipsilaterally in the most medial corner of the dorsal lateral funiculus to terminate in the lateral cervical nucleus. This nucleus is located just lateral to the dorsal horn of the first and second cervical segments (see Figure 1.5). The axons of these cells cross the spinal cord to join the contralateral medial lemniscus and, with it, terminate within the thalamus. The fibres of the entire lateral cervical system conduct very rapidly.

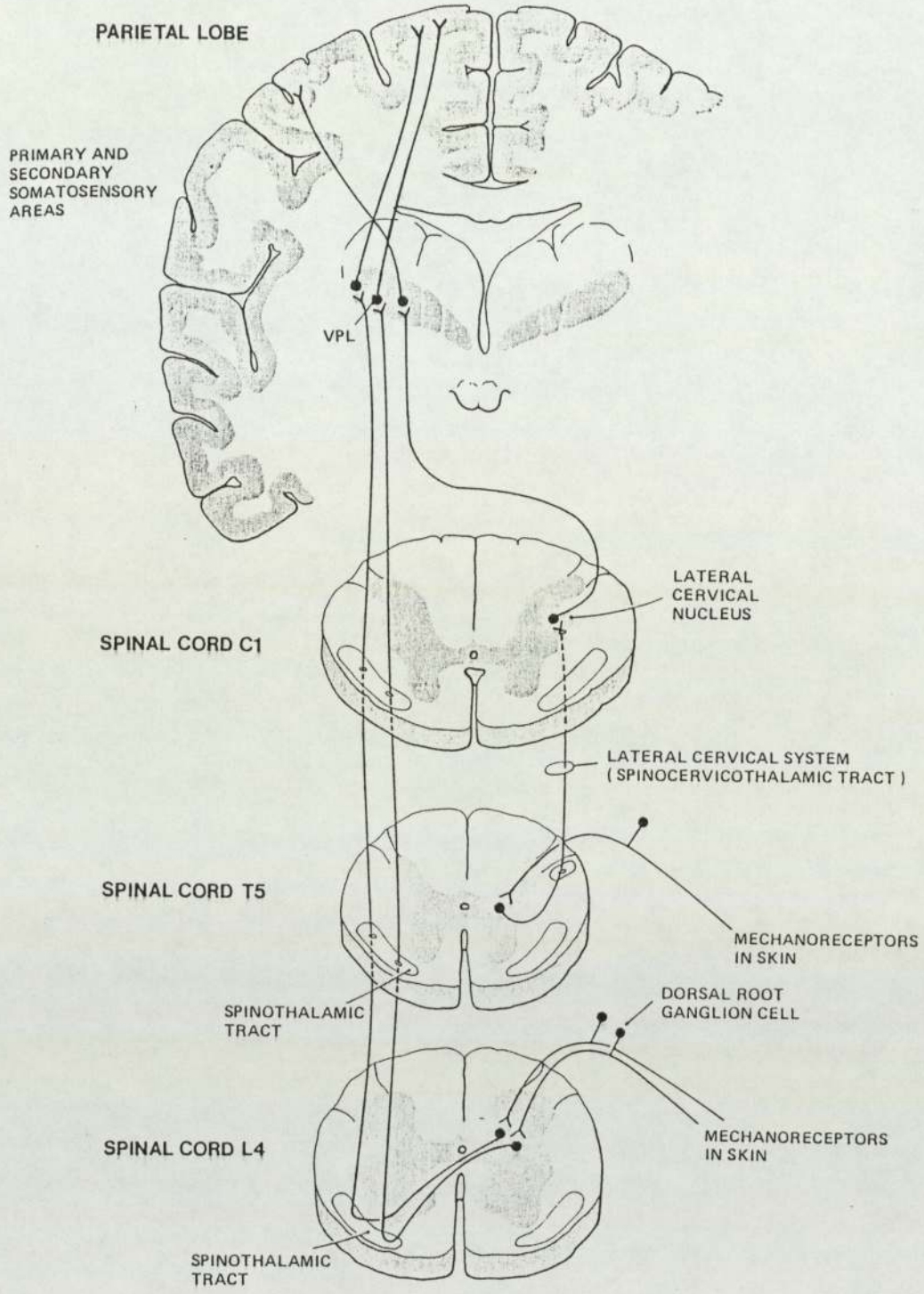

Figure 1.5 The central nervous system pathways mediating tactile sensation except for the lemniscal system. The lateral and ventral components of the lateral spinothalmic tract are shown.
Adapted from Gilman and Newman (1987).

1.5.0. Thalamic Nuclei

The ventral group of thalamic nuclei form a craniocaudal sequence of three main nuclei; the Ventralis anterior (VA), the Ventralis Intermedius (VI), also known as the Ventralis Lateralis (VL) and the Ventralis Posterior (VP). The latter can be subdivided into the Ventralis Posterior Lateralis (VPL) and the Ventralis Posterior Medialis (VPM). There are additional nuclei in this group which are inferior and oral in position (Figure 1.6)

The terminations of the medial lemniscus and spinothalamic tract fibres show contrasting features. The lemniscal fibres are wholly crossed, originating exclusively in the gracile and cuneate nuclei of the opposite side and their terminals are confined to the VPL. Whilst the majority of the spinothalamic tract fibres are also crossed, an appreciable number ascend on the same side and terminate in the ipsilateral thalamus.

VPL cells are highly specific for both the type of stimulus and the bodily site of origin. In monkeys, units respond to contralateral stimulation of the skin or hairs, or joint movement or static joint position or sinusoidal tissue vibration, but never to two of these varieties. Receptive fields from medial lemniscus activity are small and sharply localized, the smallest being recorded by stimulation of the terminal segments of the limbs. Units responding to spinothalamic tract activity in general show rather larger receptive fields and are somewhat less modality specific.

Transmission in the nuclei may be modulated by activity in descending corticothalamic fibres.

The main thalamocortical radiations from the VPL and VPM proceed through the posterior limb of the internal capsule to the primary somatic sensory areas of the cerebral cortex. Throughout this radiation the precise somatotopic organisation continues to be preserved. The same cortical projection areas project cortico-thalamic fibres back to the nuclei. Unfortunately, the thalamic projections to the secondary somatic sensory areas cannot yet be regarded as settled.

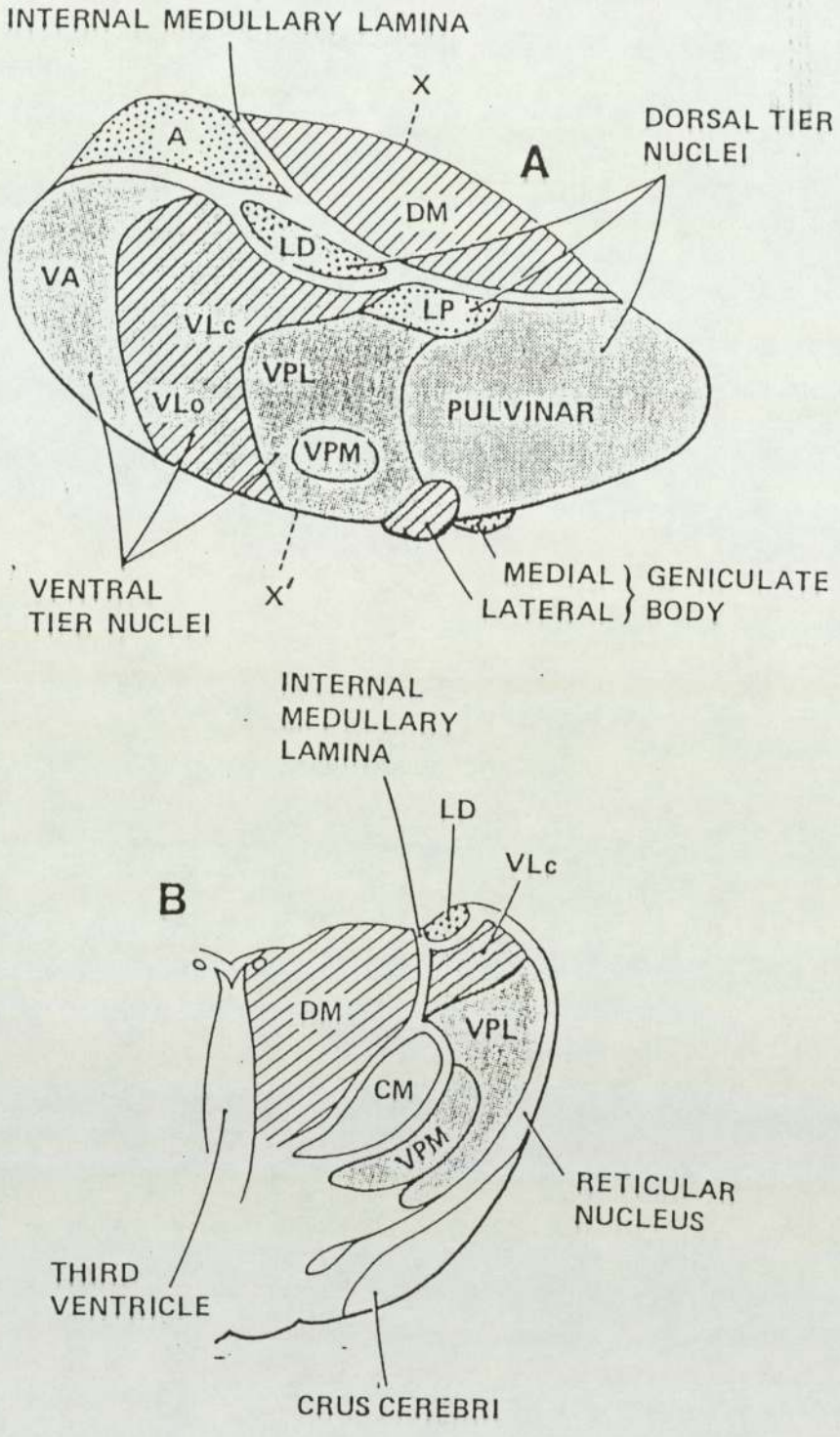

Figure 1.6. Thalamic nuclei. (A) A schematic dorsolateral view of the thalamus, which has been dissected from the left side of the brain, showing the boundaries of the thalamic nuclei. (B) A coronal section through the thalamus and subthalamus, showing the plane of a section through X-X' in A.
A= anterior nuclear group; CM= centromedian nucleus; DM= dorsomedial nucleus; LD= lateral dorsal nucleus; LP= lateral posterior nucleus; VA= ventral anterior nucleus; VLc= ventral lateral pars caudalis; VLo= ventral lateral pars oralis; VPL= ventral posterolateral nucleus; VPM= ventral posteromedial nucleus. Adapted from Gilman and Newman (1987).

1.6.0. Thalamo - Cortical and Cortico - Cortical Projections

A schematic view of the thalamocortical connections to the primary somatosensory / somatomotor areas are shown in Figure 1.7.

The thalamo-cortical tracts end in the layer IV of the cortex where synapses are found especially with stellate cells. From here the information is transported to the layers II and III and V and VI respectively. From the upper layers, the so-called U-fibres emerge, making contact with adjacent areas. From the lower layers large myelinated fibres emerge to the structures that are relatively far away as, for example, the cortex of the other hemisphere, crossing the corpus callosum.

Evidence over the last 30 years has shown that the areas receiving or originating projection fibres for somasthesis are much more extensive than the initial classical studies indicated. Furthermore, the division into 'receiving' and 'originating' projection areas is by no means so distinct as at first appeared. The postcentral gyrus is not the only area to which a somatosensory thalamic projection is directed and the distinction of motor and sensory areas still favoured in simplistic description is erroneous. In 1933 Dusser de Barenne demonstrated motor responses to stimulation of the 'sensory' areas, and projection of efferent pyramidal fibres from the same postcentral area were described by Levin and Bradford in 1938.

It is more appropriate to use the term sensorimotor in describing these areas. The first *predominantly* motor area in the precentral gyrus we will term **MsI (somatomotor area)** - this area receives fibres from the cerebellum, which relay in the nucleus ventralis lateralis of the thalamus, and these are distributed particularly to its anterior region (Brodmann area 6) and to the prefrontal area (area 8). It also receives afferents concerned in other sensory modalities, probably via the thalamus also, but in addition from the hypothalamus and from other parts of the cortex.

On the medial surface of the cerebrum, located in the medial frontal gyrus in man, is a further sensorimotor area,which being largely motor, is called the **supplementary motor area, MsII**.

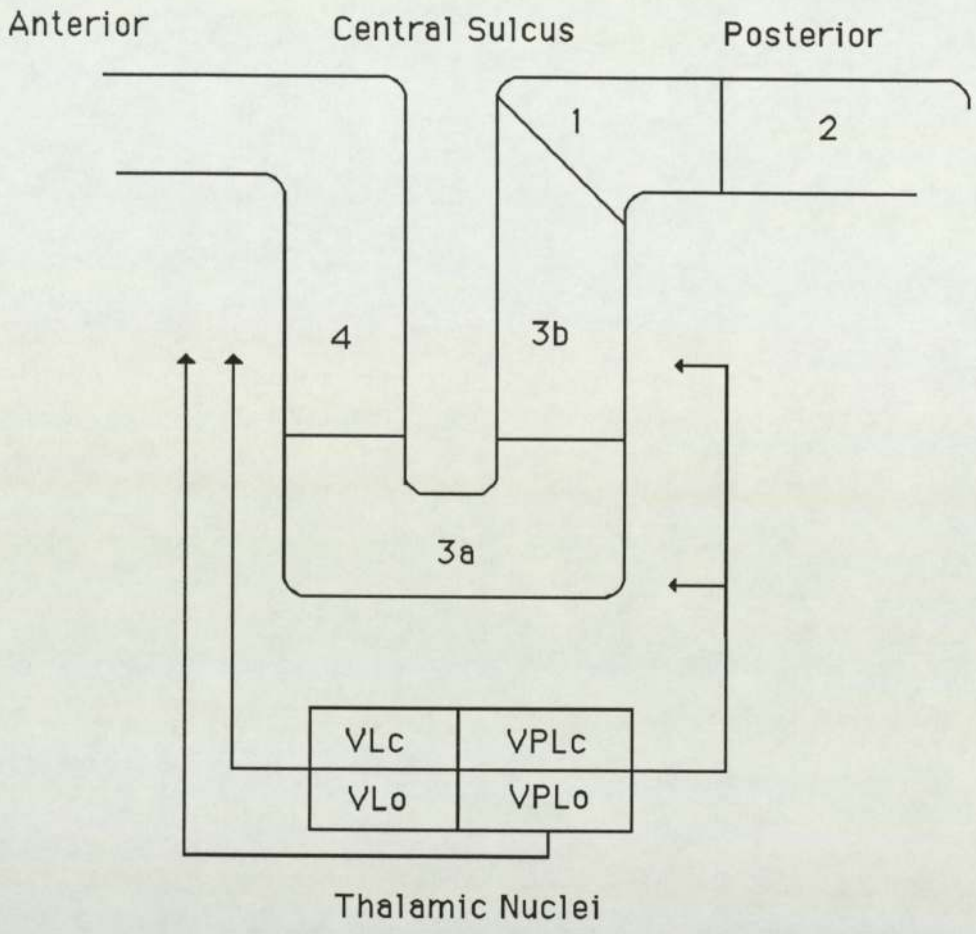

Figure 1.7. Schematic transverse cross section of the central sulcus showing Brodman areas and thalamocortical projections in the human brain.
VLc= ventral lateral pars caudalis; VLo= ventral lateral pars oralis;
VPLc= ventral posterolateral pars caudalis; VPLo= ventral posterolateral pars oralis.

Movements of the contralateral limbs can be elicited from the supplementary motor areas in monkeys and in man. There is a bilateral projection to the thalamus and to the gracile, cuneate and pontine nuclei, contrasting with the similar but unilateral projections from the primary somatomotor cortex. Efferent fibres from this area have been traced into the spinal column in cats. Much is still to be discovered of the complete nature of this area.

In the postcentral gyrus **SmI (somatosensory)** is the primary sensory area. Much work has been done using ablation techniques to study the projections of this area of cortex. In the main somatic areas, as in the visual sensory areas, it is apparent that there is an anatomical segregation of "building blocks" of different types in that neurons with similar response properties tend to be grouped in different architectonic subdivisions of the primary sensory areas. A schematic transverse section of the central sulcus showing the relative locations of the Brodmann classification of this area is shown in Figure 1.7.

Its anterior part (Brodmann area 3), borders the central sulcus and extends into its depths to meet the agranular cortex of area 4. It is of the granular type but also contains numbers of scattered medium and small pyramidal cells.

The posterior part of the postcentral gyrus (areas 1 and 2) differs particularly in its smaller content of less densely packed granular or stellate cells. The precise boundary, if such exists, between the pre and post central areas in the central sulcus (area 3a) is still subject to much experimentation.

The primary somatosensory cortex, as previously mentioned, receives its main input from the thalamic ventrobasal complex. In the monkey the projection to area 3b is heavy and made up of singularly coarse fibres, whereas the fibres to areas 1 and 2 are much fewer in number and finer in calibre (Hyvarinen. J. 1982). It is possible that the fibres to areas 1 and 2 are branches of the coarser fibres passing to area 3b (Jones and Powell 1969a). The most anterior part of SmI, area 3a, also receives a projection from the ventrobasal complex from the subnucleus ventralis posterolateralis, pars oralis (VPLo), (Jones and Porter 1980). Area 3a differs from the

more posterior part of SmI in that it receives a strong afferent input from muscles (Phillips et al. 1971), whereas the muscles have little or no representation in areas 3b and 1.

The number of neurones with complex cutaneous receptive fields increase posteriorly within SmI. Most movement sensitive neurones that do not differentiate between directions are located in area 1. The more complex cell types specifically sensitive to direction of movement or to orientation of an edge are not observed in area 3b and their number increase posteriorly (Hyvarinen 1982). Anatomical data therefore suggests that an increase in the complexity of the information handled occurs in the cytoarchitectural subdivisions of SmI with successive intracortical projection steps from area 3 to areas 1 and 2.

Inferior to SmI lies **SmII**, found in the superior lip of the posterior limb of the lateral fissure. Evoked potentials indicate a somatotopic organisation in SmII, with the face area most anterior and the leg at the posterior or caudal end of the area. Single units associated with tactile and vibration senses have been identified, and stimulation of Pacinian corpuscles evokes higher potentials than in the primary somatosensory area (McIntyre et al 1967). This second somatosensory area projects to the thalamus, but its connections and their reciprocal nature have not yet been studied in detail. It also projects to the dorsal column nuclei.

1.6.1. Ipsilateral Cortical Connections

The primary somatosensory cortex is organised strictly somatotopically. Its neurons have rather small receptive fields that facilitate accurate localisation of stimuli, and they respond briskly, indicating precisely the timing of sensory events. Moreover, in SmI different submodalities are segregated in columns giving a localizational basis for stimulus quality.

Jones and Powell (1969a) demonstrated in the monkey that SmI and SmII areas are connected with one another and with area 4 in a reciprocal organised manner and that each has a further projection to the supplementary motor area, MsII. SmI alone sends fibres outside the sensorimotor region - to area 5. The fibres passing from SmI to the above areas arise in all three of its architectonic subdivisions (areas 3,1 and 2). In addition, areas 3,1 and 2 are interconnected with one another and with the transitional field between sensory and motor

cortex, area 3a, by intracortical association fibres. Functional columns in area 3, the majority of which respond preferentially to light tactile stimuli are firmly and reciprocally interconnected with those areas 1 and 2 which respond mainly to deep stimuli, that is pressure or rotation of a joint (Powell and Mountcastle 1959; Hyvarinen 1982)

SmII receives fibres from areas 3,1 and 2 and from the ventrobasal complex of the thalamus.

It seems possible that area 3a may be a specific cortical projection area in SmI for Group I muscle afferents (E.G.Jones and R.Porter 1980) in much the same way as area 3 is the main receiving area for cutaneous afferents and areas 1 and 2 for afferents from deep tissues.

Area 2 represents a transitional zone between the anterior postcentral gyrus and the posterior parietal area 5. The latter is an associative somasthetic area that combines inputs from the joints with input from various submodalities to represent different somatosensory patterns arising during movement.

1.6.2. Contralateral Cortical Connections

It has been demonstrated in the monkey that in both SmI and SmII areas, only the parts of the cortex containing the representation of regions close to the mid-line are connected commissurally. In SmI, at least, those regions of cortex containing the representation of the distal, freer parts of the limbs neither receive nor send callosal fibres (Jones and Powell 1969b, Pandya and Vignolo 1968).

Projections from SmI and SmII are restricted to somatic sensory regions in the opposite cortex, SmI projecting in a topographically organised manner to both SmI and SmII of the contralateral side. The precise organisation of the commissural fibres may respect both the topographic and functional properties of individual cell columns. SmII, on the other hand, may be a region for interhemispheric convergence for all somatic sensory modalities.

CHAPTER 2.

THE SOMATOSENSORY EVOKED POTENTIAL

2.0. Introduction

In the next two Chapters we will consider a range of studies which have been employed over the 40 year period following the initial description of a scalp recorded somatosensory related evoked potential. These studies have made an attempt to discover more of the precise nature and origin of these potentials; which receptors originate them; which pathways mediate them and the precise cortical areas that generate them. All of these facets are essential to our understanding of the somatosensory evoked potential (SEP) and our interpretation of them in the study of normal man and in pathology.

In this Chapter we will consider some early pioneering recordings; studies that have related receptor activity to the scalp SEP and finally to review a range of studies on the effect of known lesions of the pathways of somesthesis on the SEP.

2.1.0. Morphology

It was over 40 years ago that Dawson (1947) first described the form of the SEP. Through a number of studies (1950; 1954 and 1956) he described how the early part of the cerebral response appears over the contralateral Rolandic area, with a maximum some 6-7 cm lateral to the midline for the upper limb.

In the 1960's, studies in both America and Europe began to document the morphology and normal ranges of the Somatosensory evoked potential in man. Most notable of these were Allison 1962; Goff et al 1962; Shagass and Schwartz 1964; Debecker and Desmedt 1964; Giblin 1964 and Desmedt et al 1965. There was considerable agreement between the authors results and their data has been substantiated since by many other authors.

It was Giblin though in 1964 who first observed a possible dual configuration of the postrolandic evoked potential in normal controls and described the waveforms as being of the V or W type. Like many studies at that time, and indeed still utilized in many clinics today, Giblin employed electrical shocks applied to the contralateral median or ulnar nerves at the wrist. Recording electrodes were placed over the "hand" area of the post-central gyrus which was calculated as being 7 cm lateral and 2 cm posterior to the vertex point (Cz), according to the international 10-20 system of electrode placement (Jasper 1958), with a mid-frontal reference (Fz).

The first component of the response described was a brief negative potential with onset at 14-16 msec and a peak at 17-20 msec after the stimulus. Allison (1962) and Goff et al (1962) both observed that this component was sometimes preceded by a small amplitude positive potential which peaks at 14 to 15 msec. This small waveform was to prove the centre of much future experimentation and is now regarded as being of sub-cortical origin. It was following the initial negativity that Giblin observed a duplicity of form. He found that while records of 18 of 25 healthy subjects showed a single positive potential with peak latencies ranging from 23 to 31 msec (mean 26.8 msec, standard deviation 2.2 msec), the records of the remaining 7 subjects showed two distinct brief positive potentials within the same range (see Figure 2.1). Giblin suggested that, in all subjects, both positive peaks at 22 and 31 msec are generated in the somatosensory cortex; both are recorded by electrodes on the scalp in some subjects, but in the majority they merge to give a single positive wave whose peak latency is intermediate between the two.

Following this single or double early positive component there is another negative going wave which peaks between about 30 and 40 msec. This is followed by an equally consistent positive deflection which peaks between 40 and 50 msec.

Comparison of the responses of the right and left hemispheres evoked by stimulation of the contralateral median nerves shows that, for components occurring during the first 50 msec, the responses are usually indistinguishable .

2.1.1. Nomenclature

Although there is reasonably good agreement about the data concerning the sequence of components and their latencies, there was not any uniformity of nomenclature until the system suggested by Vaughan (1969) and recommended by the Committee on Methods at the International symposium on Evoked Potentials in Man (Brussels, 1974) was widely adopted. In this system, each component is named by its polarity and mean latency or range of latencies. Thus in describing the waveforms of Giblin (1964) the V configuration would be described as consisting of N19, P26, N36, P45 components; the W configuration of N18, P22, N26, P30, N39, P49 components.

2.2.0 Stimulus

Satisfactory SEP's can be recorded with stimulation of almost any nerve trunk at various levels in the limb. The largest and most consistent results have been obtained from stimulation of the median or ulnar nerves with the cathode placed just proximal to the wrist over the nerve trunk and with cathode proximal to the anode. Digital stimulation employing ring electrodes is also effective (Dawson 1956).

With stimulation of a peripheral mixed nerve innervating both muscle and skin, changes in the cerebral potential are often correlated with defects in cutaneous sensation, though the strongest correlations exist between SEP changes and alteration of joint position sense (Halliday and Wakefield 1963; Giblin 1964; Larson et al 1966 and Williamson et al 1970). The problem of correlating receptors with SEP components is attributable to the dilemma of which receptors are responsible for mediating joint position sense; a point still debated in the literature (see section 1.1.1 - Receptors of proprioceptive activity).

Three different methods have been adopted to try to ascertain the specific contribution of groups of afferents to the scalp recorded SEP.

1. Digital and/or 'physiological' stimuli..
2. Interfering stimuli.
3. Single fibre stimulation

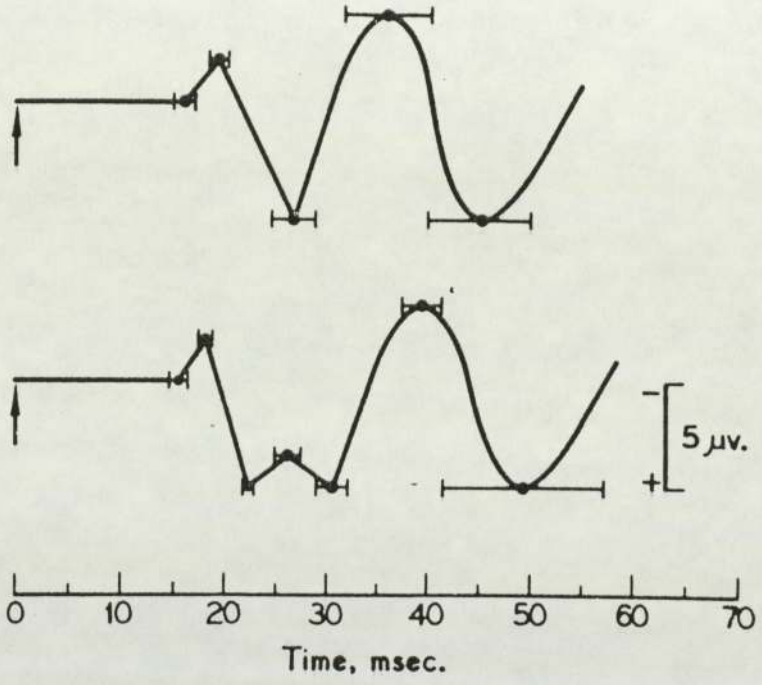

Figure 2.1 Morphological variations of the postcentral somatosensory evoked potential to median nerve stimulation and employing an Fz reference site, as described by Giblin (1964). Upper curve is the V configuration recorded in 18 subjects, and the lower curve is the W configuration recorded in 7 subjects. Horizontal bars represent 1 standard deviation on either side of the mean.

2.2.1 Digital and Physiological stimuli

Stimulation of digital nerve branches of the median or ulnar nerve avoids stimulation of Group Ia motor afferents as well as providing the ability to study individual dermatomes. The study of digital nerve SEP's have therefore provoked much interest.

In 1971, Calmes and Cracco investigated the SEP to median nerve and digital nerve stimulation using abrupt electrical pulses. They reported that although certain components of the cerebral response evoked by median nerve stimulation were not clearly apparent in the response to digital nerve stimulation in some subjects, there were not consistent differences in the response configuration among subjects. This suggests that no component of the SEP response is specific to Group Ia afferents. They also reported on the myogenic enhancement of the scalp potentials from proximal muscle groups and described this phenomenon as the somatomotor response, again demonstrating that this phenomenon is independent of Group Ia motor afferent fibres.

Topographical studies using digital stimulation, either electrical or mechanical (Duff 1980; Ishiko et al 1980; Pratt and Starr 1981; Kakigi and Shibasaki 1984) were in broad agreement with the topographic studies of Goff el al 1977 who employed electrical stimulation to the median nerve at the wrist. This area is explored more extensively in the Topography section in Chapter 3.

In 1980, Pratt et al compared the responses from the cortex to both electrical stimulation and mechanical tap delivered to the digits. They concluded that the mechanical responses were initiated by the fast conducting 'on' cutaneous nerve fibres but were of smaller amplitude and had fewer components than the electrically evoked potentials. Differences were explained by the smaller number and types of fibres activated by the mechanical tap. These authors also compared the effect of increasing stimulation rate on digital electrical, digital mechanical and median nerve electrical evoked SEP's. The similarity of the waveform of the potential evoked by 50msec and 5 msec duration mechanical pulses led them to conclude that these potentials are initiated primarily by the fast adapting 'on' cutaneous nerves. In general, the results of this

study indicated that a stimulus rate of 4/sec may be optimum but that a stimulus rate of 8/sec may be used without significant sacrifice in the ability to define the early components of the SEP.

In 1984 Kakigi and Shibasaki employed electrical, tactile and painful stimuli in a thorough study comparing latency, amplitude and topography to all three modalities. Their findings were similar to previous workers with the wave forms of the mechanical SEP not significantly differing from the painful stimulus but that these were 1-4 ms longer than the electrical SEP. It was suggested that this latency difference between the two might be due to the time lag from the beginning of the stimulation to the actual excitation of the receptor. Nakanishi et al (1973), had proposed that there was a difference in the maximal conduction velocity between the impulse evoked mechanically and electrically.

In 1974, by studying patients with different types of sensory disturbance, Nakanishi et al reported that afferent impulses responsible for the mechanically stimulated SEP's travel by the ventro-lateral tracts. Kakigi and Shibasaki (1984) disagreed with this observation since they felt that the conduction velocity of the mechanical SEP was still too fast to travel by the small fibres of this tract.

2.2.2 Interfering stimuli

In 1982 Burke et al reported complete suppression ('gating') of the cerebral potential evoked by stimulation of muscle or cutaneous afferents when a 'conditioning' afferent volley in a different nerve or in a different fascicle in the same nerve was applied. It was concluded that transmission of cutaneous or muscle afferent volleys to cortex can be profoundly altered in normal subjects by conditioning activity. Cutaneous, muscle and joint afferents from the upper limbs are known to converge onto common populations of neurons at different levels of the neuraxis, particularly the dorsal column nuclei, and active inhibitory mechanisms are documented at these levels (Bystrzycka et al 1977).

Cohen and Starr (1985) reported attenuation of cerebral potentials to both mechanical tap and electrical stimulation when muscle contraction was applied. This latter technique had been employed by earlier workers (Abbruzzese et al 1980; Jones 1981).

Tapia et al (1987) described how selective the 'gating' mechanism can be in an experiment where movement of individual digits was seen to attenuate digital SEP's while SEP's of uninvolved digits were preserved.

The scalp topography of an interfering light touch stimulus to median nerve stimulation was described by Jones and Power (1984) and Kakigi and Jones (1985). These authors reported altered scalp responses to the median nerve shock with preservation of peripheral and cervical potentials and therefore postulated modification at brain stem level. Moreover, a P32 and an N36 component was identified using subtraction techniques, that were thought to be generated within the central sulcus and specifically concerned with the processing of input from cutaneous mechanoreceptors.

2.2.3 Single fibre studies

Gandevia et al (1984) reported cortical SEP's from motor fascicle stimulation of the median nerve at the wrist. Latencies of these components were described as being of similar or shorter latency than SEP's evoked by cutaneous fascicle stimulation although amplitudes were similar. These authors concluded therefore that muscle afferent contribution may dominate the cerebral potential following median nerve stimulation at the wrist.

However Halonen et al (1988) could not reproduce their findings and reported very poorly defined low amplitude cortical responses to stimulation of motor nerves whereas cutaneous and/or mixed nerve stimulation yielded large amplitude responses. Moreover it was pointed out that of the total cross sectional funicular area of the median nerve at the wrist, only 6% is occupied by nerve fascicles (Sunderland and Bedbrook 1949) which would make the predicted amplitude of any purely motor potential very small.

2.3.0 Lesion Studies

A large amount of data pertaining to the nature, origin and clinical utility of the scalp recorded SEP has been obtained from studies on patients with localized lesions of the primary somatosensory pathways.

It has been established by several authors that the evoked response is unaffected by lesions causing loss of pain - temperature sensation, but was lost, diminished or delayed where there was loss of joint position sense (Halliday and Wakefield 1963; Giblin 1964; Bergamini et al 1966; Larson et al 1966). It was therefore concluded that since pain - temperature sensation is mediated via the ventro-lateral spinal tracts and proprioception by the posterior column pathways, that the integrity of the latter is essential for normal generation of the scalp SEP.

Various lesions involving peripheral nerves or the subcortical pathways were shown to increase the SEP onset latencies (Laget et al 1967; Desmedt 1971; Noël and Desmedt 1975;1980; Anziska and Cracco 1980; Chiappa et al 1980; Jones and Halliday 1982). The characteristic feature in patients with cortical lesions however was that the onset was either equal to control or only slightly increased, while changes in amplitude or duration of cortical SEP components could be rather marked (Noël and Desmedt 1980; Mauguière et al 1982).

As far back as 1958, Alajouanine had reported SEP abnormalities in 5 patients with parietal lesions. Between 1970 and 1988 a number of similar studies were performed to try and determine the possible generator sites of the increasingly large number of scalp SEP components described. Many studies attempted to correlate the site of lesion with both SEP abnormality and symptomatology. The following is a summary of the most important of their findings:

2.3.1 Correlation with clinical data

In common with earlier studies, the majority report SEP abnormalities occurring in patients with cortical lesions who present with moderate to severe sensory deficits with or without hemiplegia (Williamson et al 1970; Nakanishi et al 1978; Obeso et al 1980; Mauguière et al

1983; Yamada et al 1984; Tsuji et al 1988). SEP's in these patients were reduced in amplitude or eliminated and generally with good correlation between the severity of symptoms and the degree of SEP abnormality if the degree of loss of joint position sense was used as a criterion (Williamson et al 1970). Halliday and Wakefield (1963) had noted that touch sensibility was a poor criterion for judging sensory loss of the fine discriminating type and had relied solely on joint position sense because the latter is an uncomplicated index of the integrity of dorsal column function; touch sensation could be affected by lesions of either dorsal column or ventro-lateral pathways (Rose and Mountcastle 1959).

There are several examples in the literature where correlations with sensory symptoms are poor. Abnormal SEP's have been reported in patients exhibiting only mild sensory deficits or simply asterognosis with preserved tactile and deep sensation (Williamson et al 1970; Nakanishi et al 1978; Mauguière et al 1983). Similarly Okasaki et al 1971, Shibasaki et al 1977 and Yamada 1984 describe abnormal SEP's in patients with cortical lesions but without sensory deficit . Conversely, Giblin (1964) reported seven patients with moderate to severe "cortical" sensory impairment but normal SEP's, although 34 other patients revealed good correlation between the sensory deficit and the SEP abnormality. Occasionally, patients presenting with symptoms mainly of impairment of pain-temperature sensation have also produced SEP abnormality (Tsumoto et al 1973; Obeso et al 1980; Yamada et al 1984).

De Weerd (1985) performed studies on 20 patients with unilateral cerebral ischaemia and follow ups were performed to see if there was a correlation between the SEP and clinical change. Two patients with a completed stroke, who presented with the most abnormal SEP's, showed no changes in the SEP abnormalities in the course of two weeks; in 5 patients with milder cerebral ischaemia, changes were seen in this period.

In some of the patients who recovered from their strokes there was no correlation between the changes in the SEP and the overall clinical improvement and 2 patients with stable clinical condition presented with deterioration of their SEP's. Only one patient with transient ischaemic attacks and reversible ischaemic neurological deficits achieved complete

normalization of the SEP on follow-up. It was therefore considered that in the other patients in this category the SEP provided detection of subclinical abnormalities after recovery.

In summary it may be concluded that while generally we expect to see SEP abnormalities in lesions of the dorsal column pathways and primary somatosensory cortex where moderate to severe sensory loss occurs (particularly loss of joint position sense), there are sufficient exceptions to this golden rule to prevent 100% correlations to be made. The same may be said of the prognostic value of the SEP in lesion evaluation.

2.3.2 Correlation with lesion site

Several scalp recorded SEP components had been described which because of their far field nature (i.e. of similar morphology and amplitude wherever recorded on the scalp) were thought to originate sub-cortically whereas components recorded at discrete sites on the scalp were thought to be of cortical origin. Studies in patients with known discrete lesions have done much to further our knowledge of possible generator sites of the scalp recorded SEP.

The following sections present a summary of SEP findings in patients with discrete lesions of the somatosensory pathway.

2.3.2.1 Thalamic or sub-cortical lesions.

Most authors agree that in patients with lesions at or above the thalamic level,with stimulation of the affected side the P15 potential can be of normal configuration and latency while all other scalp components are abolished. In patients with lesions in the brain-stem or in the cervical cord, P15 similarly can be absent. These findings and the short latency of the P15 potential suggest that it may be the result of activity of the medial lemniscal systems from the medulla to the thalamus (Noël and Desmedt 1975 Domino et al. (1965); Nakanishi et al 1978; Anziska and Cracco 1980; Mauguière et al 1982,1983). Mauguière et al (1983b) published findings of a bilateral N18 of long duration (19 msec) recorded in patients with a unilateral

thalamic and / or suprathalamic lesion that eliminated the parietal N20-P27-P45 and prerolandic P22-N30 SSEP components (Figure 2.2). The N18 component had been documented by Desmedt and Cheron (1981b) and was best displayed by using a non-cephalic reference. Due to the polarity and duration of this potential it was hypothesized that it must represent a far-field potential whose neural generators would not be a conducted spike volley, but activity in an 'open-field' system in the brain stem and/or some uninvolved parts of the thalamus.

2.3.2.2 Cortical lesions.

As stated earlier, patients with cortical lesions typically present with SEP's whose onset is either equal to control (control group latency or preserved hemisphere data) or only slightly increased, while changes in amplitude or duration of cortical SEP components can be rather marked (Noël and Desmedt 1980; Mauguière et al 1982).

In 1983 Mauguière investigated 22 patients with unilateral cortical lesions. This important study indicated that when recording from multiple sites on the scalp it was possible to show a dissociated loss of frontal or parietal components that correlated well with the site of the lesion. A precentral lesion presenting with hemiplegia, for example, could result in the elimination of frontal components while all parietal components were intact and normal. Conversely, an anterior parietal lesion presenting with hemianaesthesia without hemiplegia could show an augmentation of frontal components co-existing with an elimination of all parietal components (Figure 2.3) .

Important conclusions from this study were twofold:

1) Provided evidence that there are multiple generator sites involved in the formation of postcentral and precentrally recorded potentials.

2) An abnormality could manifest itself as a dissociated augmentation of discrete components as well as an attenuation or elimination.

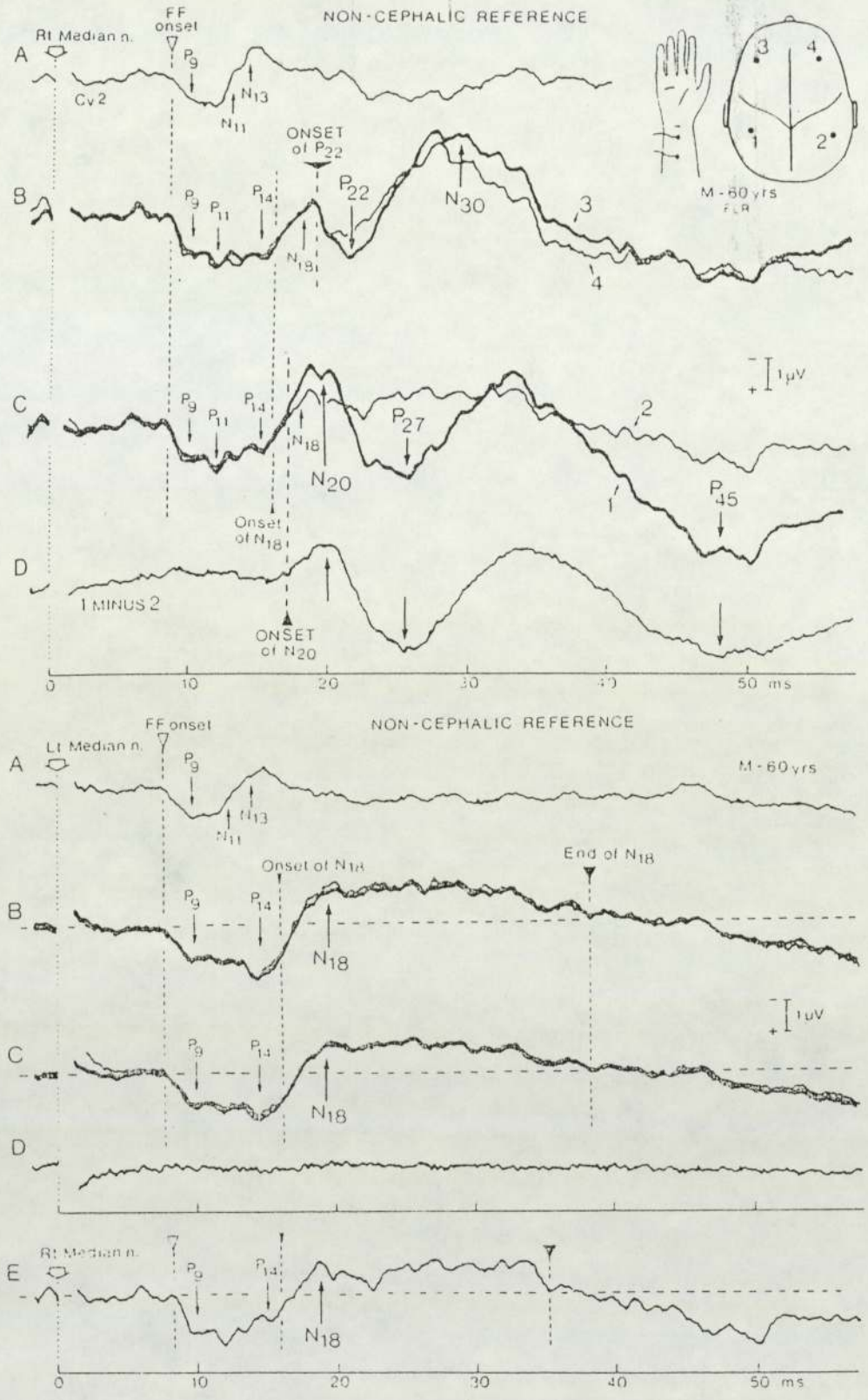

Figure 2.2. Non-cephalic reference recordings in a patient with a unilateral thalamic lesion that eliminated the parietal N20-P27-P45 and prerolandic P22-N30 SEP components. An N18 component of long duration can be discerned.
Upper traces from the unaffected hemisphere represent: A:- active electrode over the spinous process of the second cervical vertebra. B:- superimposed traces from the contralateral and ipsilateral frontal scalp. C:- superimposed traces from the contralateral and ipsilateral parietal scalp. D:- algebraic subtraction of the ipsilateral parietal trace from the contralateral parietal trace. Lower traces A-D represent same recording derivations but from the affected hemisphere. Figures from Mauguière et al (1983b).

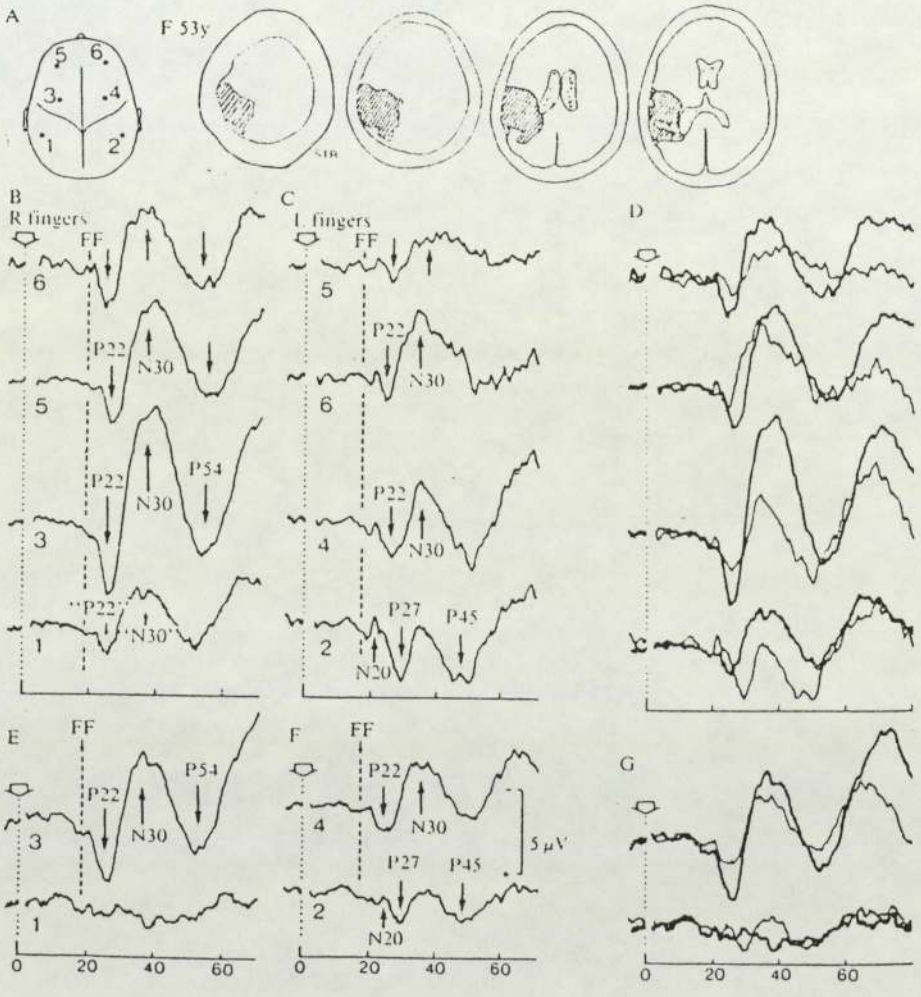

Figure 2.3. 53 year old female with a complete lesion of the left parietal region since the age of 5 years and a complete contralateral hemianaesthesia. Electrical stimulation of fingers II-III at intensities three times threshold (B,C) or near threshold (D,E) of the normal side. From Mauguière et al (1983), Figure 7.

Stejskal et al (1985) also reported augmentation in components where lesions were remote from the PSMA (3 middle frontal gyrus, 3 occipital lobe and 9 head of caudate nucleus). See Figure 2.4.

Both the studies by Obeso et al (1980) and Stejskal et al (1985) employed only single channel recordings with a parietal electrode referenced to precentral site and this therefore confounds any observations that might have been made regarding dissociated component effects in the manner of Mauguière et al (1983a).The latter authors theorized that the increase in voltage of their precentral P22-N30 components in patients with chronic parietal lesions may be due to 'sensitization' by deafferentation of the motor cortex through degeneration of the cortico-cortical connections from areas 2 and 5. An additional possibility proposed was that a postcentral cortical lesion could result in changes of the functional organization in the VPLo relay neurons projecting to the motor cortex.

Obeso et al (1980) hypothesized that the enhancement of components observed in patients with lesions remote from the PSMA could be due to neuronal hypersynchronism secondary to metabolic alterations of the PSMA neurones.

The experiences of Halliday et al (1967 and 1970) gained from patients suffering from epilepsy led them to propose that potential enhancement in this group could be due to epileptiform discharges arising in the reticular formation of the lower brain-stem, influencing sensory input to the cerebral cortex at the level of the thalamic relay nuclei. Halliday and Wakefield (1963) had also described patients with brain-stem lesions, with or without associated sensory loss, with abnormally large SEP's. Laget et al (1967) and Williamson et al (1970) describe SEP enhancement in cases of cerebral tumour causing focal epileptic seizures. Jones (1982) and Stejskal et al (1985) proposed that SEP enhancement in neurological conditions other than epilepsy may be due to interference with tonic inhibitory mechanisms at brain-stem, thalamic or cortical level. The disinhibition of the somatosensory cortex would be via the pallidum and ventral group of thalamic nuclei.

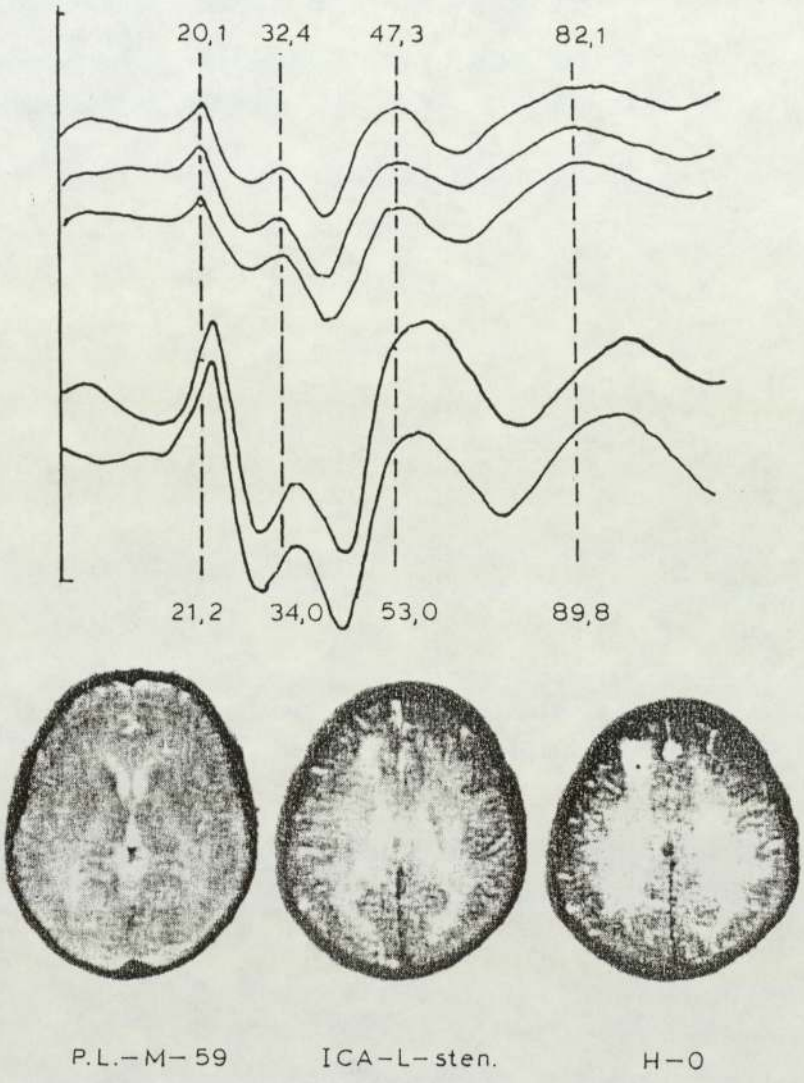

Figure 2.4. An increase in amplitude of the N1/P1 complex on the left by 200% (lower traces) with delayed latency of N1-N3. A limited lesion in the left frontal lobe was discerned.

Yamada et al (1984), De Weerd et al (1985) and Tsuji et al (1988) employed topographical techniques to examine patients with cortical lesions.The type of SEP abnormalities obtained varied considerably but they all described independent changes of frontal or parietal components (Figure 2.5).

In the investigations by De Weerd (1985), where only patients with ischaemic disorders were investigated, patients with transient cerebral ischaemia and reversible ischaemic neurological disorders did not have abnormalities in the parietal region; all abnormalities were located in the frontal region. Moreover, among those with mild but permanent neurological symptoms, there were more SEP abnormalities in the frontal region (8 of the 11 patients) than in the parietal region (5 of the 11 patients). They concluded that the potentials that are predominant in the frontal regions are probably generated in cerebral structures that are susceptible to cerebral dysfunction or are those first affected when ischaemia develops in the area supplied by the middle cerebral artery.

2.4.0. Summary

The morphology of the scalp recorded SEP described by Giblin (1964) is familiar in clinics around the world today, many of whom employ the same recording techniques used by this author. This involved the use of an electrode placed over the "hand" area of the post central gyrus which was calculated as being 7cm lateral and 2cm posterior to the vertex point (Cz), according to the international 10-20 system of electrode placement (Jasper 1958), with a mid-frontal reference (Fz).

Giblin described a duplicity of morphology with a so-called V type characterized by a negative peak at 17-20msec, a positive peak ranging from 23-31 msec, a second negativity peaking from 30-40msec and a second positivity between 40-50msec. A so-called W morphology typing was used to describe the observation that the second positivity was seen to sub-divide in some individuals into a positive-negative-positive configuration.

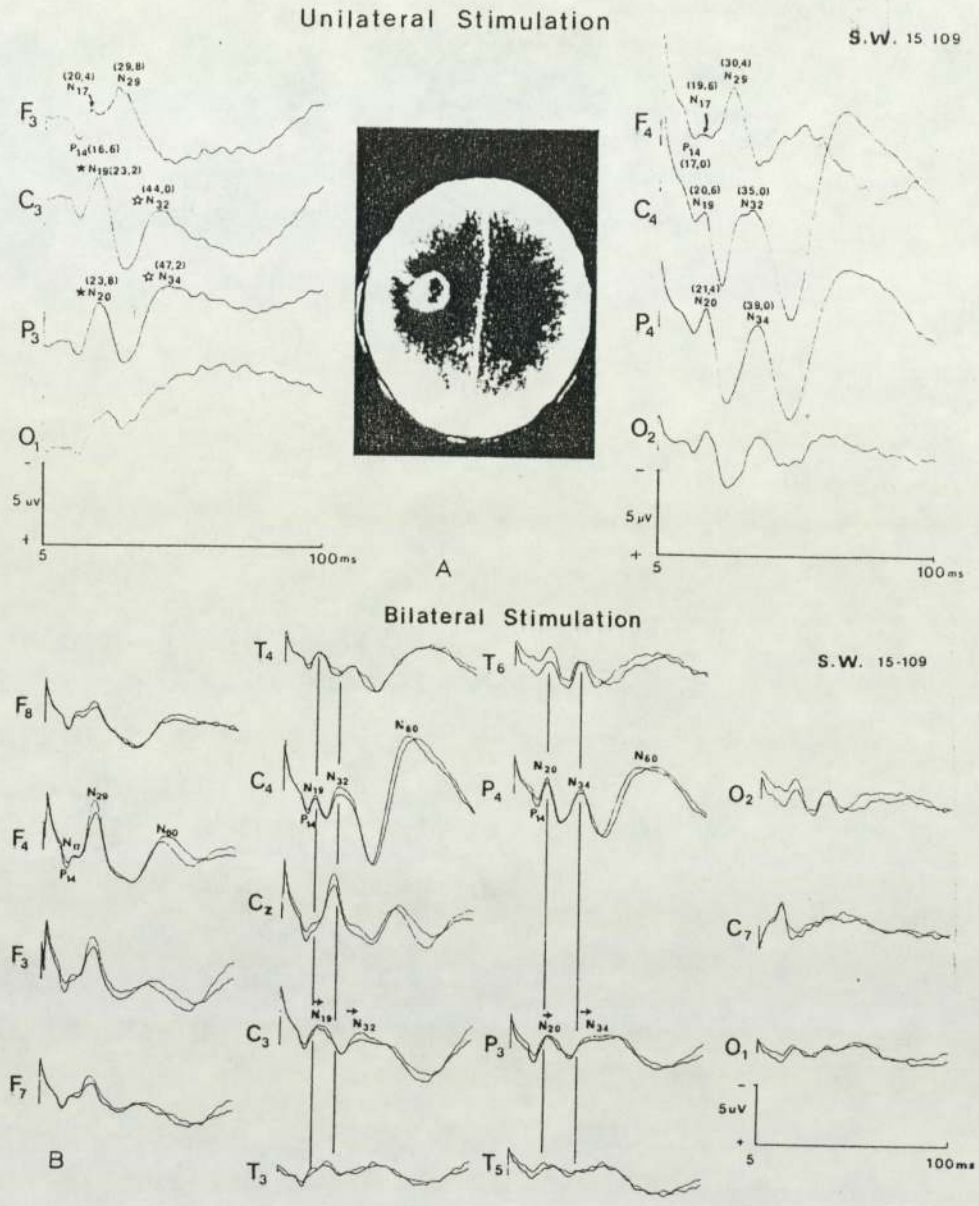

Figure 2.5. Data from Yamada et al (1984). A patient with a lesion in the left frontoparietal lobes. With right-sided stimulation (left column in A), frontal peaks were normal, but central N19, parietal N20 (black stars) were delayed. Also centroparietal N32 and N34 (white stars) were probably abnormal. The same findings were observed by bilateral stimulation (B).

Allison (1962) and Goff et al (1962) both observed that the first scalp recorded negativity was sometimes preceded by a small amplitude positive potential peaking at 14-15msec.

The largest and most consistent results have been obtained from stimulation of the median and ulnar nerve trunks, commonly at the wrist. Digital and other physiological stimuli have been employed with success.

No component of the SEP appears to be specific to Group Ia afferents, though the strongest correlations exist between SEP changes and alteration of joint position sense (Halliday and Wakefield 1963; Giblin 1964; Bergamini et al 1966; Larson et al 1966). Indeed, it seems clear that the integrity of the dorsal column pathways that mediate proprioception are essential for the generation of the scalp recorded SEP's.

In patients with lesions at or above the thalamic level,with stimulation of the affected side the P15 potential can be of normal configuration and latency while all other scalp components are abolished. In patients with lesions in the brain-stem or in the cervical cord, P15 similarly can be absent. These findings and the short latency of the P15 potential suggest that it may be the result of activity of the medial lemniscal systems from the medulla to the thalamus (Noël and Desmedt 1975 Domino et al. (1965); Nakanishi et al 1978; Anziska and Cracco 1980; Mauguière et al 1982;1983).

Patients with cortical lesions typically present with SEP's whose onset is either equal to control or only slightly increased, while changes in amplitude or duration of cortical SEP components can be rather marked (Noël and Desmedt 1980; Mauguière et al 1982).

SEP abnormalities frequently occur in patients with cortical lesions who present with moderate to severe sensory deficits with or without hemiplegia (Williamson et al 1970; Nakanishi et al 1978; Obeso et al 1980; Mauguière et al 1983; Yamada et al 1984; Tsuji et al 1988). SEP's in these patients were reduced in amplitude or eliminated and generally with good correlation between the severity of symptoms and the degree of SEP abnormality if the degree of loss of joint position sense was used as a criterion (Williamson et al 1970).

Other important conclusions from SEP studies on patients with cortical lesions have been:

1) Provided evidence that there are multiple generator sites involved in the formation of postcentral and precentrally recorded potentials (Mauguière et al 1983).

2) An abnormality could manifest itself as a dissociated augmentation of discrete components as well as an attenuation or elimination. Augmentation of components has been reported in patients whose lesions were in close proximity to the primary somatomotor cortex and also in those whose lesions were remote from this area (Obeso et al 1980; Stejskal et al 1985).

CHAPTER 3

CORTICAL GENERATORS - IDENTIFICATION / METHODOLOGY

3.0. Introduction

A number of recording techniques have been employed over the last 40 years in attempting unravel the possible cortical and subcortical generator sites of the scalp recorded SEP.

Soon after the first description of the SEP in man by Dawson (1947), recordings were made from the cortical surface (Woolsey 1949). In the ensuing years ever greater numbers of recording electrodes were employed for both scalp and cortex recordings and different reference sites employed. Computer enhanced techniques - 'brain mapping' - then entered the fray - initially for scalp recordings and then for cortex recordings. In recent years workers have used neuromagnetic recording techniques in their armoury to enable depth assessments to be made.

In this Chapter the contribution of these latter developments to our knowledge of the possible cortical generators of the SEP will be analyzed. The Chapter is divided into four general sections; 1. Reference electrodes. 2. Topographic studies 3. Brain mapping. 4. Neuromagnetic studies.

3.1.0. Reference electrodes

In an attempt to discern possible multi-generators in the somatosensory cortex, and indeed to study far-field potentials, several authors had employed the use of a non-cephalic reference electrode (Cracco and Cracco 1976; Desmedt and Cheron 1981). The precise nature of this electrode varies from group to group. Several authors have employed electrodes placed on a limb or trunk and relied on artefact rejection systems to eliminate the high amplitude electrocardiogram (ECG) that is an inevitable consequence of such a reference site (Cracco and Cracco 1976; Yamada et al 1982; Maccabee et al 1983).

Techniques have been employed to reduce or eliminate the ECG from a non-cephalic reference input. Stephenson and Gibb (1951) described a simple potentiometer device whose input was derived from a frontal trunk electrode (i.e. sternoclavicular junction) and a posterior trunk electrode (i.e. 7th cervical vertebra). The remaining ECG signal from this combined input was reduced by adjustment of the potentiometer.

An apparently bilateral distribution of the early scalp negativity when a non-cephalic reference is employed (Kritchevsky and Wiederholt 1978) appeared to conflict with the view of the interpretation of the N20 component as reflecting the contralateral 'primary' response.

In an extension of their earlier normative study, Desmedt and Cheron (1981) using the dorsum of the wrist reference described a broad N18 component which had a widespread scalp distribution and was a distinct component separate from the N20. Because of its wide distribution, if a scalp reference is employed then N18 is cancelled out and is almost cancelled when earlobe references are used (Figure 3.1). The authors explained the findings of Kritchevsky and Wiederholt (1978) on this basis.

In calculating conduction velocity from thalamus to cortex and because of its widespread distribution, Desmedt and Cheron hypothesised that N18 was of sub-cortical, probably thalamic, origin. There were two interesting points of debate on this however. Firstly, the observation that N18 presents a sizeable amplitude on the ipsilateral scalp is interesting since the thalamocortical radiation potentials are elicited only from the hemithalamus contralateral to the side stimulated (Ohye et al 1972). Secondly, the negative sign of N18 is interesting since all other far field potentials present a positive deflection, as indeed is to be expected for volume conduction beyond the structure generating the nerve volley (Arezzo et al 1981).

In a report on the morphological and topographical differences of the cortical SEP components using different reference sites, Tsuji and Murai (1986) showed extremely similar waveforms independent of the reference sites used - these included linked ears, contralateral shoulder, left ear alone and right ear alone (Figure 3.2). It should be noted however that the

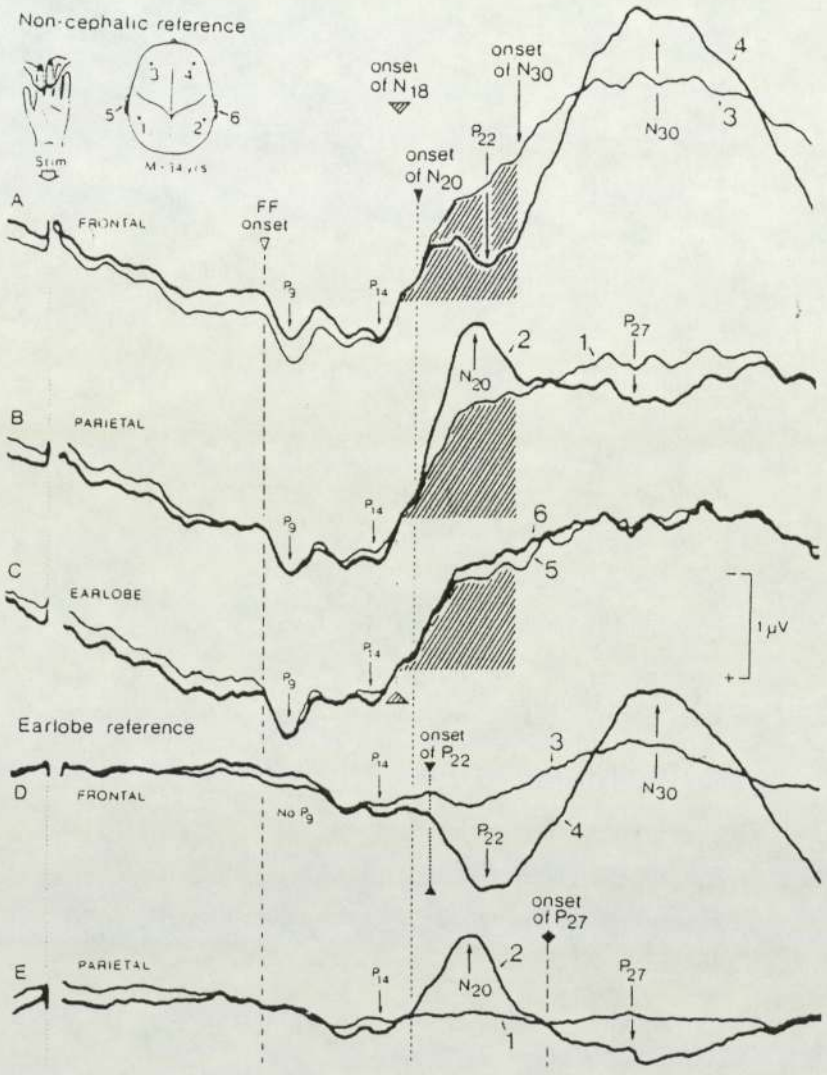

Figure 3.1. Comparison of SEP's with non-cephalic or earlobe reference in a normal male of 34 years (from Desmedt and Bourguet 1985). The non-cephalic reference recording at frontal (A) or parietal scalp (B) or earlobes (C) respectively. Thicker contralateral traces are superimposed on thinner ipsilateral traces. Electrode positions and traces are numbered 1-6. Waveforms labelled D-E show data from the same scalp sites with earlobe reference whereby the far-fields and N18 are markedly reduced through cancellation.

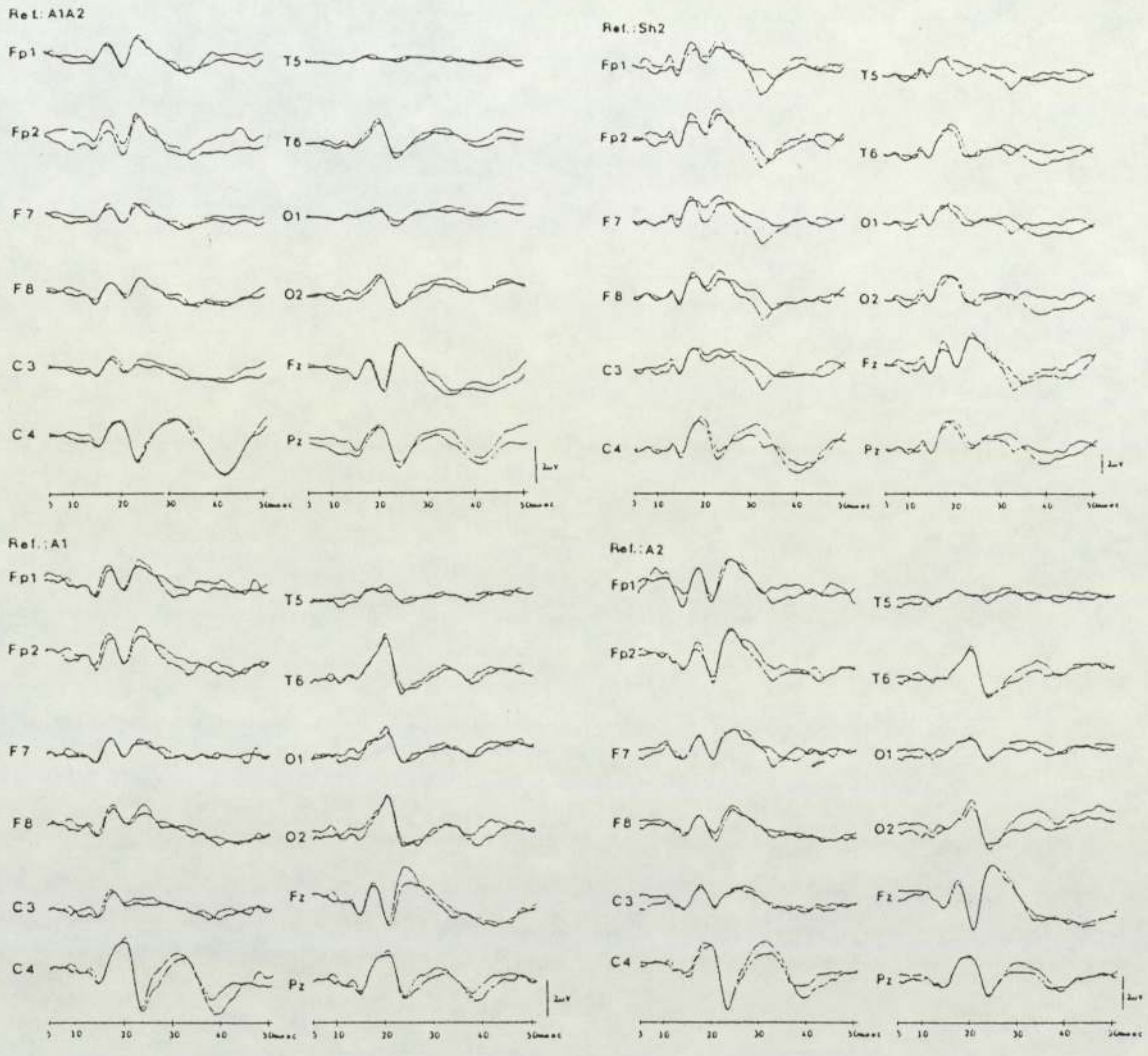

Figure 3.2. Comparison of SEP's recorded with different reference electrodes (A1A2, A1, A2 and contralateral shoulder). The morphologies and distributions of cortical SEP's were extremely similar independent of the reference electrode. Left median nerve stimulation; number of stimuli = 1024; A1A2 = linked ears; Sh2 = right shoulder; A1 = left ear; A2 = right ear; filter settings = 32-300Hz.

filter settings used in this study were 32-300Hz which would undoubtedly have produced an attenuation of the N18 component in their shoulder reference waveforms.

3.2.0. Topographic Studies; scalp surface and invasive recordings.

One of the first and still most effective of the few tools available to the Clinical Neurophysiologist for identification of possible generators of the SEP is the study of the cortical and/or scalp topography of its components.In 1977 Goff et al studied the scalp topography of the SSEP to median nerve stimulation at the wrist and displayed the results in a series of isopotential line maps.

Electrodes were placed according to the 10-20 system and an earlobe reference contralateral to the stimulus was employed. The topography of a number of components were described. P15 had a widespread distribution as expected but with a frontal emphasis. Early components N20, P25, and P30 were well localised to the posterior quadrant contralateral to the stimulated side as was P45, although its field was more diffuse. N20 and P25 had the most localized fields which were almost identical and within the larger fields of P30 and P45. N35 had a frontal bilateral distribution (see Figure 3.3.)

As Giblin (1964) had shown, Goff et al observed only a single positivity in some subjects in the latency range 24-28 msec., leading to uncertainty as to whether it should be classified as P25 or P30. Additionally they observed a clear polarity inversion across the central sulcus of N20 and P30 components. P25 did not show a clear phase reversal; was seen in less than half of their subjects and like the cortical recordings of Giblin (1964), was localized to a small region near the central sulcus. Therefore in quantifying the scalp potentials they assumed that the anterior positive potential at 20 msec (P20) was a polarity inversion of N20 rather than a P25 or P30 potential of shorter latency.

A single large widespread posterior positivity in the 25-35 msec range was P30. In a few subjects frontal "N30", a clear polarity inverted version of P30 was recorded, but in most subjects such a distinct relationship could not be seen.

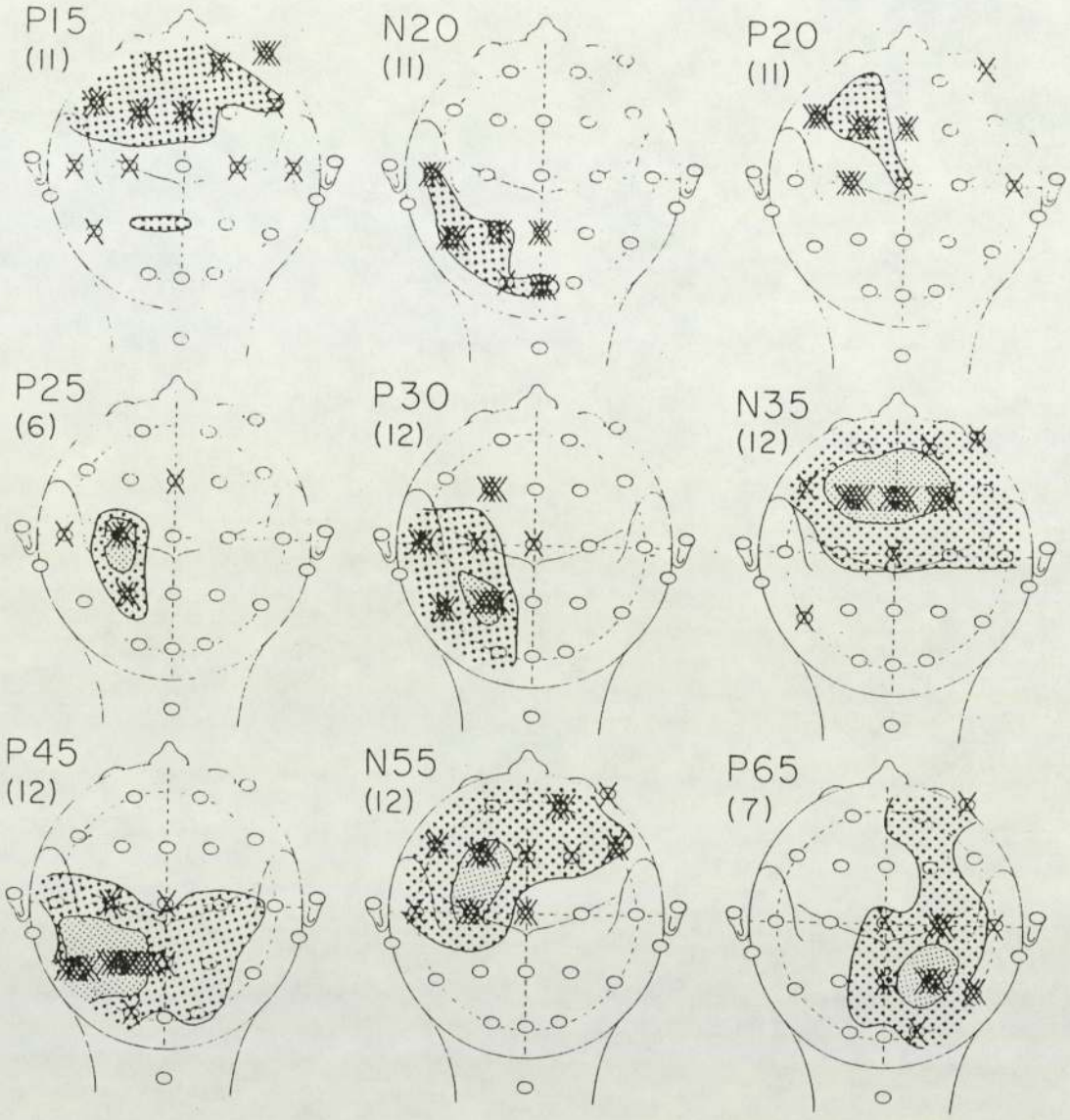

Figure 3.3. Topography of the scalp recorded SEP as described by Goff et al 1977. In cases where there is no fine-stippled area, the median value did not exceed 75% at any location; locations where the median value was 100% is indicated in black. Crosses indicate all locations at which the component was 90% or more of its maximal amplitude in any subject. The number of subjects on which a given map was based is indicated in parentheses.

Goff et al (1977) gave three reasons why they could not make presumptions as to the intracranial location of these potentials:

i. Between subject variability in topography of some components is too great to allow any conclusions as to source location.

ii. Origin of a component cannot necessarily be inferred from its scalp topography. An amplitude maximum will correctly predict the location of a source only if it is a cortical generator whose dipole orientation is approximately perpendicular to overlying scalp.

iii. Ear reference electrodes, while widely used in EP studies, are active for some components and would yield misleading inferences about source locations.

Topographical studies using digital stimulation, either electrical or mechanical (Duff 1980; Ishiko et al 1980; Pratt and Starr 1981; Kakigi and Shibasaki 1984) were in broad agreement with the maps of Goff et al (1977).

In 1980, Desmedt and Cheron, again using digital stimulation, studied the scalp topography of the SSEP in both young normal controls (20-30 years) and in a group of healthy octogenarians (80-90 years). The 'W pattern' described in this study should not be confused with that of Giblin (1964). Desmedt and Cheron used the W shape to describe the morphology of the waveform caused by the typical parietal N20, P25, N35, P45, N60 components and is compatible with the V waveform of Giblin. Desmedt and Cheron however, went on to describe the occurrence of a single positivity only following the N20 component at a latency of over 30 msec. They observed that the so called 'typical W pattern' was seen in only 12 out of the 25 normal adults of mean age 22 years, but was clearly seen in 17 out of 19 octogenarians.

They observed that both the negative peaks (postcentral N25 and N38 versus frontal N33 and N47) and the positive peaks (postcentral P32 and P49 versus frontal P26) presented markedly different latencies that were stable throughout their respective areas.

These respective areas did not normally merge or overlap in the region of the central sulcus and it was impossible to join by a straight line the peaks of precentral and postcentral components of the same polarity. This was a leading argument for suggesting separate pre and post rolandic generators for these potentials.

The lack of ipsilateral early SSEP components for stimulation of distal upper limb was documented by Desmedt and Robinson (1977). This was explained by the lack of callosal connections for the primary receiving areas representing the distal limb (Jones and Powell 1969b). When early potentials are recorded by scalp electrodes over the ipsilateral hemisphere with latencies nearly identical to those of the contralateral SEP, it is probable that they are generated by volume conduction.

3.2.1. Dipole models calculated from topographical studies

In the early 1980's, great efforts were made to describe and explain the possible cortical generators of the increasingly well defined pre and post rolandic SEP scalp components discerned from topographical studies.

Broughton (1969) had proposed a dipole model which was later elaborated by Allison (1980) to explain the nature of these waveforms. It was suggested that an active area of cortex located in the posterior bank of the central sulcus (corresponding to Brodmann area 3b), with the neuronal columns oriented roughly antero-posteriorly in a horizontal plane, would give rise to field potentials of similar latency but opposite polarity over the post central area and the frontal scalp (see Figure 3.4.) . Allison et al (1980) developed this model to account for four SEP components. N20 and P30 posteriorly and P20 and N30 anteriorly . Additionally Allison and his colleagues described an intermediate P25 potential recorded over the central sulcus and proposed that Brodmann area 1, located on the crown of the postcentral gyrus was a likely source (see Figure 3.5).

This model was disputed however on the grounds that P20 is of consistently longer latency than N20 (Papakostpoulos and Crow 1980; Desmedt and Cheron 1980; Desmedt and Bourguet 1985). These latter investigators have proposed that the frontal and parietal potentials reflect activity of separate radially oriented sources in motor or supplementary cortex frontally and somatosensory cortex parietally.

In 1984, Jones and Power used a technique of an interfering tactile stimulus applied to a hand receiving electrical stimulation to try and discern localised generator areas in the cerebral cortex. In this study they reported the presence of an N22 peak, maximal at frontal and prefrontal scalp locations and recognised as a distinct component from prerolondic P20. The latency of N22 was almost identical to that of P22 (central contralateral distribution), suggesting the possibility of a common generator. They proposed that this generator was located at the bottom and in the anterior bank of the central sulcus, Brodmann area 3a (see Figure 3.5).

Their findings concerning the N30/P30 dipole of Allison et al (1980) was limited since, as acknowledged by Allison, P30 is barely identifiable in many subjects.

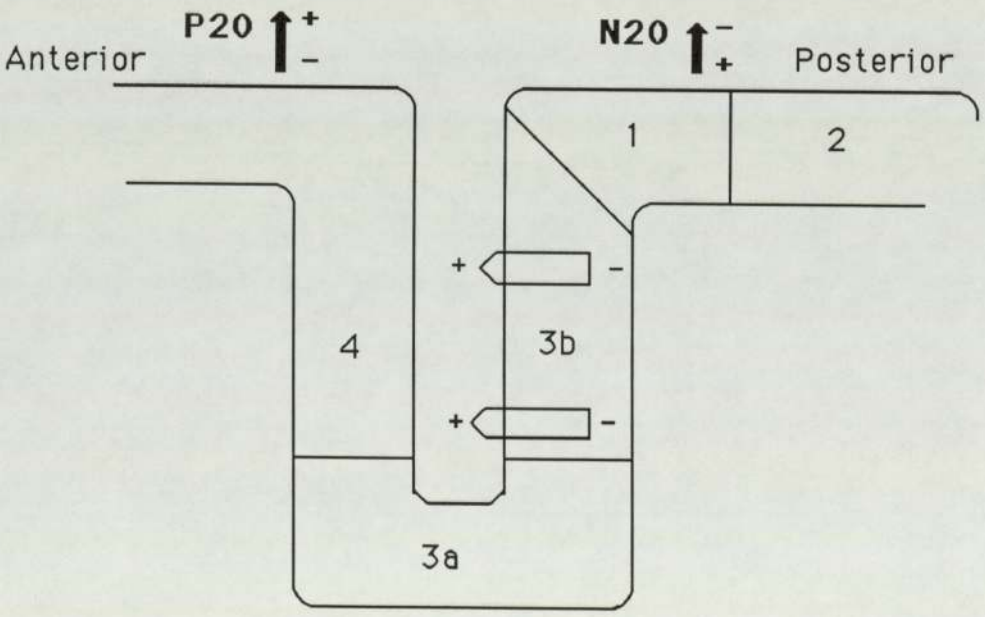

Figure 3.4 Dipole Model in central sulcus as suggested by Broughton (1969)

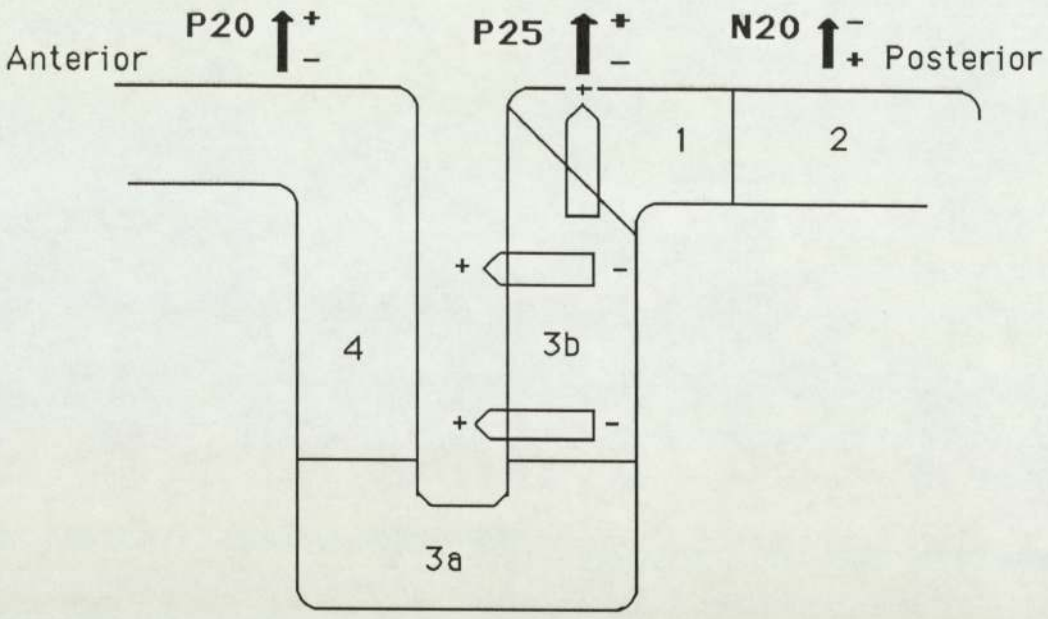

Figure 3.5. Dipole Model in central sulcus as suggested by Allison et al (1980)

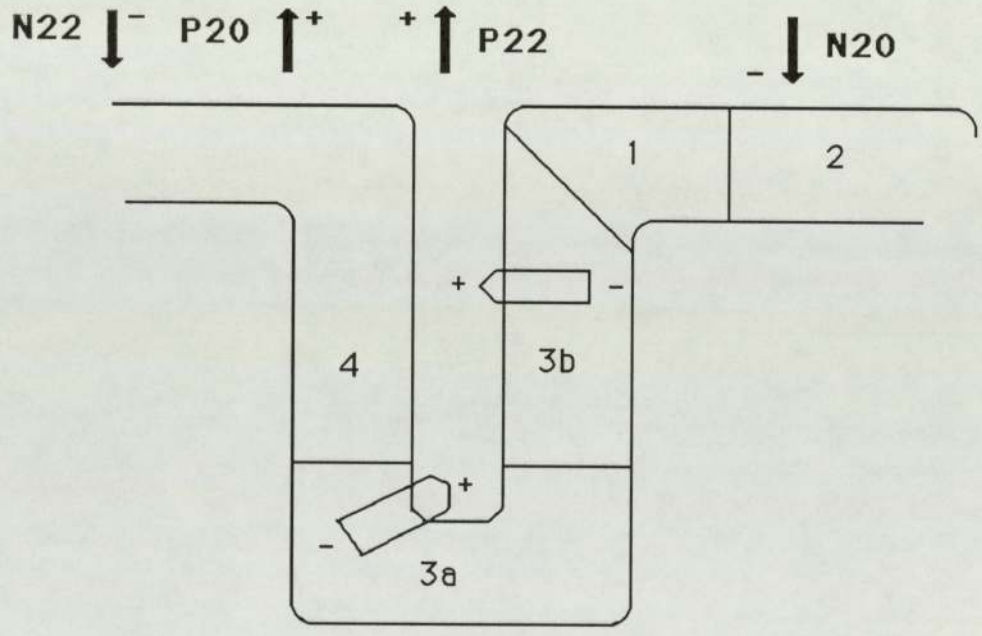

Figure 3.6. Dipole Model as suggested by Jones and Power (1984)

3.2.2 Thalamic and subcortical recordings

Cracco and Cracco (1976) first succeeded in recording three scalp positive potentials (P9, P11, P14) using a non-cephalic reference such as the dorsum of the hand. These initial components were recorded all over the scalp and were therefore considered as not being of cortical origin (near field potentials), but of sub-cortical origin (far-field potential).

In 1979 Celesia described findings from electrodes targeted at the thalamic nucleus ventralis posterolateralis (VPL) as well as the those from the surface of the cortex and the scalp. Median nerve stimulation at the wrist was employed using a frontal bone reference and he described a monophasic or diphasic potential from the VPL with mean onset latency of 13.8 ms.

In 1984 Suzuki and Mayanagi, in an attempt to examine the origins of these short latency potentials, examined 17 patients who needed intracranial or intraspinal operation. The recording sites were the spinal cord in 2 cases, the brain-stem in 8 cases, the thalamus in 3 cases and the third ventricle in 5 cases. The dorsum of the hand was used as a reference generally, with a mid-frontal reference used occasionally for intracranial recording. From several sites at the ventral surface of the brain stem, three positive waves were recorded (P'9, P'11, P'14) like the initial positive components of the scalp SEP's. The latency and amplitude of P'9 and P'11 were approximately the same as those of scalp P9, P11. The peak latencies of P'14 recorded at the medulla and pons were shorter than that of scalp P14 by 0.7-0.8msec and 0.2-0.5msec respectively. The peak latency of P'14 at the midbrain was almost the same as that of P14 and it was therefore suggested that the midbrain represents the rostral end of the origin of P14. By measuring the distance between the recording electrodes in the brainstem and peak latency difference of P'14, the fastest lemniscal conduction velocity was estimated as 56 m/sec.

Responses from the thalamus, targeted at the nucleus Ventralis intermedius (Vim), were reported as a negative wave preceded by a positivity. The negative peak was approximately 2

msec prior to that of the scalp N20 and the peak latency of the positive wave was almost identical to that of P14.

Several workers have agreed that P9 represents a volume conducted potential generated in the stimulated nerve proximal to the axilla (Cracco and Cracco 1976; Kritchevsky and Wiederholt 1978; Anziska and Cracco 1980; Desmedt and Cheron 1980). Suzuki and Mayanagi (1984) concurred with these conclusions and also that the onset of P11 indicates the arrival of the afferent volley at the cord entry, and the peak latency of P11 its arrival at C1-2 level dorsal column. Additionally they concluded that the onset latency of P14 indicates the onset of postsynaptic events in cuneate nucleus neurons and the peak latency of P14, arrival at the midbrain.

Further studies were undertaken to understand the nature of the P14 far-field component. Albe-Fessard et al (1986) performed recordings in the thalamus of 13 patients . As in previous studies, the VPL nucleus was targeted and scalp electrode sites C3 and C4 referenced to earlobe used. Waveforms similar in morphology to those of Suzuki and Mayanagi (1984) were obtained from the thalamus with both an initial positive and subsequent pronounced negative phase. Latencies of this thalamic positivity were very similar to those described by Celesia (1979) with an onset ranging from 11 to 15.2 msec and a peak from 17 to 18.4 msec.

These values were very similar to those obtained simultaneously from the scalp and led the authors to conclude that at least part of the scalp positivity had its origin in a thalamic far-field. However, they did agree that the bilateral scalp representation of this potential, and its disappearance after a brain-stem lesion (Noël and Desmedt 1975) supports a significant brain-stem contribution.

In 1987, Katayama and Tsubokawa used electrode arrays implanted within the VPL and medial lemniiscus (ML) to study possible multi-generators and/or contribution of volume conducted activity to the thalamic and scalp response. Their results suggested that the scalp P14 was a potential reflecting the activity of ML fibres and that the subsequent negativity may

reflect the activity of thalamocortical radiations and the sum of local postsynaptic activity occurring in broad areas of the brain stem and thalamus.

Further intraoperative procedures have proposed the cuneate nucleus (Møller et al 1986) and an area rostral to the junction of the cervical cord and the medulla (Jacobson and Tew 1988) as sources of the scalp recorded P14 component.

3.2.3 Cortical recordings

The first recording of evoked potentials from the human postcentral gyrus was carried out by Woolsey et al (1949). Since then, stable potentials have been obtained from the postcentral gyrus both by electrical stimulation of limb nerves and/or tactile stimulation of the skin.

Penfield and Jasper (1954) had reported sensory responses by stimulation of both postcentral and precentral gyri.

Celesia (1979) described findings from electrodes targeted at the thalamic nucleus ventralis posterolateralis (VPL) as well as the those from the surface of the cortex and the scalp. From the cortex he described a double positive deflection (P1 - mean latency 20.8, and P2 - mean latency 57.1), separated by a negative hump (N1- mean latency 37.7). P1 was frequently preceded by a small negative hump (No - mean latency 20.2). A close correlation was observed between the waves recorded directly from the postcentral gyrus and the scalp, with peak latencies of the first two positive waves differing only by 1-2.5ms between scalp and cortex. The dissimilarity between thalamic potentials and cortical potentials led this author to believe that P1 and P2, recorded over both the precentral and postcentral gyri, were of cortical origin and that the somatosensory information converges to the motor cortex.

Kelly and Goldring (1965) and Stohr and Goldring (1969) described similar P1 and P2 waves which showed polarity reversal between pial surface and white matter over the precentral and postcentral gyri and therefore also had concluded that these potentials were of cortical origin.

Between 1967 and 1969 Broughton described a series of important studies analysing and comparing scalp and cortex surface recorded somatosensory evoked potentials. Many cortex studies had preceded this work but this was the first to describe the tempero-spatial aspects

of the SEP recorded from the cortex of patients with normal sensori-motor function and compare these potentials with scalp recorded SEP's in the same patients.

These cortex to bone reference SEP recordings in unanaesthetised temporal lobe epileptics showed absence of the P15 component observed in scalp recordings but otherwise all major scalp components (N19, P25, N35 and P45) were seen. N19 and P25 components were regularly present on the postcentral gyrus where direct electrical cortical stimulation produced sensation referred to the contralateral thumb/index finger. A waveform of inverted polarity and identical or 1-2 msec longer latencies was regularly recorded precentrally.

Cortex versus scalp recorded waveform differences included amplitude reduction, spatial averaging and relative suppression of localized waveforms (see Figure 3.7)

The work of Allison et al (1980) agreed with the findings of Broughton that in both scalp and cortical surface recordings, the predominant potentials in the 20 - 30 msec range are contralateral and consist of an N20-P30 sequence recorded in the parietal area and a P20-N30 sequence recorded in the frontal area. Both authors concluded that these potentials are generated by a single dipolar source layer located in the posterior bank of the central sulcus in area 3b (see Figure 3.8)

Additionally Allison and his colleagues described an intermediate P25 potential recorded over the central sulcus and proposed that Brodmann area 1, located on the crown of the postcentral gyrus was a likely source.

Papakostopoulos and Crow (1980) also described a precentral P20 and postcentral N20 from cortical surface recordings. These authors considered that the consistent later peak time of frontal P20 compared to postcentral N20 suggested separate generators.

Slimp et al (1986) described SEP studies in a patient with a discrete resection of part of the postcentral somatosensory cortex as a treatment for epilepsy. Although removal of a 3.5cm section of tissue changed postcentral SEP's, precentral SEP's were remarkably unaltered.This led the authors also to conclude that precentral components have separate generators. Malis et al (1953) had earlier shown that somatic sensory evoked responses in the

motor cortex of monkeys survive the ablation of the postcentral gyrus. Goldring and Ratcheson (1972) had recorded from single neurons in the hand area of the motor cortex: they found sensory cells being selectively activated by active and passive hand movements. These single neuron recordings conclusively proved kinaesthetic projection to the motor cortex of man.

In 1988, Wood et al employed a 64 electrode array to study the topography of the cortical surface recorded SEP over the sensorimotor hand area. As in the studies of Broughton (1969) and Allison et al (1980), SEP's with approximately mirror image waveforms were recorded at electrode sites in the hand area on opposite of the central sulcus (P20-N30 precentrally and N20-P30 postcentrally). Additionally they described a P25-N35 complex recorded from the postcentral gyrus as well as a small region of the precentral gyrus in the immediate vicinity of the central sulcus. This waveform was largest on the postcentral gyrus about 1 cm medial to the focus of the 20- and 30- msec potentials (see Figure 3.8).

A crucial test of the contribution of area 3b to these potentials would be to record transcortically from area 3b in man. This cannot be done, but in monkeys such recordings show polarity inversion of frontal P10-N20 ("surface") and parietal N10-P20 ("white matter") potentials which likely correspond respectively to the human P20-N30 and N20-P30 sequences (Arezzo et al 1981).

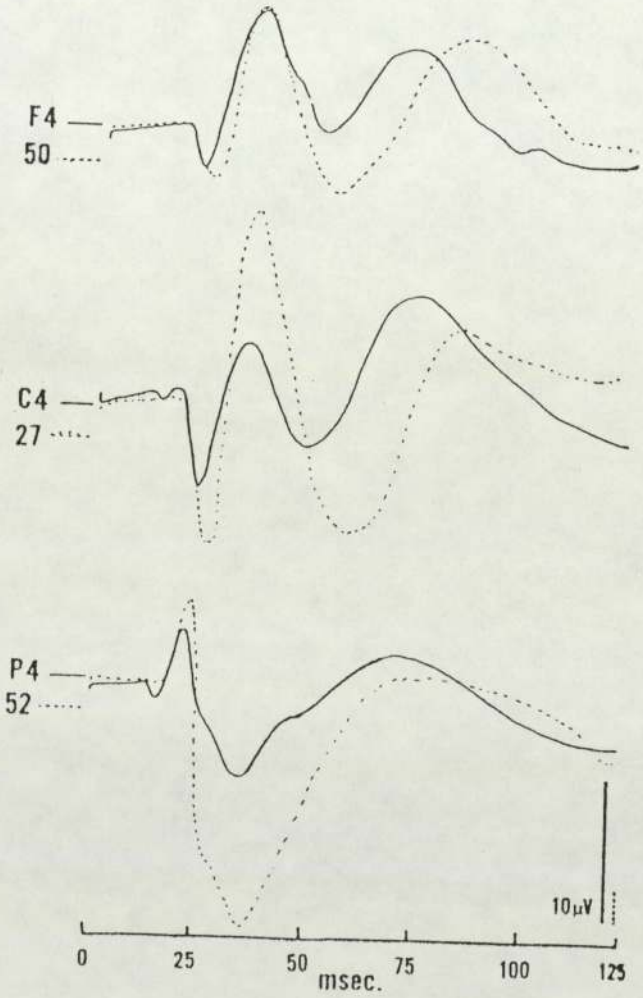

Figure 3.7. Comparison of cortical and scalp SEP's. Note the increased latencies and amplitudes of the (stippled) cortical components. From Broughton et al (1969).

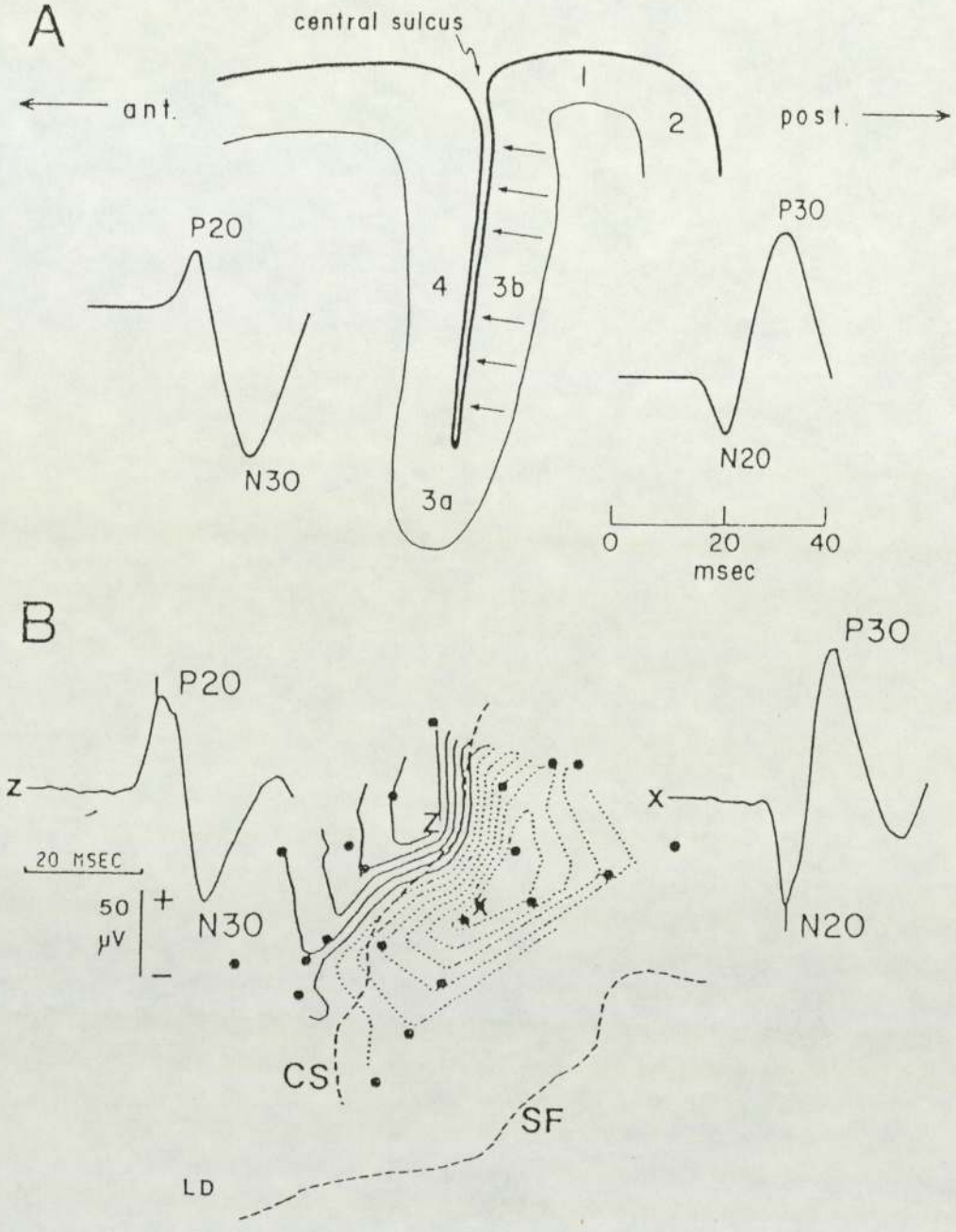

Figure 3.8. Schematic short latency potentials recorded at locations anterior and posterior to the central sulcus (A). Taken from Allison et al (1980), Figure 1. Cortical surface recordings from electrode locations in relation to central sulcus (CS) and Sylvian fissure (SF) determined from photographs made during surgery. A computer-generated isopotential map (solid line denote positive potential; dashed lines, negative) shows the distribution of activity at the latency (20ms) indicated by the cursors.

3.4.0. Brain Mapping

3.4.1 Background

Colour contour mapping now entered the fray in an attempt to enhance the increasing volume and complexity of data that was necessary in these topographical studies.

The concept of mapping the activity of the brain however is not a new one. As early as 1949, Brazier described the electrical fields recorded at the surface of the head during sleep.

In the early fifties some research groups developed topographic displays for visualizing spatio-temporal details of the EEG. For example, Walter and Shipton (1951) devised a toposcope consisting of 22 small cathode ray tubes; each tube displayed information from a bipolar EEG derivation and the arrangement of the tubes corresponded to the placement of electrode pairs. The frequency and phase of the EEG were directly indicated on the apparatus, this being achieved by means of a radial time base common to all tubes and rotated by means of a simple servo-mechanism.

Rémond (1965) developed a method for the spatio-temporal mapping of EEG and EP data by measuring the voltages from a row of 8 electrodes equidistantly placed in a region on the scalp. The equipotential maps, called chronotopograms, were estimated by a second order interpolation procedure. The display of chronotopograms has been used to give information on the underlying generators of the spontaneous EEG and of the EP components in relation to sensory, motor and cognitive processes.

Studies now began to develop into a two pronged attack; those who employed increasingly large numbers of electrodes with the conventional 10-20 montage system and those who localized the electrodes with their own arrays in areas of interest. For example, Lehmann (1971) studied equipotential fields of the human alpha EEG recorded from the scalp using a 48 channel system. The maps reflected a relatively high uniformity of the potential fields.

Bourne et al (1971) applied a spatio-temporal mapping technique to investigate the characteristics of the visual evoked potentials (VEP) recorded from 17 electrodes on the occipital scalp.

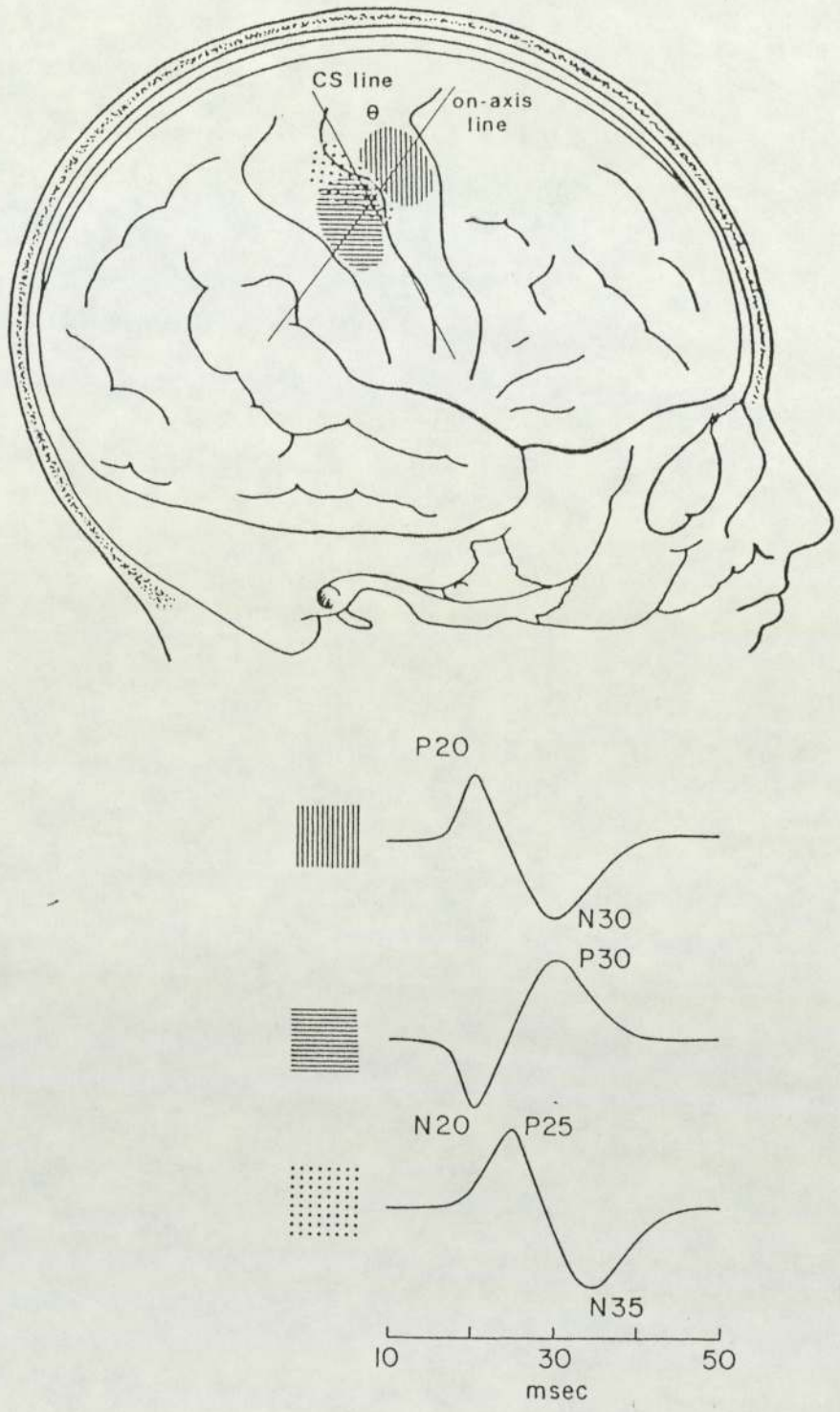

Figure 3.9. Schematic summary of the waveform, latency and topography of the somatosensory evoked potentials from the cortical surface recordings of Wood et al (1988). From Figure 10 of this publication.

We have already described how Goff et al (1977) and Allison et al (1980) reported on their studies of the scalp topography of the human somatosensory evoked responses. Their primary goal was to describe the spatial and temporal properties of all detectable EP components. For their general experimental and clinical studies, the standard 10-20 electrode placement using the earlobe as a common reference appeared to provide adequate spatial resolution of components.

Several authors (Ragot and Rémond 1978; Harner and Ostergren 1978 and Dubinsky and Barlow 1980) reported display methods of equipotential or grey-scale scalp distributions of EEG and EP activity

It was the work Duffy et al (1979, 1981 and 1982) who did much to 'popularise' the technique of topographical mapping with the utilisation of the so called 'Brain Electrical Activity Mapping' (BEAM) system. They described the processing of up to 28 channels of EEG or EP data, displaying the computed maps as a series of colour images with the use of a linear triangular interpolation method. The system permits the user to compare an individual topographic map with normative data of an age-related control group, and to display the statistically significant differences between the maps.

Buchsbaum et al (1982) and Coppola et al (1982) developed a topographic mapping system with two-dimensional so-called equal area projection of the curved left lateral surface of the human cortex. The left lateral projection was made using 12 electrodes of the standard 10-20 system for electrode placement and 4 additional electrodes in the region of the posterior cortex. It was reported that linear interpolation between the four nearest electrode positions gave the best results on the average when comparing actually measured data values with interpolated values.

Nuwer (1985) described a method for displaying the multichannel EEG and EP data as coloured bars where colour indicates voltage and the time axis is the same as in the waveforms. This method gives a useful display of EP latency shifts over the scalp.

3.4.2 Electrode number and montages

The number of electrodes for topographic mapping of electrical brain activity depends on the scalp area where the electrical activity of the underlying cortex is studied. For practical reasons, as few electrodes as possible are preferred while not losing important information. With respect to the information content, Gevins (1981) reported results which indicate a spacing of at least one electrode every 2 to 2.5 cm on the scalp; this would require more than 60 electrodes if the whole scalp were to be covered. Kahn et al (1988) reported that for total scalp recording, map quality would degrade when the number of electrodes fell below 19 Chatrian et al (1985) proposed an 81 electrode system, a so-called ten percent electrode system for topographic studies of EEG and EP activity.

Desmedt et al (1987) reviewed a number of important points in relation to electrode number and placement:

1. The number of channels should not exceed a manageable set i.e. 21 or so as in the standard EEG.

2. Both hemispheres should be recorded concomitantly to image EP fields that extend across the midline (Desmedt and Bourguet 1985) and recording only one hemisphere at a time (Coppola et al 1982; Giard et al 1985) is not sufficient.

3. For imaging the peak values of any potential field, an electrode must be near the field culmination since electrodes around that focal site only record smaller potentials (Duff 1980). This requires either using many electrodes at focal sites (say 64 up) or optimizing electrodes at focal sites.

3.4.3 Reference electrodes

Topographic mapping of the potential distributions across the scalp requires the signals from all electrodes to be referred to a common reference. Two main methods employed for SEP mapping are; i) A single or double-linked electrode as a common reference e.g. cervical electrode, earlobe electrode or other non-cephalic sites.

ii) The common reference can be defined by the average of the signals recorded at all electrodes - the Average Reference (Offner 1950).

Techniques for using the non-cephalic electrodes can be sub-divided into workers who have relied simply on artefact rejection systems to eliminate the unwanted ECG signal and those who have employed special recording methods to ensure elimination of this signal from the reference input. Workers in the first grouping include King and Green (1979) - contralateral hand reference; Wiederholt et al (1982) - Erbs point reference; Yamada et al (1982) - knee reference; Maccabee et al (1983) - contralateral shoulder.
Workers in the second grouping include Nakanishi et al (1983) and Desmedt and Huy (1984). These authors describe the technique whereby through monitoring the ECG, electrical stimuli were applied percutaneously during the minimal ECG activity with a time delay of 0.4-0.7 seconds following each QRS complex . The non-cephalic reference was the contralateral hand.

Most commonly used reference for SEP mapping is the single or linked ear electrode unless subcortical potentials are being studied when a non-cephalic electrode reference is required. Using this latter reference the sub-cortical N18 potential (Desmedt and Cheron 1981; Mauguière et al 1983) drives all scalp traces negative for nearly 20 msec and can cause difficulty in identification of peaks during this period. Since N18 occurs at the earlobes, using an earlobe reference subtracts N18 from the scalp traces and this negative shift is cancelled out or greatly reduced (Desmedt and Cheron 1981). Refer to section 3.1.

3.4.4 Interpolation

For topographic mapping of the electrical activity of the brain, an interpolation technique has to be used to estimate the values between the positions of the electrodes on the two-dimensional scalp projection. The choice of an interpolation method implies a number of

assumptions about the potential distribution between electrode positions; there are essentially two forms:

In linear interpolation methods, the distances of any point to 3 or 4 electrodes positions of a triangular or rectangular grid determine the weighting coefficients for the grid points. Buchbaum et al (1982) and Coppola et al (1982) reported that linear interpolation between the four nearest electrode positions gave the best results when comparing actually measured data values with interpolated values.

In the inverse distance interpolation method, the weighting coefficients are determined by the inverse linear, quadratic or cubic distances of a grid point to the nearest electrode positions. Several authors argue that this latter method provides the more optimum topographic maps

(Estrin and Uzgalis 1969; Desmedt et al 1987). Desmedt et al 1987 employed a range of powers in their algorithms and concluded that the third power of distance best disclosed peak foci and field contours. The same authors further maintained that the mapping algorithm should not impose restrictions like, for example, that scalp electrodes are evenly spaced which would prevent the desired flexibility in deciding electrode sites.

Perrin et al (1987) have proposed an alternative spline interpolation algorithm which fits a surface to the measured voltages, producing more accurate maps as maxima are no longer restricted to the electrode site. However, the greater accuracy is achieved at the expense of increased computation.

3.4.5 Statistical mapping

Topographic maps of an individual patient or subject offer limited information if not compared with maps of normative data of control groups in a statistical way.

The so-called Z statistic has been applied to compare individual data with normative data of a control group (Duffy et al 1982). Pre-requisites for use of this statistic are that the control

group population number exceeds 30 and that values are normally distributed (see Chapter 4).

The Student's t-test is also commonly employed to discriminate between the mean maps of two groups e.g. a mean map of data of normal subjects and a mean map of data of patients.

3.5.0 SEP using Brain Mapping techniques

In 1985, Desmedt and Bourguet applied a 'brain mapping' technique to re-assess the functional organisation of the somatosensory system. Sixteen electrodes were placed over both sides of the scalp and the common reference was the right earlobe. The SSEP components could now be assessed in a series of frozen colour display maps at short time intervals and the spatio-temporal properties of each component carefully examined.

Their data substantiated views about the distinct cortical generators for N20, P27 and P22 respectively. The N20 and P27 fields were restricted to the contralateral parietal scalp and did not appear ipsilaterally. The prerolandic P22 field appeared about 1 msec after the N20 onset and its offset was not synchronous with that of N20. The P22 field was also clearly distinct in

timing and scalp location from P27. P22 thus involved prerolandic neuron populations at a time when no P27 had yet appeared, and P27 involved other parietal neuron populations at a later time. They hypothesized therefore that P22 may be generated in the motor area 4 and the supplementary motor area.

As in the study of Goff et al (1977), the mapped N30 field was quite extensive over the precentral region on both sides. The P45 field was found to be inconstant in young adults and quite variable in its extent.

Deiber et al (1986) employed colour bit- mapping to study the topography of the SEP to digital stimulation. An array of 16 electrodes were concentrated in the contralateral centro-parietal region. Their maps clearly showed that the parietal negative N20 component has a frontal positive P20 counterpart and that this configuration was consistent with the dipole

model as suggested by Broughton (1969) and Allison (1980). Indeed, magnetic recordings supported this view of such a tangential oriented dipolar source in the somatosensory cortex (Okada et al 1984; Wood et al 1985). However, Deiber et al expands this further by describing a P22 central positivity distinct in time and space from the earlier N20/P20 configuration. Indeed they found that the peak of P22 was found to shift in space according to the stimulated finger, suggesting a somatotopic organization of the somatosensory projections upon the precentral motor cortex. This somatotopically organized distribution of the central positivity, previously observed by Duff (1980), suggests that the radially oriented P22 generator is situated close to the surface, thus generating a narrow spread potential field on the scalp. A schematic representation of their dipole model is shown in Figure 3.10.

They failed however to record the frontal/prefrontal N22 as described by Jones and Power (1984) and suggested that this was because the muscle spindle afferents to area 3a are not activated by digital stimulation as they would be by median nerve stimulation at the wrist.

In 1987, Desmedt et al used an improved brain mapping protocol (namely a 27 channel system with optimized electrode placement), and concurred with the observations of Deiber et al (1986) on the likely dipolar model.

Allison et al (1989) applied colour bit-mapping techniques to cortical surface recordings to further support their previously outlined dipole models - shown particularly clearly in the study of Wood et al (1988) illustrated in Figure 3.9.

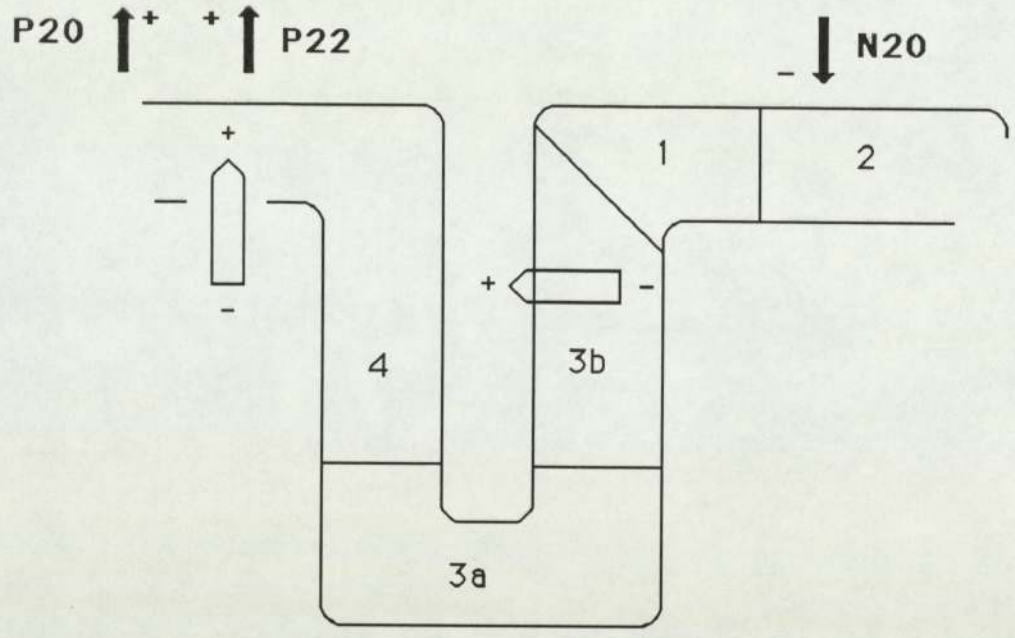

Figure 3.10 Dipole Model as suggested by Deiber et al 1986

3.6.0 Neuromagnetic recordings

Neuromagnetic recordings of somatosensory evoked activity have been of interest in assessing dipole models and therefore possible generators because of a number of inherent properties of evoked fields that differ from evoked potentials. The most important of these differences are:

1. Surface evoked potentials are more sensitive to radial than to tangential sources, whereas evoked fields are sensitive mainly to the tangential component of a source current.

2. Evoked potentials have greater relative sensitivity to deep sources than evoked fields.

3. The inhomogenous conductivities of the dura, skull and scalp have little influence on surface evoked fields, whereas they decrease the spatial resolution of surface evoked potentials.

4. The spatial distribution of evoked field and evoked potential activity on the surface differ in orientation by 90 degrees.

(Kaufman and Williamson 1980; Cuffin and Cohen 1979; Williamson and Kaufman 1981 and Cohen and Cuffin 1983).

A number of workers have recorded the human somatically evoked field using liquid helium cooled SQUIDs (Superconducting Quantum Interference Devices).

Brenner et al (1978) showed that electrical stimulation of the median nerve produces steady state magnetic responses, the topography of which indicates a current source at the contralateral primary somatosensory cortex (SI). Later, Kaufman et al (1981), Okada et al (1981), Hari et al (1984) and Huttenen et al 1987 reported that transient responses elicited by median nerve stimulation were also localized near the contralateral rolandic fissure at latencies of 20 - 250 msec. Sutherling et al 1988 measured the magnetoencephalogram (MEG), electroencephalogram (EEG) and electrocorticogram (ECoG) after stimulation of contralateral median nerve in four patients with partial epilepsy evaluated for surgery. Isopotential fields were plotted for each modality. Each of the three fields appeared to give a different picture of the underlying cortical currents in active somatosensory cortex. MEG was simplest, showing good fits to a single tangential dipole at 20 and 30 msec. EEG detected what the MEG did and in addition detected approximately radial currents at 25msec which required a second dipole for good fit to the data. However, these authors reported that the MEG appeared more sensitive than previous investigators had expected in detecting in two patients the tangential part of a current source that was predominantly radial electrical fields. They postulated that there may be a need to modify the assumptions that MEG is insensitive to approximately radial currents on top of the gyri in the usual background noise in most laboratories

Depth of the source can be estimated. An approximate procedure is to determine the locations of the field extrema from a plot of an isofield map and to measure the arc length between the extrema. The depth can then be determined for a current dipole by the arc length and the radius of the sphere whose surface has the same curvature of the head near the somatosensory area. Employing this technique, magnetic recordings of peri-rolandic SEP's 20 msec after median nerve stimulation confirmed the absence of an ipsilateral

response and provided evidence of a contralateral response seen as an equivalent dipole at a depth of 25mm +/- 2mm from the scalp surface (Kaufman et al 1981)

Two important studies, Wood (1982) and Wood et al (1985) applied the magnetic field theories to the problem of possible multiple generators in the somatomotor cortex. In the earlier paper, Wood looked at dipole localization methods and the application of electrical field theory to the identification of electrical sources in the human body and the solution of what is termed the INVERSE problem - that is to calculate the sources within a volume conductor given the empirical potential field on the surface. In order to attempt a solution to this problem, a number of assumptions must be made about the geometry and conductivity of the skull, brain and other tissues:

1. The head is assumed to consist of a sphere corresponding to the brain, surrounded by two concentric shells corresponding to the skull and scalp.

2. Each region is assumed to be homogeneous in which capacitative and reactive effects are assumed to be negligible; in such a medium electrical effects will propagate instantaneously.

3. The brain and scalp are assumed to be equal in resistivity (220Ω/cm), with the skull 80 times greater (a so called three sphere model).

4. The surface potential field at a given instant in time is assumed to approximate that generated by a dipole source.

Taking these assumptions into account several workers (Darcey et al 1980 and Sidman et al 1978) have applied numerical minimization algorithms to achieve dipole localization - the D.L.M. (Dipole Localization Methods).

Application of this DLM has been made to the SEP complex described by Broughton (1969) and Allison(1980) ; that of a P20-N30 complex at frontal locations and an N20-P30 complex at parietal locations. Broughton and Allison hypothesised that these potentials originate in a source buried in the posterior bank of the central sulcus. Sidman et al (1978) reported DLM results for the P30-N30 field in which the location of the best fitting equivalent dipole correspond closely to that predicted by the Broughton - Allison hypothesis . For the earlier

N20 - P20 potentials, the Sidman et al DLM results yielded unstable solutions with a poor fit to the obtained data (see Figure3.11). If N20-P20 and P30-N30 are generated by equivalent dipole sources with the same location and opposite orientation as the Broughton - Allison hypothesis suggests, then they should have exactly the same scalp distribution with opposite polarity. One explanation for the different dipolar fields seen would be the summation of a somatosensory cortex source with a more broadly distributed subcortical negativity.

An alternative hypothesis for the origins of these potentials is to assume separate precentral and postcentral generators for N30 and P30 instead of a single tangentially oriented source (Papakostopoulos and Crow 1980; Desmedt and Cheron 1980).

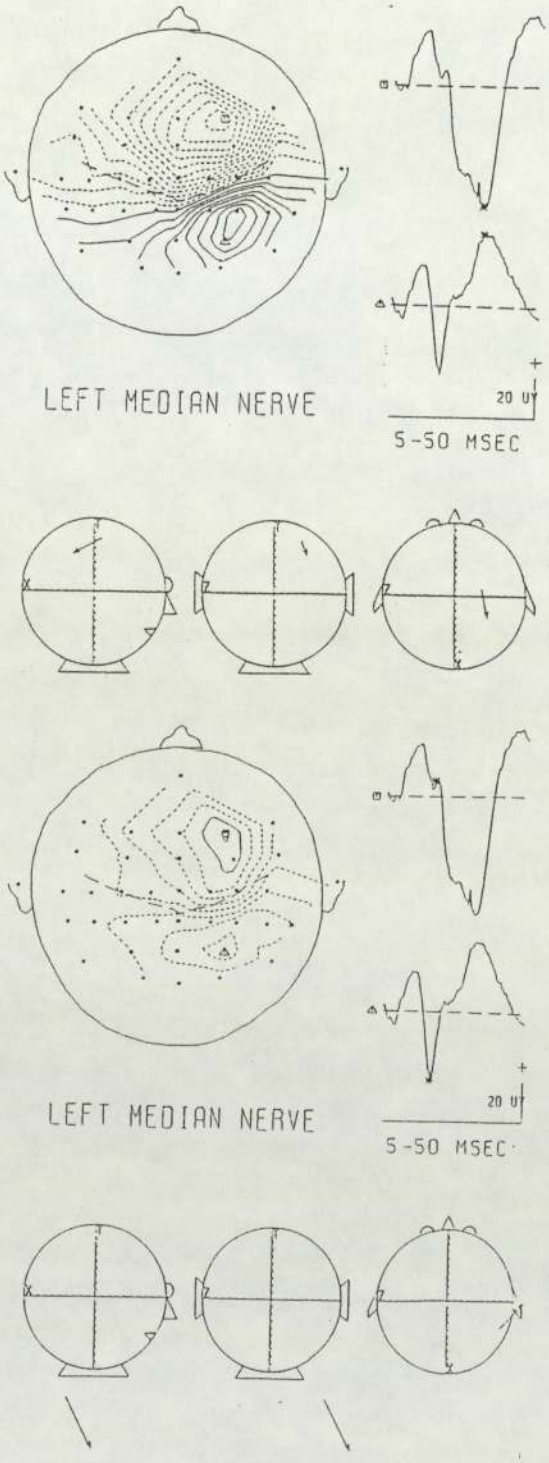

Figure 3.11. Dipole localisation models applied to the N30-P30 complex of Allison et al (1980) (**Top**) and the N20-P20 complex (**Bottom**).

CHAPTER 4

STUDY OF THE TOPOGRAPHY OF THE UPPER LIMB SOMATOSENSORY EVOKED POTENTIAL IN THE HEALTHY HUMAN ADULT

4.1.0 Introduction

Although there have been studies on the scalp distribution of upper limb SEP components in normal man (Goff et al 1977; Desmedt and Bourguet 1985 and Desmedt et al 1987), and descriptions of the differential effect on SEP components of discrete cortical lesions (Mauguière et al 1983); there have been few descriptions of the clinical application of an SEP control population database using 'brain mapping' systems. Duffy et al 1981 has described the use of the Z - score map as an aid for detection of significant topographic differences between a control population and an individual (refer to Figure 4.1).

The purpose of this first study was twofold; First to study the morphology and topography of the first 56ms of scalp recorded SEP activity from a broad age range of normal control volunteers. This short epoch was selected to record only the so called 'primary cortical ' responses with high resolution since there is evidence that later potentials are modified by cognitive factors (Desmedt et al 1983). The second purpose of the initial study was to collate a normative database in order that this may be used to investigate the effectiveness of such a database in the detection of pathology.

Previous methods for studying the scalp topography of SEP components can be described as falling into three groups.The first group consists of authors who have employed electrodes placed widely over the scalp according to the 10-20 method of electrode placement (e.g. Goff et al 1977). The second group consists of studies where the 10-20 system has been employed with the addition of extra 'optimumly' placed electrodes (e.g. Desmedt et al 1987). The third group consists of authors who have clustered the electrodes over one somatosensory/somatomotor cortex (Duff 1980 and Deiber et al 1986).

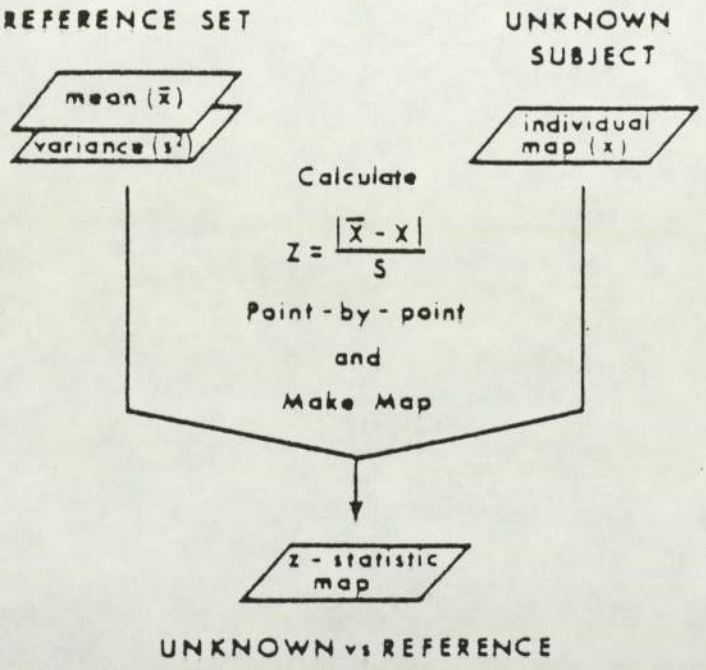

Figure 4.1. The Z-statistic measures the deviation of an individual mapping matrix from the mean of a set of mapping matrices. The Z-transform (the number of standard deviations by which an individual observation differs from the mean of a reference set) is calculated for each pixel in a colour contour mapping image. These transformed scores compare the individual subject to the mean and variance mapping images of a reference population. For example, a mapping image representing the spatial voltage distribution at a given latency for an unknown subject may be compared with the mapping image for the same latency derived from a population of control subjects. The result of this point-by point Z-transformation is a new matrix of Z values retaining the spatial framework of the original mapping image. Clusters of high Z values will then define regions in which the individual subject statistically differs from the reference population.
Pre-requisites for use of this statistic are that the control group population number exceeds 30 and that it is normally distributed.
From Duffy (1982).

Due to the number of recording channels available for this study (a maximum of 20), it was decided to use two methods; the first, for the study of the total scalp distribution of the upper limb SEP and in the construction of a normative database, employed electrodes placed according to the International 10-20 system (Jasper 1958); the second, which will be described in a later Chapter, using a polar projection system of placement (Drasdo and Furlong 1988) to study the SEP components with greater spatial resolution.

In this Chapter we will consider the methods and results obtained from the 10-20 system study.

4.2.0 Method

Thirty five volunteers gave informed consent to be involved in the study and all presented with no current or past history of neurological illness. They were selected from undergraduate, postgraduate and staff members of the University of Aston or from visiting members of the public involved with groups providing subjects for the University on a regular basis. Ethical Committee approval was given.

In each subject the head was measured according to the International 10-20 system (Jasper 1958) and points located and marked on the scalp using a wax pencil. The 20 points included Fp1, Fp2, F3, F4, F7, F8, Fz, T3, T4, T5, T6, C3, C4, Cz, P3, P4, Pz, O1, O2, Oz. Electrodes were also attached to the right and left earlobes to serve as linked reference sites. Selection of this reference, as opposed to a non-cephalic site (see section 3.1.0), was based on findings of Desmedt et al (1981). These authors reported a widespread and prolonged N18 component which was best seen using a non-cephalic reference; this component could obscure the morphology and certainly the topography of the earlier cortical components. Since the N18 component was greatly reduced by employing an earlobe reference, and since this site was relatively silent for the early cortical component, it was considered to be an ideal reference location for this study. Electrodes were also applied to the right and left Erbs points to enable monitoring of the peripheral signal.

Prior to electrode placement the scalp was prepared at each location with the application of Omniprep™ paste which was applied with a cotton wool bud. This mildly abrasive paste was used to lower the skin resistance. Electrodes were then applied at the prepared locations and fixed in position with Blenderm™ tape. Dracard™ electrode gel was then inserted into the scalp/electrode gap using a syringe and 1mm blunt ended needle.

Electrodes were plugged into the headbox of a 20 channel Biologic Brain Atlas III™ system. Scalp electrode resistances were measured on the system with the ground electrode, reference electrode and an individual scalp electrode forming a resistance bridge. A 1KHz 2uA signal was used to measure the impedance to the nearest 1KΩ.

The Biologic Brain Atlas III™ system is based on an NEC microprocessor with a central processing unit containing a 16 MHz 80386 16-bit floating point processor and 1000KB of dynamic RAM. A 10 MB Bernoulli cartridge was available for data storage and processing. An 8-bit analog to digital converter with a conversion time of 1.2 uS was incorporated. The system contained its own amplifiers; these had a common mode rejection ratio of 100 dB at 60Hz and an input impedence of greater than 100 MΩ. Noise levels were 0.6 uV RMS, 1.5 uV peak to peak.

Amplifiers were set to a gain of 30,000 and an automatic artefact rejection system based on amplitude employed. The system would therefore allow signals of up to plus or minus 82uV to be incorporated into the average. Filters were set to a high turnover frequency of 1500 Hz (-3dB down point, roll-off 12dB/octave) and a low turnover frequency of 10 Hz (-3dB down point, roll-off 12dB/octave) .

The time window was 64 ms in total but included 7.5 ms of pre-stimulus data. There were 256 data points covering this epoch which gave a resolution of 0.25ms per point.

Subjects were seated in a Parker-Knoll™ reclining chair. Wrists were swabbed with acetone to lower the skin resistance. At the patient end the stimulator incorporated two saline soaked pads which slotted onto contact plates mounted in a plastic applicator. This device was held in

place on the wrist by means of a Velcro™ strap and ensured that the cathode was 2.5 cm from the anode; the latter always being placed distal to the cathode on the subject.

The choice of limb order to be stimulated was made on a pseudo-random basis between subjects.

The stimulus was delivered via a constant current stimulator and consisted of a 0.1 ms duration square wave pulse delivered at a rate of 2.7 per second. The subjective threshold of the pulse was initially determined and the pulse increased until a regular moderate contraction of the thenar muscle was obtained. The current required to achieve this was invariably between x2 or x3 the subjective threshold current and so if no twitch was observed at x3 threshold current this would imply incorrect positioning of the wrist stimulator pads and these would therefore be repositioned until a contraction was observed.

Once adequate stimulus levels were obtained the subjects were instructed to close their eyes and to keep them still and to relax muscles as much as possible . Particular attention was paid to ensure relaxation of neck and jaw muscles as well as the stimulated hand and arm. This was assisted by fully reclining the chair.

Two reliable recordings were achieved before repositioning the stimulus onto the opposite limb.

On subjects who tolerated the stimulus well and upon whom additional recording time would be well tolerated, Erbs point electrodes were located and additional runs recorded substituting Oz recording electrode for the peripheral one. This technique was employed in order to establish an estimate of normal peripheral to central conduction time and to control for peripheral differences.

Prior to each recording session two forms of calibration were undertaken. The first internal calibration involved a 100uV square wave signal passed through each amplifier and a measurement of the issuing voltage and D.C. offset of each displayed for inspection.

The second, external check, involved connecting a test loop from the auditory stimulator of the system (jack plug) to pins of a 25 way connector at the headbox. This enabled a

predefined signal to be passed through every input of the complete system and the resultant waveforms displayed for analysis. Comparison of mapping continuity across channels could also be checked along with amplifier and headbox integrety. Commonly a 500 Hz signal with a 10ms rise/fall time and 30ms plateau was employed with a 10ms pre-stimulus delay. A 64ms time window and filter settings of 10Hz to 1500 Hz were used.

Once data was recorded, each of the 20 channels were inspected for artefact and then stored onto cartridge for subsequent analysis. Analysis would involve the measurement of peak latencies, base line to peak and peak to peak amplitudes and the creation of colour isopotential contour maps. The latter was achieved by aligning a cursor onto the peaks of interest and using the software of the system, representing the base line to peak voltage from each channel as a colour on a scale ranging from red (positive deflections) to blue (negative deflections). These colours were then superimposed onto a two dimensional representation of the scalp surface.

Since the voltage at each electrode location only were known, the colours (and hence voltages) of the intermediate pixels were determined by a linear interpolation algorithm using the voltage and the distance of the four nearest electrodes for the calculation, as shown overleaf.

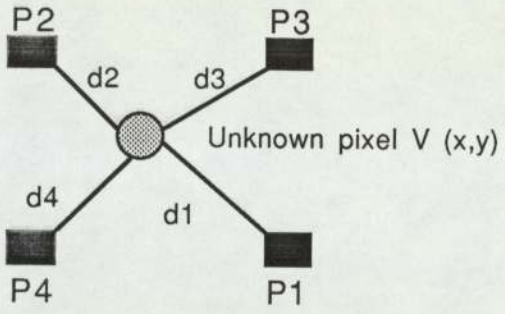

$$V(x,y) = \frac{\sum_{i=1}^{4} Pi \; d\,i^{b}}{\sum_{i=1}^{4} d\,i^{b}}$$

Figure 4.2 Interpolation algorithm.
Pi = voltage of the ith electrode at chosen latency
di = distance from pixel to the ith electrode
b =1,2,3 or 4 depending on coefficient for interpolation. Will equal 1 for linear interpolation.

The Biologic Brain Atlas III™ system employs the Canon PJ1080A ink jet for hard copy of the isopotential colour contour maps. However, in order to obtain a higher quality image for this thesis, it was decided to use the printing facility and therefore the mapping software of a Nicolet Pathfinder II™ system employing an Hitachi colour thermal printer. Once again, the presentation of the contour maps were within a circular two dimensional representation of the scalp surface.

The mapping algorithms of both systems were the same and calculated from the electrode co-ordinates represented on a square grid. The Pathfinder II™ software enabled the electrodes to be placed within this grid in an unequal or non-equidistant fashion whereas the Biologic Atlas III™ software assumes equidistance between electrodes. This latter system was adopted and no attempt was made to represent any apparent non-linearity of distance caused by scalp curvature. Base line to peak voltages recorded from the Biologic system were entered into

the mapping software of the Pathfinder II™ system manually. The base line in each case was determined by the amplifier zero level of the recording system and **no** base line adjustment of the waveforms relative to this baseline were made. However, the 7.5 ms of pre-stimulus averaged data was used as an indicator of possible unequal D.C. offset of waveforms relative to the baseline which might lead to false apparent maxima.

Component isopotential maps were calculated in two ways; firstly, group mean waveforms were calculated by averaging each of the 256 datapoints from the 20 channels of the 35 control subjects. From the resultant waveforms, isopotential field maps were calculated for the main components and referred to as **group mean waveform maps**. Secondly, isopotential field maps were calculated individually from each component of each subject and these maps were averaged together. These maps were referred to as **group mean component maps.** This exercise was performed because it was considered that due to latency variations of peaks between individuals that topographic representation from group mean waveforms may lead to misrepresentation of components, some of which could be purely artefacts of the averaging process. Group mean component maps however represent essentially a latency independent topographic representation of each individually identified component.

Comparisons between the two types of map generation were performed using the Z statistic, where;

$$Z = \frac{(x - m)}{s}$$

x= mean component map data, m= mean waveform data and s= variance of waveform data.

Z is given in standard deviations from the control group waveform data.

The result of this point-by point Z-transformation is a new matrix of Z values retaining the spatial framework of the original mapping image. Clusters of high Z values will then define regions in which the individual component map statistically differs from the reference

population. This data can therefore be represented topographically on colour contour maps where colour ranges now indicate standard deviation.

Initial analysis of data involved the examination of group mean waveform and group mean maps to discover which electrodes should be used for subsequent component data analysis. Waveform nomenclature throughout this study was based on the suggestions of Vaughan (1969) and recommended by the Committee on Methods at the International Symposium on Evoked Potentials in Man (Brussels 1974). In this system, each component is named by its polarity and mean latency or range of latencies - i.e. the mean latency of the component peak prefixed by either N (for negative) or P (for positive) - for example - N20.

Statistical analysis was performed on an Apple MacIntosh™ microcomputer using the Statsworks™ and Statview™ software. All statistical summaries and graphical representations of data were based on the analysis of right limb data only, with the exception of right versus left differences. This was to avoid the use of two correlated measures from the same subject.

Linear and multiple regression analysis were used to determine correlations of peak and interpeak latency and amplitude with age and height. These regression methods assume normal linearity and homoscedasticity. Significance of correlation was based on t-test analysis where the null hypothesis (Ho) assumes that the regression correlation coefficient (r) equals zero; thus

$$t = r\sqrt{N-2} / \sqrt{1-r^2}$$ where (N-2) equals the degrees of freedom.

4.3.0 Results

Recordings were made from 35 control volunteers:

The mean age of the group was 44.91 years; Standard deviation 25.47; Range 17 years to 86 years.

The mean height of the group was 170.11 cm; Standard deviation 11.39; Range 151cm - 193 cm.

For analysis of age related changes throughout this study, the control group was divided into :

a). Young age group: N=17; Mean age= 23.59 years; Standard Deviation= 4.03; Minimum age= 17 years; Maximum age= 30 years.

b). Old age group: N= 13; Mean age= 75.62 years; Standard Deviation= 8.05; Minimum age= 60 years; Maximum age= 86 years.

4.3.1 Group mean waveforms and group mean maps

Group mean waveforms for both right and left limb stimulation were plotted. These are shown in **Figures 4.3-4.5.** Nine major components were identified from these traces and isopotential maps were plotted for each of them. This data is shown in a series of eight maps (components N20 and P20 feature on the same map) in Figures 4.6-4.13. Analysis of these group mean waveform maps revealed the electrode locations at which these components were maximal. To assess whether the nature in which the maps were calculated affected this distribution, the corresponding components in each individual were mapped and averaged as a group. Maximal amplitudes at electrode sites were noted for right and left limb data and the right limb comparisons shown in Table 4.1 overleaf.

It can be seen from Table 4.1 that for right limb stimulation, each component was represented at 85% amplitude or greater on electrodes F3, C3 or P3 no matter how the map was constructed. The same was true for the corresponding electrodes on the right hemisphere for left limb stimulation. For further calculation of peak latency, peak to peak amplitude and interpeak data therefore, only data from these electrodes were used to represent the appropriate cortical area i.e. F3/F4 for frontal data, C3/C4 for central data and P3/P4 for parietal data.

TABLE 4.1. ELECTRODE SITES OF 85% OR GREATER AMPLITUDE REPRESENTATION (RIGHT LIMB)

COMPONENT	GROUP MEAN WAVE/MAP ELECTRODE SITE	GROUP MEAN MAP ELECTRODE SITE
P14	**Fz**, F7, Fp1, F4, Cz	**Fz**,Fp1,FpZ,F7,F4,Cz
N20	**P3**, T5.	**P3**, T5.
P20	**Fz**, F3	**Fz**, F3
P22	**C3.**	**C3.**
P27	**P3**, T3.	**P3**, T3.
N30	**F3**, Fz, C3, Cz.	**F3**, Fz,
N31	**C3**	**C3**
N33	**C3**	**C3**
P42	**C3**	**C3,** P3

Bold figures indicate 100% amplitude representation

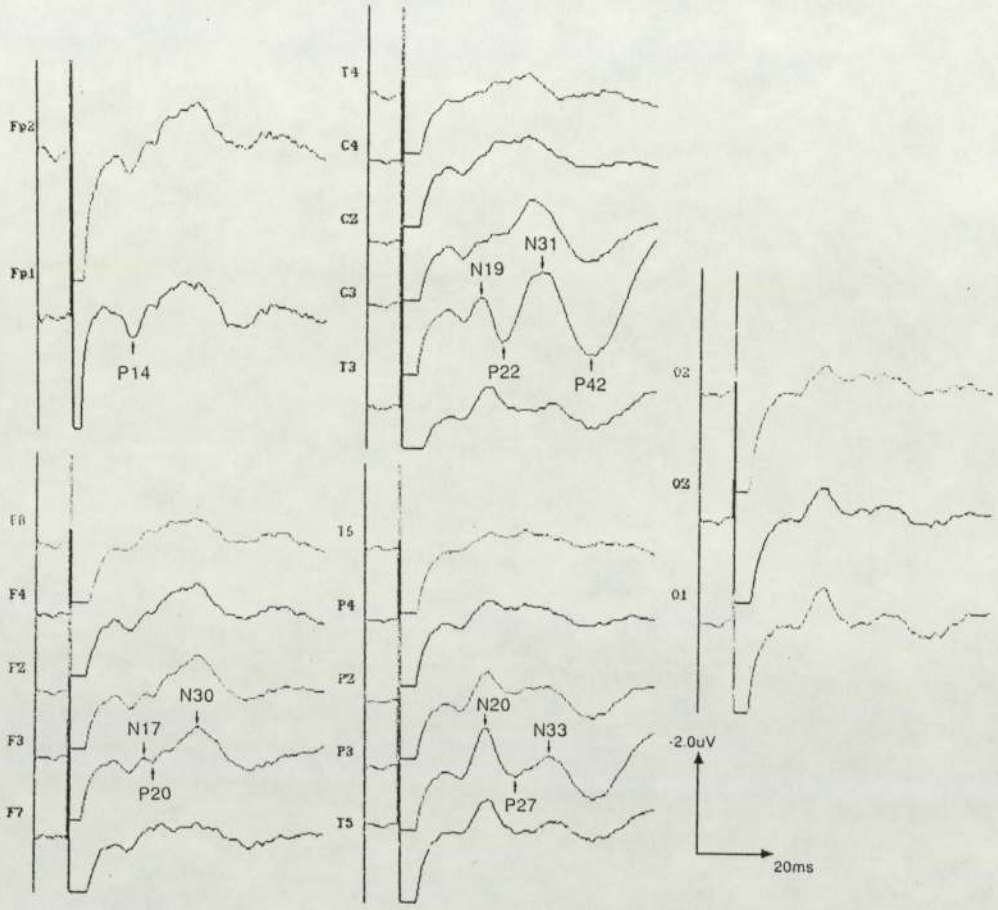

Figure 4.3. Group mean waveforms for right limb stimulation.

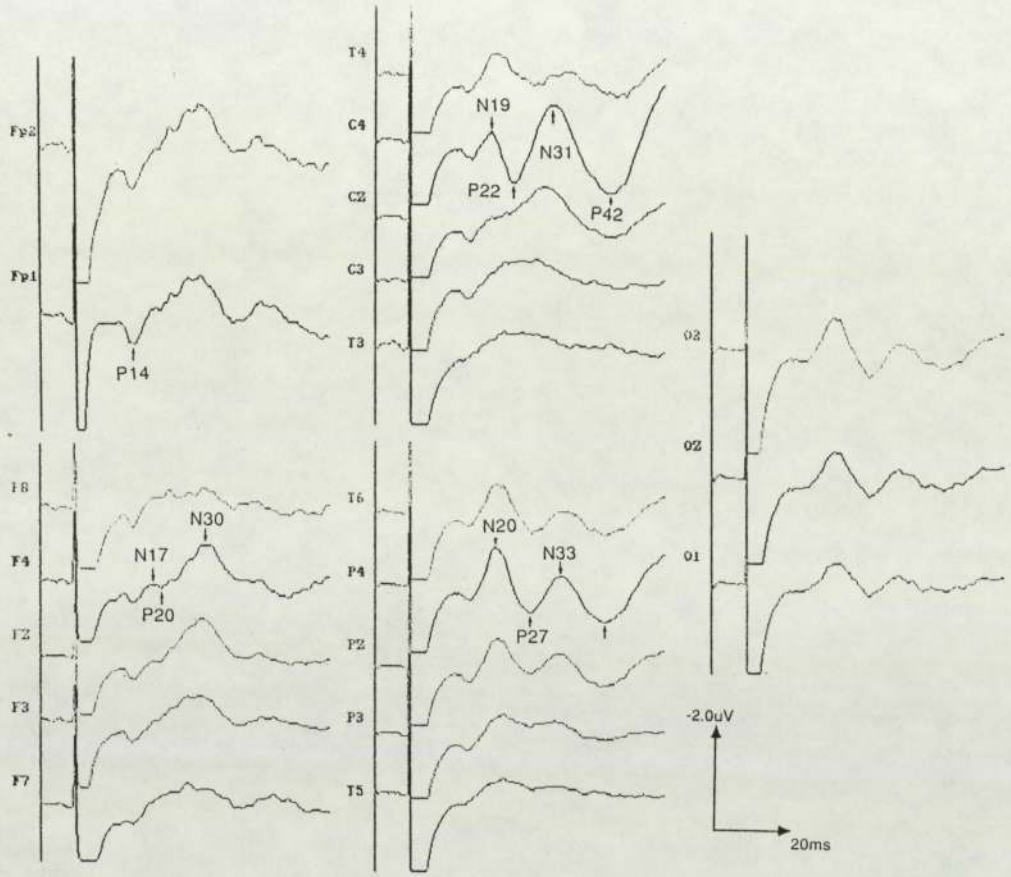

Figure 4.4. Group mean waveforms for left limb stimulation

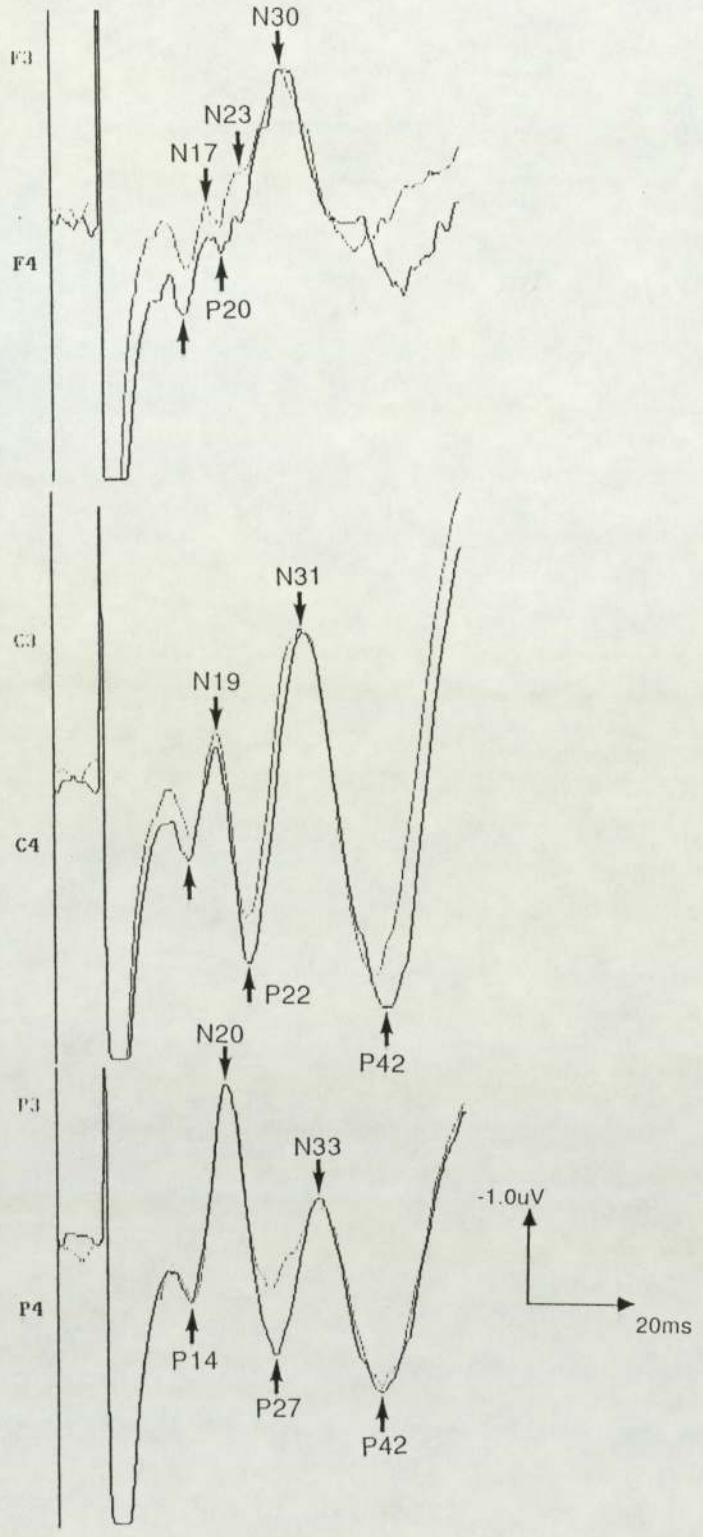

Figure 4.5. Group mean waveforms for right and left limb stimulation. Key electrode sites F3/F4, C3/C4 and P3/P4 are shown. Every scalp recorded component was represented at 85% or greater of their total amplitudes at these locations.

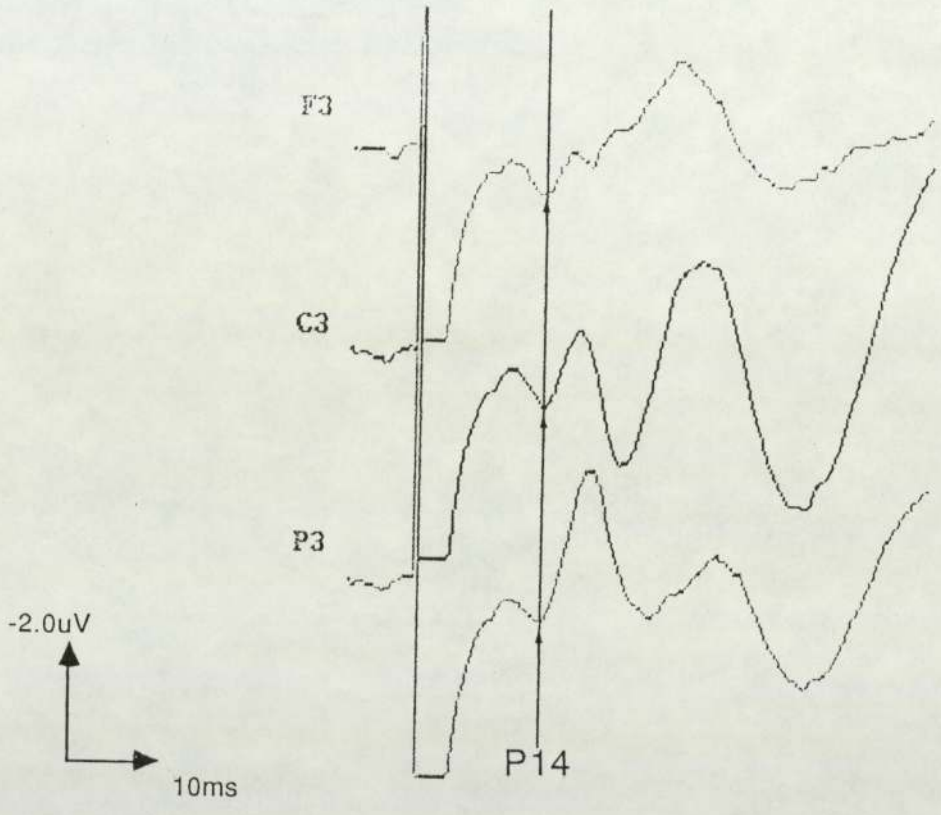

Figure 4.6 (Above). Group mean waveforms from right limb data. Cursor point indicates latency at which the P14 group mean waveform map was constructed (see overleaf).

Figure 4.6.1 (Overleaf)

Topographic maps (from left to right) indicate P14 component group mean waveform map (P14W), group mean map (P14M) and Z statistic map of the comparison of the two .

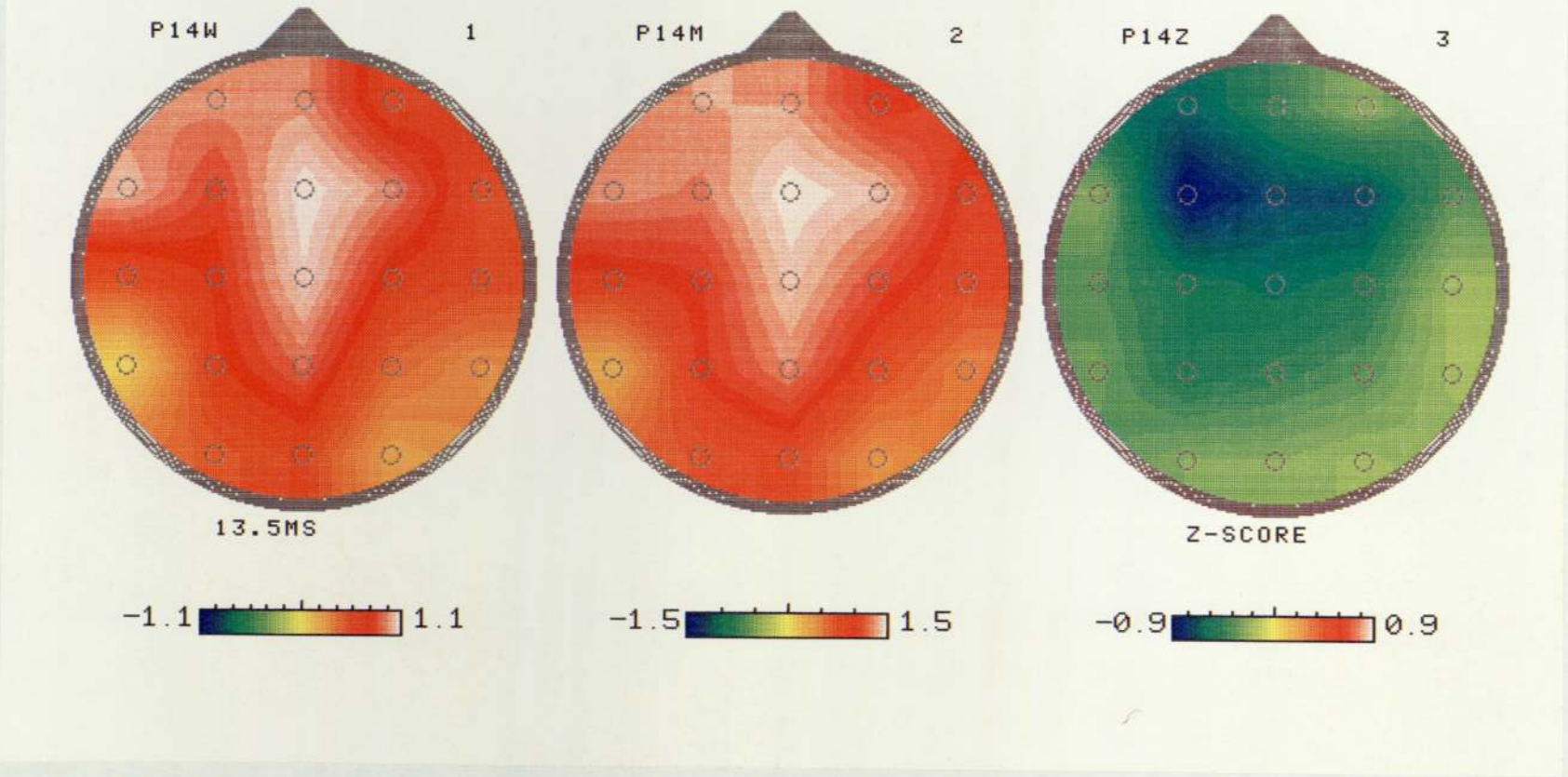
P14W
1
13.5MS
-1.1
1.1
P14M
2
-1.5
1.5
P14Z
3
Z-SCORE
-0.9
0.9

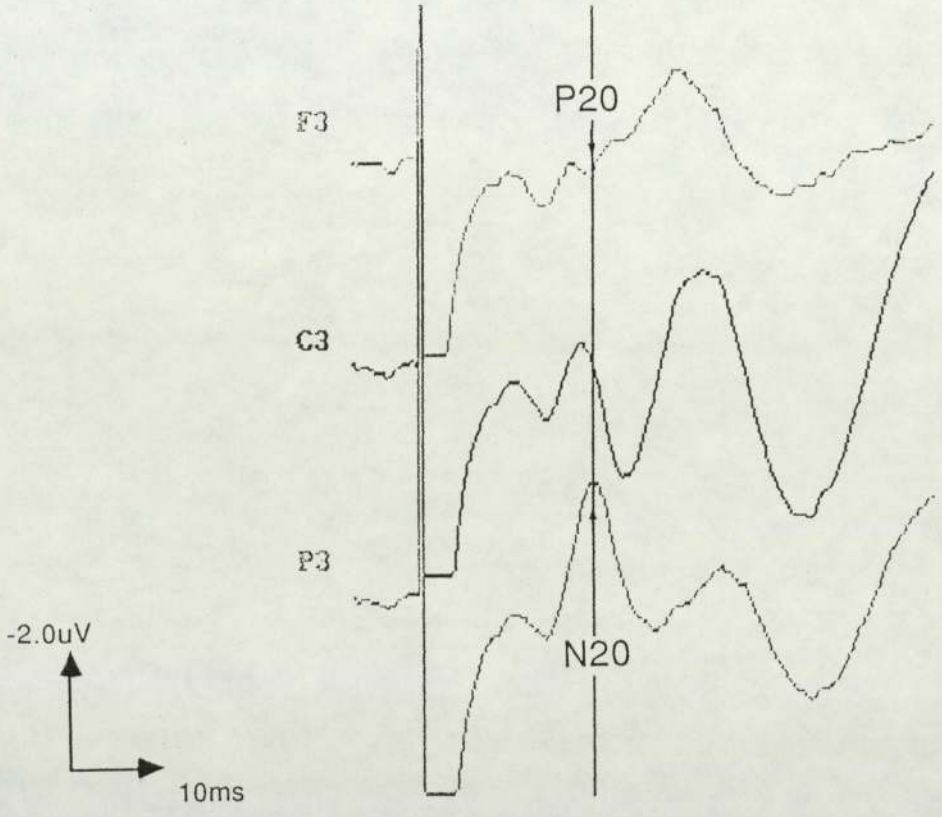

Figure 4.7 (Above). Group mean waveforms from right limb data. Cursor point indicates latency at which the N20/P20 group mean waveform map was constructed (see overleaf).

Figure 4.7.1 (Overleaf)

Topographic maps (from left to right) indicate N20/P20 component group mean waveform map (N20W), group mean map (N20M) and Z statistic map of the comparison of the two .

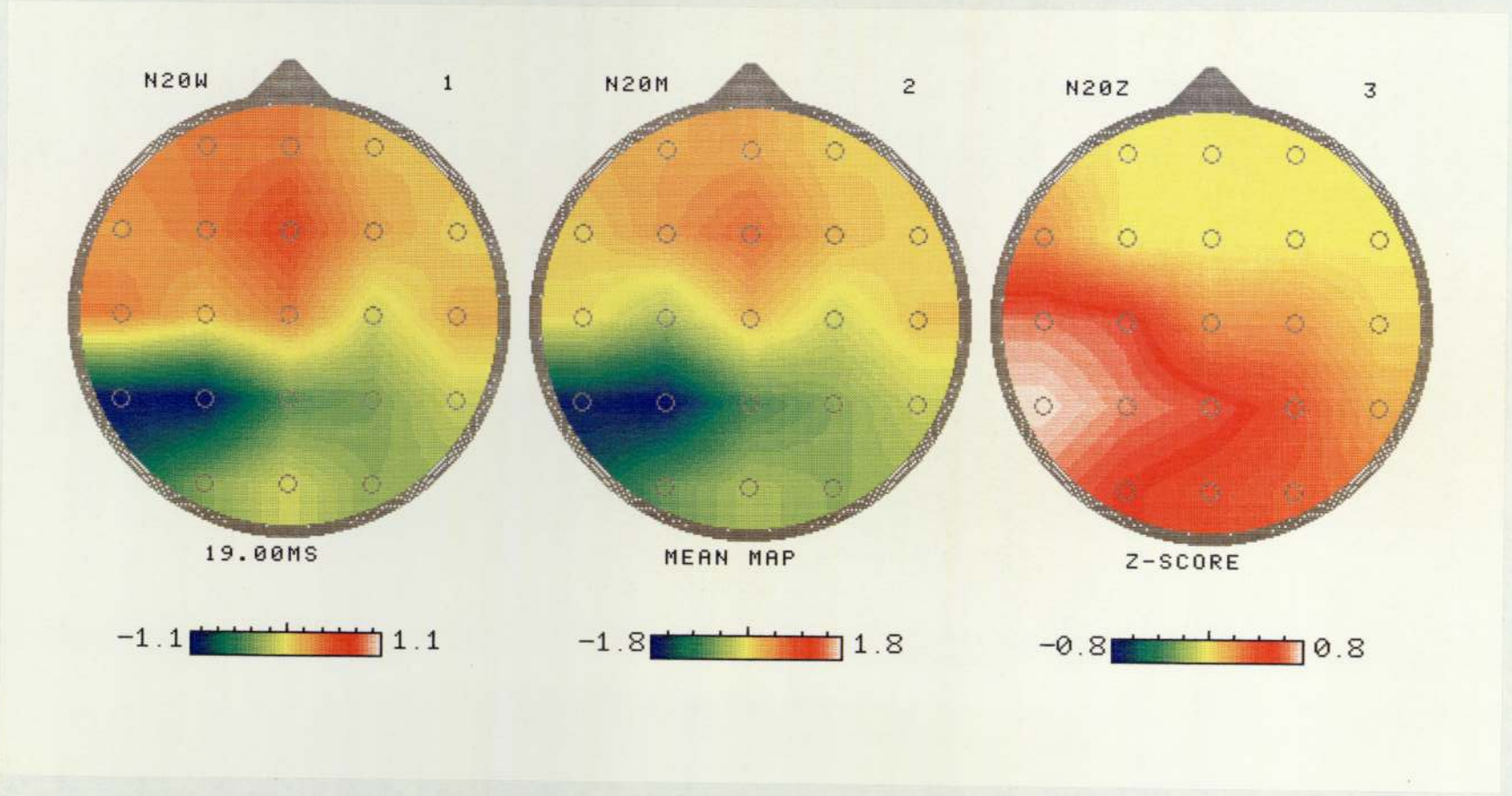
N20W
1
19.00MS
-1.1
1.1
N20M
2
MEAN MAP
-1.8
1.8
N20Z
3
Z-SCORE
-0.8
0.8

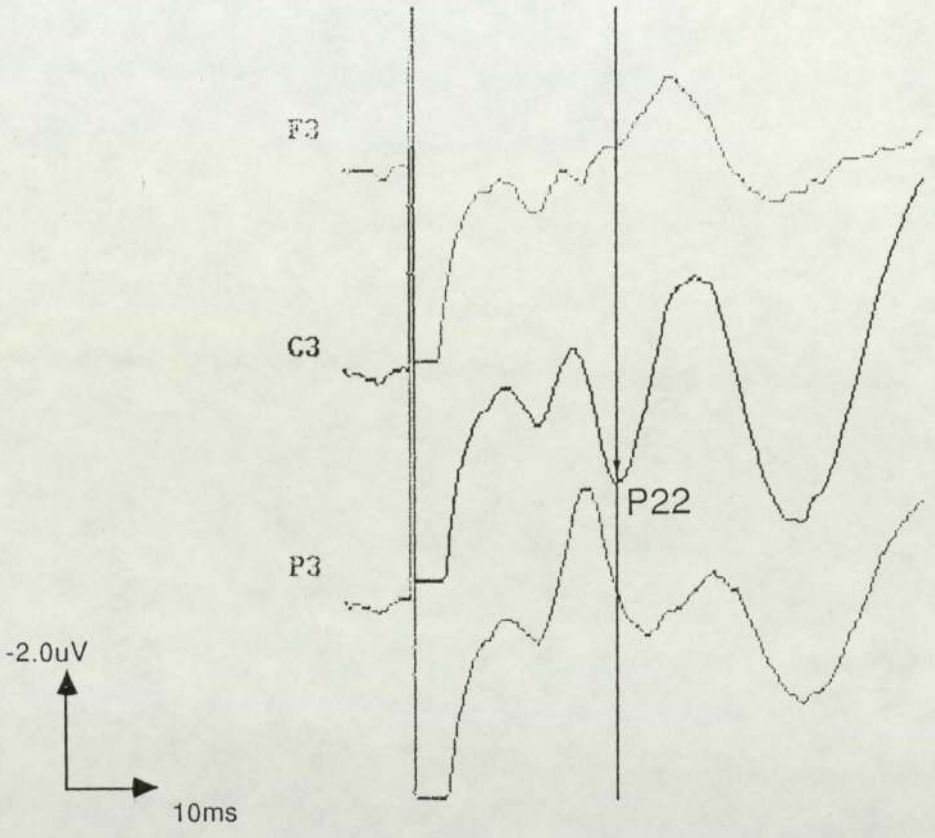

Figure 4.8 (Above). Group mean waveforms from right limb data. Cursor point indicates latency at which the P22 group mean waveform map was constructed (see overleaf).

Figure 4.8.1 (Overleaf)

Topographic maps (from left to right) indicate P22 component group mean waveform map (P22W), group mean map (P22M) and Z statistic map of the comparison of the two .

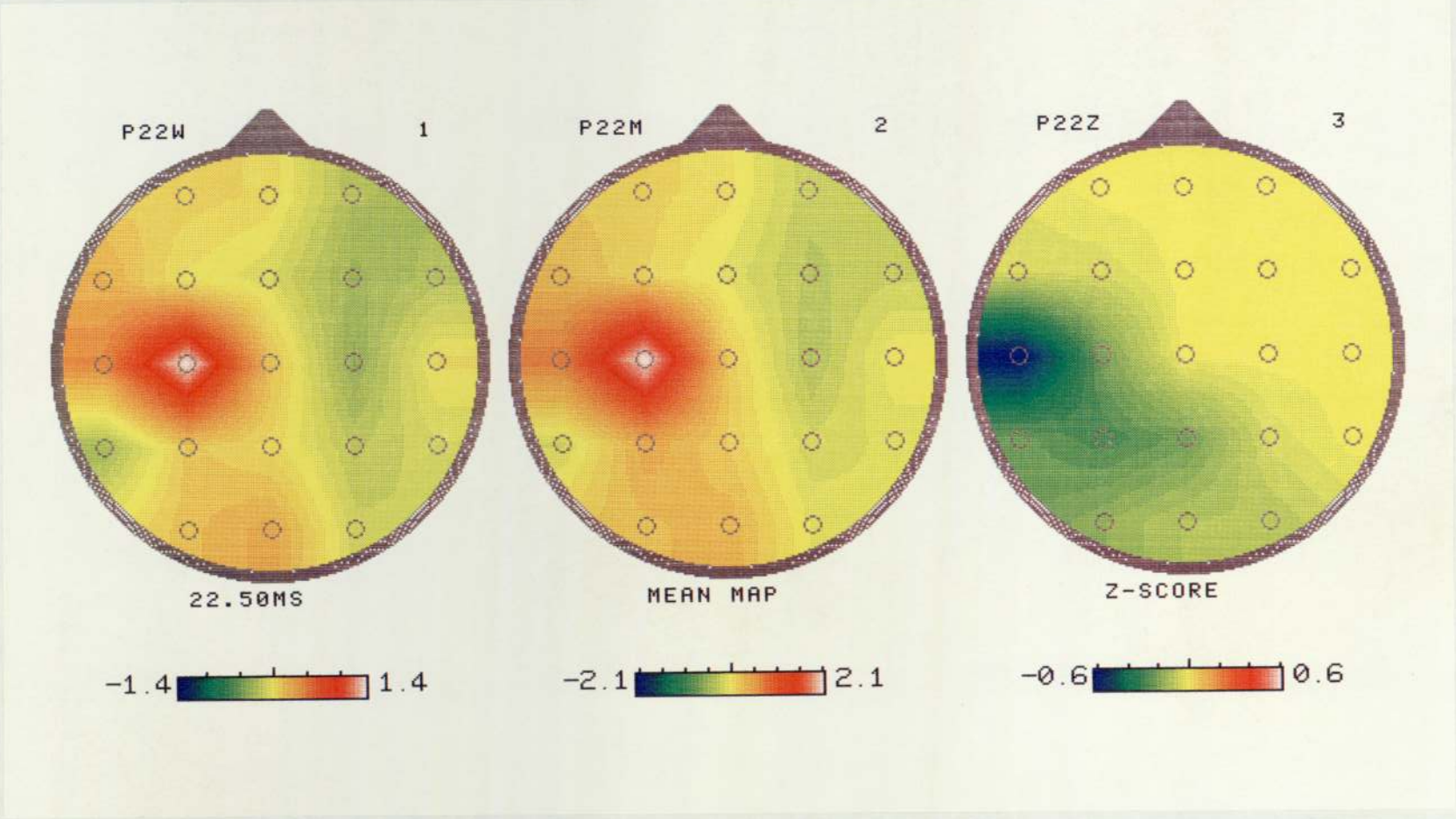
P22W
1
22.50MS
-1.4
1.4
P22M
2
MEAN MAP
-2.1
2.1
P22Z
3
Z-SCORE
-0.6
0.6

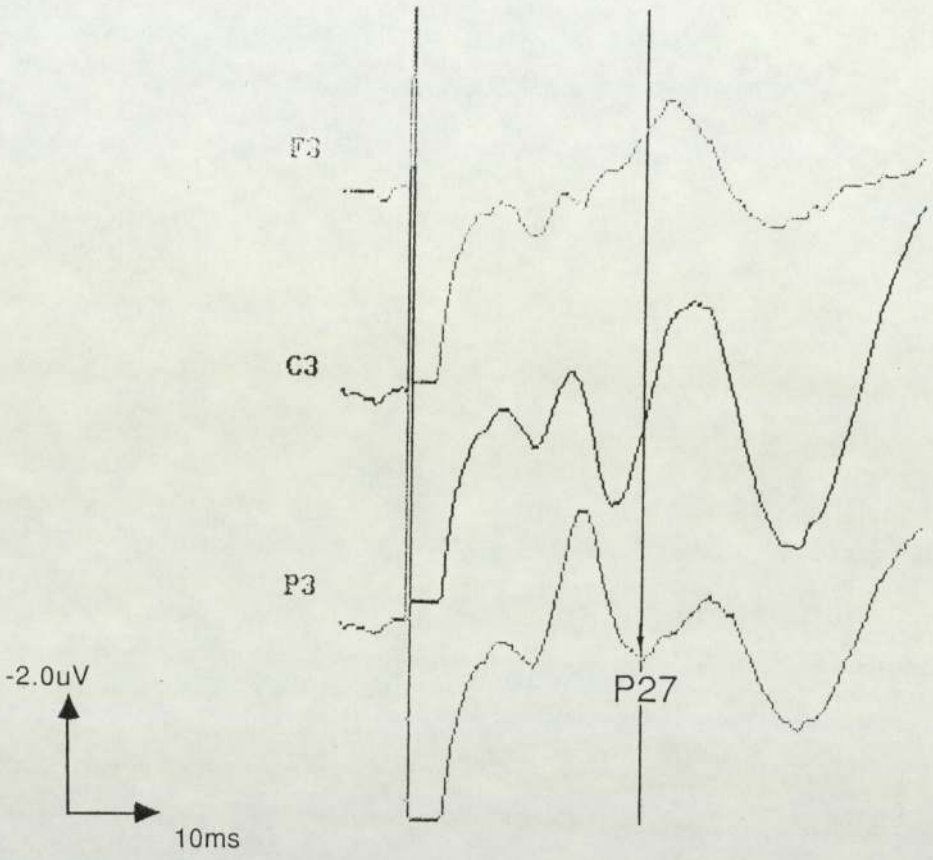

Figure 4.9 (Above). Group mean waveforms from right limb data. Cursor point indicates latency at which the P27 group mean waveform map was constructed (see overleaf).

Figure 4.9.1 (Overleaf)

Topographic maps (from left to right) indicate P27 component group mean waveform map (P27W), group mean map (P27M) and Z statistic map of the comparison of the two .

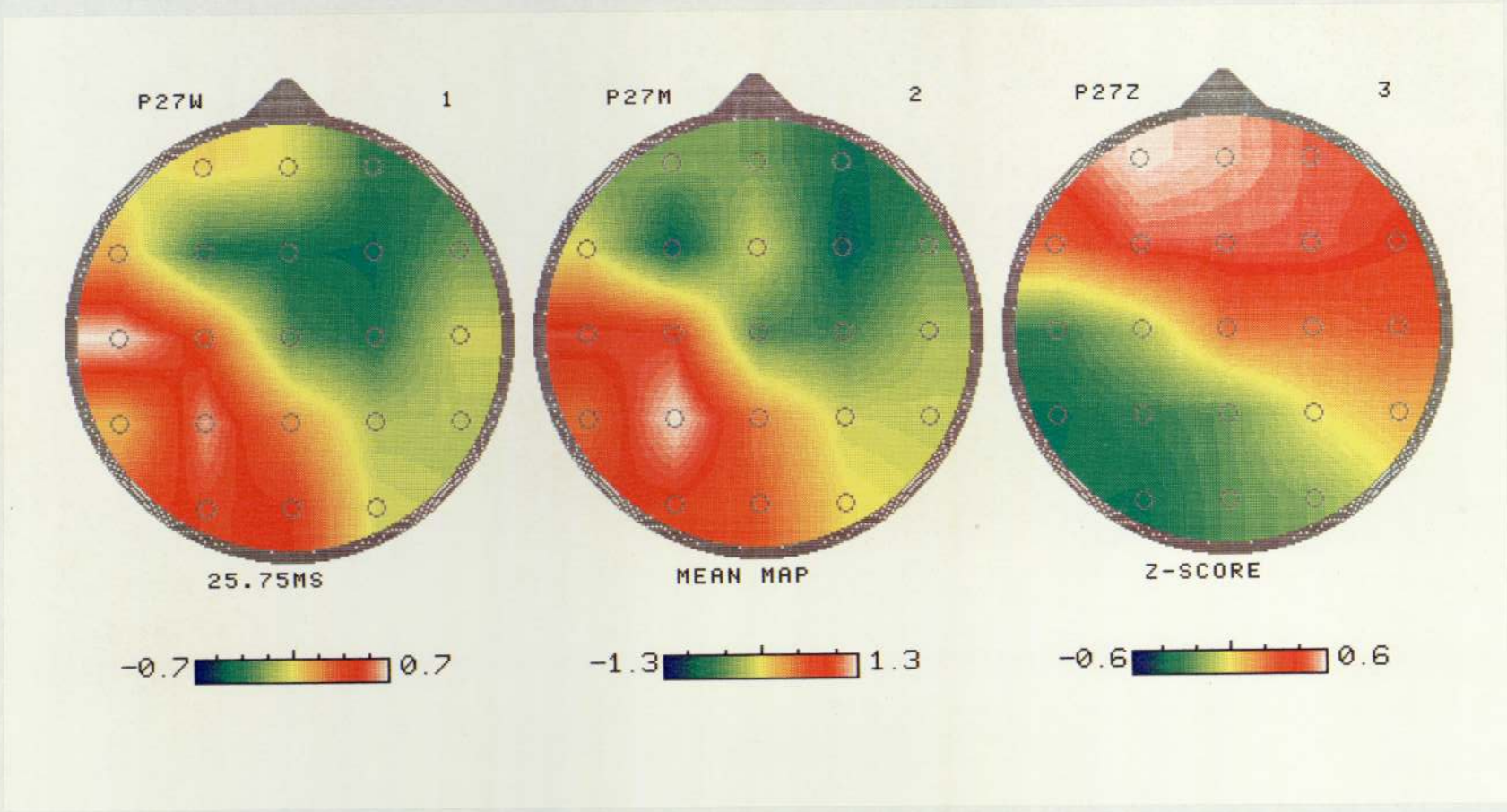
P27W
1
25.75MS
-0.7
0.7
P27M
2
MEAN MAP
-1.3
1.3
P27Z
3
Z-SCORE
-0.6
0.6

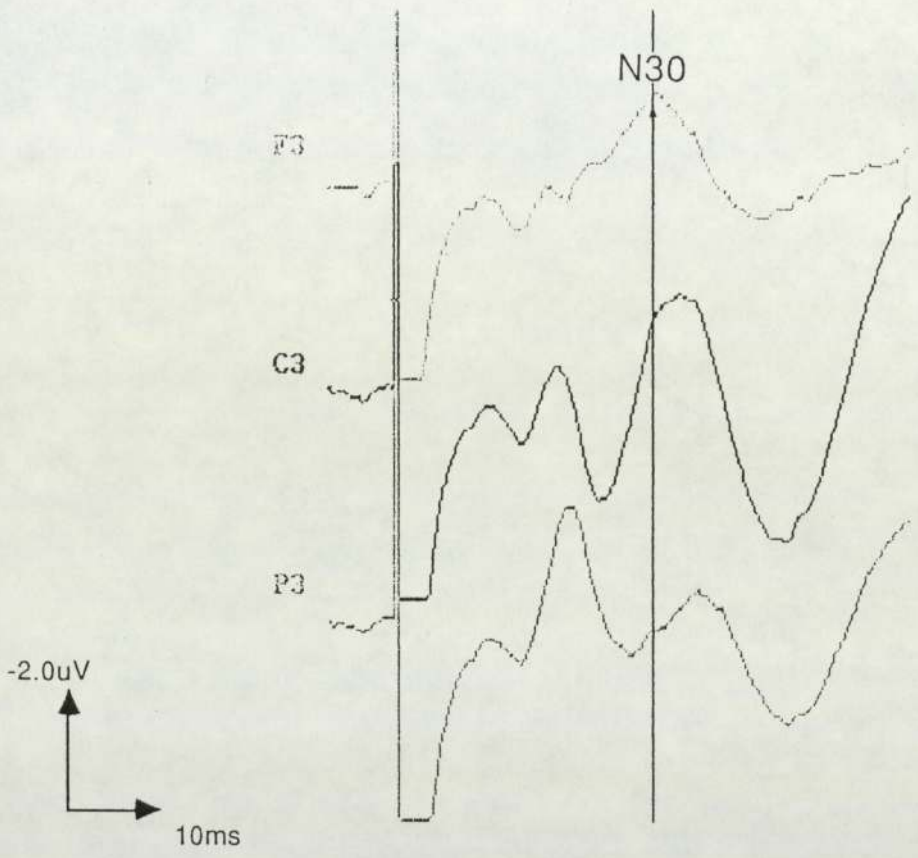

Figure 4.10 (Above). Group mean waveforms from right limb data. Cursor point indicates latency at which the N30 group mean waveform map was constructed (see overleaf).

Figure 4.10.1 (Overleaf)

Topographic maps (from left to right) indicate N30 component group mean waveform map (N30W), group mean map (N30M) and Z statistic map of the comparison of the two .

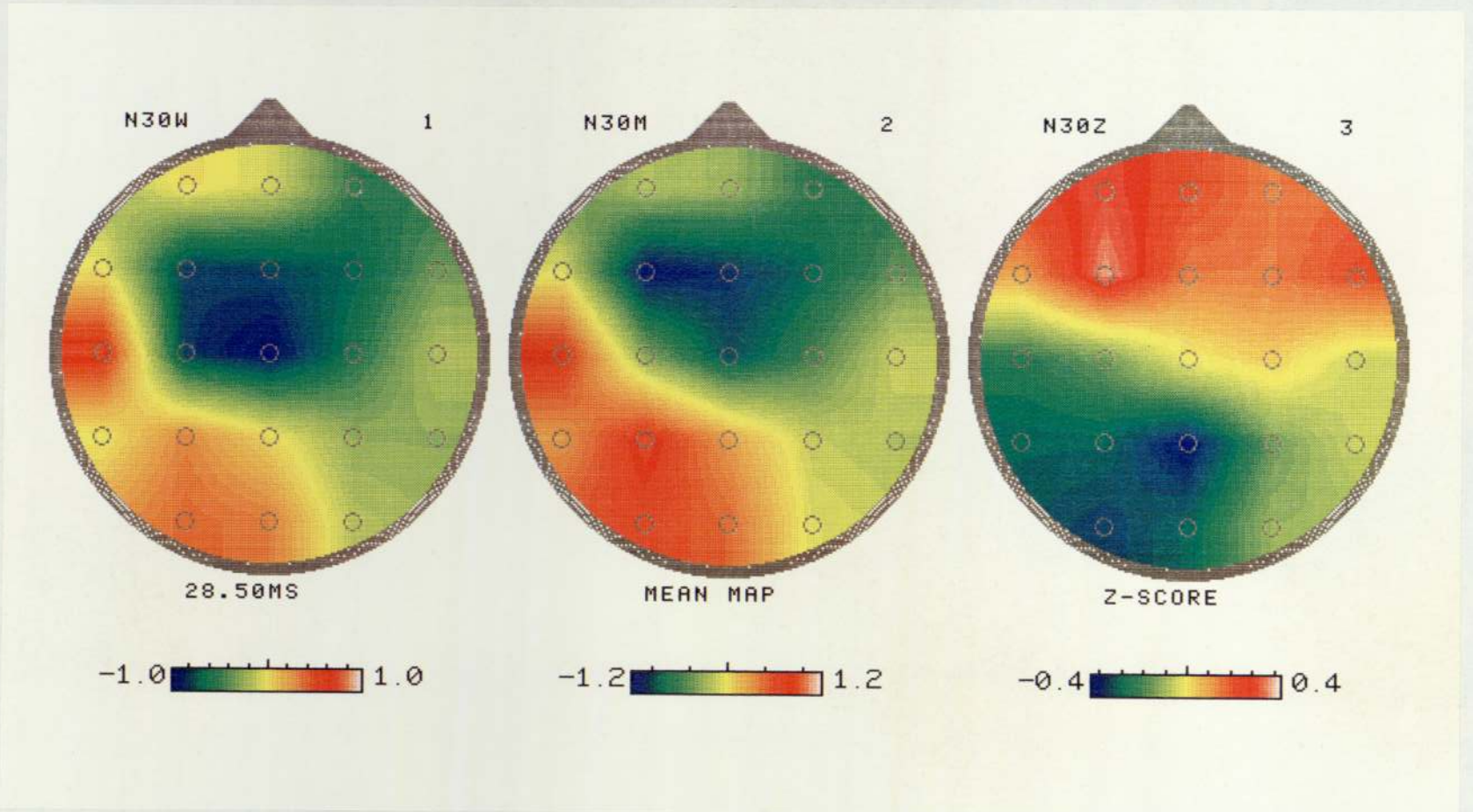
N30W
1
28.50MS
-1.0
1.0
N30M
2
MEAN MAP
-1.2
1.2
N30Z
3
Z-SCORE
-0.4
0.4

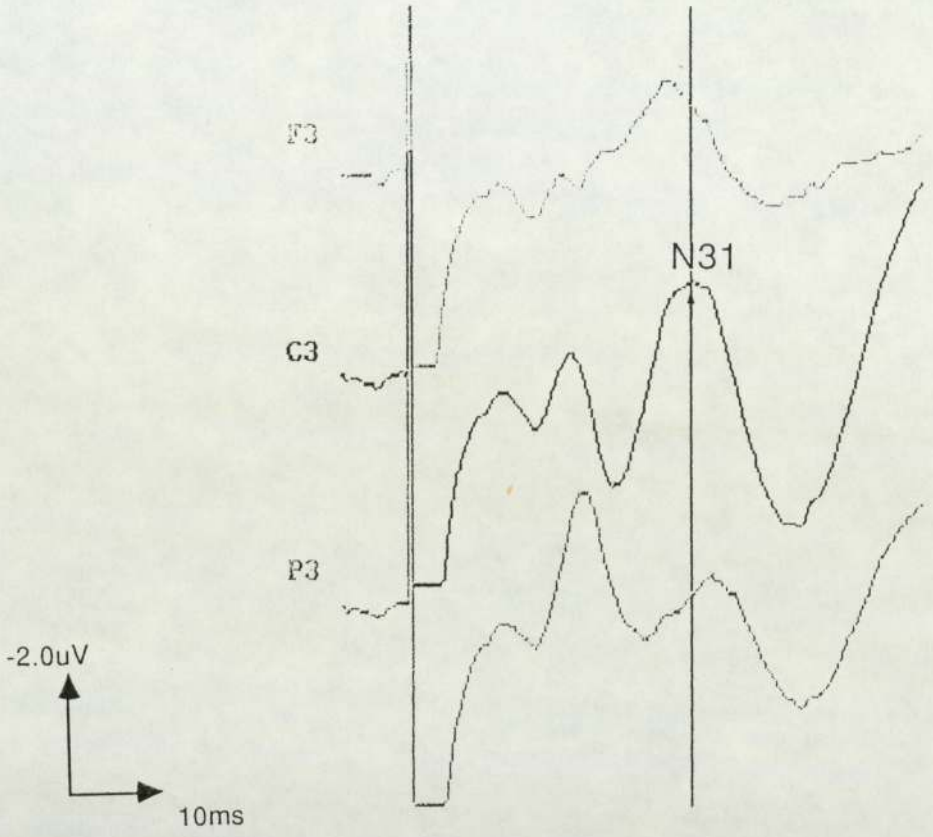

Figure 4.11 (Above). Group mean waveforms from right limb data. Cursor point indicates latency at which the N31 group mean waveform map was constructed (see overleaf).

Figure 4.11.1 (Overleaf)

Topographic maps (from left to right) indicate N31 component group mean waveform map (N31W), group mean map (N31M) and Z statistic map of the comparison of the two .

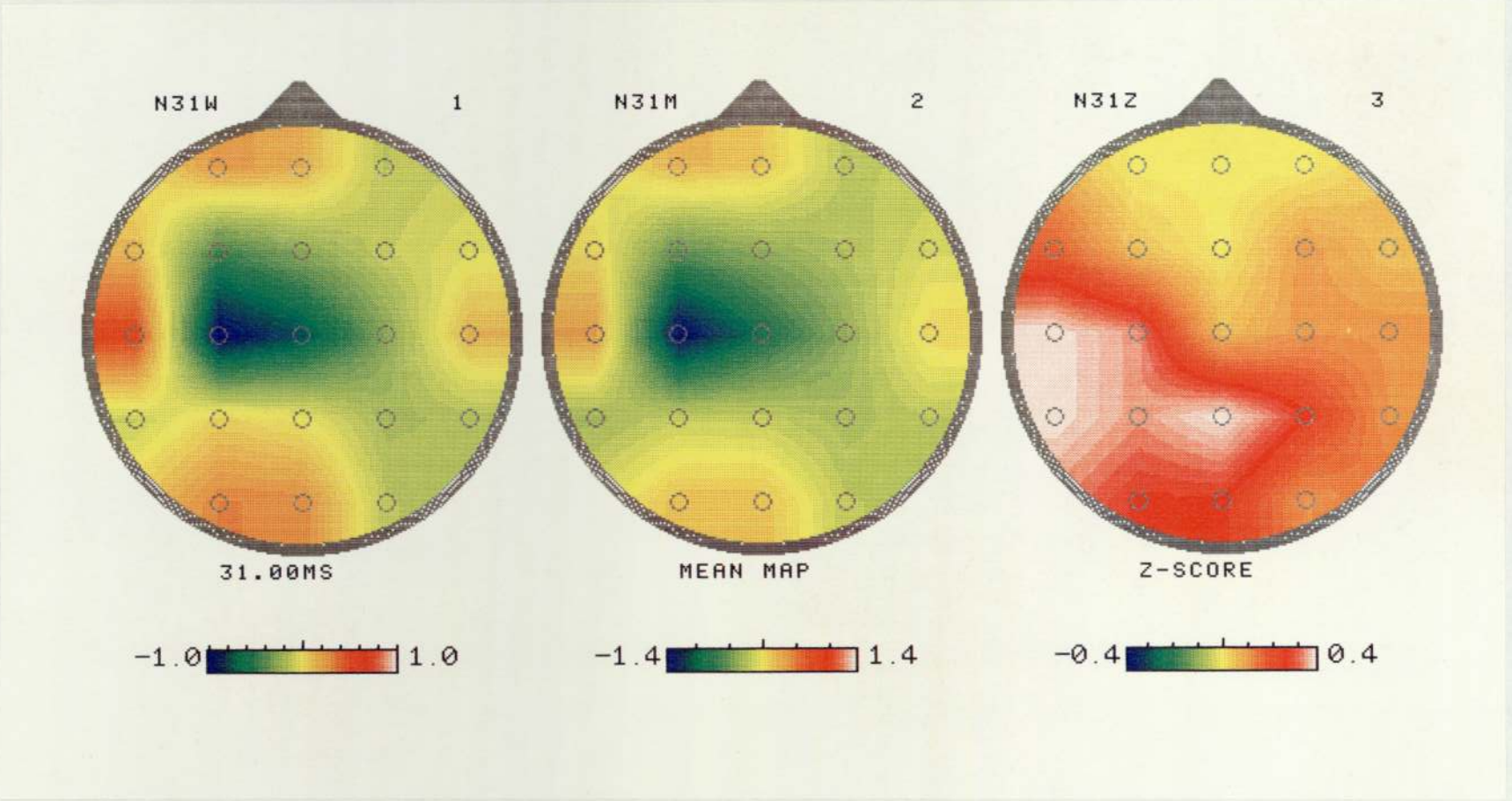
N31W
1
31.00MS
-1.0
1.0
N31M
2
MEAN MAP
-1.4
1.4
N31Z
3
Z-SCORE
-0.4
0.4

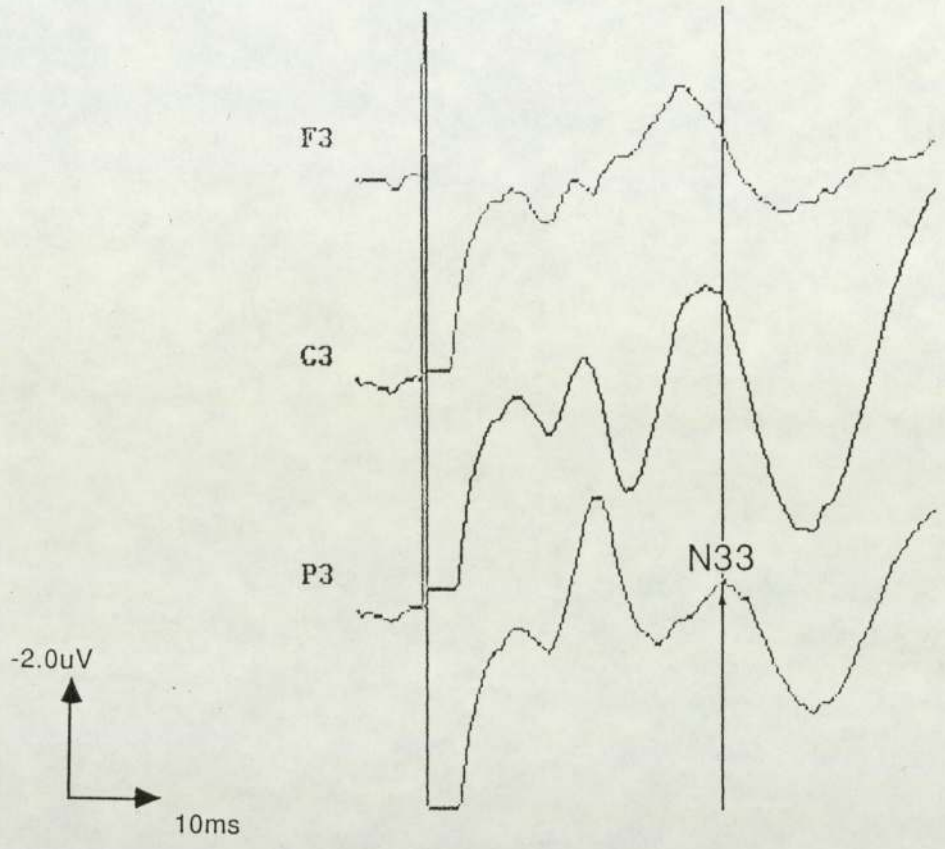

Figure 4.12 (Above). Group mean waveforms from right limb data. Cursor point indicates latency at which the N33 group mean waveform map was constructed (see overleaf).

Figure 4.12.1 (Overleaf)

Topographic maps (from left to right) indicate N33 component group mean waveform map (N33W), group mean map (N33M) and Z statistic map of the comparison of the two .

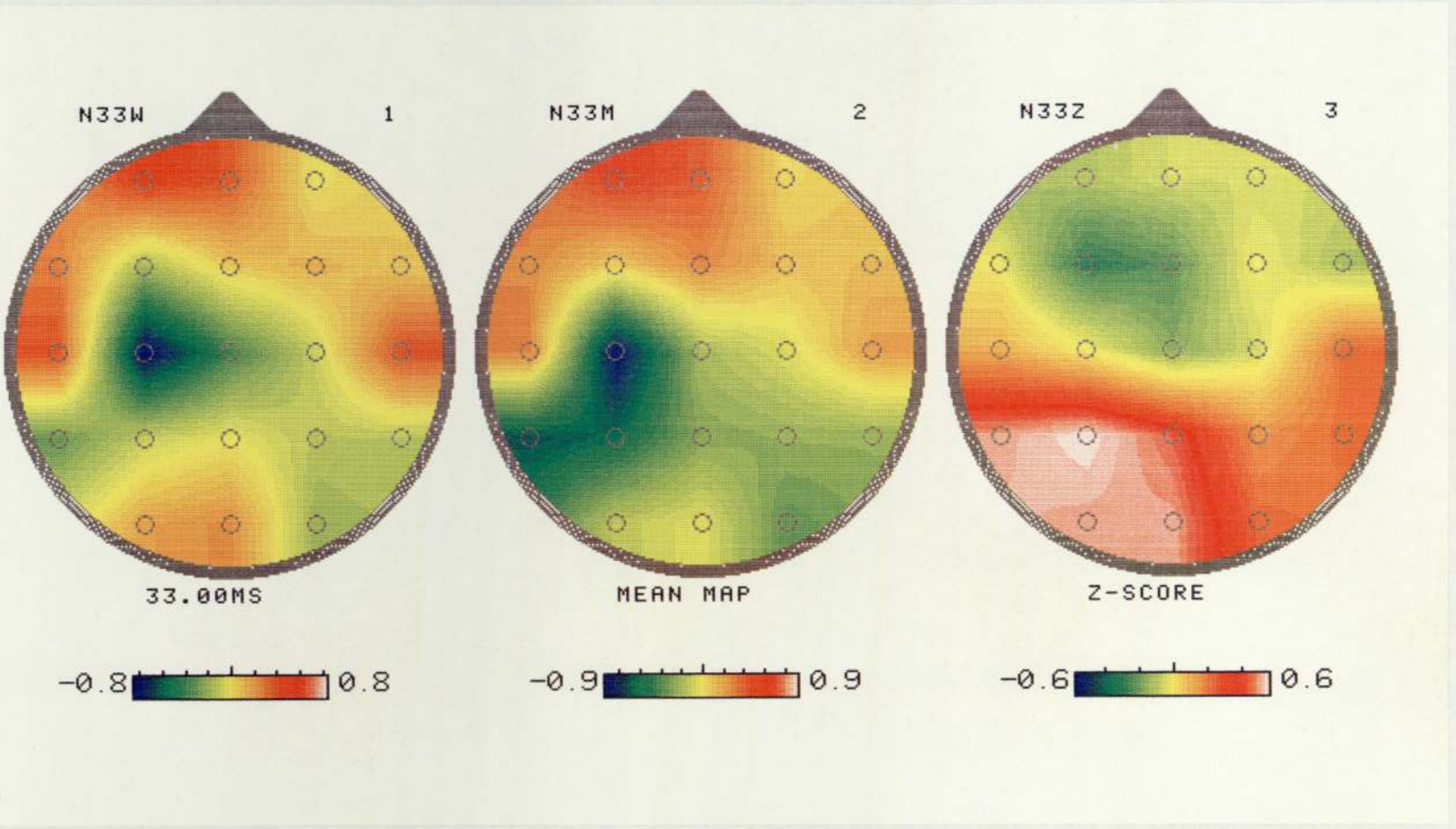
N33W
1
33.00MS
-0.8
0.8
N33M
2
MEAN MAP
-0.9
0.9
N33Z
3
Z-SCORE
-0.6
0.6

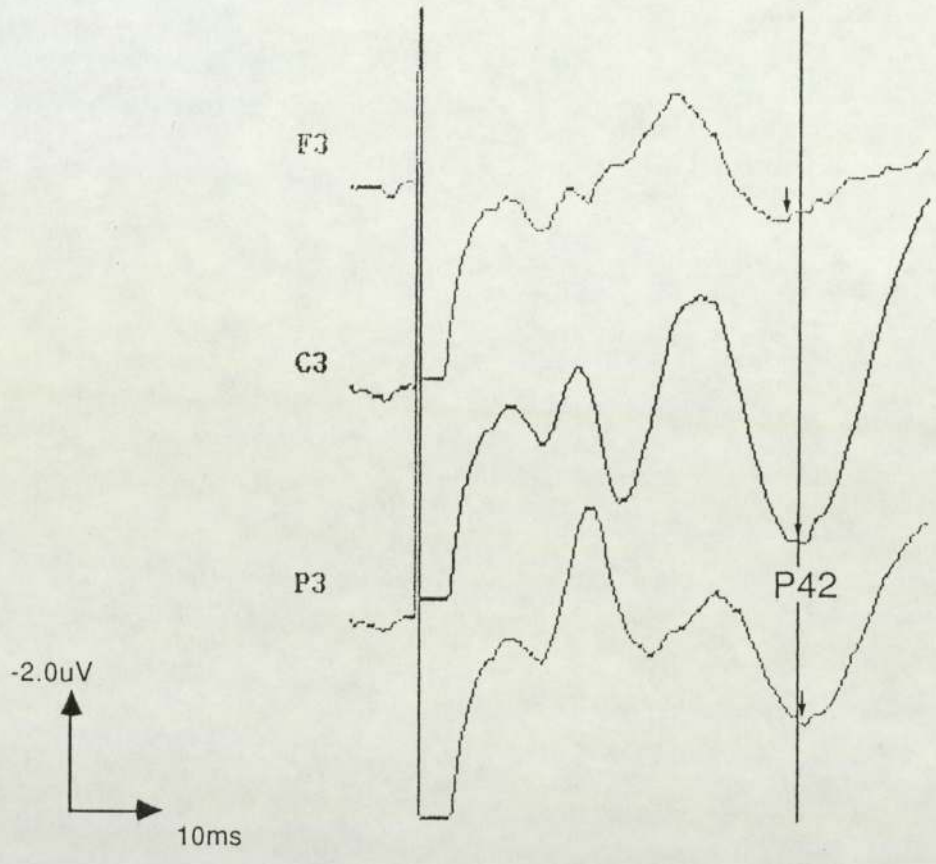

Figure 4.13 (Above). Group mean waveforms from right limb data. Cursor point indicates latency at which the P42 group mean waveform map was constructed (see overleaf).

Figure 4.13.1 (Overleaf)

Topographic maps (from left to right) indicate P42 component group mean waveform map (P42W), group mean map (P42M) and Z statistic map of the comparison of the two .

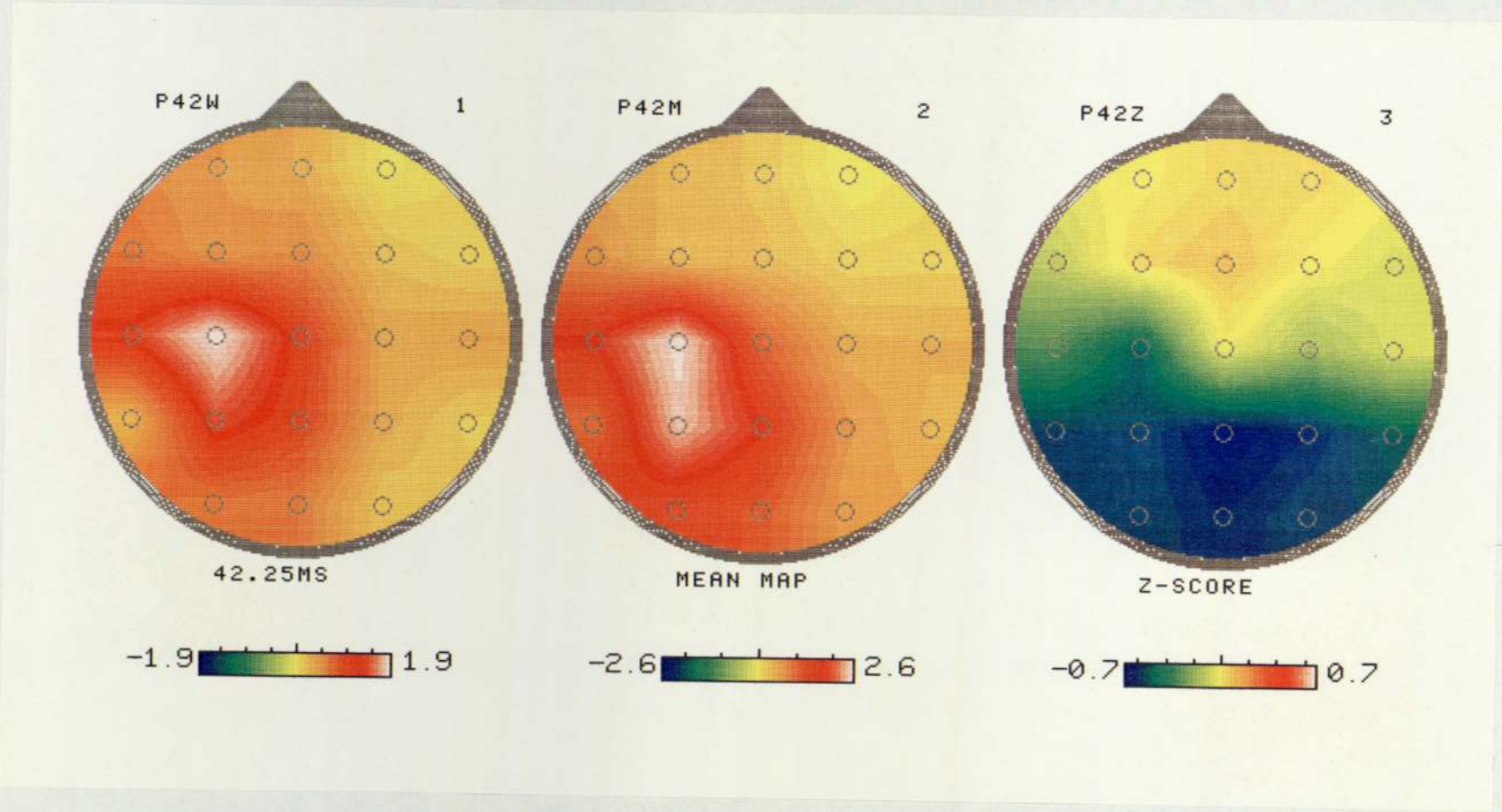
P42W
1
42.25MS
-1.9
1.9
P42M
2
MEAN MAP
-2.6
2.6
P42Z
3
Z-SCORE
-0.7
0.7

In order that a more quantitative assessment of topographic variations between group mean wave/maps and group mean maps could be made, the two map types were compared for each component using the Z statistic. Each pair of maps and their subsequent Z scores , also plotted topographically, are displayed in Figures 4.6.1 to 4.13.1. It can be seen from subjective comparison of the maps shown in these Figures, and confirmed by Z score analysis, that there was no significant difference in topographic distribution of components between the two types of map generation ($Z < 1$ standard deviation at every electrode site and for each component).

As would be predicted, amplitudes in the group mean maps were greater than those at comparable electrode sites of group mean waveform maps, since the decremental effect of latency scatter was absent in the group mean map generation.

With the exception of Erb's point and P14 components, data will now be examined in terms of scalp location i.e. Frontal, Central and Parietal component data. Topographical data will also be presented in each of these relevant sections

4.3.1.1 Erb's point and P14 components

4.3.1.2 Erb's and P14 Group Mean Data

The P14 component was observed as a short duration positive transient in 30 of the control subjects (86%) and occurring bilaterally in 26 (74.3%). In those subjects where P14 was present, it was observed in each of the 20 electrode sites. Inspection of the group mean waveforms (Figures 4.3-4.5) clearly reveals its consistent form.

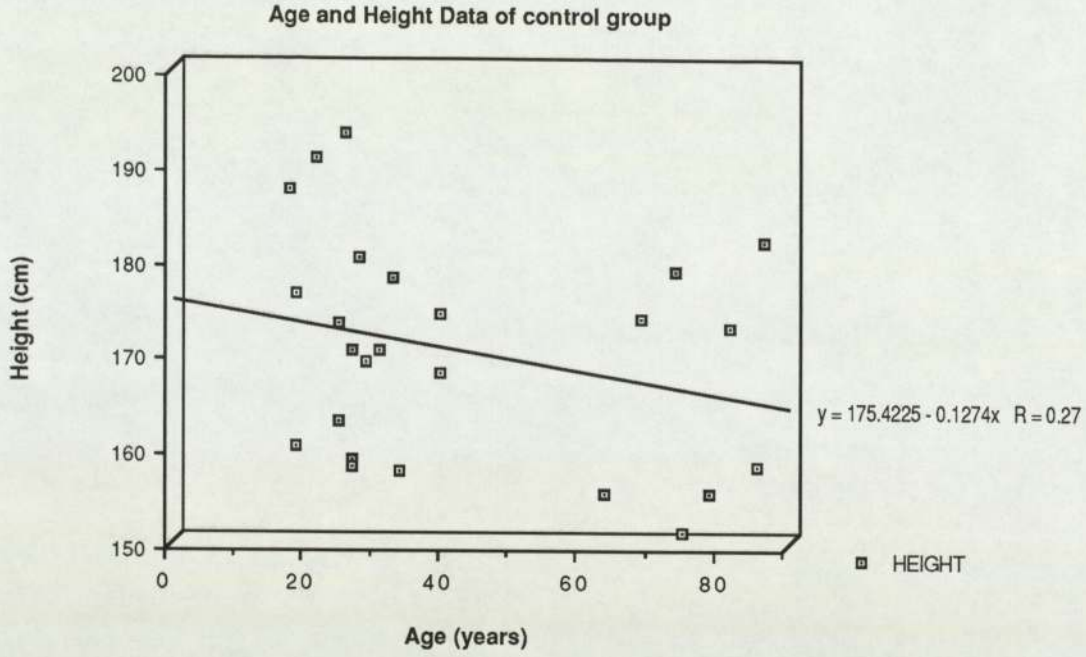

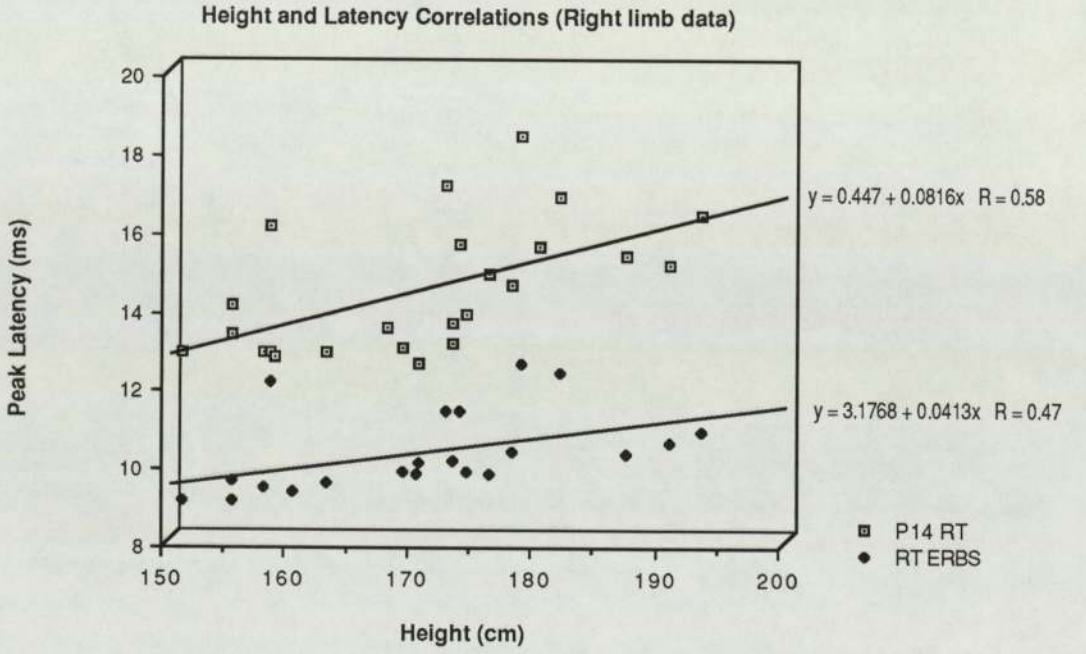

Figure 4.14. Age and height and height and latency correlations for Erbs and P14 potentials.
Significance of correlation coefficient where Ho: r=0;
Age v Height; not significant ($p>0.05$).
Height v Erbs; significant ($p<0.05$).
Height v P14; significant ($p<0.01$).

Student t-test analysis revealed a significant latency and amplitude difference between right and left limb data if analysed in pairs ($p<0.01$). Unpaired analysis revealed a significant amplitude difference ($p< 0.05$) between limbs. It should be noted that for right v left limb data, there were no significant differences in Erb's potential latency ($p >0.05$) or indeed in Erb's to P14 interpeak latency ($p >0.05$).

All group mean data is shown in Appendix 1, Tables A1 - A6.1.

4.3.1.3 Correlation of Erb's and P14 latency and amplitude with age and height.

An initial important observation from linear regression analysis of height and age of the control subjects was that these two variables were not significantly correlated with each other (Figure 4.14; Ho: $r=0;p>0.05$).

Student t-testing between a young age grouping (17-30 years; N=17) and old age grouping (60-86 years; N=13) revealed a significant increase in latency and decrease in amplitude of P14 in the old age group ($p<0.05$)

Linear regression analysis and student t-test revealed significantly high correlations of Erb's and P14 component latency with both age and height independently (where Ho: $r=0$; $p<0.02$).See Figures 4.14 and 4.15. Multiple regression analysis involving both age and height predictably yielded a significantly greater correlation (where Ho: $r=0$; $p<0.001$) and therefore multiple regressions were subsequently used for prediction of upper limits of normality for latency (see Table 4.3, section 4.3.5).

Erb's to P14 interpeak latency data was not significantly correlated with either age (see Figure 4.15) or height independently ($p>0.05$) but multiple regression analysis revealed a significant correlation with age and height in combination ($p<0.01$).

It is also important to note that there was a significant increase in the right versus left limb/hemisphere latency difference of P14 in the old age group ($p<0.01$).

Age related group mean data is shown in Appendix 1Tables A2 - A6.1.

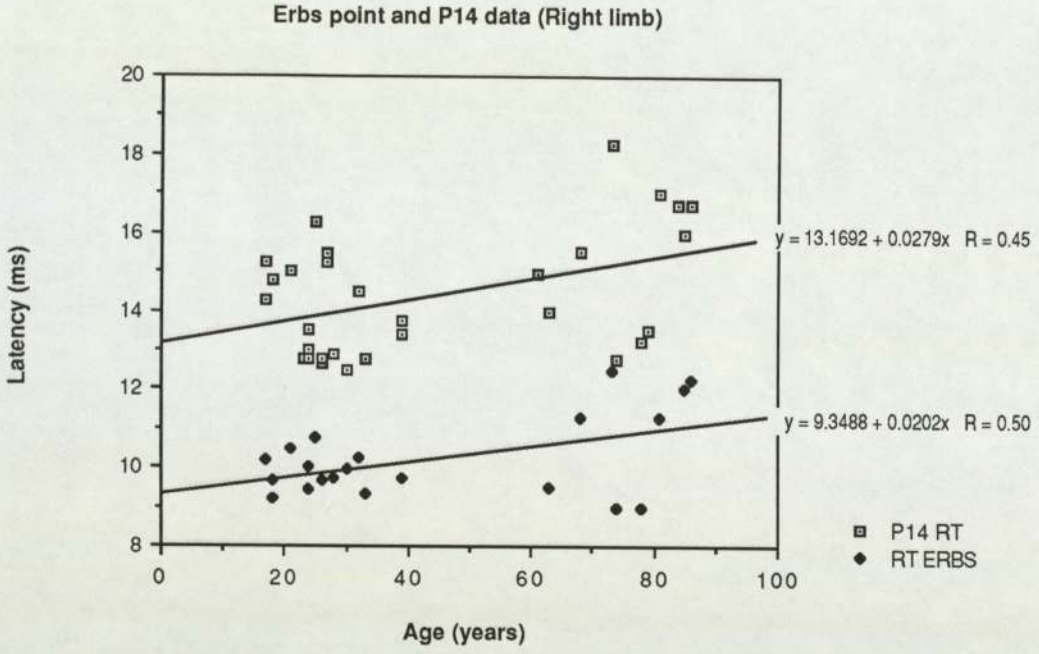

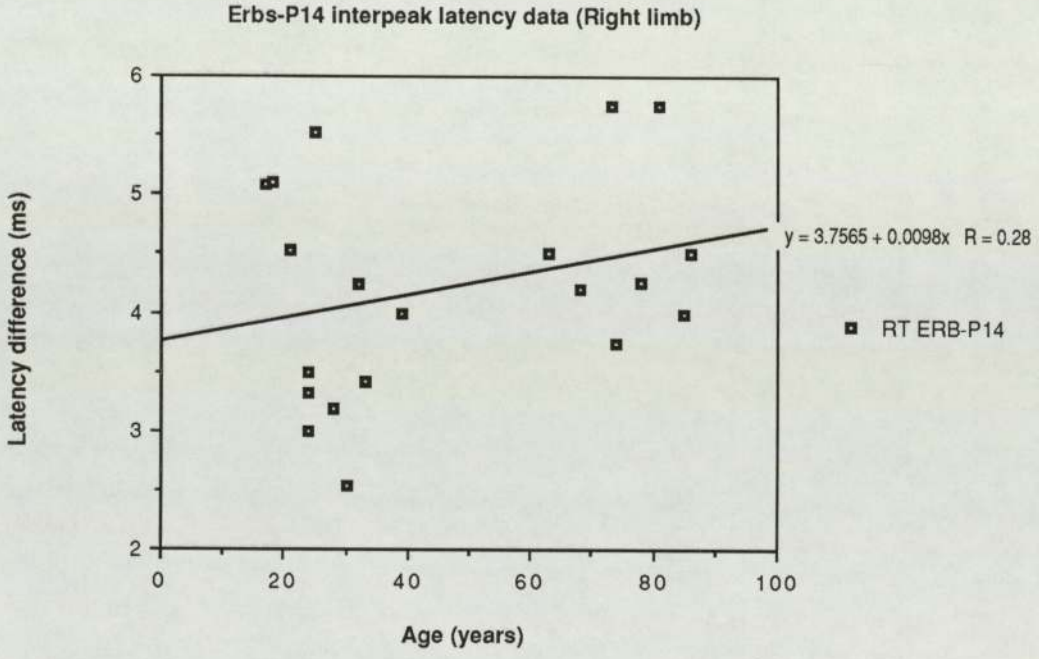

Figure 4.15 Age correlations for Erbs point and P14 latencies
Erbs and P14 were significantly correlated with age ($p<0.02$)
Erbs-P14 interpeak latency was not significantly correlated ($p>0.05$)
Ho: $r=0$.

4.3.1.4 Topography of the P14 component

Examination of topographic maps confirmed the analysis of baseline to peak amplitudes indicating that although P14 was a widespread component, evident at all 20 scalp locations, it invariably showed a greater amplitude at anterior scalp locations (see Figure 4.6.1 and Appendix 1 Tables A1 - A6). The mean amplitude at the F3 electrode (1.6uV) being significantly different to the mean amplitude at the P3 electrode (0.76uV) ($p<0.01$).

Since there was no significant peak latency difference ($p<0.01$) between frontal, central or parietal P14 components, no further mention of the P14 data will be made under these separate headings.

4.3.2.0 Frontal Components

4.3.2.1 Frontal Group Mean Data

Six components were consistently recorded at the F3 and F4 electrode positions to right and left limb stimulation. From the mean latency data, these components were given the following labels -P14, N17, P20, N23, N30 and P42. From inspection of each individuals waveforms, it became clear that in some individuals two further temporally distinct components had to be recognised - P35 (N=12) and N43 (N=9).

Actual mean peak data is shown in Appendix 1 Tables A1 and A1.1 with a latency and amplitude schematic shown in Figure 4.16.

There was no significant difference ($p>0.05$) between right and left limb data for peak latencies, or peak to peak amplitudes of any components, with the exception of P14 discussed in the previous section. N17-P42 interpeak latency was significantly different to unpaired analysis ($p<0.01$) but not to paired analysis ($p>0.01$)

The least frequently occurring component was N43; present in 26% of subjects and occurring bilaterally in only 9%.

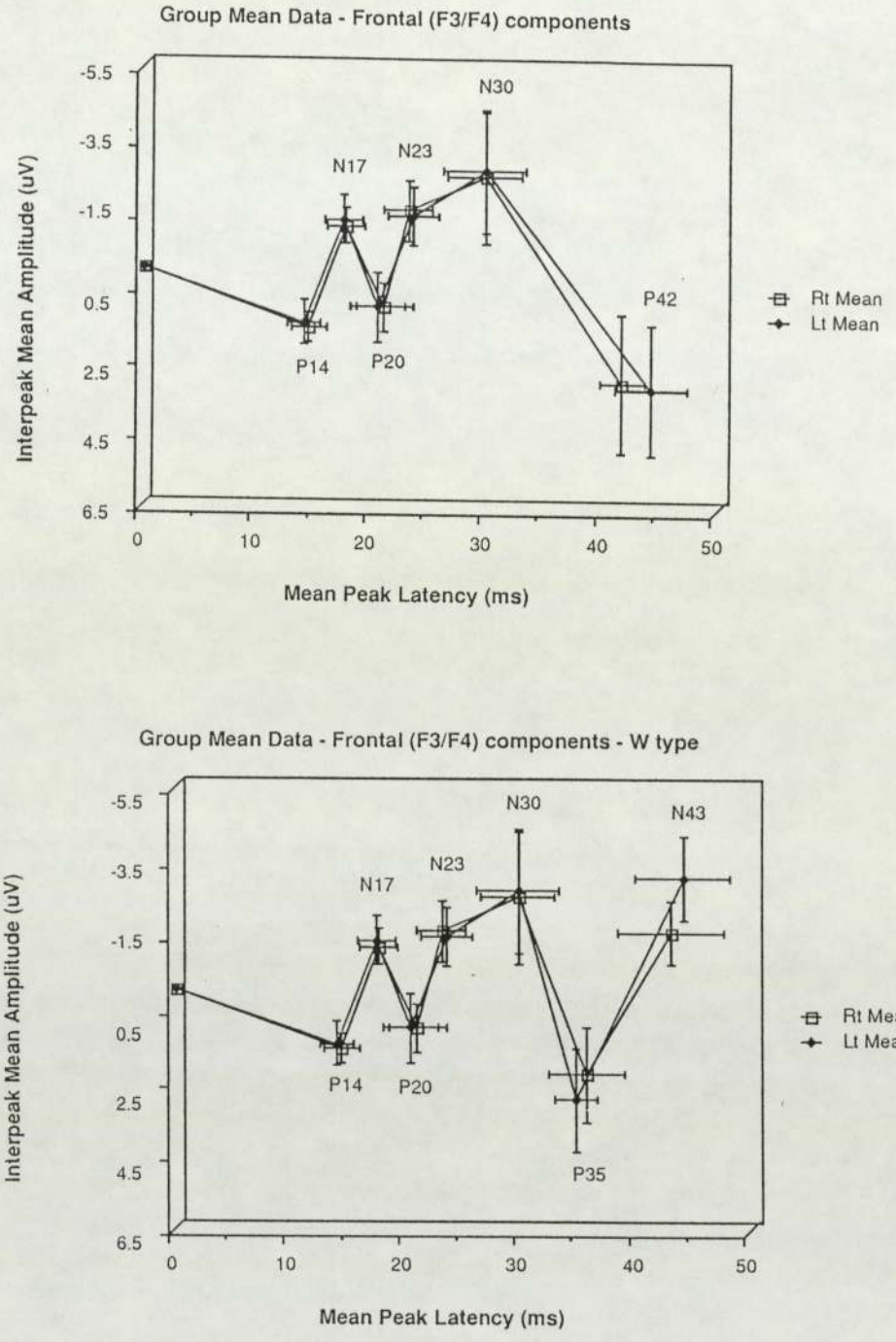

Figure 4.16. Amplitude and latency schematic constructed from the group mean data of components recorded from F3/F4 electrode sites. Error bars indicate 1 standard deviation.

4.3.2.2 Frontal component morphology

Three main morphological variations were observed for components up to and including the N30 component. These appeared to be caused by the presence and/or amplitude variations of the N23 component. In subjects in whom it did not occur this was known as frontal variation 1 or F type I. A typical example is shown in Figure 4.17. This was the most commonly occurring form

(seen in 47% of recordings); this may in part be due to the fact that N23 was most often seen as a deflection on the negative going limb of a more dominant N30 component and it is possible that in many subjects this latter component obscured it. In subjects where N23 was observed in this second form as a small clearly defined negativity on the rising edge of N30 (Figure 4.17), this was labelled as F type II and was present in 26% of recordings.

The final and least frequently occurring variation (9% of recordings) was F type III. In these subjects, N23 appeared to be the dominant component following the P20 deflection i.e. of greater amplitude than the following broad N30 component (Figure 4.17).

Following the N30 component, two further morphological variations were seen to occur. Firstly, a broad single positivity, the P42 component, was seen in 34% of recordings. This was referred to as a V type configuration. Secondly, a positive-negative complex was seen in 24% of recordings formed by the P35 and N43 components and referred to as a W type configuration.

It should be noted that in 18% of recordings, no clear frontal morphology typing could be established for components up to the N30 potential, either because of low amplitude poorly formed potentials and/or because of artefactual contamination. This figure rose to 41% for the post N30 components (P35, N43 and P42).

A full breakdown of morphology typing is shown in Table 4.4.

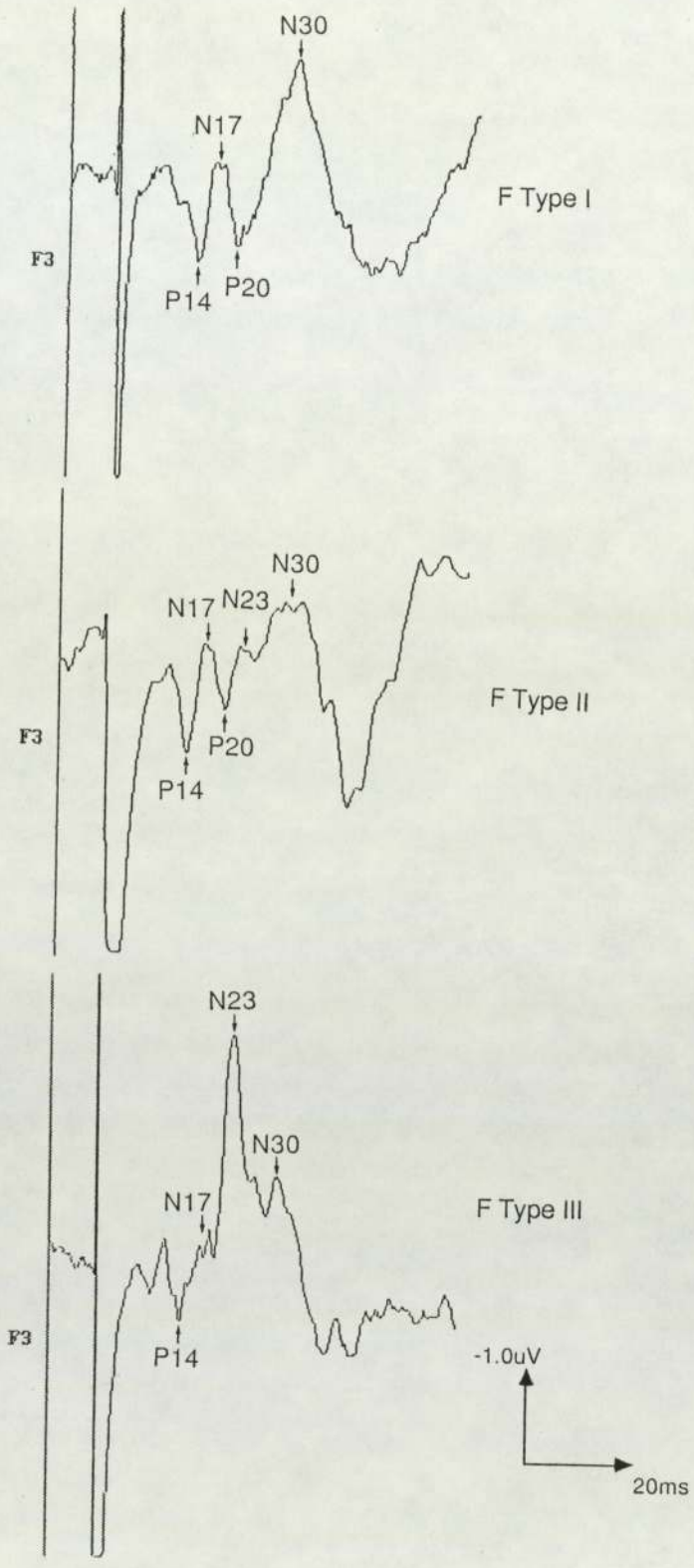

Figure 4.17. Frontal component morphology variations.

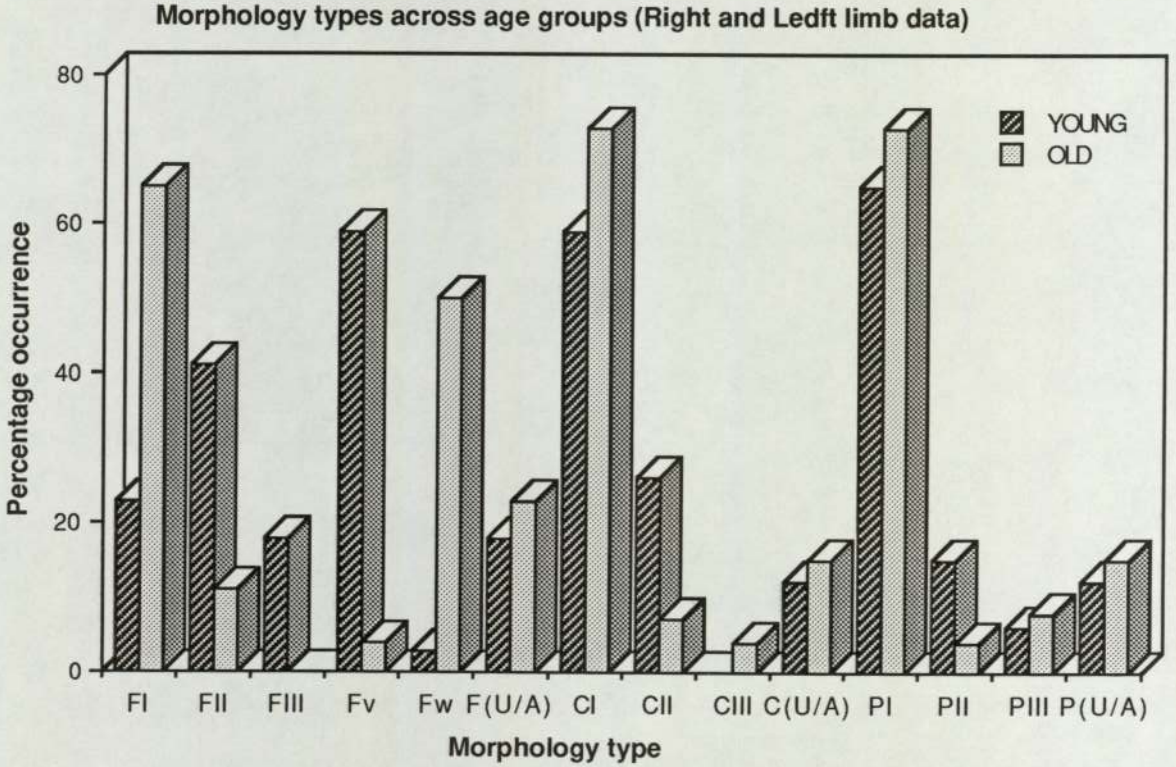

Figure 4.18. Age related morphology types.
Young age group = 17-30 years (N=17); Old age group = 60-86 years (N=13)
F=Frontal C=Central P=Parietal U/A=unclear or artefactual

4.3.2.3 Correlation of frontal morphology with age

The distribution of morphology types between a young age grouping (17-30 years; N=17) and an old age grouping (60-86 years; N=13) are shown graphically in Figure 4.18.

It was clear that F type I was the most commonly occurring variation in the old age group (65% of recordings) whereas F type II was the most commonly occurring variation in the young (14%). F type I occurred in only 23% of young age group recordings while F type III (which is the extreme version of F type II) was only seen in the young age group, occurring in 18% of their recordings.

Comparison of frontal V and W type variations caused by the P42 or P35/N43 complexes revealed a striking age related correlation; with the exception of one young individual, the W configuration was seen exclusively in the old or middle age group. Equally, with the exception of one old age individual, the V configuration was seen exclusively in the young or middle age groups; thus -

TABLE 4.2 % OCCURRENCE OF V AND W MORPHOLOGY TYPES WITH AGE

GROUP	V TYPE	W TYPE	UNCLEAR
Young (N=17)	59	03	38
Middle (N=5)	20	30	50
Old (N=13)	04	50	46

4.3.2.4 Correlation of frontal component latency and amplitude with age and height.

Peak latencies of P14, N17, P20 and N23 were significantly longer in the old age group (60-86 years) compared to the young (17-30 years). In the case of N23 however, only 2 observations of this component were made compared to 11 in the young.

Linear regression analysis revealed that N17 was more significantly correlated with height than age whilst with P20 the reverse was true (see Figure 4.19). For both components, multiple

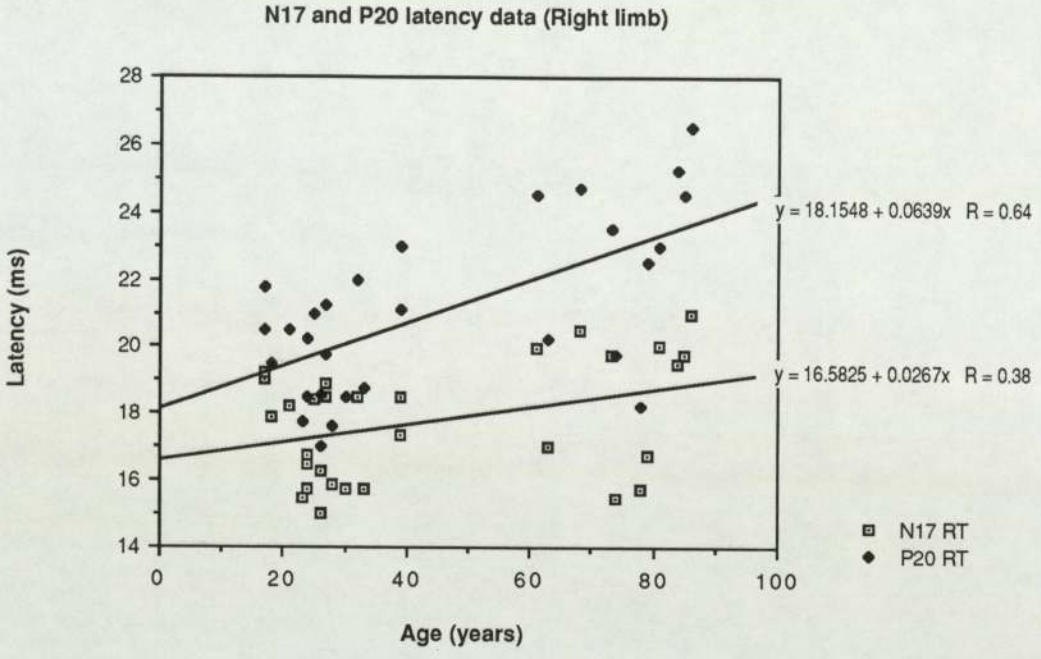

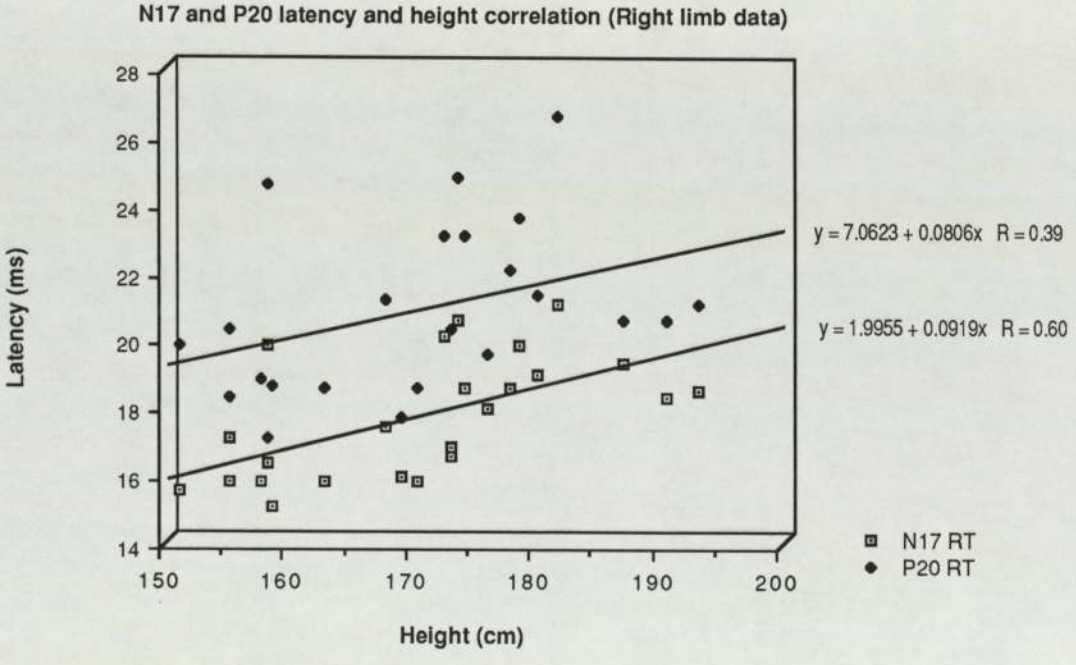

Figure 4.19 Age v Latency correlations for frontal components N17 and P20.
Significance of correlations; Ho: r=0;
N17 v Age; significantly correlated ($p<0.05$).
P20 v Age; significantly correlated ($p<0.001$).
N17 v Height; significantly correlated ($p<0.01$).
P20 v Height; not significantly correlated ($p>0.05$).

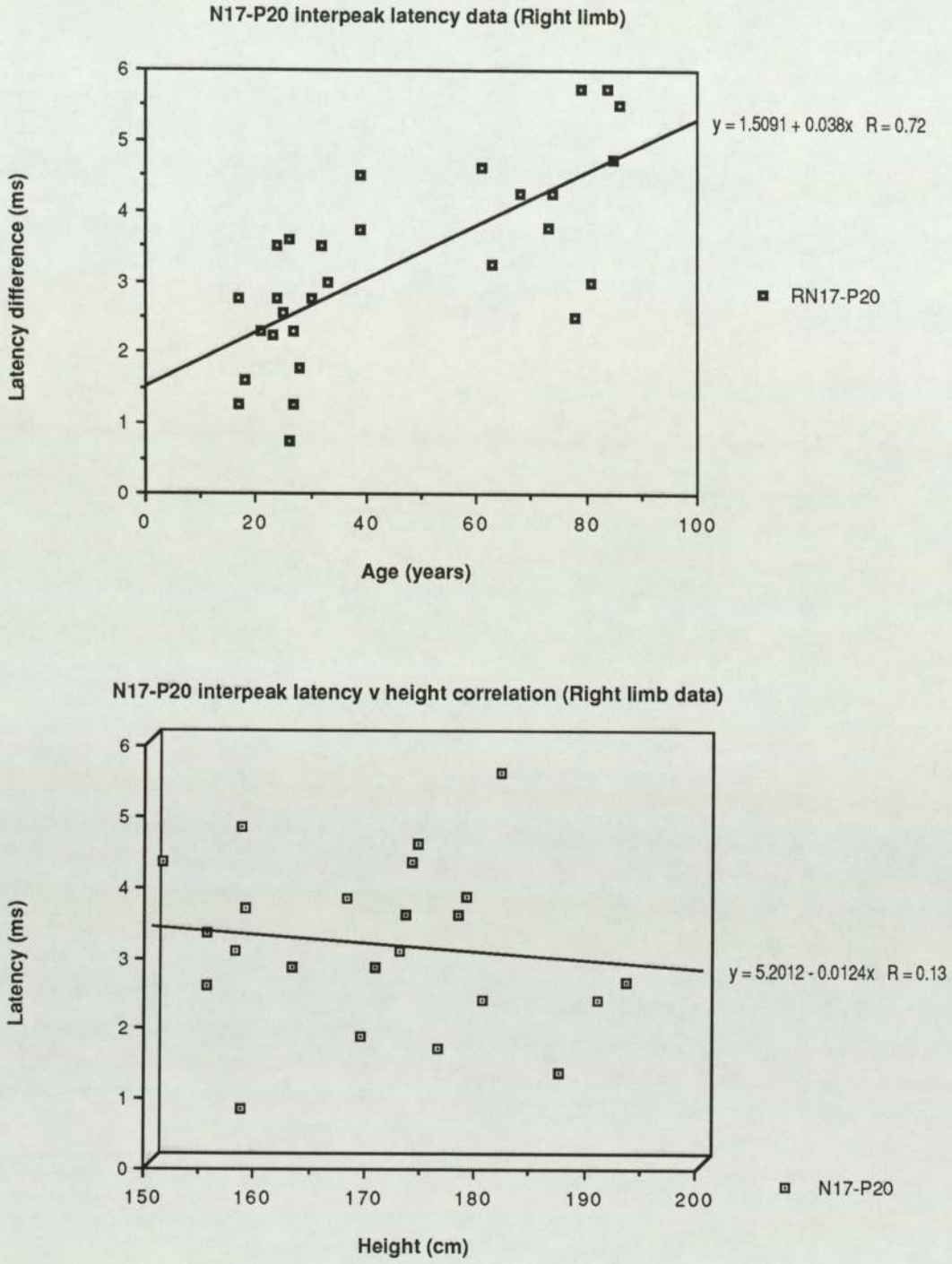

Figure 4.20. Frontal components N17 to P20 interpeak latency difference data.
Simple Linear regressions indicate regression coefficient (R).
Significance of regressions; Ho: r=0;
N17-P20 interpeak latency v Age; significant ($p<0.001$).
N17-P20 interpeak latency v Height ; not significant ($p>0.05$).

regression prediction of latency were highly correlated with age and height combined (Ho:r=0; p<0.001).

N30 was not significantly correlated with either age or height or the combination (p>0.05).

P35 and N42 were clearly 'old age' related components while P42 could be classified a young age group related potential.

N17 to P20 interpeak latency was highly correlated with age (r=0.72; p<0.001) but not significantly correlated with height (r=0.13; p>0.05) as shown in Figure 4.20.

No peak to peak amplitudes were significantly different between age groups.

Detailed age related data is shown in Appendix 1 Tables A2 and A2.2 as well as Figure 4.32.

4.3.2.5 Topography of frontal components

Clear mean topographic distributions of N17 and N23 frontal potentials could not be derived from the group mean waveforms or maps because of the greater amplitude of other components at other scalp locations of similar or overlapping latency. The onset of the N17 component arose concurrently with central N19 and parietal N20 components immediately following the P14 peak. In each individual, the amplitude of N20 was always greater than that of N17.

In the case of N23, as indicated earlier, this was most commonly seen on the ascending limb of the larger and broad N30 component. However, in the cases of four young group control individuals in whom an F type III morphology occurred i.e. a dominant N23 compared to N30, some analysis could be made. This was achieved by forming a mean N23 map (from right limb data) from F type III individuals (N=3); this is shown in Figure 4.21. A clear opposing negative-positive field pattern was observed with the negative field lying frontally and bilaterally with a maxima at the F3 and Fz electrodes and the positive field lying centro-parietally with distinct contralateral lateralisation to the stimulus. This positive field was centred over the P3 electrode.

The P20 component also formed a similar opposing polarity field pattern in group mean maps (Figure 4.7.1) with the Fz location providing the positive P20 maxima frontally to both right and

left limb stimulation. It is worth noting however that with right limb stimulation, the P20 amplitude was greater at the F3 than the F4 electrode while with left limb stimulation the reverse was true.

The concomitant positive field, caused by the parietal N20 component was distinctly contralateral to the stimulus and was maximal at P3 and P4 electrodes respective to stimulation; this will be described in more detail under parietal component data, section 4.3.4.

Maps of the broad bilateral frontally distributed N30 component (Figure 4.10.1) showed a similar relationship to that of P20 ; the F3 electrode providing the largest amplitude N30 to right limb stimulation and the F4 electrode to left limb stimulation. It would appear therefore that for both P20 and N30 components, despite a generally bilateral distribution frontally, that some contralateral emphasis was preserved.

Two morphological variations were observed following the N30 component in individuals. Firstly, (and most commonly seen in the young age grouping) a broad P42 concomitant with central and parietal P42 components was seen. Secondly, (and most commonly seen in the old age grouping) a clear phase inversion formed by the temporal relationship of parietal N33 with frontal P35 and parietal P42 with frontal N43 was observed.

To examine this apparent age related difference topographically, the control waveforms for right limb stimulation were divided into the young age grouping (17-30 years) and old age grouping (60-86 years). The waveforms of each group were then averaged separately. Three wave/maps were then generated; from the young group a P42 map and from the old group a P35/N33 and N43/P42 map. Waveforms and maps are shown in Figures 4.22 and 4.22.1 respectively.

Frontal P42 in the young group rose concomitantly with the dominant central P42 and a smaller parietal P42. The map therefore presented a single locus of positivity centred over the C3 electrode and extending anteriorly.

Frontal N43 of the old age group rose concomitantly with central and parietal P42 components; the resultant map presented a clear dipolar field pattern with the positive maxima

occurring at contralateral location P3 and the negative maxima at ipsilateral location F4, although the 85% amplitude isocontour for N43 extended bilaterally whilst the central and parietal P42 remained exclusively contralateral.

Frontal P35 rose concomitantly with the parietal N33 component in the old age grouping producing a similar phase inversion on either side of the central sulcus as the N43/P42 complex just described. However, maps of the P35/N33 complex were confused by the temporal overlap of the dominant central N31 component and so a less clear dipolar pattern emerged.

Figure 4.21 (Overleaf) Group mean waveform map (left) and group mean map (right) of dominant N23 component from three F type III individuals.

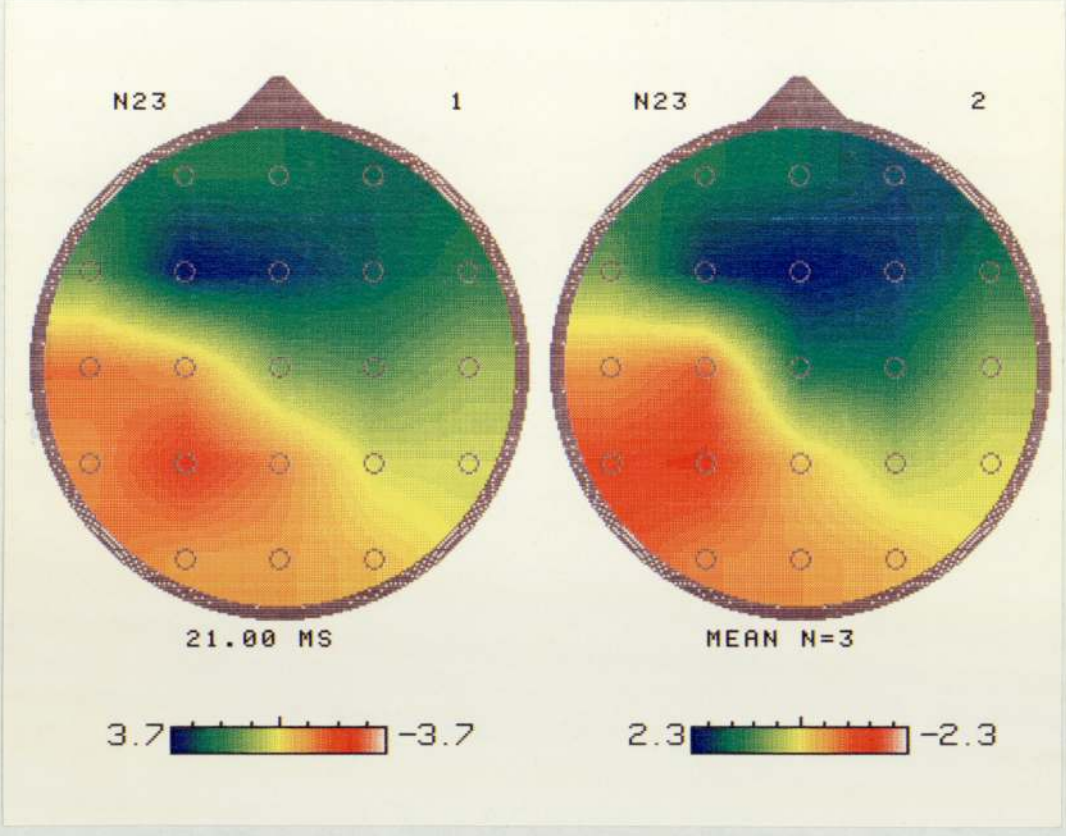
N23
1
21.00 MS
3.7
-3.7
N23
2
MEAN N=3
2.3
-2.3

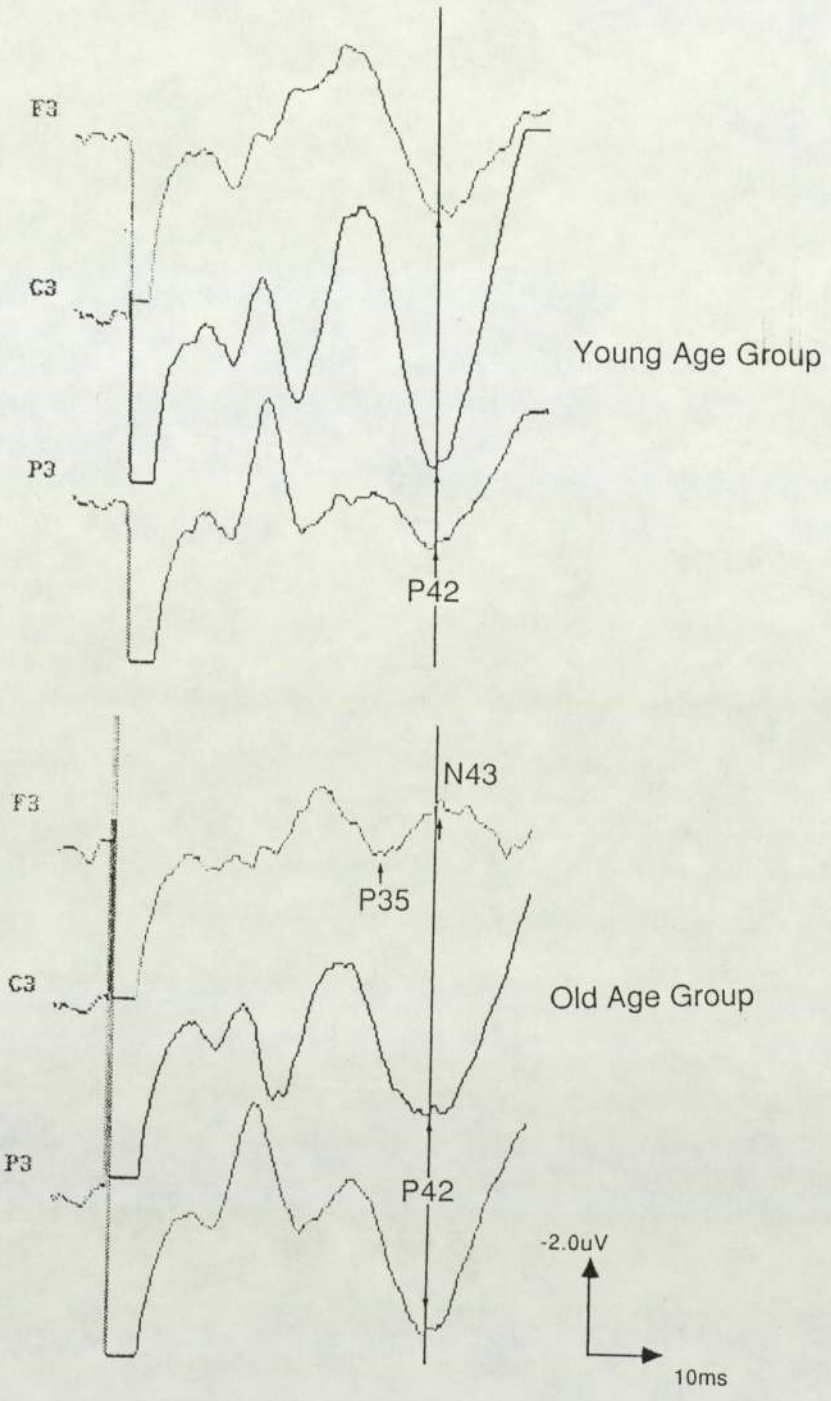

Figure 4.22 (Above) Group mean waveforms for young age group (top) and old age group (bottom). Cursors indicate latencies at which topographic maps (overleaf) were generated.

Figure 4.22.1 (Overleaf)

Group mean waveform maps for the 'young P42' (left), the 'old N43/P42 complex (right).

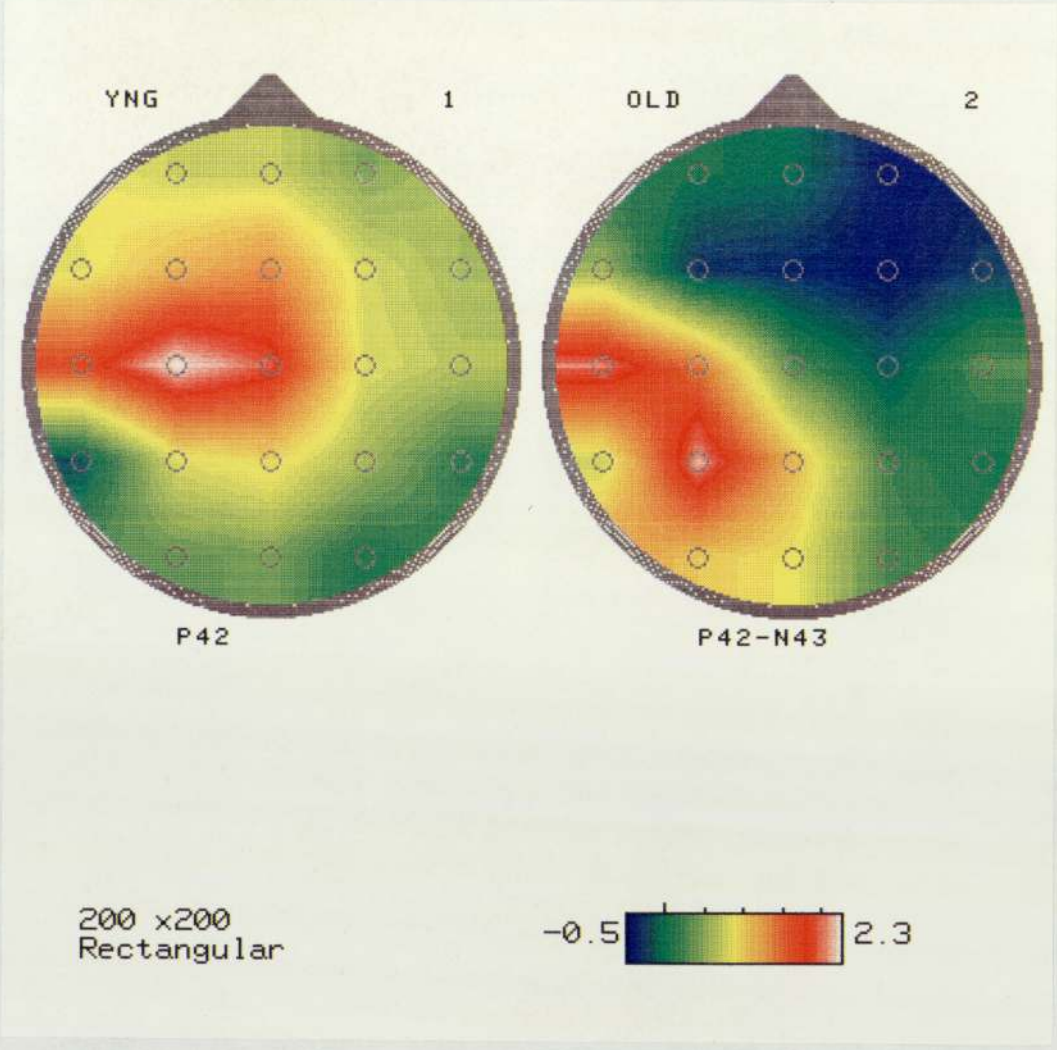
YNG
1
OLD
2
P42
P42-N43
200 x200
Rectangular
-0.5
2.3

4.3.3.0. Central Component Data

4.3.3.1 Central component group mean data

Seven components were consistently recorded at the C3 and C4 electrode positions; from mean latency data these were given the following labels - P14, N19, P22, N24, P26, N31 and P42.

Actual mean peak data is shown in Appendix 1 Tables A3 and A3.1 with latency and amplitude shown in two schematics (Figure 4.23) for clear representation.

There was no significant differences in peak latency or peak to peak amplitude of any component when comparing right and left limb stimulation ($p>0.05$), with the exception of P14 as outlined earlier.

Least frequently occurring components were N24 and P24, appearing in only 17% of recordings compared to 80% or more for all others. N24 and P26 were the only components not evident in the group mean waveforms (Figures 4.3-4.5)

Largest mean amplitude component was the N31-P42 peak.

4.3.3.2. Morphology of central components

Three morphological variations of central components were observed in the normal control group and were labelled C types I, II and III.

C type I presented a clear W shaped waveform formed by the N19, P22, N31 and P42 components - a typical example is shown in Figure 4.24. This was the commonest presentation of central components in the control group, comprising 69% of recordings.

C type II occurred in 19% of recordings and an example is also shown in Figure 4.24 . This variation was formed by the separation of the P22 peak into a positive-negative-positive complex formed by N24 and P26 components. The establishment of the true existence of these components and not as myogenic or otherwise artefactual components, was on the basis of trail/re-trial reproducability and the absence of significant EMG contamination in these or neighbouring channels.

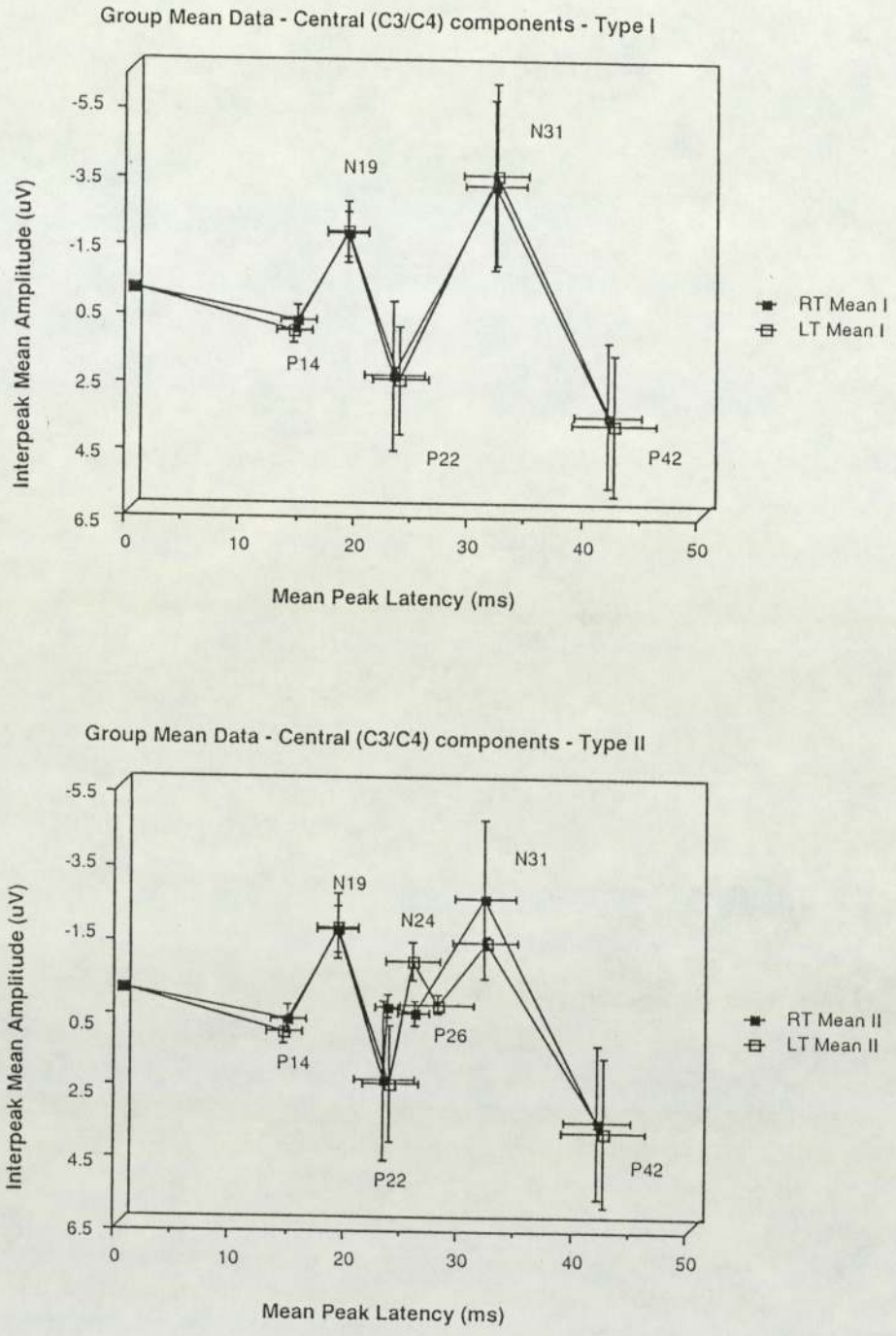

Figure 4.23. Latency and amplitude schematics constructed from group mean data of components recorded at C3/C4 electrode sites. Split into two graphs for clear presentation only. Error bars indicate 1 standard deviation.

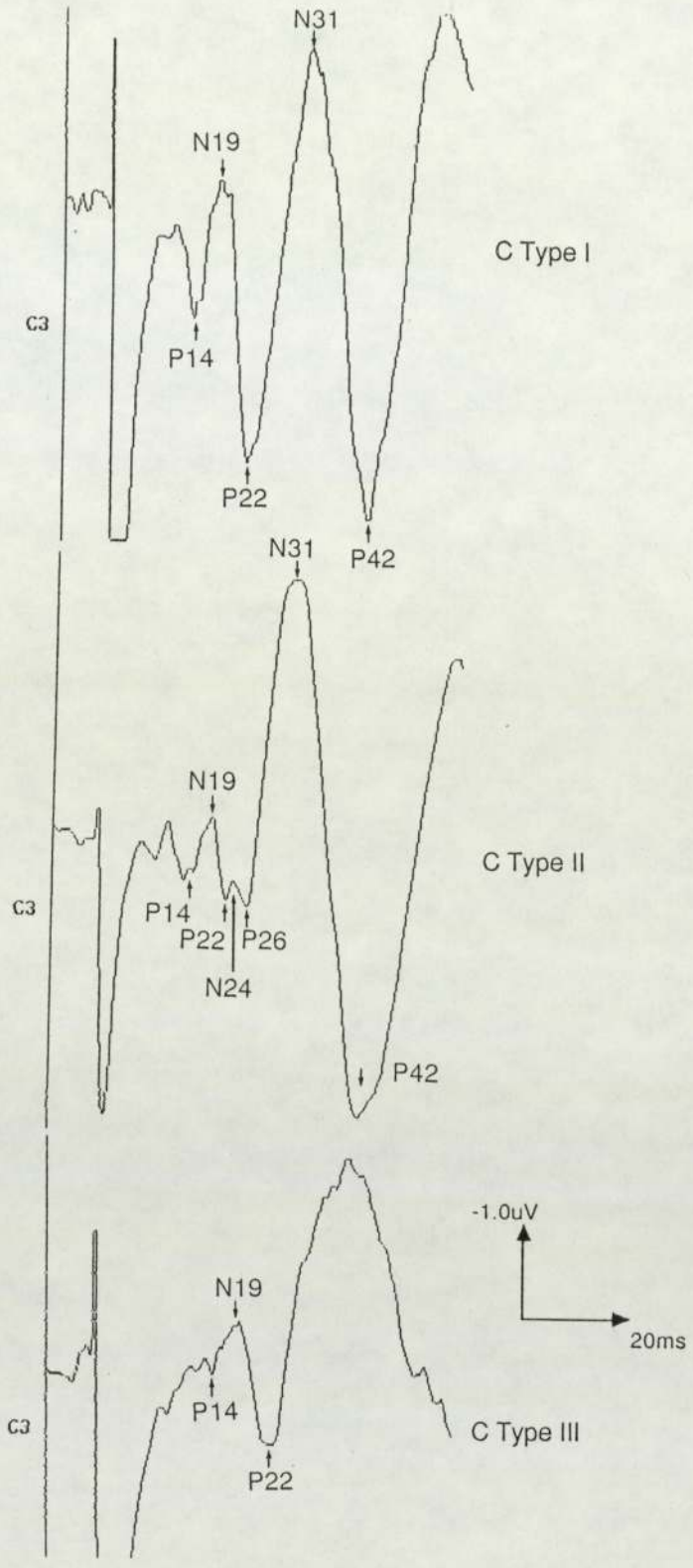

Figure 4.24. Morphological variations of central components.

C type III occurred only in subject N30 and is shown in Figure 4.24. As can be seen, this was formed by the usual N31-P42 complex apparently replaced by a broad negativity of peak latency 39.75ms. This morphology could be explained as a prolonged version of C type I, i.e. with P22 and N31 occurring at longer latencies than seen in the young and P42 therefore not occurring within the acquired epoch.

4.3.3.3. Correlation of central morphology with age

The occurrence of C type I was very similar between the young age group (17-30 years; N=17) at 59% and the old age group (60-86 years; N=13) at 73%. C type II occurred slightly more frequently in the young group (26%) than the old (7%) whilst C type III only occurred once and that in the old age group (4%).

Unclear or artefactual data occurred with similar frequency in both young (12%) and old (15%).

4.3.3.4. Correlation of central component latency and amplitude with age and height.

There was a significant latency increase of N19 and P22 components as well as the N19-P22 interpeak latency in the old age group ($p<0.01$) when compared to the young grouping. All amplitudes and other component latencies showed no significant changes to age or height ($p>0.05$). Related data is shown in Appendix 1 Tables A3 and A3.1.

Linear regression analysis revealed that N19 latency was significantly correlated to age ($p<0.01$) and height ($p<0.05$) (Figure 4.25) and highly correlated to the multiple regression of the combination ($r=0.87$; $p<0.001$).

P22 latency was highly correlated to age ($p<0.001$) but not height ($p>0.05$) (Figure 4.25) although highly correlated to the multiple regression line combining both ($r=0.90$; $p<0.001$).

N19-P22 interpeak latency was significantly correlated to age only ($r=0.68$; $p<0.001$) (Figure 4.26).

Detailed age related data is shown in Appendix 1Tables A4 and A4.1 .

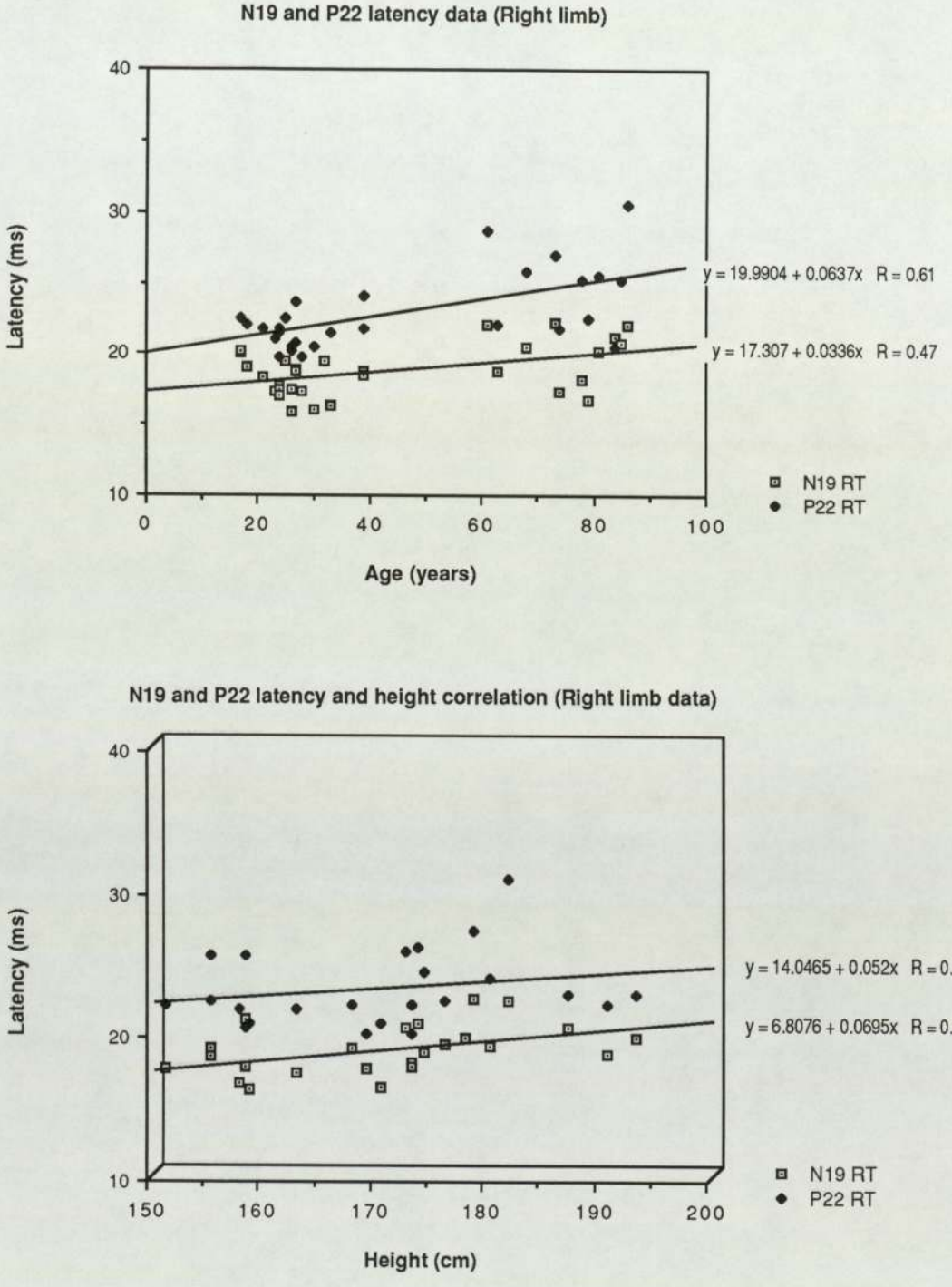

Figure 4.25 Age and height v Latency correlations for central components N19 and P22. Simple linear regressions with regression coefficients (R) are shown. Significance of correlations; Ho: R=0; N19 v Age; significant ($p<0.01$). P22 v Age ; significant ($p<0.001$). N19 v Height; significant ($p<0.05$). P22 v Height ; not significant ($p>0.05$).

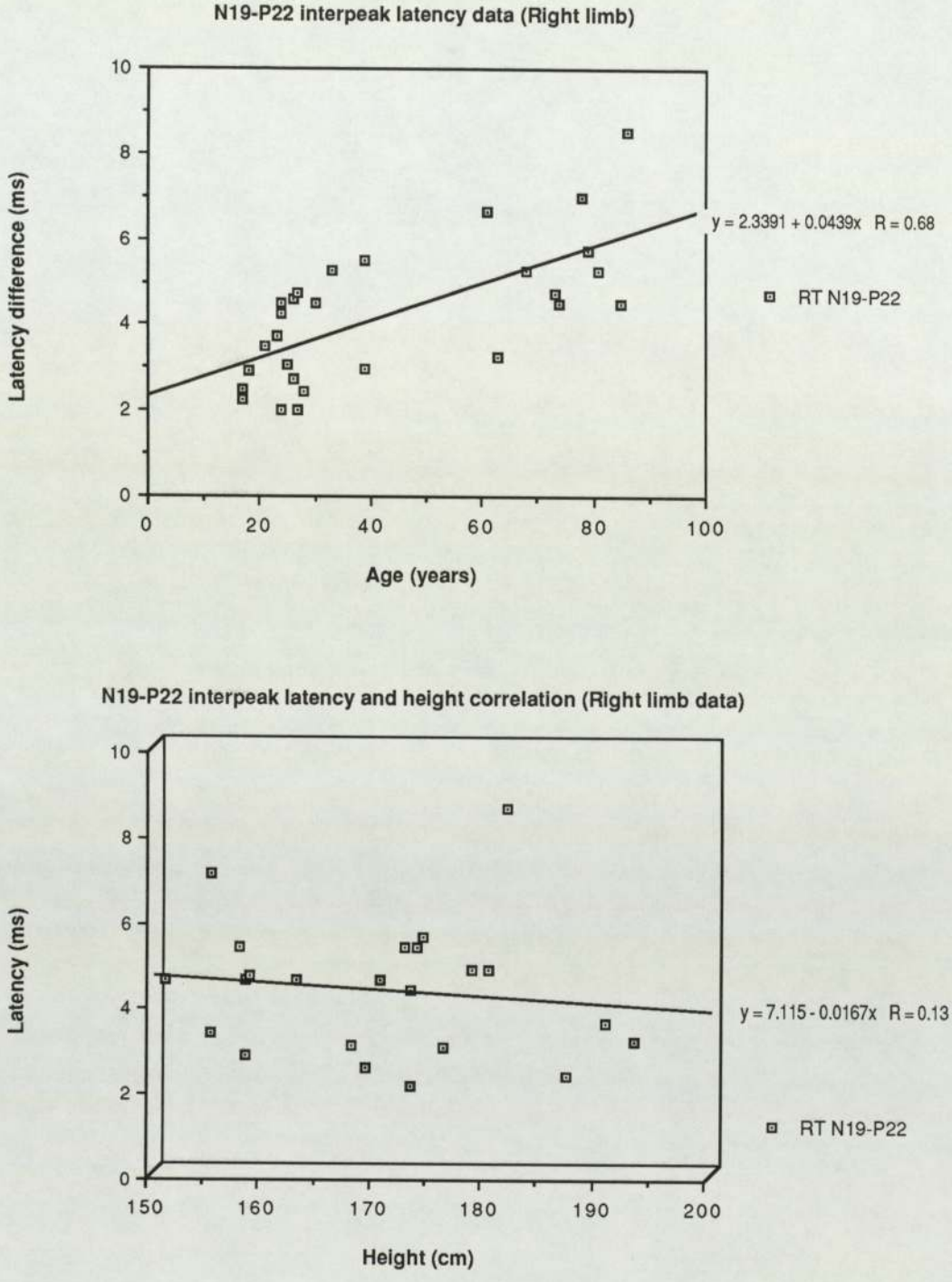

Figure 4.26. Central components N19 to P22 interpeak latency difference data.
Simple Linear regressions indicate regression coefficient (R).
Significance of correlations; Ho: R=0;
N19-P22 v Age; significant ($p<0.001$).
N19-P22 v Height; not significant ($p>0.05$).

4.3.3.5. Topography of central components.

Distinct topographic maps could not be derived for N19, N24 or P26 peaks because of their overlap with components of similar latency and greater amplitude.

Group mean waveform maps and group mean maps were plotted for P22, N31 and P42 components (Figures 4.8.1, 4.11.1 and 4.13.1). The distributions for each component were very similar; that of a single circumscribed locus of activity centred over the C3 electrode for right limb stimulation and C4 for left limb, with very little spread to other electrodes and no clear opposite polarity field patterns occurring elsewhere on the scalp. This was particularly true for the P22 and N31 components; for P42, this component was also seen spreading to the parietal electrode P3 (right limb) or P4 (left limb). In the group mean maps these electrodes fell within the 90% amplitude isocontour for this component.

4.3.4.0. Parietal Component Data

4.3.4.1. Parietal Group Mean Data.

Seven components were consistently recorded at the P3 and P4 electrode positions; from mean latency data their peaks were given the following labels - P14, N20, P22, N25, P27, N33 and P42. Actual mean peak data is shown in Appendix1 Tables A5 and A5.1 with latency and amplitude schematics shown in Figure 4.27.

There were no significant differences in peak latency or peak to peak amplitudes for any component when comparing right with left limb data ($p>0.05$), with the exception of P14 as previously outlined.

Least frequently occurring components were P22 and N25, seen in 17% of right limb recordings and 6% of left limb. All other components occurred in 71% or more of the total recordings.

Largest mean peak to peak amplitude component was that of N20-P27.

4.3.4.2. Morphology of parietal components.

Three morphological variations of parietal components were observed in the normal control group and were labelled P types I, II, or III.

P type I was the commonest presentation, comprising 70% of recordings. It appeared, like C type I, as a W shaped waveform formed by the N20, P27, N33 and P42 peaks. A typical example is illustrated in Figure 4.28.

P type II was formed by the apparent separation of the P27 peak into a positive-negative-positive complex caused by the P22, N25 and P27 components. An example is shown in Figure 4.28. 11% of recordings included these intermediate peaks.

P type III occurred in 6% of recordings and was formed by the N33-P42 complex apparently 'replaced' by a broad negativity following a normal P27 peak. An example is shown in Figure 4.28.

13% of parietal recordings were categorised as unclear and/or artefactual.

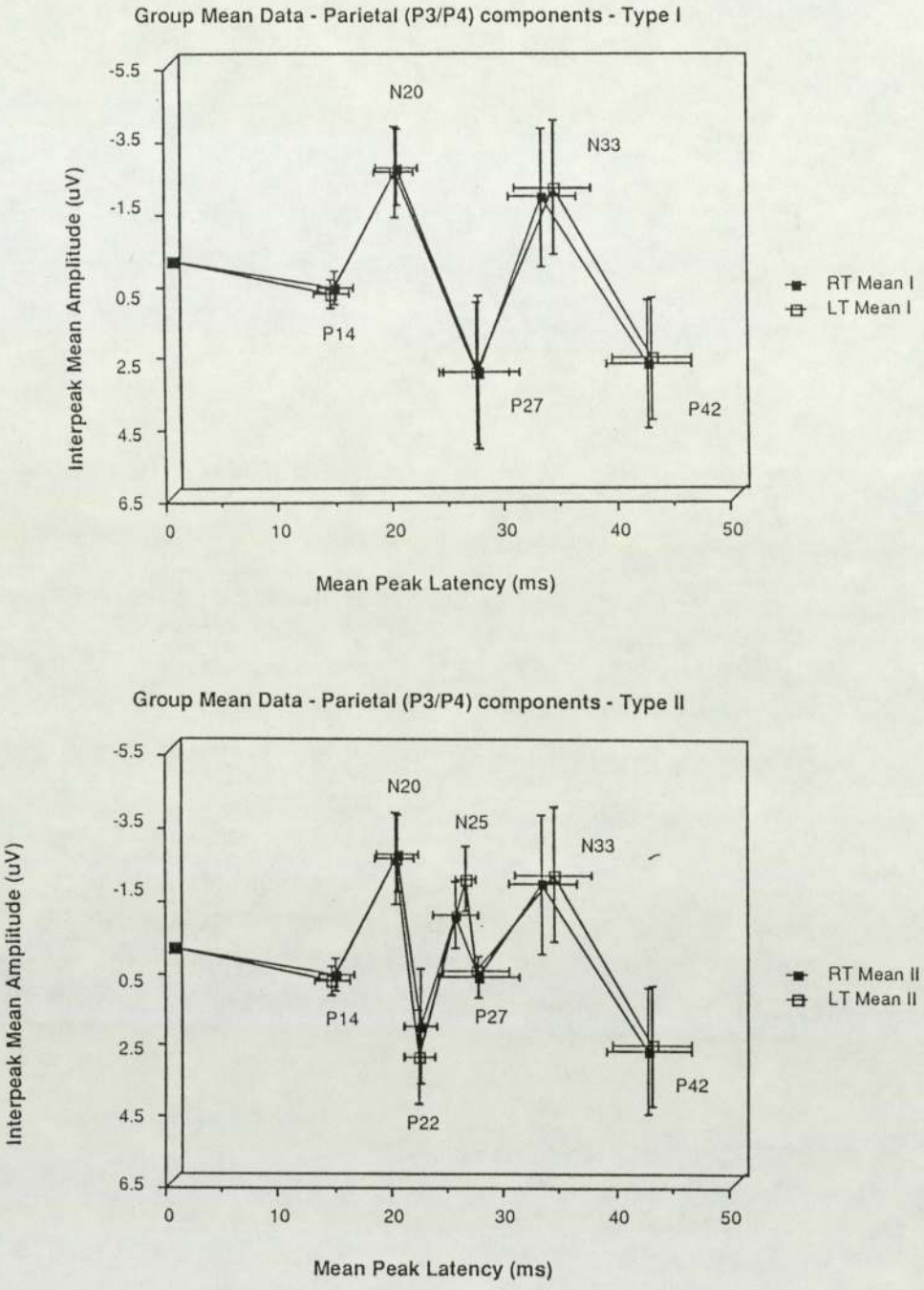

Figure 4.27. Latency and amplitude schematics constructed from group mean data of parietal P3/P4 electrode locations. Shown as two graphs for clear representation only. Error bars indicate 1 standard deviation.

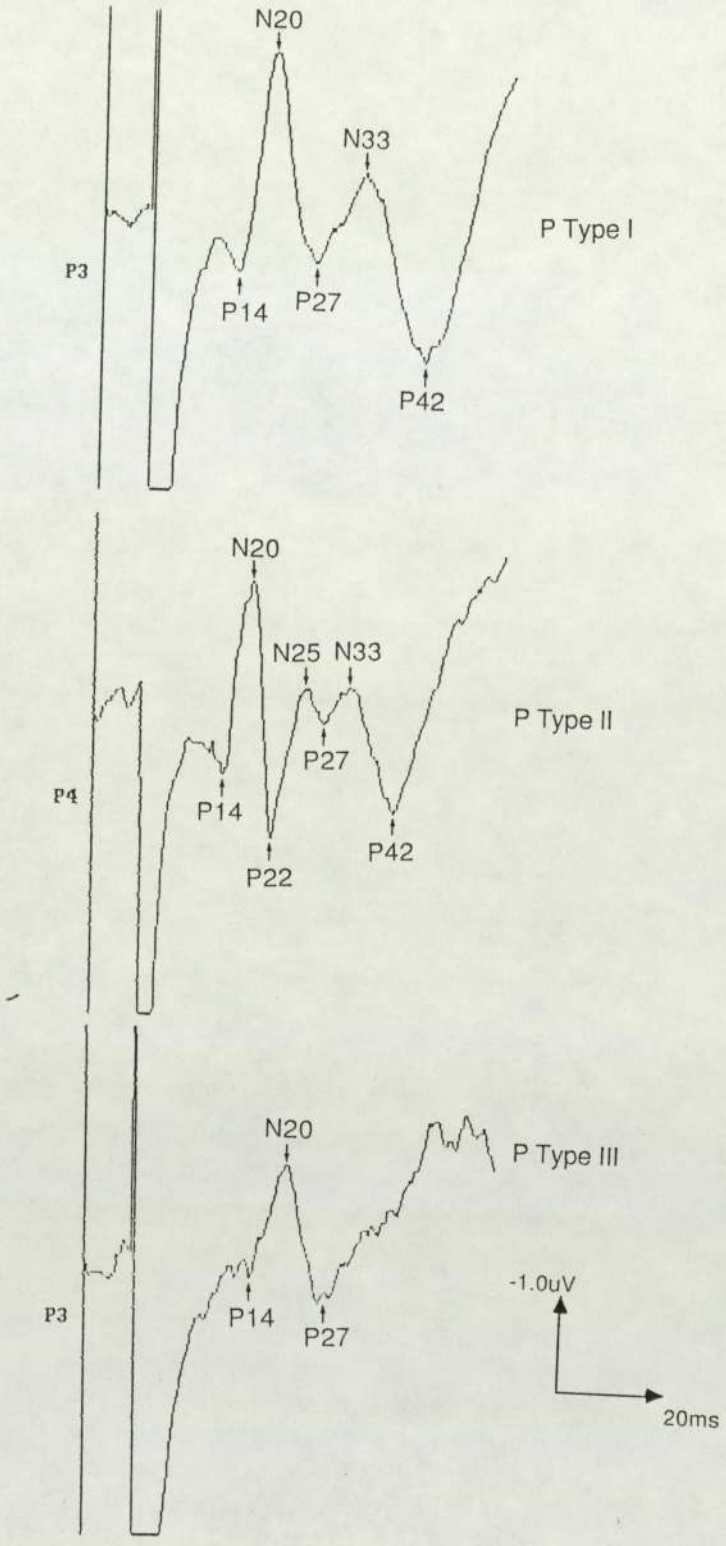

Figure 4.28 Morphological variations of parietal components.

4.3.4.3. Correlation of morphology of parietal components with age.

P type I was by far the most frequently occurring variation in both the young (65%) and the old (73%) age groups. P II was more commonly seen in the young age group (15%) than the old (4%) whilst the rarely occurring P III variation was seen in 6% of young recordings and a similar 8% of the old.

Unclear or artefactual data preventing precise morphology typing occurred with similar frequency in both young (12%) and old (15%) age groups.

4.3.4.4. Correlation of parietal component latency and amplitude with height and age.

Student t-test revealed a significant increase in peak latency of the P14 and N20 components in the old age group compared to the young ($p<0.01$) as well as a significant increase in the P14-N20 interpeak latency.

Linear regression analysis revealed that the N20 peak latency was significantly correlated to age ($r=0.61$; $p<0.001$) and to a lesser extent to height ($r=0.43$; $p<0.05$) (see Figure 4.29), and was therefore predictably highly correlated to a multiple regression line combining both variables ($r=0.87$;$p<0.001$).

P14-N20 interpeak latency was significantly correlated to a linear regression with age ($p<0.01$) but not height ($p>0.05$) - see Figure 4.30. Multiple regression analysis did not yield a correlation of greater significance.

A significant peak to peak amplitude increase of the N33-P42 component was observed in the old age group compared to the young ($p<0.01$), and a significant correlation with linear regression (Figure 4.31) was also found ($r=0.52$; Ho: $r=0$; $p<0.01$).

Detailed age related data is shown in Figure 4.32 as well as Appendix 1 Tables A6 and A6.1 .

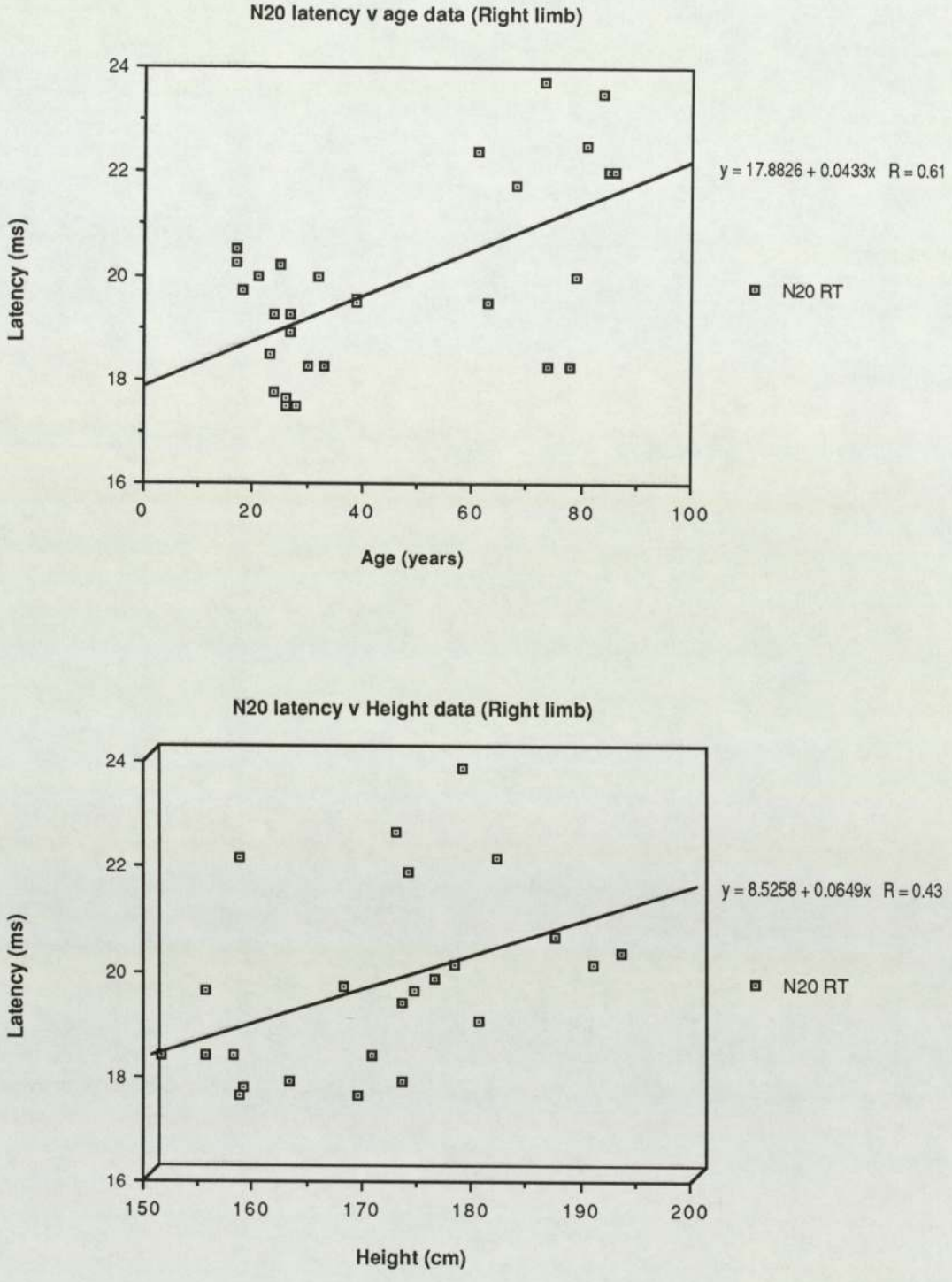

Figure 4.29. Simple Linear regression analysis of N20 component latency with age and height.
Significance of correlation; Ho: R=0;
N20 v Age; significant ($p<0.001$).
N20 v Height; significant ($p<0.05$).

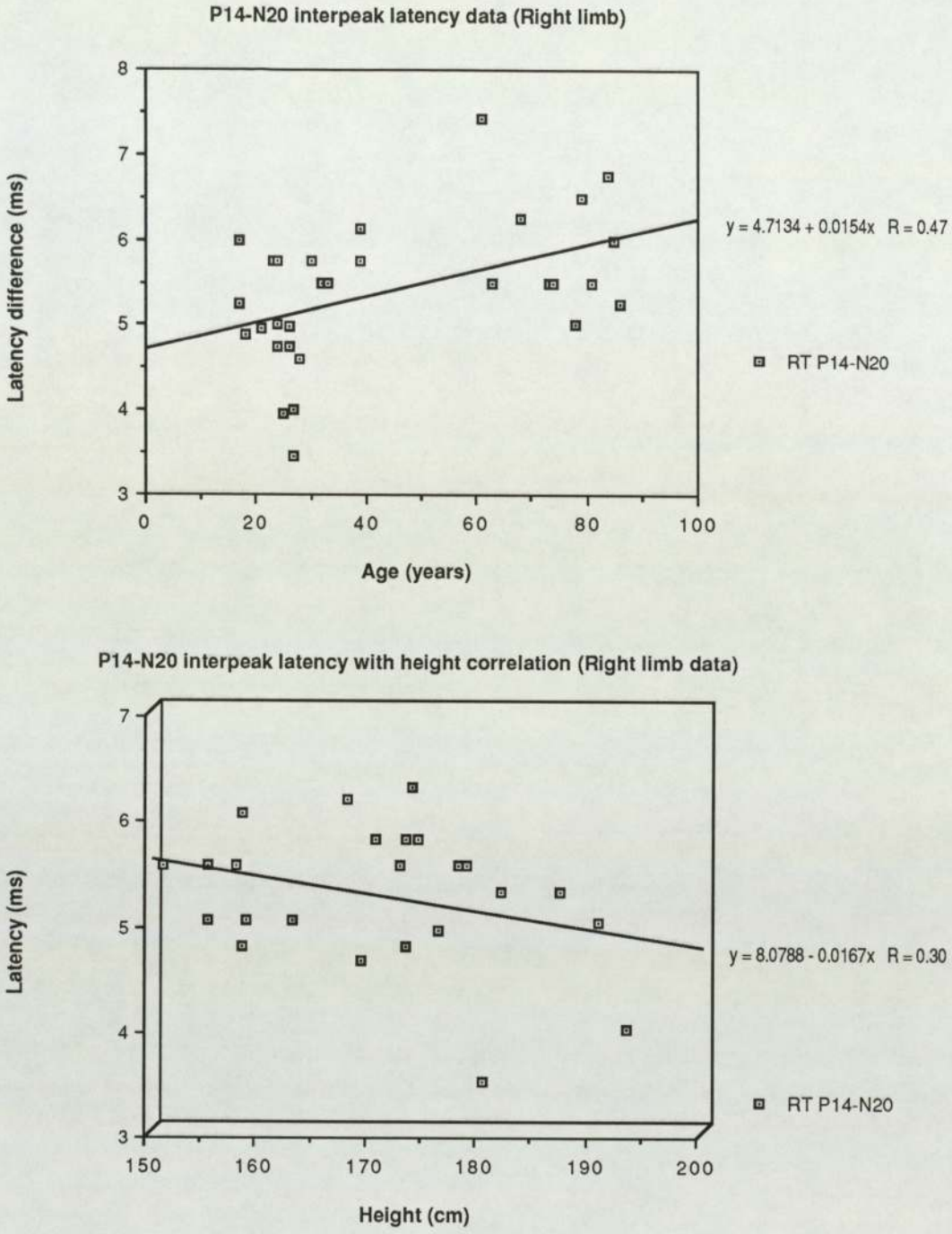

Figure 4.30. P14-N20 interpeak latency correlation with age and height. Simple linear regressions with regression coefficients (R) are shown.
Significance of correlations; Ho: R=0;
P14-N20 v Age; significant ($p<0.01$).
P14-N20 v Height; not significant ($p>0.05$).

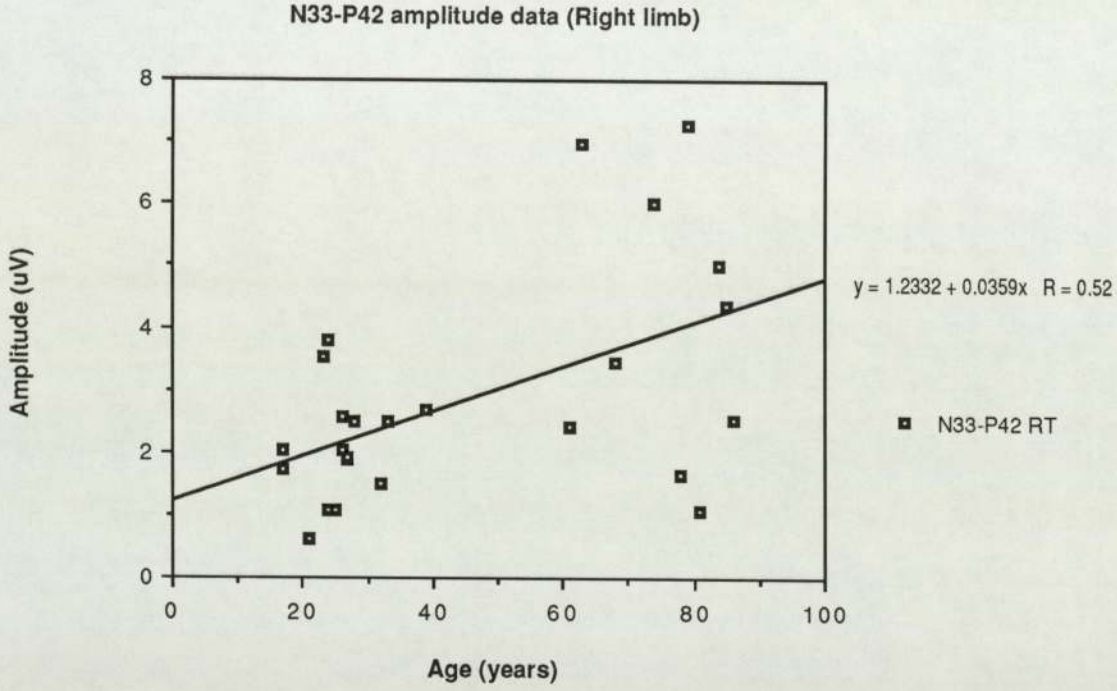

Figure 4.31. N33-P42 amplitude correlation with age. Simple linear regression (R) was significantly correlated where; Ho: R=0; $p<0.01$.

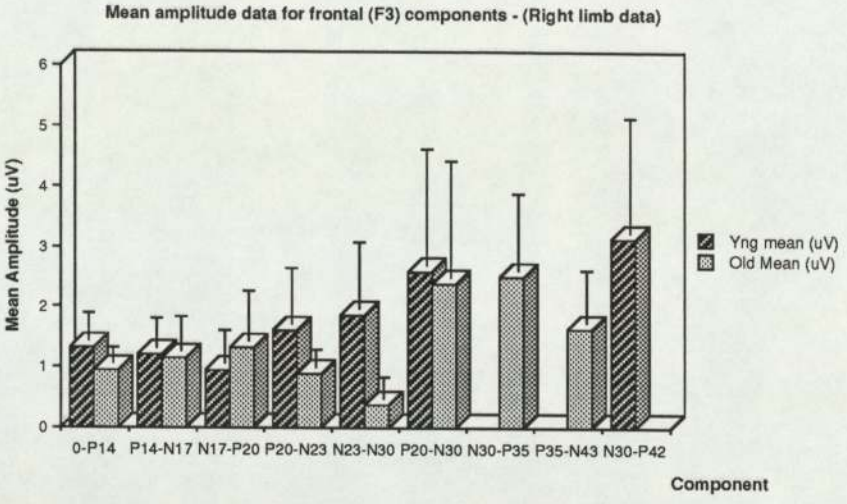

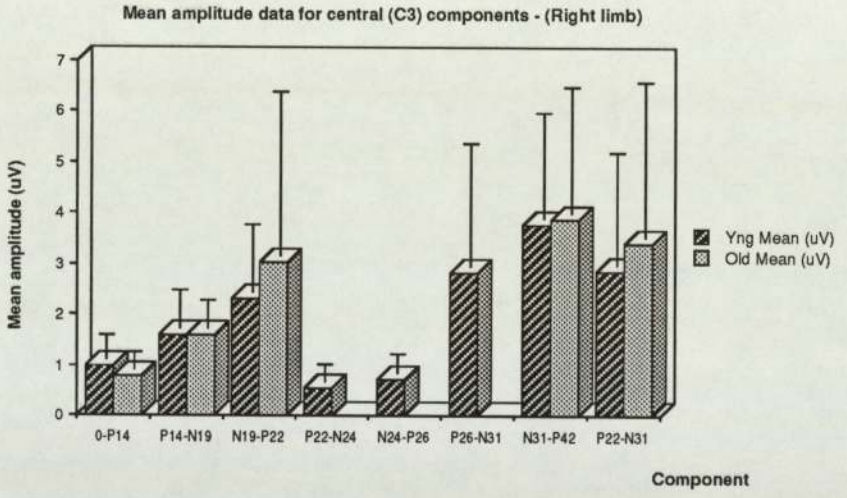

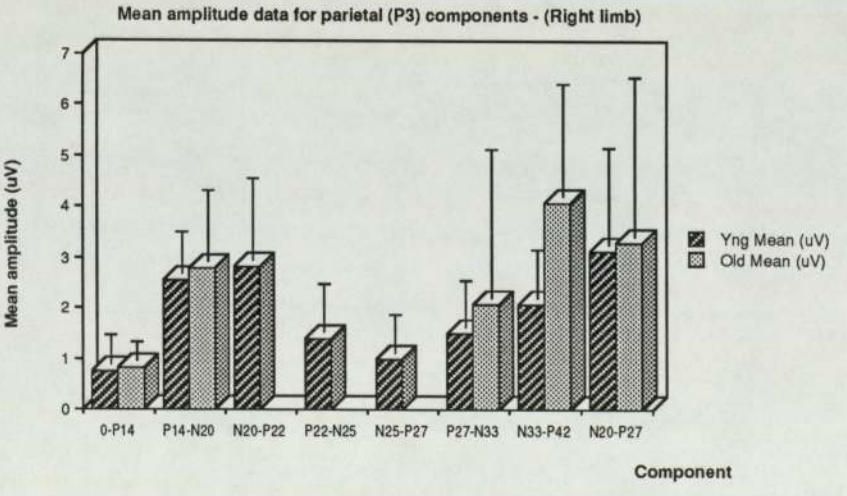

Figure 4.32. Group mean amplitude data from young (17-30 years) and old (60-86 years) age groupings. Only parietal N33-P42 component peak amplitude was significantly different between these groups ($p<0.01$).

4.3.4.5. Topography of parietal components.

Group mean waveform maps and group mean maps were plotted for N20 (Figure 4.7.1) and P27 (Figure 4.9.1). Maps for both components revealed two fields of opposite polarity with an antero-posterior relationship. In the case of N20 the negative maxima occurred at P3 (for right limb stimulation, P4 for left) and the positive maxima at Fz (for both right and left limb stimulation).

For P27, the positive maxima was also centred around the P3 (or P4) electrode site with the negative maxima at Fz for mean maps and F4 for the right limb mean waveform map.

No clear topographic maps could be derived for parietal P22, N25 or N33 because of their overlap with components of similar latency and greater amplitude. Parietal P22 and N25 were coincidental with a higher amplitude central P22 component; parietal N33 overlapped with the higher amplitude central N31 component.

In the case of the parietal P42 component, its mean latency was not significantly different to that of the central P42 ($p>0.05$), although the latter component was frequently of higher amplitude.

As discussed in section 4.3.2.0., a clear topographic difference of P42 was seen between a young and old age grouping with the tangentially oriented dipolar like field of the old age group 'enhanced' by the significant N33-P42 amplitude increase.

4.3.5.0. Upper Limits of normality

In total, 17 discrete components were consistently recorded in the control group. Analysis of the component correlations of latency with age and height provided optimum methods for determination of upper limits of normality. This was important in providing an accurate method for comparison with, and subsequent detection of pathology.

See overleaf for tabulation of employed methods (Table 4.3)

Where linear regression was the proven method of determination, the following formula was employed:- **L = a + bx + c**

where **L** = Latency in msec

a = y intercept

b = regression coefficient

x = age in years

c = 2.5 x (Standard Estimate of Error)

Where multiple regression was the optimum method of determination, then the following formula was employed:- **L = aA +bH + c + d**

where **L** = latency in msec; **a** and **b** = regression coefficients; **A** = age in years; **H** = height in cm; **c** = y intercept; **d** = 2.5 x (Standard Error of Estimate).

TABLE 4.3 PREDICTION OF UPPER LIMITS OF NORMALITY FOR LATENCY

COMPONENT	METHOD	AGE/COEFF	HEIGHT/COEFF	Y-INTERCEPT	S.E.E
ERB'S	Multiple	0.030	0.064	-2.015	0.573
P14	Multiple	0.048	0.114	-7.151	0.786
N17	Multiple	0.050	0.126	-5.905	0.909
N19	Multiple	0.055	0.107	-1.976	0.896
N20	Multiple	0.057	0.104	-0.600	0.891
P20	Multiple	0.080	0.134	-5.573	1.359
P22	Multiple	0.097	0.116	-1.119	1.194
N23	Multiple	0.101	0.122	-1.336	1.309
P27	2.5 x S.D.				
N30	2.5 x S.D.				
N31	Multiple	0.054	0.143	+4.733	2.027
N33	2.5 x S.D.				
P35	2.5 x S.D.				
P42	2.5 x S.D.				
N43	2.5 x S.D.				
Erbs-P14	Multiple	0.020	0.053	- 5.783	0.703
N17-P20	Linear	0.038		+1.509	0.938
N19-P22	Linear	0.044		+2.339	1.184
P14-N20	Linear	0.015		+4.713	0.745

Multiple = Multiple Regression analysis

Linear = Linear Regression analysis

2.5 x S.D. = 2.5 x Standard Deviation of group mean

U.L.N. = Upper Limit of Normality in msec.

S.E.E. = Standard Error of Estimate

Only the N33-P42 component revealed a significant amplitude age related change; in general however, although one may easily predict upper limits of normality from group mean data for both latency and amplitude, for the amplitude measure there was difficulty in applying the 2.5 standard deviation limiter for the lower limit since this would frequently take the value below zero. An alternative measure would be to assume abnormality on any value which was less than 50% of the amplitude of the smallest value obtained from our 35 normal control subjects (Jones 1982), but these values would fall between only 1 and 2 standard deviations from the mean.

4.3.5.1. Normality limits of Fz derived potentials.

By subtraction of Fz potentials from the appropriate parietal potentials using the software of the Brain Atlas III™ system, the following normality limits for these Fz derived potentials were calculated.

TABLE 4.3.1.

LATENCY

	Right Limb		Left Limb	Latency Difference	
Component	Mean (S.D.)	U.L.N.	Mean (S.D.)	Mean (S.D.)	U.L.N.
N20	20.07 (1.86)		19.65 (1.74)	0.43 (0.47)	
P27	27.17 (3.43)		27.30 (3.06)	1.00 (1.14)	
N33	34.53 (3.60)		34.00 (3.34)	1.32 (1.98)	
P42	42.67 (4.83)		42.67 (3.81)	2.80 (2.03)	

AMPLITUDE

	Right Limb		Left Limb	Amplitude Difference	
Component	Mean (S.D.)	U.L.N.	Mean (S.D.)	Mean (S.D.)	U.L.N.
0-N20	2.81 (1.46)	6.46	2.41 (1.52)	0.77 (0.60)	
20-27	5.45 (3.58)	14.40	4.66 (3.18)	1.94 (1.42)	
27-33	3.80 (3.02)	11.35	3.52 (3.20)	1.85 (1.57)	
33-42	3.35 (2.40)	9.35	3.57 (3.14)	1.45 (1.24)	

S.D. = Standard Deviation; U.L.N. = Upper Limit of Normality, calculated as the mean + (2.5x standard deviation).

Lower limits of amplitude were calculated as 50% of the amplitude of the lowest recorded control group value, thus: 0-N20 = 0.32uV; N20-P27 = 0.50uV; P27-N33 = 0.44uV; N33-P42 = 0.24uV.

4.3.6.0. Combination of morphology types across scalp

Morphology type combinations across the scalp are shown in Tables 4.4 and 4.5 overleaf. The commonest combinations can be summarised thus:-

FI with CI	46% of F and C type combinations
FI with PI	43% of F and P type combinations
CI with PI	57% of C and P type combinations
FI + CI +PI	41% of total combinations

Points of note were:-

1. FI,CI,PI combination occurred in 61% of old age group but only 21% of young age group.
2. Frontal V type morphology occurred in 59% of young recordings and only 4% of old.
3. Frontal W type morphology occurred in 3% of young group recordings but in 50% of the old group.
4. CII occurred most frequently with FII.
5. FII occurred equally frequently with PI and PII
6. CIII only occurred with FII and PIII.
7. PIII only occurred with CII and CIII.

TABLE 4.4 COMPONENT MORPHOLOGY TYPES OF CONTROL GROUP

Control No	Age	F Type RT	F Type LT	C Type RT	C Type LT	P Type RT	P Type LT
N1	18	FII + V	FII + V	CII	CII	PIII	PIII
N2	21	FII + V	FII + V	CII	CI	PI	PI
N3	18	U/A	FII + U	U/A	CI	A	U
N4	25	FII + V	U/A	CII	U/A	PI	A
N5	26	FI + V	FII + V	CI	CI	PI	PI
N6	41	FI + U	FI + U	CI	CI	PII	PI
N7	39	U/A	FII + V	CII	CI	PII	PI
N8	27	FII + V	FI + V	CI	CI	PII	PI
N9	26	U/A	U/A	U/A	U/A	U/A	U/A
N10	28	FIII + V	FI + V	CI	CI	PI	PI
N11	60	FI + W	U	CI	CII	PI	PI
N12	24	FIII + V	FIII + U	CII	CII	PI	PI
N13	17	U	FII + V	CI	CII	PI	PI
N14	17	FIII + U	FIII + U	CI	CI	PI	PI
N15	24	FII + V	FI + V	CI	CI	PII	PII
N16	24	FII + V	FI + V	CI	CI	PI	PI
N17	30	FII + V	FIII + V	CI	CI	PII	PII
N18	23	FI + U	FI + U	CI	CI	PI	PI
N19	27	FII + V	FII + U	CII	CII	PI	PI
N20	26	FI + W	U/A	CI	CI	PI	PI
N21	32	FI + W	FI + U	CI	CII	PI	PI
N22	33	FI + V	FI + V	CI	CI	PI	PI
N23	84	FI + W	FI + W	CI	CI	PI	PI
N24	79	FI + U	FI + V	CI	CI	PI	PI
N25	79	U	U	U	U	U	U
N26	78	FI + U	FI + W	CI	CI	PI	PI
N27	85	FI + W	U + W	CI	CI	PI	PI
N28	81	FII + W	FI + U	CI	CI	PI	PI
N29	63	FI + W	FI + W	CI	CI	PII	PI
N30	73	FII + U	FII + U	CIII	CII	PIII	PIII
N31	72	U/A	U/A	U/A	U/A	U/A	U/A
N32	74	FI + W	FI + W	CI	CI	PI	PI
N33	39	FI + W	FI + W	CI	CI	PI	PI
N34	68	FI + U	FI + W	CI	CI	PI	PI
N35	86	FI + W	FI + U	CI	CI	PI	PI

KEY F= FRONTAL C=CENTRAL P=PARIETAL

U/A indicates where components were Unclear and/or Artefactual

V = V type morphology formed by frontal N30-P42 complex

W = W type morphology formed by frontal N30-P35-N43 complex

TABLE 4.5 COMPONENT MORPHOLOGY TYPES FOR YOUNG AGE GROUP (17-30 YEARS)

Control No	Age	F Type RT	F Type LT	C Type RT	C Type LT	P Type RT	P Type LT
N1	18	FII + V	FII + V	CII	CII	PIII	PIII
N2	21	FII + V	FII + V	CII	CI	PI	PI
N3	18	U/A	FII + U	U/A	CI	U/A	U
N4	25	FII + V	U/A	CII	U/A	PI	U/A
N5	26	FI + V	FII + V	CI	CI	PI	PI
N8	27	FII + V	FI + V	CI	CI	PII	PI
N9	26	U/A	U/A	U/A	U/A	U/A	U/A
N10	28	FIII + V	FI + V	CI	CI	PI	PI
N12	24	FIII + V	FIII + U	CII	CII	PI	PI
N13	17	U	FII + V	CI	CII	PI	PI
N14	17	FIII + U	FIII + U	CI	CI	PI	PI
N15	24	FII + V	FI + V	CI	CI	PII	PII
N16	24	FII + V	FI + V	CI	CI	PI	PI
N17	30	FII + V	FIII + V	CI	CI	PII	PII
N18	23	FI + U	FI + U	CI	CI	PI	PI
N19	27	FII + V	FII + U	CII	CII	PI	PI
N20	26	FI + W	U/A	CI	CI	PI	PI

COMPONENT MORPHOLOGY TYPES FOR OLD AGE GROUP (60-86 YEARS)

Control No	Age	F Type RT	F Type LT	C Type RT	C Type LT	P Type RT	P Type LT
N11	60	FI + W	U	CI	CII	PI	PI
N23	84	FI + W	FI + W	CI	CI	PI	PI
N24	79	FI + U	FI + V	CI	CI	PI	PI
N25	79	U	U	U	U	U	U
N26	78	FI + U	FI + W	CI	CI	PI	PI
N27	85	FI + W	U + W	CI	CI	PI	PI
N28	81	FII + W	FI + U	CI	CI	PI	PI
N29	63	FI + W	FI + W	CI	CI	PII	PI
N30	73	FII + U	FII + U	CIII	CII	PIII	PIII
N31	72	U/A	U/A	U/A	U/A	U/A	U/A
N32	74	FI + W	FI + W	CI	CI	PI	PI
N34	68	FI + U	FI + W	CI	CI	PI	PI
N35	86	FI + W	FI + U	CI	CI	PI	PI

KEY F= FRONTAL C=CENTRAL P=PARIETAL

U/A indicates where components were Unclear and/or Artefactual

V = V type morphology formed by frontal N30-P42 complex

W = W type morphology formed by frontal N30-P35-N43 complex

4.3.7.0. Latency comparison of components

Student t-tests were performed on components with closely matching latencies but occurring at different scalp locations. The data is listed in Table 4.6 below.

TABLE 4.6 **COMPONENT LATENCY COMPARISON**

	RT LIMB		**LT LIMB**	
	T-test	**P-value**	**T-test**	**P-value**
Components	Paired (No. of pairs)	Unpaired	Paired (No. of pairs)	Unpaired
(F)P20 v (P)N20	0.000 (29)	0.036	0.002 (25)	0.205
(F)P20 v (C)P22	0.000 (28)	0.011	0.000 (25)	0.000
(C)P22 v (P)P22	**0.786 (06)**	0.385	0.015 (03)	0.259
(C)P22 v (F)N23	0.000 (14)	0.780	**0.138 (11)**	0.881
(F)N30 v (C)N31	0.001 (29)	0.015	0.006 (25)	0.027
(F)N30 v (P)P27	0.000 (28)	0.004	0.000 (24)	0.003
(C)N31 v (P)N33	0.003 (27)	0.145	0.000 (26)	0.020
(P)N33 v (F)P35	0.034 (10)	0.019	0.035 (07)	**0.456**
(C)P42 v (P)P42	**0.088 (24)**	0.473	**0.313 (25)**	0.784
(P)P42 v (F)N43	**0.941 (08)**	0.019	**0.498 (04)**	0.390
(F)P42 v (C)P42	**0.597 (12)**	**0.904**	**0.178 (12)**	**0.115**
(F)P42 v (P)P42	**0.284 (10)**	**0.623**	**0.335 (10)**	**0.157**

Bold figures indicate data **not** significantly different at the 0.05 level.

4.4.0. Discussion and Conclusions

4.4.1. Component topography and dipole models

4.4.1.1. P14 component

This component appeared with equal latency over the entire scalp. Topographic mapping revealed an anterior amplitude emphasis. These findings are in agreement with previous authors, such as Goff et al 1977 (their P15), Jones and Power 1984 (their P14) and Tsuji and Murai 1986 (their P12).

I concur with these authors that the nature of the topographic distribution of this potential is that of a far field component with a generator of sub-cortical origin.

4.4.1.2. N17 and N19 components

Clear topographic distributions for these components were not obtained in this study because of their smaller amplitude and similar latency to the larger parietal N20 component.

Maps of such components have been achieved in other studies by adjustment of the recording baseline; Tsuji and Murai (1986) reported a frontal N16 component (equivalent to our N17) and produced a topographic map revealing a broad bilateral fronto-central distribution. However this map reflected the amplitudes from a baseline placed at the peak of a P12 component (equivalent to our P14), i.e. presented a peak to peak amplitude distribution. Baseline manipulation was avoided in our study; it was not possible to discover from either inspection of waveforms or maps, whether the frontal N17 or N19 components were spatially discrete components.

Desmedt and Cheron (1981) and Mauguière et al (1983b) have reported the presence of a broad, long duration N18 component best revealed by a non-cephalic reference and thought to be of thalamic origin. This N18 component would be greatly attenuated, but not totally eliminated by the use of an earlobe reference. It is therefore conceivable that the N17 and

N19 peaks were produced at least in part by the superimposition of frontal P20 and central P22 peaks over a subcortically generated N18.

Iwayama et al 1988 suggested an origin of N15 (equivalent to our N17) as above the level of the thalamus.

4.4.1.3. N20 and P20 components

Paired t -testing of P20 and N20 peak latencies revealed a significant difference ($p<0.001$) between these two components although not to unpaired analysis. Inspection of group mean waveform and group mean maps however revealed a close relationship between these components with P20 producing a diffuse frontal positivity concomitant with the parietal negativity of N20. The line of equipotentiality dividing these fields approximated to that of the Rolandic fissure.

These findings equate to a common generator producing an equivalent dipole oriented tangentially to the scalp surface; these findings are in agreement with several authors - notably Broughton 1969; Goff et al 1977, and Allison et al 1980;1989. The precise nature of the dipole equivalent generators of these components were clouded by studies by Papakostopoulos and Crow 1980 and Desmedt and Cheron 1980. These authors disputed the single equivalent dipole model on the grounds that P20 were of consistently longer latency than N20. They therefore proposed that the frontal and parietal potentials reflected activity of separate radially oriented sources in motor or supplementary cortex frontally and somatosensory cortex parietally. This model appeared to be further supported by the findings of Mauguière et al (1983) who reported an apparently preserved P22-N30 complex in patients with cortical lesions in whom N20 had been abolished. However Goff et al 1977 and Allison et al 1980 had previously described a peri-rolandic P25 component and Deiber et al 1986 a P22 component which could be differentiated both spatially and temporally from an N20-P20 complex. This data was supported subsequently by Desmedt and Bourguet 1985 and Desmedt et al 1987 whose latterly modified dipole model supported a single tangentially

oriented source for the N20-P20 complex and a radially oriented source for a P22 component.

Data in this study does support the findings of Papakostopoulos and Crow (1980) in so far as the mean peak latency of P20 (21.04 ms +/- 2.54ms) was greater than that of N20 (19.81 ms +/- 1.8ms) ; as mentioned earlier, whilst the means were not significantly different, significance was indicated with paired analysis ($p<0.001$).However, it has been argued that such latency differences do not preclude a single generator model (Cracco 1976).

I concur with those authors who suggest that the likely source of the N20-P20 complex is Brodmann area 3b located in the posterior bank of the central sulcus (see Figure 3.6 Chapter 3); this model has been supported by magnetic recordings (Okada et al 1984; Wood et al 1985) indicating a source some 25mm +/- 2mm from the scalp surface.

4.4.1.4. P22 component

Postulation on the likely source of this dipole falls into two camps. Maugiuère et al 1983, supported subsequently by Deiber et al 1986 and Desmedt et al 1987, have proposed Brodmann area 4 as the most likely source. Mauguière et al had described a prerolandic P22 component which had been eliminated by a precentral lesion associated with a severe hemiplegia. Moreover, the P22 component reappeared in conjunction with the clinical regression of the motor deficit after surgical excision of the tumour. However, it is worth noting that these authors did not describe or dissociate P22 from a P20 component.

The alternative proposal comes most notably from Allison et al 1980;1989 and Wood et al 1988. In the two latter papers, topographic mapping techniques have been applied to electrode arrays placed on the surface of the cortex . These authors, in describing their P25 component indicated that this was largest on the postcentral gyrus about 1 cm medial to the focus of the 20 and 30 msec potentials. They therefore proposed that Brodmann area 1 was the most likely source for this intermediate component.

A third alternative model has been proposed by Jones and Power (1984). In their discussion on the likely origin of the P22 component, they felt that there was a tangential orientation of

the likely dipole equivalent source based on the relationship of P22 with a bifrontal N22 component . They proposed Brodmann area 3a as a possible common source for these potentials.

Results in this study support the argument that P22 can be spatially and temporally differentiated from closely related components, notably N20, P20 and P27. Inspection of group mean maps reveal potential fields for P22 which could be explained by a radially oriented dipole in or at very close proximity to the Rolandic fissure. The very confined fields of this potential also lead one to speculate that the generators are likely to be located at the surface of a gyrus rather than in the depths of the sulcus. However, the precise variation of orientation of possible generators for this potential must bring into consideration the nature of the N23 component recorded at precentral locations. This will now be discussed.

4.4.1.5. N23 component

Jones and Power (1984) were the first authors to speculate on the nature and importance of an N22 component (equivalent to our N23) seen in all nine of their normal controls (aged 22-35 years) with a bilateral and frontal/prefrontal distribution. They were not the first authors however to reveal this component in their data. Goff et al 1977 described an N30 component which was often obscured by a larger N35 and was not treated as a separate component. Desmedt and Cheron (1980) described a frontal N28 component (digital nerve stimulation) which occurred in close relationship to an N40 component (equivalent to our N30 component).

Jones and Power (1984) reported that the mean latency of their N22 component was almost identical to that of the P22 suggesting the possibility of a common generator. Initial inspection of our mean data would tend to suggest the same, although right limb N23 and P22 latencies were significantly different ($p<0.05$)

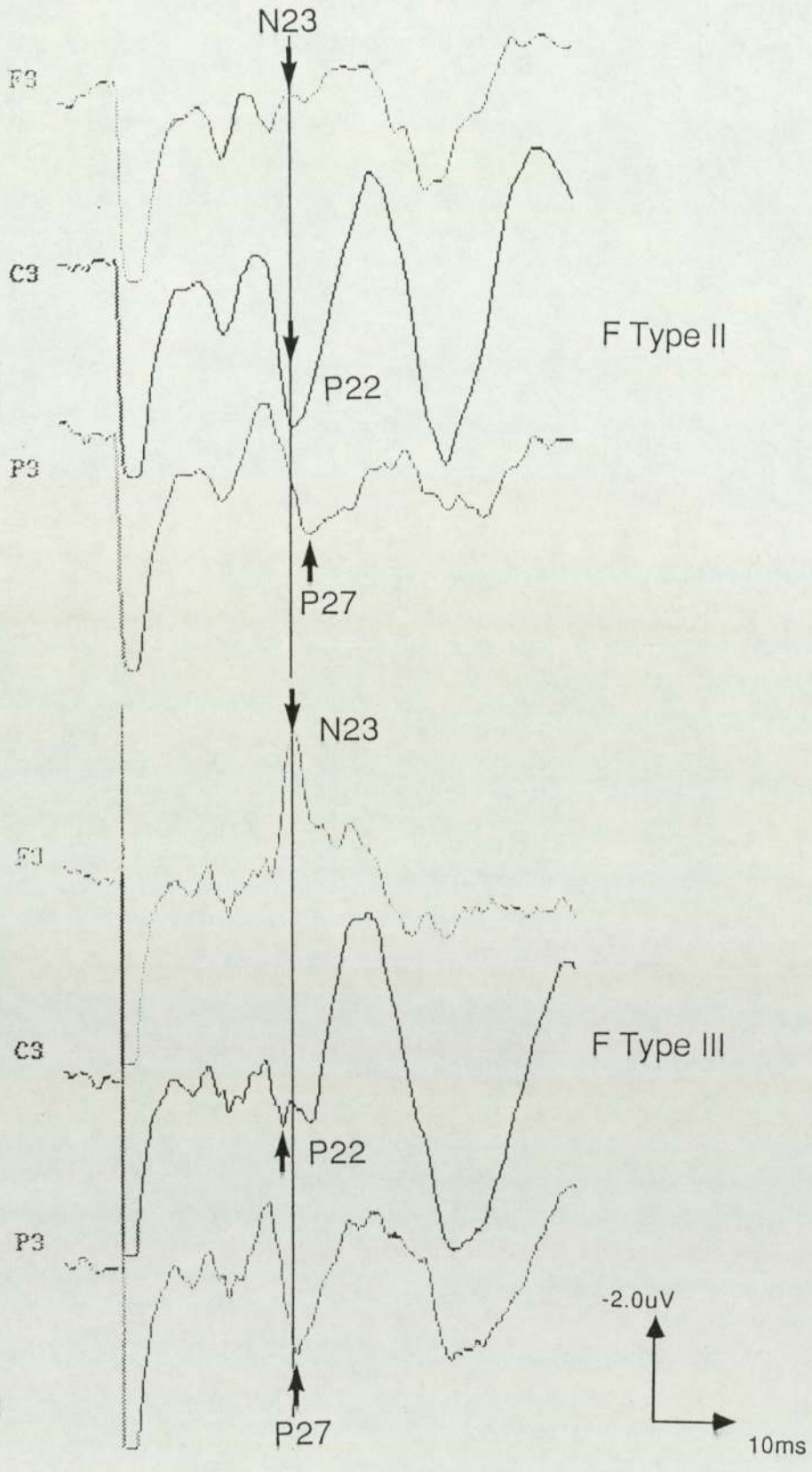

Figure 4.33. Frontal N23 component relationship with central P22 and parietal P27 components in both F type I I and F type III individuals.

Table 4.7. Group mean peak latency for right limb data

COMPONENT	TOTAL GROUP LATENCY/(STD DEV)	YOUNG AGE GROUP LATENCY/(STD DEV.)	OLD AGE GROUP LATENCY/(STD. DEV.)
P22	22.28 (2.67)	21.38 (1.15)	24.97 (3.08)
N23	23.08 (2.14)	22.71 (1.50)	26.38 (2.65)
P27	27.06 (3.56)	26.26 (4.53)	28.15 (2.43)

Examination of F type II waveforms further supported the P22/N33 relationship (Figure 4.33); however examination of the waveforms of F type III individuals in whom an apparently large N23 component existed, suggested that in these subjects there was a closer relationship with the parietal P27 component (see Figure 4.33). If the appearance of an N23 component was dependent on the temporal relationship of central P22 and/or parietal P27 to frontal N30 component, it would be important to reveal any significant difference of P22-N30, P27-N30 or P22-P27 interpeak latencies between morphology types. The following comparisons were made taking care to match morphology types between groups as closely as possible:-

Mean interpeak data
P22-N30
(F type I + C type I)
individuals
Latency: 5.31 ms
Std. Dev: 4.2
Obs: 15

Mean interpeak data
P22-N30
(F type II+ C type I)
individuals
Latency: 8.87 ms
Std. Dev: 2.12
Obs: 5

Mean interpeak data
P22-N30
(F type III + C type I)
individuals
Latency: 7.92 ms
Std Dev: 5.42
Obs: 2

Mean interpeak data
P22-P27
(F ,C and P type I) individuals
Latency: 3.03 ms
Std. Dev: 2.48
Obs: 12

Mean interpeak data
P22-P27
(F type II+ C&P type I)
Latency: 3.13 ms
Std. Dev: 2.30
Obs: 2

Mean interpeak data
P22-P27
(F type III+ C&P type I)
Latency: 0.69
Std Dev: 0.08
Obs: 2

Std.Dev = Standard Deviation; Obs. = Number of observation.

None of the mean latencies differed significantly between morphology groups ($p>0.05$) with student t-test analysis. However, the data still suggested that in subjects where no N23 was evident (F type I individuals), that this may have been due to the merging of the N23/N30 complex caused by a variable temporal relationship between P22, P27 and N30 generators.

An alternative or possibly parallel model would be that the equivalent dipole orientation for the intermediate P22 component varied between subjects; where a more tangential orientation occurred then a frontal N23 component was observed. Were this true then evidence of the P22 component might be seen at parietal locations; this model could explain the P type II morphology where a P22 component occurred at P3/4 locations. However, F types II and III were as frequently seen in P type I as P type II individuals. The most likely explanation therefore is that the morphological variations are subject to both slight temporal variations as well as orientation of dipole equivalent generators. F type III for example could be explained on the basis of close temporal relationship of P22 and P27 components with an increased tangential orientation of P22; these factors combine to give the large dominant N23 frontal component.

4.4.1.6 P27 and N30 components

P27 contour maps revealed a close similarity to those of N20 and of course were concomitant with N23 fields in F type III individuals as already described. The dipole model suggested for N20 therefore could explain all three of these components, at least in some subjects.

Several authors, most notably Allison et al 1980 and Wood et al 1988, have presented data indicating a clear N30-P30 relationship on either side of the central sulcus which, due to the similarity of their dipole-like field patterns, implied a common generator with that of the N20-P20 complex.

Data of this study, in common with that of Goff et al 1977, indicated that whilst the contralateral parietal P27 could present such a simple dipole field pattern (P type III morphology seen in 6% of records), our N30 component (equivalent to the N35 of Goff et al) presented a less clear relationship in the majority of subjects.

As discussed in the preceding section, the temporal relationship of N30 with P27, P22 and N23 are variables that contribute to the debate. It would appear that whilst the P27 component may present a dipolar field pattern which contributes greatly to the amplitude of the subsequent N30 component, the long duration and broad bilateral distribution of the latter component would indicate other generators contributing to this complex. Frontal activity as a result of cortico-cortical interactions may also be involved. Nöel and Desmedt (1980) had shown that N30 could be affected by lesions of the precentral cortex while the P30 component was preserved.

Desmedt and Bourguet (1985) went on to propose the supplementary motor area as a possible generator of this component and this has been supported by Rossini et al (1989) who described attenuation of N30 in a patient with a meningioma located in the left supplementary motor area.

4.4.1.7. N31 N33 and P35 components

Maps of N31 were closely similar to those of P22 and thus suggestive of a common source.

Due to the greater amplitude of N31 over N33 and their close temporal relationship, it was difficult to differentiate these two components spatially in group mean maps and in many individuals. In F type W individuals however, in whom a P35 component arose concomitantly with the parietal N33 (seen clearly in the old age group mean waveforms, Figure 4.22), provided evidence of a tangentially oriented dipole for these latter components. Thus it would appear that N31 and N33 indeed have separate generators.

It was interesting to observe that whereas central N31 and parietal N33 latencies were significantly different ($p<0.01$), the same was not true of frontal N43 and parietal P42 or indeed central and parietal P42 ($p>0.05$).

4.4.1.8. P42 component

This component appeared to have a slightly broader distribution in group mean wave/maps than P22 and N31 with the P3/P4 electrode falling within the group mean 85% amplitude isocontour. However, as with P22 and N31 no clear dipolar pattern, such as that seen with the

N20 and P27 component maps, was evident. Examination of P42 maps of old and young age groups however revealed a striking difference, with a dominantly tangentially oriented generator indicated for the old group and a radial generator for the young. This data suggests that central and parietal P42 components indeed have separate generators; possibly the same generator as P22 for the central P42 component whose field is most closely matched, and the proposed N20/P20 generator for the parietal P42.

P42 fields of the control group mean waveform and component maps are more closely related to the findings of Jones and Power (1984) in their description of a P40 component than the findings of Goff et al (1977) and Desmedt and Bourguet (1985) who describe a much broader distribution for their P45 component.

4.4.1.9. Summary of proposed dipole models

From analysis of group mean waveforms and maps as well as group mean data, the following dipole models are proposed.

Figure 4.34 overleaf shows a single dipolar source located in the posterior bank of the central sulcus responsible for N20/P20 components as well as P27 and possibly a significant part of the N30 component. However it is proposed that N30 is also contributed to by other generators, possibly located in the supplementary motor area (MSII).

It is clear from the maps that P22 can be spatially and temporally differentiated from the N20/P20 complex and thus a separate generator is indicated. This theory is further supported by the lesion studies of Mauguière et al 1983 although these authors did not differentiate between the peri-rolandic P22 and frontal P20 as described by authors such as Deiber et al (1986). Cortical surface recordings of Wood et al (1988) and Allison et al (1989) confirm the presence of an intermediate (P25) component but suggest Brodmann area 1 as being the likely generator of this component. In this study the P22 component consistently revealed a well circumscribed locus of activity centred over the C3/C4 electrodes. Studies such as Homan et al (1987) and Steinmetz et al (1989) have shown that these electrodes are most commonly located over the precentral gyrus.

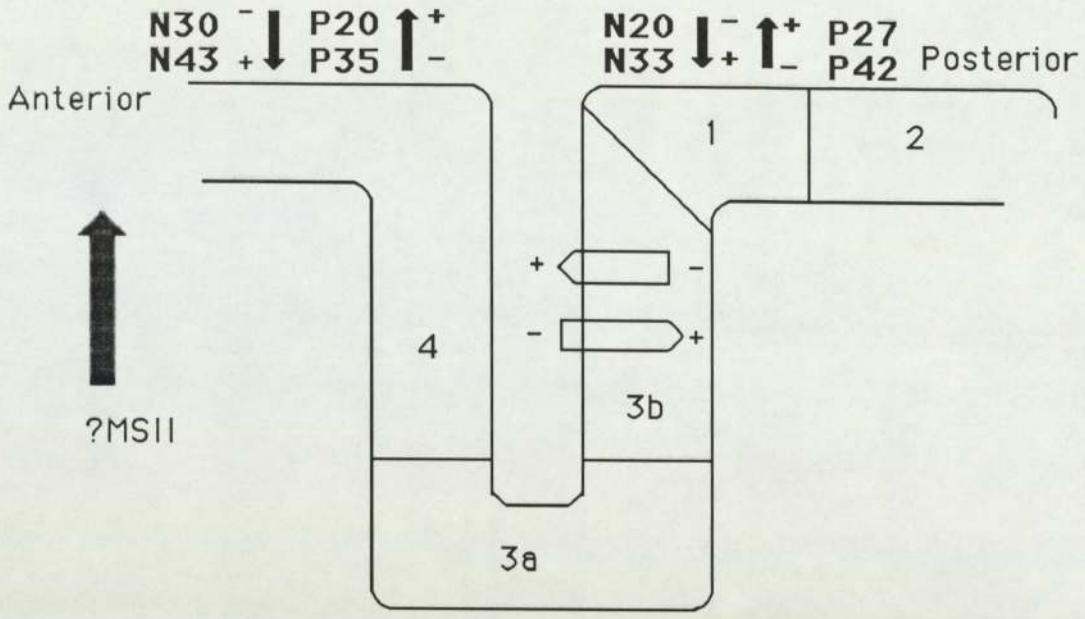

Figure 4.34. Possible dipole equivalent generators located in the central sulcus responsible for N20 / P20, P27 / N30, N33 / P35 and P42 / N43 components.

Given the amplitude and radial nature of the P22 component we have considered Brodmann area 4 or area 1 on either 'lip' of the central sulcus as the most likely source locations. It is the relationship of the P22 component with frontal N23 which leads us to propose the variable extension of the P22 generator into the anterior bank of the central sulcus in Brodmann area 4 (see Figure 4.35 overleaf). Jones and Power (1984) have suggested area 3a at the base of the central sulcus as being a likely source for such a dipole model but the relatively large amplitude of this component and the confined locus of its scalp surface electrical field are possible contraindications.

Given the spatial and temporal properties of N31, it is proposed that this component has the same generator as P22.

Parietal N33 showed a clear 'phase inversion' relationship with frontal P35 in the old age group and thus suggests the same generator that produced the similar N20/P20 field patterns; namely Brodmann area 3b.

Two distinct P42 fields may be discerned between age groups; a radial field pattern similar to P22 and N31 in the young age grouping and a tangential field type pattern similar to that seen in the control group wave/map N20/P20 complex for the old age grouping. This generator suggests that two generators co-exist; a tangentially oriented generator producing the parietal P42 and frontal N43 (Figure 4.34), and a radially oriented generator producing the central P42 (Figure 4.35). The tangential field patterns of the elderly group may become apparent because of an attenuation of frontal components co-existing with a preserved or enhanced N33-P42 parietal complex.

Allison et al (1989b) proposed Brodmann area 3b as the likely source for their P45 component and Brodmann area1 as a source for a P50 potential. The peak latencies of these cortical surface components however may have been prolonged by anaesthetic effects and therefore precise comparisons are difficult.

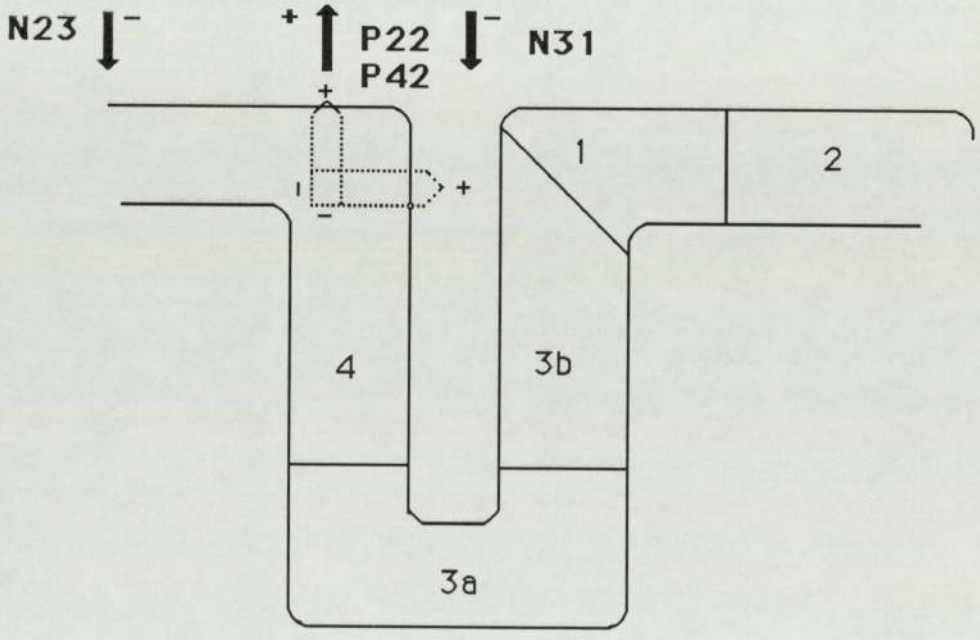

Figure 4.35. Possible dipole equivalent generators located in or around the central sulcus responsible for central P22, N31 and P42 and frontal N23 components.

4.4.2.0. Morphology and age variations

Several authors have reported on the importance of age, height and gender effects on the calculation of upper limits of normality of latency of scalp recorded SEP components (Allison et al 1983;1984; Mervaala et al 1988). Our data supports the view that age and height factors are essential elements in these calculations for P14, N17, N19, N20, P20, P22, N23 and N31 components. This may reflect the fact that these components arise as a direct result of the initial volley at the primary somatosensory cortex (with the exception of P14) and are not influenced by secondary cortical processing; thus they are more likely to directly reflect peripheral influences.

Morphological variables and age changes in relation to scalp topography are both areas which have not been dealt with extensively by previous authors. A notable exception is the work of Desmedt and Cheron (1980;1981) in their examination of a group of octogenarians in comparison to a young control group. They observed that parietally, the W pattern formed by their N22-P30-N35-P45 components to digital nerve stimulation was recorded in only 12 of 25 unselected normal adults of mean age of 22 years (48%) but in 17 of 19 octogenarians (89%) of mean age 82.3 years. This W pattern equates to the P type I morphology of this study which occurred in 65% of the young age group (mean age 23.6 years) and 73% of the old age group (mean age 75.5 years). It is worth noting however that the combination of the FI with CI with PI morphology types across the scalp occurred in 61% of the old age group but only 21% of the young.

Several authors have observed significant latency and amplitude changes between age groups. Shagass and Schwartz (1965) described an enlargement of amplitudes and lengthening of latencies with increasing age in a population ranging from 15 to 80 years of age.

Lüders (1970) described the effect of aging in components over a 500msec time period in subjects ranging from 19 to 69 years of age. Waveforms were measured from the contralateral cerebral hemisphere from needle electrodes fixed on the parasaggital line 7cm lateral to the

vertex and 2cm posterior to the mid-coronal line. The reference electrode was sited on the ipsilateral earlobe. They described four principal components with the following latencies: P1= 23.7 +/- 0.42; P2= 42.0 +/- 0.35; P3= 93.4 +/-4.7 and P4= 213.8 +/- 9.9. Latencies of the earliest and latest components presented no significant alteration, but the intermediate components lengthened significantly with older age. Amplitudes described a U shaped curve - decreasing at the 30-45 year age level and increasing again in the older age. These findings were consistent with those of Shagass and Schwartz whose amplitude / age curve 'bottomed' out in the 20-39 year age group.

Desmedt and Cheron (1980) reported a significant increase of all postcentral SEP latencies in the octogenarians. They also reported that the mean increases of amplitude were significant (at $p<0.025$) for the postcentral N22, P30 and N35 as well as for P45 ($p<0.001$). The authors only included data from subjects with the same morphology type for comparison.

Data from our study contrasts with that of previous authors in so far as postcentrally, only P14 and N20 components revealed significant increases in latency in the old age group and only the N33-P42 component amplitude revealed a significant increase in the old. Differences may exist because of the older mean age of subjects in the study of Desmedt and Cheron (1980), and in contrast to the studies of Lüders and Shagass and Schwartz, the present study had few subjects in the 31-59 age group (N=5) for comparison.

However, the findings are consistent with reports indicating that the peripheral nerve sensory conduction velocity exhibits a tendency to decrease with age (Desmedt and Cheron 1978). It would appear that peripheral effects may be directly reflected onto all cortical components with peaks occurring up to approximately 30 msec (with the exception of parietal P27 and frontal N30). Later components tended to be broader, although precise quantitative measure was difficult due to the inability to accurately gauge component onset times. Certainly, greater inter-individual variability in peak latency occurred in the later components; this may reflect secondary cortical processing.

The increase in amplitude of cortical components with age is difficult to reconcile with data suggesting a loss of cortical neurones reaching some 50% for the superior frontal gyrus for the eigth decade of life (Brody 1970). Desmedt and Cheron (1980) had reported attenuation of the frontal N30 component as a process of normal aging co-existing with augmentation of postcentral components. The authors reflected that this may indicate a differential aging effect across the cortex.

Lack of morphological variation in our old age group may reflect neurone loss. Broader duration of components with increasing age could lead to greater component summation or enhanced 'synchronisation' of remaining neurones and result in amplitude increases, although we have no data from this study to substantiate these latter theories.

Variation in P42 topography with age seen in this study could however support the argument of differential rates of neurone loss across the cortex.

CHAPTER 5

SOMATOSENSORY EVOKED POTENTIALS IN PATIENTS WITH KNOWN CORTICAL LESIONS.

5.1.0. Introduction

Several workers have turned their attention in recent years to the use of isopotential colour contour maps to help illustrate and unravel the complexities of the spatial and temporal relationships of scalp recorded evoked potentials. The technique appears to be particularly useful in the analysis of SEP components (Desmedt and Bourguet 1985; Deiber et al 1986; Desmedt et al 1987).

When topographical techniques have been employed in the study of SEP's in patients with unilateral cortical lesions, independent changes of frontal or parietal components have been observed (Mauguière et al 1983; Yamada et al 1984; De Weerd et al 1985 and Tsuji et al 1988).

Other workers have reported on the validity of statistical brain mapping techniques in the detection of pathology - notably Duffy et al 1981 and Duffy 1982. Commercial mapping systems became available providing software capable of performing the Z statistic which gave ease of comparison of patient data with a control group database. Despite the popularity of such statistical mapping methods and the well publicised findings of Duffy and co-workers since the early 1980's, there remains few reports by other workers of the success or otherwise of such methods in the detection of pathology .

The purpose of the study described in this Chapter was twofold: Firstly, to discover whether the study of discrete cortical lesions using brainmapping techniques would shed further light on the nature and origin of the scalp recorded SEP components.

Secondly, to discover whether the use of an SEP topographical mapping database and statistical mapping methods was useful in the detection of abnormalities associated with such lesions.

5.2.0. Method

Patients referred to the Neurology department at New Cross hospital in Wolverhampton and suspected or known to have a unilateral cortical lesion based on the neurological exam and possibly CT scan evidence, were referred to the Clinical Neurophysiology Unit at Aston University in for SEP investigation. The evoked potential recordings were made as soon after the neurological exam as possible.

The neurological exam included assessment of upper and lower limb muscle power, tone and reflex. Assessments of pain and temperature sensation were made along with touch, two point discrimination and vibration. Position sense was assessed by flexion of distal digits and stereognosis was assessed by the ability of the patient to identify an object such as a coin by touch alone as well as the ability to recognise figures inscribed on the palm of the hand. Wherever possible, follow up data indicating clinical change subsequent to SEP recordings were made.

The method used for the evoked potential recording was identical to that employed for the normal control study described in the previous Chapter. Assessments of the patient data were then performed. Peak latency and peak to peak amplitude data was noted for the components recorded at the frontal (F3/F4), central (C3/C4) and parietal (P3/P4) electrode sites contralateral to the limb stimulated. This data was then compared to the upper and lower limits of normality calculated from the control group by multiple regression, linear regression or from the +/- 2.5 standard deviation from group mean points as described in section 4.3.5.0 in Chapter 4.

Morphology of components were classified using the system and nomenclature described for the normal control group - namely FI, FII or FIII morphology types occurring frontally with an

additional V or W classification; CI, CII or CIII morphology types occurring centrally and PI, PII or PIII types occurring parietally.

Comparisons were made of each data point of each of the 20 channels of recordings made from the patient to the group mean control waveforms using the Z statistic software of the Brain Atlas III™ system. The subsequent colour contour maps indicated the variation of patient to control group in standard deviations.

The second type of topographical map analysis to be performed was the comparison of individual component maps from the patient to the mean component maps of the control group . Again the Z statistic was employed so that the subsequent variations could be generated topographically in standard deviations.

Having completed the three stages of analysis of the patient data, an attempt was made to assess the correlation between clinical findings, SEP analysis using the conventional method of peak latency and peak to peak amplitude, and the data generated by the statistical mapping techniques. A final stage to assist this process was the formation of an Fz reference derived potential using P3 and P4 locations as 'active' electrodes to closely approximate the recording technique most commonly used in the clinical environment. This enabled an assessment of whether the changes seen using mapping techniques may have been detected using more conventional recording protocols. The Fz derived potentials were achieved by subtraction of the Fz potential from the appropriate parietal potential using the Brain Atlas III™ software. Data was compared to that of the Fz derived potentials of the control group (Chapter 4, section 4.3.5.1.)

5.3.0. Results

Twelve patients were referred for SEP mapping assessment over a twelve month period.

The mean age of the patient group was 52.17 years; standard deviation 16.49 years. This compares with a mean age of 44.91 years; standard deviation 25.47 years, for the control group. Student t-test comparison of these two means yielded a non-significant p value of 0.364.

Similarly, the mean height of the patient group was 175.3cm; standard deviation 7.12cm, compared with a mean height for the control group of 170.11cm; standard deviation 11.39cm. Student t-test comparison of these two means yielded a non-significant p value of 0.190.

The results of each patient will now be presented individually with the patients identified by the nomenclature P followed by a numeral, i.e. P1, P2 etc.

5.3.1.0. Patient 1 (P1) results.

5.3.1.1. P1 Clinical presentation.

This 62 year old gentleman suffered a left hemisphere cerebro-vascular accident in July 1982. A CT scan confirmed a left parieto-occipital infarction. When reviewed in clinic in July 1988, he presented with no clear upper limb signs but reported some weakness in the right lower limb. He was also subject to the occasional tonic-clonic seizure - the last one occurring in June 1988. Neurological examination revealed only an upward going plantar reflex in the right leg (Table 5.1).

Medication consisted of Phenytoin (500mg) and Nifedipine (200mg b.d.).

Table 5.1 Clinical Summary for Patient P1

	UPPER LIMB		LOWER LIMB	
	Right	Left	Right	Left
Power	Normal	Normal	Normal	Normal
Tone	Normal	Normal	Normal	Normal
Reflex	Normal	Normal	Plantar ↑	Normal
Pain	Normal	Normal	Normal	Normal
Temp.	Normal	Normal	Normal	Normal
Touch	Normal	Normal	Normal	Normal
Vibration	Normal	Normal	Normal	Normal
Position	Normal	Normal	Normal	Normal
2 Point dis.	Normal	Normal	Normal	Normal
Stereognosis	Normal	Normal	Normal	Normal

Direction of arrow indicates an increase (upward) or decrease (downward) of sensory or motor function.
In the case of reflex activity an upward arrow indicates an upward going reflex.

5.3.1.2. P1 SEP results.

SEP's were recorded in July 1988.

Subjective inspection of frontal waveforms showed an FI V type morphology occurring to both right and left limb stimulation. There was a morphology difference between central components; at the C3 electrode to right limb stimulation a type CI with small P22-N31 but large N31-P42 component was observed. At C4 to left limb stimulation, a CII morphology type, with P22-N25-P27 complex was observed.

Parietally there was an attenuation of the P27-N33-P42 complex at the P3 electrode location to right limb stimulation compared to the P4 left limb counterparts. Precise location of the P42 peak to right limb stimulation was difficult due to a broad and poorly formed morphology. Waveforms are shown in Figure 5.1

Analysis of peak latency and peak to peak amplitude revealed no significant differences for any components(<2.5 standard deviation). This data is shown in Table 5.2.

Comparison of the patients waveforms with the control group mean waveforms was performed using the Z statistic. This analysis revealed a maximum standard deviation of 1.87 for right limb stimulation (occurring at the F3 location) and 1.75 for left limb (T3 location). See Figure 5.2.

The temporal relationship of central N31 with parietal P27 (both peaks occurring at 27.50ms) to right limb stimulation was an unusual one and therefore the topographic map at this latency was compared with the control group mean P27 map using the Z statistic. As can be seen in Figure 5.3, no location exceeded 1.75 standard deviations (T3 location providing the maximum deviation).

Subjective comparison of P3 and P4 to Fz reference derivations as seen in Figure 5.1 clearly reflected the attenuation of the post - N20 parietal components, however all peak latency and peak to peak amplitudes for the Fz derived potentials were within normal limits.

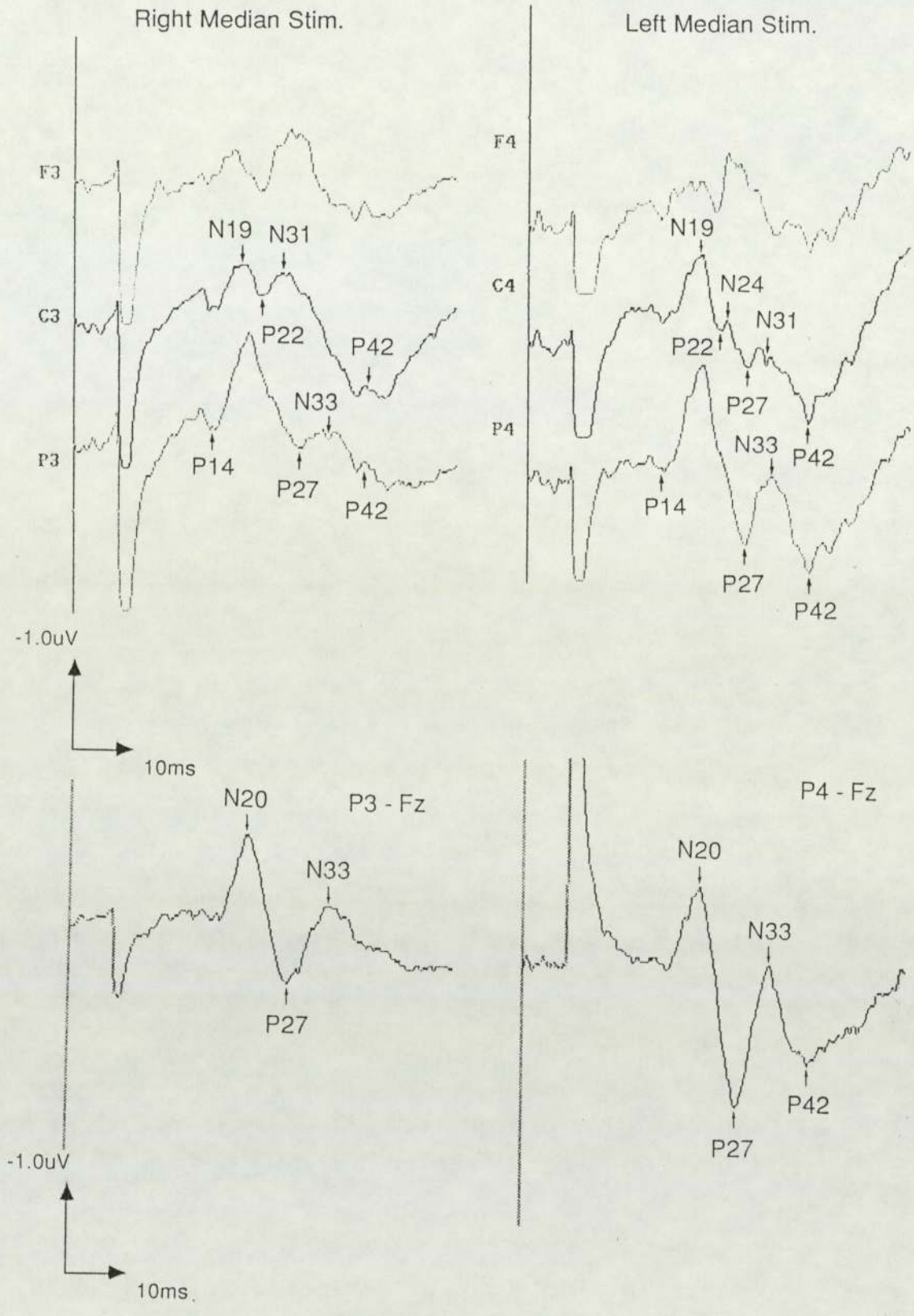

Figure 5.1. SEP waveforms for Patient 1 (P1) for right and left median nerve stimulation. Fz reference derived potentials are shown beneath the original earlobe reference recordings.

Patient: P1
Age (years): 63
Height (cm): 173

Component	Patient Data (ms)		Upper limit	Interhemisphere Latency	Interhemisphere Latency Diff.
	Right limb	Left limb	of normality	Difference (ms)	Upper Limit (ms)
Erbs	10.50	10.75	12.38	-0.25	0.49
P14	15.50	15.00	17.56	0.50	1.61
N17	19.00	19.50	21.32	-0.50	1.83
N19	20.50	21.00	22.24	-0.50	1.70
N20	21.75	21.50	23.21	0.25	1.72
P20	23.75	23.75	26.05	0.00	3.56
P22	24.00	24.50	28.05	-0.50	3.79
N23	-	-	29.41	0.00	1.79
P27	30.25	29.25	35.96	1.00	4.32
N30	28.75	27.25	37.85	1.50	4.64
N31	27.50	31.00	37.94	-3.50	3.90
N33	35.00	33.25	40.52	1.75	4.23
P35	-	-	43.89	0.00	2.40
P42(Part)	41.75	39.50	51.58	2.25	3.84
N43	-		54.34	0.00	4.68
Erbs-P14	5.00	4.25	6.40		
N17-P20	4.75	4.25	6.25		
N19-P22	3.50	3.50	8.07		
P14-N20	6.25	6.50	7.52		
N20-P42	20.00	18.00	31.43	2.00	4.30

Component Amplitude	Patient Data (uV)		Lower limit	Interhemisphere Amplitude	Interhemisphere Amp. Diff.
	Right limb	Left limb	of normality	Difference (uV)	Upper Limit (uV)
Frontal comps					
0-P14	0.09	0.56	0.09	-0.47	1.54
P14-N17	0.29	0.31	0.12	-0.02	1.31
N17-P20	0.35	0.27	0.04	0.08	1.52
P20-N30	0.56	0.39	0.08	0.17	2.55
Central comps					
0-P14	0.24	0.22	0.09	0.02	1.27
P14-N19	1.13	0.58	0.06	0.55	1.94
N19-P22	1.03	0.66	0.22	0.37	3.04
P22-N31	0.23	0.13	0.01	0.10	3.31
N31-P42	1.27	0.70	0.28	0.57	5.32
Parietal comps					
0-P14	0.48	0.27	0.02	0.21	1.35
P14-N20	1.09	0.96	0.36	0.13	2.73
N20-P27	1.33	1.62	0.41	-0.29	3.34
P27-N33	0.11	0.61	0.08	-0.50	4.12
N33-P42	0.54	0.86	0.30	-0.32	3.78

Table 5.2 Comparison of latencies and amplitudes with normality limits from control group. Lower limit of normality for amplitude of control group calculated as 50% of minimum recorded value.
U = unclear peak - no precise latency and morphology determination.
Ab = component peak appears to be entirely absent.
Bold figures indicate data which exceeds upper limits of normality.
Interhemisphere differences calculated as (Right-Left) limb data.

Patient: P1 **Fz reference derived potentials**
Age (years): 63
Height (cm): 173

Component	Patient Data (ms)		Upper limit	Interhemisphere Latency	Interhemisphere Latency Diff.
	Right limb	Left limb	of normality	Difference (ms)	Upper Limit (ms)
N20	21.75	21.75	24.16	0.00	1.61
P22			25.22		0.55
N25			26.77		1.42
P27	28.75	28.25	35.74	0.50	3.85
N33	36.00	33.25	43.53	2.75	6.27
P42	U	40.00	54.75		7.88

Component Amplitude	Patient Data (uV)		Lower limit	Interhemisphere Amplitude	Interhemisphere Amp. Diff.
	Right limb	Left limb	of normality	Difference (uV)	Upper Limit (uV)
0-N20	1.17	0.42	0.32	0.75	2.27
N20-P27	1.55	1.95	0.50	-0.40	5.49
P27-N33	0.80	1.27	0.44	-0.47	5.78
N33-P42		0.90	0.24		4.55

Table 5.2.1

Comparison of latencies and amplitudes with normality limits from control group.
Lower limit of normality for amplitude of control group calculated as 50% of minimum recorded value.
U = unclear peak - no precise latency and morphology determination.
Ab = component peak appears to be entirely absent.
Bold figures indicate data which exceeds upper limits of normality.
Interhemisphere differences calculated as (Right-Left) limb data.

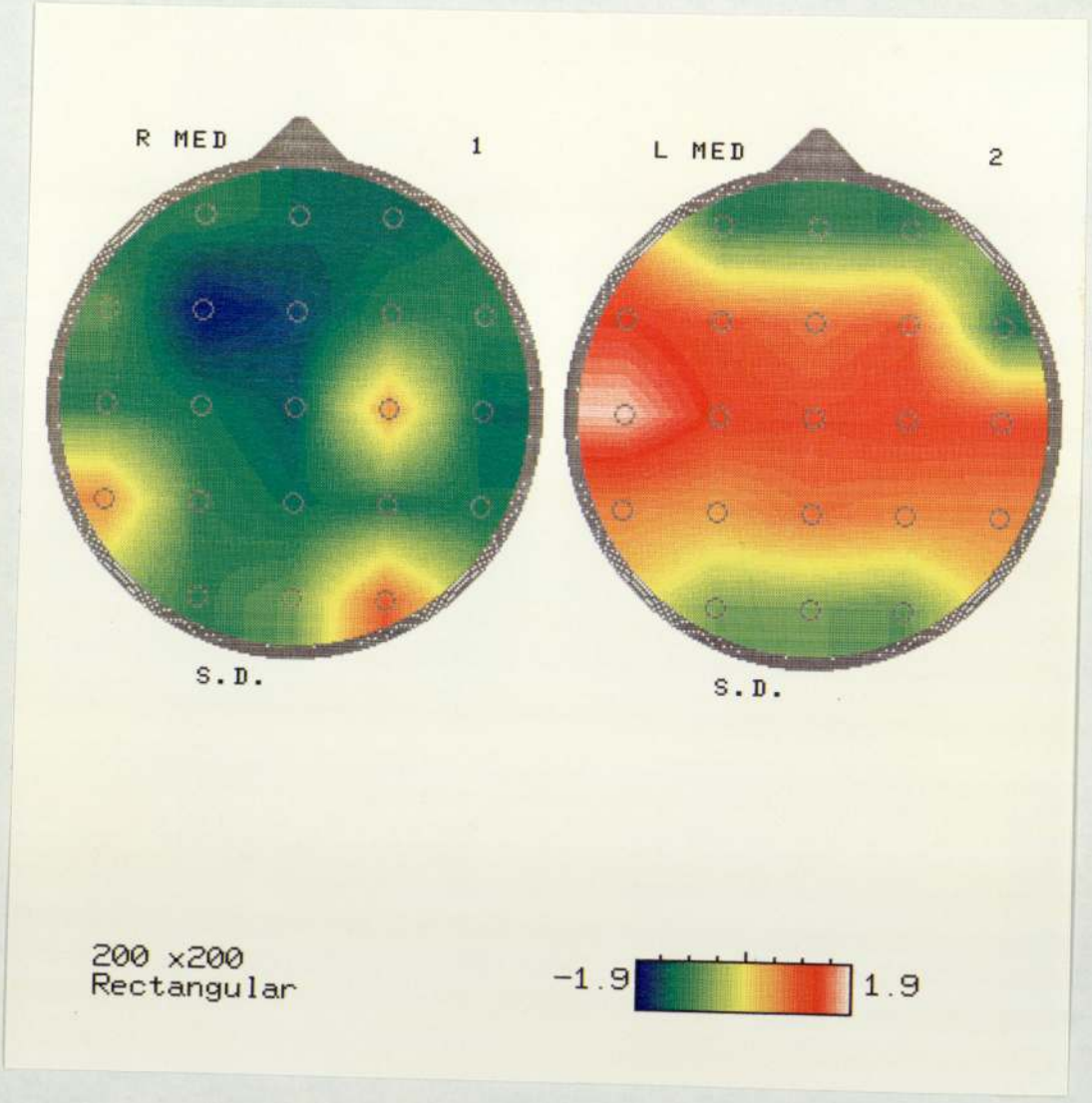

Figure 5.2. Statistical mapping of patient P1.

Maps indicate (from left to right) maximum standard deviation across entire waveform for right median and left median stimulation compared to the control group mean waveform.

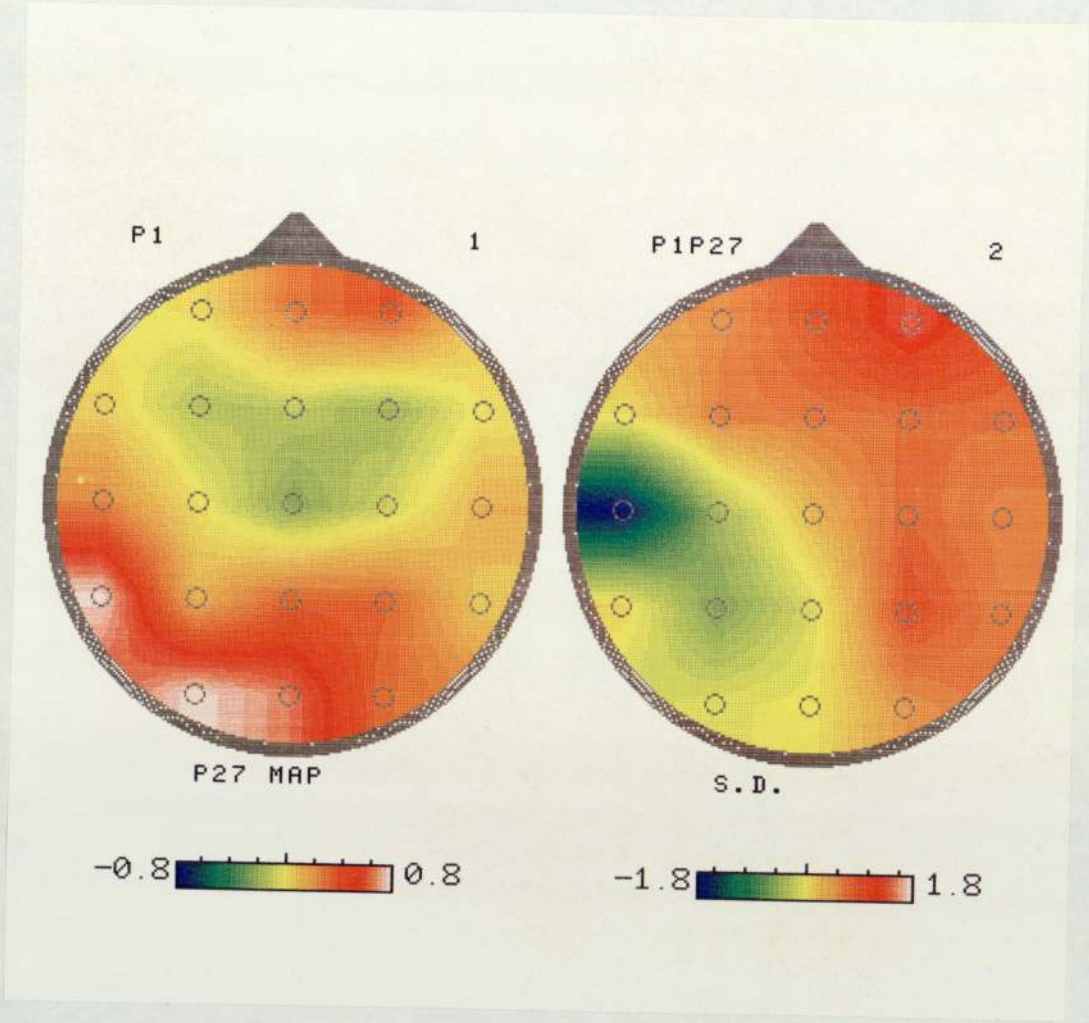

Figure 5.3. The first map (left) indicates the distribution of potential of the patients (P1) P27 component map to right median nerve stimulation. The second map (right) indicates the distribution of standard deviation when comparing the patient map to the control group mean P27 map.

5.3.1.3. Summary and conclusion of P1 results.

The left hemisphere parieto-occipital infarction seen in this patient may have resulted in the attenuation of the P27-N33-P42 complex recorded in this hemisphere and possibly modified the morphology of the central components. The degree of attenuation seen did not exceed limits of normality of the control group data however. No abnormality of waveform or map was indicated from the statistical mapping employed from the control group databases.

5.3.2.0 Patient 2 (P2) results.

5.3.2.1. P2 Clinical presentation.

This 38 year old male patient was admitted to hospital in October 1987 presenting with left sided weakness and some loss of sensation most notably in the left lower limb. A CT scan revealed a right hemisphere internal capsular area infarction (Figure 5.4). Angiography failed to reveal evidence of a lesion.

When reviewed as an outpatient in August 1988 there had been an improvement in clinical condition. There was no evidence of any sensory deficit although some weakness was detected in the left upper limb with brisk reflexes in both the left upper and lower limb. This data is summarised in Table 5.3.

Table 5.3 Clinical Summary for Patient P2

	UPPER LIMB		LOWER LIMB	
	Right	Left	Right	Left
Power	Normal	4/5	Normal	Normal
Tone	Normal	Normal	Normal	Normal
Reflex	Normal	▲	Normal	▲
Pain	Normal	Normal	Normal	Normal
Temp.	Normal	Normal	Normal	Normal
Touch	Normal	Normal	Normal	Normal
Vibration	Normal	Normal	Normal	Normal
Position	Normal	Normal	Normal	Normal
2 Point dis.	Normal	Normal	Normal	Normal
Stereognosis	Normal	Normal	Normal	Normal

Direction of arrow indicates an increase (upward) or decrease (downward) of sensory or motor function.
In the case of reflex activity an upward arrow indicates hyperreflexia.

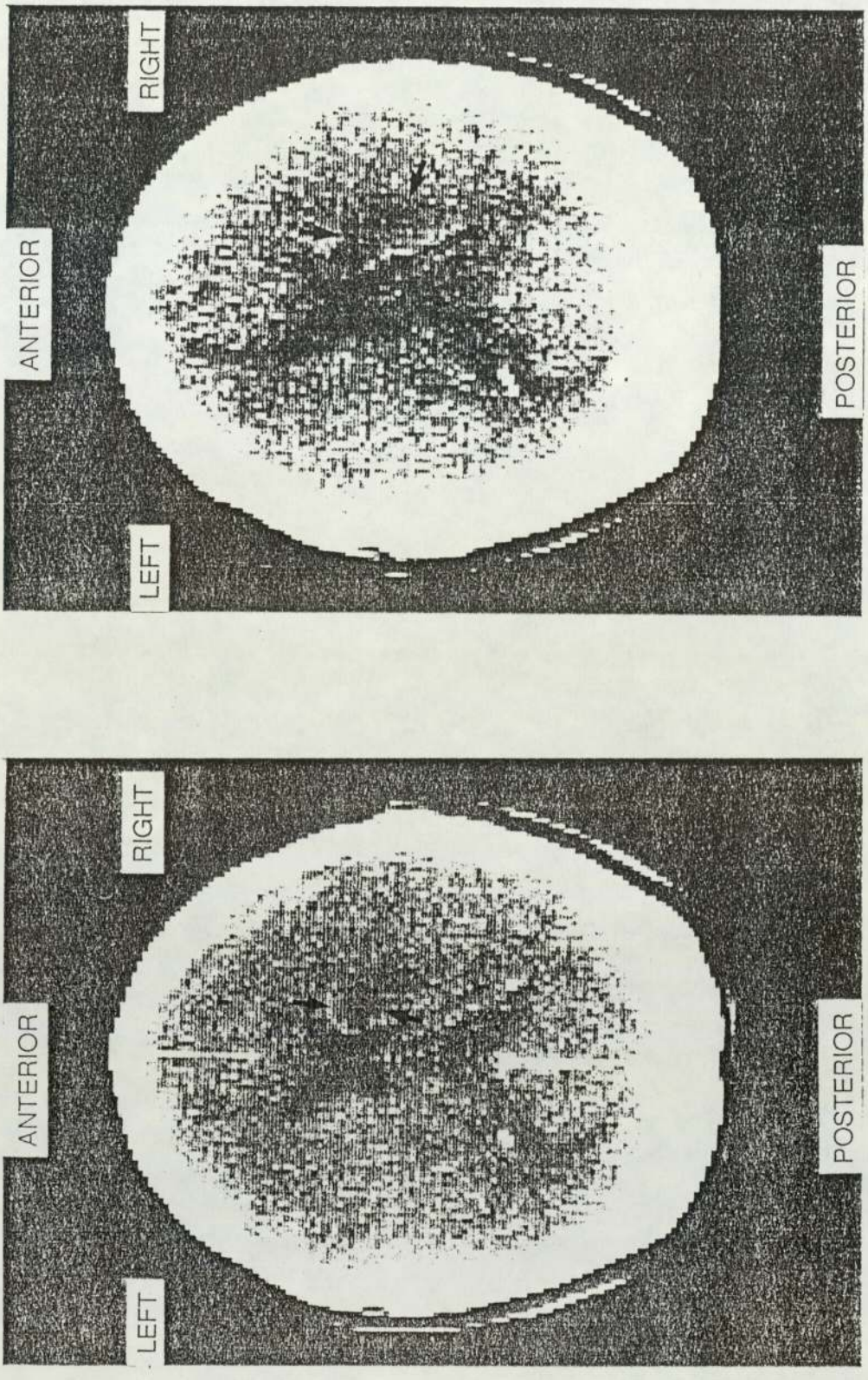

Figure 5.4. CT Scan for patient P2. Arrows indicate lesion site.

5.3.2.2. P2 SEP results.

SEP's were recorded from this patient in August 1988.

Subjective inspection of waveforms (Figure 5.5) revealed poorly formed frontal components bilaterally with P14, N17 and N43 the only clear components. C and P types I occurred bilaterally.

No obvious asymmetries were observed and this was confirmed by component latency and amplitude analysis tabulated in Table 5.4 where no abnormalities were seen (<2.5 standard deviation).

Comparison with group mean waveforms using the Z statistic revealed a maximum standard deviation to right limb stimulation of 2.50 (P4 location) and 2.25 standard deviations at the O1 electrode location to left limb stimulation (Figure 5.6).

Fz reference derivations also seen in Figure 5.5 reflected the basic symmetry between waveforms if slightly 'noisier' with right limb stimulation. All peak latency and peak to peak amplitudes of these components were within normal limits.

5.3.2.3. Summary and conclusion of P2 results.

Normal SEP waveforms and contour maps in this patient coincided with left upper limb weakness and brisk reflexes but normal sensation caused by a right hemisphere cerebral infarction.

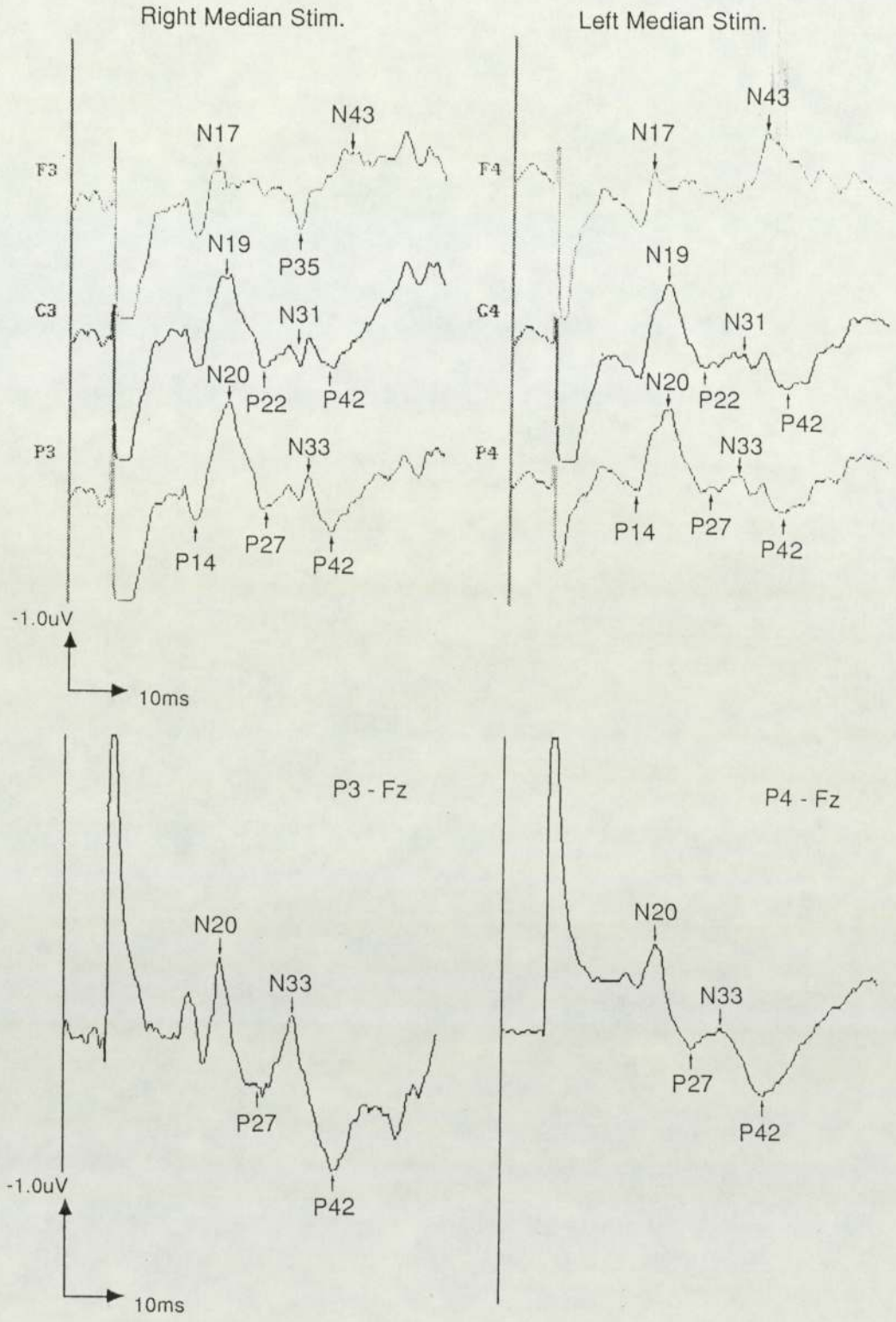

Figure 5.5. SEP waveforms for Patient 2 (P2) for right and left median nerve stimulation. Fz reference derived potentials are shown beneath the original earlobe reference recordings.

Patient: P2
Age (years): 39
Height (cm): 173

Component	Patient Data (ms)		Upper limit	Interhemisphere Latency	Interhemisphere Latency Diff.
	Right limb	Left limb	of normality	Difference (ms)	Upper Limit (ms)
Erbs	10.25	10.25	11.66	0.00	0.49
P14	14.00	14.00	16.41	0.00	1.61
N17	17.25	16.00	20.12	1.25	1.83
N19	18.75	18.75	20.92	0.00	1.70
N20	19.50	19.00	21.84	0.50	1.72
P20	19.75	19.00	24.13	0.75	3.56
P22	25.50	25.00	25.72	0.50	3.79
N23	-	-	26.98	0.00	1.79
P27	26.25	26.50	35.96	-0.25	4.32
N30	U	U	37.85	0.00	4.64
N31	33.25	30.75	36.65	2.50	3.90
N33	33.25	31.00	40.52	2.25	4.23
P35	-	29.25	43.89		2.40
P42(Part)	37.25	39.00	51.58	-1.75	3.84
N43	-	35.50	54.34		4.68
Erbs-P14	3.75	3.75	5.92		
N17-P20	2.50	3.00	5.34		
N19-P22	6.75	6.25	7.02		
P14-N20	5.50	5.00	7.16		

Component Amplitude	Patient Data (uV)		Lower limit	Interhemisphere Amplitude	Interhemisphere Amp. Diff.
	Right limb	Left limb	of normality	Difference (uV)	Upper Limit (uV)
Frontal comps.					
0-P14	1.02	0.98	0.09	0.04	1.54
P14-N17	0.84	1.20	0.12	-0.36	1.31
N17-P20	0.22	0.31	0.04	-0.09	1.52
P20-N30	U	U	0.08	0.00	2.55
Central comps.					
0-P14	0.83	1.22	0.09	-0.39	1.27
P14-N19	1.62	2.10	0.06	-0.48	1.94
N19-P22	1.60	1.83	0.22	-0.23	3.04
P22-N31	0.53	0.24	0.01	0.29	3.31
N31-P42	0.57	0.68	0.28	-0.11	5.32
Parietal comps.					
0-P14	1.04	0.53	0.02	0.51	1.35
P14-N20	2.18	1.75	0.36	0.43	2.73
N20-P27	1.87	1.63	0.41	0.24	3.34
P27-N33	0.49	0.24	0.08	0.25	4.12
N33-P42	0.98	0.81	0.30	0.17	3.78

Table 5.4 Comparison of latencies and amplitudes with normality limits from control group. Lower limit of normality for amplitude of control group calculated as 50% of minimum recorded value.
U = unclear peak - no precise latency and morphology determination.
Ab = component peak appears to be entirely absent.
Bold figures indicate data which exceeds upper limits of normality.
Interhemisphere differences calculated as (Right-Left) limb data.

Patient: P2 **Fz reference derived potentials**
Age: 39
Height: 173

Component	Patient Data (ms)		Upper limit	Interhemisphere Latency	Interhemisphere Latency Diff.
	Right limb	Left limb	of normality	Difference (ms)	Upper Limit (ms)
N20	19.25	18.75	23.01	0.50	1.61
P22			25.22	0.00	0.55
N25			26.77	0.00	1.42
P27	26.50	25.00	35.74	1.50	3.85
N33	31.50	29.50	43.53	2.00	6.27
P42	39.00	37.00	54.75	2.00	7.88

Component	Patient Data (uV)		Lower limit	Interhemisphere Amplitude	Interhemisphere Amp. Diff.
Amplitude	Right limb	Left limb	of normality	Difference (uV)	Upper Limit (uV)
0-N20	1.00	1.64	0.32	-0.64	2.27
N20-P27	2.36	2.22	0.50	0.14	5.49
P27-N33	2.78	0.39	0.44	2.39	5.78
N33-P42	2.88	1.49	0.24	1.39	4.55

Table 5.4.1

Comparison of latencies and amplitudes with normality limits from control group.
Lower limit of normality for amplitude of control group calculated as 50% of minimum recorded value.
U = unclear peak - no precise latency and morphology determination.
Ab = component peak appears to be entirely absent.
Bold figures indicate data which exceeds upper limits of normality.
Interhemisphere differences calculated as (Right-Left) limb data.

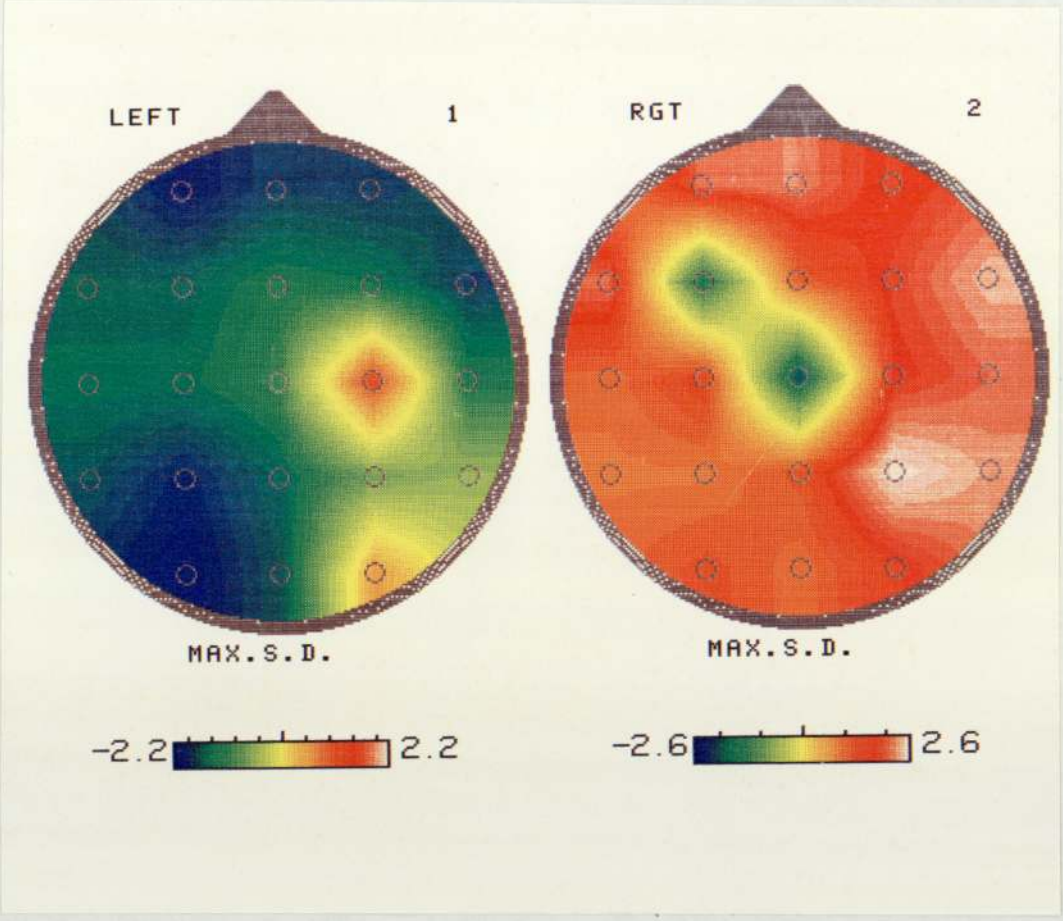

Figure 5.6. Statistical mapping of P2.

Maps indicate (from left to right) maximum standard deviation across entire waveform for right median and left median stimulation.

5.3.3.0. Patient 3 (P3) results.

5.3.3.1. P3 clinical presentation.

This 75 year old gentleman presented in August 1988 with a history of paraesthesia and involuntary movements of the left thumb and index finger. There was no Jacksonian progression although the patient reported occasional twitching of the left side of the neck unassociated with the twitching in the hand. On examination, there was a loss of position sense and 2 point discrimination in the left hand with a possible slight loss of stereognosis (Table 5.5.). A CT scan at high convexity revealed a right centro-parietal lesion with oedema (Figure 5.7).

On the 15th of August, the tumour was excised through a craniotomy. The histology showed a highly cellular poorly differentiated malignant tumour. Following surgery, he developed a mild hemiparesis and the sensory deficit remained unchanged.

5.3.3.2. P3 SEP results.

Subjective inspection of waveforms showed attenuation of frontal and parietal components to left median nerve stimulation compared to the right (Figure 5.8). There appeared to be no significant difference in morphology of the frontal components but both central and parietal locations reveal marked morphological differences between hemispheres. The familiar C type I and P type I components recorded from right median nerve stimulation are replaced by C type III and P type III components with left limb stimulation.

The dominant feature however was the marked amplitude increase of the left limb P22 component co-existing with the relative attenuation of all other components compared to their right limb component counterparts.

Analysis of component latency and amplitude data shown in Table 5.6 indicates the significant peak latency difference of the N31 and N33 components between hemispheres.

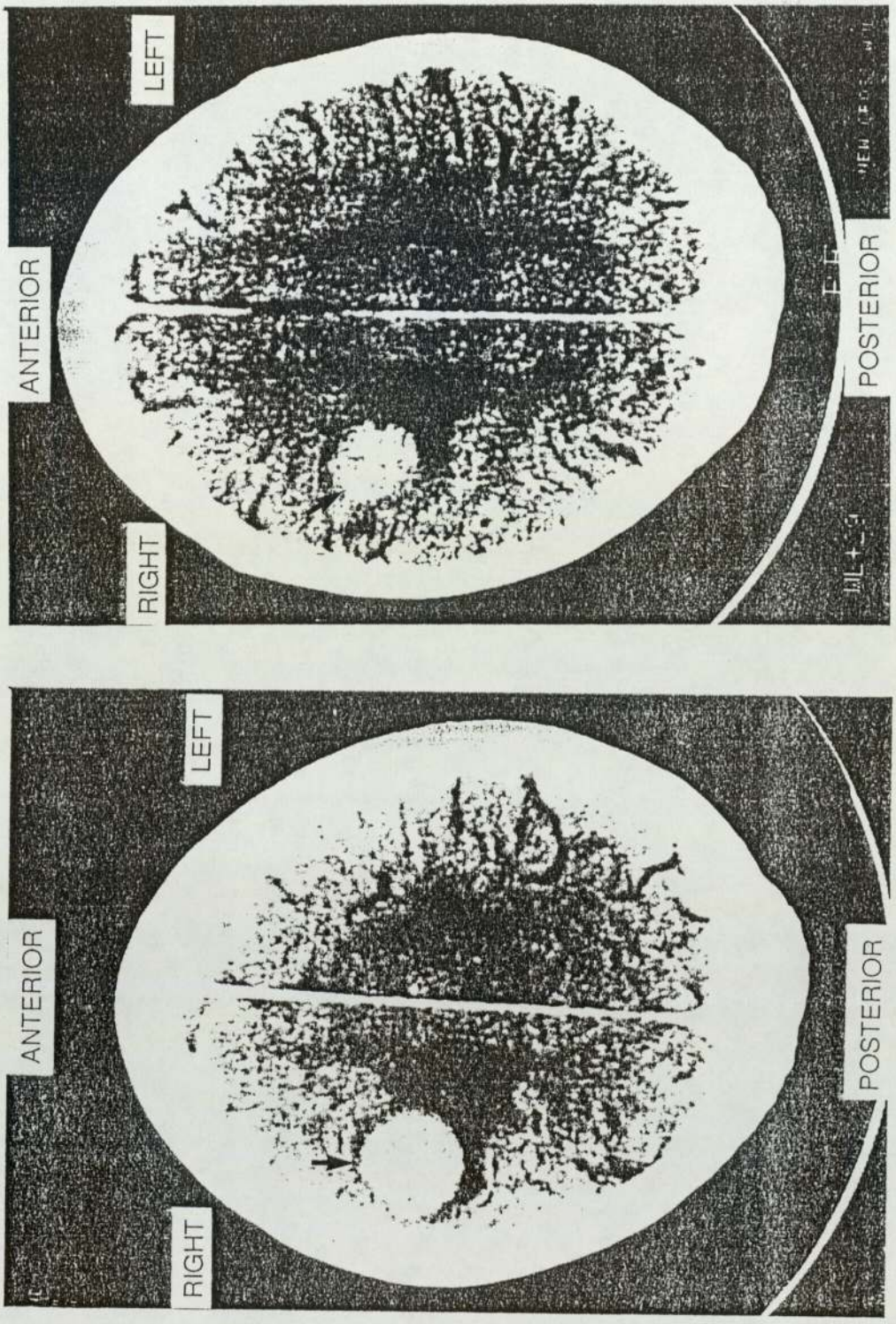

Figure 5.7. CT Scans for patient P3. Arrows indicate site of lesion.

Table 5.5 Clinical Summary for Patient P3

	UPPER LIMB		LOWER LIMB	
	Right	Left	Right	Left
Power	Normal	Normal	Normal	Normal
Tone	Normal	Normal	Normal	Normal
Reflex	Normal	Normal	Normal	Normal
Pain	Normal	Normal	Normal	Normal
Temp.	Normal	Normal	Normal	Normal
Touch	Normal	Normal	Normal	Normal
Vibration	Normal	Normal	Normal	Normal
Position	Normal	↓	Normal	Normal
2 Point dis.	Normal	↓	Normal	Normal
Stereognosis	Normal	↓ ?	Normal	Normal

Direction of arrow indicates an increase (upward) or decrease (downward) of sensory or motor function.
A question mark alongside a category indicates inconsistent findings on a trial / re-trial basis.

In the amplitude domain, the difference between the right and left N19-P22 complex was within normal limits whereas the P22-N31 amplitude and right/left amplitude difference was markedly abnormal.

All other other amplitudes were within normal limits.

Comparison of the patient waveforms with the control group mean waveforms was made using the Z statistic. The standard deviation map to left median stimulation revealed a focus of abnormality at the C4 electrode corresponding to the peak of the P22 component (3.5 standard deviations) and also for the peak of the delayed N31 component (3.43 standard deviations). See Figure 5.9.

For comparison, the P22 map was compared to the group mean control P22 map, again using the Z statistic, and the resultant standard deviation map is shown in Figure 5.10. Interestingly, the standard deviation at C4 was 1.87 using this analysis with the greatest deviation occurring at the T4 electrode (2.93 standard deviations). The same procedure was adopted for comparison of the left median N31 component with the control group mean N31 map. Here, the standard deviation at the C4 electrode was 1.50 with the maximum standard deviation of 2.18 occurring at P3.

Analysis of the waveforms to right median nerve stimulation (Figure 5.11) revealed two points of abnormality - at the P3 electrode location (2.75 standard deviations) and Pz (3.06 standard deviations) coinciding with the parietal P27 component. The patient P27 component map was therefore compared to the group mean control P27 map - with this analysis no standard deviation exceeded 1.87 (Figure 5.11).

Inspection of the P3-Fz and P4-Fz reference derivations revealed the relative attenuation of the parietal components and morphology difference of right limb components compared to left, with the baseline to peak of N20 amplitude difference measure between limbs being abnormally great (>2.5 s.d.). There was of course no indication of the focal augmented P22 potential (Figure 5.12).

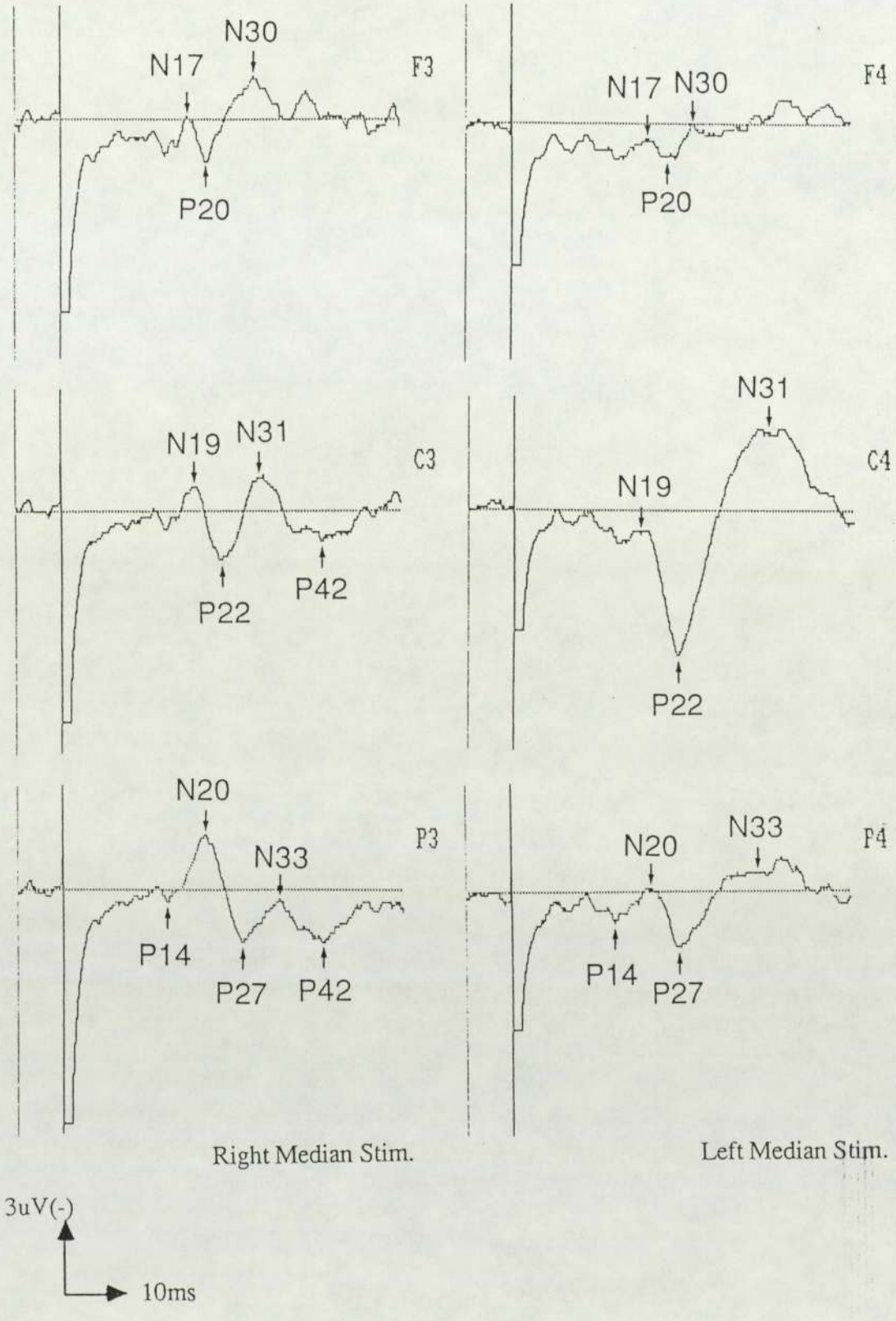

Figure 5.8. SEP waveforms for Patient 3 (P3) for right and left median nerve stimulation.

Patient: P3
Age (years): 75
Height (cm): 183

LATENCY DATA

Component	Patient Data (ms)		Upper limit	Interhemisphere Latency	Interhemisphere Latency Diff.
	Right limb	Left limb	of normality	Difference (ms)	Upper Limit (ms)
Erbs	11.75	11.50	13.38	0.25	0.49
P14	17.25	17.00	19.28	0.25	1.61
N17	21.00	22.25	23.18	-1.25	1.83
N19	21.75	20.75	23.97	1.00	1.70
N20	23.25	22.50	24.93	0.75	1.72
P20	24.00	25.75	28.35	-1.75	3.56
P22	26.25	27.00	30.37	-0.75	3.79
N23	26.00		31.84		1.79
P27	29.75	27.75	35.96	2.00	4.32
N30	32.00	30.00	37.85	2.00	4.64
N31	33.00	42.50	40.02	**-9.50**	3.90
N33	35.75	40.25	40.52	**-4.50**	4.23
P35			43.89	0.00	2.40
P42	43.25	Ab	51.58		3.84
N43			54.34	0.00	4.68
Erbs-P14	5.50	5.50	7.17		
N17-P20	3.00	3.50	6.70		
N19-P22	4.50	6.25	8.60		
P14-N20	6.00	5.50	7.70		

AMPLITUDE DATA

Component	Patient Data (uV)		Upper limit	Interhemisphere Amplitude	Interhemisphere Amp. Diff.
Amplitude	Right limb	Left limb	of normality	Difference (uV)	Upper Limit (uV)
Frontal comps.					
0-P14	1.49	1.61	2.61	-0.12	1.54
P14-N17	1.49	0.92	2.38	0.57	1.31
N17-P20	1.89	0.73	2.75	1.16	1.52
P20-N30	3.70	1.32	7.00	2.38	2.55
Central comps.					
0-P14	0.73	1.47	1.93	-0.74	1.27
P14-N19	1.81	0.41	3.20	1.40	1.94
N19-P22	3.14	5.14	8.05	-2.00	3.04
P22-N31	3.48	**9.46**	9.32	**-5.98**	3.31
N31-P42	2.72	Ab	9.03		5.32
Parietal comps.					
0-P14	0.46	1.22	1.89	-0.76	1.35
P14-N20	2.72	1.22	5.23	1.50	2.73
N20-P27	4.44	2.36	8.29	2.08	3.34
P27-N33	1.76	3.13	6.60	-1.37	4.12
N33-P42	1.88	Ab	7.38		3.78

Table 5.6 Comparison of latencies and amplitudes with normality limits from control group.
Lower limit of normality for amplitude of control group calculated as 50% of minimum recorded value.
U = unclear peak - no precise latency and morphology determination.
Ab = component peak appears to be entirely absent.
Bold figures indicate data which exceeds upper limits of normality.
Interhemisphere differences calculated as (Right-Left) limb data.

Patient: P3 **Fz reference derived potentials**
Age: 75
Height: 183

Component	Patient Data (ms)		Upper limit	Interhemisphere Latency	Interhemisphere Latency Diff.
	Right limb	Left limb	of normality	Difference (ms)	Upper Limit (ms)
N20	23.50	23.75	25.84	-0.25	1.61
P22			25.22	0.00	0.55
N25			26.77	0.00	1.42
P27	30.00	29.00	35.74	1.00	3.85
N33	36.25	39.25	43.53	-3.00	6.27
P42	42.00	U	54.75		7.88

Component	Patient Data (uV)		Upper limit	Interhemisphere Amplitude	Interhemisphere Amp. Diff.
Amplitude	Right limb	Left limb	of normality	Difference (uV)	Upper Limit (uV)
0-N20	4.04	1.11	6.46	**2.93**	2.27
N20-P27	6.73	3.35	14.40	3.38	5.49
P27-N33	2.24	3.52	11.35	-1.28	5.78
N33-P42	1.98	-	9.35		4.55

Table 5.6.1

Comparison of latencies and amplitudes with normality limits from control group.
Lower limit of normality for amplitude of control group calculated as 50% of minimum recorded value.
U = unclear peak - no precise latency and morphology determination.
Ab = component peak appears to be entirely absent.
Bold figures indicate data which exceeds upper limits of normality.
Interhemisphere differences calculated as (Right-Left) limb data.

Figure 5.9. **Overleaf**. Maps show left median P22 map for patient 3 (top left), the distribution of standard deviation compared to the control group mean waveform (top right), the patient N31 map (bottom left) and the distribution of standard deviation compared to the control group mean waveform (bottom right).

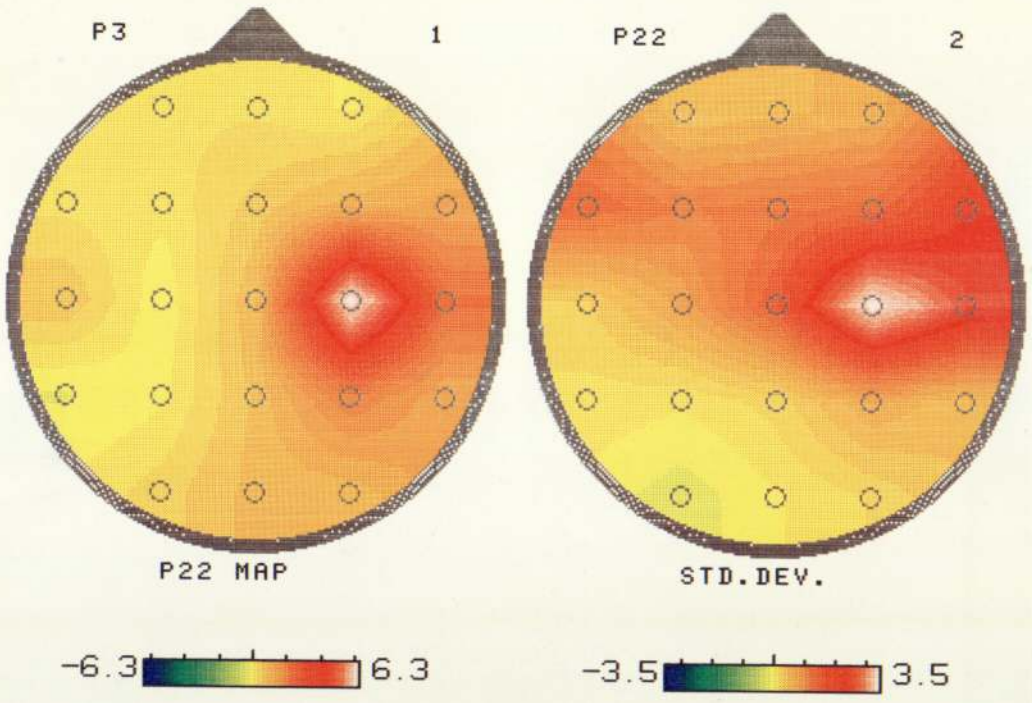
P3
1
P22
2
P22 MAP
STD.DEV.
-6.3
6.3
-3.5
3.5

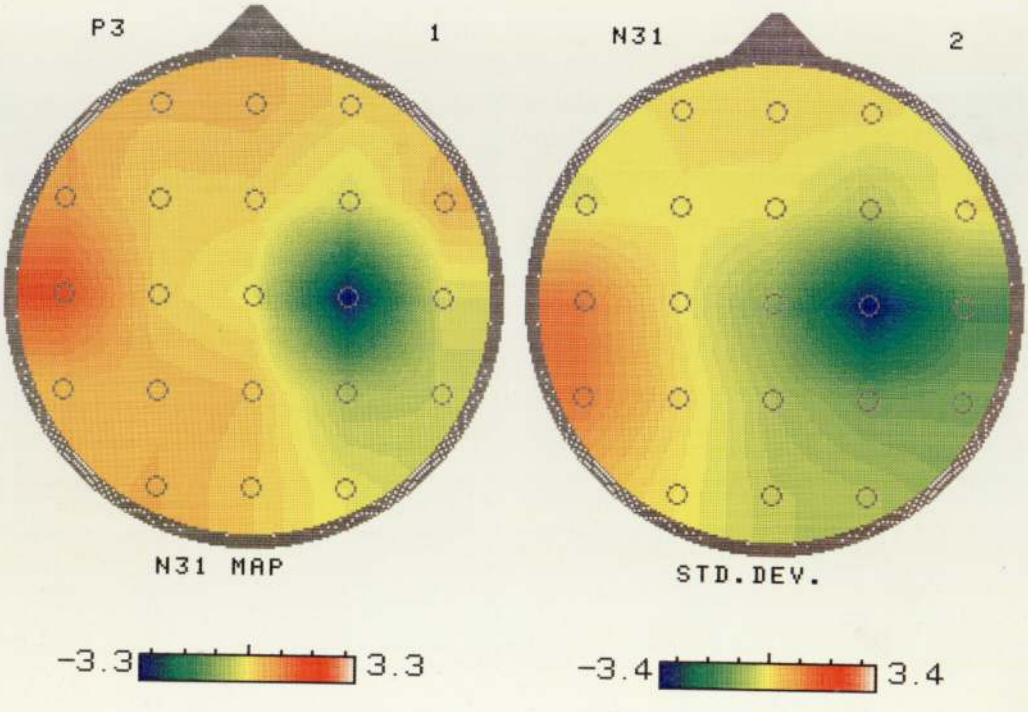
P3
1
N31
2
N31 MAP
STD.DEV.
-3.3
3.3
-3.4
3.4

Figure 5.10. Overleaf. Maps show left median P22 map for patient 3 (top left); the distribution of standard deviation compared to the control group mean P22 map (top right); the patient N31 map (bottom left) and the distribution of standard deviation compared to the control group mean N31 map (bottom right).

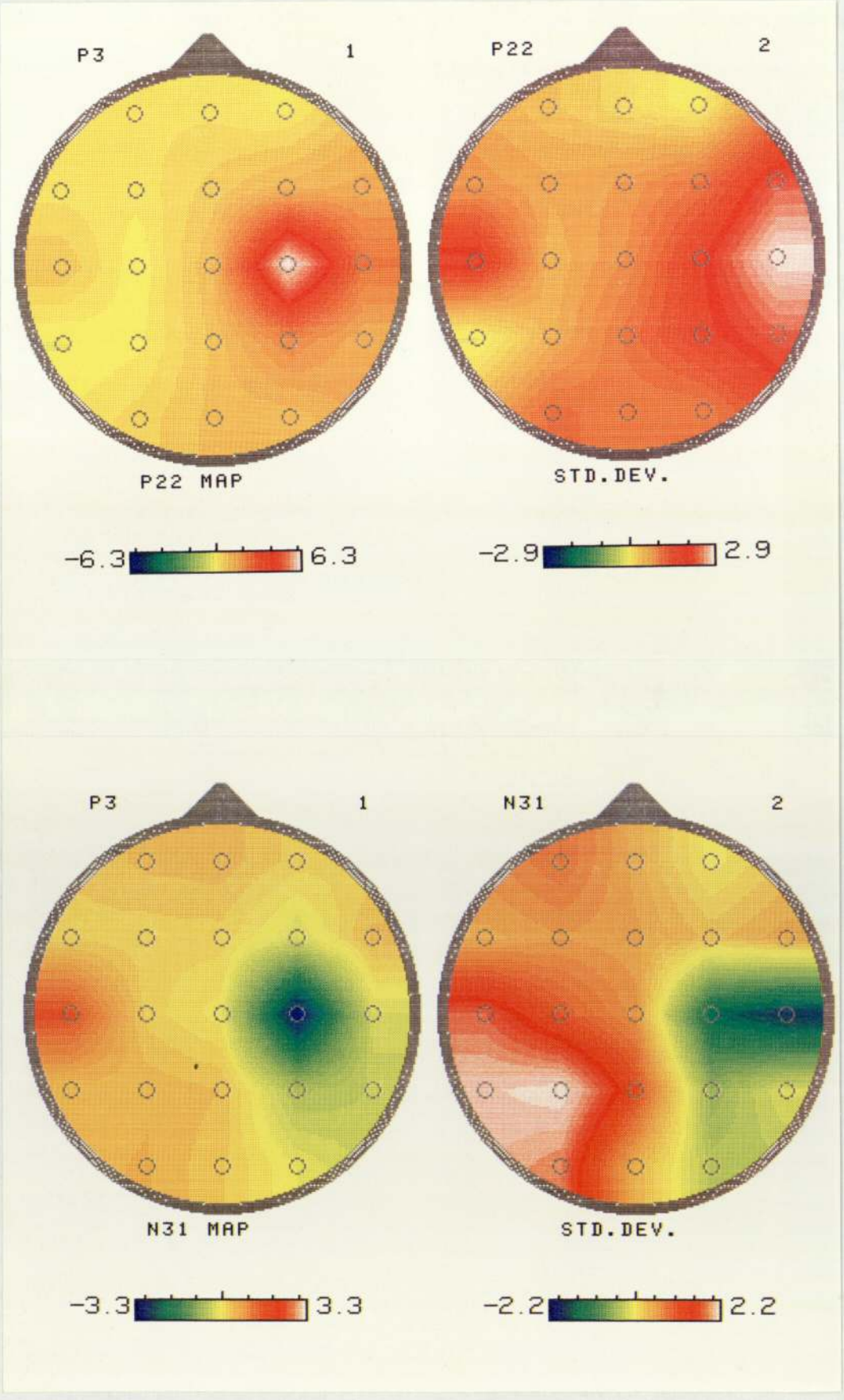
P3
1
P22
2
P22 MAP
STD.DEV.
-6.3
6.3
-2.9
2.9
P3
1
N31
2
N31 MAP
STD.DEV.
-3.3
3.3
-2.2
2.2

Figure 5.11. Overleaf. Maps show right median P27 map for patient 3 (left), the distribution of standard deviation compared to the control group mean waveform (middle) and the distribution of standard deviation compared to the control group mean P27 map.

P3
1
P27 MAP
-2.2
2.2
P27
2
WAVE S.D.
-3.1
3.1
P27
3
MAP S.D.
-1.9
1.9

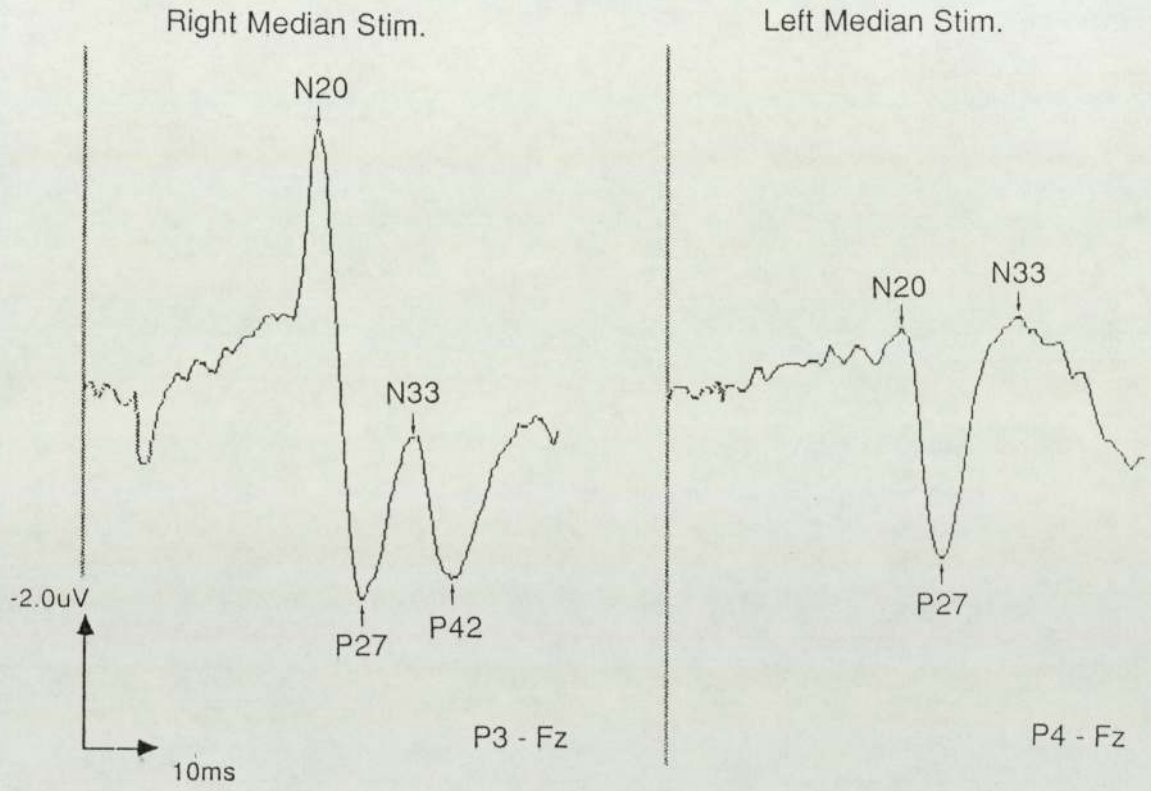

Figure 5.12. Fz derived potentials for patient P3.

5.3.3.3. Summary and conclusion of P3 results.

This patient presented with a large right hemisphere peri-rolandic space occupying lesion resulting in a decrease of position sense, two point discriminative touch and stereognosis in the left upper limb. Involuntary movement of the left thumb and index finger was reported.

SEP abnormalities were an augmentation of the right hemisphere P22 component co-existing with relative attenuation of all other right hemisphere components. Right hemisphere central N31-P42 and parietal N33-P42 complexes were 'replaced' with single negativities whose peak latencies were significantly delayed compared to their left hemisphere counterparts. The augmented P22-N31 complex represented a 'giant' potential in relation to the control group (>2.5 standard deviations).

It is important to note that the morphology difference seen between right and left hemisphere central and parietal components was not seen in any control individual.

Statistical mapping using the control group mean waveform data indicated the significant abnormality of the right hemisphere P22 and N31 components (>3.0 standard deviations). However, statistical mapping using the control group P22 and N31 maps revealed a shift in the locus of abnormality in the case of P22 from C4 to T4. In the case of N31, no abnormality was detected at any location with a maximum standard deviation of 2.18 occurring at the ipsilateral site P3.

Some disparity between the maps may be explained by comparing the age and height of this particular patient with that of the control group. At 75 years of age, patient P3 would clearly fall into the control group 'old age' category; the mean height of the old age grouping was 165.6cm with a maximum recorded height of 181cm. Patient P3 measured 183cm. The standard deviations indicated by the waveform statistical mapping for P22 was invariably the product of both the unusual amplitude and latency of this component in comparison to the control group.We know from the control group data that the latency of P22 is dependent on both age and height factors. The base line to peak amplitude of the augmented P22 was not significantly great at the C4 electrode (<2.5 standard deviations), and this is reflected in the

group mean map analysis where with this 'latency independent measure' the augmentation only reached significance at the adjacent electrode (T4).

These findings would explain the disparity between control data, statistical waveform maps and statistical component maps for the left hemisphere P27 component, i.e. the apparent P27 abnormality seen on waveform analysis was an 'artefact' caused by the disparity of patient age and height with that of the control group.

5.3.4.0. Patient 4 (P4) results.

5.3.4.1. P4 clinical presentation.

This 34 year old male patient presented in August 1988 with sudden onset of weakness and numbness of the left limbs. As well as some unco-ordination of left arm movement, there was deterioration of vision in the right eye. A summary of clinical findings are shown in Table 5.7.

Angiography and a CT scan revealed multiple small vessel infarctions in the patients right cerebral hemisphere.

A diagnosis of embolic infarctions affecting the territory of the right middle cerebral artery together with a right retinal artery embolism was made.

The patient was later to undergo an endarterctomy.

Table 5.7 Clinical Summary for Patient P4

	UPPER LIMB		LOWER LIMB	
	Right	Left	Right	Left
Power	Normal	↓	Normal	↓
Tone	Normal	↓	Normal	↓
Reflex	Normal	↑	Normal	↑
Pain	Normal	Normal	Normal	Normal
Temp.	Normal	Normal	Normal	Normal
Touch	Normal	Normal	Normal	Normal
Vibration	Normal	Normal	Normal	Normal
Position	Normal	↓	Normal	Normal
2 Point dis.	Normal	↓	Normal	Normal
Stereognosis	Normal	Normal	Normal	Normal

Direction of arrow indicates an increase (upward) or decrease (downward) of sensory or motor function.
In the case of reflex activity an upward arrow indicates hyperreflexia.

5.3.4.2. P4 SEP results.

SEP recordings in this patient (August 1988) were slightly marred by a large stimulus artefact tending to drive the baseline in a negative (upward) direction in the early part of the potentials. However, clear components were consistently recorded and the artefact did not prevent component classification to be made (Figure 5.13).

The morphology of the frontal components were very similar between right and left limb stimulation - that of the FI V type. Centrally and parietally there appeared to be a marked morphology difference with C type I and P type I occurring to right limb stimulation and C type III and P type III to left median stimulation. Thus, centrally the N19 components were bilaterally very similar but to left median stimulation, P22 and N31 components appeared shifted in latency compared to the right limb counterparts as did the P27 and N33 components parietally. It should be noted that in both right and left limb / hemisphere P22 and P27 components, a notch was seen in the descending limb of each waveform. This feature was not however consistently seen in repeat trials and peaks were identified as accurately as possible on the trail -re-trial basis. It was considered that the identified peaks equated to the correct counterpart in the opposite hemisphere.

The component differences were highlighted in Table 5.8 where the left limb P22 component latency was abnormally prolonged as were the N33 peak latency and N19-P22 interpeak latency. There was a significant latency difference between sides of the N31 and N33 components. P27 was not significantly delayed with a difference of 3.5ms between sides.

Comparison of the patient right and left limb waveforms with control group mean waveforms using the Z statistic yielded no data point which exceeded 2.5 standard deviations (except for the artefactual epoch between the stimulus and P14 component which was ignored). It was considered that the P22 map to left median stimulation might deviate significantly from the group mean P22 map, but comparison using the Z statistic revealed a maximum deviation of 2.43 and that at the ipsilateral P3 location (see Figure 5.14).

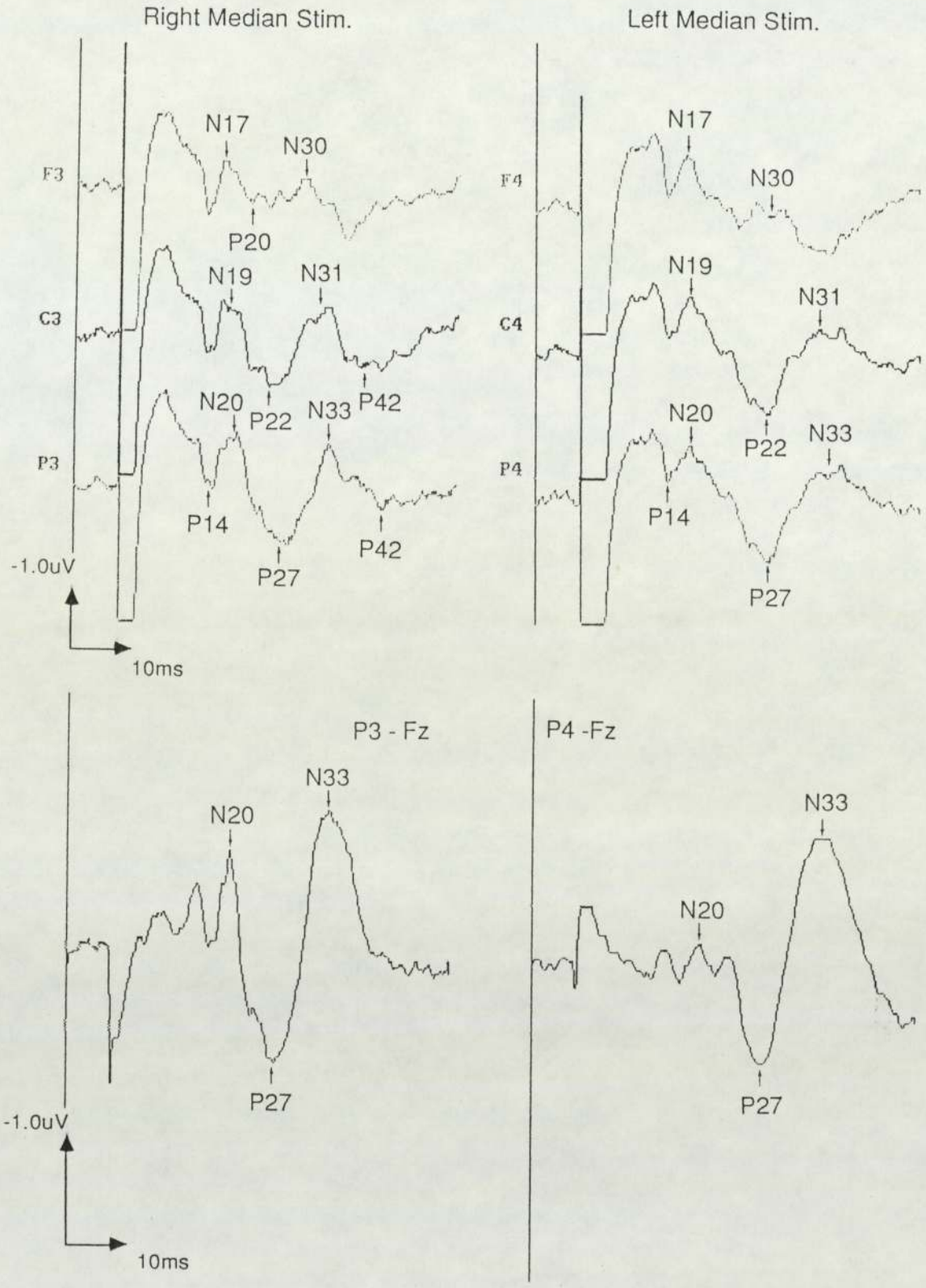

Figure 5.13. SEP waveforms for Patient 4 (P4) for right and left median nerve stimulation.Fz reference derived potentials are shown beneath the original earlobe reference recordings.

Patient: P4
Age (years): 34
Height (cm): 180

LATENCY DATA

Component	Patient Data (ms)		Upper limit	Interhemisphere Latency	Interhemisphere Latency Diff.
	Right limb	Left limb	of normality	Difference (ms)	Upper Limit (ms)
Erbs	11.00	10.50	11.96	0.50	0.50
P14	15.00	14.50	16.97	0.50	1.61
N17	17.25	17.75	20.75	-0.50	1.83
N19	18.50	18.25	21.39	0.25	1.70
N20	19.25	18.25	22.29	1.00	1.72
P20	21.50	U	24.66		3.56
P22	23.75	**30.75**	26.04	**-7.00**	3.79
N23		U	27.33	0.00	1.79
P27	27.50	31.00	35.96	-3.50	4.32
N30	30.50	31.25	37.85	-0.75	4.64
N31	34.50	39.75	37.38	**-5.25**	3.90
N33	35.00	**41.25**	40.52	**-6.25**	4.23
P35		39.75	43.89		2.40
P42	43.75	Ab	51.58		3.84
N43			54.34		4.68
Erbs-P14	4.00	4.00	6.19		
N17-P20	4.25	U	5.15		
N19-P22	5.25	**12.50**	6.80		
P14-N20	4.25	3.75	7.09		

AMPLITUDE DATA

Component Amplitude	Patient Data (uV)		Lower limit	Interhemisphere Amplitude	Interhemisphere Amp. Diff.
	Right limb	Left limb	of normality	Difference (uV)	Upper Limit (uV)
Frontal comps.					
0-P14	0.26	0.10	0.09	0.16	1.54
P14-N17	0.72	0.70	0.12	0.02	1.31
N17-P20	0.73	1.20	0.04	-0.47	1.52
P20-N30	0.47	1.49	0.08	-1.02	2.55
Central comps.					
0-P14	0.24	0.10	0.09	0.14	1.27
P14-N19	0.62	0.81	0.06	-0.19	1.94
N19-P22	0.98	2.12	0.22	-1.14	3.04
P22-N31	1.03	1.52	0.01	-0.49	3.31
N31-P42	0.91	Ab	0.28		5.32
Parietal comps.					
0-P14	0.09	0.03	0.02	0.06	1.35
P14-N20	0.76	0.66	0.36	0.10	2.73
N20-P27	1.78	2.05	0.41	-0.27	3.34
P27-N33	1.69	1.47	0.08	0.22	4.12
N33-P42	1.12	Ab	0.30		3.78

Table 5.8 Comparison of latencies and amplitudes with normality limits from control group. Lower limit of normality for amplitude of control group calculated as 50% of minimum recorded value.
U = unclear peak - no precise latency and morphology determination.
Ab = component peak appears to be entirely absent.
Bold figures indicate data which exceeds upper limits of normality.
Interhemisphere differences calculated as (Right-Left) limb data.

Patient: P4 **Fz reference derived potentials**
Age: 34
Height: 180

Component	Patient Data (ms)		Upper limit	Interhemisphere Latency	Interhemisphere Latency Diff.
	Right limb	Left limb	of normality	Difference (ms)	Upper Limit (ms)
N20	19.50	20.25	23.54	-0.75	1.61
P22			25.22	0.00	0.55
N25			26.77	0.00	1.42
P27	27.00	30.50	35.74	-3.50	3.85
N33	36.25	40.50	43.53	-4.25	6.27
P42	A	A	54.75		7.88

Component Amplitude	Patient Data (uV)		Lower limit	Interhemisphere Amplitude	Interhemisphere Amp. Diff.
	Right limb	Left limb	of normality	Difference (uV)	Upper Limit (uV)
0-N20	1.22	0.42	0.32	0.80	2.27
N20-P27	1.89	1.05	0.50	0.84	5.49
P27-N33	2.27	2.01	0.44	0.26	5.78
N33-P42	-		0.24	0.00	4.55

Table 5.8.1

Comparison of latencies and amplitudes with normality limits from control group.
Lower limit of normality for amplitude of control group calculated as 50% of minimum recorded value.
U = unclear peak - no precise latency and morphology determination.
Ab = component peak appears to be entirely absent.
Bold figures indicate data which exceeds upper limits of normality.
Interhemisphere differences calculated as (Right-Left) limb data.

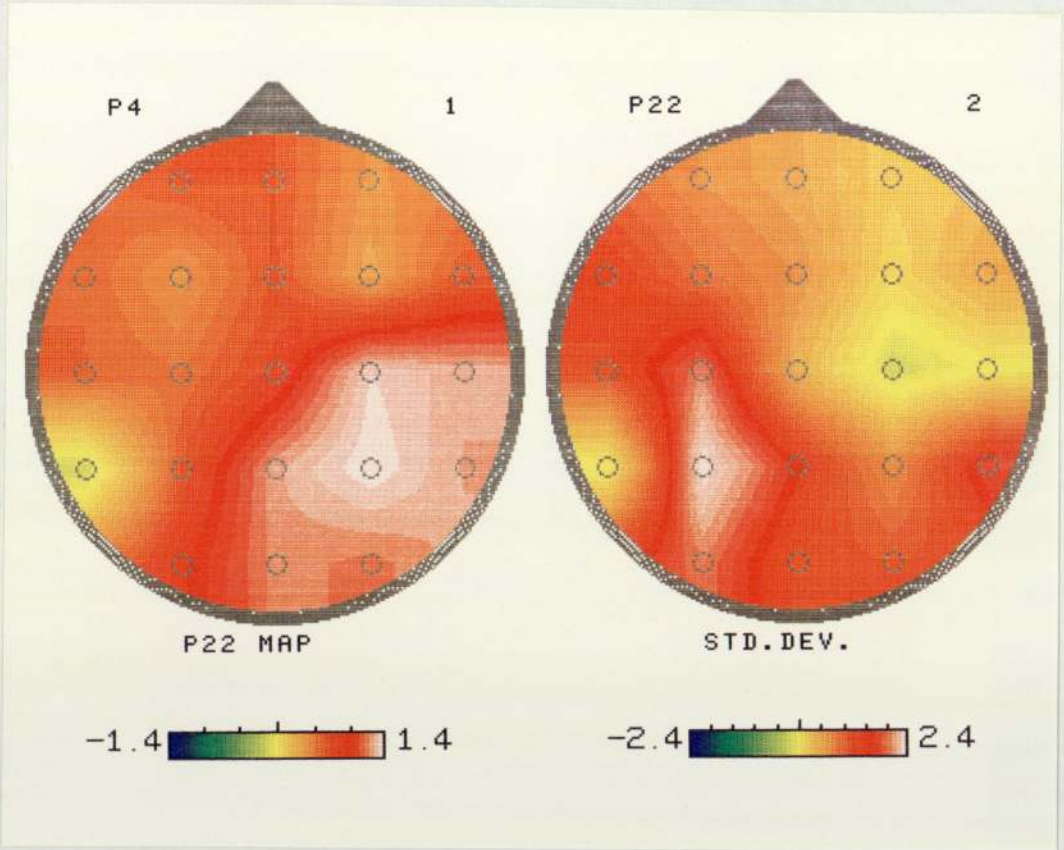

Figure 5.14. Patient P4 P22 map (left) and standard deviation map formed by comparison with control group mean P22 map (right).

Subjective analysis of Fz reference derivations reflected the latency shift seen to left median stimulation (Figure 5.13). Actual peak latency and peak to peak amplitudes were all within normal limits.

5.3.4.3. Summary and conclusions of P4 results.

Left limb weakness with some sensory loss caused by multiple small infarctions in the right hemisphere coincided with the delay (or possibly loss) of the right hemisphere P22 component and delay of the following N31 component centrally . Parietally a slight but non significant P27 delay was followed by an abnormally delayed N33 component (>2.5 standard deviations).

It is possible to interpret the P22 and N31 delay as possibly the loss of the P22-N31 complex which has been 'replaced' by volume conduction by the parietal P27-N33 complex.

It is again important to note that the morphology difference seen between right and left hemisphere central and parietal components was not seen in any control individual.

Statistical mapping yielded no abnormality.

5.3.5.0. Patient 5 (P5) results.

5.3.5.1. P5 clinical presentation.

This 22 year old lady presented in late July 1988 with a 4 day history of loss of some motor and sensory function of the left side of the body. There was some improvement in her condition over the next few days when a CT scan and evoked potentials were recorded at New Cross hospital (August 4th 1988). The CT scan revealed a small zone of abnormality in the right parietal area close to the internal capsule (Figure 5.15). It was considered likely that this was a zone of infarction although demyelination could not be excluded at this time.

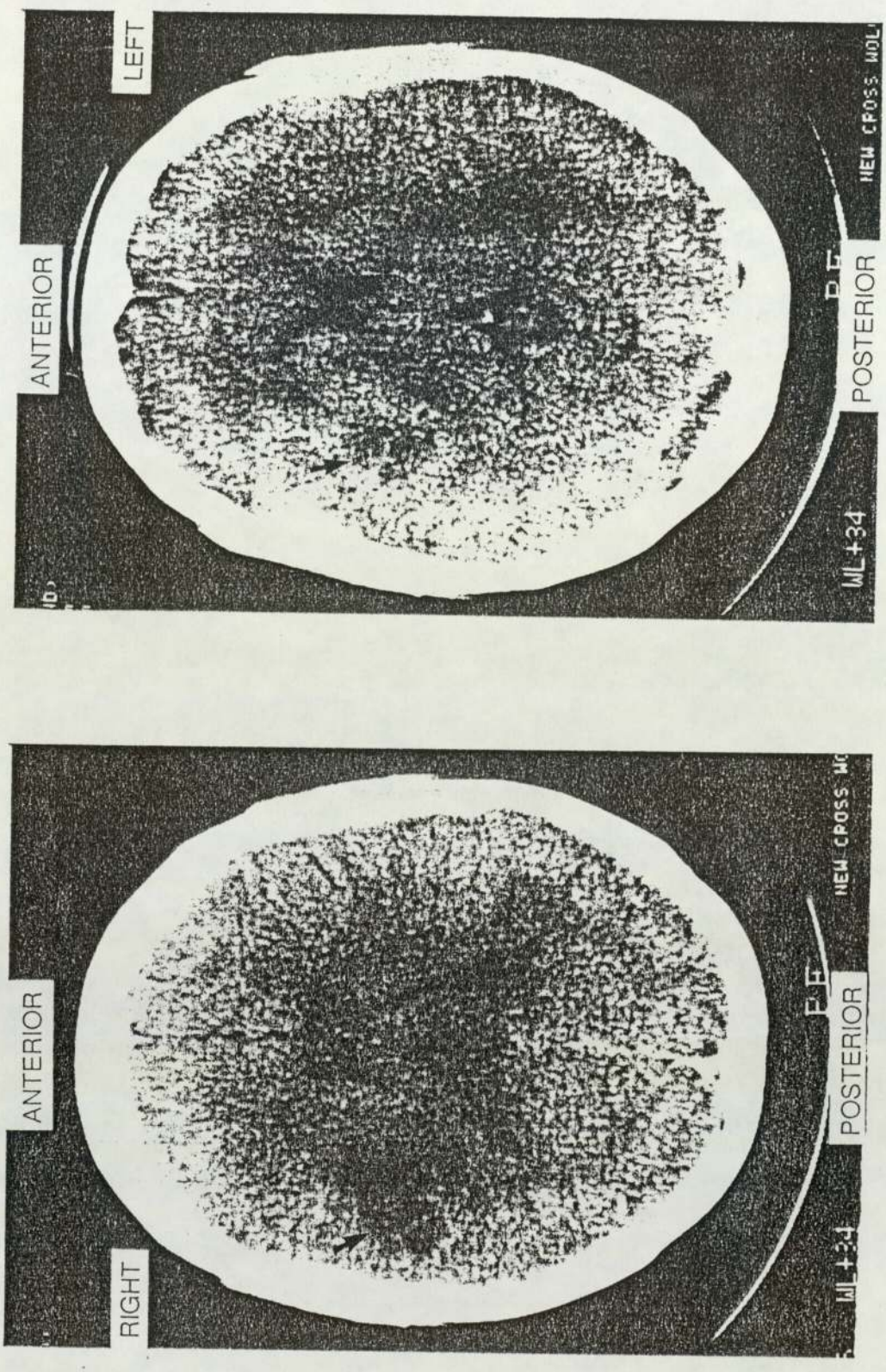

Figure 5.15. CT scan of patient P5. Arrows indicate site of lesion.

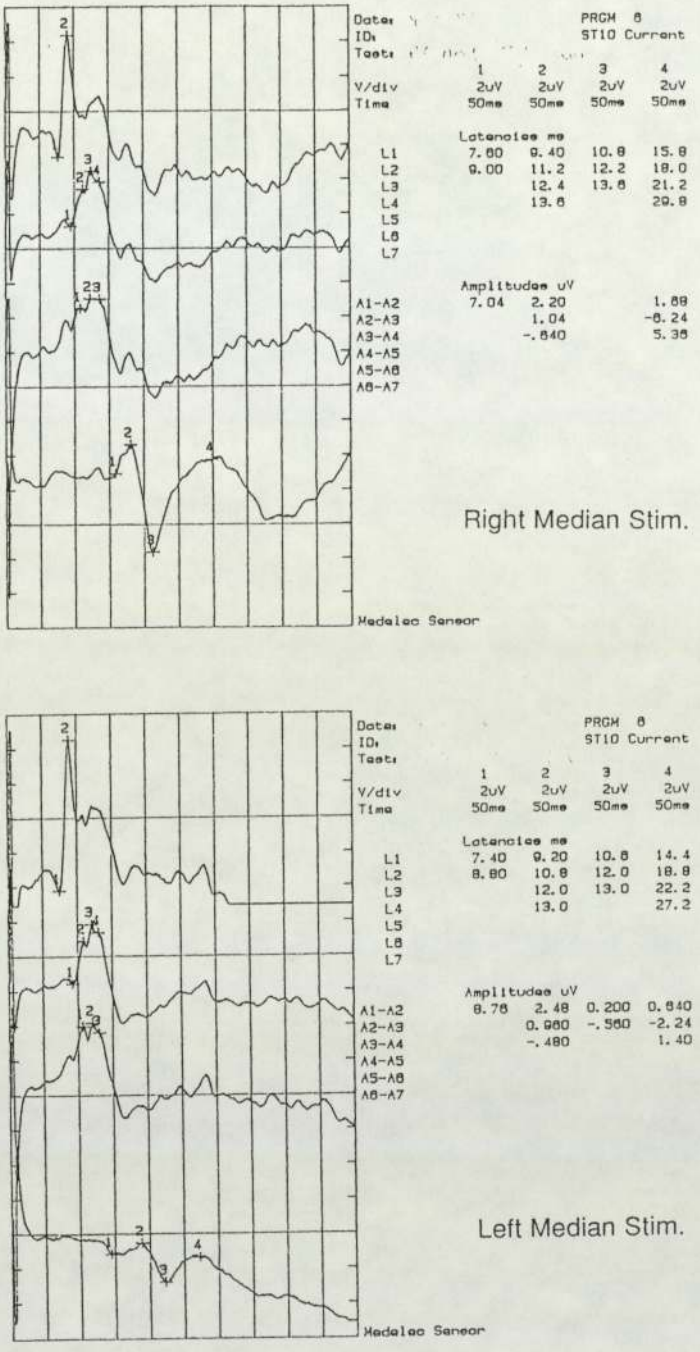

Figure 5.16. Upper limb SEP's recorded shortly after onset of symptoms. Channels for each limb stimulated are 1. (top) Erbs point - Fz. 2. Cv2 - Fz. 3. Cv7 - Fz. 4. Cortex - Fz. Cortical sites determined as 7cm lateral and 2cm posterior to Cz.

Data courtesy of the Neurophysiology Department, New Cross Hospital.

Table 5.9 Clinical Summary for Patient P5

	UPPER LIMB		LOWER LIMB	
	Right	Left	Right	Left
Power	Normal	4/5	Normal	4/5
Tone	Normal	↓	Normal	↓
Reflex	Normal	↑	Normal	↑
Pain	Normal	↓	Normal	↓
Temp.	Normal	↓	Normal	↓
Touch	Normal	↓	Normal	↓
Vibration	Normal	↓	Normal	↓
Position	Normal	↓	Normal	↓
2 Point dis.	Normal	Normal	Normal	Normal
Stereognosis	Normal	Normal	Normal	Normal

Direction of arrow indicates an increase (upward) or decrease (downward) of sensory or motor function.
In the case of reflex activity an upward arrow indicates hyperreflexia.
Motor data indicated as a fraction represents degree of loss compared to opposite limb.A question mark alongside a category indicates inconsistent findings on a trial / re-trial basis.

Upper and lower limb SEP's were reported as showing normal latencies but there was a marked decrease in amplitude of all right hemisphere components to left median nerve stimulation (Figure 5.16). A clinical summary taken at this time is shown in Table 5.9.The patient was referred to Aston University for SEP mapping which was performed on August 18th 1988.

She was reviewed again in clinic on September 9th 1988 where some improvement in condition was seen. Power in upper limbs were 95% normal and sensory findings were normal. Power in lower limbs remained 3-4/5 and she could walk unaided but with a spastic gait. A repeat CT scan was performed on September 27th and revealed a continuing abnormality in the right parietal area but showing less enhancement than previously. It was considered that these changes excluded a neoplastic process.

5.3.5.2. P5 SEP results.

Subjective inspection of the waveforms revealed two obvious morphological right versus left hemisphere differences (Figures 5.17 and 5.18). Firstly, whichever limb was stimulated, the frontal morphology of components presented as type FIII i.e. a larger N23 component than N30. The most striking difference however was that to right limb stimulation, the post N30 frontal morphology was a V type (a single clear P42 component) but to left limb stimulation a W type morphology, with a clear N43 component was seen. These observations were unusual on two counts; no normal control subjects presented with a V and W morphology type co-existing in the same individual; secondly, it was rare to see a W type morphology occurring in a young individual.

The second morphological difference was seen at the central C3/C4 locations where the N19 component was much broader than its right limb counterpart.

Analysis of component peak latency and amplitude data shown in Table 5.10 confirmed the significant interhemisphere latency difference of the N19 component, being relatively delayed to left limb stimulation, although all absolute peak latencies were within normal limits. The interhemisphere P14-N19 latency difference was also abnormally prolonged.

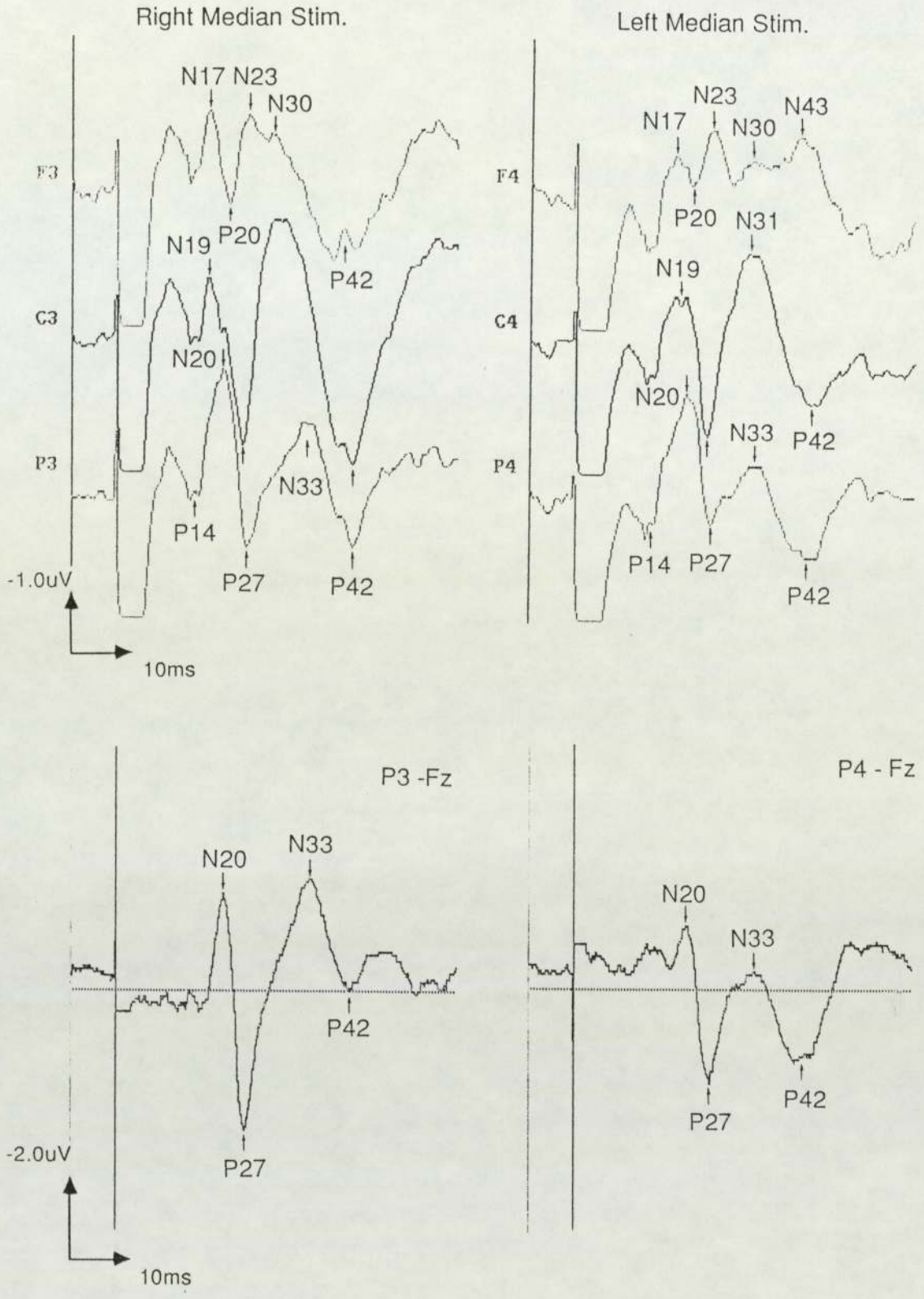

Figure 5.17. SEP waveforms for Patient 5 (P5) for right and left median nerve stimulation.Fz reference derived potentials are shown beneath the original earlobe reference recordings.

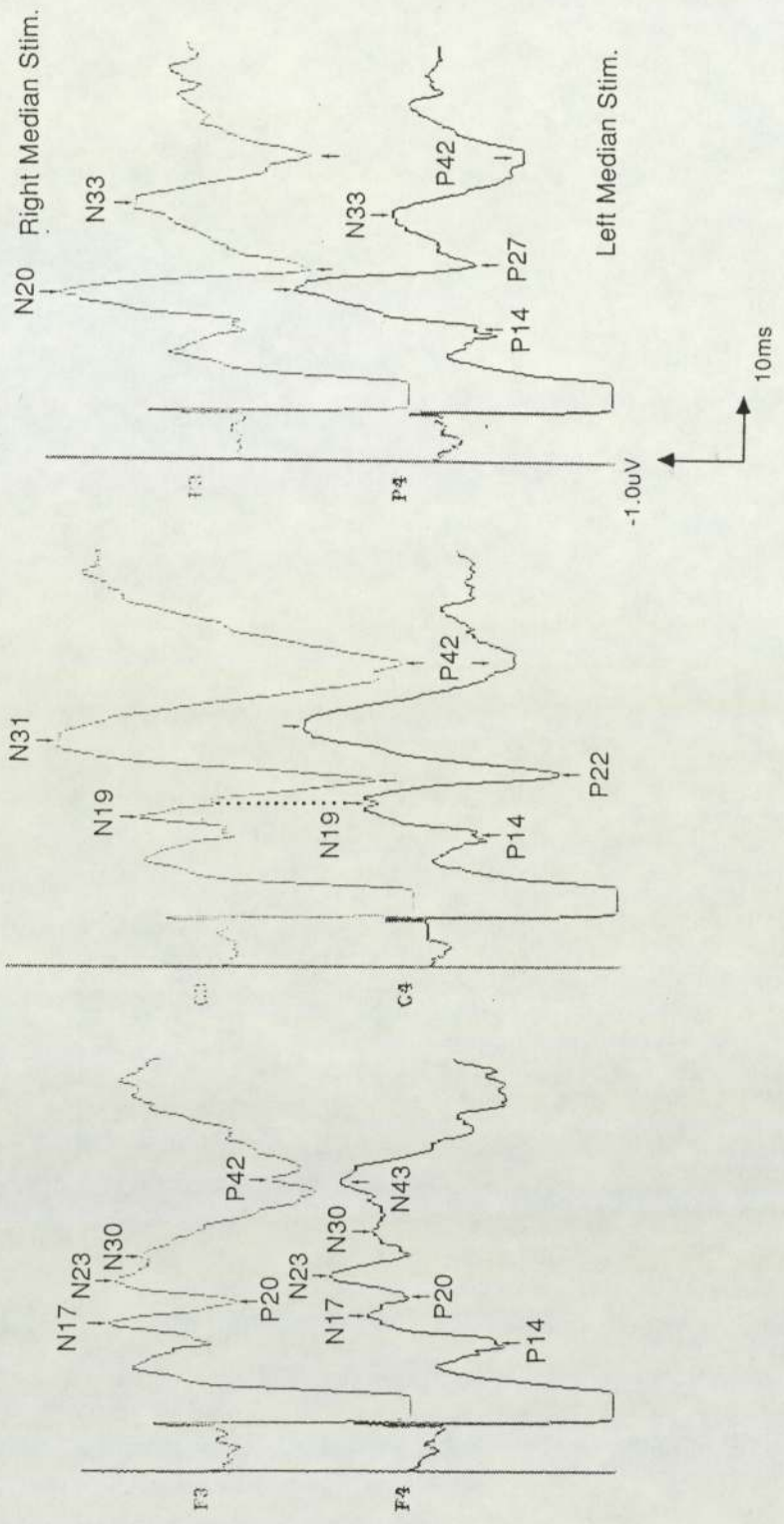

Figure 5.18. Waveforms of patient P5 to right median (upper traces) and left median (lower traces) nerve stimulation.

Patient: P5
Age (years): 22
Height (cm): 157

LATENCY DATA

Component	Patient Data (ms)		Upper limit	Interhemisphere Latency	Interhemisphere Latency Diff.
	Right limb	Left limb	of normality	Difference (ms)	Upper Limit (ms)
Erbs	9.25	8.75	10.13	0.50	0.49
P14	13.00	12.50	13.77	0.50	1.61
N17	15.25	16.50	17.25	-1.25	1.83
N19	15.25	17.50	18.27	**-2.25**	1.70
N20	17.75	18.50	19.21	-0.75	1.72
P20	18.75	19.25	20.62	-0.50	3.56
P22	21.00	22.00	22.21	-1.00	3.79
N23	22.00	22.75	23.31	-0.75	1.79
P27	21.50	22.50	35.96	-1.00	4.32
N30	25.75	29.50	37.85	-3.75	4.64
N31	27.00	29.25	33.44	-2.25	3.90
N33	31.50	29.75	40.52	1.75	4.23
P35			43.89	0.00	2.40
P42(Part)	39.00	39.00	51.58	0.00	3.84
N43		37.25	54.34		4.68
Erbs-P14	3.75	3.75	4.74		
P14-N17	2.25	4.00	5.44	-1.75	2.49
N17-P20	3.50	2.75	4.69		
P14-N19	2.25	5.00	6.62	**-2.75**	2.01
N19-P22	5.75	4.50	6.27	1.25	4.24
P14-N20	4.75	6.00	6.91	-1.25	1.70

AMPLITUDE DATA

Component Amplitude	Patient Data (uV)		Lower limit	Interhemisphere Amplitude	Interhemisphere Amp. Diff.
	Right limb	Left limb	of normality	Difference (uV)	Upper Limit (uV)
Frontal comps.					
0-P14	0.24	1.04	0.09	-0.80	1.54
P14-N17	1.06	1.63	0.12	-0.57	1.31
N17-P20	1.64	0.53	0.04	1.11	1.52
P20-N23	1.54	0.98	0.02	0.56	3.08
P20-N30	1.21	0.36	0.08	0.85	2.55
Central comps.					
0-P14	0.12	0.73	0.09	-0.61	1.27
P14-N19	1.03	1.24	0.06	-0.21	1.94
N19-P22	2.95	2.34	0.22	0.61	3.04
P22-N31	3.98	3.25	0.01	0.73	3.31
N31-P42	4.35	2.82	0.28	1.53	5.32
Parietal comps.					
0-P14	0.30	0.81	0.02	-0.51	1.35
P14-N20	2.15	2.28	0.36	-0.13	2.73
N20-P27	3.13	2.28	0.41	0.85	3.34
P27-N33	2.19	1.05	0.08	1.14	4.12
N33-P42	2.19	1.64	0.30	0.55	3.78

Table 5.10 Comparison of latencies and amplitudes with normality limits from control group. Lower limit of normality for amplitude of control group calculated as 50% of minimum recorded value.
U = unclear peak - no precise latency and morphology determination.
Interhemisphere differences calculated as (Right-Left) limb data.
Bold figures indicate data which exceeds upper limits of normality.

Patient: P5 **Fz reference derived potentials**
Age: 22
Height: 157

Component	Patient Data (ms)		Upper limit	Interhemisphere Latency	Interhemisphere Latency Diff.
	Right limb	Left limb	of normality	Difference (ms)	Upper Limit (ms)
N20	17.75	18.50	20.43	-0.75	1.61
P22			25.22		0.55
N25			26.77		1.42
P27	21.25	22.25	35.74	-1.00	3.85
N33	32.00	29.75	43.53	2.25	6.27
P42	38.50	37.00	54.75	1.50	7.88

Component	Patient Data (uV)		Lower limit	Interhemisphere Amplitude	Interhemisphere Amp. Diff.
Amplitude	Right limb	Left limb	of normality	Difference (uV)	Upper Limit (uV)
0-N20	2.03	0.87	0.32	1.16	2.27
N20-P27	4.99	3.81	0.50	1.18	5.49
P27-N33	5.33	2.22	0.44	3.11	5.78
N33-P42	2.38	1.83	0.24	0.55	4.55
0-N20	1.68	0.64		1.04	
N20-P27	6.24	2.24		4.00	
P27-N33	5.36	1.40		3.96	

Table 5.10.1

Comparison of latencies and amplitudes with normality limits from control group.
Lower limit of normality for amplitude of control group calculated as 50% of minimum recorded value.
U = unclear peak - no precise latency and morphology determination.
Interhemisphere differences calculated as (Right-Left) limb data.
Bold figures indicate data which exceeds upper limits of normality.

In the amplitude domain, all peak to peak measures and interhemisphere differences were within normal limits. Whilst the P20 component to left median nerve stimulation was slightly attenuated

compared to its right limb counterpart, this may have in part been due to the broader and relatively delayed left limb N17 component.

Comparison was made of these waveforms with the group mean control waveforms using the Z statistic. Interestingly, no data point exceeded 2.5 standard deviations to left median stimulation whilst to right limb stimulation, levels exceeding 3 standard deviations were seen at frontal electrodes F7, F3, Fz and F4 (Figure 5.19). These levels of deviation coincided with the large N17 component seen in this patient, although as already stated all peak to peak measures were within normal limits.

Comparison with Fz reference derived potentials (Figure 5.17) revealed an attenuation of the N20 component to left limb stimulation as well as N20-P27 and P27-N33 complexes. Comparison of right and left limb parietal components with Fz components confirms that these differences were mainly caused by change in the frontal components i.e. the 'so called' reference electrode in these recordings. All differences observed in these potentials however fell within normal limits when compared to control group data.

To highlight the differences in scalp potentials in this patient, maps were constructed at latencies coincident with the N20, P27 and P42 potentials for both right and left limb stimulation. These maps were paired for comparison and shown, with waveforms in Figures 5.20 and 5.21. The clearest difference in maps was not surprisingly that of P42 where to right limb stimulation a clear radial field pattern was obtained whereas to left limb stimulation the P42 map more closely approximates to the P27 field map - that of a dipolar field pattern. Each of the P42 maps were compared to the control group P42 maps - neither yielded levels exceeding 2 standard deviations.

5.3.5.4. Summary and conclusions of P5 results.

Left upper and lower limb weakness with sensory impairment was seen in this young lady whose CT scan revealed a small zone of infarction in the right centro-parietal area.

All parietal SEP components were within normal limits whilst the peak latency of the central N19 component to left median stimulation was prolonged. Frontal components revealed a marked morphological difference between stimulated limbs - this difference was not seen in any individual of the control population. A case could be argued that in fact the N30-P42 complex to left limb stimulation was absent and therefore the N23 and N43 components dominated.

Fz reference derivations yielded an asymmetry of amplitude between sides (although <2.5 s.d.) - topographical mapping revealed that the Fz derived left limb/right hemisphere attenuation was caused mainly by changes at the Fz 'reference' electrode.

Interestingly, statistical mapping indicated no abnormality of left limb/right hemisphere components but yielded abnormally high standard deviations coincidental with the peak of the frontal N17 component to right limb stimulation. This is odd since the peak to peak value of the left median P14-N17 at 1.64uV was greater than its right limb counterpart at 1.06uV and all amplitudes and latencies fell well within normal limits. The explanation appeared to lie in the fact that with right limb stimulation, the entire P14-N17 complex lay above the baseline with P14 peaking at -0.24uV thus yielding an apparent N17 peak voltage of -1.54uV. Whilst this in itself did not present a 'giant' N17 potential, at 15.25ms it exceeded 2.5 standard deviations of the control group mean voltage.

Inspection of the left median P14-N17 complex revealed that this 'straddled' the baseline with P14 at +1.04uV and N17 at -0.59uV. These voltages fell well within normal limits of the control group at 16.50ms. The conclusion therefore is that the right median 'frontal abnormality' represented a false positive of statistical mapping.

One would have predicted that neither of the P42 maps generated by right and left limb stimulation would have yielded an abnormality since both the V and W morphology types.

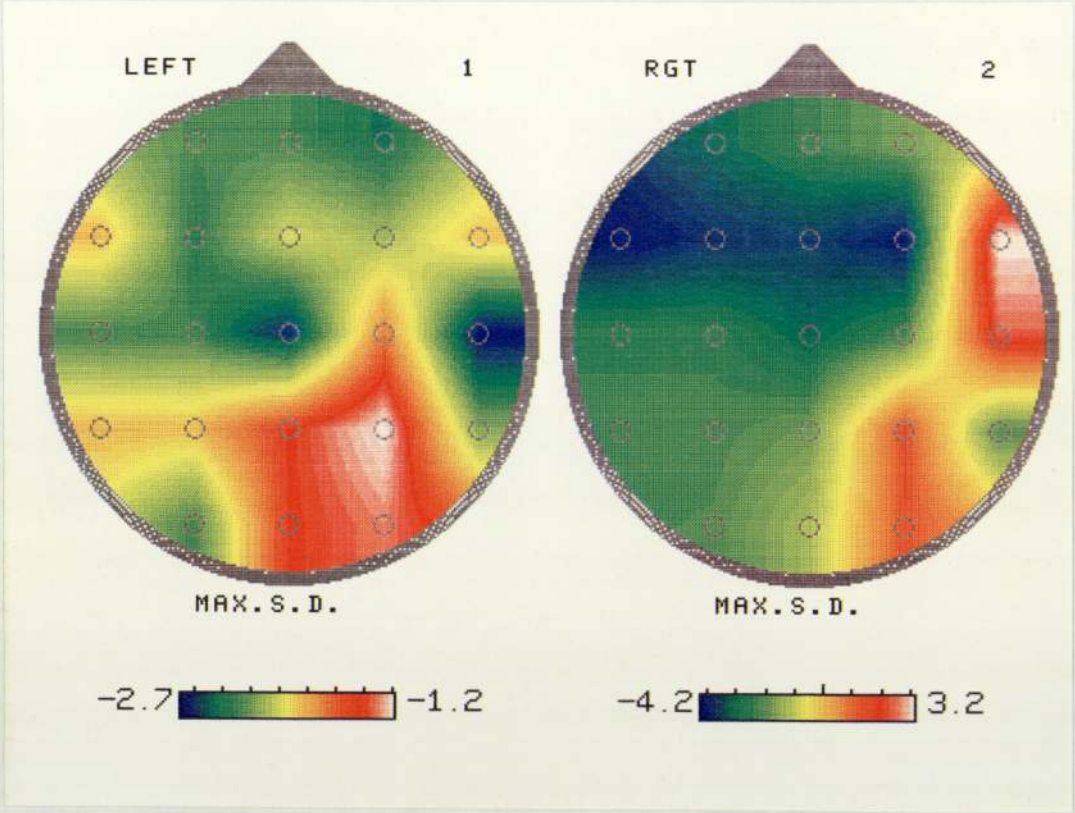

Figure 5.19. Statistical mapping of P5.

Maps indicate (from left to right) maximum standard deviation across entire waveform for right median and left median stimulation.

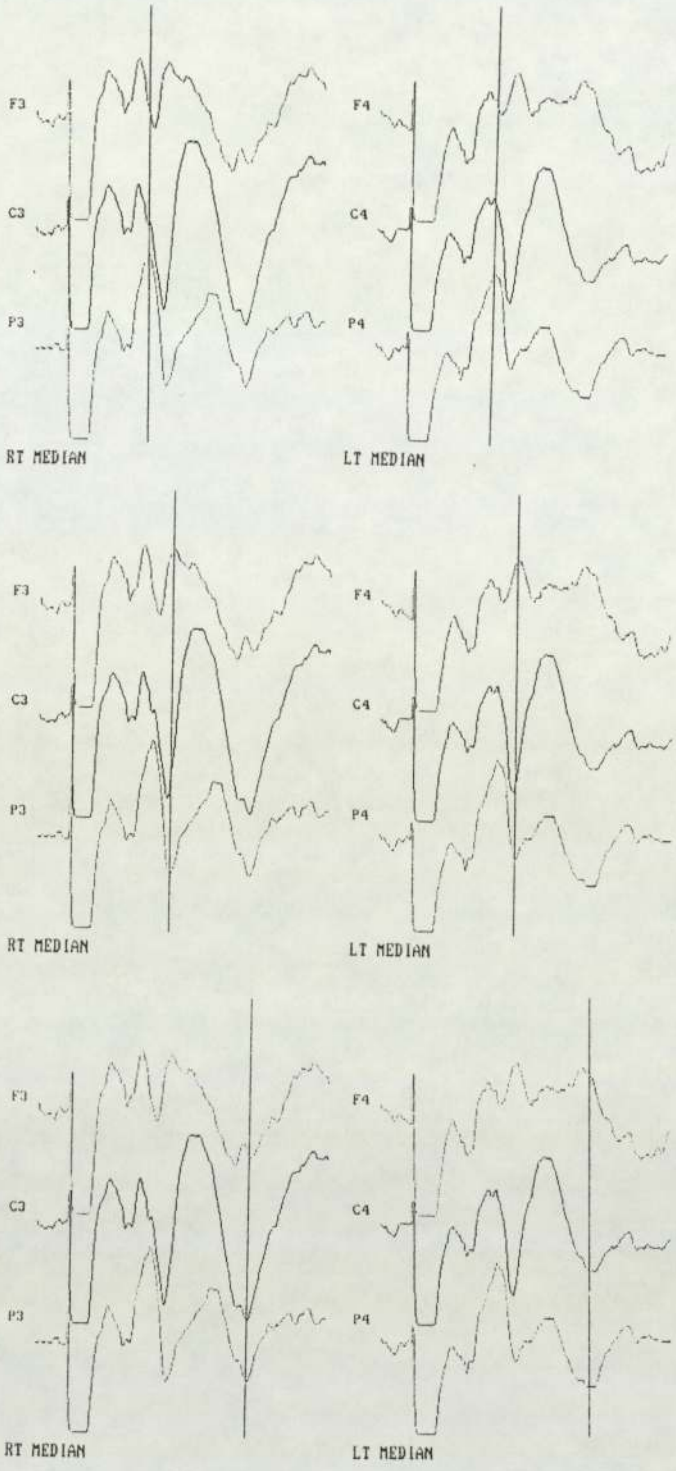

Figure 5.20. Patient P5 waveforms indicating (top) latencies at which N20 maps generated; (middle) latencies at which P27 maps generated and (bottom) latencies at which P42 maps generated. These maps are shown in:-

Figure 5.21. Overleaf. Patient P5; right and left median N20 and P27 maps.

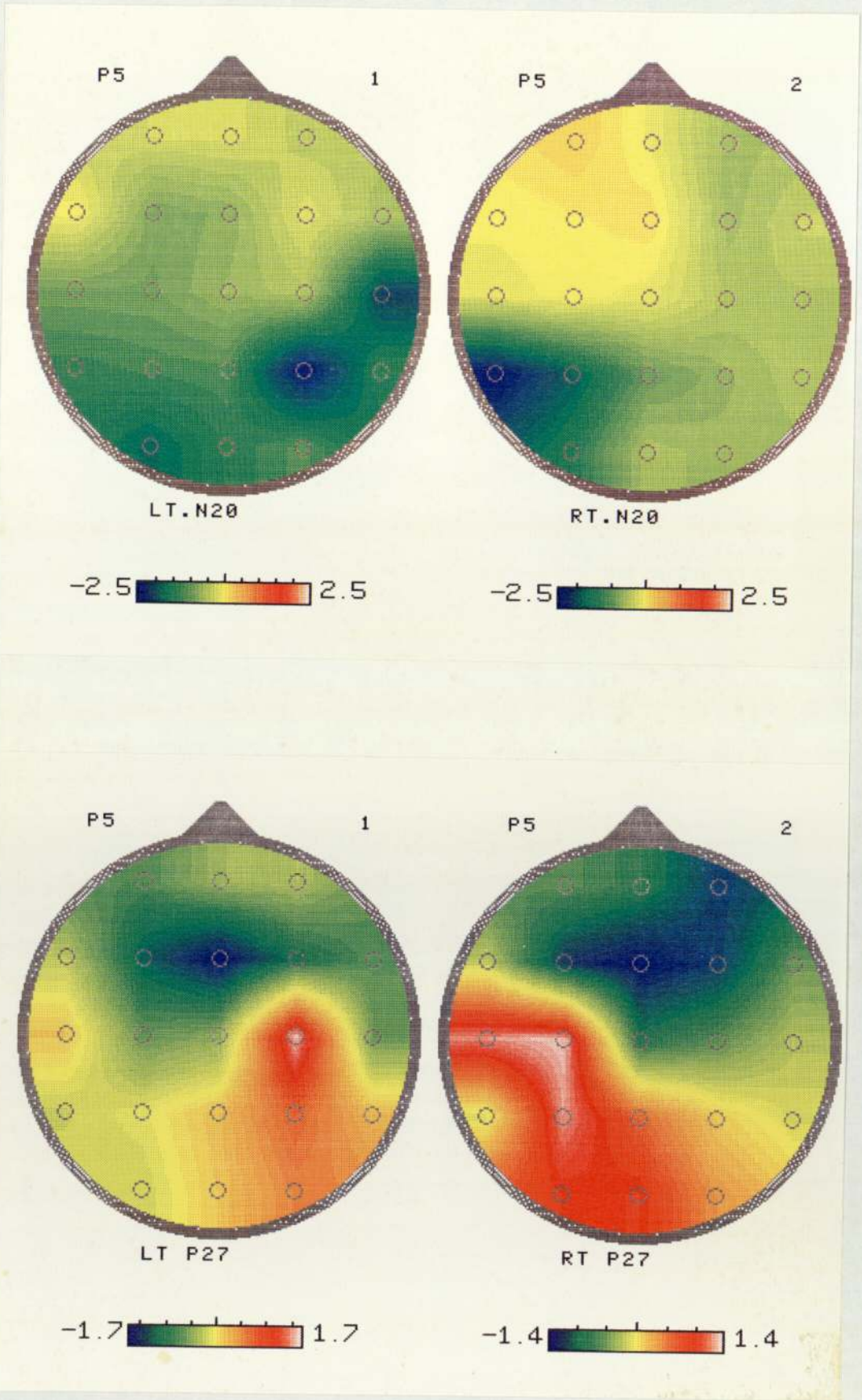
P5
1
LT.N20
-2.5
2.5
P5
2
RT.N20
-2.5
2.5
P5
1
LT P27
-1.7
1.7
P5
2
RT P27
-1.4
1.4

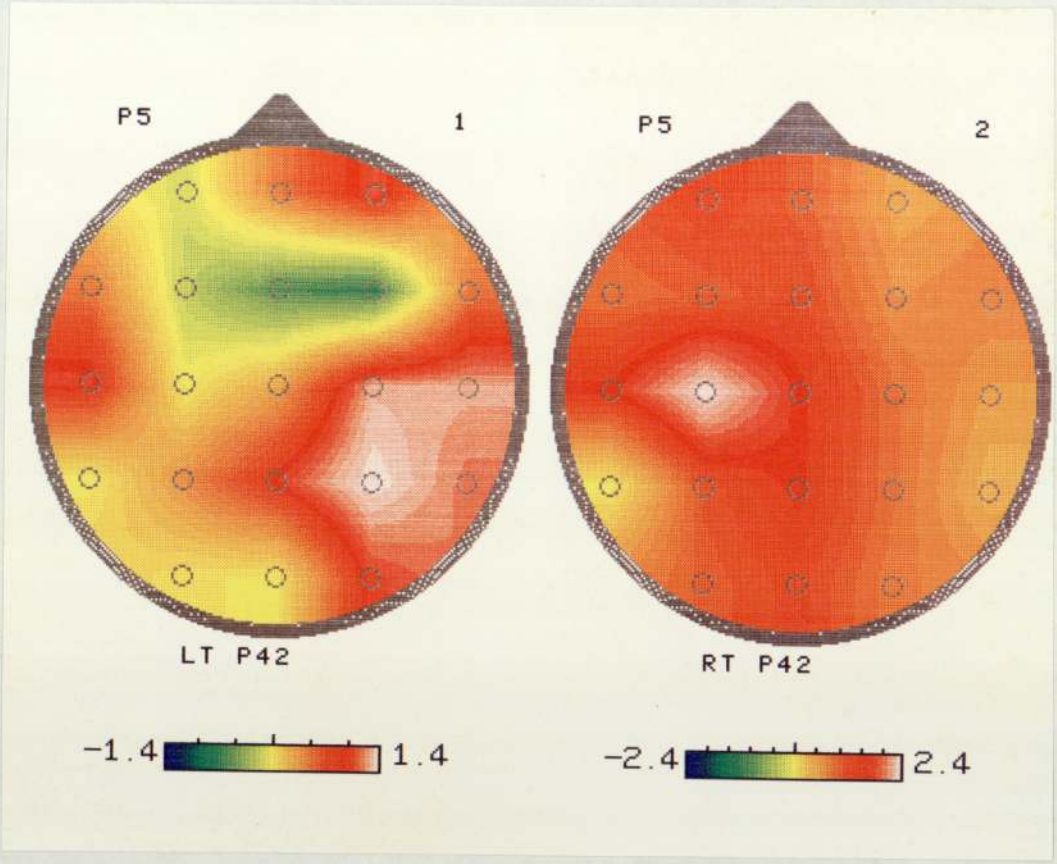

Figure 5.21.1. Patient P5. Right and left median P42 maps.

occurred separately in the control group. The abnormality in this case was that these types occurred within the same individual between limbs/hemispheres.

5.3.6.0. Patient 6 (P6) results.

5.3.6.1. P6 clinical presentation.

This 37 year old male patient presented in November 1985 with an epileptic seizure following a cerebral haemorrhage. A CT scan revealed a left intracerebral haemorrhage in the tempero-parieto-occipital area. When seen for review in September 1988, he presented with bilaterally brisk reflexes in both upper and lower limbs (Table 5.11). Other signs were a quadrantic hemianopia. Medication consisted of Epilim (300mg daily).

5.3.6.2. P6 SEP results.

SEP mapping was performed in September 1988. Subjective inspection of waveforms revealed low amplitude potentials, somewhat poorly formed, particularly frontally where the FIII morphology type occurred bilaterally (see Figure 5.22). Centrally and parietally, C type I and P type I morphology types also occurred bilaterally. Most obvious feature of note was a large 'N50' component occurring at frontal and central locations and again recorded bilaterally .

Analysis of the peak latencies and peak to peak amplitudes (Table 5.12) revealed that all component values, with the exception of the unusual N50, were within normal limits.

Comparison of these components with the control group mean waveforms using the Z statistic revealed no data point exceeding 2.5 standard deviations bilaterally except at F4 to left median nerve stimulation where the peak of the large amplitude N50 was recorded at 3.06 standard deviations from the control group mean voltage at this latency (see Figure 5.23).

Inspection of the Fz reference derived potentials (Figure 5.22) revealed comparable symmetry between components to right and left stimulation although a slight attenuation of the N20 component was seen to left limb stimulation (<2.5 s.d.).

Table 5.11 Clinical Summary for Patient P6

	UPPER LIMB		LOWER LIMB	
	Right	Left	Right	Left
Power	Normal	Normal	Normal	Normal
Tone	Normal	Normal	Normal	Normal
Reflex	↑	↑	↑	↑
Pain	Normal	Normal	Normal	Normal
Temp.	Normal	Normal	Normal	Normal
Touch	Normal	Normal	Normal	Normal
Vibration	Normal	Normal	Normal	Normal
Position	Normal	Normal	Normal	Normal
2 Point dis.	Normal	Normal	Normal	Normal
Stereognosis	Normal	Normal	Normal	Normal

Direction of arrow indicates an increase (upward) or decrease (downward) of sensory or motor function.
In the case of reflex activity an upward arrow indicates hyperreflexia.

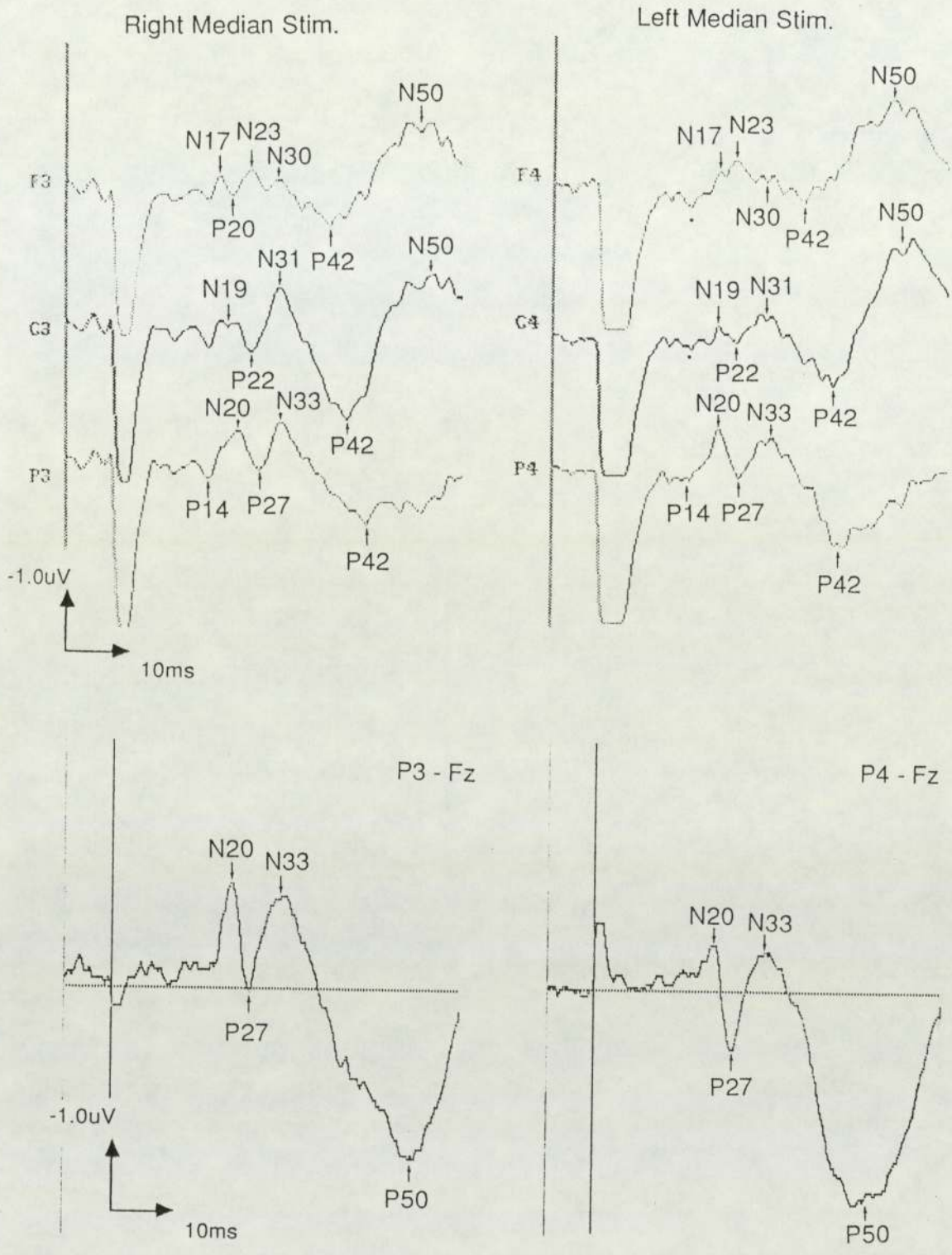

Figure 5.22. SEP waveforms for Patient 6 (P6) for right and left median nerve stimulation.Fz reference derived potentials are shown beneath the original earlobe reference recordings.

Patient: P6
Age (years): 37
Height (cm): 178

LATENCY DATA

Component	Patient Data (ms)		Upper limit	Interhemisphere Latency	Interhemisphere Latency Diff.
	Right limb	Left limb	of normality	Difference (ms)	Upper Limit (ms)
Erbs	10.25	10.25	11.92	0.00	0.49
P14	15.00	14.25	16.88	0.75	1.61
N17	17.00	17.50	20.65	-0.50	1.83
N19	18.25	19.25	21.35	-1.00	1.70
N20	19.75	19.25	22.25	0.50	1.72
P20	19.00	U	24.64		3.56
P22	22.00	22.00	26.10	0.00	3.79
N23	22.00	22.00	27.39	0.00	1.79
P27	23.25	22.50	35.96	0.75	4.32
N30	26.50	27.00	37.85	-0.50	4.64
N31	26.75	27.00	37.25	-0.25	3.90
N33	26.75	27.75	40.52	-1.00	4.23
P35			43.89	0.00	2.40
P42	40.75	38.75	51.58	2.00	3.84
N43			54.34	0.00	4.68
Erbs-P14	4.75	4.00	6.15		
N17-P20	2.00	4.50	5.26		
N19-P22	3.75	2.75	6.93		
P14-N20	4.75	5.00	7.13		

AMPLITUDE DATA

Component Amplitude	Patient Data (uV)		Lower limit	Interhemisphere Amplitude	Interhemisphere Amp. Diff.
	Right limb	Left limb	of normality	Difference (uV)	Upper Limit (uV)
Frontal comps.					
0-P14	0.14	0.10	0.09	0.04	1.54
P14-N17	0.48	0.24	0.12	0.24	1.31
N17-P20	0.38	U	0.04	0.38	1.52
P20-N30	0.33	U	0.08		2.55
Central comps.					
0-P14	0.19	0.29	0.09	-0.10	1.27
P14-N19	0.45	0.43	0.06	0.02	1.94
N19-P22	0.50	0.28	0.22	0.22	3.04
P22-N31	1.31	0.45	0.01	0.86	3.31
N31-P42	2.76	1.65	0.28	1.11	5.32
Parietal comps.					
0-P14	0.17	0.02	0.02	0.15	1.35
P14-N20	1.34	1.05	0.36	0.29	2.73
N20-P27	0.81	1.03	0.41	-0.22	3.34
P27-N33	0.98	0.89	0.08	0.09	4.12
N33-P42	2.14	2.25	0.30	-0.11	3.78

Table 5.12 Comparison of latencies and amplitudes with normality limits from control group. Lower limit of normality for amplitude of control group calculated as 50% of minimum recorded value.
U = unclear peak - no precise latency and morphology determination.
Ab = component peak appears to be entirely absent.
Bold figures indicate data which exceeds upper limits of normality.
Interhemisphere differences calculated as (Right-Left) limb data.

Patient: P6 **Fz reference derived potentials**
Age: 37
Height: 178

Component	Patient Data (ms)		Upper limit	Interhemisphere Latency	Interhemisphere Latency Diff.
	Right limb	Left limb	of normality	Difference (ms)	Upper Limit (ms)
N20	19.25	19.25	23.47	0.00	1.61
P22			25.22	0.00	0.55
N25			26.77	0.00	1.42
P27	22.00	22.25	35.74	-0.25	3.85
N33	27.25	28.00	43.53	-0.75	6.27
P42/P50	48.00	43.25	54.75	4.75	7.88

Component Amplitude	Patient Data (uV)		Lower limit	Interhemisphere Amplitude	Interhemisphere Amp. Diff.
	Right limb	Left limb	of normality	Difference (uV)	Upper Limit (uV)
0-N20	1.31	0.92	0.32	0.39	2.27
N20-P27	1.38	1.32	0.50	0.06	5.49
P27-N33	1.18	1.22	0.44	-0.04	5.78
N33-P42	3.24	3.04	0.24	0.20	4.55

Table 5.12.1

Comparison of latencies and amplitudes with normality limits from control group.
Lower limit of normality for amplitude of control group calculated as 50% of minimum recorded value.
U = unclear peak - no precise latency and morphology determination.
Ab = component peak appears to be entirely absent.
Bold figures indicate data which exceeds upper limits of normality.
Interhemisphere differences calculated as (Right-Left) limb data.

Figure 5.23. Overleaf. Statistical mapping for patient P6; maps indicate maximum standard deviation for left median nerve data (top left) and right median nerve data (top right).

Maps below indicate N50 component maps for left median (left) and right median nerve stimulation (right),

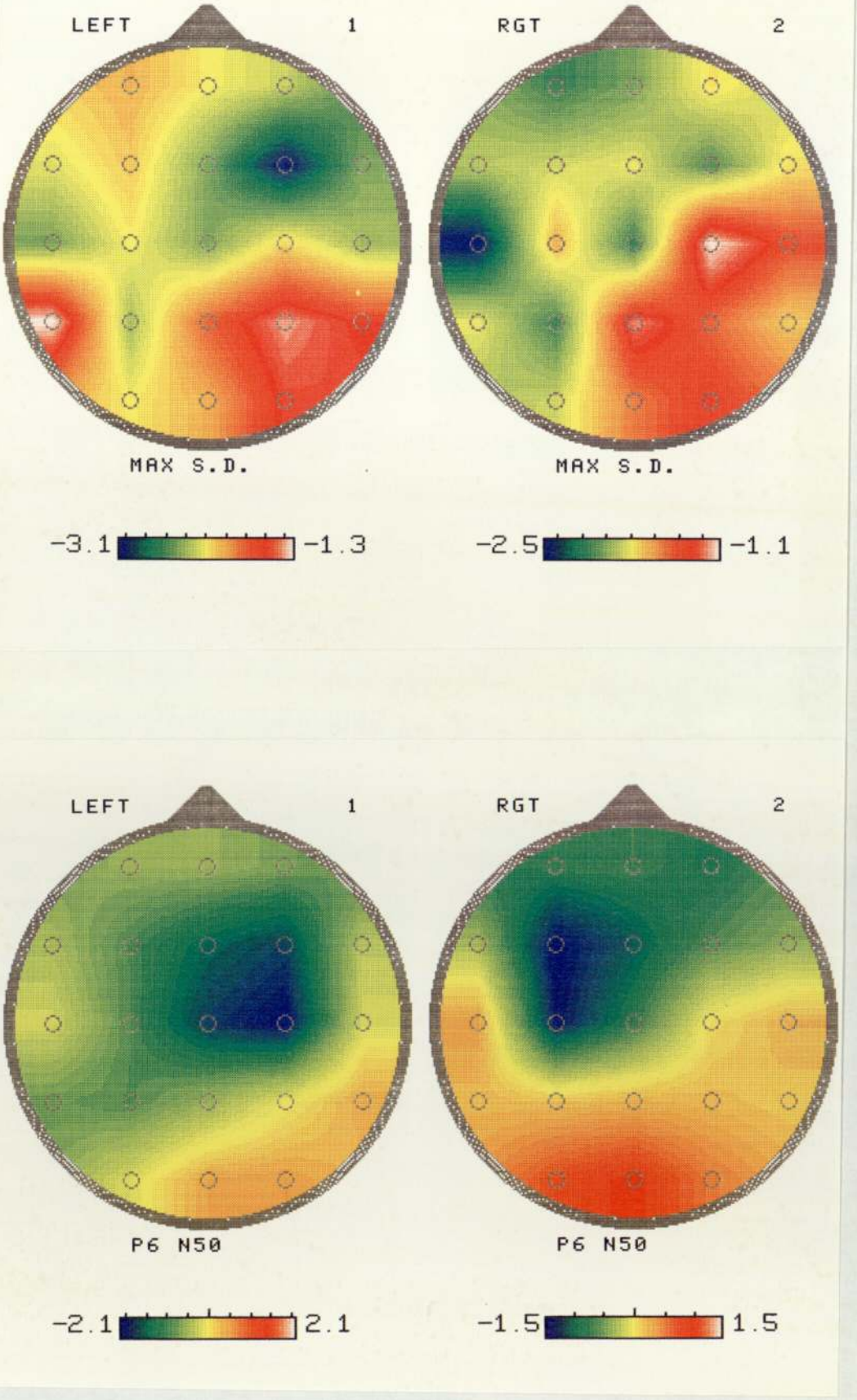
LEFT
1
RGT
2
MAX S.D.
MAX S.D.
-3.1
-1.3
-2.5
-1.1
LEFT
1
RGT
2
P6 N50
P6 N50
-2.1
2.1
-1.5
1.5

5.3.6.3. Summary and conclusion for P6.

This patient presenting with bilaterally brisk upper and lower limb reflexes but no sensory deficit produced poorly formed SEP's with rather an unusual dominant N50 component. This bilaterally occurring component was the only feature of note in an otherwise normal recording. Statistical mapping revealed an area of abnormality concomitant with the peak of this N50 potential to left median stimulation only.

The bilateral appearance of the unusual morphology make these findings of doubtful clinical significance.

The frontal emphasis of the N50 components yielded an unusual large P50 component in the Fz derived potentials.

5.3.7.0. Patient 7 (P7) results.

5.3.7.1. P7 clinical presentation.

This 67 year old gentleman presented with intermittent paraesthesia affecting the left hand following a right parietal CVA in January 1988. At the time of the SEP mapping recordings in August 1988, no symptoms were present.

There was a previous history of cerebrovascular accident affecting the left hemisphere.

5.3.7.2. P7 SEP results.

Subjective inspection of waveforms revealed relative attenuation of most components to right limb stimulation compared to their left limb counterparts (Figure 5.24). Most marked attenuation appeared to be the frontal P20-N30 complex and parietal P14-N20 and N20-P27. It was not surprising therefore that Fz reference derivations reflected a relative right limb component attenuation of the N20-P27 complex (Figure 5.24), but this attenuation was within normal limits (<2.5 s.d.).

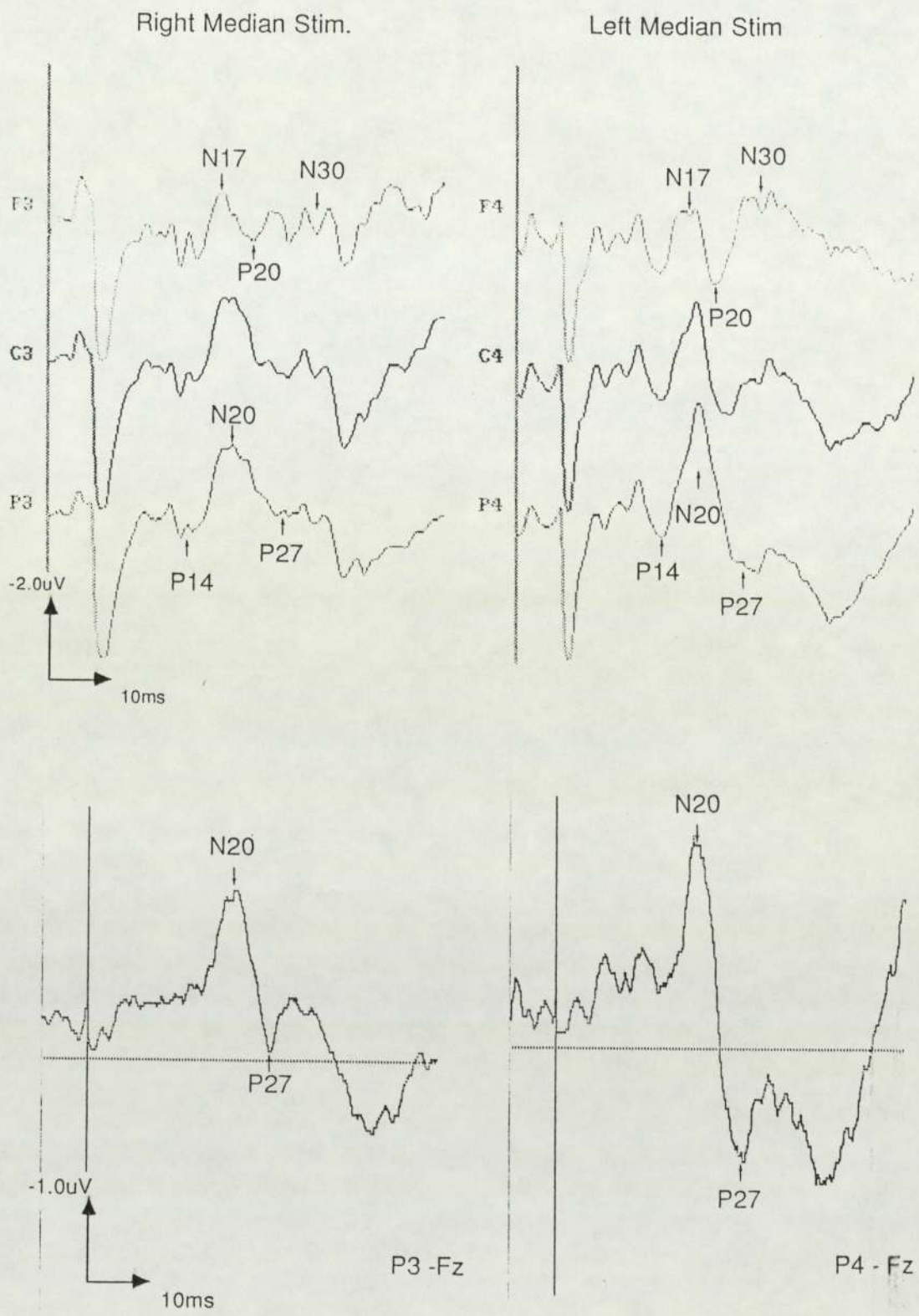

Figure 5.24. SEP waveforms for Patient 7 (P7) for right and left median nerve stimulation.Fz reference derived potentials are shown beneath the original earlobe reference recordings.

Analysis of peak latency and amplitude data in Table 5.13 showed that here too the amplitude asymmetry of components fell within normal limits as did all peak values.

Comparison of these waveforms with the control group mean waveforms using the Z statistic revealed that no data point exceeded 2.5 standard deviations for either right or left limb data (Figure 5.25).

Statistical mapping of patient component maps to control group mean maps, particularly at latencies of obvious relative attenuation such as the P27 component to right median nerve stimulation, revealed no component that exceeded 1 standard deviation.

5.3.7.3. Summary and conclusion of P7.

This patient presented in January 1988 with a right hemisphere stroke and at the time of the SEP recordings in the August of the same year presented with intermittent mild paraesthesia of the left fingertips. However, there was evidence on CT scan of a previous CVA affecting the left hemisphere. Clear correlation with the SEP and clinical data was thus confused. However the slight asymmetry of the SEP's were essentially within normal limits to peak latency and amplitude data and statistical mapping revealed no abnormality.

Patient: P7
Age (years): 67
Height (cm): 178

LATENCY DATA

Component	Patient Data (ms)		Upper limit	Interhemisphere Latency	Interhemisphere Latency Diff.
	Right limb	Left limb	of normality	Difference (ms)	Upper Limit (ms)
Erbs	12.25	12.25	12.82	0.00	0.49
P14	15.25	15.50	18.32	-0.25	1.61
N17	20.50	20.00	22.15	0.50	1.83
N19	21.75	21.25	23.00	0.50	1.70
N20	21.75	21.75	23.96	0.00	1.72
P20	25.50	24.50	27.04	1.00	3.56
P22	28.25	26.00	29.01	2.25	3.79
N23	29.00		30.42		1.79
P27	30.50	29.75	35.96	0.75	4.32
N30	34.00	33.25	37.85	0.75	4.64
N31	33.75	33.25	38.87	0.50	3.90
N33	33.75	35.00	40.52	-1.25	4.23
P35			43.89	0.00	2.40
P42	40.25	43.00	51.58	-2.75	3.84
N43			54.34	0.00	4.68
Erbs-P14	3.00	3.25	6.75		
N17-P20	5.00	4.50	6.40		
N19-P22	6.50	4.75	8.25		
P14-N20	6.50	6.25	7.58		

AMPLITUDE DATA

Component Amplitude	Patient Data (uV)		Lower limit	Interhemisphere Amplitude	Interhemisphere Amp. Diff.
	Right limb	Left limb	of normality	Difference (uV)	Upper Limit (uV)
Frontal comps.					
0-P14	0.36	0.95	0.09	-0.59	1.54
P14-N17	0.76	0.91	0.12	-0.15	1.31
N17-P20	0.84	1.10	0.04	-0.26	1.52
P20-N30	0.36	1.60	0.08	-1.24	2.55
Central comps.					
0-P14	0.14	0.57	0.09	-0.43	1.27
P14-N19	1.22	1.71	0.06	-0.49	1.94
N19-P22	1.02	1.93	0.22	-0.91	3.04
P22-N31	0.20	0.95	0.01	-0.75	3.31
N31-P42	1.68	1.61	0.28	0.07	5.32
Parietal comps.					
0-P14	0.26	0.38	0.02	-0.12	1.35
P14-N20	1.38	2.34	0.36	-0.96	2.73
N20-P27	1.08	2.89	0.41	-1.81	3.34
P27-N33	0.12	1.17	0.08	-1.05	4.12
N33-P42	1.28	1.18	0.30	0.10	3.78

Table 5.13 Comparison of latencies and amplitudes with normality limits from control group.
Lower limit of normality for amplitude of control group calculated as 50% of minimum recorded value.
U = unclear peak - no precise latency and morphology determination.
Ab = component peak appears to be entirely absent.
Bold figures indicate data which exceeds limits of normality.
Interhemisphere differences calculated as (Right-Left) limb data.

Patient: P7 **Fz reference derived potentials**
Age: 67
Height: 178

Component	Patient Data (ms)		Upper limit	Interhemisphere Latency	Interhemisphere Latency Diff.
	Right limb	Left limb	of normality	Difference (ms)	Upper Limit (ms)
N20	23.75	22.50	24.91	1.25	1.61
P22			25.22	0.00	0.55
N25			26.77	0.00	1.42
P27	29.50	30.00	35.74	-0.50	3.85
N33	35.00	36.00	43.53	-1.00	6.27
P42	45.25	43.25	54.75	2.00	7.88

Component Amplitude	Patient Data (uV)		Lower limit	Interhemisphere Amplitude	Interhemisphere Amp. Diff.
	Right limb	Left limb	of normality	Difference (uV)	Upper Limit (uV)
0-N20	1.77	2.08	0.32	-0.31	2.27
N20-P27	1.72	3.18	0.50	-1.46	5.49
P27-N33	0.45	0.47	0.44	-0.02	5.78
N33-P42	1.26	0.74	0.24	0.52	4.55

Table 5.13.1

Comparison of latencies and amplitudes with normality limits from control group.
Lower limit of normality for amplitude of control group calculated as 50% of minimum recorded value.
U = unclear peak - no precise latency and morphology determination.
Ab = component peak appears to be entirely absent.
Bold figures indicate data which exceeds limits of normality.
Interhemisphere differences calculated as (Right-Left) limb data.

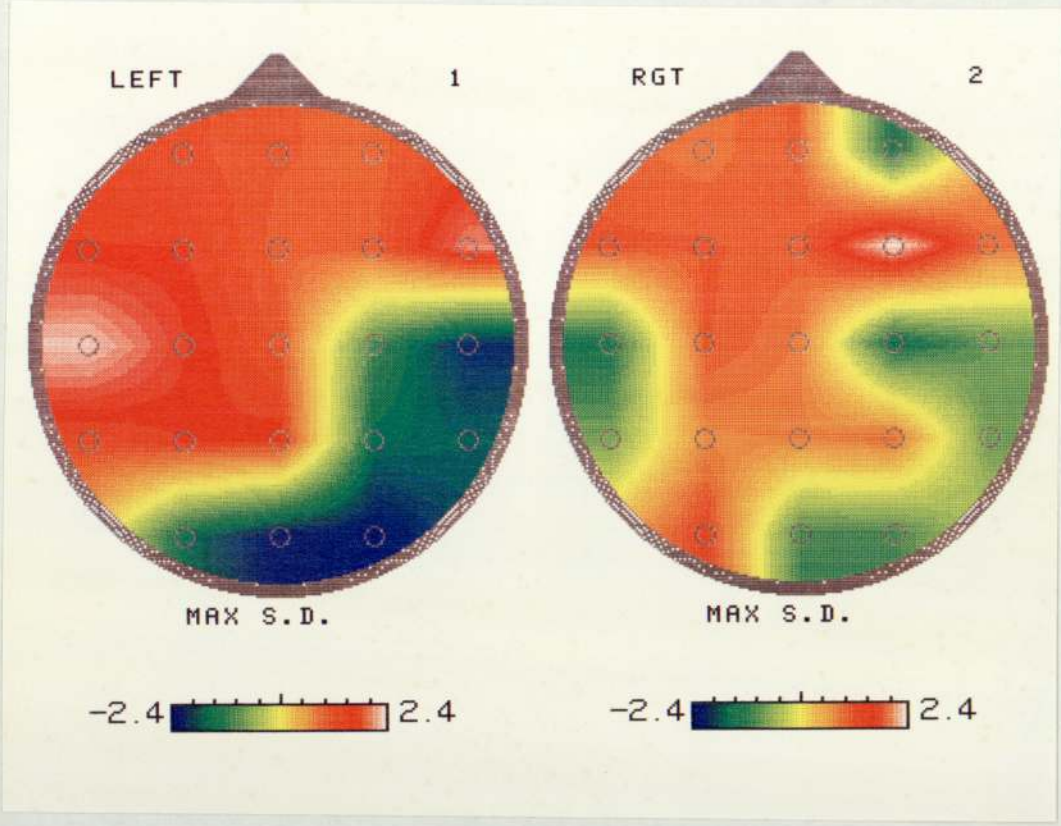

Figure 5.25. Statistical mapping for patient P7; maps indicate maximum standard deviation for left median nerve data (left) and right median nerve data (right).

5.3.8.0. Patient 8 (P8) results.

5.3.8.1. P8 clinical presentation.

This 63 year old male patient presented in mid - August 1988 with a two week history of loss of consciousness. Neurological examination revealed no abnormality.

A CT scan revealed a large non-enhancing density with a surround of oedema in the left parietal region (Figure 5.26). There was also evidence on a plain run of a small round density with a surround of oedema in the right frontal lobe. A diagnosis of right frontal infarction with a left parietal haematoma and secondary epilepsy was made.

5.3.8.2. P8 SEP results.

The dominant feature of this patients SEP's was a large unilateral negative potential occurring at 40.25ms (N40) to left median stimulation with its maximum amplitude centred at the C4 electrode (Figure 5.27). The morphology of the waveforms were FI V type, C type III and P type III to right median stimulation and FI W type, C type III and P type III to left median stimulation. Centrally therefore the waveforms were of similar morphology type till the peak of the respective N31 components but the broad N40 negativity following the P22-N31 complex to left median nerve stimulation was entirely absent to right median stimulation. The N31 component to left median stimulation appeared as a notch on the ascending limb of the N40 component in fact.

The appearance of the N40 component at frontal electrodes also changed the morphology type from a V type seen with right median stimulation to the W morphology type (N30-P35-N43) seen particularly in many elderly control subjects. No control subject presented with similar morphology differences between limbs/hemispheres. Indeed, none of the control subjects presented with a central negativity at this latency - the P42 component was the dominant component centrally in all control subjects regardless of the appearance of an N43 or P42 component frontally.

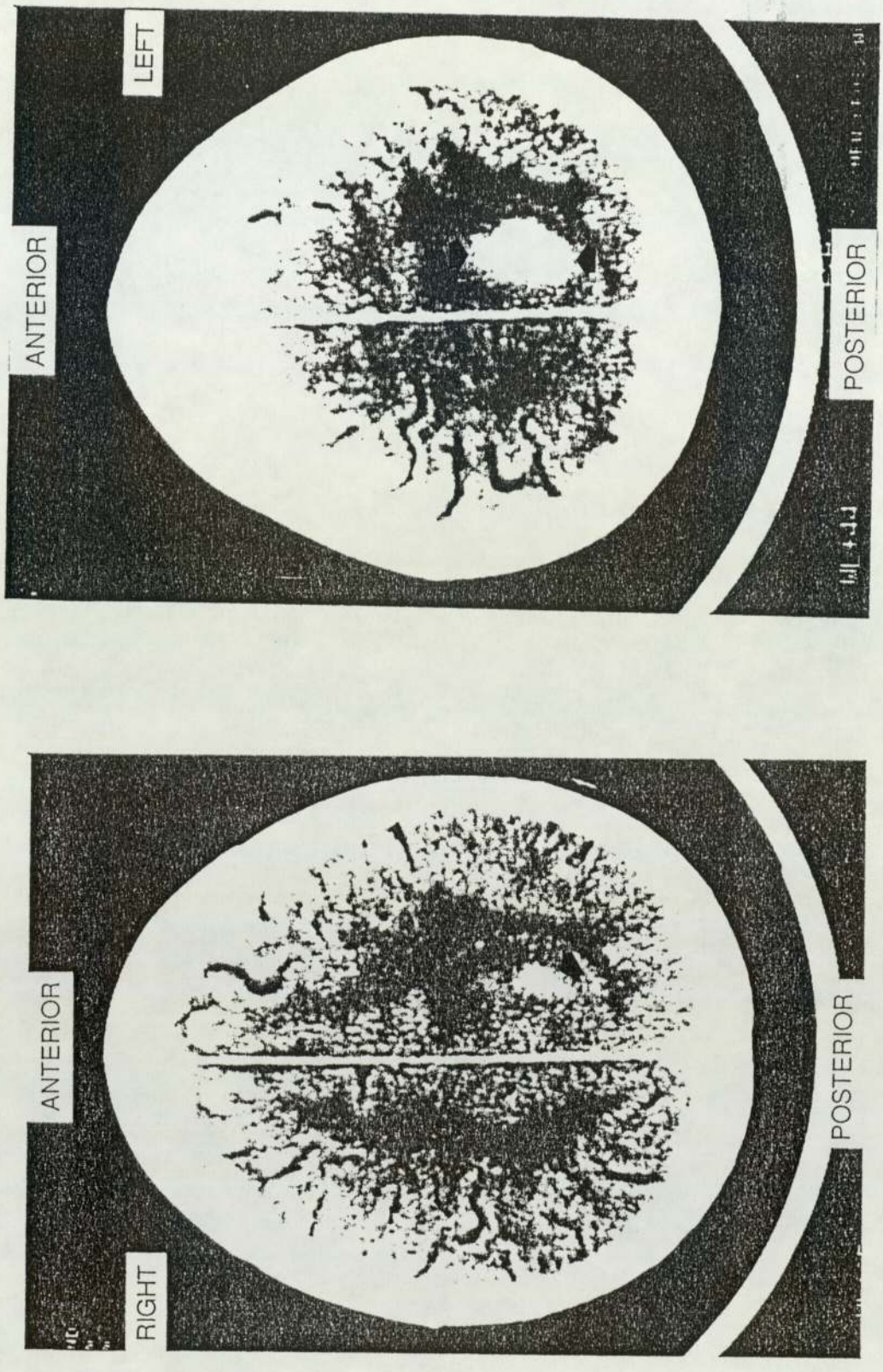

Figure 5.26. CT scans of patient P8. Arrows indicate site of lesion.

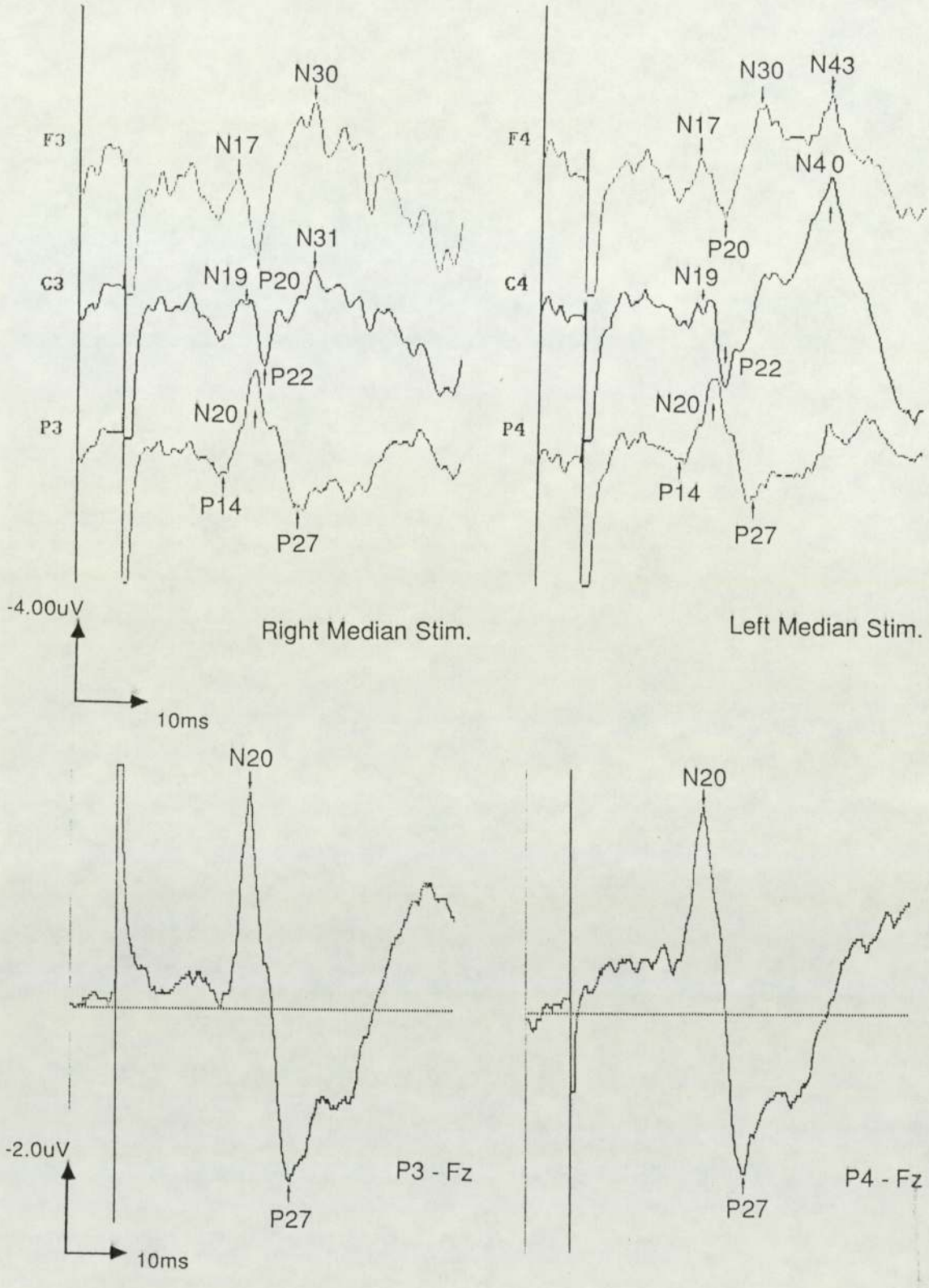

Figure 5.27. SEP waveforms for Patient 8 (P8) for right and left median nerve stimulation.Fz reference derived potentials are shown beneath the original earlobe reference recordings.

With the exception of this unusual and large unilateral N40 component all other peak latencies and peak to peak amplitudes in this patient were within normal limits compared to the control group (Table 5.14).

Patient waveforms were compared with the control group mean waveforms using the Z statistic. Two clear areas of abnormality were indicated. Not surprisingly a standard deviation of 3.56 was recorded at the C4 electrode to left median stimulation concomitant with the peak of the spurious N40 component (Figure 5.28). More surprisingly was a standard deviation of 3.56 at the C3 electrode to left median stimulation concomitant with the latency of a normal P22 potential at the C4 electrode (see Figure 5.29). Closer examination of the 'ipsilateral P22' in comparison to the control group mean ipsilateral potential revealed a marked difference (Figure 5.30). In fact examination of the ipsilateral central potential in the individual control subjects confirmed that the ipsilateral potential would normally consist of a broad negativity with either little or no indication of the corresponding positivity in the contralateral hemisphere. Therefore at +1.22uV, the 'ipsilateral P22' represented a significant variation from normal. This was confirmed by comparing the patient P22 map with the control group mean P22 map, again using the Z statistic (Figure 5.29); the resultant map also indicated a significant variation at the ipsilateral C3 site (3.18 standard deviations).

Inspection of the 'N40' map revealed a potential field closely similar to the familiar P22 map also seen in this patient (Figure 5.28).

Fz derived potentials produced closely similar potentials (Figure 5.27) which fell within normal limits.

Patient: P8
Age (years): 63
Height (cm): 175

LATENCY DATA

Component	Patient Data (ms)		Upper limit	Interhemisphere Latency	Interhemisphere Latency Diff.
	Right limb	Left limb	of normality	Difference (ms)	Upper Limit (ms)
Erbs	12.25	12.00	12.51	0.25	0.49
P14	15.75	16.00	17.79	-0.25	1.61
N17	18.75	18.75	21.57	0.00	1.83
N19	20.00	19.75	22.45	0.25	1.70
N20	21.75	21.75	23.42	0.00	1.72
P20	22.00	23.25	26.31	-1.25	3.56
P22	23.25	23.50	28.28	-0.25	3.79
N23			29.65	0.00	1.79
P27	29.50	28.25	35.96	1.25	4.32
N30	31.50	29.00	37.85	2.50	4.64
N31	31.75	30.50	38.23	1.25	3.90
N33	35.00	31.75	40.52	3.25	4.23
P35			43.89	0.00	2.40
P42(Part)	39.25	38.50	51.58	0.75	3.84
N43			54.34	0.00	4.68
Erbs-P14	3.50	4.00	6.51		
N17-P20	3.25	4.50	6.25		
N19-P22	3.25	3.75	8.07		
P14-N20	6.00	5.75	7.52		

AMPLITUDE DATA

Component Amplitude	Patient Data (uV)		Lower limit	Interhemisphere Amplitude	Interhemisphere Amp. Diff.
	Right limb	Left limb	of normality	Difference (uV)	Upper Limit (uV)
Frontal comps.					
0-P14	2.28	1.47	0.09	0.81	1.54
P14-N17	1.39	1.31	0.12	0.08	1.31
N17-P20	2.90	2.16	0.04	0.74	1.52
P20-N30	5.70	3.95	0.08	1.75	2.55
Central comps.					
0-P14	1.63	0.93	0.09	0.70	1.27
P14-N19	1.39	0.40	0.06	0.99	1.94
N19-P22	2.25	2.69	0.22	-0.44	3.04
P22-N31	3.42	3.91	0.01	-0.49	3.31
N31-P42	U	0.12	0.28	-0.12	5.32
Parietal comps.					
0-P14	1.30	0.12	0.02	1.18	1.35
P14-N20	3.83	2.25	0.36	1.58	2.73
N20-P27	4.98	4.25	0.41	0.73	3.34
P27-N33	0.98	0.89	0.08	0.09	4.12
N33-P42	0.04	0.07	0.30	-0.03	3.78

Table 5.14 Comparison of latencies and amplitudes with normality limits from control group. Lower limit of normality for amplitude of control group calculated as 50% of minimum recorded value.
U = unclear peak - no precise latency and morphology determination.
Ab = component peak appears to be entirely absent.
Bold figures indicate data which exceeds upper limits of normality.
Interhemisphere differences calculated as (Right-Left) limb data.

Patient: P8 **Fz reference derived potentials**
Age: 63
Height: 175

Component	Patient Data (ms)		Upper limit	Interhemisphere Latency	Interhemisphere Latency Diff.
	Right limb	Left limb	of normality	Difference (ms)	Upper Limit (ms)
N20	22.00	22.00	24.38	0.00	1.61
P22			25.22	0.00	0.55
N25			26.77	0.00	1.42
P27	29.00	28.75	35.74	0.25	3.85
N33	34.25	34.75	43.53	-0.50	6.27
P42	37.25	37.75	54.75	-0.50	7.88

Component	Patient Data (uV)		Lower limit	Interhemisphere Amplitude	Interhemisphere Amp. Diff.
Amplitude	Right limb	Left limb	of normality	Difference (uV)	Upper Limit (uV)
0-N20	4.57	4.36	0.32	0.21	2.27
N20-P27	8.26	7.80	0.50	0.46	5.49
P27-N33	1.78	1.78	0.44	0.00	5.78
N33-P42	0.09	0.08	0.24	0.01	4.55

Table 5.14.1

Comparison of latencies and amplitudes with normality limits from control group.
Lower limit of normality for amplitude of control group calculated as 50% of minimum recorded value.
U = unclear peak - no precise latency and morphology determination.
Ab = component peak appears to be entirely absent.
Bold figures indicate data which exceeds upper limits of normality.
Interhemisphere differences calculated as (Right-Left) limb data.

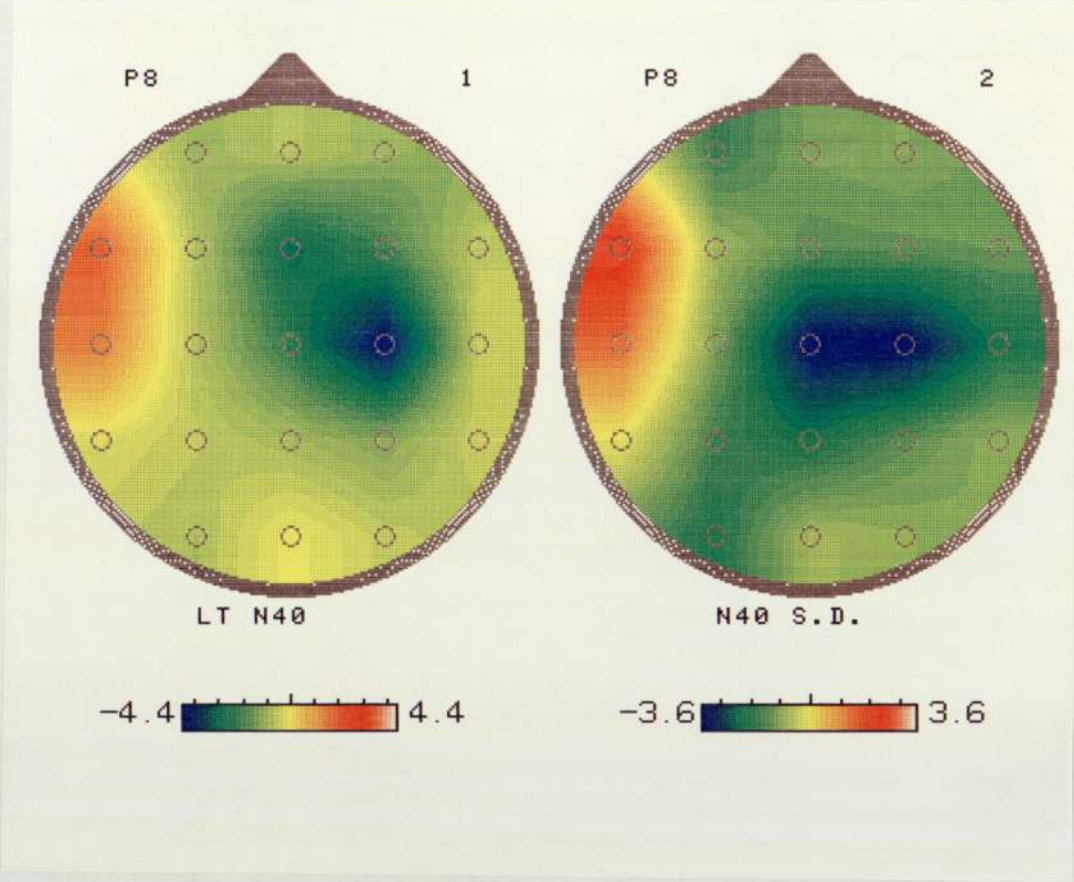

Figure 5.28. Patient P8 N40 component map recorded to left median stimulation (left);Standard deviation map concomitant with peak of N40 at 40.25ms (right) using Z transform with control group mean waveforms.

Figure 5.29. Overleaf. P22 component map for patient P8 (left);

Standard deviation map generated by Z transform analysis with control group mean waveforms (centre);

Standard deviation map generated by Z transform analysis with control group mean P22 component map (right).

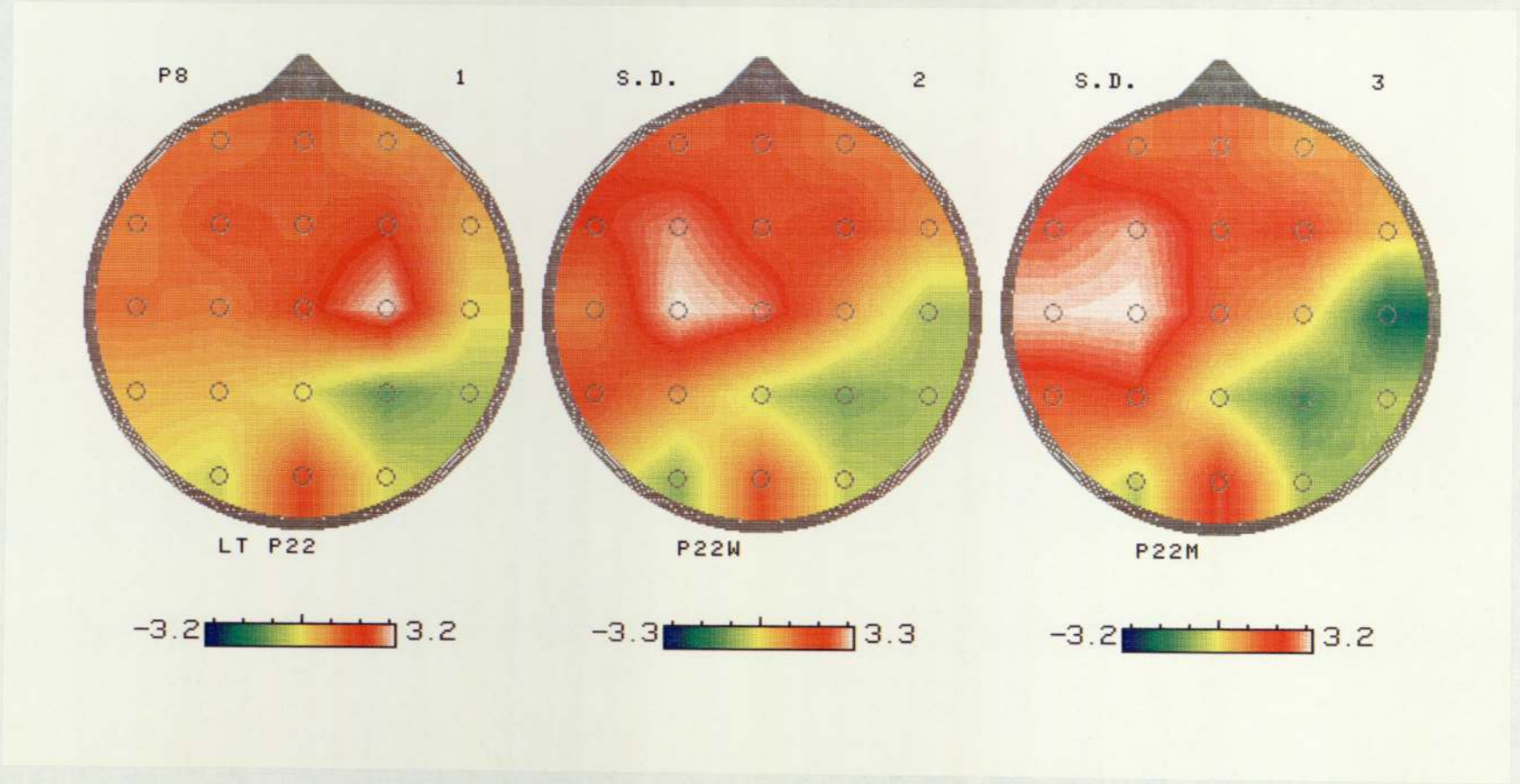
P8
1
LT P22
-3.2
3.2
S.D.
2
P22W
-3.3
3.3
S.D.
3
P22M
-3.2
3.2

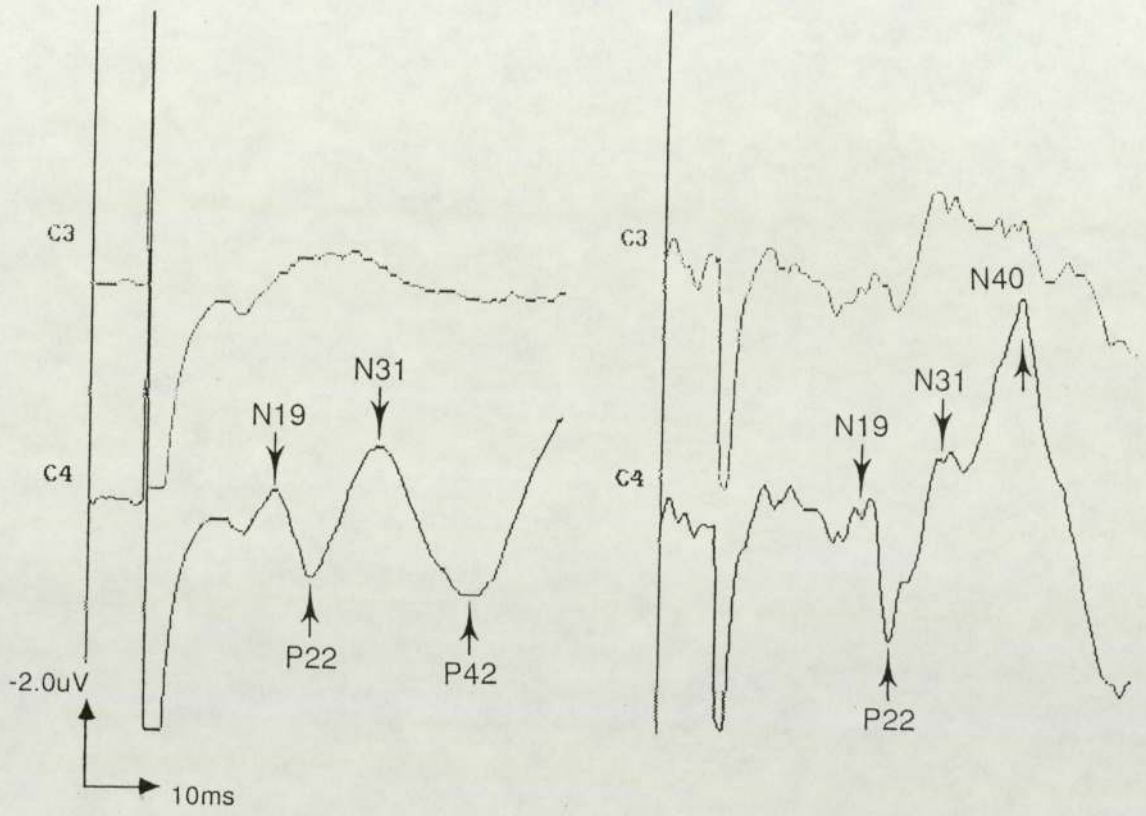

Figure 5.30. Control group mean ipsilateral and contralateral central waveforms to left median nerve stimulation (left) shown in comparison to patient P8 waveforms.

5.3.8.3. Summary and conclusion of P8 results.

This patient presented with no obvious neurological signs despite CT scan evidence of a large left parietal haematoma. There was also CT scan evidence of infarction in the right frontal lobe. The patient had a history of recurrent loss of consciousness.

SEP's revealed an unusual and large central N40 component in the right hemisphere to left median stimulation which was not present in right limb/left hemisphere recordings. A similar component morphology was recorded bilaterally in patient 6 (N50).

Statistical mapping confirmed the N40 component as a significant deviation from the control group and also indicated that the ipsilateral P22 recorded to left median stimulation also deviated significantly.

The diagnostic significance of the ipsilateral P22 abnormality in left median recordings determined by statistical mapping was difficult to interpret. Mauguière et al (1983) described how components could be 'volume conducted' to areas where the normal component was absent due to a lesion, although in all the cases described, this 'replacement' was always in the same cortical hemisphere.

However, could it be possible that the unusual appearance of the ipsilateral P22 was caused by the presence of the left hemisphere lesion blocking normal ipsilateral conduction of potentials thus allowing contralateral volume conduction to prevail?.

Interpretation of this data is difficult given evidence of both right and left hemisphere lesions. The N40 component for example could be explained as being evidence of an aberrant potential caused by the right frontal infarction or indeed as a normal, if unusual variant, which has been lost in the left hemisphere due to the large parietal infarction.

It is interesting to note however that whichever way the data is interpreted, peak latency and peak to peak amplitude data of the Fz reference derived potentials failed to reveal evidence of an asymmetry.

5.3.9.0. Patient 9 (P9) results.

5.3.9.1. P9 clinical presentation.

In February 1989, this 59 year old male patient suffered a right cerebral hemisphere infarction. He presented with left sided weakness, left hemianaesthesia and a left hemianopia (clinical summary Table 5.15). A CT scan revealed a large right tempero-parietal infarction (Figure 5.31).

SEP mapping was performed in March 1989. A follow up examination three months later indicated an improvement in weakness and sensory loss with the hemianopia persisting.

5.3.9.2. P9 SEP results.

Components to right median stimulation presented F type I W, C type I and P type I morphology using the control group classification. All peak latencies and peak to peak amplitudes on this side were within normal limits. Components to left median stimulation were markedly different. Classification of frontal morphology was difficult on this side because of a broad and 'broken' N30 potential which did not allow precise peak identification. However, P14, N17 and P20 components were clearly evident and closely similar to their right median counterparts.

Centrally, the P22-N31-P42 complex seen to right median stimulation was 'replaced' by a simple positive- negative complex giving a C type III classification. A closely similar P type III was seen at parietal locations. Waveforms are shown in Figures 5.32 and 5.33.

Analysis of peak latency and peak to peak data (Table 5.16) revealed a significant right versus left limb/hemisphere P22 latency difference. Absolute interpeak latencies of N19-P22 and P14-N20 were significantly prolonged to left median stimulation (>2.5 standard deviations).

Table 5.15 Clinical Summary for Patient P9

	UPPER LIMB		LOWER LIMB	
	Right	Left	Right	Left
Power	Normal	4/5	Normal	4/5
Tone	Normal	↑	Normal	Normal
Reflex	Normal	↑	Normal	↑
Pain	Normal	↓	Normal	↓
Temp.				
Touch	Normal	↓	Normal	↓
Vibration	Normal	↓	Normal	↓
Position	Normal	Normal	Normal	Normal
2 Point dis.	Normal	↓	Normal	↓
Stereognosis	Normal	↓	Normal	Normal

Direction of arrow indicates an increase (upward) or decrease (downward) of sensory or motor function.
In the case of reflex activity an upward arrow indicates hyperreflexia.
Motor function shown as a fraction indicates degree of loss compared to the other limb.

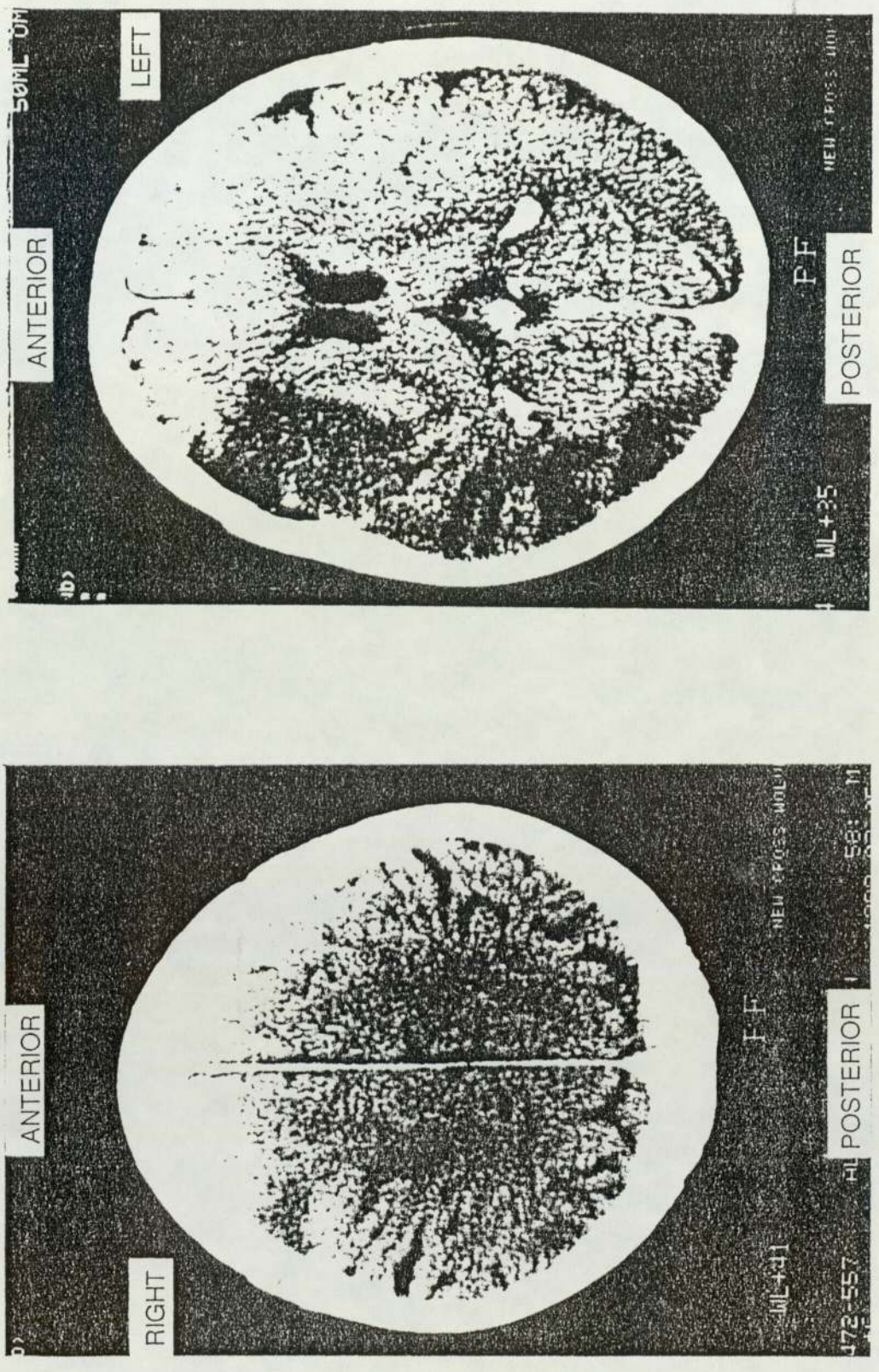

Figure 5.31. CT scans of patient P9. Arrows indicate site of lesion.

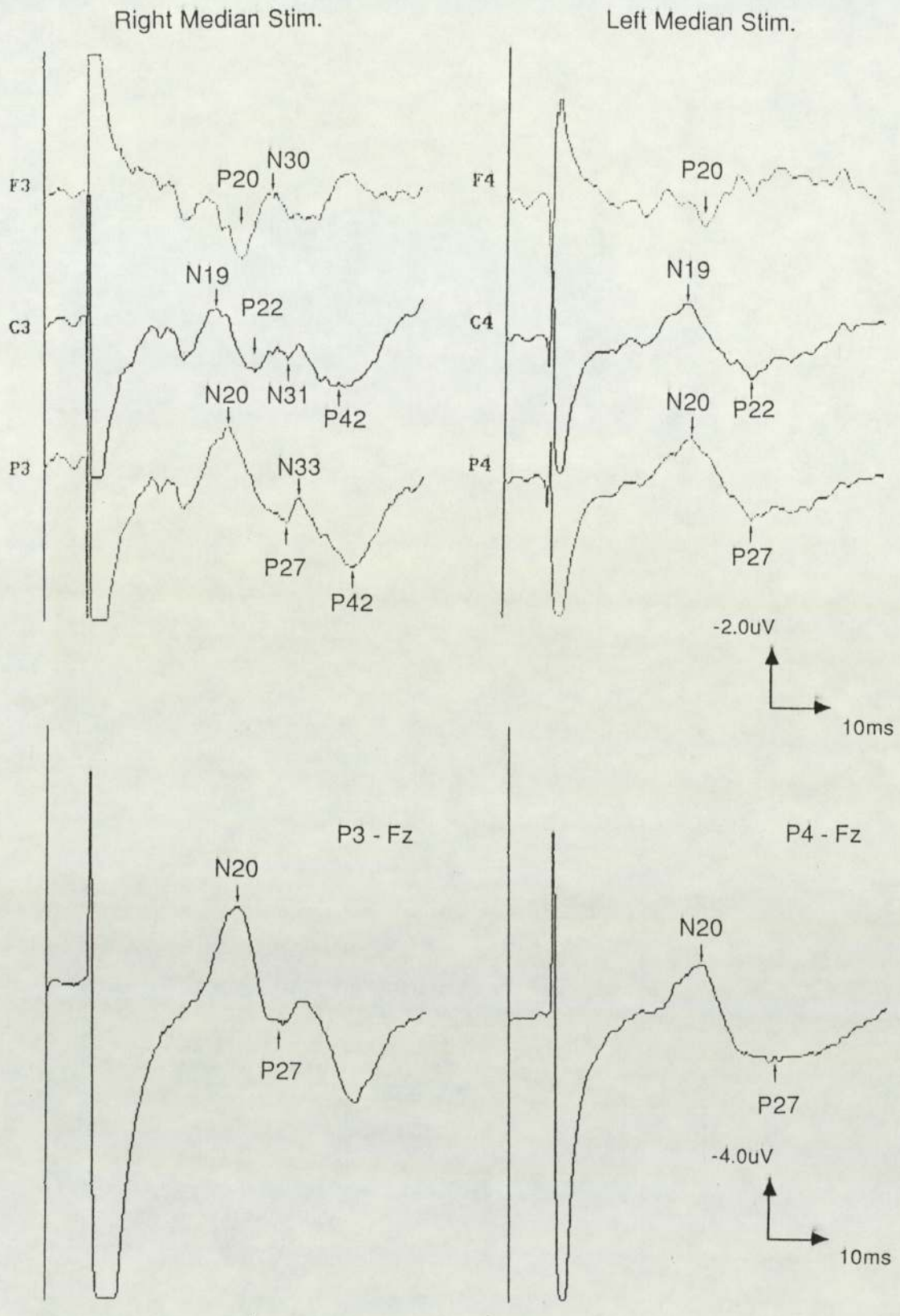

Figure 5.32. SEP waveforms for Patient 9 (P9) for right and left median nerve stimulation.Fz reference derived potentials are shown beneath the original earlobe reference recordings.

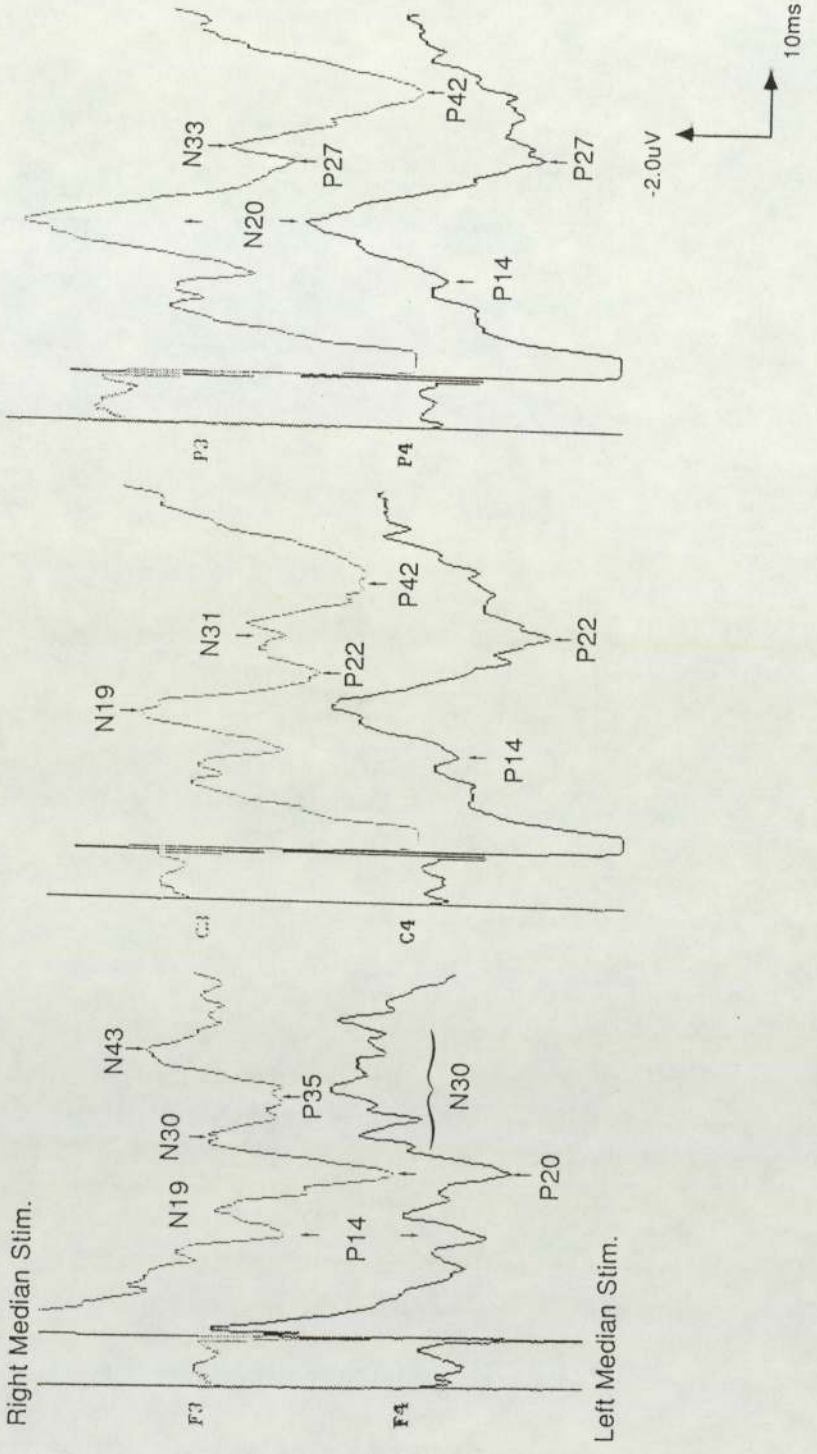

Figure 5.33. Waveforms of patient P9 to right median (upper traces) and left median (lower traces) nerve stimulation.

Patient: P9
Age (years): 59
Height (cm): 178

LATENCY DATA

Component	Patient Data (ms)		Upper limit	Interhemisphere Latency	Interhemisphere Latency Diff.
	Right limb	Left limb	of normality	Difference (ms)	Upper Limit (ms)
Erbs	11.50	11.25	12.58	0.25	0.49
P14	16.00	15.50	17.94	0.50	1.61
N17	19.75	19.50	21.75	0.25	1.83
N19	21.25	22.50	22.56	-1.25	1.70
N20	23.25	23.75	23.50	-0.50	1.72
P20	25.25	25.50	26.40	-0.25	3.56
P22	27.50	34.00	28.24	**-6.50**	3.79
N23		31.50	29.61		1.79
P27	32.75	34.25	35.96	-1.50	4.32
N30	30.75	**38.50**	37.85	**-7.75**	4.64
N31	33.50	U	38.44		3.90
N33	35.25	U	40.52		4.23
P35	36.50		43.89		2.40
P42(Part)	44.25	Absent	51.58		3.84
N43	44.25		54.34		4.68
Erbs-P14	4.50	4.25	6.59		
N17-P20	5.50	6.00	6.10		
N17-N30	11.00	19.00	19.33		
N19-P22	6.25	**11.50**	7.90		
P14-N20	7.25	**8.25**	7.46		

AMPLITUDE DATA

Component Amplitude	Patient Data (uV)		Lower limit	Interhemisphere Amplitude	Interhemisphere Amp. Diff.
	Right limb	Left limb	of normality	Difference (uV)	Upper Limit (uV)
Frontal comps.					
0-P14	0.95	0.89	0.09	0.06	1.54
P14-N17	0.85	0.77	0.12	0.08	1.31
N17-P20	2.25	1.32	0.04	0.93	1.52
P20-N30	2.23	2.26	0.08	-0.03	2.55
Central comps.					
0-P14	0.81	0.40	0.09	0.41	1.27
P14-N19	1.81	1.54	0.06	0.27	1.94
N19-P22	0.29	2.71	0.22	-2.42	3.04
P22-N31	0.44	U	0.01		3.31
N31-P42	1.01	U	0.28		5.32
Parietal comps.					
0-P14	1.05	0.28	0.02	0.77	1.35
P14-N20	2.91	1.73	0.36	1.18	2.73
N20-P27	3.41	2.96	0.41	0.45	3.34
P27-N33	0.83	U	0.08		4.12
N33-P42	2.54	U	0.30		3.78

Table 5.16 Comparison of latencies and amplitudes with normality limits from control group. Lower limit of normality for amplitude of control group calculated as 50% of minimum recorded value.
U = unclear peak - no precise latency and morphology determination.
Ab = component peak appears to be entirely absent.
Bold figures indicate data which exceeds upper limits of normality.
Interhemisphere differences calculated as (Right-Left) limb data.

Patient: P9 **Fz reference derived potentials**
Age: 59
Height: 178

Component	Patient Data (ms)		Upper limit	Interhemisphere Latency	Interhemisphere Latency Diff.
	Right limb	Left limb	of normality	Difference (ms)	Upper Limit (ms)
N20	24.25	24.50	24.52	-0.25	1.61
P22			25.22	0.00	0.55
N25			26.77	0.00	1.42
P27	31.50	33.75	35.74	-2.25	3.85
N33	35.75	A	43.53		6.27
P42	44.25	A	54.75		7.88

Component Amplitude	Patient Data (uV)		Lower limit	Interhemisphere Amplitude	Interhemisphere Amp. Diff.
	Right limb	Left limb	of normality	Difference (uV)	Upper Limit (uV)
0-N20	3.83	1.87	0.32	1.96	2.27
N20-P27	4.15	3.34	0.50	0.81	5.49
P27-N33	0.71	A	0.44		5.78
N33-P42	3.62	A	0.24		4.55

Table 5.16.1

Comparison of latencies and amplitudes with normality limits from control group.
Lower limit of normality for amplitude of control group calculated as 50% of minimum recorded value.
U = unclear peak - no precise latency and morphology determination.
Ab = component peak appears to be entirely absent.
Bold figures indicate data which exceeds upper limits of normality.
Interhemisphere differences calculated as (Right-Left) limb data.

Statistical mapping yielded no data point or electrode site that exceeded 2.5 standard deviations from the control group mean waveforms. Comparison of the patient map at the latency of central P22 and parietal P27 components to left median stimulation with the control group P22 and P27 maps similarly revealed no location that exceeded 2.5 standard deviations (Figure 5.34).

Fz reference derived potentials (Figure 5.32) revealed a left median N20 attenuation compared to its right median counterpart, although this fell within normal limits. The familiar P27-N33-P42 complex was seen to right limb stimulation was replaced by a broad simple V complex to left limb stimulation.

5.3.9.3. Summary and conclusion of P9.

This patient, presenting with a large right tempero- parietal infarct producing left sided weakness and sensory loss, produced a number of left median/right hemisphere SEP abnormalities. It is tempting to describe these abnormalities as loss of the central P22 -N31-P42 and parietal N33-P42 complexes as well as the concomitant frontal P35-N43 complex. Again, it may be possible that the 'lost' central components were 'replaced' by forward volume conduction of the parietal P27 component. This is a more seductive argument than interpreting the abnormal P22 asymmetry as simple delay of the right hemisphere component since the right hemisphere P22 presented with the identical latency and morphology to the parietal P27 which was not itself abnormally prolonged.

Statistical mapping would be interpreted as yielding a false negative finding in this case.

Figure 5.34. Overleaf.P22/P27 component map for patient P9 at 32.25ms (left);
Standard deviation map generated by Z transform analysis
with control group mean P22 component map (centre);
Standard deviation map generated by Z transform analysis
with control group mean P27 component map (right).

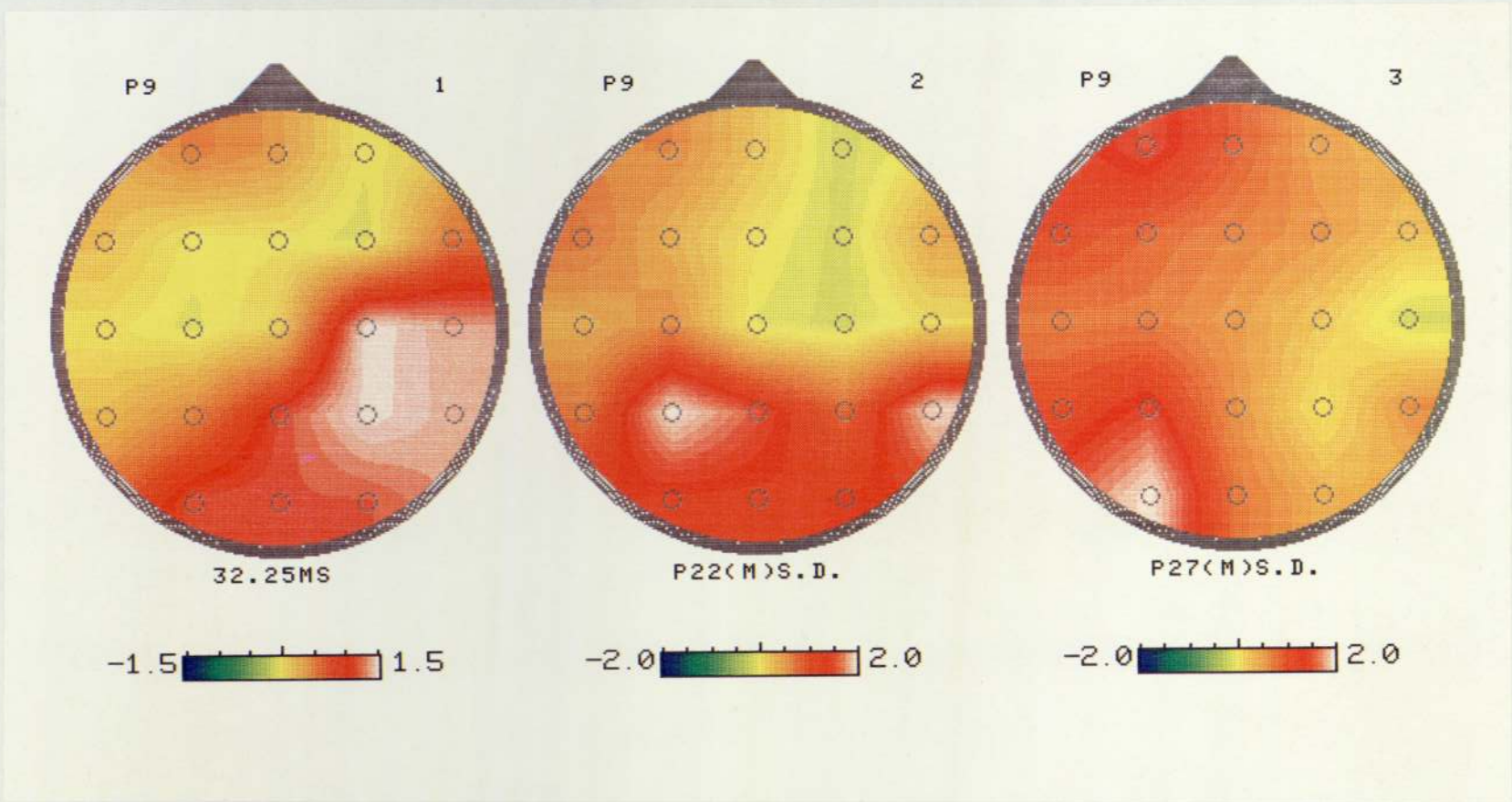
P9
1
32.25MS
-1.5
1.5
P9
2
P22(M)S.D.
-2.0
2.0
P9
3
P27(M)S.D.
-2.0
2.0

5.3.10.0. Patient 10 (P10) results.

5.3.10.1. P10 clinical presentation.

This 55 year old patient presented on the 12th May 1989 with right lower limb weakness and difficulty with speech but no sensory loss or upper limb signs. Towards the end of May the patient became subject to occasional myoclonic jerking of the toes of the right foot. These focal fits occasionally spread to involve the right arm and face.

A CT scan revealed a tiny focal lesion in the left precentral area close to the Falx.

Neurological exam immediately prior to SEP mapping revealed increased muscle tone on the right with right pyramidal weakness affecting the right leg. Sensation was normal. Right reflexes were brisker than let with right extensor plantar (Table 5.17). Three weeks had elapsed since onset of symptoms.

5.3.10.2. P10 SEP results.

Subjective inspection of the patient waveforms revealed closely similar morphology types between sides - F type II V, C type I and P type I to right median stimulation and F type II V, C type I and P type II to left median nerve stimulation (Figure 5.35). The main distinguishing features between the two hemisphere responses were amplitude asymmetry, with P22, P27 and N30 components in the right hemisphere to left median stimulation being much smaller in amplitude than the left hemisphere/right median counterparts (see also Figure 5.36). Analysis of peak to peak amplitude data (Table 5.18) revealed that the N19-P22 and P22-N31 central complexes and P27-N33 parietal complex to right median stimulation were abnormally large potentials compared to the control group data (>2.5 standard deviations).

Predictably therefore each of these potentials yielded abnormally large interhemisphere amplitude differences (>2.5 standard deviations).

All peak and interpeak latency data was within normal limits.

Table 5.17 Clinical Summary for Patient P10

	UPPER LIMB		LOWER LIMB	
	Right	Left	Right	Left
Power	Normal	Normal	2/5	Normal
Tone	Normal	Normal	↑	Normal
Reflex	Normal	Normal	↑	Normal
Pain	Normal	Normal	Normal	Normal
Temp.	Normal	Normal	Normal	Normal
Touch	Normal	Normal	Normal	Normal
Vibration	Normal	Normal	Normal	Normal
Position	Normal	Normal	Normal	Normal
2 Point dis.	Normal	Normal	Normal	Normal
Stereognosis	Normal	Normal	Normal	Normal

Direction of arrow indicates an increase (upward) or decrease (downward) of sensory or motor function.
In the case of reflex activity an upward going arrow indicates hyperreflexia.

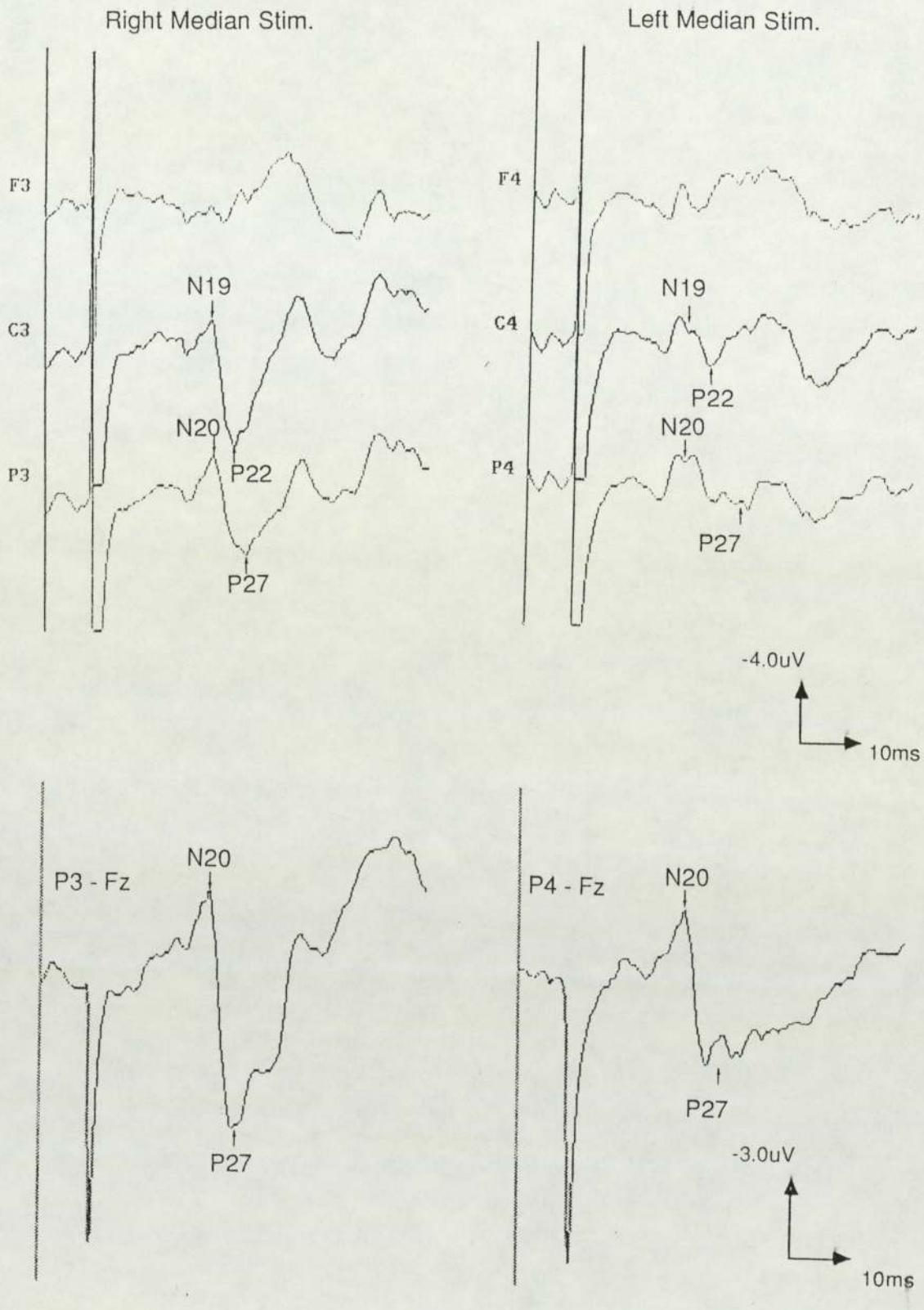

Figure 5.35. SEP waveforms for Patient 10 (P10) for right and left median nerve stimulation.Fz reference derived potentials are shown beneath the original earlobe reference recordings.

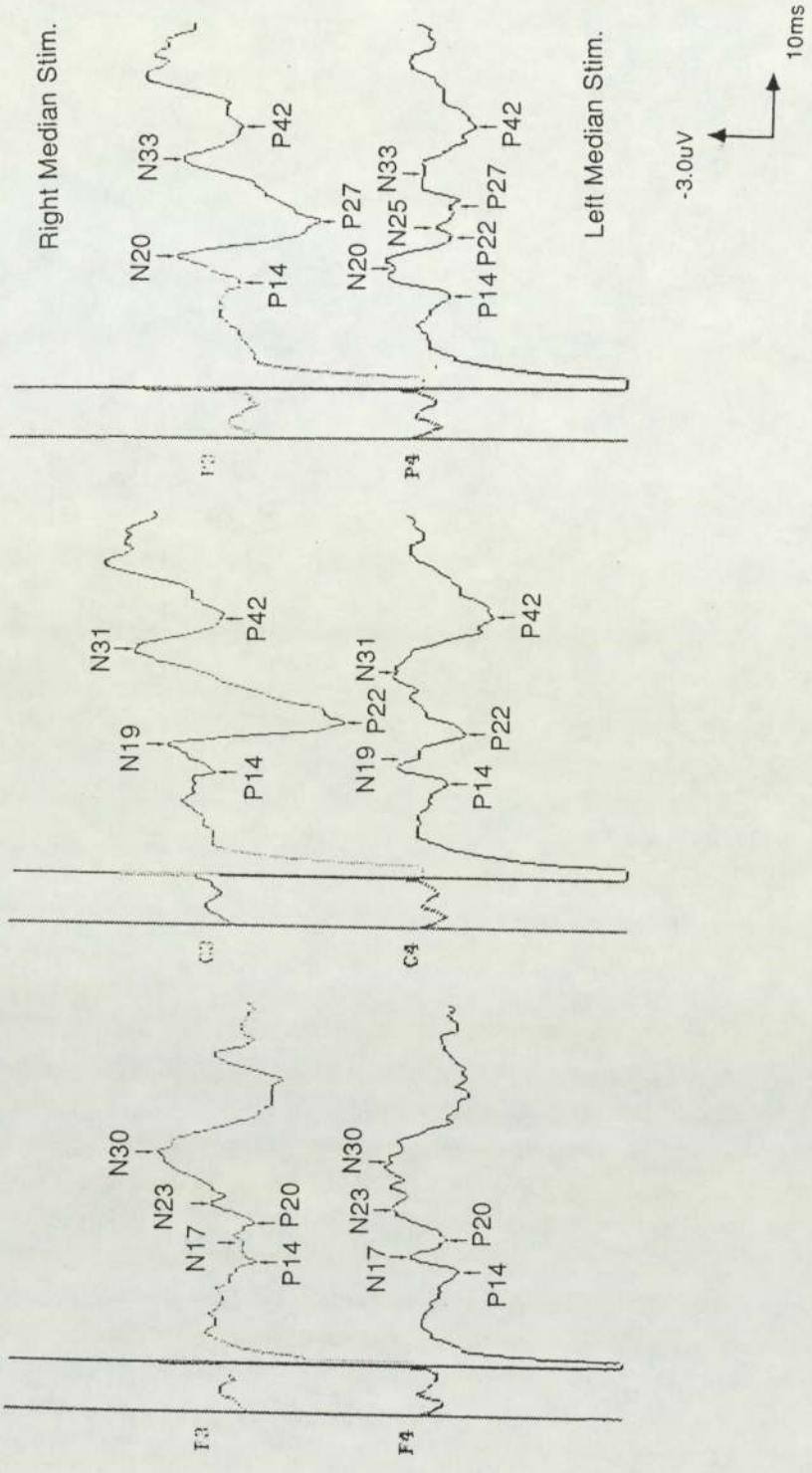

Figure 5.36. Waveforms of patient P10 to right median (upper traces) and left median (lower traces) nerve stimulation.

Patient: P10
Age (years): 55
Height (cm): 178

LATENCY DATA

Component	Patient Data (ms)		Upper limit	Interhemisphere Latency	Interhemisphere Latency Diff.
	Right limb	Left limb	of normality	Difference (ms)	Upper Limit (ms)
Erbs	10.50	10.25	12.46	0.25	0.49
P14	16.00	14.50	17.75	1.50	1.61
N17	19.75	17.00	21.55	2.75	1.83
N19	20.00	19.00	22.34	1.00	1.70
N20	20.25	19.00	23.27	1.25	1.72
P20	22.00	19.75	26.08	2.25	3.56
P22	24.00	22.25	27.85	1.75	3.79
N23	24.75	24.50	29.21	0.25	1.79
P27	25.75	28.00	35.96	-2.25	4.32
N30	32.75	31.00	37.85	1.75	4.64
N31	34.50	31.25	38.22	3.25	3.90
N33	35.25	33.25	40.52	2.00	4.23
P35			43.89	0.00	2.40
P42(Part)	40.25	40.50	51.58	-0.25	3.84
N43			54.34	0.00	4.68
Erbs-P14	5.50	4.25	6.51		
N17-P20	2.25	2.75	5.94		
N19-P22	4.00	3.25	7.72		
P14-N20	4.25	4.50	7.40		

AMPLITUDE DATA

Component Amplitude	Patient Data (uV)		Upper limit	Interhemisphere Amplitude	Interhemisphere Amp. Diff.
	Right limb	Left limb	of normality	Difference (uV)	Upper Limit (uV)
Frontal comps.					
0-P14	1.86	1.86	2.61	0.00	1.54
P14-N17	1.13	2.42	2.38	-1.29	1.31
N17-P20	1.05	1.92	2.75	-0.87	1.52
P20-N30	4.94	4.31	7.00	0.63	2.55
Central comps.					
0-P14	0.93	1.11	1.93	-0.18	1.27
P14-N19	2.42	1.49	3.20	0.93	1.94
N19-P22	**8.94**	2.47	8.05	**6.47**	3.04
P22-N31	**10.59**	3.78	9.32	**6.81**	3.31
N31-P42	4.31	5.00	9.03	-0.69	5.32
Parietal comps.					
0-P14	1.07	1.30	1.89	-0.23	1.35
P14-N20	3.25	2.94	5.23	0.31	2.73
N20-P27	7.12	2.92	8.29	**4.20**	3.34
P27-N33	**6.78**	1.23	6.60	**5.55**	4.12
N33-P42	2.94	2.54	7.38	0.40	3.78

Table 5.18 Comparison of latencies and amplitudes with normality limits from control group. Lower limit of normality for amplitude of control group calculated as 50% of minimum recorded value.
U = unclear peak - no precise latency and morphology determination.
Ab = component peak appears to be entirely absent.
Bold figures indicate data which exceeds upper limits of normality.
Interhemisphere differences calculated as (Right-Left) limb data.

Patient: P10 **Fz reference derived potentials**
Age: 55
Height: 178

Component	Patient Data (ms)		Upper limit	Interhemisphere Latency	Interhemisphere Latency Diff.
	Right limb	Left limb	of normality	Difference (ms)	Upper Limit (ms)
N20	20.25	19.75	24.33	0.50	1.61
P22		23.50	25.22		0.55
N25		26.00	26.77		1.42
P27	25.00	28.50	35.74	-3.50	3.85
N33	35.75	A	43.53		6.27
P42	39.25	A	54.75		7.88

Component Amplitude	Patient Data (uV)		Upper limit	Interhemisphere Amplitude	Interhemisphere Amp. Diff.
	Right limb	Left limb	of normality	Difference (uV)	Upper Limit (uV)
0-N20	2.89	2.99	6.46	-0.10	2.27
N20-P27	8.39	5.63	14.40	2.76	5.49
P27-N33	6.86	-	11.35		5.78
N33-P42	0.79	-	9.35		4.55

Table 5.18.1

Comparison of latencies and amplitudes with normality limits from control group.
Lower limit of normality for amplitude of control group calculated as 50% of minimum recorded value.
U = unclear peak - no precise latency and morphology determination.
Ab = component peak appears to be entirely absent.
Bold figures indicate data which exceeds upper limits of normality.
Interhemisphere differences calculated as (Right-Left) limb data.

Comparison of the patient left limb waveforms to control group mean waveforms using the Z statistic revealed no data point or electrode location that exceeded 2.5 standard deviations. Right limb waveform analysis however revealed a broad area of abnormality to statistical mapping over the left centro-parietal area with a maxima at C3 of 5.93 standard deviations (Figure 5.37). Examination of peaks concomitant with standard deviation maxima confirmed that P22 and P27 components to right median stimulation were abnormally large in amplitude. Comparison of these component maps with the respective control group mean maps revealed a shift in the scalp locations of standard deviation maxima compared to the waveform analysis. In the case of the P22 component map, the standard deviation at C3 had fallen from 5.93 to 2.60 with the new maxima at P3 of 3.43 standard deviations (Figure 5.38). For P27, the C3 maxima of 5.62 seen in waveform analysis fell to 3.06 with a new maxima at T3 and a standard deviation of 4.81 (Figure 5.39).

Fz reference derived potentials reflected the right versus left amplitude asymmetry (Figure 5.35), although all peak to peak amplitude measures of N20 and P27 were within normal limits. There was no comparable N33-P42 complex to left limb stimulation for direct comparison to the right.

5.3.10.3. Summary and conclusion of P10 results.

This patient presented with CT scan evidence of a tiny lesion in the left precentral region. The patient had been subject to right focal fits and presented with some lower limb weakness but no upper limb motor or sensory signs.

The SEP waveforms were characterised by 'giant' P22 and P27 components in the left hemisphere with right median nerve stimulation.

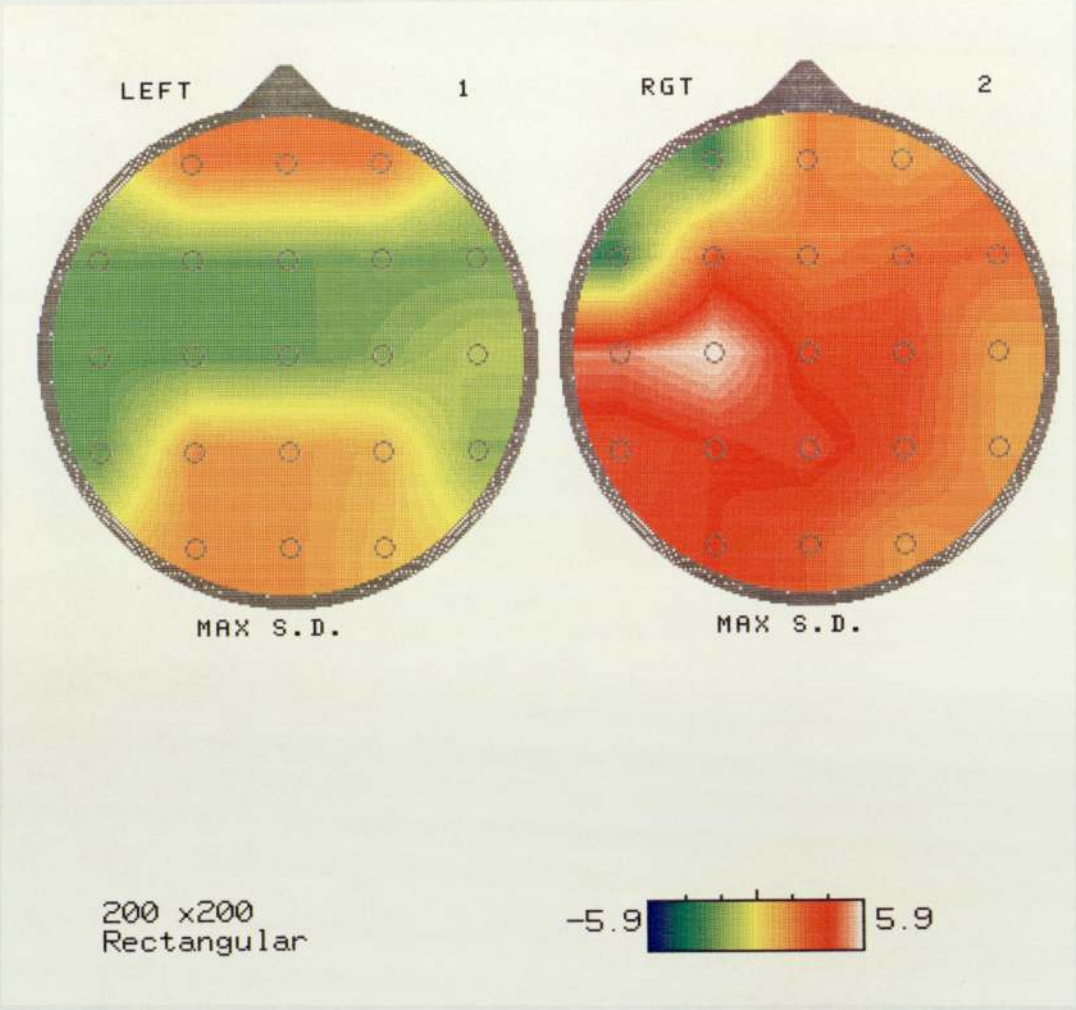

Figure 5.37. Patient 10 statistical mapping; maps indicate maximum standard deviation for left median nerve data (left) and right median nerve data (right).

Figure 5.38. Overleaf. P22 component map for patient P10 (left);
Standard deviation map generated by Z transform analysis
with control group mean waveforms (centre);
Standard deviation map generated by Z transform analysis
with control group mean P22 component map (right).

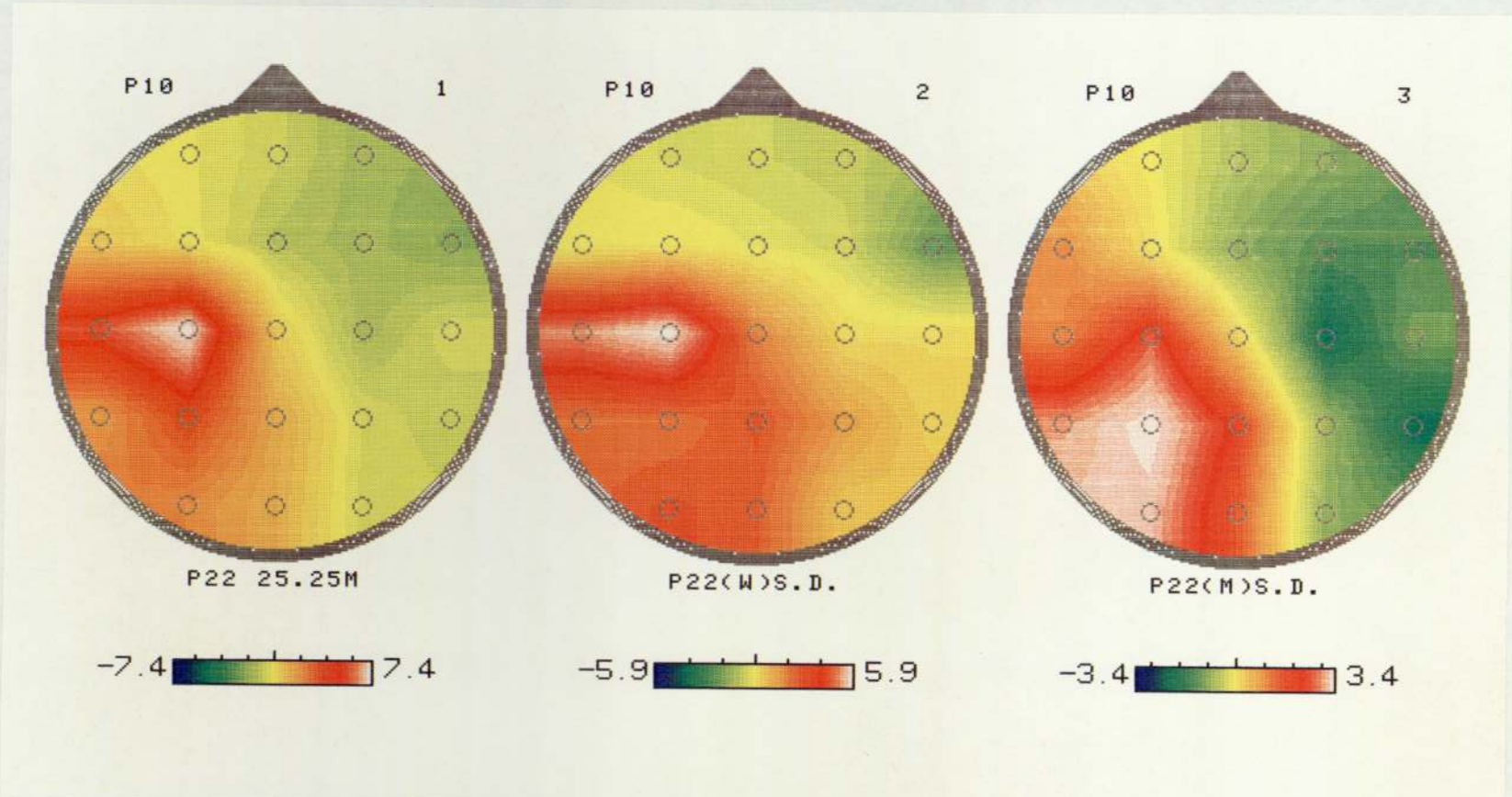
P10
1
P22 25.25M
-7.4
7.4
P10
2
P22(W)S.D.
-5.9
5.9
P10
3
P22(M)S.D.
-3.4
3.4

Figure 5.39. Overleaf. P27 component map for patient P10 (left);
Standard deviation map generated by Z transform analysis
with control group mean waveforms (centre);
Standard deviation map generated by Z transform analysis
with control group mean P27 component map (right).

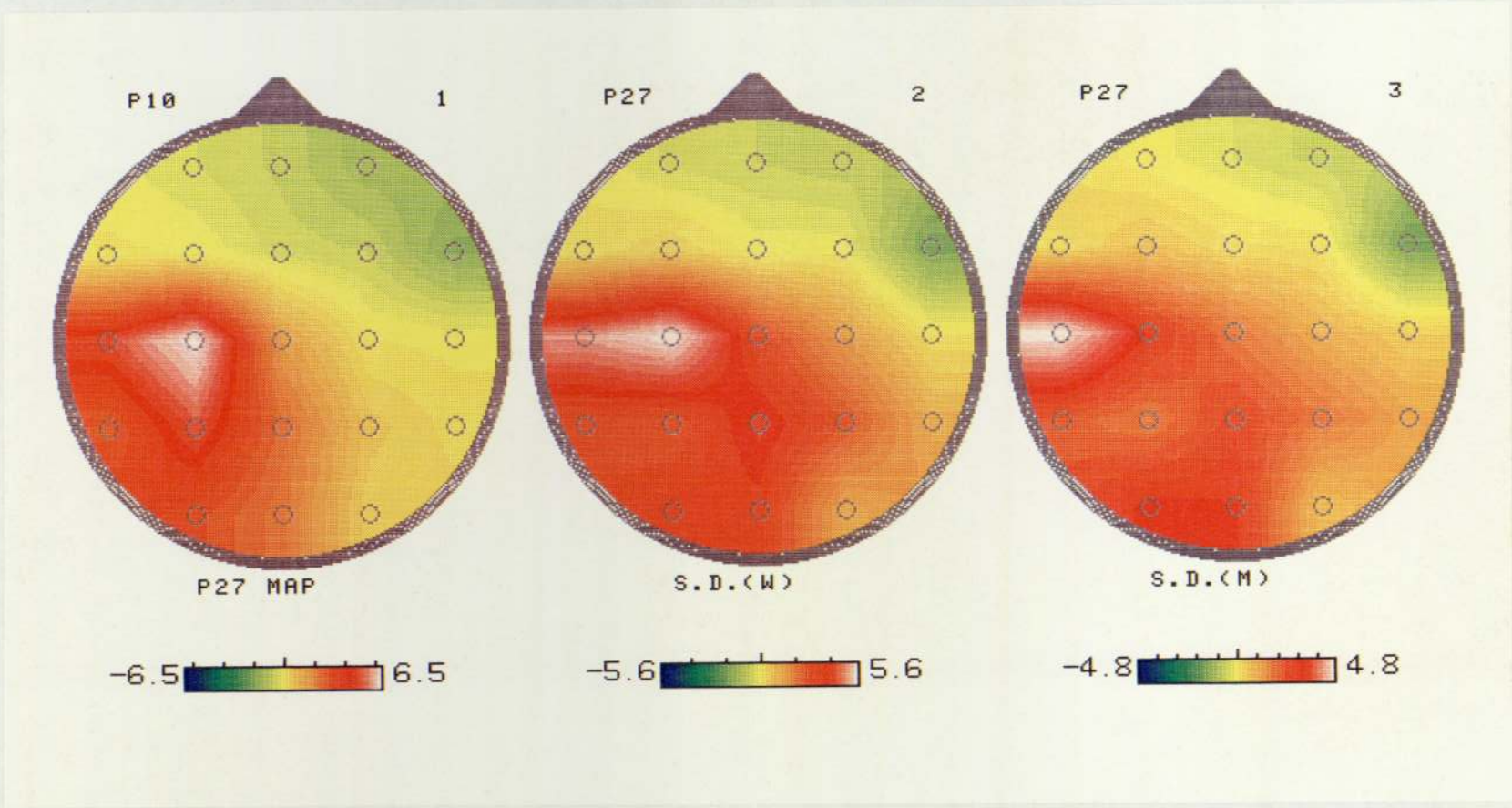
P10
1
P27 MAP
-6.5
6.5
P27
2
S.D.(W)
-5.6
5.6
P27
3
S.D.(M)
-4.8
4.8

These results were similar to the findings of patient 3 where a lesion in close proximity to the primary somatosensory/somatomotor cortex causing an 'irritative' effect on the cortex i.e. epileptogenic, produced focal discrete augmentation of components.

In the case of patient 3 however, the augmentation co-existed with attenuation of all other components whereas in the case of patient 10, all other potentials were of similar amplitude to their normal opposite hemisphere counterparts. The fact that the P42 complexes that followed the giant P22 and P27 components were of normal amplitude possibly suggests that they therefore arose from different generators.

Whilst it would be predicted that the standard deviation of the patient's 'giant' potentials would be smaller in group mean component maps compared with group mean waveform maps with statistical mapping (component peaks were always of larger amplitude in control group mean maps than the group mean waveform counterparts), the difference in the locus of abnormality between the two types of analysis could not easily be predicted.

It is of interest to note that the right versus left N20-P27 interpeak amplitude difference fell within normal limits of control data for the Fz derived potentials.

5.3.11.0. Patient 11 (P11) results.

5.3.11.1. P11 clinical presentation.

A 68 year old male patient presented with episodic sensory disturbance of the right hand with occasional cramp like spasms. EMG examination was normal but clinically there was some evidence of wasting of this limb (Table 5.19).

A CT scan showed evidence of a left parietal lesion. An E.E.G. showed a slow wave abnormality in the left fronto-parietal area but no spikes were seen.

A diagnosis of a left parietal infarction with focal epilepsy was made.

Table 5.19 Clinical Summary for Patient P11

	UPPER LIMB		LOWER LIMB	
	Right	Left	Right	Left
Power	↓	Normal	Normal	Normal
Tone	Normal	Normal	Normal	Normal
Reflex	Normal	Normal	Normal	Normal
Pain	Normal	Normal	Normal	Normal
Temp.	Normal	Normal	Normal	Normal
Touch	Normal	Normal	Normal	Normal
Vibration	Normal	Normal	Normal	Normal
Position	Normal	Normal	Normal	Normal
2 Point dis.	↓	Normal	Normal	Normal
Stereognosis	Normal ?	Normal	Normal	Normal

Direction of arrow indicates an increase (upward) or decrease (downward) of sensory or motor function.
A question mark alongside a category indicates inconsistent findings on a trial / re-trial basis.

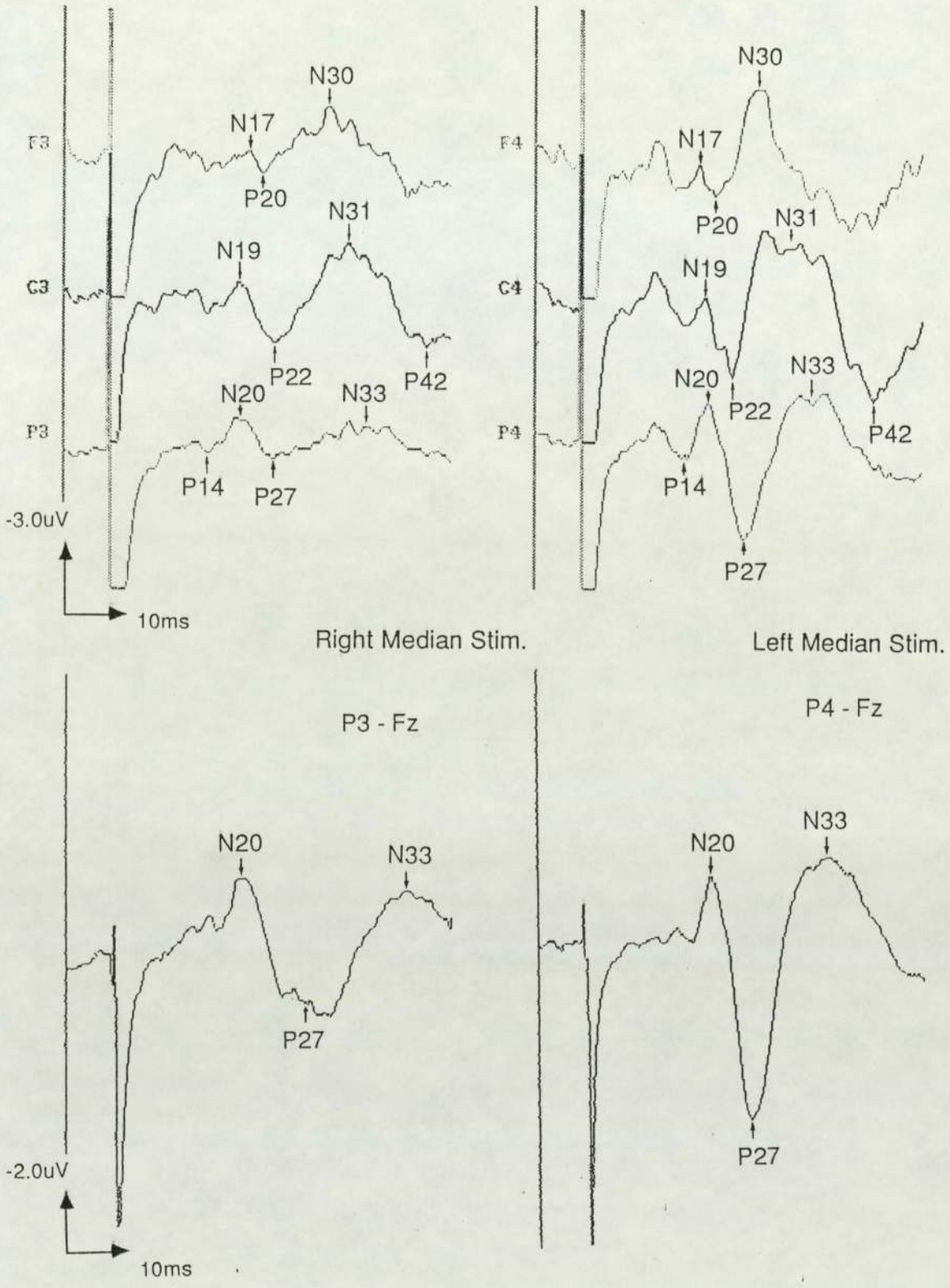

Figure 5.40. SEP waveforms for Patient 11 (P11) for right and left median nerve stimulation.Fz reference derived potentials are shown beneath the original earlobe reference recordings.

5.3.11.2. P11 SEP results.

Initial visual inspection of the waveforms revealed attenuation and prolongation of many of the SEP components in the left hemisphere to right median stimulation compared to the right hemisphere/left median potentials (Figure 5.40).Analysis of the patient peak latency and peak to peak amplitude data (Table 5.20) highlighted a number of abnormalities. Peak latencies of right median N31, N33 and central P42 components were abnormally prolonged compared to the control group (>2.5 standard deviations). Interpeak latencies were prolonged for N19-N31 and N20-N33 measures on the same side. Interhemisphere latency differences were also abnormal for N33 and central P42 components. It should be noted that precise identification of parietal P42 peaks could not be determined for right median stimulation.

The amplitude difference of the N20-P27 complex between hemispheres was abnormally large.

Comparison of patient waveforms with the control group mean waveforms using the Z statistic yielded no data point or scalp location that exceeded 2.5 standard deviations for either right or left median nerve stimulation (Figure 5.41). This was equally true for component map comparison with control group mean maps.

Fz reference derived potentials (Figure 5.40) reflected the abnormal attenuation of the N20-P27 complex with right median nerve stimulation compared to left (>2.5 s.d.). There was also an abnormally great inter-hemisphere peak latency difference of the N33 components.

5.3.11.3. Summary and conclusion of P11 results.

Patient 11 presented with a similar case history to two previously described patients (P3 and P10) with a discrete unilateral cortical lesion with episodic motor symptoms (jerking and clenching) affecting the contralateral upper limb. Unlike the previous two patients however, both of whom produced augmentation of at least one discrete potential - no augmentation was seen in the affected hemisphere in this patient, only attenuation and prolongation of potentials. Statistical mapping failed to detect an abnormality and would thus count as a false negative finding.

Patient: P11
Age (years): 68
Height (cm): 173

LATENCY DATA

Component	Patient Data (ms)		Upper limit	Interhemisphere Latency	Interhemisphere Latency Diff.
	Right limb	Left limb	of normality	Difference (ms)	Upper Limit (ms)
Erbs	12.00	12.00	12.53	0.00	0.49
P14	16.00	16.50	17.80	-0.50	1.61
N17	21.50	19.50	21.57	**2.00**	1.83
N19	21.50	20.25	22.52	1.25	1.70
N20	21.75	21.00	23.50	0.75	1.72
P20	25.00	22.00	26.45	3.00	3.56
P22	27.00	25.00	28.53	2.00	3.79
N23			29.91	0.00	1.79
P27	27.00	26.75	35.96	0.25	4.32
N30	36.00	29.25	37.85	6.75	4.64
N31	**39.25**	36.00	38.21	3.25	3.90
N33	**42.50**	38.25	40.52	**4.25**	4.23
P35			43.89	0.00	2.40
P42(Cent)	**52.50**	48.25	48.72	**4.25**	3.84
N43			54.34	0.00	4.68
Erbs-P14	4.00	4.50	6.50		
N17-P20	3.50	2.50	6.44		
N19-P22	5.50	4.75	8.29		
P14-N20	5.75	4.50	7.60		
N19-N31	**17.75**	15.75	17.69		
N20-N33	**20.75**	17.25	20.37		

AMPLITUDE DATA

Component Amplitude	Patient Data (uV)		Lower limit	Interhemisphere Amplitude	Interhemisphere Amp. Diff.
	Right limb	Left limb	of normality	Difference (uV)	Upper Limit (uV)
Frontal comps.					
0-P14	0.57	1.24	0.09	-0.67	1.54
P14-N17	0.43	0.79	0.12	-0.36	1.31
N17-P20	0.51	1.12	0.04	-0.61	1.52
P20-N30	1.81	3.89	0.08	-2.08	2.55
Central comps.					
0-P14	0.55	0.88	0.09	-0.33	1.27
P14-N19	1.06	0.89	0.06	0.17	1.94
N19-P22	2.08	2.78	0.22	-0.70	3.04
P22-N31	3.53	4.79	0.01	-1.26	3.31
N31-P42	3.63	5.71	0.28	-2.08	5.32
Parietal comps.					
0-P14	0.36	0.51	0.02	-0.15	1.35
P14-N20	1.21	1.94	0.36	-0.73	2.73
N20-P27	1.38	5.31	0.41	**-3.93**	3.34
P27-N33	1.12	4.80	0.08	-3.68	4.12
N33-P42	U	U	0.30	0.00	3.78

Table 5.20 Comparison of latencies and amplitudes with normality limits from control group. Lower limit of normality for amplitude of control group calculated as 50% of minimum recorded value.
U = unclear peak - no precise latency and morphology determination.
Ab = component peak appears to be entirely absent.
Bold figures indicate data which exceeds upper limits of normality.
Interhemisphere differences calculated as (Right-Left) limb data.

Patient: P11 **Fz reference derived potentials**
Age: 68
Height: 173

Component	Patient Data (ms)		Upper limit	Interhemisphere Latency	Interhemisphere Latency Diff.
	Right limb	Left limb	of normality	Difference (ms)	Upper Limit (ms)
N20	21.75	21.00	24.40	0.75	1.61
P22			25.22	0.00	0.55
N25			26.77	0.00	1.42
P27	28.75	27.50	35.74	1.25	3.85
N33	49.25	40.00	43.53	**9.25**	6.27
P42			54.75	0.00	7.88

Component Amplitude	Patient Data (uV)		Lower limit	Interhemisphere Amplitude	Interhemisphere Amp. Diff.
	Right limb	Left limb	of normality	Difference (uV)	Upper Limit (uV)
0-N20	1.59	2.93	0.32	-1.34	2.27
N20-P27	2.24	8.79	0.50	**-6.55**	5.49
P27-N33	3.83	9.40	0.44	-5.57	5.78
N33-P42			0.24	0.00	4.55

Table 5.20.1

Comparison of latencies and amplitudes with normality limits from control group.
Lower limit of normality for amplitude of control group calculated as 50% of minimum recorded value.
U = unclear peak - no precise latency and morphology determination.
Ab = component peak appears to be entirely absent.
Bold figures indicate data which exceeds upper limits of normality.
Interhemisphere differences calculated as (Right-Left) limb data.

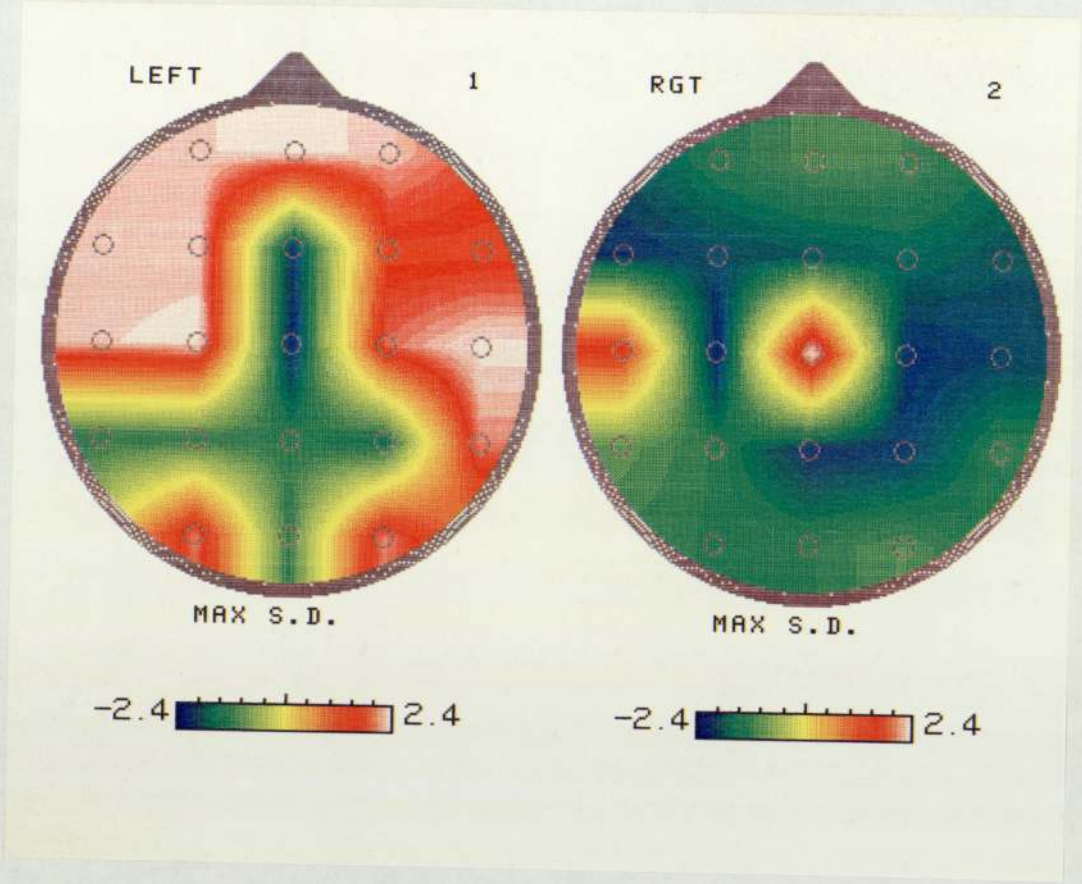

Figure 5.41. Patient 11 statistical mapping; maps indicate maximum standard deviation for left median nerve data (left) and right median nerve data (right).

5.3.12.0. Patient 12 (P12) results.

5.3.12.1. P12 clinical presentation.

This 44 year old lady presented with a chronic right sided hemiparesis since childhood and a history of tonic-clonic seizures. She was able to walk unaided - indeed the weakness and sensory deficit were described as minimal (Table 5.21). She had suffered no fits for several months at the time of recording.

Her drug regime consisted of Phenobarbitone (60mg), Tegretol (400mg b.d.) and Phenytoin (100mg nocte).

CT scan revealed a low density area in the left internal capsule and in the anterior parietal area (Figure 5.42).

Her condition had remained unchanged for many years.

5.3.12.2. P12 SEP results.

Clear SEP's were recorded to left median nerve stimulation with all peak latencies and peak to peak amplitudes falling within normal limits. Morphology types were F type I W, C type II and P type I.

No clearly consistent SEP components could be discerned with right median nerve stimulation. A small negative peak seen on all channels and occurring at a similar latency to the N20 parietal component recorded with left limb stimulation was seen in some trials. This peak was superimposed on top of a long duration negative shift of the baseline (Figure 5.43).

5.3.12.3. Summary and conclusion of P12 results.

No consistent right median SEP components could be discerned in this lady with a mild chronic right hemiparesis. A tiny 'N20' component seen in some trials superimposed on top of a long duration negative shift in the baseline might have in part been contributed to by the sub-cortical N18 component described by Desmedt and Cheron (1981) and Mauguière et al (1983).

Table 5.21 Clinical Summary for Patient P12

	UPPER LIMB		LOWER LIMB	
	Right	Left	Right	Left
Power	↓	Normal	↓	Normal
Tone	↑	Normal	↑	Normal
Reflex	↑	Normal	↑	Normal
Pain	Normal	Normal	Normal	Normal
Temp.	Normal	Normal	Normal	Normal
Touch	Normal	Normal	Normal	Normal
Vibration	↓	Normal	↓	Normal
Position	↓	Normal	↓	Normal
2 Point dis.	10 mm	2 mm	↓	Normal
Stereognosis	Normal	Normal	Normal	Normal

Direction of arrow indicates an increase (upward) or decrease (downward) of sensory or motor function.
In the case of reflex activity an upward arrow indicates hyperreflexia.

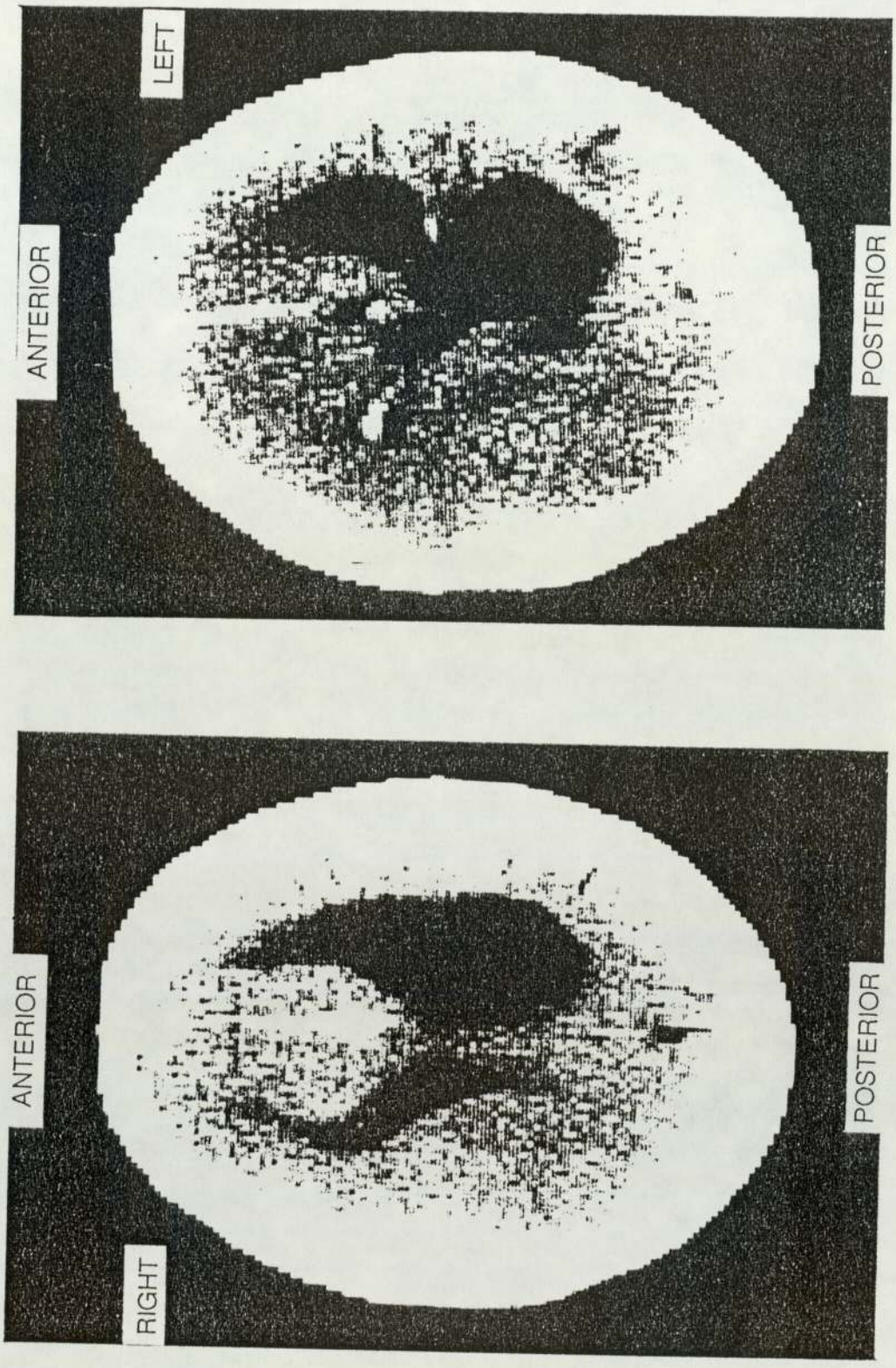

Figure 5.42. CT scans of patient P12.

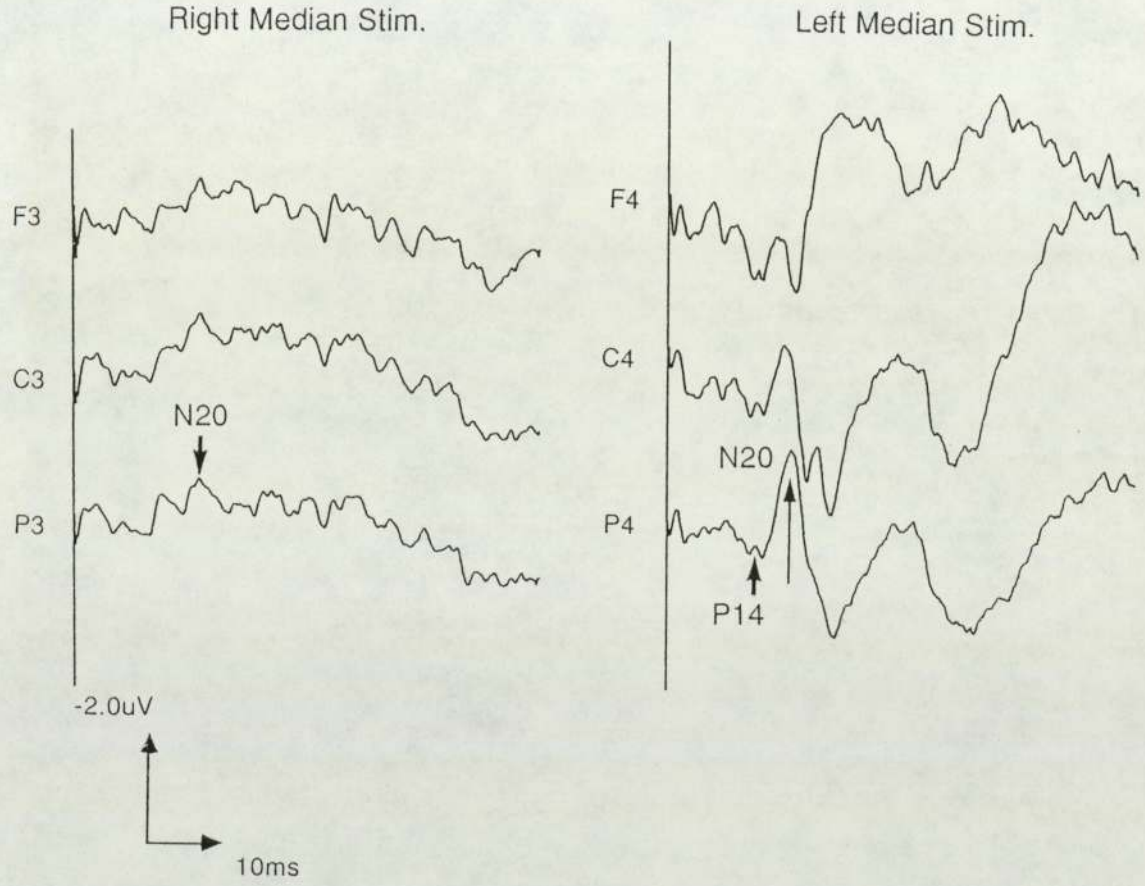

Figure 5.43. SEP waveforms for Patient 12 (P12) for right and left median nerve stimulation.

5.4.0. Summary and Conclusions.

Twelve patients were referred to the Clinical Neurophysiology Unit at Aston University for SEP recordings. Each were referred on the basis of evidence of cortical lesions on clinical grounds and CT scan evidence.

Analysis of patient mean height and age with those of the control group using Student t-test revealed no significant difference.

Nine of the twelve lesions were known to be cerebrovascular in nature; one was proven to be space occupying and one of unknown aetiology.

Tables 5.22 and 5.23 present a summary of the findings in these patients.

5.4.1. Correlation with clinical symptoms.

The following table presents a further summary of the correlation between patient upper limb symptoms and the occurrence of SEP abnormalities:

SYMPTOM TYPE	SEP NORMAL	SEP ABNORMAL
No upper limb symptoms	1	1
Sensory impairment only	1	
Motor impairment only	2	1
Motor and Sensory impairment	0	6

It should be noted that involuntary motor jerking was classified as motor impairment for the purposes of this summary.

Patient	Lesion	Symptoms	SEP Results	Stats. Mapping
P1	Left hemisphere Parieto-occipital infarction. (1982)	Right lower limb weakness	Slight left hemisphere attenuation of the P27-N33-P42 complex Peak to peak amplitudes all within normal limits. (July 1988)	Equivocal.
P2	Right hemisphere internal capsule infarction. (Oct. 1987)	Left upper limb weakness with brisk reflexes.	Normal (Aug 1988)	Equivocal
P3	Right hemisphere perirolandic space occupying lesion. (Aug 1988)	Decrease in position and two point sense. Possible slight loss of stereognosis. Twitching of left thumb and index finger.	Augmentation of right hemisphere P22 comp., co-existing with attenuation of all other right hemisphere SEP components. (Aug 1988)	Positive correlation.
P4	Multiple small right hemisphere infarctions. (Aug 1988)	Left limb weakness with sensory loss.	Delay or loss of right hemisphere P22 and delay of N31 centrally. Parietal delay of N33 component. (Aug 1988)	False negative
P5	Small zone of infarction in the right parietal area. (July 1988)	Left upper and lower limb weakness with sensory impairment.	Prolonged N19 comp. Marked morphology difference between frontal components. (Aug 1988)	False positive.
P6	Left hemisphere haemorrhage in tempero-parietal occipital area. (Nov 1985)	Bilaterally brisk upper and lower limb reflexes.	Unusual bilateral N50 component. (Sept 1988)	Positive correlation.

Table 5.22. Summary of patient findings.
Dates (in brackets) indicate the date of onset of illness and the date on which SEP's performed. Symptoms are those presented at time of SEP recording.
Statistical mapping categorised on the basis of agreement with peak latency and amplitude data of control group.

Patient	Lesion	Symptoms	SEP Results	Stats. Mapping
P7	Right hemisphere stroke in Jan.1988. Evidence of old left hemisphere CVA.	Intermittent paraesthesia of the left fingerips.	Normal (Aug 1988)	Equivocal.
P8	Large left hemis., parietal haematoma. Infarction right frontal lobe. (Sept 1988)	No clear neurological signs.	Large right hemisphere central N40 component. (Sept 1988)	Positive correlation.
P9	Right hemisphere tempero-parietal infarct. (Feb 1989)	Left upper and lower limb weakness and sensory loss.	Loss of right central P22-N31-P42 and parietal N33-P42 as well as frontal P35-N43 complexes. (March 1989)	False negative.
P10	Small left anterior parietal lesion. (May 1989)	Right upper limb focal twitching. Right lower limb weakness..	Giant central P22 and parietal P27 components. (May 1989)	Positive correlation.
P11	Left parietal infarction. (Oct 1988)	Episodic jerking and clenching of right hand with slight sensory signs.	Prolonged right hemis., N31, N33 and P42 comps. Abnormal N20-P27 amplitude difference between hemispheres. (July 1989)	False negative.
P12	Left anterior parietal and internal capsule lesions. (Since childhood)	Chronic right hemiparesis with mild sensory signs in right upper and lower limbs.	Absent left hemisphere components. (Sept 1988)	*

Table 5.23. Summary of patient findings.
Dates (in brackets) indicate the date of onset of illness and the date on which SEP's performed. Symptoms are those presented at time of SEP recording.
Statistical mapping categorised on the basis of agreement with peak latency and amplitude data of control group.

If one examines the type of sensory loss in relation to SEP results one observes that 5 patients with abnormal SEP's presented with impairment of joint position sense - only one patient (P9) with preserved joint position sense (but impaired touch/vibration sense) produced abnormal SEP's. Patient P7 presented with similar symptomatology to patient P9 but produced normal SEP findings.These findings therefore are in broad agreement with Halliday and Wakefield (1963) and Williamson et al (1970) who described a generally good correlation between the severity of symptoms and the degree of SEP abnormality if the degree of loss of joint position sense was used as a criterion.

5.4.2. SEP abnormalities

It has been stated in previous studies that that the characteristic feature in patients with cortical lesions was that the latency of onset of components was either equal to control (contralateral hemisphere or control mean data) or slightly increased, while changes in amplitude or duration of cortical SEP components could be rather marked (Laget et al 1967: Nöel and Desmedt 1980; Mauguière et al 1983). These facts are generally borne out by our study but it must be said that the precise calculation of component onset times was difficult to determine in comparison to peak latency. Moreover, in several examples it was difficult, if not impossible, to discern whether a particular component was delayed or whether this component was indeed missing and had been 'replaced' by a neighbouring component of differing latency by volume conduction. This phenomenon has been described previously by Mauguière et al (1983).

Mijoshi et al (1971), in contrast to the findings of Williamson et al (1970), reported in a detailed study of 34 patients with sensory impairment caused by cerebrovascular lesion, that some SEP components were found to be less vulnerable than others. They reported that the first negativity (N20) was of normal amplitude and latency in 50% of records classified as severely abnormal by other criteria. The most sensitive component was that labelled P2 (equivalent to our parietal P42), which was delayed in 6 out of 11 records classified as slightly abnormal and

apparently of abnormally short latency in 3 others. It is worth noting that in serial recordings they revealed a gradual restoration of the SEP alongside clinical improvement, but even when clinical sensory recovery was complete there was frequently a residual delay of P2 and later potentials.

It is interesting to correlate this data with that of our study. In the 8 patients with abnormal SEP's (and one borderline case, P1), in only one case of discrete component change was a component earlier than P22 implicated. This was in patient P5 where a prolonged N19 component was observed. On this basis it is worth reporting that, of the abnormalities recorded, the P22-N31 complex was abnormal in four patients, the N33-P42 complex in 3 patients and an abnormality of P27 in two.

The phenomenon of SEP enhancement by pathological processes has long been recognized. In fact it was this process that first enabled Dawson (1947) to record SEP's from the surface of the human scalp. The components most often described lay in the 30-40msec range, and in patients with progressive myoclonic epilepsy amplitudes of up to ten times those of normal subjects have been reported (Halliday 1967), although a lesser degree of enhancement may be encountered in other conditions. Laget et al (1967) and Williamson et al (1970) describe SEP enhancement in cases of cerebral tumour causing focal epileptic attacks.

Mauguière et al (1983) described a patient with hemianaesthesia without hemiplegia who showed an augmentation of frontal P22-N30 components co-existing with an elimination of all parietal components.

Data from our study contributes to current knowledge in two ways; firstly two patients with discrete cortical lesions leading to focal epileptic episodes (P3 and P10) resulted in the augmentation of discrete cortical potentials - not only augmentation compared to the opposite hemisphere as described by Mauguière, but 'giant' potentials compared to a control group. The second most important aspect of these observations was that the one component

involved in each case was the peri-rolandic P22 component which has been subject to much debate in recent literature. In patient P3, the P22 -N31 complex was greatly augmented compared to both the contralateral hemisphere of the patient and also in comparison to the control group. The fact that this phenomenon co-existed with attenuation of all other parietal and frontal components in the affected hemisphere provided convincing evidence that the P22-N31 complex has separate generators than those responsible for the N20-P27-N33 components parietally and P20-N30 components frontally.

Although Mauguière et al (1983) described augmentation of a pre-frontal P22-N30 complex, they did not differentiate between a frontal P20-N30 complex and a peri-rolandic P22-N31 complex. The differential affect of lesions on these components seen in our study therefore provides important evidence that these are discrete and, in part at least, independent components.

It is clear therefore that the P22 and N31 components are important measures to examine in cases of lesions affecting the primary somatosensory/somatomotor cortex. Furthermore, topographic maps of patients with augmented P22-N31 complexes further supports the hypothesis of the essential radial orientation of the generators of these components.

In this study, augmentation of components was only seen with lesions in close proximity to the primary somatosensory/somatomotor (PSMA) cortical areas. Obeso et al (1980) and Stejskal et al (1985) both reported augmentation of components in patients with lesions remote form the PSMA. However both groups employed only single channel recordings with a precentral reference electrode site.

The experiences of Halliday et al (1967 and 1970) gained from patients suffering from epilepsy led them to propose that potential enhancement in this group could be due to epileptiform discharges arising in the reticular formation of the lower brain-stem, influencing sensory input to the cerebral cortex at the level of the thalamic relay nuclei. Halliday and Wakefield (1963) had also described patients with brain-stem lesions, with or without associated sensory loss, with abnormally large SEP's. Jones (1982) and Stejskal et al (1985)

proposed that SEP enhancement in neurological conditions other than epilepsy may be due to interference with tonic inhibitory mechanisms at brain-stem, thalamic or cortical level. The disinhibition of the somatosensory cortex would be via the pallidum and ventral group of thalamic nuclei.

Desmedt and Cheron (1980) had proposed the hypothesis that some SEP changes seen in octogenarians reflected differential neuronal loss across the cortex. As was seen from the study described in the last Chapter, there was an interesting morphological and topographical difference of frontal components seen between an old age grouping and a young age grouping. This difference was essentially that a frontal N43 component was commonly seen in the old age group replacing the frontal P42 component commonly seen in the young.

It seems most relevant to note therefore that in two patients, P42 and N43 components were observed in opposite hemispheres, a situation that did not occur in any control individual. N43 was observed in a young female patient (P5) in the same hemisphere where a centro-parietal lesion had caused a significant delay in the peak latency of N19. A frontal P42 was seen in the unaffected hemisphere. In patient P8, both right and left hemisphere lesions were detected, but a frontal N43 was observed with a right frontal lobe infarction and a frontal P42 was observed in the left hemisphere where a parietal haematoma was seen.

A final relevant observation was that in patient P10 in whom giant central P22 and parietal P27 components were observed, the ensuing P42 components at these locations were of closely similar amplitude to those recorded in the preserved hemisphere.

These findings lead one to speculate as to whether P42 is generated by both pre and post central generators and indeed by generators other than those responsible for P22 and P27 complexes. The presence of a frontal N43 component would be consistent with either a degree of neuronal loss in the frontal lobe or loss of direct input via cortico-cortical relay mechanisms to the frontal lobe.

5.4.3. Value of statistical mapping.

If one takes the findings of statistical mapping in each of the patients and compares this with the more conventional 'manual' analysis of peak latency, peak to peak amplitude and morphology data, by using the SEP data as the 'true analysis', the performance of statistical mapping can be summarised as seen below.

STATS. MAPPING V SEP DATA.	NO. OF FINDINGS.
Equivocal	3
False negative	3
False positive	1
Positive correlation.	4

where equivocal = normal SEP and normal map; false negative = abnormal SEP and normal map; false positive = normal SEP and abnormal map; positive correlation = abnormal SEP and abnormal map.

Patient 12 who presented with absent SEP's did not have statistical mapping performed.

In percentage terms, this data may be interpreted by saying that statistical mapping correlated well with SEP topographical data in 64% of cases, failed to reflect an SEP abnormality in 27% of cases and yielded a false positive in 9%.

One major difference of course between the conventional data measures and statistical mapping measures was that amplitudes were measured conventionally with peak to peak data whereas map data was collated using a baseline to peak measure. The relationship of any transient in relation to the baseline must therefore be taken into consideration when interpreting data. One method that was of benefit here was the use of the 7.5ms pre-stimulus epoch; the relationship of this measure to the baseline provided a useful assessment of any waveform to baseline offset caused by artefacts of any kind. However, it should be noted that in the case of the one false positive finding caused by a transient lying entirely above the

baseline, the pre-stimulus epoch was normally located along the level of the baseline and therefore this 'first line of defence' proved inadequate.

In the case of the three false negative findings, one at least could be explained on the basis that the abnormalities consisted of prolonged interpeak and/or interhemisphere measures. The inherent weakness of the database employed in this study was that no assessment could be made of interhemisphere differences. This was indeed a major weakness in a system used to detect cortical lesions. It was considered that one might employ a bilateral limb stimulation protocol as has been advocated by Yamada et al (1984), and create a database accordingly. Indeed, this is the method adopted by Duffy et al (1981) for their BEAM™ system and statistical probability mapping. Whilst this would be effective in many cases, in patients showing an abnormality of frontal components there would possibly be difficulties in interpretation since many of the frontal components, notably N30, are markedly bilateral in distribution. In the case of patient 5 in our study for example, the morphological variations of the frontal components would most certainly be lost with bilateral stimulation.

Another weakness of statistical mapping using control group mean waveforms for analysis was that whilst the observer may assess from the patient data that a particular component may be lost or delayed, providing the datapoints of the relevant epoch fell within the normal range calculated from the control database, these changes would of course not be detected. The system was therefore unable to 'recognise' morphological variation which is another important tool in the armoury of the detection of cortical lesions. In order to overcome this, a form of template waveform would need to be generated, but to create adequate templates at 20+ locations would undoubtedly be a complex and prohibitive task in terms of computational time.

The second method of statistical mapping, namely comparing the patient's individual component maps to the control group mean component maps also had difficulties. Whilst this technique provided an important ' latency free' measure, it was reliant on the observer selecting the appropriate map for comparison; it was difficult to make a valid judgement on a

suitable matrix for analysis when a component was deemed to be 'missing', and indeed 'replaced' by a different neighbouring component by volume conduction.

During the course of these studies it was considered important that both types of statistical mapping were employed in order to assess the true validity of the findings. It should be noted however that the software of the each of the commercial systems used for the studies adopted one method or the other, but not both.

It was also clear from our study that correct matching of both age and height of patient with control group was essential. Although there was no significant difference of age and height between patient group and control group, the present control databases need extending in both the numbers of subjects within the old and young age groupings and also the range of heights within these groupings. These failings were clearly highlighted in two cases; patient P3, an elderly tall gentleman whose height exceeded that of any individual within the old age grouping yielded poor latency correlation. Patient P5, a young lady who presented with a frontal N43 component; this finding being most unusual at this age would possibly have been detected as an abnormality if a statistically large young control group could have been accessed for statistical mapping in isolation from the old.

In general terms it has to be reported that the interpretation of standard deviation maps created by the Z transform software of the Brain Atlas III™ system required much time and an intimate knowledge of the data used in the compilation of the control database. It most certainly would not be recommended as a tool for the uninformed clinician seeking a 'quick answer'.

5.4.4. Fz reference derived potentials.

In 8 of the 12 patients (66%) the Fz derived potentials were in agreement with topographic studies, whether normal or abnormal. In the other four patients (33%), the Fz derived potentials were within normal limits despite abnormalities of central or frontal components recorded topographically.

In the case of patient P3, the Fz derived potentials were abnormally reduced in the affected hemisphere, in line with the attenuation of parietal and frontal components, but gave no indication of the augmentation of central components.

A similar finding was seen in the case of patient P10. Here, both P22 and P27 components were abnormally large in amplitude in the topographic study whilst the N20-P27 amplitude of the Fz derived potentials were within normal limits. However it should be remarked that the morphology of the post P27 components were markedly asymmetric in these latter potentials.

In summary therefore, it can be stated that whilst the Fz derived potentials were effective in detecting lesions affecting the generators of the parietal and therefore some frontal components, focal lesions in close proximity to the PSMA but not affecting those generators in the posterior bank of the central sulcus, may be missed in these recordings.

5.4.5. Summary of the value of SEP mapping.

In 1986 Oken and Chiappa stated; 'It is important to differentiate between (1) the ability of a statistical method to classify a patient whose diagnosis is uncertain into either a normal or a specific disease group and (2) an analysis that shows statistically significant differences between two groups, such as normal controls and patients with verifiable disease. The latter analysis is generally helpful only in understanding the pathophysiological characteristics of the disease, whereas the former ability is critical to the clinical utility of a test.

To be substantiated as useful, a newly proposed clinical test that classifies patients into either a normal or diseased state must be evaluated by its false-positive and false negative rates, and by comparison with other available diagnostic tests.'

In agreement with these observations it is worth reflecting that our topographical studies of the SEP confirmed abnormalities shown by clinical examination and/or CT scanning in 66% of patients. Statistical mapping using the Z transform correlated well with topographic SEP mapping in 64% of cases. In isolation, statistical mapping yielded a detection rate of 27% compared to clinical exam and CT scan.

Half of the patients with topographic SEP abnormalities failed to produce an abnormality when the Fz derived potentials were viewed in isolation. This equates to a detection rate of 36% compared with clinical exam and CT scan.

The conclusions from the study therefore are

1.Topographic studies of the scalp recorded SEP increase the detection rate of cortical lesions affecting the PSMA over conventional single channel Fz reference derived recordings.

2. The value of the control database for statistical mapping in its current form is low.

This has been a post-hoc study. The SEP abnormalities have been determined with full knowledge of neurological exam and CT scan findings. The full value of the techniques outlined will only be determined by the ability to detect pathology in patients in whom the diagnosis is uncertain or in whom clinical exam or other diagnostic techniques have been equivocal. This is a study still to be undertaken.

The value of the current control database may be increased by including data obtained by bilateral median nerve stimulation and extending the numbers of subjects within each age range.

The Z transform is a univariate statistic and the value of statistical probability mapping would undoubtedly be extended by the incorporation of multivariate analysis into the existing systems.

CHAPTER 6

THE USE OF A NEW COORDINATE SYSTEM IN THE MEASUREMENT OF THE SOMATOSENSORY EVOKED POTENTIAL IN THE HEALTHY HUMAN ADULT.

6.1.0. Introduction.

When recording all types of evoked potentials, it is common practice to place electrodes at or near sites determined by the 10-20 system of electrode location (Jasper 1958). This system was originally designed to standardize placement of electrodes for recording EEG and makes use of percentage distances (usually 10 and 20%) to compensate for different head sizes and shapes. Locations are determined by measuring from nasion to inion along the anterior to posterior axis, and from pre-auricular points, through the vertex, along the coronal axis.

A major problem with using the 10-20 electrode placements for recording evoked potentials is that the sites and spacing of electrodes are not optimal for displaying all types of responses. The locus of maximum activity of evoked potentials often falls in the non-linear space between projected 10/20 electrodes which introduces an element of uncertainty.

Picton et al (1978) described a modification of the 10-20 system to allow specification of positions of more closely spaced electrodes. Other workers have used such intermediate electrode sites to enhance their whole of scalp studies (Buchsbaum et al 1982; Thickbroom et al 1984). See Figure 6.1.

Many methods have been reported which provide for more localised mapping of scalp potentials. Rémond and Torres (1964) proposed a system of coordinates with the poles located at the nasion and inion. Electrodes were then positioned at the intersection of the lines and designated by numerical and alphabetic symbols (Figure 6.2). Estrin and Uzgalis (1969) regarded the head as a unit sphere and used solid geometry coordinates to provide a conical projection forming a rectangular matrix from electrodes on a small area of the scalp.

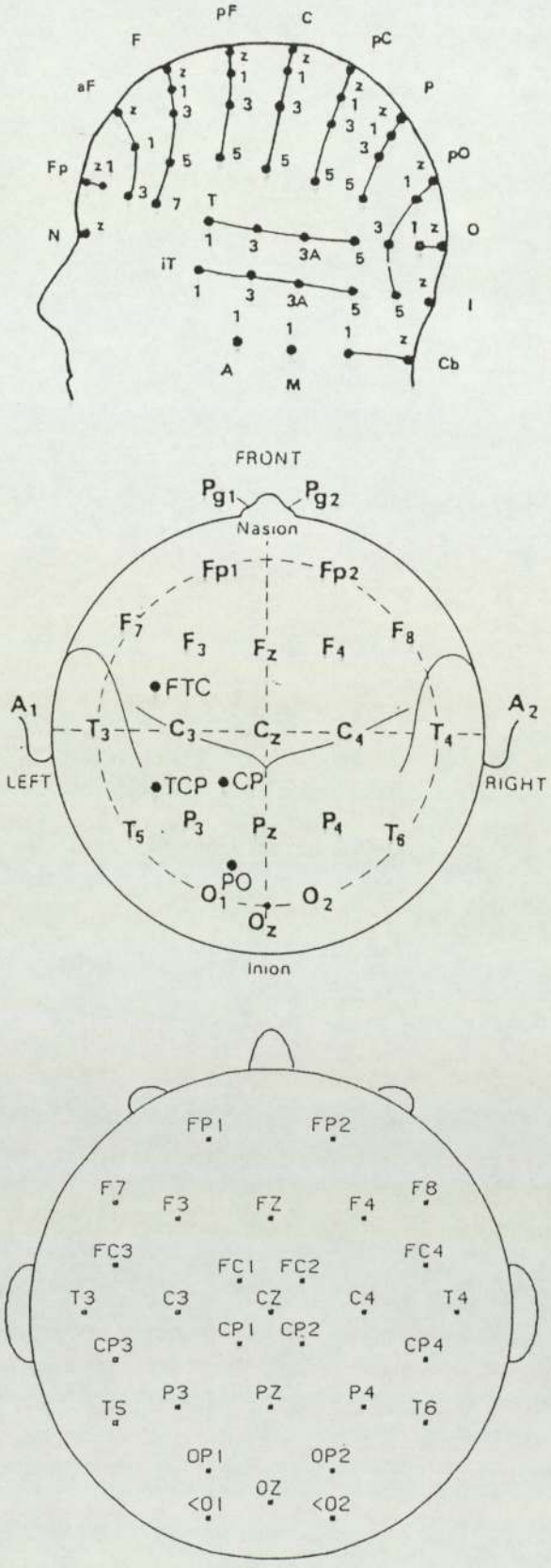

Figure 6.1. Electrode placement systems employing the 10-20 method and/or modified intermediate sites. Illustrations taken from Picton et al (1978), top; Buchsbaum et al (1982), middle; Thickbroom et al (1984), bottom.

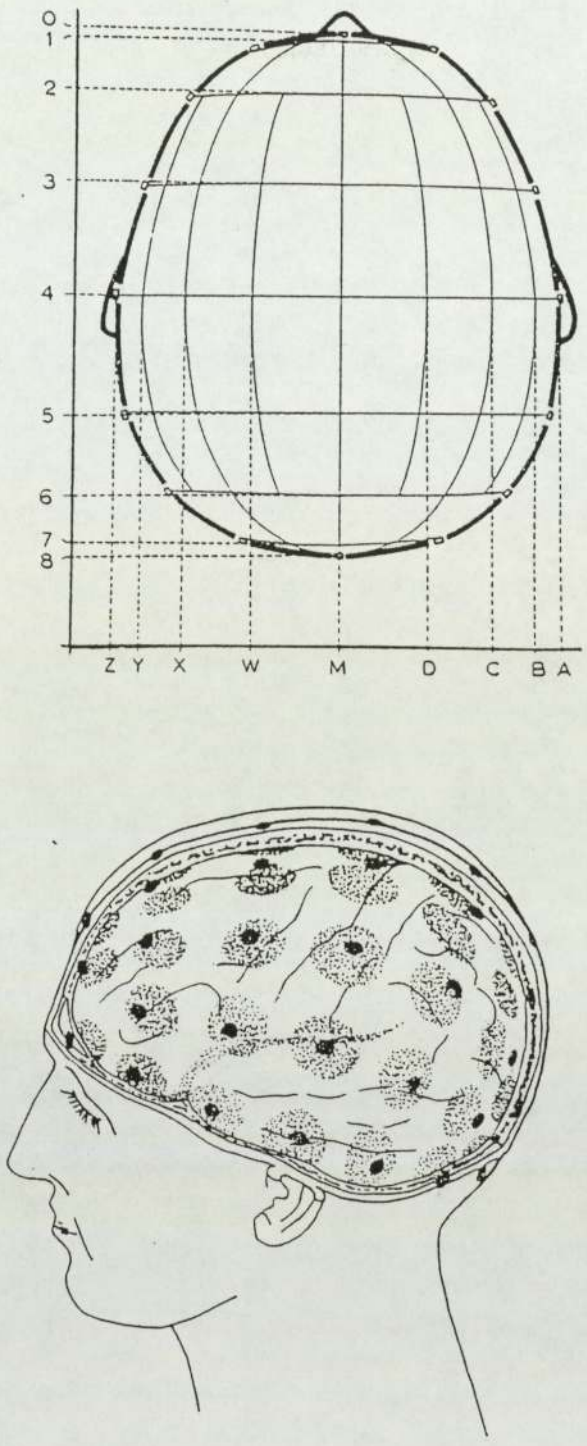

Figure 6.2. Electrode placement system proposed by Rémond and Torres (1964). This system is based upon the determination of 9 meridiens, crossed perpendicularly at regular intervals by 7 parallels.

Duff (1980) applied a rectangular matrix of 36 electrodes at a position specified by two of the 10-20 system and Lemieux et al (1984) similarly described a 4 x 4 equidistant grid array centred over areas of interest (Figure 6.3). Ary et al (1981) used spherical coordinates to display evoked potentials from 52 electrodes located on a shell fitted to the individual head. Coppola et al. (1982) devised an equal area projection and MacKay (1984) used triangular matrix for source density mapping on the occipital scalp. Desmedt and Huy (1984) treated the neck as a perfect cylinder with a rectangular electrode array in studies of sub-cortical potentials and Thickbroom et al. (1986) projected the scalp onto a sphere and presented orthoscopic views. Rectangular graticules are almost universal in local geographic maps and their advantages for local mapping were clearly recognised in the above reports.

In SEP topographical studies, two basic techniques have been employed. The first has been the use of whole of scalp electrode placements according to the 10-20 system (Goff et al 1977) or to slightly modify the location of some of these electrodes (Deiber et al 1986; Desmedt et al 1987). See Figure 6.4. The second method has been to cluster all of the recording electrodes over one hemisphere in a widely spaced array (Deiber et al 1986) or in a very close matrix (Duff et al 1980). See Figure 6.3.

Problems caused by the use of such arrays in these latter methods were:- (a) difficulties in communicating precise electrode locations and/or (b) where fixed interelectrode distances were used, the non-proportionality of this measure prevents precise reproducabilty across all head sizes.

Deiber et al(1986) employed their localised mapping matrices to support the hypothesis of separate cortical generators for the peri-rolondic P22 component and to show that the locus of this component varied according to the somatotopic organization of the cortex.

Recently we have devised a method for projecting the scalp onto a rectangular graticule (Drasdo and Furlong 1988). The purpose of the study described in this Chapter was to

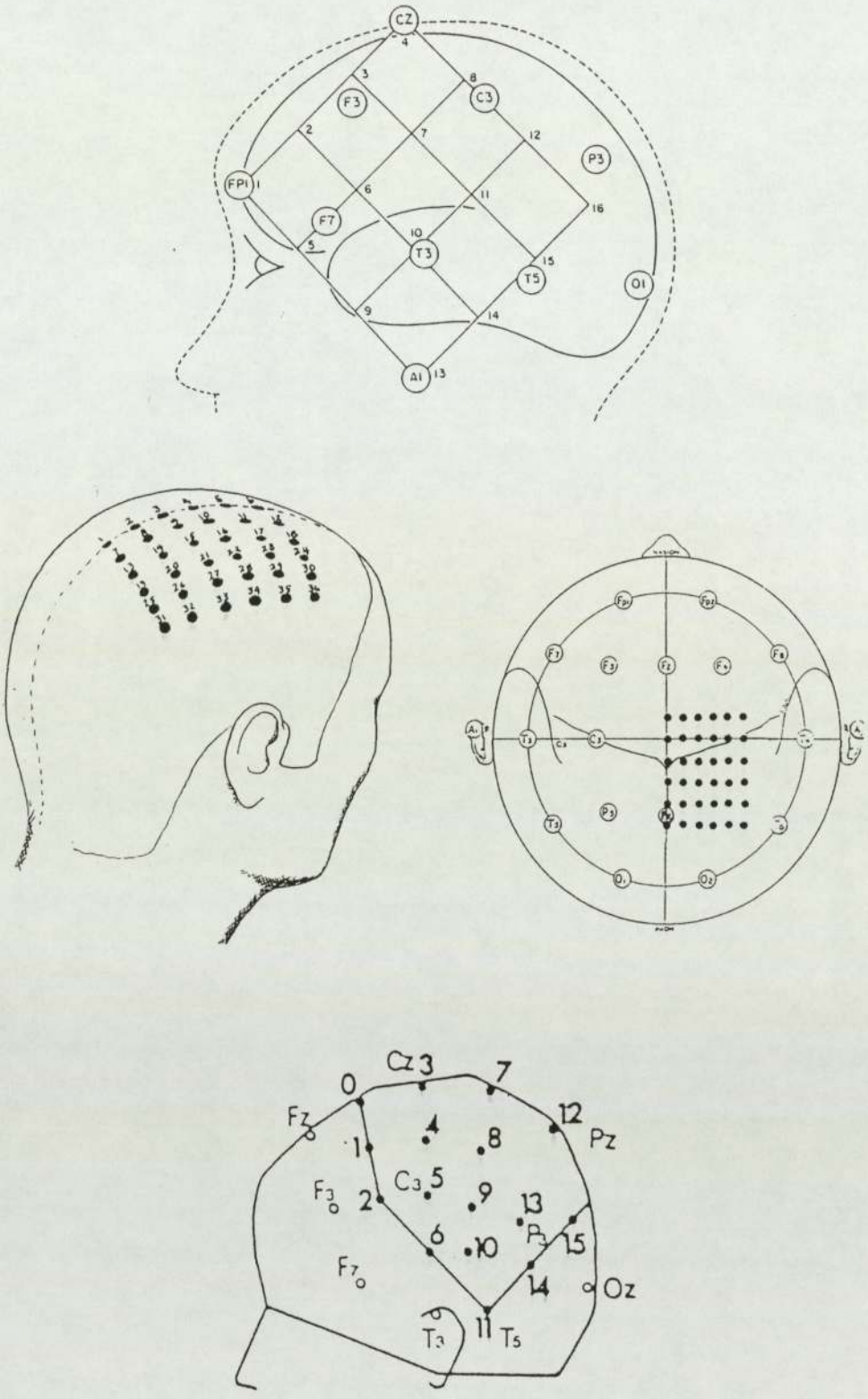

Figure 6.3. Localized electrode arrays. Illustrations taken from Lemieux et al (1984), top; Duff et al (1980), middle, and Deiber et al (1986), bottom.

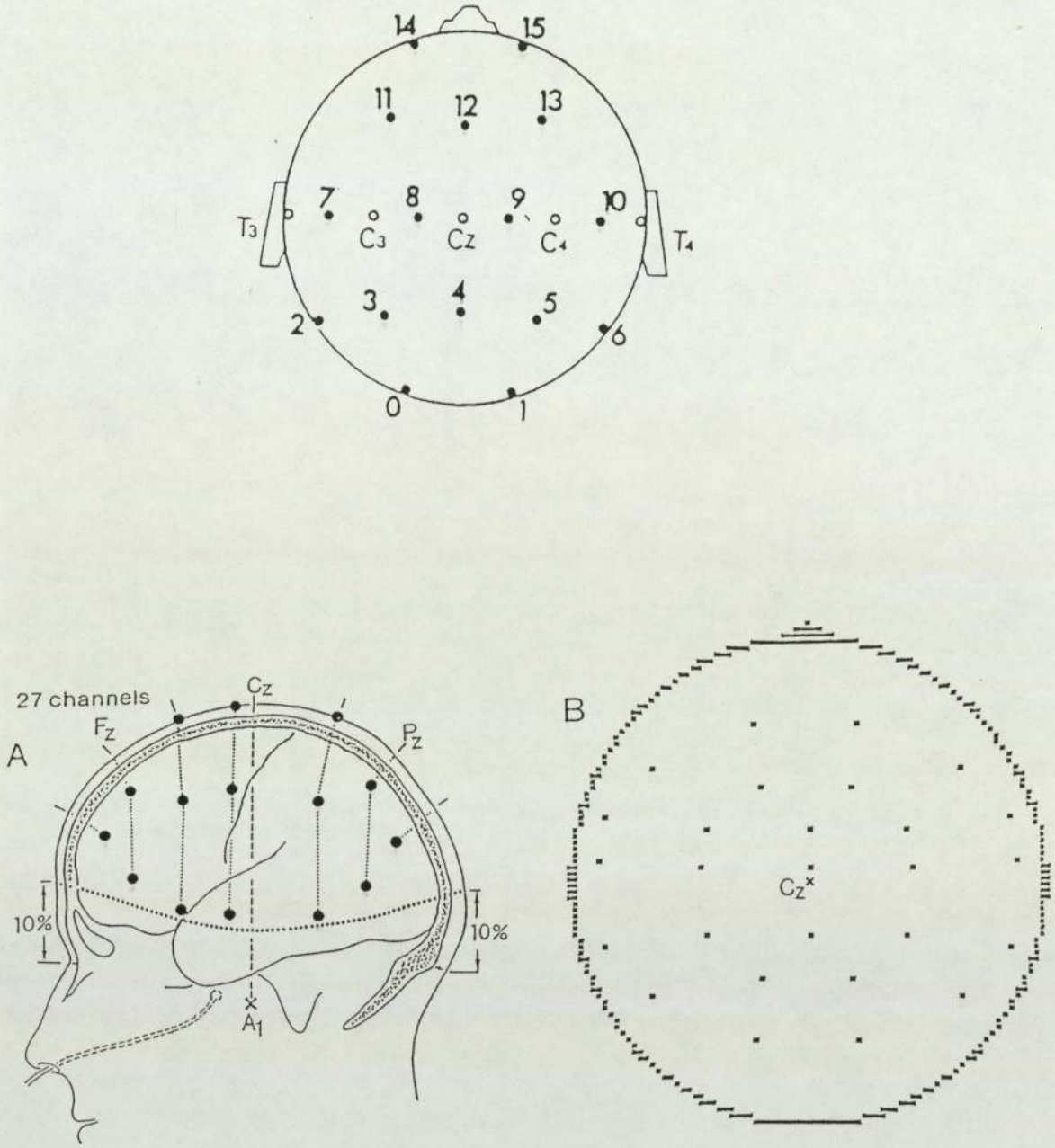

Figure 6.4. Electrode arrays used for SEP mapping which have employed modified or intermediate 10-20 system sites. Examples taken from Deiber et al (1986), top, and Desmedt et al (1987), bottom.

employ the sagittal polar co-ordinate system to the study of the temporal and spatial relationship of a rangeof SEP components in control subjects. It was hoped that the increased spatial resolution that such a technique would provide would give further evidence as to the origin of some of the SEP components.

6.2.0. Theory and method.

According to the principles of conventional cartography, mapping is achieved by defining coordinates and a projection (Steers 1985). The simple cylindrical projection or plate carree is of particular interest. The lines of latitude and longitude are projected onto a surrounding cylindrical surface, which is opened out to provide a flat map without distortion of vertical or equatorial distances. Latitude and longitude are projected as a rectangular graticule. To apply a similar concept to the scalp, however, it is first necessary to define a system of scalp coordinates.

For a projection with the axis in a sagittal direction, points defined by the inion and nasion form the poles. The frame of coordinates form a series of lines diverging from the inion and converging upon the nasion, like those of Rémond and Torres (1964). For our purposes however, continuous distances along these lines are required, specified in terms of percentage of each inion/nasion distance. Each polar line is identified on a scale of 0-50 units, relating to its surface distance along the intersecting curved lines, from the median plane. The baseplane therefore contains the inion and nasion and is equidistant from the zygomatic temporal process. To establish electrode placement, the inion, nasion and vertex are located as for the 10/20 system. The first coordinate denoting a polar line is marked on the equator which is equidistant from inion and nasion and extends from vertex to baseplane roughly occupying a coronal plane. The second coordinate, the polar distance, is then marked along the polar line in say 10% intervals of the nasion-inion distance, thus locating the electrode or signal position. It is easy to specify any position on the scalp, even below the baseplane. An example is shown is Figure 6.5 where the point on the scalp can be accurately defined by the

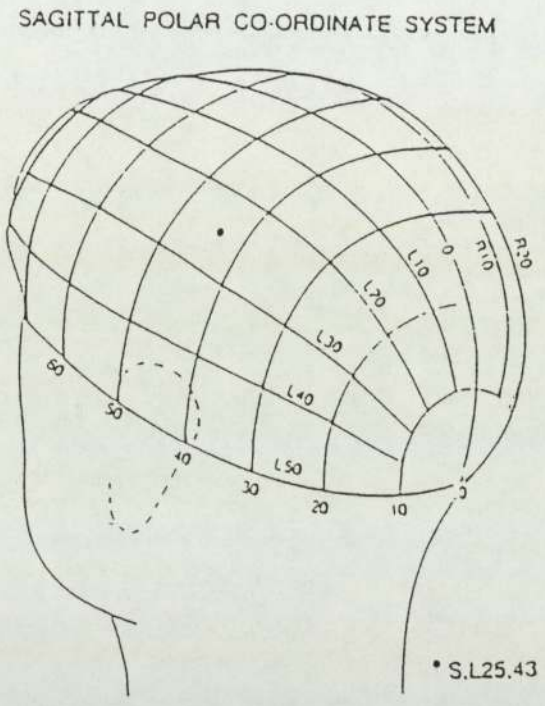

Figure 6.5. Sagittal polar projection. The point on the scalp can be accurately defined by the coordinates S L25,43 - where S indicates a sagittal projection, L indicates the left hemisphere, 25, the polar line and 43 the polar distance.

coordinates S L25,43 - where S indicates a sagittal projection, L indicates the left hemisphere, 25, the polar line and 43 the polar distance.

Six normal control volunteers had a 21 point grid measured on their left hemispheres according to the sagittal polar coordinate system. The bottom row of the grid was taken as 10% above the baseplane i.e on polar line L40 and the midline of the grid taken as 50% of the nasion-inion baseplane distance. Thus the bottom row mid-line point of the grid could be defined as S L40,50. Subsequent points were therefore calculated at 10% intervals of nasion-inion baseplane distance (polar distances) and 10% of the vertex-baseplane measure (polar lines). Precise locations of the grid are shown in Figure 6.6.

The reference electrode site was taken as the right earlobe. In all other respects the patient preparation and recording parameters were identical to that described in the Methods in Chapter 4 (Section 4.2.0).

Several averages were taken from each subject to ensure reproducability of data.

6.3.0. Results

Group mean waveforms were constructed from the data by averaging the six sets of control group waveforms using the software of the Biologic Brain Atlas III™ system. These waveforms are shown if Figure 6.7. Main components were then identified - namely P14, N20, P20, P22, P27, N30, N31, N33 and P42. Colour contour maps were then constructed at latencies concomitant with the peaks of each of these components. These waveform maps are shown in Figure 6.8 .

To compare and contrast this data, component maps were constructed from each control individual. This enabled group mean component maps also to be constructed (Figures 6.9-6.16).

To provide ease of comparison between the three sets of data, dipole comparison maps were constructed. This was achieved by drawing equivalent dipoles onto a schematic head. Where

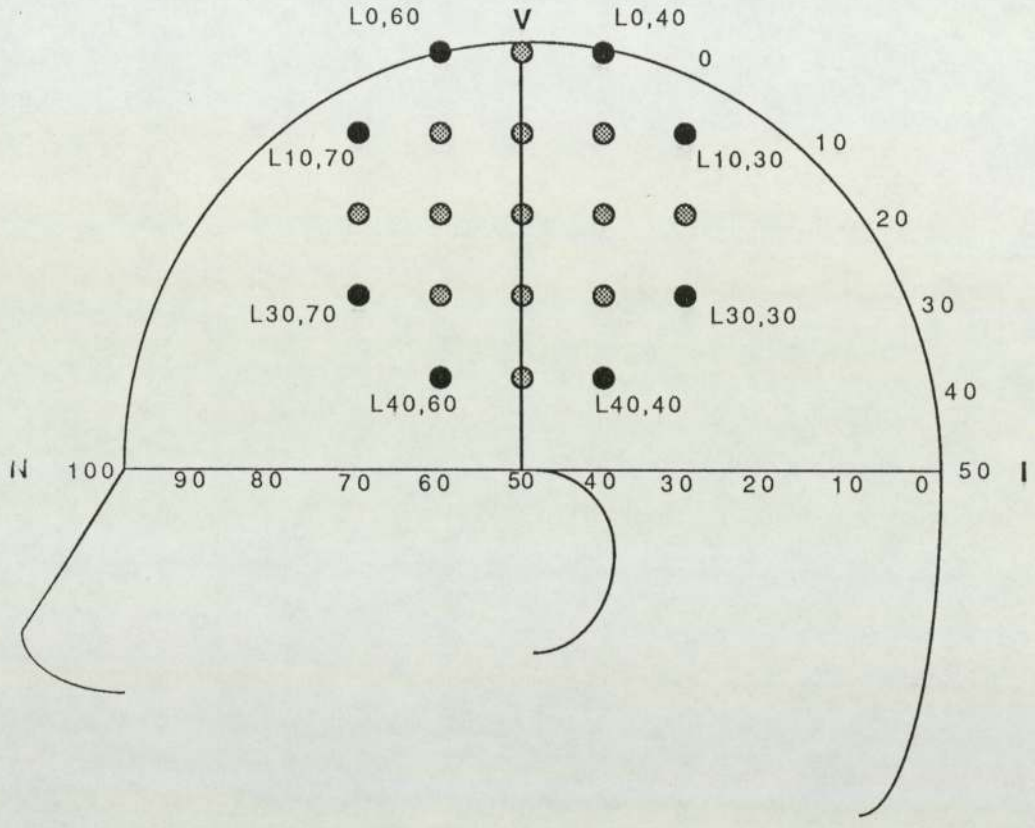

Figure 6.6. Sagittal polar projection of electrodes onto the left hemisphere using a 10% electrode spacing based on nasion-inion distance and vertex to baseline distance. Baseline is determined by the nasion-inion plane.
N = Nasion; I = Inion; V = Vertex.

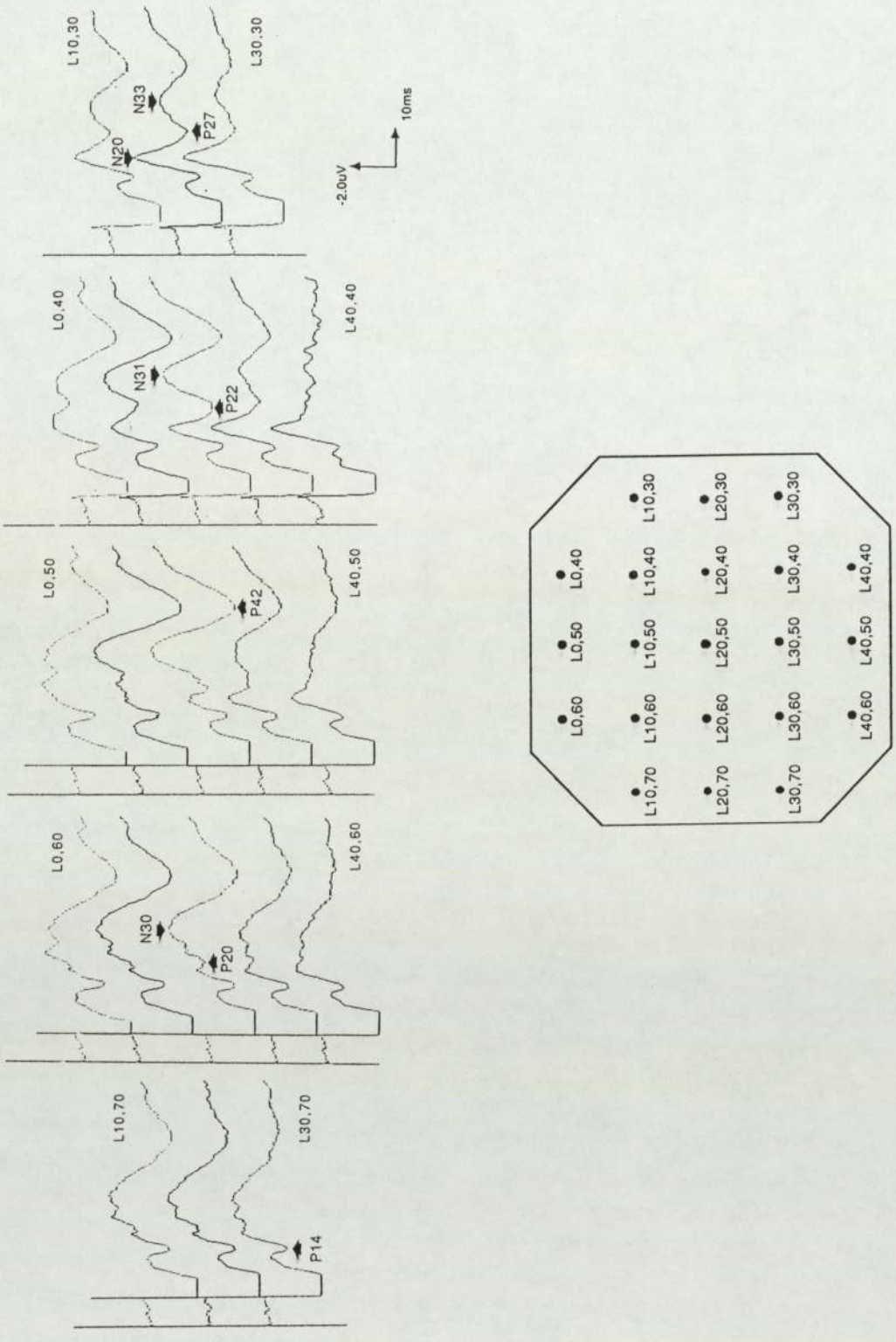

Figure 6.7. Group mean waveforms constructed from six control individuals. Figures adjacent to waveforms represent electrode location on the sagittal polar projection.

Figure 6.8. **Overleaf**. Maps constructed from components of group mean control waveforms.

Topographic Mapping

into SCRATCH file

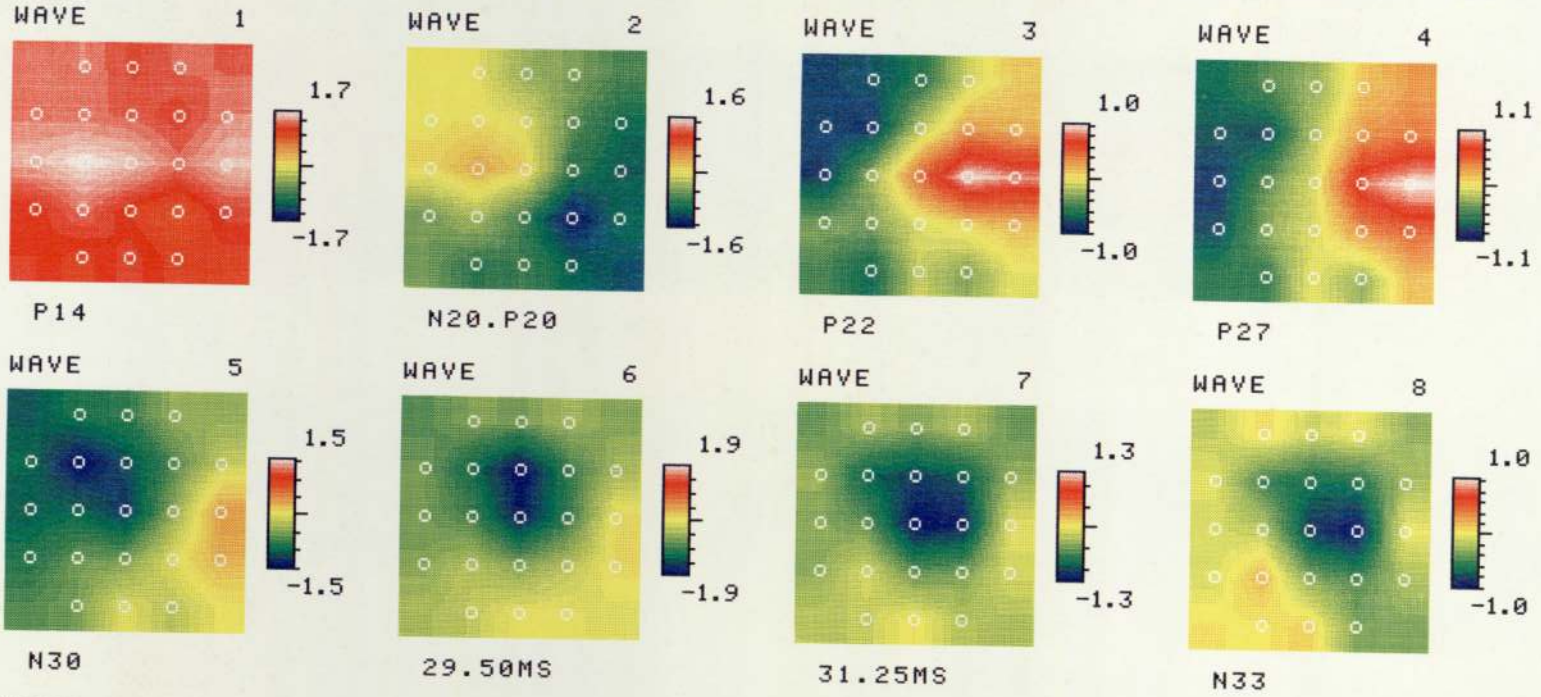

100 x100
Rectangular

MAP
Nicolet Pathfinder TMAP

a tangential dipole - like field was observed i.e. where two clear areas of concomitant opposite polarity were observed, an arrow would point from maximum negativity to maximum positivity. Alternatively, if a radial dipole like field was observed i.e. a well circumscribed locus of activity with no concomitant field of opposite polarity, then the appropriate electrode site on the schematic head would be shaded. Such diagrams were constructed for each main component and are shown in Figures 6.17 and 6.18.

The following observations from this data were made:-

6.3.1. P14 Maps

Each control individual showed a positivity at every electrode site with the largest deflections seen along the 60% polar distance line. Both group mean waveform map (Figure 6.8) and group mean component map (Figure 6.9) showed the maximum positivity occurring at L20,60.

6.3.2. N20/P20 Maps

Each control individual showed a clear post-central negativity and pre-central positivity concomitant with the peak of the N20/P20 components (Figure 6.10). Lines connecting the sites of maximum negativity and positivity in each individual revealed a consistent diagonal alignment of the dipolar fields (Figure 6.17). This alignment is reflected in the group mean N20/P20 component map where the maximum negativity occurred at L40,30 and maximum positivity at L0,60.

6.3.3. P22 Maps

Only three of the six control individuals produced P22 components that could be temporally differentiated from a P27 component.

Two of the three P22 waveform maps revealed radial dipole like fields with the locus of positivity occurring at L20,50 (subject N1) and L10,50 (subject N3). In subject N5, the P22 map revealed a tangential dipole-like field with maximum positivity at L20,40 and maximum negativity at L10,60. Due to the much greater amplitude of this latter data, the group mean component map for P22 reflected the dipole field of this subject (Figure 6.11).

6.3.4. P27 Maps

P27 maps were obtained in each of the six control individuals, although as already stated, in three subjects there was no temporal separation of P22 and P27 components (subjects N2, N4 and N6). Categorisation of these maps into P22 and P27 representations were thus based on the latencies of these components.

Distributions of P27 maps were broadly similar to N20/P20 maps although the former revealed slightly differing loci of negativity and positivity than their opposite polarity N20/P20 counterparts.

This is reflected in both the group mean component and waveform maps where the maximum positivities occurred at L20,30 and the maximum negativities at L10,60 (Figures 6.8 and 6.12).

6.3.5. N30, N31 and N33 Maps.

N30 maps revealed a wide inter-individual variation in dipole field types and orientations in five control subjects. Subjects N1 and N2 produced radial dipole-like fields whereas subjects N3, N4 and N5 revealed clear tangential dipole-like fields. In subject N3, there was no temporal separation between N30 and N31 components.

In control subject N6, no clear N30 map could be discerned - in this case a dominant N23 component was observed consistent with the FIII classification described in Chapter 4. It was interesting to note in this case that the appearance of the dominant N23 component coincided with a close temporal relationship of P22 and P27 complexes. This was consistent with the observations of the occurrence of the dominant N23 in the control group as described in Chapter 4. The topographic map concomitant with N23 in this subject could not be distinguished from that of the P27 component map shown for this subject in Figure 6.12.

In each individual, the maximum negativity was observed at either central or pre-central locations.The group mean N30 component map also revealed a closely similar topographical distribution to that seen for the P27 group mean maps.

Figure 6.9. **Overleaf**. P14 component maps from control individuals. Large map represents the group mean topographic distribution of P14.

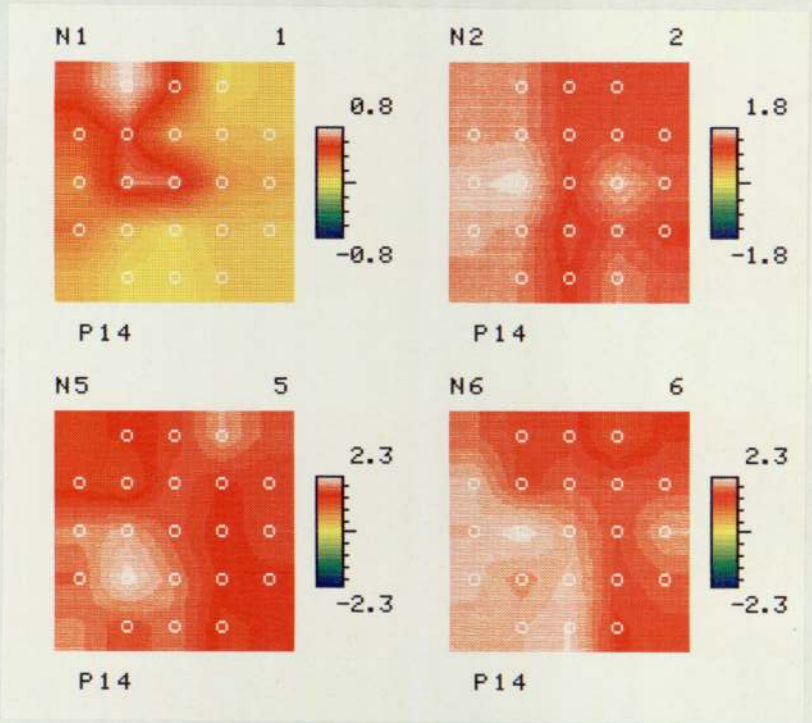
N1
1
0.8
-0.8
P14
N2
2
1.8
-1.8
P14
N5
5
2.3
-2.3
P14
N6
6
2.3
-2.3
P14

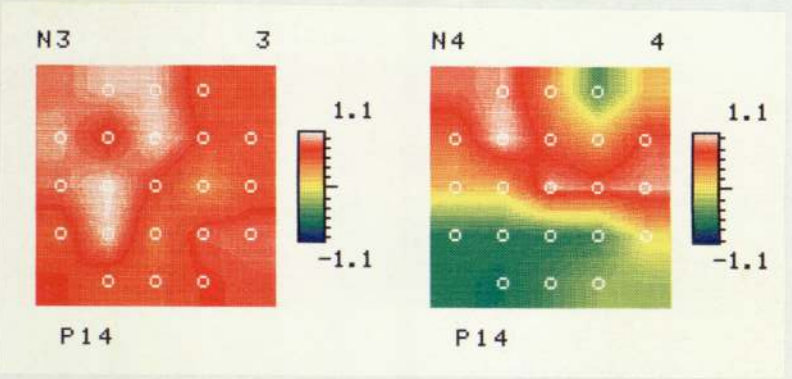
N3
3
1.1
-1.1
P14
N4
4
1.1
-1.1
P14

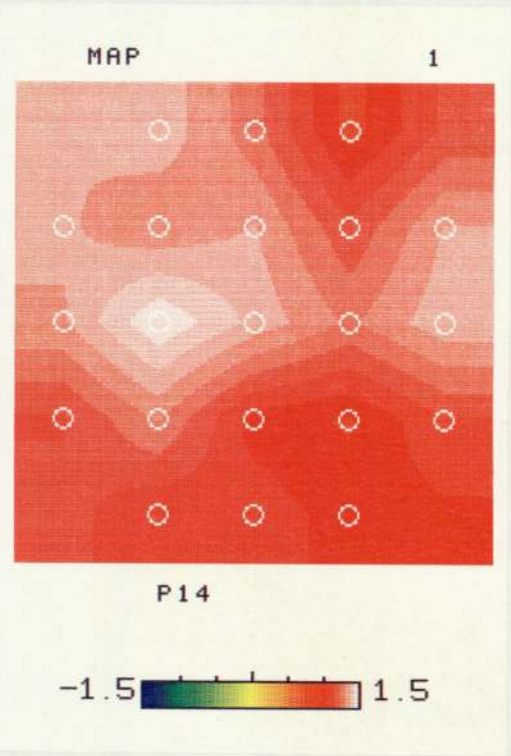
MAP
1
P14
-1.5
1.5

Figure 6.10. Overleaf. N20/P20 component maps from control individuals. Large map represents the group mean component topographic distribution of N20/P20.

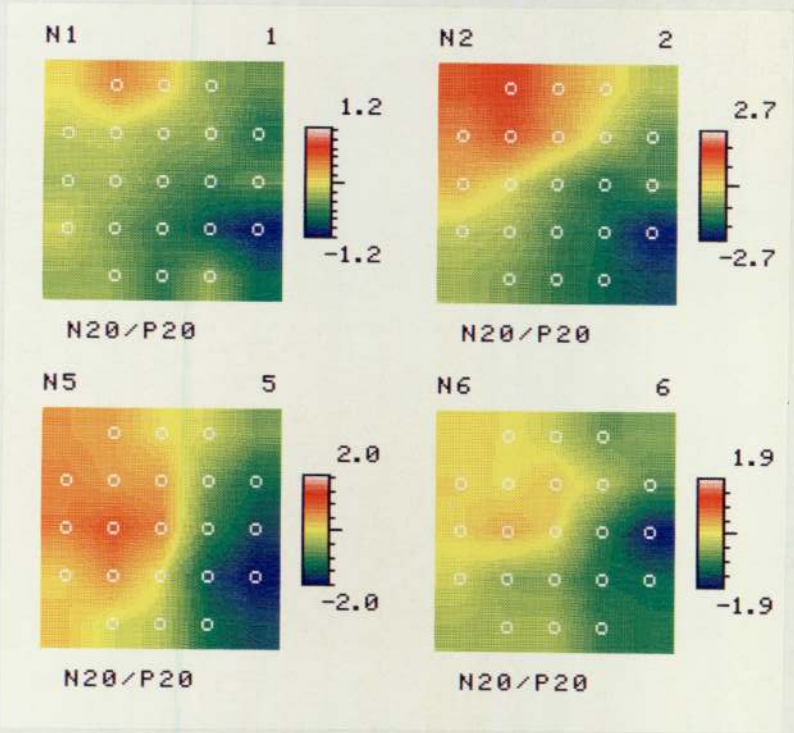
N1
1
1.2
-1.2
N20/P20
N2
2
2.7
-2.7
N20/P20
N5
5
2.0
-2.0
N20/P20
N6
6
1.9
-1.9
N20/P20

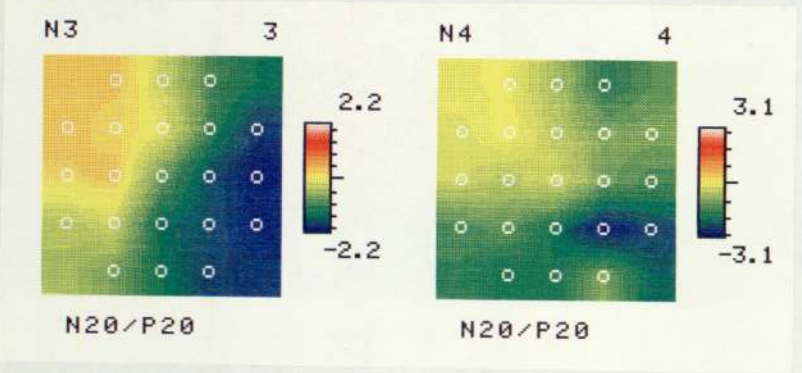
N3
3
2.2
-2.2
N20/P20
N4
4
3.1
-3.1
N20/P20

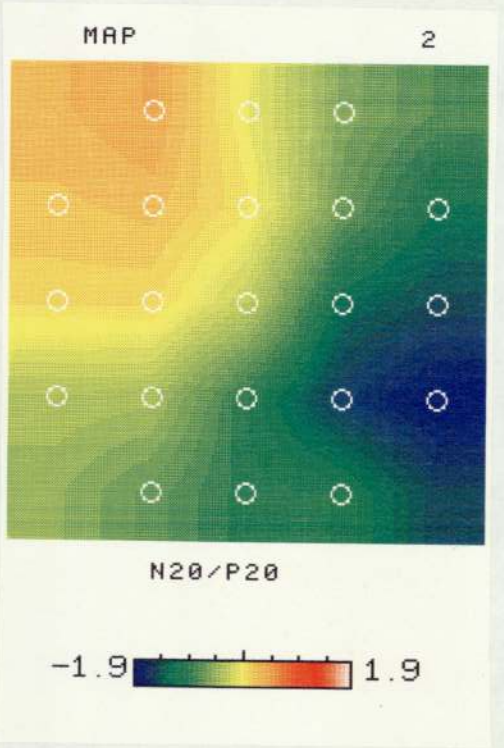
MAP
2
N20/P20
-1.9
1.9

Figure 6.11. Overleaf. P22 component maps from control individuals. Large map represents the group mean component topographic distribution of P22.

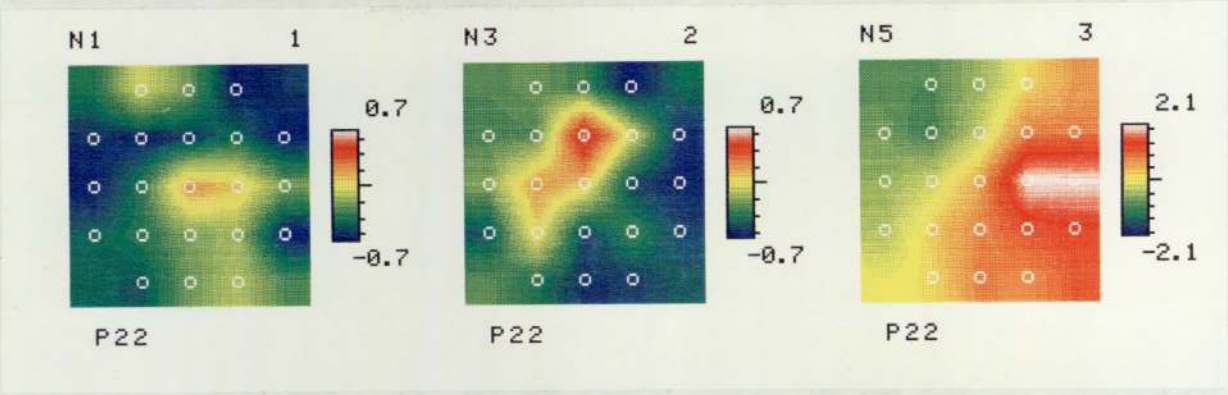
N1
1
0.7
-0.7
P22
N3
2
0.7
-0.7
P22
N5
3
2.1
-2.1
P22

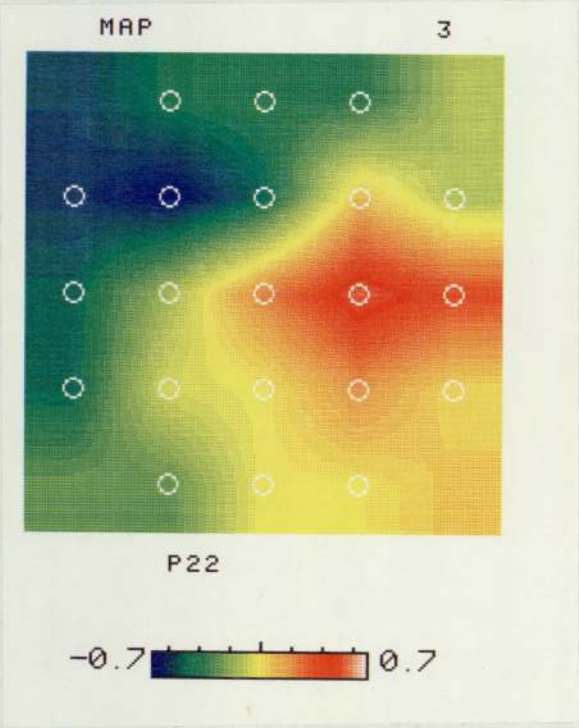
MAP
3
P22
-0.7
0.7

Whilst most components of the group mean waveforms had clear spatial and temporal properties that enabled easy identification, the peak of N31, and hence an accurate contour map, was more difficult to discern. N30 clearly peaked at 27.00ms with maximum negativity occurring at precentral L10,60. At 29.50ms a second negative locus was observed at central L20,50 which remained the maxima despite the general posterior shift of negative contours until 32.25ms where the postcentral N33 component was seen to peak at L20,40. Contour maps were therefore constructed at 29.50ms and 31.25ms to represent the possible N31 maxima (Figure 6.8).

Only two control individuals produced N31 components that could be temporally discerned from N30 and N33 components. N31 maps in these two individuals (subjects N1 and N5) revealed clear radial dipole-like fields centred over electrode site L20,50 (Figure 6.14).

Five control individuals produced N33 components although in two of these it was difficult to clearly discern temporally between N31 and N33 components. As with N30 maps, a wide variability of field distributions were observed. Subjects N1 and N2 produced radial dipole-like fields centred over electrode site L20,50 as seen with the two N31 components. In the remaining three subjects however, clear tangential dipole-like fields were observed with widely differing orientations (Figures 6.15 and 6.18) although the maximum negativity was either central or post-central in location.

6.3.6. P42 Maps.

P42 components were clearly discerned in all six control subjects, and while the radial dipole field type was observed in all six subjects, P42 was the only component whose maxima was observed at pre-central, central and post-central electrode locations. The positive locus of P42 obtained from the group mean waveform map was L10,50 (Figure 6.8) and for the group mean component map, L20,50 (Figure 6.16).

In two control individuals (N4 and N6), there was a latency difference between P42 occurring at pre-central locations and the P42 component occurring at central and post-central locations. In subject N4, frontal P42 occurred at 36.25ms compared to central and

Figure 6.12. Overleaf. P27 component maps from control individuals. Large map represents the group mean component topographic distribution of P27.

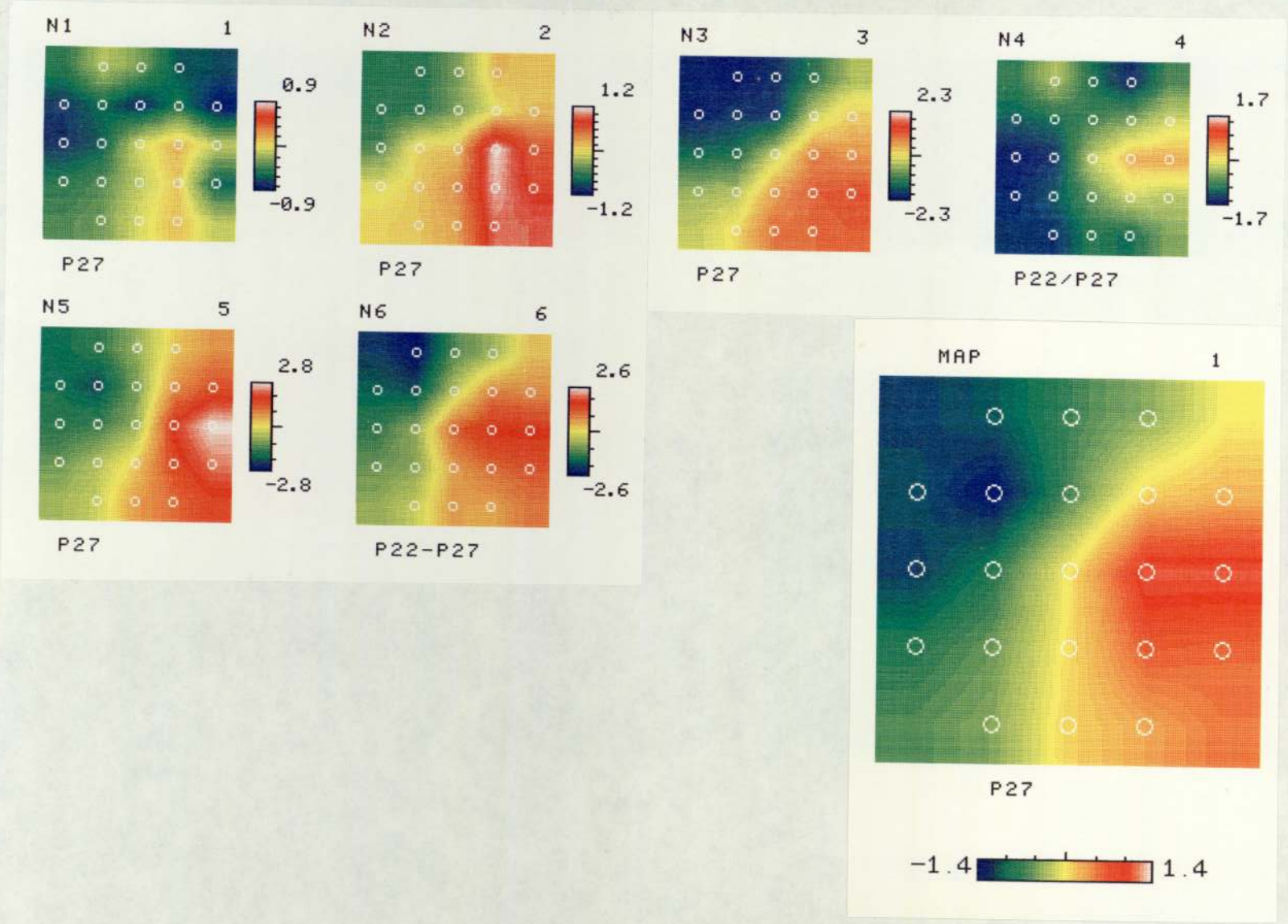
N1
1
0.9
-0.9
P27
N2
2
1.2
-1.2
P27
N3
3
2.3
-2.3
P27
N4
4
1.7
-1.7
P22/P27
N5
5
2.8
-2.8
P27
N6
6
2.6
-2.6
P22-P27
MAP
1
P27
-1.4
1.4

Figure 6.13. Overleaf. N30 component maps from control individuals. Large map represents the group mean component topographic distribution of N30.

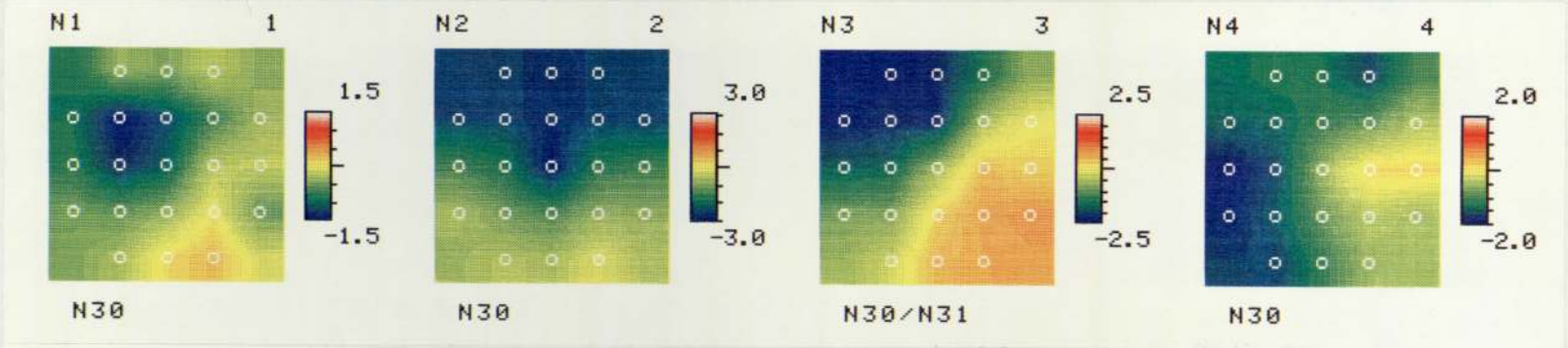
N1
1
1.5
-1.5
N30
N2
2
3.0
-3.0
N30
N3
3
2.5
-2.5
N30/N31
N4
4
2.0
-2.0
N30

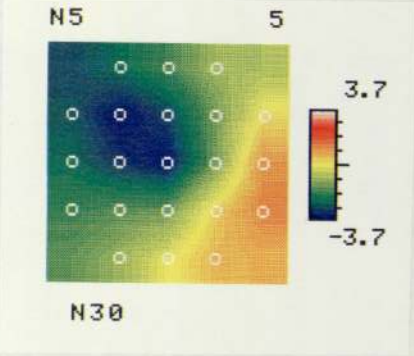
N5
5
3.7
-3.7
N30

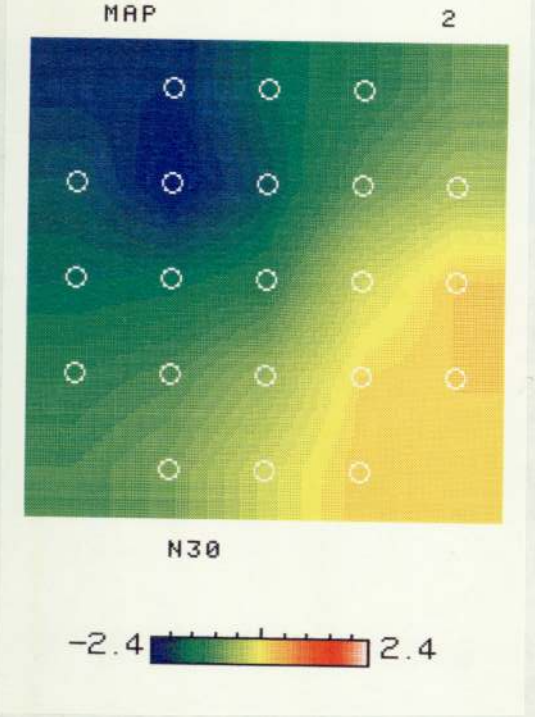
MAP
2
N30
-2.4
2.4

Figure 6.14. Overleaf. N31 component maps from control individuals. Large map represents the group mean component topographic distribution of N31.

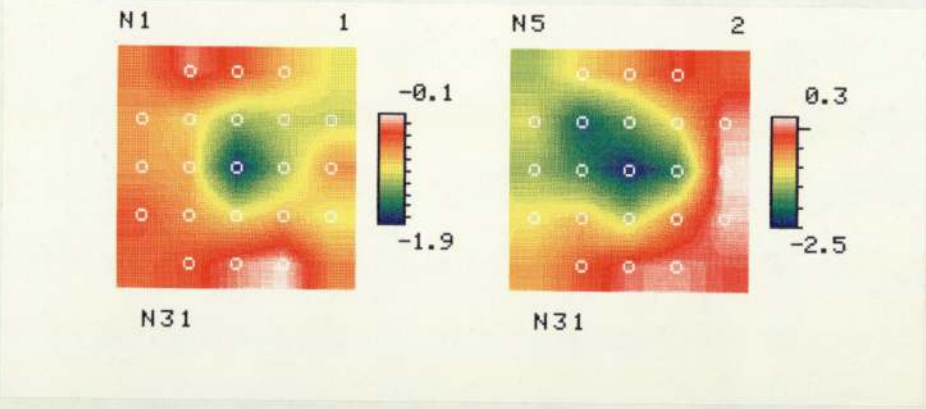
N1
1
-0.1
-1.9
N31
N5
2
0.3
-2.5
N31

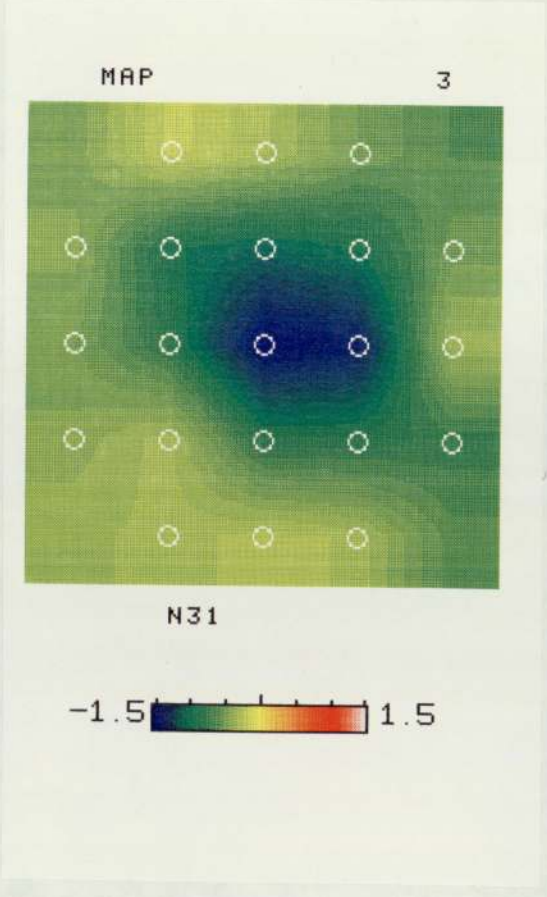
MAP
3
N31
-1.5
1.5

Figure 6.15. Overleaf. N33 component maps from control individuals. Large map represents the group mean component topographic distribution of N33.

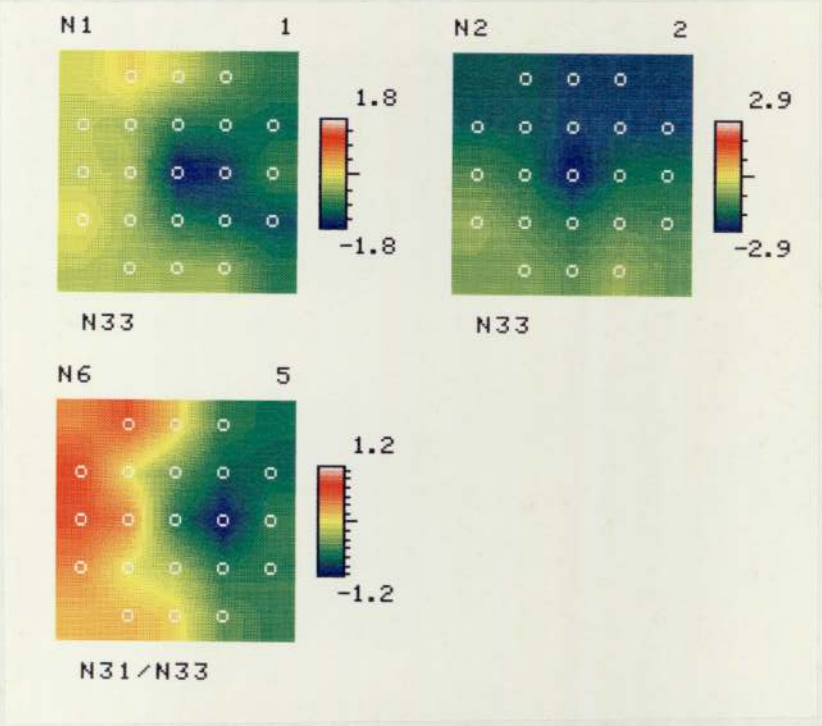
N1
1
1.8
-1.8
N33
N2
2
2.9
-2.9
N33
N6
5
1.2
-1.2
N31/N33

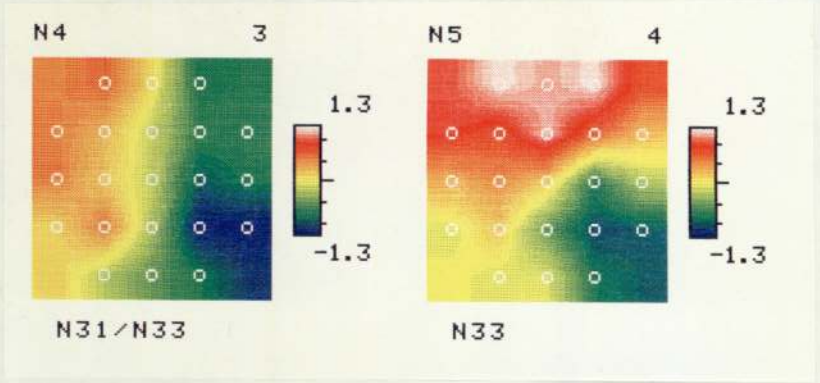
N4
3
1.3
-1.3
N31/N33
N5
4
1.3
-1.3
N33

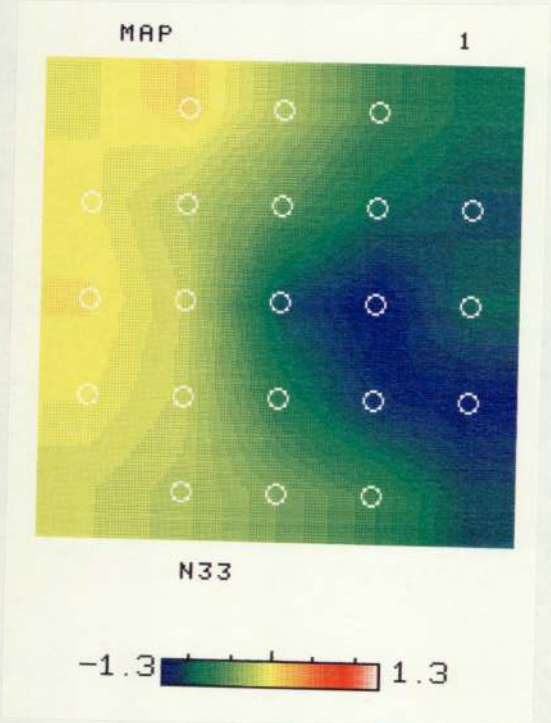
MAP
1
N33
-1.3
1.3

Figure 6.16. Overleaf. P42 component maps from control individuals. Large map represents the group mean component topographic distribution of P42.

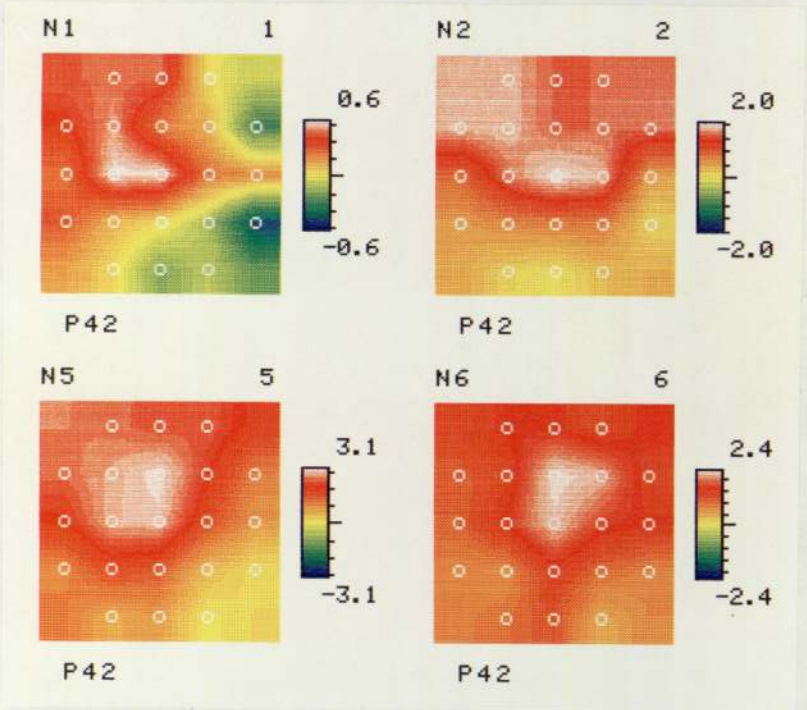
N1
1
0.6
-0.6
P42
N2
2
2.0
-2.0
P42
N5
5
3.1
-3.1
P42
N6
6
2.4
-2.4
P42

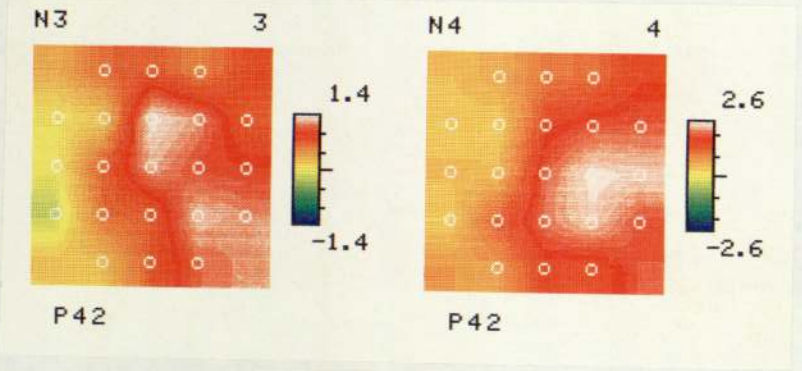
N3
3
1.4
-1.4
P42
N4
4
2.6
-2.6
P42

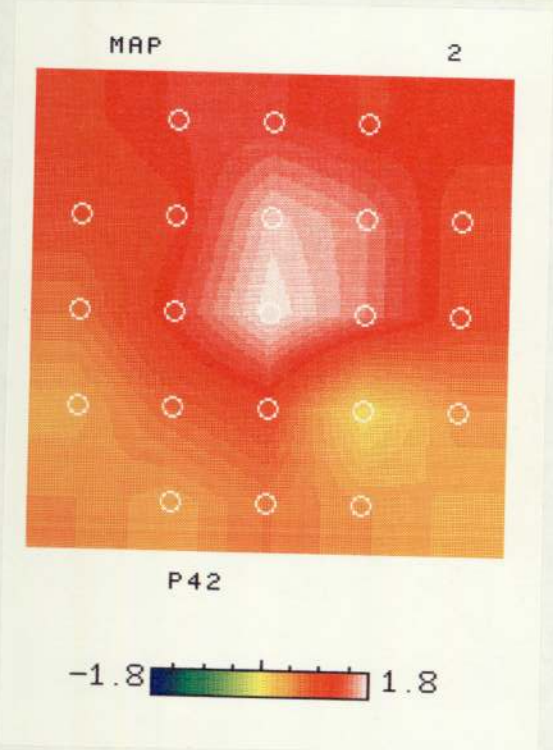
MAP
2
P42
-1.8
1.8

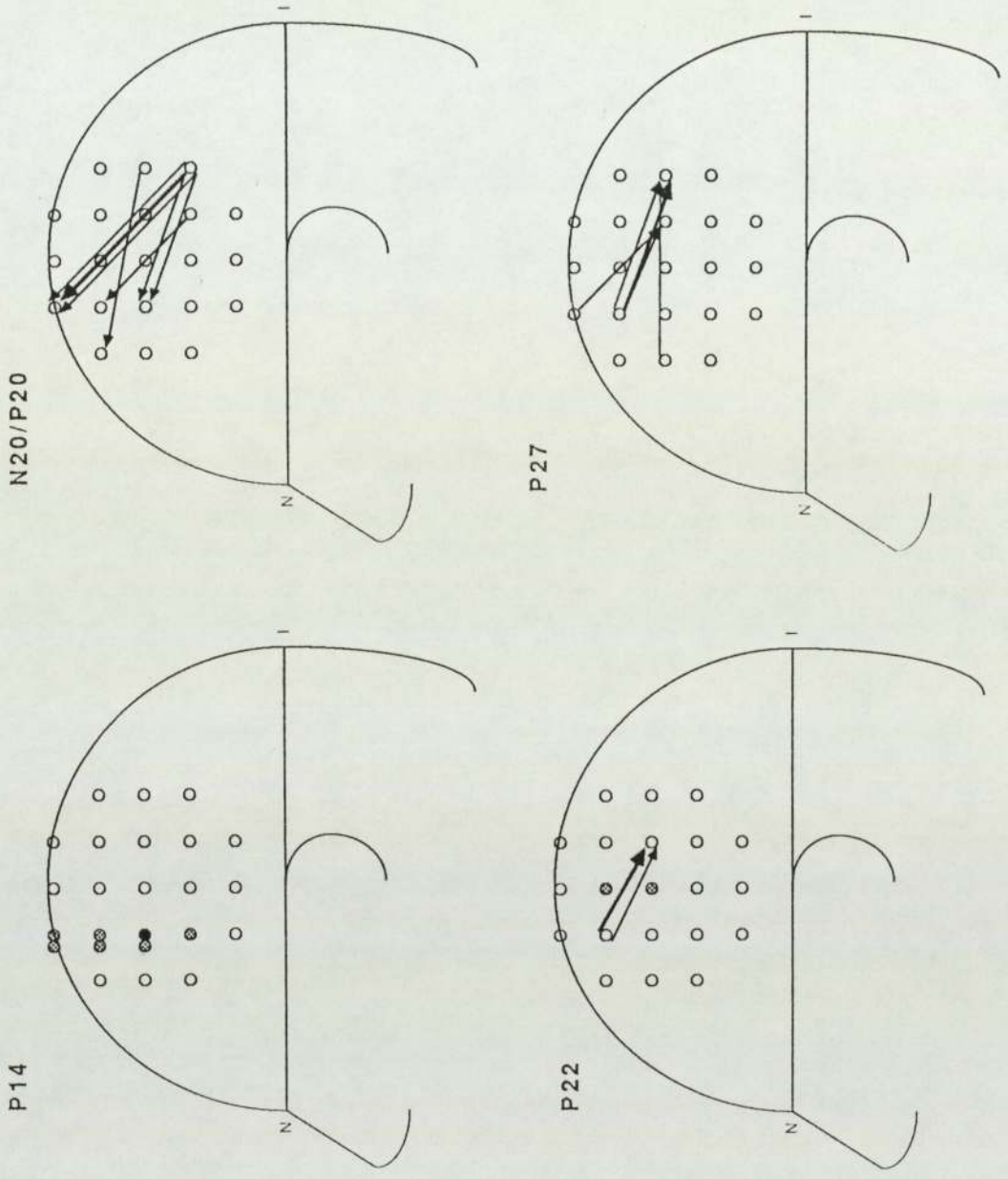

Figure 6.17. Schematic alignment of dipole fields for P14, N20/P20, P22 and P27 components. Arrows drawn from maximum negativity to maximum positivity where tangential dipole-like fields were observed. Shaded electrode sites represent maximum locus of radial dipole-like fields. Bold shading or arrows represent alignment of group mean dipole field (from group mean component maps).

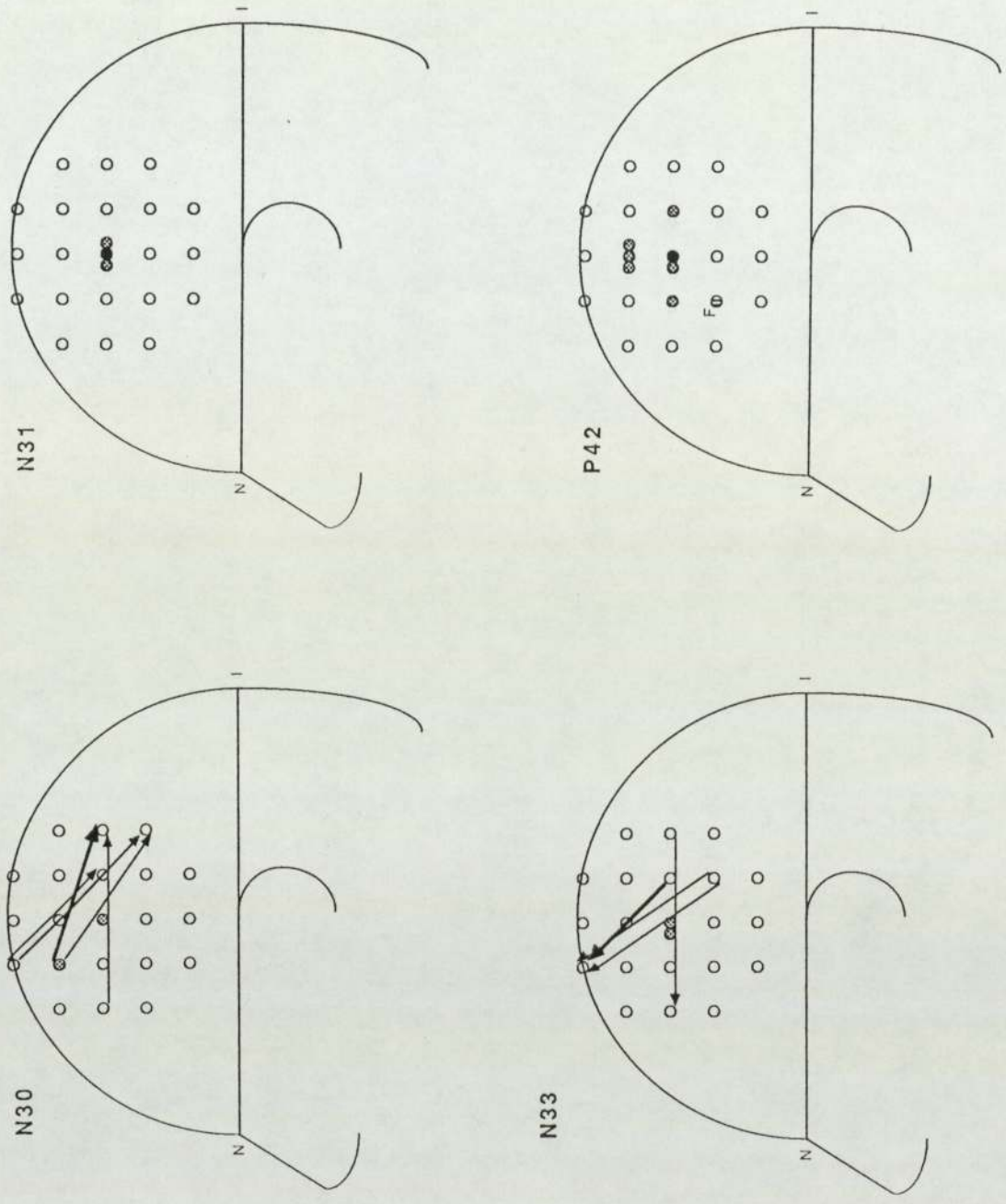

Figure 6.18. Schematic alignment of dipole fields for N30, N31, N33 and P42 components. Arrows drawn from maximum negativity to maximum positivity where tangential dipole-like fields were observed. Shaded electrode sites represent maximum locus of radial dipole-like fields. Electrode marked F on P42 model indicates locus of a Frontal P42 that differed spatially and temporally from the central/parietal conterpart.
Bold shading or arrows represent alignment of group mean dipole field (from group mean component maps).

post-central P42 occurring at 41.75ms. In subject N6, frontal P42 occurred 1.5ms after the central/post-central P42 at 37.00ms. Maps generated at the peak of the frontal P42 produced a different topographical distribution for control subject N4 with the locus of positivity occurring at L30,60.

6.4.0. Summary and Conclusion.

The sagittal polar projection employed in this study provided a system that was both easy to employ and whose points could easily and effectively be communicated. The 10% spread of electrodes provided optimum cover of all important components without extending too far over the scalp and thus incurring measurement distortion due to excessive curvature of the skull. The proportionality of measurements employed allowed for group mean data to be acquired.

With all systems of electrode placement that employ measurements of external cranial landmarks to locate electrodes on the scalp, there is a basic assumption that there is consistent correlation between the scalp locations and underlying cerebral structures. Binnie et al (1982) cast doubt on this assumption in relation to the 10-20 system. They observed that the quadrants bounded by the nasion, inion and preauricular points varied in size by more than 10% in the majority of normal subjects. These observations were supported by Homan et al (1987) who employed CT scans to determine the cortical correlation of electrode markers placed according to the 10-20 system. They reported that in seven of twelve subjects investigated 2 hemispheric and 12 quadrant asymmetries of 10% or greater were observed. They also reported a precentral location for the C3/C4 electrode sites in most of the 12 adults studied, however, direct identification of cortical areas was not possible in their study.

Steinmetz et al (1989) using nuclear magnetic resonance techniques (NMR) observed the lateral end-points of the central sulci lay approximately 1cm superior to the cortical

Figure 6.19. Overleaf. Map (left) indicates control group mean potential distribution concomitant with N20/P20 components as described in Chapter 4.
The arrow in the central schematic diagram was constructed to illustrate the sites of maximum positivity to maximum negativity and thus represent the theoretical neuronal alignment responsible for the dipolar field.
The diagram (right) is taken from Steinmetz et al (1989) and represents the relationship of the central sulcus to Cz and C3/C4 electrode sites in 16 healthy volunteers.

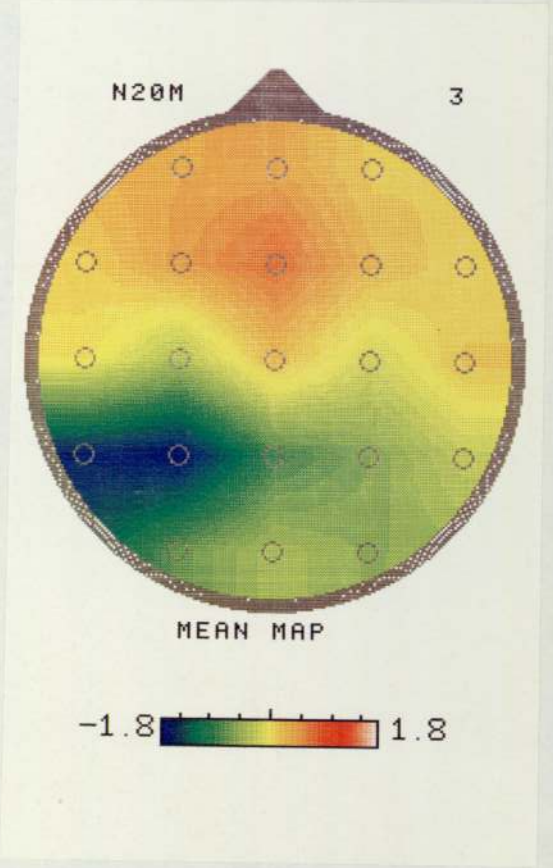
N20M
3
MEAN MAP
-1.8
1.8

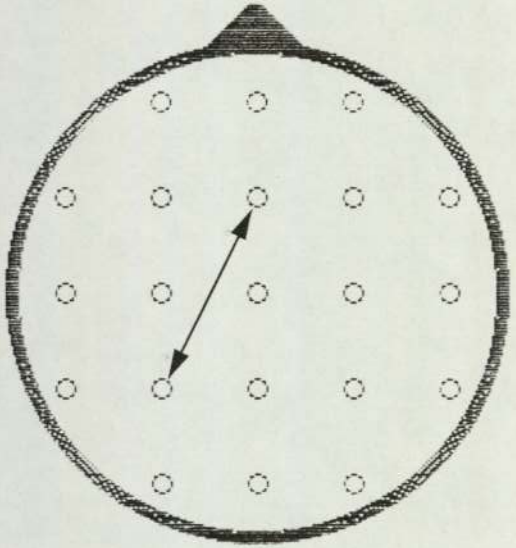

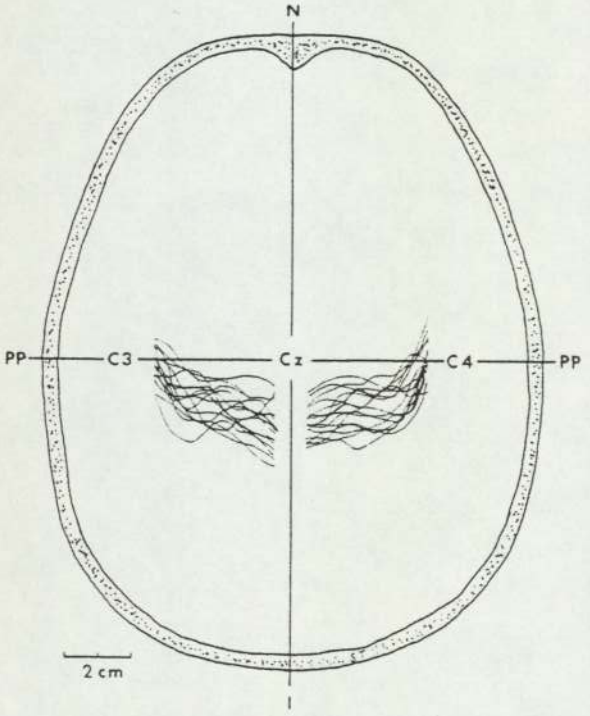
N
PP
C3
Cz
C4
PP
2 cm
I

Figure 6.20. Overleaf. Map (left) indicates control group mean potential distribution concomitant with N20/P20 components as earlier in this Chapter.
The arrows in the central schematic diagram (top right) were constructed to illustrate the sites of maximum positivity to maximum negativity in the six control subjects and thus represent the theoretical neuronal alignment responsible for the dipolar fields. The bold arrow indicates the alignment of the field shown in the group mean map.
The diagram (right lower) is taken from Steinmetz et al (1989) and represents the relationship of the central sulcus to Cz electrode site in 16 healthy volunteers.

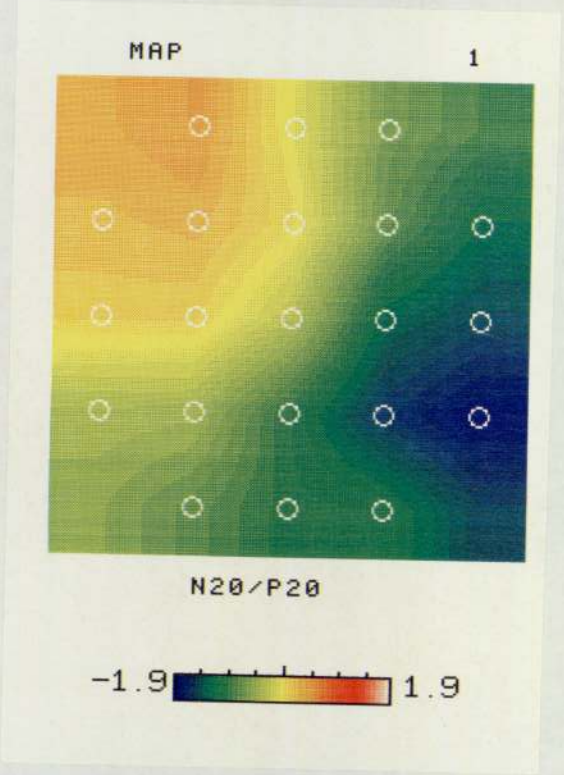
MAP
1
N20/P20
-1.9
1.9

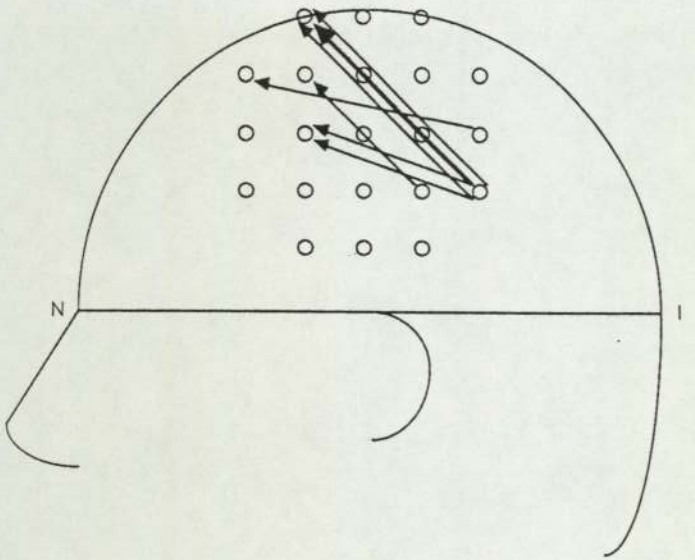
N20/P20
N
I

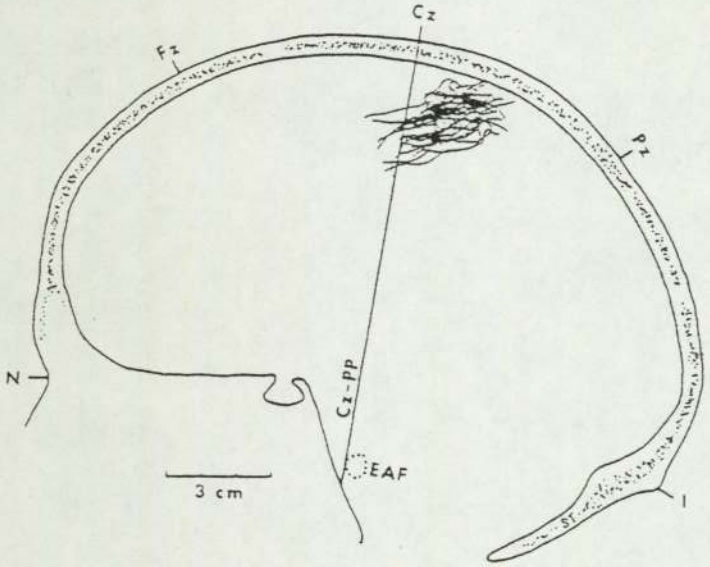
Cz
Fz
Pz
N
C1-PP
EAF
3 cm
I

representation of C3/C4 and that these electrode placement sites overlay the pre or post - central cortex depending on individual anatomy .

It is interesting to compare the dipole orientation of SEP components obtained in this study to the sulcus/electrode orientations reported by Steinmetz and co-workers. As can be seen in Figures 6.19 and 6.20, the orientation of the N20/P20 complexes would appear to correlate well with the argument that generators of these potentials lie within the posterior bank of this sulcus.

Radial dipole-like fields for P22 and N31 components as opposed to tangential dipole-like fields for N20 and P27 supports observations made in the previous two Chapters relating to separate generators of the scalp recorded SEP components. However, the temporal overlap of components - particularly P22 with P27, N30 with N31 and N31 with N33 in the young control subjects often prevented the precise topographic patterns of distribution of these components to be determined.

When averaging data from closely spaced electrode matrices, the variation in component topography caused by individual variation of underlying cortical features may be more greatly reflected than in recordings derived from greater interelectrode distances. For this reason, group mean component maps may be more meaningful than group mean waveform maps in this study.

A valuable observation that could be made equally well from the group mean waveforms as from inspection of individual subject waveforms was that component latency and morphology could change markedly between adjacent electrode locations for several components. Consider the group mean waveform recorded at electrode site L20,40 for example (Figure 6.8). Waveforms seen at all adjacent electrode locations whether anteriorly, posteriorly, inferiorly or superiorly, were markedly different in latency and/or morphology, most notably at the latency concomitant with the P22 complex. This sudden change of latency and morphology is consistent with components reflecting the activity of discrete and separate generators rather than arising by volume conduction from more distant generators. For such

components one does not observe the so -called travelling wave phenomenon (Cracco 1976) which predicts a gradual shifting of components in time along a longitudinal series of scalp electrodes .

The increased spatial resolution of the 10% electrode matrix confirmed the previous observation that components such as P22 and N31 are extremely focal in nature and are likely therefore to be generated by radially oriented generators located near the cortex surface.

The polar distance line linking vertex to baseline (i.e. L0,50 to L50,50) appeared to be an important 'interface' between what might be regarded as pre-central components- namely P20-N30 complexes, and post-central components such as N20-P27. Thus the peri-rolandic P22-N31 complexes were seen either on or at close proximity to this line. However, without NMR scans on the individuals recorded, one cannot say conclusively whether this line fell pre- or post rolandically.

It appears likely from the data recorded in this study is that P42 components were formed by multiple pre and post central generators. This would account for the variable and broad distribution of the component as well as the occasional temporal shift observed between pre and post central components.

In discussion on the placement of electrodes for satisfactory mapping of all scalp SEP components, Desmedt et al (1987) recommended the use of a 27 channel (whole of scalp) montage at sites related to the 10-20 system with additional coronal rows of electrodes at 10% either in front or behind the vertex . They reported that the central coronal plane itself was critical for early SEP responses in the precentral region. On evidence that anatomical correlations had shown the standard EEG C3 and C4 electrodes to usually overlap the precentral gyrus in different subjects (Jasper 1958; Hellström et al 1964; Blume et al 1974), they placed the central coronal row 1 or 1.5cm in front of Cz to ensure that C3' and C4' sites (20% from midline) overlapped the motor strip in front of the central fissure (Figure 6.4).

Data from this study concurs with the observation that the central coronal plane was critical for recording the pericentral P22 and N31 components. However, this study also indicates that a shift of 10% pre-centrally may result in the failure to adequately record these components in some individuals and therefore cannot support the view for the need to shift the central coronal plane for SEP recordings. It would appear desirable however to illicit recordings from 10% intervals around the central C3/C4 electrode locations to accurately reflect the activity of the peri-rolandic potentials. This latter argument is supported by the work of Spitzer et al (1989) who employed closely spaced coronal and sagittal rows of electrodes to record the SEP. By Fourier transform analysis of SEP components and applying the Nyquist criterion (samples should be taken at 1/(2B) second intervals, where B is the recording bandwidth) , they proposed that the optimum interelectrode distance for SEP recordings should be 3cm or less. They concluded that the use of larger interelectrode recording distances such as employed in the 10-20 system of electrode placement, and where linear interpolation techniques were used could result in erroneous amplitude, location and contour results of potentials. This would be particularly true for focal components such as P22.

CHAPTER 7

SOMATOSENSORY EVOKED POTENTIALS IN SCHIZOPHRENIA. A LATERALIZATION STUDY

7.1.0. Introduction

In all the studies of both normal subjects and patients with specific lesions so far discussed in this thesis, comparisons have frequently been made between contralateral and ipsilateral responses to the stimulus. As a further development of this technique it was decided to analyse reported differences in lateralisation between patients with schizophrenia and normal controls.

In 1970, Hardin and Castelucci hypothesized that the latency difference between selected components of the ipsilateral and contralateral somatosensory evoked potential (SEP) could be interpreted as representing commisural delay. Salamy (1978) performed SEP recordings over a wide age range employing a vibro-tactile stimulus and recording electrodes over both somatosensory "hand areas" referenced to the vertex (Cz) electrode, and observed an ipsilateral response of longer latency and lower amplitude than the contralateral response. This difference in latency decreased with age and was said to reflect maturation in somatosensory commisural transmission.

The origin of the ipsilateral somatosensory evoked response remains open to question. Although it may arise from an afferent volley originating from the contralateral cortex mediated via an inter-hemispheric pathway - the corpus callosum - the potentials could equally result from volume conduction from contralateral cortex, or by direct uncrossed pathways arising in the thalamus. Several years previously, Rosenthal and Biggelow (1972) had shown a 20% thickening of the corpus callosum in a postmortem study of schizophrenic subjects.

Jones and Miller (1981) inspired by the previous studies set out to investigate the relationship between ipsilateral and contralateral SEP components in schizophrenics. Using a recording

protocol similar to that employed by Salamy they found that the ipsilateral response in controls was small in amplitude and delayed in onset compared with the contralateral response. In schizophrenics, however, no delay was seen on the ipsilateral hemisphere and it was suggested that ipsilateral pathways originated in the brainstem, rather than in a non-conducting corpus callosum. It was further proposed that schizophrenia might arise from agenesis of the corpus callosum.

In criticism of this work Connolly (1982) observed that the technique employed would only assess the small number of myelinated callosal axons. Generalisation from this small group to conclusions of total callosal block were felt to be ill-advised. However, in view of the potential importance of these findings, Shagass et al. (1983) carried out a replication study after certain methodological faults had been removed. In Jones and Miller's original study SEPs had been recorded with a vertex (Cz) electrode used as reference. This electrode can be active and a spurious ipsilateral response could be recorded (Desmedt and Brunko 1980). For this reason Shagass et al., employed linked ears as well as a vertex reference site. Their findings showed contralaterally higher amplitude SEPs in both controls and schizophrenics. They found no difference in the latencies between the ipsilateral and contralateral SEPs in either groups.

These and further conflicting studies (Tress et al 1983; Fenwick et al 1983), encouraged Cooper et al.,(1985) to investigate the matter further. SEP's arising from a complex vibro-tactile stimulus to the forefingers, similar to that employed by Jones and Miller, were further studied. The stimulus, mainly of movement and to a lesser extent touch, was modified to give an optimal tracing. Eight patients with affective disorder (3 depressive and 5 manic) all had the expected contralateral hemisphere lateralisation as did 12 out of 15 normals. Three normals and 3 schizophrenics had a loss of lateralisation of the evoked response to stimulation of one hand and normal lateralisation when the other hand was stimulated (unilateral abnormality). Ten out of 21 schizophrenic patients had an abnormal lack of lateralisation response whichever hand was stimulated (bilateral abnormality). The wave forms were characterised by

major positive peaks with a latency of approximately 30 milliseconds and 45 milliseconds. In control groups, the response recorded ipsilaterally was invariably too small to reliably identify peaks. Judgements on the degree of lateralisation were made subjectively by visual inspection. Lateralisation characteristics were evident only for the earliest part of the responses and at longer latencies there were often similarities in amplitude between the wave forms recorded over the two hemispheres.

Cooper et al (1985) felt that the nature of the stimulus employed in their study of schizophrenia was of major importance. Such a stimulus would achieve consistency with previous authors in this field who had employed either vibro-tactile or similar mechanical stimulation (Jones and Miller 1981, Tress et al.1983). It was also felt that such a stimulus would be less distressing and more easily tolerated by schizophrenics than conventional electrical stimulation. However, there are a number of inherent problems in the design of vibro-tactile speaker systems (Jones and Miller, 1981; Shagass et al., 1983; Cooper et al., 1985). A considerable audio-stimulus is delivered to the patient which needs to be masked.

The speaker cone is a low inertia system and subjective sensation is modified by pressure exerted from the stimulated digit. The duration of the stimulus is relatively long compared with electrical square wave constant voltage stimulation (10ms versus 100us) and this may result in poorer formed potentials.

Finally the vast majority of literature other than the schizophrenic studies employs electrical stimulation to nerve trunk or digit and it is therefore difficult to generalize from findings using the vibrating stimulus and to compare them with wider studies usually of larger groups of patients and controls.

Cooper et al., (1985), felt that their findings were probably stimulus specific. However, since whatever mediated the ipsilateral short latency cortical response (other than simple volume conduction) has to be the result of "hardwired" thalamic and/or cortico-cortical tracts, the nature of the stimulation should be relatively inconsequential, unless we challenge existing anatomical, physiological and electrophysiological knowledge.

It has been demonstrated that the integrety of the dorsal column pathways is essential for generation of cortical SEP's (Halliday and Wakefield 1963) with the small signals detected in lateral spinothalamic tracts appearing to contribute nothing to the scalp potential (Suzuki and Mayanagi 1984). These facts coupled with existing knowledge of the cytoarchitecture of the primary somatosensory cortex lead to the conclusion that cerebral locations of the SEP are unlikely to differ widely, whether the stimulus is electrical or vibro-tactile if only digital nerves are stimulated (Hyvarinen 1982, Kakigi and Shibasaki 1984); the comparative morphology of tactile and electrical evoked responses would appear to differ little (Pratt and Starr, 1981).
Given these factors and the relatively poor responses obtained on the vibro-tactile stimulus, it was decided to standardise on electrical digital stimulation.

The following study was carried out using digital electrical stimulation, with the results recorded on the Biologic Brain Atlas III System to facilitate more detailed topographic analysis of the data.

7.2.0. Method

A patient group of 19 schizophrenics, both inpatients and outpatients, were compared to a group of normal healthy volunteers. Patients were interviewed using a modified form of the Schedule of Affective Disorder in Schizophrenia (S.A.D.S.) and included in the study if they fulfilled R.D.C. and D.S.M. 3 criteria for schizophrenia. Basic demographic data and clinical details, such as the duration of illness were collected. A case note review, using the Present State Examination (PSE) symptom checklist (Wing et al 1974), allowed all patients to be classified as having nuclear schizophrenia.
Twenty electrodes were placed over the scalp according to the International 10-20 system at points Fp1,Fp2,F3,F4,F7,F8,Fz,Cz,Pz,T3,T4,T5,T6,C3,C4,P3,P4,O1,Oz and O2 with linked earlobe electrodes as the reference. The stimulus was produced by ring electrodes placed on the distal phalanx of the index finger with cathode proximal to the anode. An earth lead

held by a velcro strip was attached on the forearm; some light abrasion of the skin with the velcro beforehand produced a low resistance. Subjects were placed in a prone position, made warm and comfortable and asked to remain still with their eyes closed but to remain awake. Subjective threshold of the stimulus was ascertained and a current level three times this threshold used to elicit the SEP.Stimulus duration was 200 microseconds and current levels were typically 3-6 milliamps.

Both right and left index fingers were stimulated in each subject, the order being on a random basis between subjects. Stimulation rate was 2.7 per second and 1024 stimulus runs were averaged. Careful monitoring of the input signal with automatic artefact rejection was maintained to ensure artefact-free recordings.

The Biologic Brain Atlas III System with built-in amplifiers was employed for recording. Gains were set at 50,000 with low frequency filters at 10Hz and high frequency filters at 1500Hz (-3dB points, roll-offs 12dB-octave). Twenty channels of data were recorded and stored on a 10 megabyte disc cartridge for analysis. Isopotential colour contour maps were generated from the waveforms in the manner described in detail in Chapter 4.

7.3.0. Results

Thirteen normal control volunteers were recorded; six male and seven female, of mean age 29.9 years (spread 19-57yrs). Nineteen schizophrenic patients were recorded; fourteen male and seven female, of mean age 35.5 years (spread 17-68 years). There was a positive family history in 3 patients. The average time since onset of first illness was 10 years (spread 2-40 years) and patients had been hospitalised for an average of 59 months (spread 3 months to 24 years). All patients were currently on drug treatment.

In the control group, of the twenty six possible recordings obtainable (right and left index fingers), twenty four were actually achieved.Two recordings were lost from two right hand dominant individuals from whom no recognisable potentials to left index finger stimulation were discerned, but subsequently showed normal responses to median nerve stimulation.

In the schizophrenic group, of the possible thirty eight recordings, twenty nine were actually achieved. In four patients, no recognisable components to digital stimulation could be discerned in either hand. Each of these patients subsequently produced clearly recognisable potentials to median nerve stimulation. One patient had received major injuries to his left hand in a machine accident which had resulted in the loss of his left index finger.

Utilising the software of the Brain Atlas III™ system, group mean waveforms were calculated for the control group and schizophrenic patient group. Initial subjective analysis of the waveforms obtained from the parietal area resulted in the recognition of the W response described in earlier Chapters - the familiar P14-N20-P27-N33-P42 components obtained by median nerve stimulation. Although mean peak latencies are longer for digital stimulation than median nerve, the nomenclature for responses to median nerve stimulation was adopted for ease of communication and comparison. Actual mean peak latencies of contralateral parietal hemisphere components are shown in Table 7.1 (overleaf).

Other consistent components seen in both patient and control groups were frontal N17-P20-N30 and centro-parietal N19-P22-N31-P42 potentials . The most relevant waveforms are illustrated in Figures 7.1 and 7.2.

TABLE 1. Mean peak latencies of contralateral parietal hemisphere components

Control	**P14**	**N20**	**P27**	**N33**	**P42**
	Mean s.d	Mean s.d	Mean s.d.	Mean s.d.	Mean s.d.
Rt Index	17.0ms (2.0)	22.8ms (1.6)	29.4ms (2.5)	37.7ms (3.4)	46.8ms(4.0)
Lt Index	17.1ms (1.2)	22.3ms (1.4)	28.2ms (2.5)	36.1ms (3.0)	44.6ms(3.9)
Schizophrenic					
	Mean s.d	Mean s.d	Mean s.d.	Mean s.d.	Mean s.d.
Rt Index	17.9ms (1.7)	23.7ms (1.7)	29.8ms (1.8)	36.9ms (5.6)	45.7ms (4.5)
Lt Index	17.6ms (1.0)	22.9ms (1.4)	30.2ms (2.6)	36.9ms (3.6)	44.6ms (3.8)

Isopotential colour contour maps were plotted from the group mean waveforms of control and patient groups (Figures 7.3 -7.6). Maps were generated at latencies concomitant with the peaks of the parietal N20,P27, N33 and P42 components as well as central P22. From the control group mean data no clear spatial distinction could be made between latencies concomitant with N31 and N33 and so unlike the patient group data, no separate map was generated for the N31 component. Inspection of these maps revealed that the topography of components of control and patient groups were closely similar. Certainly, there were no differences between the groups in terms of the lateralisation of components with all components fields appearing clearly contralaterally.

In order to identify any significant group differences, the student t-test was performed (again using the Brain Atlas III ™ system software) comparing every data point of every channel of the two group mean waveforms. The subsequent results supported the subjective impression from the waveforms that there was no significant difference between the groups ($p>>0.05$).

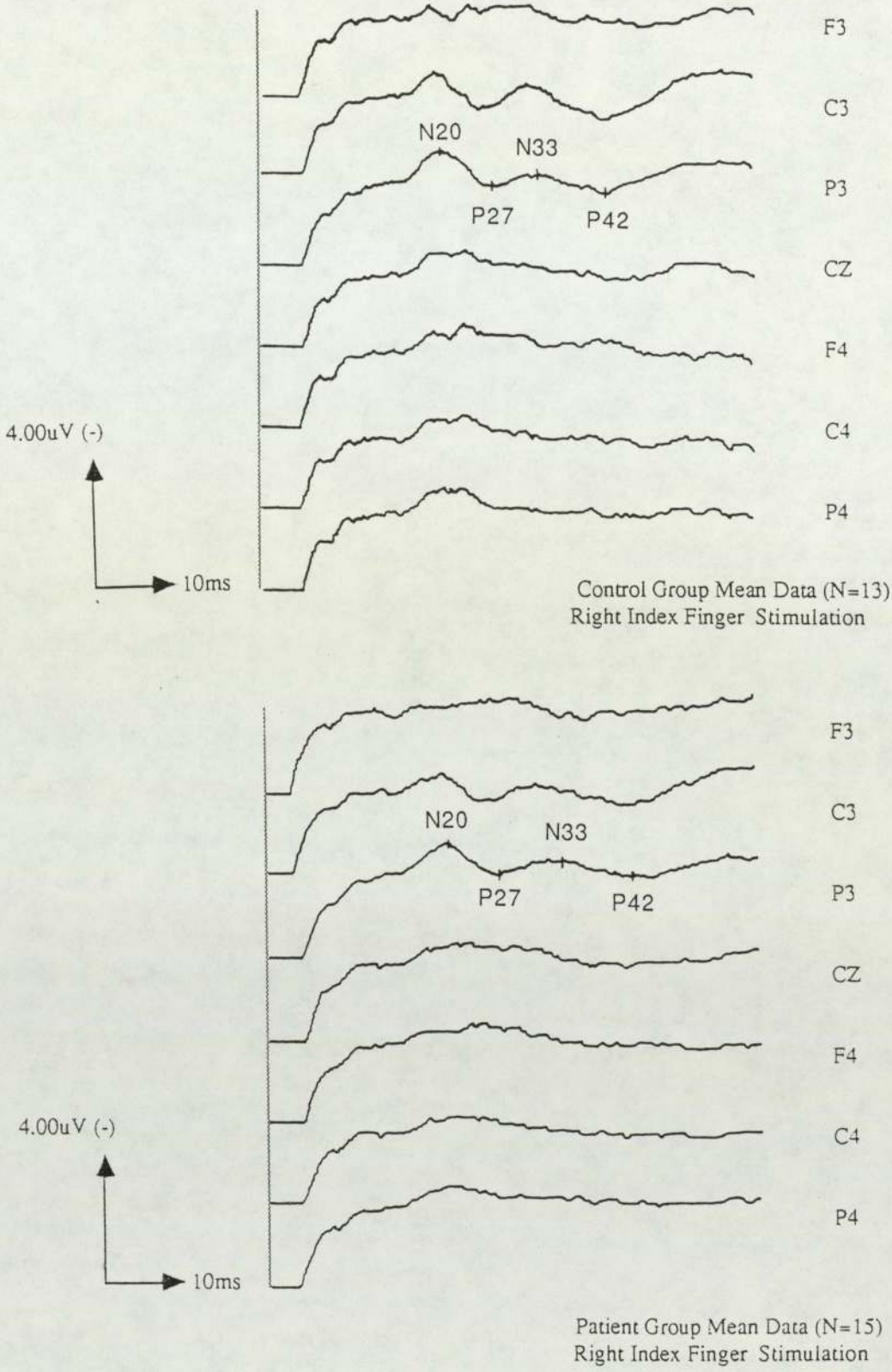

Figure 7.1. Control group mean waveforms (top) and patient group mean waveforms (bottom) for right index finger stimulation.

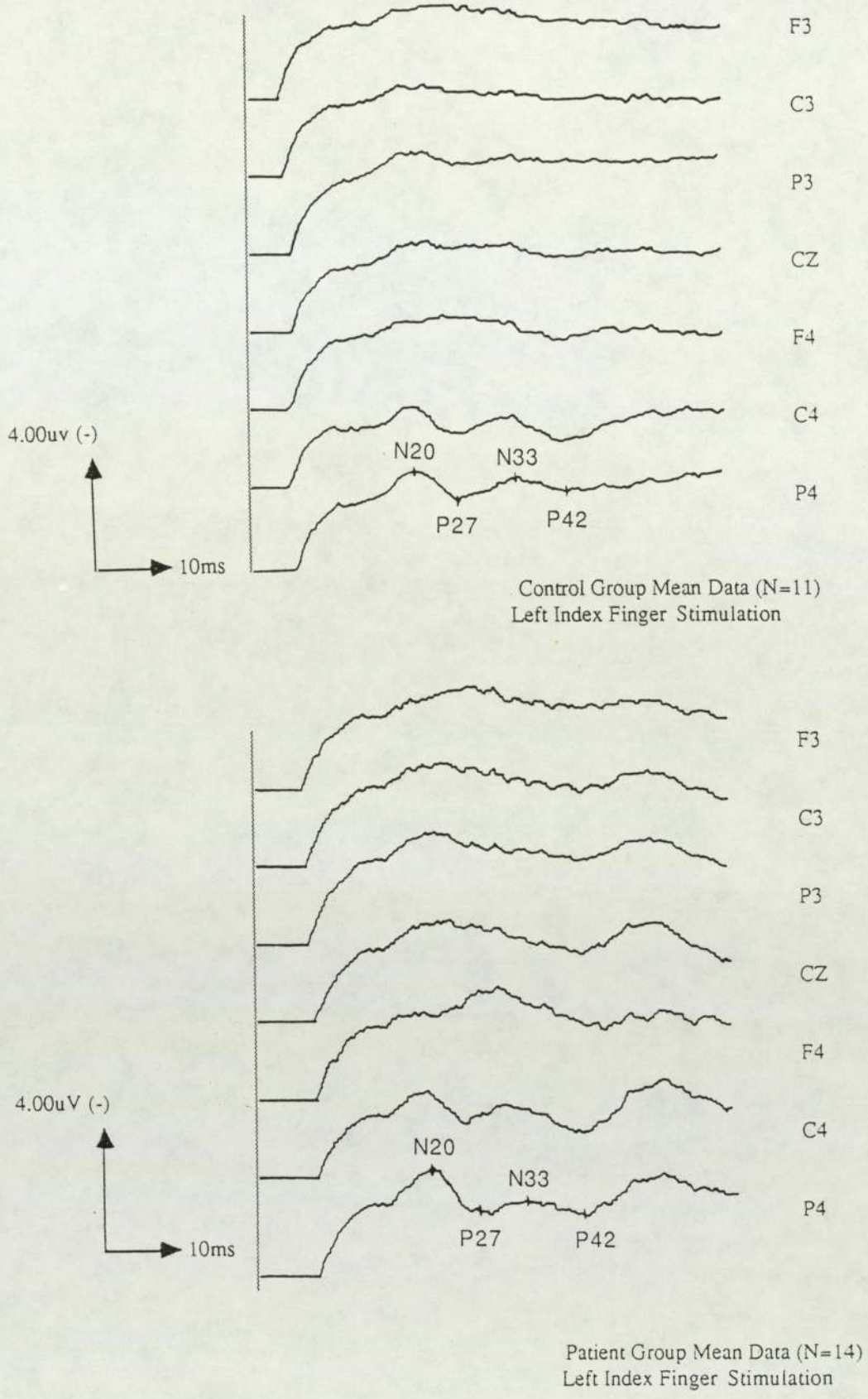

Figure 7.2. Control group mean waveforms (top) and patient group mean waveforms (bottom) for left index finger stimulation.

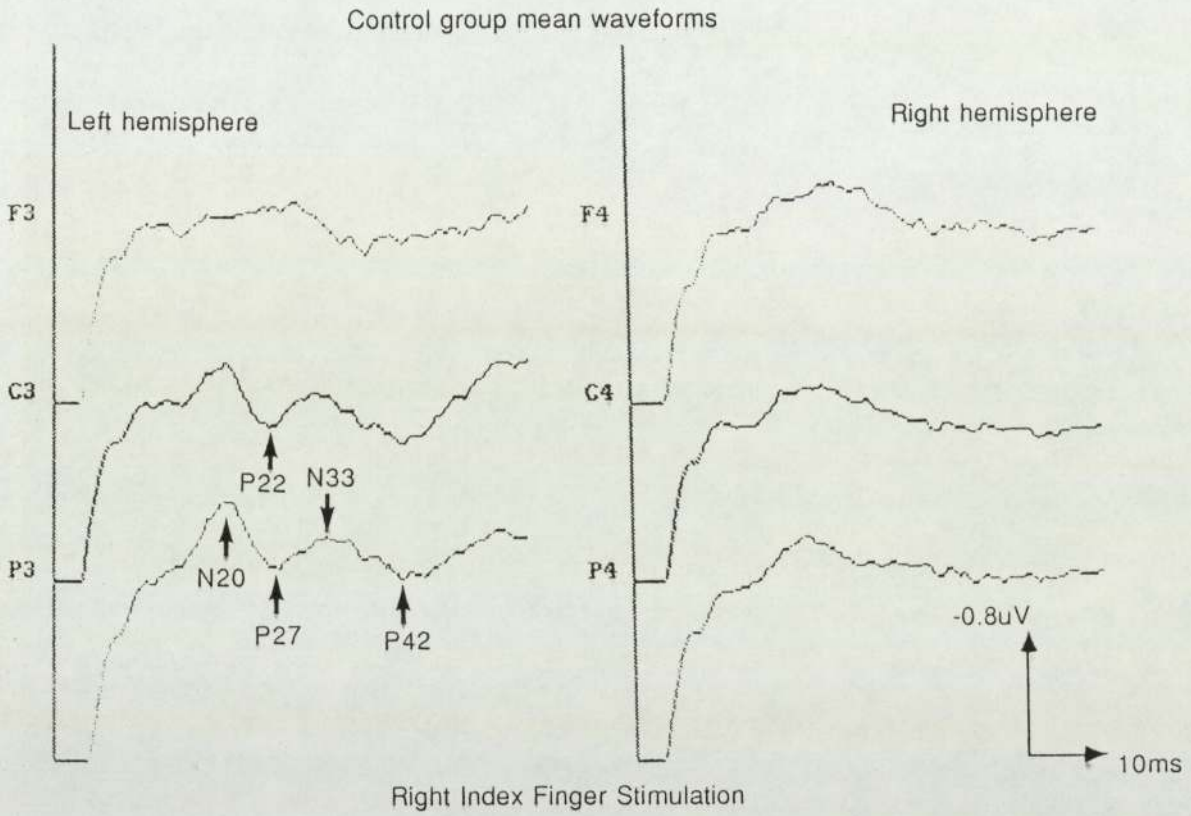

Figure 7.3. **Above.** Control group mean waveforms indicating peaks from which isopotential contour maps constructed.

Figure 7.3.1 **Overleaf**. N20/P20, P22 and P27 component maps generated from the peaks of the control group mean waveforms.

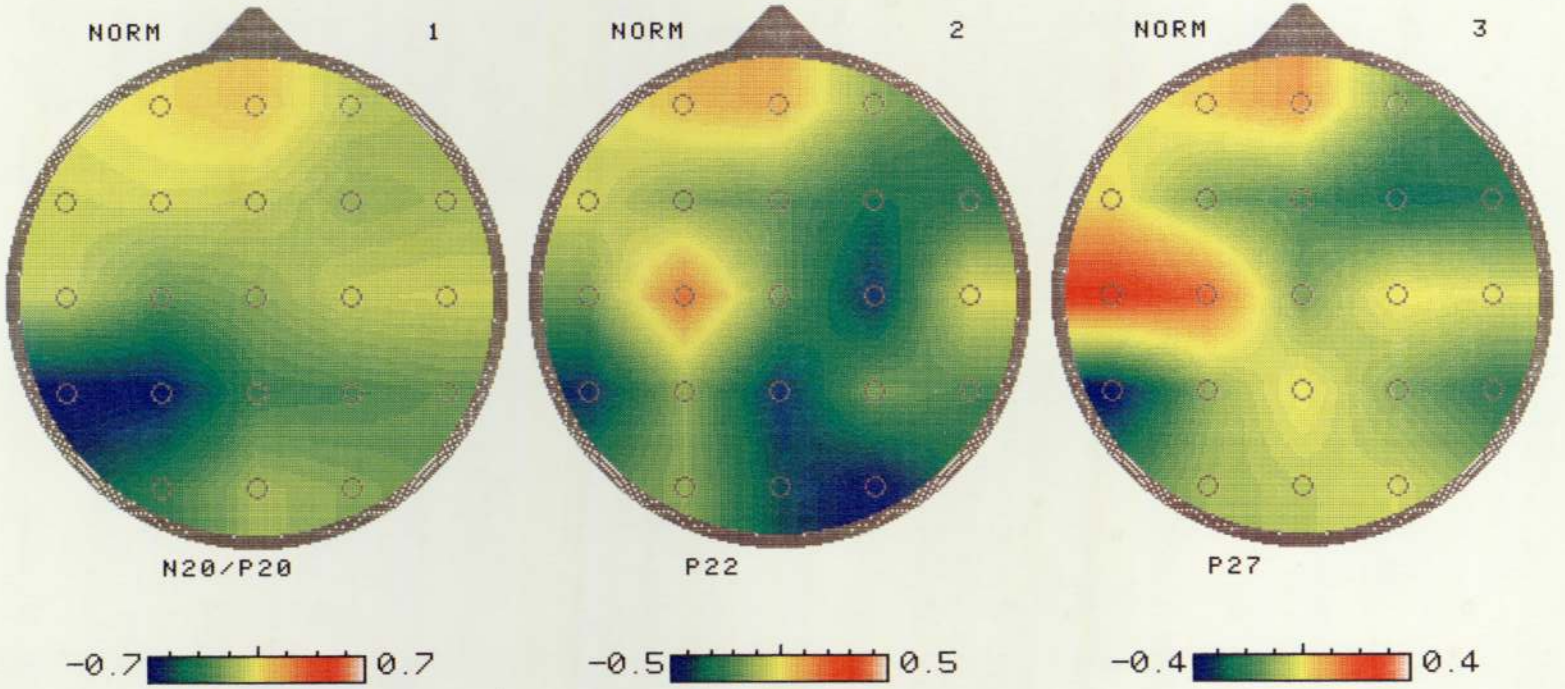
NORM 1
N20/P20
−0.7
0.7
NORM 2
P22
−0.5
0.5
NORM 3
P27
−0.4
0.4

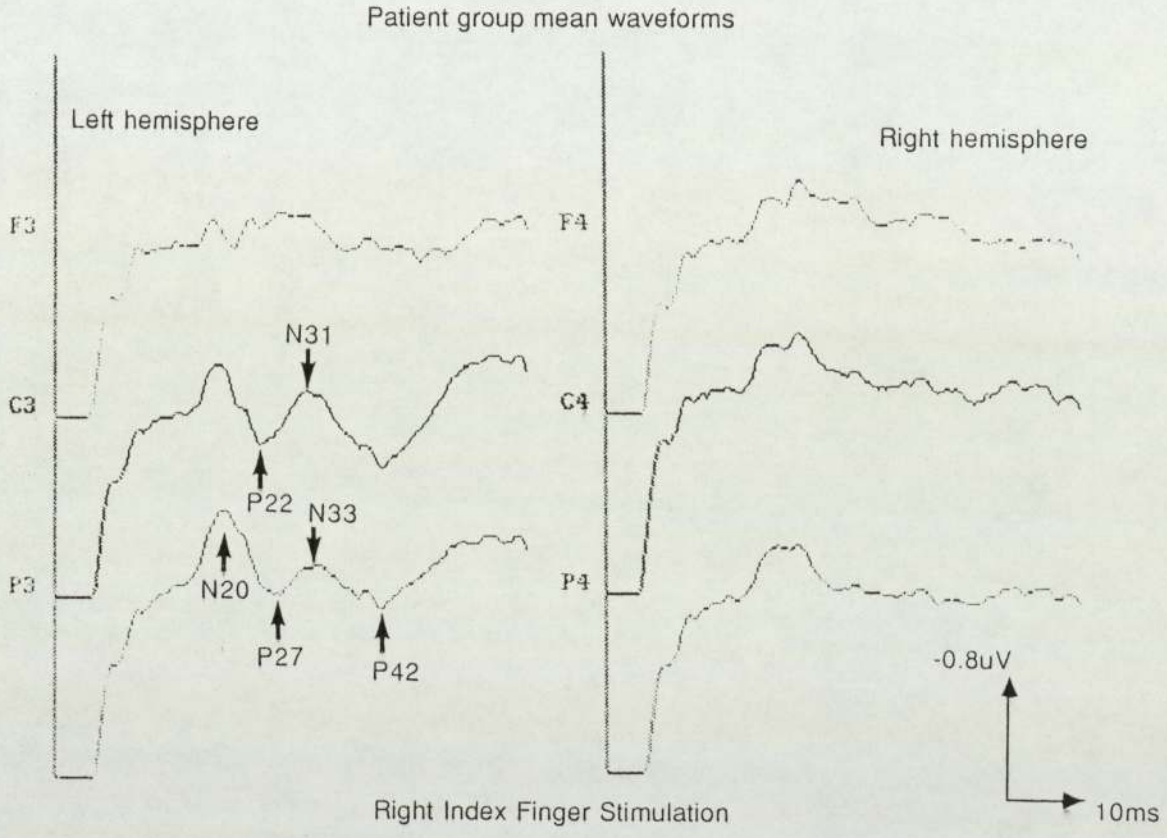

Figure 7.4. **Above.** Patient group mean waveforms indicating peaks from which isopotential contour maps constructed.

Figure 7.4.1 **Overleaf**. N20/P20, P22 and P27 component maps generated from the peaks of the schizophrenic patient group mean waveforms.

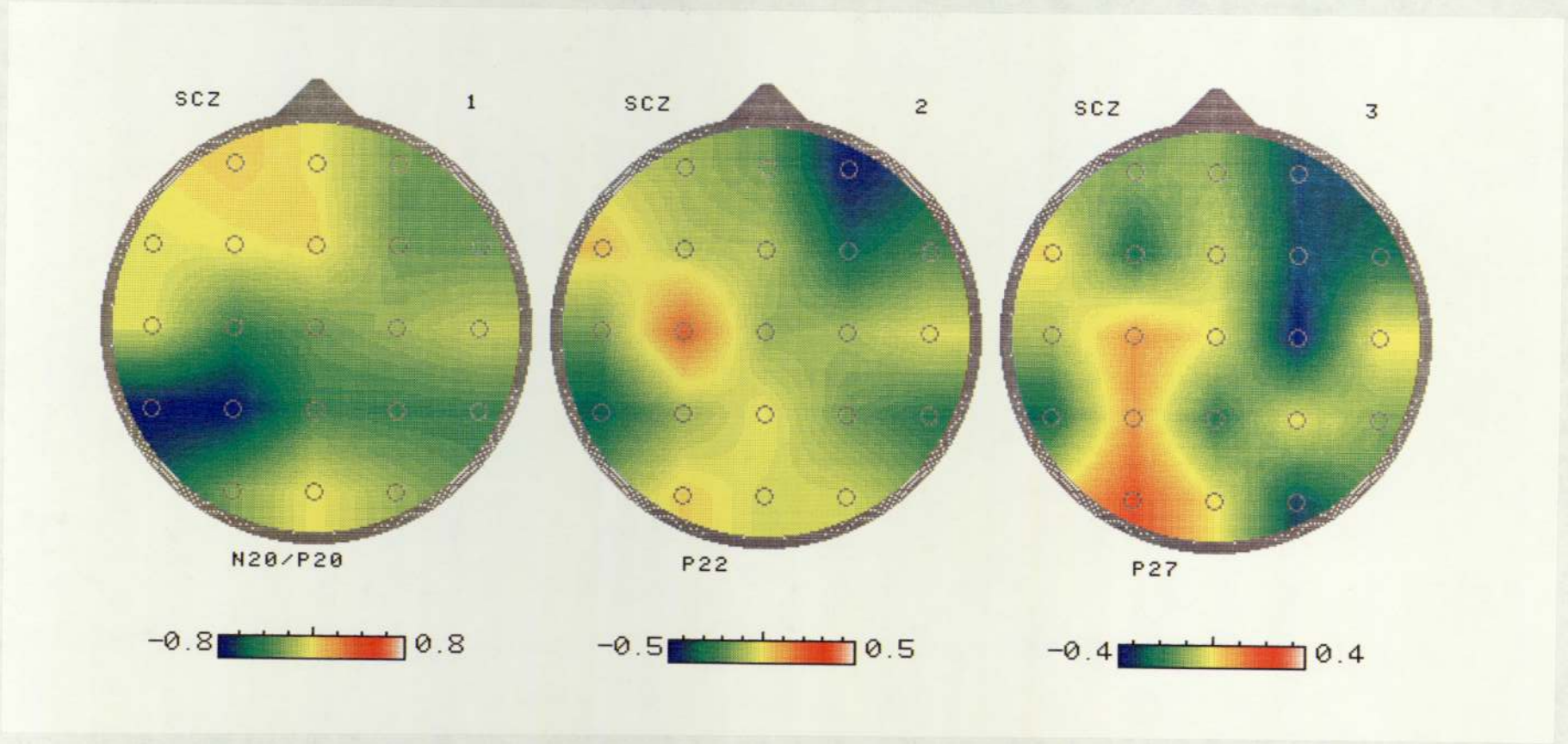
SCZ
1
N20/P20
−0.8
0.8
SCZ
2
P22
−0.5
0.5
SCZ
3
P27
−0.4
0.4

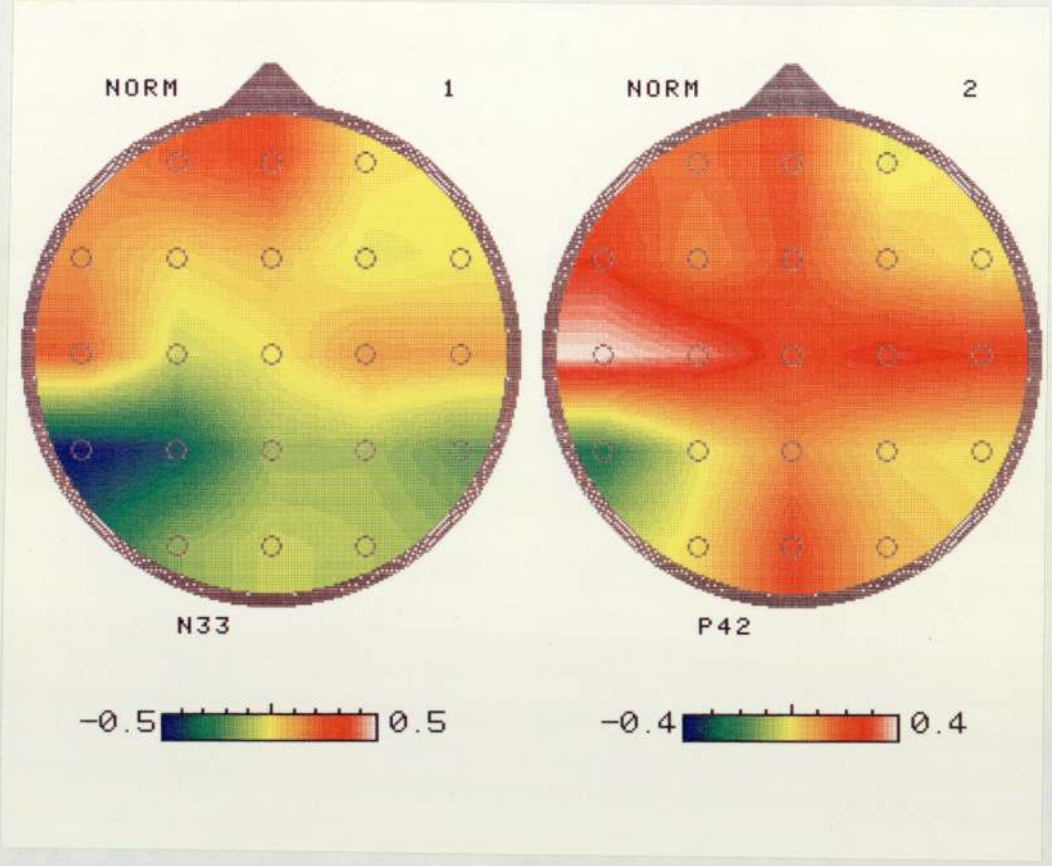

Figure 7.5. N33 and P42 component maps generated from the peaks of the control group mean waveforms (right index finger stimulation).

Figure 7.6. **Overleaf**. N31, N33 and P42 component maps generated from the peaks of the schizophrenic patient group mean waveforms (right index finger stimulation.)

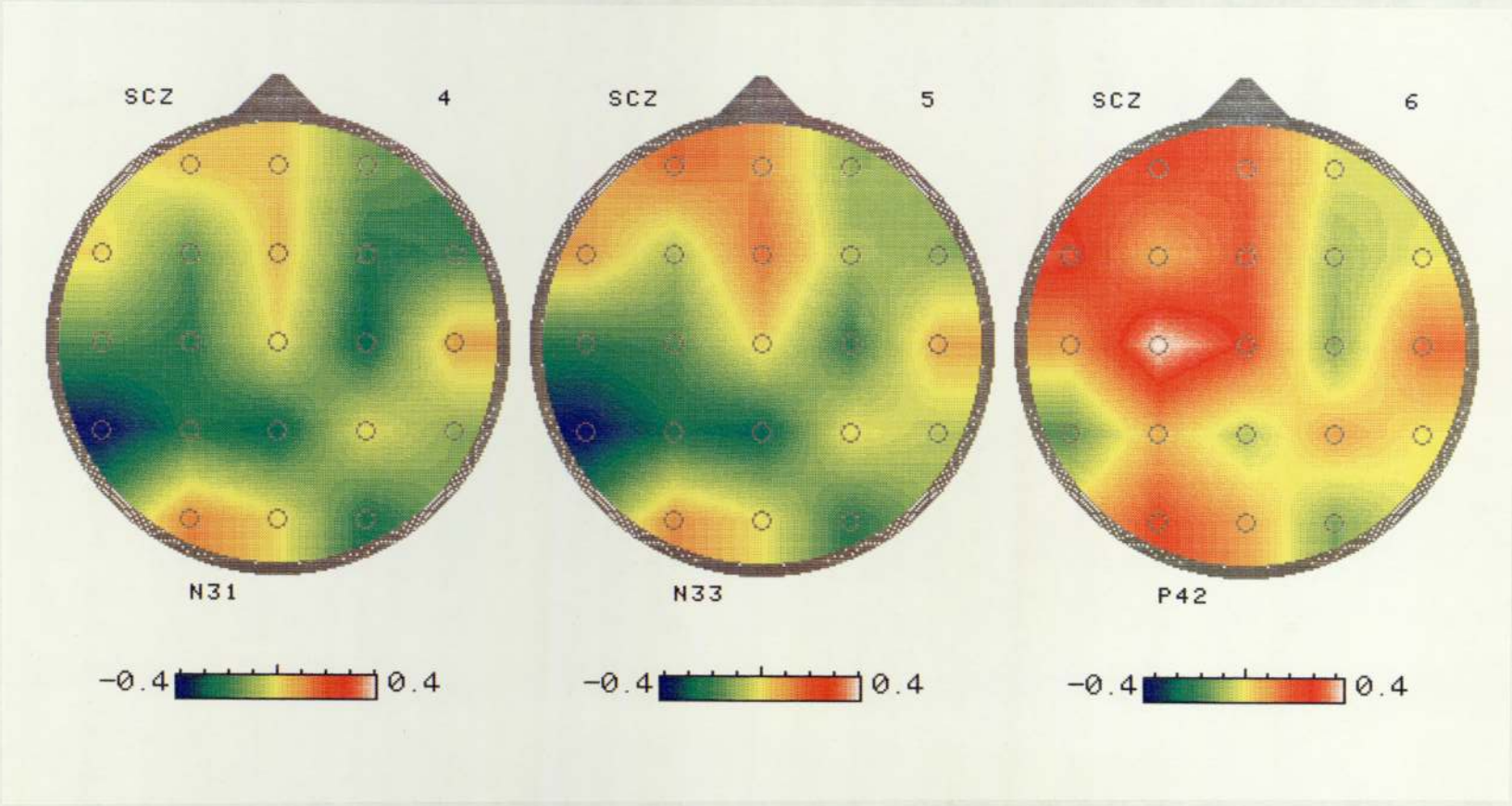
SCZ
4
N31
−0.4
0.4
SCZ
5
N33
−0.4
0.4
SCZ
6
P42
−0.4
0.4

Peak latency (Table 7.1) and peak to peak amplitude data (Figure 7.7) were recorded from the waveforms obtained at electrode sites P3 and P4 for closer comparison with previous studies (Jones and Miller 1981; Cooper et al 1985).

Statistical analysis of peak and peak to peak data was employed. Student t-test revealed no significant differences in any peak latency between patient and control group ($p>0.05$). Additionally, paired t-testing of inter-hemisphere peak latency revealed no significant differences of any parietal component ($p>0.05$).

In both patient and control groups, the post-rolandic contralateral components were always of greater amplitude than their ipsilateral counterparts, with contralateral N20-P27 consistently the highest amplitude component for both groups. Comparison of the two groups was made by t-test of the group peak amplitude means; for both right and left index finger stimulation there was no significant difference in peak amplitudes between groups ($p > 0.05$).In order to provide some objective assessment of the degree of lateralisation for each component, the following measure was used;

$$\frac{\text{(Contralateral amplitude - Ipsilateral amplitude)}}{\text{(Contralateral amplitude + Ipsilateral amplitude)}} \times 100\ \%$$

This formula provided a score which if positive (>0) indicated a degree of contralateral amplitude lateralisation and if negative (<0) then ipsilateral amplitude lateralisation.The mean percentage lateralisation for each component is shown in Figure 7.8.There was no significant difference in lateralisation between the patient and control groups ($p > 0.05$). The mean lateralisation percentages were positive indicating contralateral lateralisation for each component in both patient and controls.

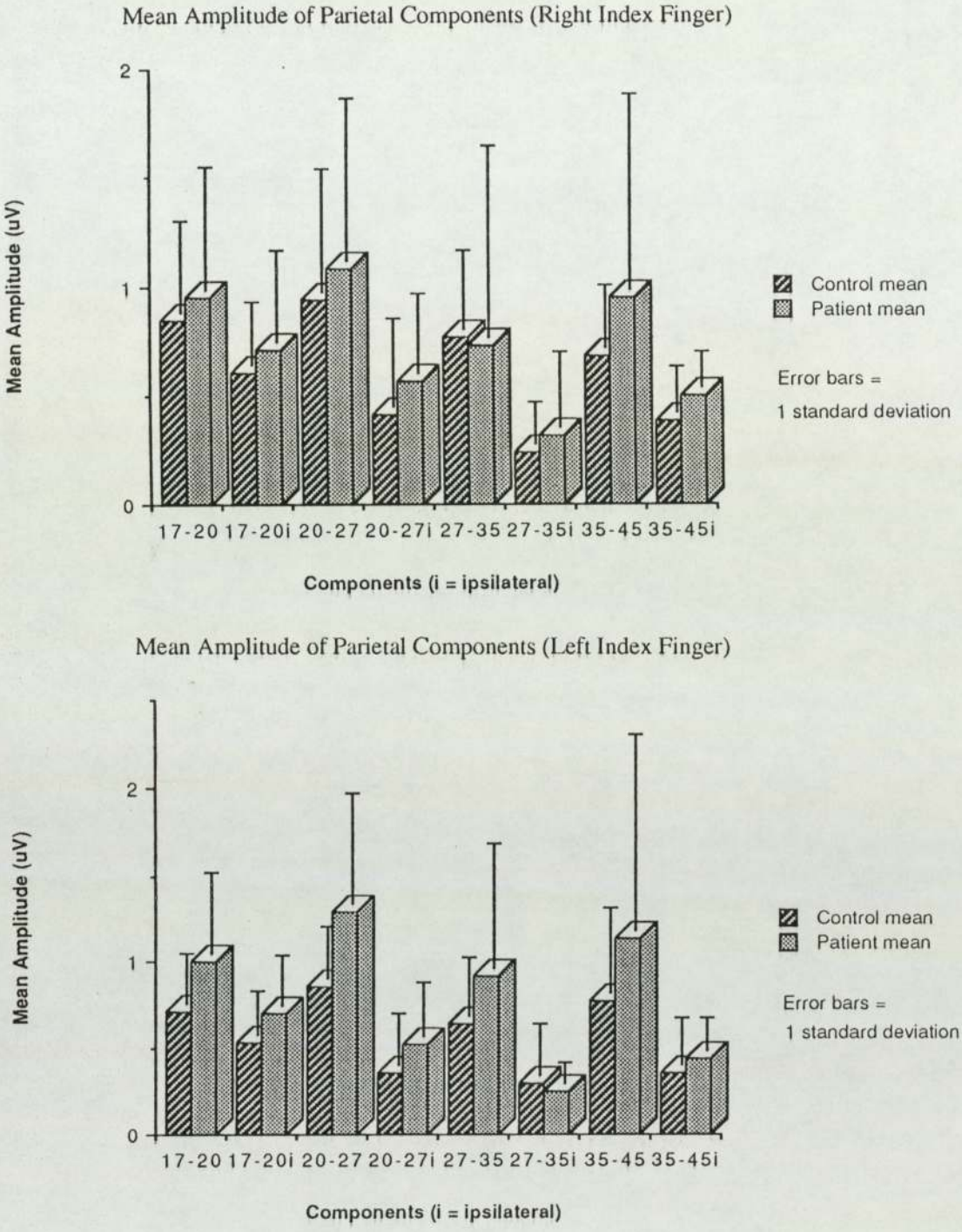

Figure 7.7. Mean peak to peak amplitude data of parietal components to right index (top) and left index (bottom) finger stimulation.

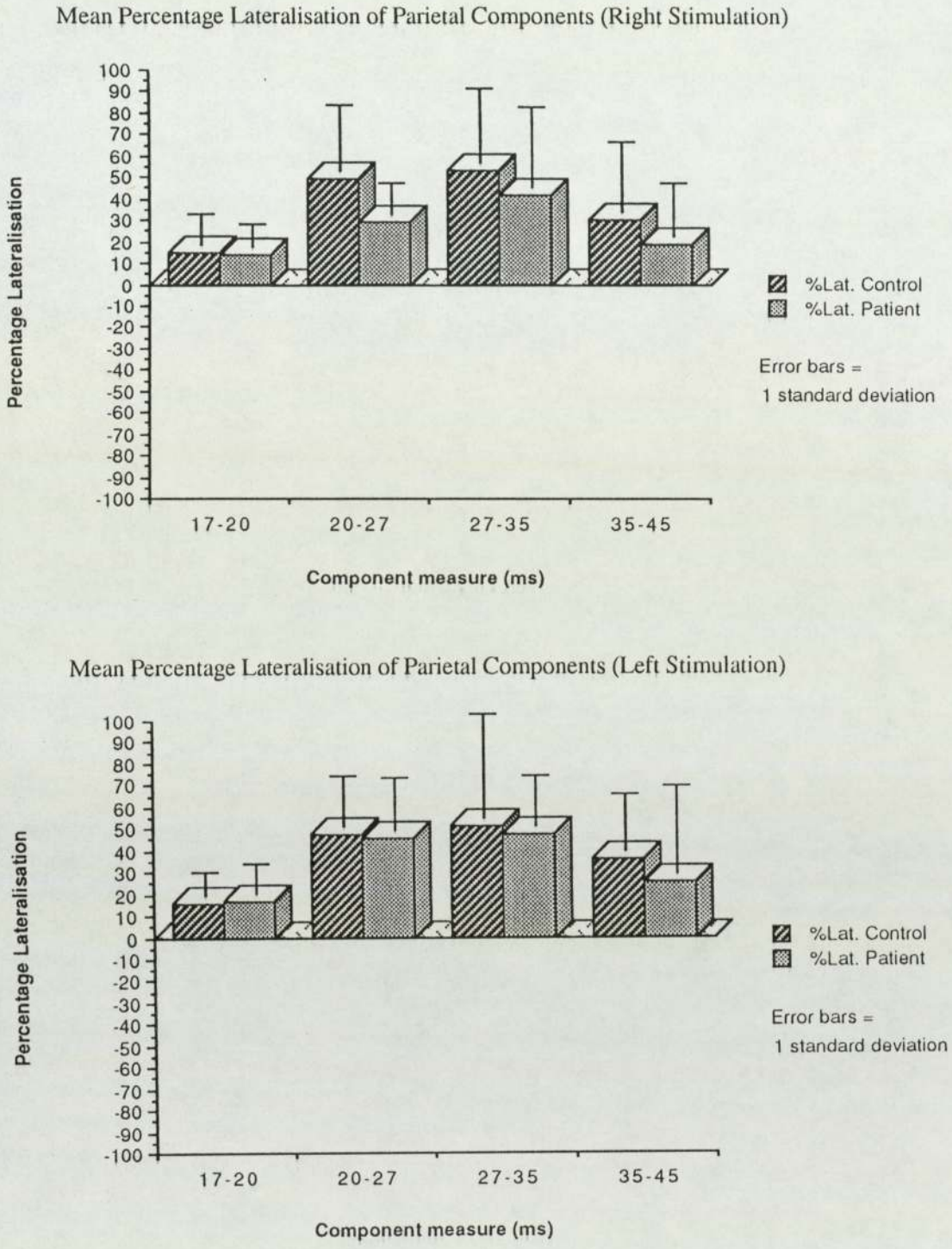

Figure 7.8. Mean percentage lateralisation of parietal components.

At other scalp locations, centro-parietal components (N19-P22-N31-P42) showed similar lateralisation features to those seen parietally in both patient and control groups. At frontal locations, components (N17-P20-N30) were bilaterally distributed in both groups. P14, although not clearly apparent on the group mean averages, was a consistently clear component in both patient and control groups.This component was recognisable in most recordings at every scalp location. These findings are in agreement with previous authors (Goff et al 1977; Kakigi and Shibasaki, 1984; Desmedt and Cheron 1980b; Duff, 1980).

One problem of comparing group mean data is that if an individual patient differed significantly from the control group, this fact may be lost when incorporated into a non-significant larger mean.

To monitor for this, each schizophrenic subject was compared to the group mean control population using the Z-score technique utilizing the Brain Atlas III™ software in the manner of Duffy (1981) as described earlier in earlier Chapters, where;

$$Z = \frac{(x - m)}{s}$$

x= individual subject data, m=control group mean data and s=control group variance. Z is given in standard deviations from the control group.

Each schizophrenic subject produced low Z scores ($Z < 2$ standard deviations) across the entire waveform and at every scalp location with the exception of one subject. Patient SXI produced a waveform which on subjective inspection appeared to be quite bilaterally symmetrical across the entire waveform particularly at parietal locations (Figure 7.9). The subsequent Z score map indicated a statistically significant deviation over the ipsilateral centro-parietal and temporal areas (Figure 7.10). The highest area of deviation however appeared to be the temporal derivations. Re-inspection of the individual waveforms revealed a higher level of EMG artefact in the ipsilateral temporal region than the contralateral (Figure 7.9).

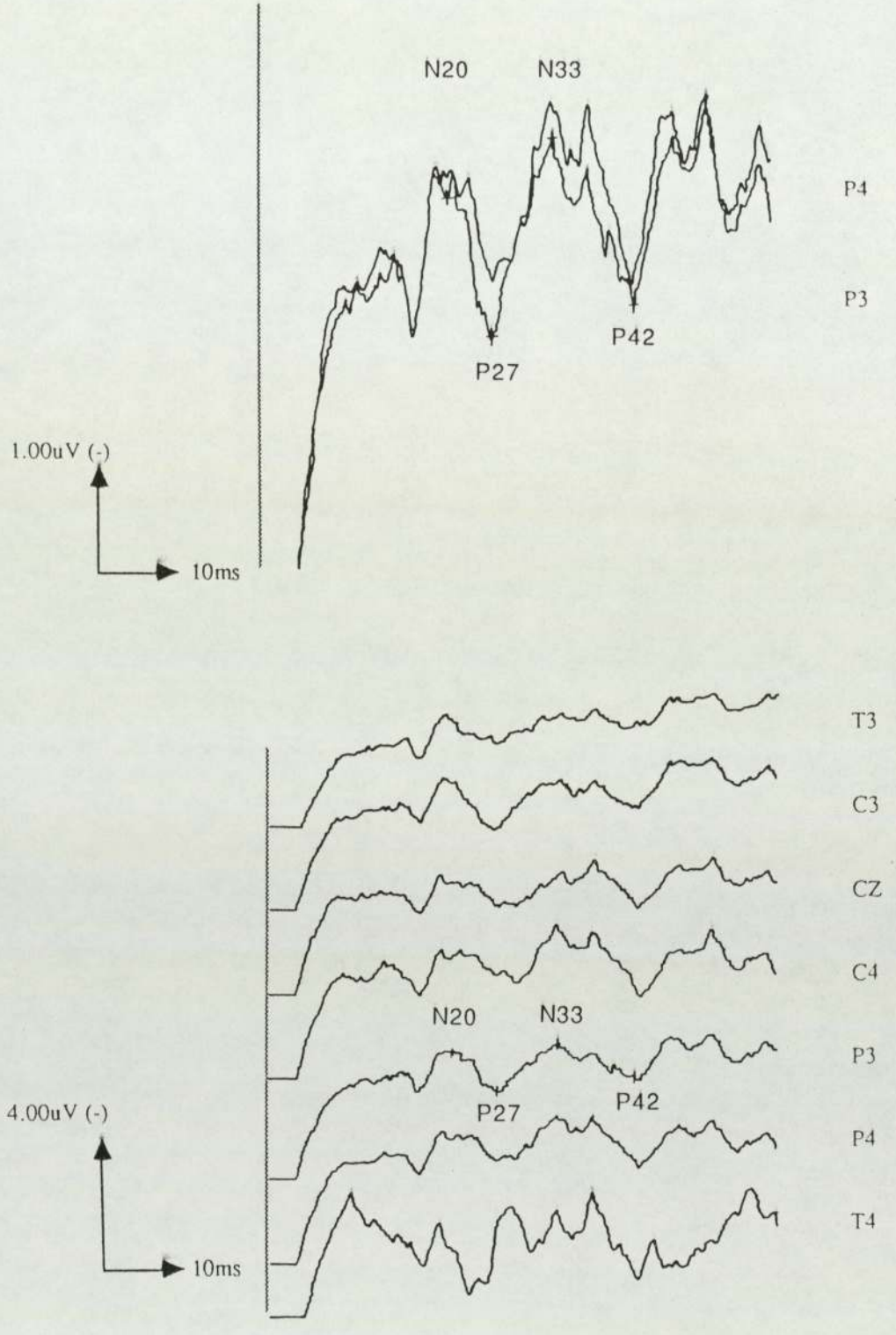

Figure 7.9. Waveforms from patient SXI showing an apparent bilateral lateralisation (top). Inspection of other waveforms reveals right temporal EMG artefact (bottom).

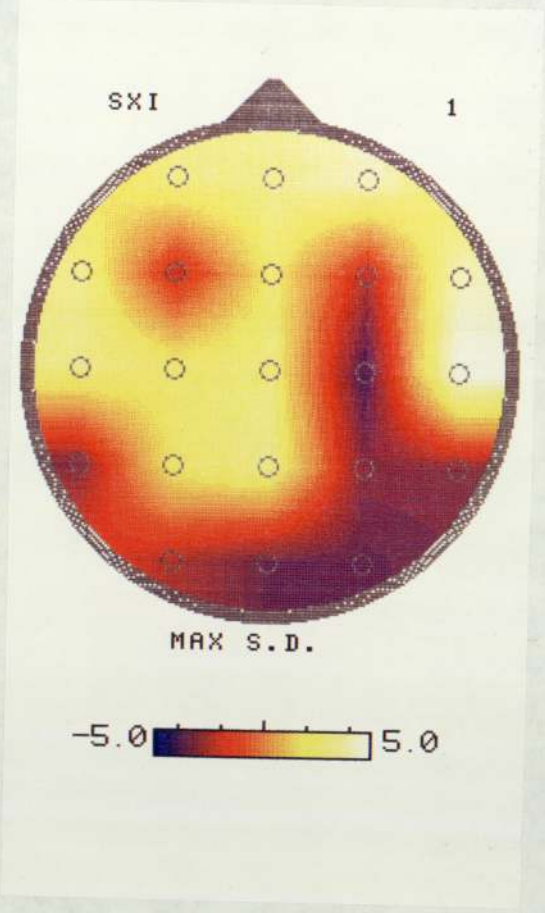

Figure 7.10 Z-score map for patient SXI.

Interpretation of the parietal component amplitudes without the benefit of knowledge of the extent of this asymmetric artefact could produce spurious conclusions. The effect of myogenic enhancement of the components on the ipsilateral hemisphere cannot be excluded (Bickford et al 1964; Calmes and Cracco 1971).

7.4.0. Discussion and Conclusion

The results of this study are summarised as follows:

1. There was no significant difference in either amplitude or morphology between the traces obtained from the control and patient group recorded from 20 scalp locations.
2. There was no significant difference in peak latency comparing patient to control group, ipsilateral and contralateral latencies for right and left index finger stimulation.
3. The mean peak-to-peak amplitudes for parietal components,were always greater for contralateral components compared to the ipsilateral counterpart.
4. The percentage lateralisation quotient, showed no lateralisation differences between the subject and control groups.
5. When the data for, each schizophrenic patient was compared to the control group data , no differences were found except in one case of asymmetric temporal EMG artefact.

Although the present study obtained adequate recordings of the somatosensory evoked potentials using a conventional digital nerve stimulus, it failed to replicate the findings of Cooper et al.; that of a loss of lateralisation in a sub-group of schizophrenics. It should be noted that the dominant components of Cooper's waveforms were positivities at approximately 30 msec and 45 msec which would equate well to the two dominant components obtained in this study, namely P27 and P45.

Cooper et al tentatively hypothesised that their findings arose from abnormality in the corpus callosum. It has been established, however, that there are no direct callosal connections between the primary somatosensory hand areas in monkeys (Jones and Powell 1969). Supporting evidence for this in man is provided by magnetic recordings to transcutaneous stimulation of the median nerve (Okada 1984), which have revealed no ipsilateral components. Regional cerebral blood flow studies (Foit et al 1980) also have failed to reveal any ipsilateral components. This suggests that ipsilateral electrical components are volume conducted from the contralateral hemisphere. This is further supported by our lack of significant latency difference between ipsilateral and contralateral components .

An abnormality of the corpus callosum would not then allow one to predict that there would be a loss of lateralisation in the somatosensory evoked potential and our findings are therefore not surprising. It is disappointing that the present study was not able to confirm the presence of a neurophysiological marker of schizophrenia, as described by Cooper et al.

It does however raise a note of caution to experimenters examining lateralising events or topographical data generally, that careful monitoring of EMG must be undertaken as well. Unfortunately recordings from the temporal region were not carried out during the study by Cooper et al., so the question as to whether myogenic activity in the temporal region produced an apparently abnormal result of their schizophrenic group, has to remain unanswered.

CHAPTER 8

SUMMARY AND CONCLUSIONS ON THE VALUE OF THE SEP USING BRAINMAPPING TECHNIQUES

8.1.0. Introduction

'As the"average" neurologist attempts to determine the legitimacy of these highly technical devices, he or she is confronted with a barrage of information including, on the one hand, exaggerated criticisms by self-proclaimed experts, many of whom have had little first-hand experience with these methods. It is difficult to discern fact from fantasy.'

Duffy F.H. Clinical value of topographic mapping and quantified Neurophysiology.

Arch. Neurol., 1989, 46, 1133-1134.

'Little research has been published on how these tests could have an impact on the treatment of individual patients. Such scientific studies ought to show that these tests offer something valuable not readily available through standard history, physical examination, and ordinary medical testing that would have been done anyway, such as magnetic resonance imaging or routine EEG.'

Nuwer M.R. Uses and abuses of brain mapping.

Arch. Neurol., 1989, 46, 1134-1136.

The two statements above were the background against which this thesis was undertaken. The question as to whether topographical techniques, colour contour mapping and statistical mapping techniques genuinely contributed to conventional recording methods used in the clinic were begging an answer. The following sections summarize the observations that were made.

8.2.0 SEP and clinical correlation

Examination of the literature reveals that no component of the SEP appears to be specific to Group Ia afferents, though the strongest correlations exist between SEP changes and alteration of joint position sense (Halliday and Wakefield 1963; Giblin 1964; Bergamini et al 1966; Larson et al 1966). Indeed, it seems clear that the integrity of the dorsal column pathways that mediate proprioception are essential for the generation of the scalp recorded SEP's.

Patients with cortical lesions typically present with SEP's whose onset is either equal to control or only slightly increased, while changes in amplitude or duration of cortical SEP components can be rather marked (Noël and Desmedt 1980; Mauguière et al 1982). SEP's in this type of patient were reduced in amplitude or eliminated and generally with good correlation between the severity of symptoms and the degree of SEP abnormality if the degree of loss of joint position sense was used as a criterion (Williamson et al 1970).

Data from this thesis is generally supportive of these observation in that If one examines the type of sensory loss in relation to SEP results (Chapter 5) one observes that 5 patients with abnormal SEP's presented with impairment of joint position sense - only one patient (P9) with preserved joint position sense (but impaired touch/vibration sense) produced abnormal SEP's. Patient P7 presented with similar symptomatology to patient P9 but produced normal SEP findings.

Observations relating to the most affected components were that in the 8 patients with abnormal SEP's (and one borderline case, P1), in only one case of discrete component change was a component earlier than P22 implicated. This was in patient P5 where a prolonged N19 component was observed. On this basis it is worth reporting that, of the abnormalities recorded, the P22-N31 complex was abnormal in four patients, the N33-P42 complex in 3 patients and an abnormality of P27 in two.

In some circumstances it was difficult to discern whether a component was delayed or is in fact absent; topographic analysis may be helpful in making this interpretation. An example of this

was seen with patient P9 in Chapter 5. This patient, presenting with a large right tempero-parietal infarct producing left sided weakness and sensory loss, produced a number of left median/right hemisphere SEP abnormalities. It was tempting to describe these abnormalities as loss of the central P22 -N31-P42 and parietal N33-P42 complexes as well as the concomitant frontal P35-N43 complex. It may be possible that the 'lost' central components were 'replaced' by forward volume conduction of the parietal P27 component. This was a more seductive argument than interpreting the abnormal P22 latency asymmetry as simply delay of the right hemisphere component since the right hemisphere P22 presented with the identical latency and morphology to the parietal P27 which was not itself abnormally prolonged.

8.3.0. Generators

Important conclusions from SEP studies on patients with cortical lesions have been:

1) Provided evidence that there are multiple generator sites involved in the formation of postcentral and precentrally recorded potentials (Mauguière et al 1983).

2) An abnormality could manifest itself as a dissociated augmentation of discrete components as well as an attenuation or elimination. Augmentation of components has been reported in patients whose lesions were in close proximity to the primary somatomotor cortex and also in those whose lesions were remote from this area (Obeso et al 1980; Stejskal et al 1985).

Data from this thesis contributes to this current knowledge in two ways; firstly two patients with discrete cortical lesions leading to focal epileptic episodes (P3 and P10) resulted in the augmentation of discrete cortical potentials - not only augmentation compared to the opposite hemisphere as described by Mauguière, but 'giant' potentials compared to a control group. The second most important aspect of these observations was that the one component involved in each case was the peri-rolandic P22 component which has been subject to much debate in recent literature. In patient P3, the P22 -N31 complex was greatly augmented compared to both the contralateral hemisphere of the patient and also in comparison to the

control group. The fact that this phenomenon co-existed with attenuation of all other parietal and frontal components in the affected hemisphere provided convincing evidence that the P22-N31 complex has separate generators than those responsible for the N20-P27-N33 components parietally and P20-N30 components frontally.

Although Mauguière et al (1983) described augmentation of a pre-frontal P22-N30 complex, they did not differentiate between a frontal P20-N30 complex and a peri-rolandic P22-N31 complex. The differential affect of lesions on these components seen in our study therefore provides important evidence that these are discrete and, in part at least, independent components.

It is clear therefore that the P22 and N31 components are important measures to examine in cases of lesions affecting the primary somatosensory/somatomotor cortex. Furthermore, topographic maps of patients with augmented P22-N31 complexes further supports the hypothesis of the essential radial orientation of the generators of these components.

In this study, augmentation of components was only seen with lesions in close proximity to the primary somatosensory/somatomotor (PSMA) cortical areas.

Desmedt and Cheron (1980) had proposed the hypothesis that some SEP changes seen in octogenarians reflected differential neuronal loss across the cortex. As was seen from the study described Chapter 4, there was an interesting morphological and topographical difference of frontal components seen between an old age grouping and a young age grouping. This difference was essentially that a frontal N43 component was commonly seen in the old age group replacing the frontal P42 component commonly seen in the young.

It seems most relevant to note therefore that in two patients, P42 and N43 components were observed in opposite hemispheres, a situation that did not occur in any control individual. N43 was observed in a young female patient (P5) in the same hemisphere where a centro-parietal lesion had caused a significant delay in the peak latency of N19. A frontal P42 was seen in the unaffected hemisphere. In patient P8, both right and left hemisphere lesions were detected,

but a frontal N43 was observed with a right frontal lobe infarction and a frontal P42 was observed in the left hemisphere where a parietal haematoma was seen.

A final relevant observation was that in patient P10 in whom giant central P22 and parietal P27 components were observed, the ensuing P42 components at these locations were of closely similar amplitude to those recorded in the preserved hemisphere.

These findings lead one to speculate as to whether P42 is generated by both pre and post central generators and indeed by generators other than those responsible for P22 and P27 complexes. The presence of a frontal N43 component would be consistent with either a degree of neuronal loss in the frontal lobe or loss of direct input via cortico-cortical relay mechanisms to the frontal lobe.

8.4.0. Statistical Mapping

Oken and Chiappa (1986) stated that 'It is important to differentiate between (1) the ability of a statistical method to classify a patient whose diagnosis is uncertain into either a normal or a specific disease group and (2) an analysis that shows statistically significant differences between two groups, such as normal controls and patients with verifiable disease. The latter analysis is generally helpful only in understanding the pathophysiological characteristics of the disease, whereas the former ability is critical to the clinical utility of a test.

To be substantiated as useful, a newly proposed clinical test that classifies patients into either a normal or diseased state must be evaluated by its false-positive and false negative rates, and by comparison with other available diagnostic tests.'

Data from this thesis showed that statistical mapping correlated well with SEP topographical data in 64% of cases, failed to reflect an SEP abnormality in 27% of cases and yielded a false positive in 9%. From this point of view, the statistical mapping was of interest in relation to comparison of patients with verifiable disease to control individuals. The performance of the technique in classification of patients with unknown diagnoses into control or disease state was not assessed in this thesis but is an important study to be done. However it must be

stated that the optimum database would be one containing 30 control individuals for each decade of life (for an adult population) and be normally distributed for both age and height. The database employed in this thesis contained 35 control individuals covering 8 decades.

Duffy (1982) stated that 'It should be emphasised that the Z or t-statistic SPM are intended to localize regional differences and are not intended to be optimal measures of overall level of group or individual difference. Overall significance is best assessed by multivariate statistical techniques.' This is an important observation and supports the view that the value of Z transform data should not be overstated or overestimated by technologist or clinician.

The conclusions from this thesis in relation to mapping techniques and the detection of cortical lesions therefore are that; 1. Topographic studies of the scalp recorded SEP increase the detection rate of cortical lesions affecting the PSMA over conventional single channel Fz reference derived recordings.

2. The value of the control database for statistical mapping in the detection of cortical lesions in its current form is low.

8.5.0. Montages

The sagittal polar projection employed in this study provided a system that was both easy to employ and whose points could easily and effectively be communicated. The 10% spread of electrodes provided optimum cover of all important components without extending too far over the scalp and thus incurring measurement distortion due to excessive curvature of the skull. The proportionality of measurements employed allowed for group mean data to be acquired.

Desmedt et al (1987) made a number of observations relating to the number and location of scalp electrodes:-

1. The number of channels should not exceed a manageable set (like the 21 or so in standard EEG) otherwise the time taken to set up and maintain adequate recording conditions becomes excessive.

2. Both hemispheres should be recorded concomitantly to image EP fields that extend across the midline and recording one hemisphere at a time is not sufficient.

3. For imaging the peak values of any potential field, an electrode must be near the field of culmination since electrodes around that focal site only record smaller potentials.

Whilst I concur with statements 1 and 3 above, there are difficulties in deciding upon a whole of scalp montage employing only a moderate number of electrodes that adequately reflects the topography of all components. Data from the study detailed in Chapter 6 concurred with the observation that the central coronal plane was critical for recording the pericentral P22 and N31 components. However, this study also indicated that a shift of 10% pre-centrally may result in the failure to adequately record these components in some individuals and therefore cannot support the recommendation by Desmedt et al (1987) for the need to shift the central coronal plane for SEP recordings. It would appear desirable however to illicit recordings from 10% intervals around the central C3/C4 electrode locations to accurately reflect the activity of the peri-rolandic potentials. This latter argument is supported by the work of Spitzer et al (1989) who employed closely spaced coronal and sagittal rows of electrodes to record the SEP. They proposed that the optimum interelectrode distance for SEP recordings should be 3cm or less. They concluded that the use of larger interelectrode recording distances such as employed in the 10-20 system of electrode placement, and where linear interpolation techniques were used could result in erroneous amplitude, location and contour results of potentials. This would be particularly true for focal components such as P22.

Given these observations it would appear desirable to target the appropriate montage according to the purpose for which the SEP is intended. If the aim is the detection of cortical lesions for example, then a whole of scalp montage is desirable and the conventional 10-20 montage adequate. Close analysis of spatio-temporal properties of individual components, particularly for research purposes may require a localised montage to be employed.

8.6.0. Conclusion

In conclusion, I would like to include this statement from a recent article:-

'Interestingly, there appear to be no studies to demonstrate what brain mapping adds to the diagnosis in an individual patient, nor indeed whether the increased information and misinformation from brain mapping is clinically better or worse than that from the stark but familiar, standard electroencephalogram.

One cannot but welcome advances in harnessing, quantification, and visual display of brain activity, but the burden of proof of the clinical usefulness of brain mapping remains with those who would make diagnosis more elaborate, complex, or costly.'

Hachinski Vladimir. Brain Mapping.

Arch.Neurol., 1989, 36, 1136.

One hopes that this thesis has taken one step in the direction towards lightening the burden.

REFERENCES

ABBRUZZESE G., ABBRUZZESE M., FAVALI E., IVALDI M., LEANDRI M. AND RATTO S. The effects of hand muscle vibration on the somatosensory evoked potential in man: an interaction between lemniscal and spino-cerebellar inputs?
*J.Neurol.Neurosurg.Psychiat., 1980, **43**, 433-437.*

ALBE-FESSARD D., TASKER R., YAMASHIRO K., CHODAKIEWITZ J. AND DOSTROVSKY J. Comparison in man of short latency averaged evoked potentials recorded in thalamic and scalp hand zones of representation.
*Electroenceph.clin.Neurophysiol., 1986, **65**, 405-415.*

ALLISON T. Recovery functions of somatosensory evoked responses in man.
*Electroenceph.clin.Neurophysiol., 1962, **14**, 331.*

ALLISON T. Scalp and cortical recordings of initial somatosensory cortex activity to median nerve stimulation in man.
*Ann. NY. Acad. Sci .,1982 ,**388**, 671-679*

ALLISON T., GOFF W.R., WILLIAMSON P.D. AND VAN GILDER J.C. On the neural origin of early components of the human somatosensory evoked potential.
*In: J.E. Desmedt (Ed.), Clinical Uses Cerebral, Brainstem and Spinal Somatosensory Evoked Potentials, Progr. Clin. Neurophysiol., **Vol. 7**, Karger, Basel 1980: 51-68.*

ALLISON T., HUME A.L., WOOD C.C., AND GOFF W.R. Developmental and aging changes in somatosensory, auditory and visual evoked potentials.
*Electroenceph.clin.Neurophysiol., 1984, **58**, 14-24.*

ALLISON T., WOOD C.C. AND GOFF W.R. Brain Stem Auditory, Pattern Reversal Visual and Short-Latency somatosensory evoked potentials: Latencies in relation to age, sex and brain and body size.
*Electroenceph.clin.Neurophysiol., 1983, **55**, 619-636*

AMINOFF M.J., DAVIS S.L., PANITCH H.S. Serial evoked potential studies in patients with definate multiple sclerosis.
*Arch. Neurol., 1984, **41**, 1197-1202.*

ANGEL R.W., QUICK W.M., CURTIS-BOYLLS C., WEINRICH M., AND RODNITZKY R.L. Decrement of somatosensory evoked potentials during repetitive stimulation.
*Electroenceph.clin.Neurophysiol., 1985, **60**, 335-342.*

ANZISKA B AND CRACCO R.Q. Short latency somatosensory evoked potentials: studies in patients with focal neurological disease.
*Electroenceph.clin.Neurophysiol., 1980, **49**, 227-239.*

AREZZO J.C., VAUGHAN H.G. AND LEGATT A.D. Topography and intracranial sources of somatosensory evoked potentials in the monkey. II. Cortical components.
*Electroenceph.clin.Neurophysiol., 1981, **51**, 1-18.*

ARY J.P., DARCEY T.M. AND FENDER D.H. A method for locating scalp electrodes in spherical coordinates.
IEEE Trans.Biomed.Eng., 1981, BME-28, 834-836.

DUSSER DE BARENNE J.G. Corticalisation of function and functional localisation in cerebral cortex.
*Archs. Neurol.Psychiat.,1933, Chicago, **30**, 884-901.*

BARTEL D.R., MARKAND O.N. AND KOLAR O.J. The diagnosis and classification of mutiple sclerosis: Evoked responses and spinal fluid electrophoresis.
*Neurol., 1983, **33**, 611-617.*

BICKFORD R.G., JACOBSON J.L. AND CODY D.T.R. Nature of Average Evoked Potentials to sound and other stimuli in man.
*Ann. N.Y. Acad. Sci., 1964, **112**, 204-223.*

BINNIE C.D., DEKKER E., SMITH A. AND VAN DER LINDEN G. Practical considerations in the positioning of EEG electrodes.
*Electroenceph.clin.Neurophysiol., 1982, **53**, 453-458.*

BLUME W.T., BUZA R.C. AND OKAZAKI H. Anatomic correlates of the 10-20 electrode placement system in infants.
*Electroenceph.clin.Neurophysiol., 1974, **36**, 303-307.*

BOURNE J.R., CHILDERS D.G. AND PERRY N.W. Topological characteristics of the visual evoked response in man.
*Electroenceph.clin.Neurophysiol., 1981, **30**, 423-436.*

BRAZIER M.A.B. The electrical fields at the surface of the head during sleep.
*Electroenceph.clin.Neurophysiol., 1949, **1**, 195-204.*

BRODY H. Structural changes in the aging nervous system.
*Interdisc.Top.Gerontol., 1970, **7**, 9-21.*

BROUGHTON R.J. Averaged Evoked Potentials.
E.Donchin & D.B.Lindsley (Eds.), 1969, 79-84.

BROUGHTON R.J., RASMUSSEN T. AND BRANCH C. Scalp and direct cortical recordings of somatosensory evoked potentials in man.
*Canad.J.Psychol., 1981, **35**, 136-158.*

BUCHSBAUM M.S., RIGAL F., COPPOLA R., CAPPELLETTI J., KING C. AND JOHNSON J. A new system for grey-level surface distribution maps of electrical activity.
*Electroenceph.clin.Neurophysiol., 1982, **53**, 237-242.*

BURKE D., GANDEVIA S., MCKEON B. AND SKUSE N.F. Interactions between cutaneous and muscle afferent projections to cerebral cortex in man.
*Electroenceph.clin.Neurophysiol., 1982, **53**, 349-360.*

BURGESS P.R. AND CLARK F.J. Characteristics of knee joint receptors in the cat.
*J.Physiol. (Lond.), **203**, 317-335.*

BYSTRZYCKA E., NAIL B.S. AND ROWE M. Inhibition of cuneate neurones: its afferent source and influence on dynamically sensitive 'tactile' neurones.
*J. Physiol. (Lond.), 1977, **268**, 251-270.*

CALMES R.L. AND CRACCO R.Q. Comparison of somatosensory and somatomotor evoked responses to median nerve and digital nerve stimulation.
*Electroenceph.clin.Neurophysiol., 1971, **31**, 547-562.*

CELESIA G.C.. Somatosensory evoked potentials recorded directly from human thalamus and Sml cortical area.
*Arch Neurol., 1979, **36**, 399-405*

CHIAPPA K.H. Pattern shift visual, brainstem auditory and short-latency somatosensory evoked potentials in multiple sclerosis.
*Neurology, 1980, **30**, 110-123.*

CHIAPPA K.H. Evoked potentials in Clinical Medicine.
Raven Press, New York, 1983.

CHIAPPA K.H., CHOI S.K. AND YOUNG R.R. Short latency somatosensory evoked potentials following median nerve stimulation in patients with neurological lesions.
*In: J.E. Desmedt (Ed.), Clinical Uses Cerebral, Brainstem and Spinal Somatosensory Evoked Potentials, Progr. Clin. Neurophysiol., **Vol. 7**, Karger, Basel 1980: 264-281.*

COHEN L.G. AND HALLETT M. Methodology for non-invasive mapping of human motor cortex with electrical stimulation.
*Electroenceph.clin.Neurophysiol., 1988, **69**, 403-411.*

COHEN L.G. AND HALLETT M. Noninvasive mapping of human motor cortex.
*Neurology, 1988, **38**, 904-909.*

COHEN L.G. AND STARR A. Vibration and muscle contraction affect somatosensory evoked potentials.
*Neurology (1985), **35**, 691-698.*

CONNOLLY J.F. The corpus callosum and brain function in schizophrenia.
*Correspondence Brit. J. Psychiat., 1982,**140**, 429-30.*

COOPER J.E., ANDREWS H. AND BARBER C. Stable abnormalities in the lateralisation of early cortical somatosensory evoked potentials in schizophrenic patients.
*Brit. J. Psychiat., 1985, **146**, 585-593.*

COPPOLA R. Topographic methods of fuctional cerebral analysis. In: A.R. Potvin and J.H. Potvin (Eds.), Frontiers of Engineering in Health Care. IEEE Press, New York, 1982: 71-78.

COPPOLA R., BUCHSBAUM M.S., RIGAL F. Computer generation of surface distribution maps of measures of brain activity.
*Comp. Biol. Med., 1982, **12**, 191-199.*

CRACCO R.Q. Travelling waves of the human scalp-recorded somatosensory evoked response.
*Electroenceph.clin.Neurophysiol., 1976 , **33**, 557-566.*

CRACCO R.Q., AND CRACCO J.B. Somatosensory evoked potentials in man: far field potentials.
*Electroenceph.clin.Neurophysiol., 1976 ,**41**, 460.*

DAWSON G.D. Cerebral responses to electrical stimulation of peripheral nerve in man.
*J. Neurol. Neurosurg. Psych., 1947, **10**,134.*

DAWSON G.D. The relative excitability and conduction velocity of sensory and motor nerve fibres in man.
*J.Physiol., **131**, 436.*

DEBECKER J. AND DESMEDT J.E. Les potentiels évoqués cérébraux et les potentiels de nerf sensible chez l'homme.
*Acta. Neurol. Belg., **64**, 1212.*

DEIBER M.P., GIARD M.H. AND MAUGIERE F. Seperate generators with distinct orientations for N20 and P22 somatosensory evoked potentials to finger stimulation?
*Electroenceph.clin.Neurophysiol., 1986, **65**, 321-334.*

DESMEDT J.E. AND BOURGUET M. Color imaging of parietal and frontal somatosensory potential fields evoked by stimulation of median or posterior tibial nerve in man.
*Electroenceph.clin.Neurophysiol., 1985, **62**, 1-17*

DESMEDT J.E. AND BRUNKO. Functional organisation of the far-field and cortical components of somatosensory evoked potentials in normal adults.
*In: J.E. Desmedt (Ed.), Clinical Uses Cerebral, Brainstem and Spinal Somatosensory Evoked Potentials, Progr. Clin. Neurophysiol., **Vol. 7**, Karger, Basel 1980: 264-281.*

DESMEDT J.E. AND CHERON G. Central somatosensory conduction in man: Neural generators and interpeak latencies of the far-field components recorded from neck and right or left scalp and earlobes.
*Electroenceph.clin.Neurophysiol., 1980, **50**, 382-403.*

DESMEDT J.E. AND CHERON G. Somatosensory evoked potentials to finger stimulation in healthy octogenarians and in young adults: Wave forms, scalp topography and transit times of parietal and frontal components.
*Electroenceph.clin.Neurophysiol., 1980b, **50**,404-425.*

DESMEDT J.E. AND CHERON G. Prevertebral (oesophageal) recording of subcortical somatosensory evoked potentials in man: the spinal P13 component and the dual nature of the spinal generators.
*Electroenceph.clin.Neurophysiol., 1981, **52**, 257-275.*

DESMEDT J.E. AND CHERON G. Non-cephalic reference recording of early somatosensory potentials to finger stimulation in adult or aging normal man: differentiation of widespread N18 and contalateral N20 from the prerolandic P22 and N30 components.
*Electroenceph.clin.Neurophysiol., 1981, **52**, 553-570.*

DESMEDT J.E., DEBECKER J. AND MANIL J. Mise en évidence d'une signe électrique cérébral associé à la détection par la sujet d'un stimulus sensoriel tactile.
*Bull. Acad. Roy.Med. Belg., 1965, **5**, 887.*

DESMEDT J.E. AND HUY N.T. Bit-mapped colour imaging of the potential fields of propagated and segmental subcortical components of somatosensory evoked potentials in man.
*Electroenceph.clin.Neurophysiol., 1984, **58**, 481-497.*

DESMEDT J.E., HUY N.T. AND BOURGUET M. The cognitive P40, N60 and P100 components of somatosensory evoked potentials and the earliest electrical signs of sensory processing in man.
*Electroenceph.clin.Neurophysiol., 1983, **56**, 272-282*

DESMEDT J.E., HUY N.T. AND BOURGUET M. Bit-mapped imaging of human evoked potentials with reference to the N20,P22,P27 and N30 somatosensory responses.
*Electroenceph.clin.Neurophysiol., 1987, **68**, 1-19.*

DESMEDT J.E. AND HUY N.T. Bit-Mapped colour imaging of the potential fields of propagated and segmental subcortical components of somatosensory evoked potentials in man.
*Electroenceph.clin.Neurophysiol., 1984, **58**, 481-497*

DESMEDT J.E., HUY N.T. AND BOURGUET M. The cognitive P40, N60 and P100 components of somatosensory evoked potentials and the earliest electrical signs of sensory processing in man.
*Electroenceph.clin.Neurophysiol., 1983, **56**, 272-282.*

DESMEDT J.E. AND ROBERTSON D. Differential enhancementnof early and late components of the cerebral somatosensory evoked potential during forced paced cognitive tasks in man.
*J. Physiol., **271**, 761-782.*

DOMINO E.F., MATSUOKA S., WALTZ J AND COOPER I.S. Effects of cryogenic thalamic lesions in the somesthetic evoked response in man.
*Electroenceph.clin.Neurophysiol., 1965,**19**, 127.*

DRASDO N. AND FURLONG P.. Coordinate sysyems for evoked potential topography.
*Electroenceph.clin.Neurophysiol., 1988, **71**, 469-473.*

DUFF T.A.. Topography of scalp recorded potentials evoked by stimulation of the digits.
*Electroenceph.clin.Neurophysiol., 1980, **49**, 452-460.*

DUFFY F.H, BURCHFIELD J.L. AND LOMBROSO C.T. Brain electrical activity mapping (BEAM): a method for extending the clinical utility of EEG and evoked potential data.
*Ann. Neurol., 1979, **5**, 309-321.*

DUFFY F.H., BARTELS P.H. AND BURCHFIEL J.L. Significance probability mapping: an aid in the topographic analysis of brain electrical activity.
*Electroenceph.clin.Neurophysiol., 1981, **51**: 455-462.*

DUFFY F.H. Topographic display of evoked potentials: Clinical applications of brain electrical activity mapping (BEAM)
*N.Y.Acad.Sci., 1982, **388**, 183-196*

DUFFY F.H. Clinical value of topographic mapping and quantified Neurophysiology.
*Arch. Neurol., 1989, **46**, 1133-1134.*

ESTRIN T. AND UZGALIS R. Computerized display of spatio-temporal EEG patterns.
IEEE Trans. Biomed. Eng., 1969, BME-16, 192-196.

FENWICK P., BRENNA D. AND PHILPOT M. Correspondence.
*Brit. J. Psychiat.,1983, **143**, 524.*

FOIT A., LARSEN B., HATTORI S., SKINHØJ E. AND LASSEN N.A.. Cortical activation during somatosensory stimulation and voluntary movement in man: a regional cerebral blood flow study.
*Electroenceph.clin.Neurophysiol., 1980, **50**, 426-436*

FOX P.T., BURTON H. AND RAICHLE M.E. Mapping human somatosensory cortex with positron emission tomography.
*J. Neurosurg., 1987, **67**, 34-43.*

GARDNER E.P., HÄMÄLÄINEN H.A., WARREN S., DAVIS J. AND YOUNG W. Somatosensory evoked potentials and cortical single unit responses elicited by mechanical tactile stimuli in awake monkeys.
*Electroenceph.clin.Neurophysiol., 1984, **58**, 537-552*

GANDEVIA S.C. AND BURKE D. Projection to the cerebral cortex from proximal and distal muscles in the human upper limb.
*Brain, 1988, **111**, 389-403.*

GANES T. A study of peripheral, cervical and cortical evoked potentials and afferent conduction times in the somatosensory pathway.
*Electroenceph.clin.Neurophysiol., 1980, **49**, 446-451.*

GEVINS A.S. The use of brain electrical potentials (BEP) to study the localization of human brain function.
*Int. J. Neurosci., 1981, **13**(1), 27-41.*

GIBLIN D.R. Somatosensory evoked potentials in healthy subjects and in patients with lesions of the nervous system.
Ann. N.Y. Acad. Sci.,1964, ***112****, 93.*

GIBLIN D.R. Scalp recorded somatosensory evoked potentials.
In: Electrodiagnosis in Clinical Neurology. (Aminoff M.J. Ed.) Churchill Livingstone 1980, 414-450.

GILMAN S AND NEWMAN S.W. Essentials of Clinical Neuroanatomy and Neurophysiology. Edition 7, F.A. Davis Company (Philedelphia) 1987.

GOLDRING S. AND RATCHESON R. Human motor cortex: Sensory input data from single neuron recordings.
Science, 1972, ***175****, 1493-1495.*

GOFF G.D., MATSUMIYA Y., ALLISON T. AND GOFF W.R. The scalp topography of human Somatosensory and Auditory Evoked Potentials.
Electroenceph.clin.Neurophysiol., 1977, ***42****, 57-76.*

GREEN J.B., NELSON A.V., AND MICHAEL D. Digital zero-phase shift filtering of short latency somatosensory evoked potentials.
Electroenceph.clin.Neurophysiol., 1986, ***63****, 384-388.*

GOFF W.R., ROSNER B.S. AND ALLISON T. Distribution of cerebral somatosensory evoked responses in normal man.
Electroenceph.clin.Neurophysiol., 1962, ***14****, 697.*

GREEN J.B. AND WALCOFF M.R. Evoked potentials in multiple sclerosis.
Arch. Neurol., 1982, ***39***

GREGORIE E.M. AND GOLDRING S. Localization of function in the excision of lesions from the sensorimotor region.
J.Neurosurg., 1984, ***61****, 1047-1054.*

GRISOLIA J.S. AND WIEDERHOLT W.C. Short latency somatosensory evoked potentials from radial,median and ulnar nerve stimulation in man.
Electroenceph.clin.Neurophysiol., 1980, ***50****, 375-381.*

GRIGG P. AND GREENSPAN B.J. Response of primate joint afferent neurons to mechanical stimulation of knee joint.
*J. Neurophysiol., 1977, **40**, 1-8.*

GULMANN N.C., WILDSCHIØDTZ G. AND ØRBAEK K. Alteration of interhemispheric conduction through the corpus callosum in chronic schizophrenia.
*Biol. Psychiat., **17**, 585-93.*

HACHINSKI V. Brain Mapping.
*Arch.Neurol., 1989, **36**, 1136.*

HALLLIDAY A.M. The electrophysiological study of myoclonus in man.
*Brain, 1967, **90**, 241-284.*

HALLIDAY A.M. AND HALLIDAY E. Cortical evoked potentials in patients with benign essential myoclonus and progressive myoclonic epilepsy.
*Electroenceph.clin.Neurophysiol., 1970, **29**, 106-107.*

HALLIDAY A.M AND MASON A.A. The effect of hypnotic anaesthesia on cortical responses.
*J.Neurol.,Neurosurg.,Psychiat., **36**, 75.*

HALLIDAY A.M. AND WAKEFIELD G.S. Cerebral evoked potentials in patients with dissociated sensory loss.
*J. Neurol. Neurosurg. Psychiat., 1963, **26**, 211.*

HALONEN J.P., JONES S.J. AND SHAWAT F. Contribution of muscle and cutaneous afferents to scalp recorded cortical SEP's following median and radial nerve stimulation in man.
*Electroenceph.clin.Neurophysiol., 1988, **71**, 331-335.*

HARI R., REINIKAINEN K., KAUKORANTA E., HÄMÄLÄINEN M., ILMONIEMI R., PENTTINEN A., SALMINENJ., AND TESZNER D. Somatosensory evoked cerebral magnetic fields from SI and SII in man.
*Electroenceph.clin.Neurophysiol., 1984, **57**, 254-263.*

HASHIMOTO I. Somatosensory evoked potentials from the human brain-stem: origins of short latency potentials.
*Electroenceph.clin.Neurophysiol., 1984, **57**, 221-227.*

HARDIN W.B., AND CASTELLUCCI V.F. Analysis of somatosensory, auditory and visual averaged transcortical and scalp responses in the monkey.
*Electroenceph.clin.Neurophysiol., 1970, **28**, 488-498*

HELLSTRÖM B., KARLSSON B AND MÜSSBICHLER H. Electrode placement in EEG of infants and anatomical relationship studied radiographically.
*Amer.J.EEG Technol., 1964, **4**, 71-76.*

HJORTH B. An on-line transformation of EEG scalp potentials into orthogonal source derivations.
*Electroenceph.clin.Neurophysiol., 1975, **39**, 526-530.*

HJORTH B. Source derivation simplifies topographical EEG interpretation.
*Am.J.EEG.Tech., **20**, 121-132.*

HOMAN R.W., HERMAN J. AND PURDY P. Cerebral location of international 10-20 system electrode placement.
*Electroenceph.clin.Neurophysiol., 1987, **66**, 376-382.*

HULLIGER M., NORDH E. AND VALLBO Å.B. The absence of position sense response in spindle afferent units from human finger muscles during accurate position holding.
*J.Physiol . (London) ,**322**, 167-179.*

HUTTUNEN J., HARI R., AND LEINONEN L. Cerbral magnetic responses to stimulation of ulnar and median nerves.
*Electroenceph.clin.Neurophysiol., 1987, **66**, 391-400.*

HYVÄRINEN J. The Parietal Cortex of Monkey and Man.
Springer-Verlag 1982

IKUTA T., FURUTA N., KONDO K., OHE S. The waveform of the group mean SEP of normal human subjects.
*Electroenceph.clin.Neurophysiol., 1980, **49**, 250-256.*

ISHIKO N., HANAMORI T. AND MURAYAMA N. Spatial distribution of somatosensory responses evoked by tapping the tongue and finger in man.
*Electroenceph.clin.Neurophysiol., 1980, **50**, 1-10.*

IWAYAMA K., MORI K., IWAMOTO K., YAMAUUCHI T., AND MASAGO M. Origin of frontal N15 component of somatosensory evoked potential in man.
*Electroenceph.clin.Neurophysiol., 1988, **71**, 125-132.*

JACOBSON G.P. AND TEW J.M. The origin of the scalp recorded P14 following electrical stimulation of the median nerve: intraoperative observations.
*Electroenceph.clin.Neurophysiol., 1988, **71**, 73-76*

JASPER H.H. Report of Committee on Methods of Clinical Examination in Electroencephalography.
*Electroenceph.clin.Neurophysiol., 1958, **10**, 370-375.*

JONES E.G. AND PORTER R. What is area 3a ?
*Brain Res. (1980) **198**, 307-321*

JONES E.G AND POWELL T.P.S. Connections of the Somatic Sensory Cortex of the Rhesus Monkey. I. - Ipsilateral Cortical Connections.
*Brain (1969) **92**, 477-502.*

JONES E.G AND POWELL T.P.S. Connections of the Somatic Sensory Cortex of the Rhesus Monkey. II. - Contralateral Cortical Connections.
*Brain (1969) **92**, 717-730.*

JONES G.H. AND MILLER J.J. Functional tests of the corpus callosum in schizophrenia.
*Brit. J. Psychiat., 1981, **139**, 553-557.*

JONES S.J. Short latency potentials recorded from the neck and scalp following median nerve stimulation in man.
*Electroenceph.clin.Neurophysiol., 1977, **43**, 853-863*

JONES S.J. Somatosensory evoked potentials: the abnormal waveform. In: A.M. Halliaday (Ed.), Evoked Potentials in Clinical Testing. Livingstone, Edinburgh, 1982, 431-470.

JONES S.J. AND POWER C.N. Scalp topography of human somatosensory evoked potentials: the effect of interfering tactile stimulation applied to the hand.
*Electroenceph.clin.Neurophysiol., 1984, **58**, 25-36.*

KAKIGI R. AND JONES S.J. Effects on median nerve SEP's of tactile stimulation applied to adjacent and remote areas of the body surface.
*Electroenceph.clin.Neurophysiol., 1985, **62**, 252-265.*

KAKIGI R. AND SHIBASAKI H. Scalp topography of mechanically and electrically evoked somatosensory potentials in man.
*Electroenceph.clin.Neurophysiol., 1984, **59**, 44-56.*

KATAYAMA Y. AND TSUBOKAWA T. Somatosensory evoked potentials from the thalamic sensory relay nucleus (VPL) in humans: correlations with short latency somatosensory evoked potentials recorded at the scalp.
*Electroenceph.clin.Neurophysiol., 1987, **68**, 187-201.*

KATZ S., MARTIN H.F. AND BLACKBURN J.G. The effects of interaction between large and small diameter fiber systems on the somatosensory evoked potential.
*Electroenceph.clin.Neurophysiol., 1978, **45**, 45-52.*

KELLY D.L., GOLDRING S. AND O'LEARY J.L. Averaged evoked somatosensory responses from the exposed cortex of man.
*Arch. Neurol., 1965, **13**, 1-9.*

KAHN E.M., WEINER R.D., BRENNER R.P., AND COPPOLA R. Topographic maps of brain electrical activity - pitfalls and precautions.
*Biol. Psychiatry, 1988, **23**, 628-636.*

KIMURA J., YAMADA Y., SHIVAPOUR E., AND DICKINS S. Neural pathways of somatosensory evoked potentials: Clinical implications.
*Kyoto Symposia, 1982, (EEG Suppl. No. **36**).*

KING D.W AND GREEN J.B. Short latency somatosensory evoked potentials in humans.
*Electroenceph.clin.Neurophysiol., 1979 ,**46**, 702-708.*

KRITCHEVSKY M. AND WIEDERHOLT W.C. Short latency evoked responses in man.
*Arch. Neurol (Chic.), 1978, **35**, 706-711.*

LAGET P., MAMO H ET HOUDART R. De l'intérêt des potentiels évoqués somesthésiques dans l'étude des lésions du lobe pariétal de l'homme. Etude préliminaire.
*Neurochirurgie, 1967, **13**, 841-853.*

LARSON S.J., SANCES A. AND CHRISTENSON P.C. Evoked somatosensory potentials in man.
*Arch. Neurol., 1966,**15**, 88.*

LEHMANN D. Multichannel topography of human alpha EEG fields.
*Electroenceph.clin.Neurophysiol., 1971, **31**, 439-449.*

LEHMANN D. AND SKRANDIES W. Reference-free identification of components of checkerboard-evoked multichannel potential fields.
*Electroenceph.clin.Neurophysiol., 1980, **48**, 609-621.*

LEHMANN D. AND SKRANDIES W. Spatial analysis of evoked potentials in man - a review.
*Progress in Neurobiology, 1984, **23**, 227-250.*

LEHTONEN J.B. AND KOIVIKKO M.J. The use of a non-cephalic reference electrode in recording cerebral evoked potentials in man.
*Electroenceph.clin.Neurophysiol., 1971, **31**, 154-156.*

LEMIEUX J.F., VERA R.S. AND BLUME W.T. Technique to display topographical evolution of EEG events.
*Electroenceph.clin.Neurophysiol., 1984, **58**, 565-568.*

LEVIN P.M. AND BRADFORD F.K. The exact origin of the cortico-spinal tract in the monkey.
J. Comp. Neurol., **68**, 411-22.

LÜDERS H. The effects of aging on the wave form of the somatosensory cortical evoked potential.
*Electroenceph.clin.Neurophysiol., 1970, **29**, 450-460.*

MACKAY D.M. Source-Density mapping of human visual receptive fields using scalp electrodes.
*Exp. Brain Res., 1984, **54**, 579-581.*

MALIS L.I., PRIBRAM K.H. AND KRUGER L. Action potentials in motor cortex evoked by peripheral nerve stimulation.
*J. Neurophysiol., 1953, **16**, 161-167.*

MATTHEWS P.B. Proprioceptors and their contribution to somatosensory mapping: complex messages require complex processing.
*Can.J.Physiol.Pharmacol., 1988, **66**, 431-438.*

MATTHEWS W.B. AND SMALL D.G. Serial recordings of visual and somatosensory evoked potentials in normal man and patients with multiple sclerosis.
*J. Neurol. Sci., 1979, **40**, 11-21.*

MAUGUIÉRE F., BRUNON A.M., ECHALLIER J.F., AND COURJON J. Early somatosensory evoked potentials in thalamo-cortical lesions of the lemniscal pathways in humans.
Clinical Applications of Evoked Potentials in Neurology, 1982, 321-338.

MAUGUIÉRE F. AND COURJON J. The origin of short latency somatosensory evoked potentials in man.
*Ann. Neurol. ,1981, **9**, 707-710.*

MAUGUIÉRE F., DESMEDT J.E. AND COURJON J. Astereognosis and dissociated loss of frontal or parietal components of somatosensory evoked potentials in hemispheric lesions.
*Brain (1983), **106**, 271-311.*

MAUGUIÉRE F., DESMEDT J.E. AND COURJON J. Neural generators of N18 and P14 far-field somatosensory evoked potentials studied in patients with lesion of thalamus or thalamo-cortical radiations.
*Electroenceph.clin.Neurophysiol., 1983, **56**, 283-292.*

MACCABEE P.J., PINKHASOV E.I. AND CRACCO R.Q. Short latency somatosensory evoked potentials to median nerve stimulation: effect of low frequency filter.
*Electroenceph.clin.Neurophysiol., 1983, **55**, 34-44*

MCNAUGHT A.B., AND CALLANDER R. Illustrated Physiology
Churchill Livingstone, 1983, 4th Edition.

MERVAALA E., PÄÄKKÖNEN A., AND PARTANEN J. The influence of height, age, and gender on the interpretation of median nerve SEP's.
*Electroenceph.clin.Neurophysiol., 1988, **71**, 109-113.*

MCCLOSKEY D.I. Position sense after surgical disconnection of the cerebral hemispheres in man.
*Brain (1973) **96**, 269-276.*

A.K.MCINTYRE, M.E.HOLMAN AND J.L.VEALE.
*Expl.Brain Res.,1967, Vol.**4**.*

MIJOSHI S., LÜDERS H., KATO M AND KUROIWA Y. The somatosensory evoked potentials in patients with cerebrovascular diseases.
*Folia psychiat. neurol. jap., 1971, **25**, 9-25.*

MILLAR J. Convergence of joint, cutaneous and muscle afferents onto cuneate neurones in the cat.
*Brain Res., 1979, **175**, 347-449.*

MOBERG ERIK. The role of cutaneous afferents in position sense, kinaesthesia, and motor function of the hand.
*Brain (1983) , **106**, 1-19.*

MØLLER A.R., JANNETTA P.J. AND BURGESS J. Neural geneartors of the somatosensory evoked potentials: recording from the cuneate nucleus in man and monkeys.
*Electroenceph.clin.Neurophysiol., 1986, **65**: 241-248.*

MORRIS H.H., LÜDERS H., LESSER R.P., DINNER D.S. AND KLEM G.H. The value of closely spaced scalp electrodes in the localization of epileptiform foci: a study of 26 patients with complex partial seizures.
*Electroenceph.clin.Neurophysiol., 1986, **63**, 107-111.*

NAKANISHI T., SHIMADA Y., SAKUTA M. AND TOYOKURA Y. The initial positive component of the scalp recorded somatosensory evoked potential in normal subjects and in patients with neurological disorders.
*Electroenceph.clin.Neurophysiol., 1978, **45**, 26-34.*

NAKANISHI T., SHIMADA Y. AND TOKOKURA Y. Somatosensory evoked responses to tactile tap in man.
*Electroenceph.clin.Neurophysiol., 1973, **34**, 1-6.*

NAKANISHI T., TAMAKI M., OZAKI Y. AND ARASAKI R. Origins of short latency somatosensory evoked potentials to median nerve stimulation.
*Electroenceph.clin.Neurophysiol., 1983, **56**,74-85*

NOEL P. AND DESMEDT J.E. Somatosensory evoked potentials after vascular lesions of the brainstem and diencephalon.
*Brain. **98**, 13.*

NUWER M.R. A comparison of the analysis of EEG and evoked potentials using coloured bars in place of coloured heads.
*Electroenceph.clin.Neurophysiol., 1985, **61**,310-313.*

NUWER M.R. Uses and abuses of brain mapping.
*Arch. Neurol., 1989, **46**, 1134-1136.*

OBESO J.A., MARTI-MASSO J.F., AND CARRERA N. Somatosensory evoked potentials: Abnormalities with focal brain lesions remote from the primary sensorimotor area.
*Electroenceph.clin.Neurophysiol., 1980, **49**, 59-65.*

OFFNER F.F. The EEG as potential mapping: The value of the average monopolar reference.
*Electroenceph.clin.Neurophysiol., 1950, **2**, 213-214.*

OHYE C., FUKAMACHI A. AND NARABAYASHI H. Spontaneous and evoked activity of sensory neurons and their organisation in the human thalamus.
*z. Neurol., 1972, **203**, 219-234.*

OKADA Y.C., TANANBAUM R., WILLIAMSON S.J. AND KAUFMAN L. Somatotopic organization of the human somatosensory cortex revealed by neuromagnetic measurements.
*Exp. Brain Res., 1984, **56**, 197-205.*

OKASAKI A., SHIOTA T. AND TERUDA C. Clinical studies on the somatosensory evoked response in neurosurgical patients.
*Electroenceph.clin.Neurophysiol., 1971, **31**, 189.*

OKEN B.S. AND CHIAPPA K.H. Statistical issues concerning computerized analysis of brainwave topography.
*Ann. Neurol., 1986, Vol.**19**, 5, 493-494.*

PANDYA D.N. AND VIGNOLO L.A. Interhemispheric projections of the parietal lobe in the rhesus monkey.
*Brain Research., 1968, **15**, 49-65.*

PAPAKOSTOPOULOS D. AND CROW H.J. Direct recording of the somatosensory evoked potential from the cerebral cortex of man and the difference between precentral and postcentral potentials.
*In: J.E. Desmedt (Ed.), Clinical Uses Cerebral, Brainstem and Spinal Somatosensory Evoked Potentials, Progr. Clin. Neurophysiol., **Vol. 7**, Karger, Basel 1980: 15-26.*

PENFIELD W. AND JASPER J. Epilepsy and the functional anatomy of the human brain.
Boston, Little Brown & Co., 1954, 52-88.

PERRIN F., PERNIER J., BERTRAND O., GIARD M.H. AND ECHALLIER J.F. Mapping of scalp potentials by surface spline interpolation.
*Electroenceph.clin.Neurophysiol., 1987, **66**, 75-81.*

PHILLIPS C.G., POWELL T.P.S. AND WIESENDANGER M. Projection from low threshold muscle afferents of hand and forearm to area 3a of babboons cortex.
*J.Physiol. (London), **217**, 419-446.*

PRATT H., POLTOSKE D. AND STARR A. Mechanically and electrically evoked somatosensory potentials in humans: effects of stimulus presentation rate.
*Electroenceph.clin.Neurophysiol., 1980, **49**, 240-249.*

PRATT H. AND STARR A. Mechanically and Electrically evoked somatosensory potentials in humans: scalp and neck distributions of short latency components.
*Electroenceph.clin.Neurophysiol., 1981, **51**, 138-147.*

PICTON T W., WOODS D., STUSS D AND CAMPBELL K. Methodology and meaning of human evoked potential scalp distribution studies.
Multidisciplinary Perspectives in Event Related Brain Potential Research. 1978, U.S. Environmental Protection Agency 600/9-77-043, p515-522. Otto, D.A. (Ed.)

POWELL T.P.S. AND MOUNTCASTLE V.B. The cytoarchitecture of the postcentral gyrus of the monkey Macaca mulatta.
*Bull. John Hopkins Hosp., **105**, 108-120.*

RAGOT R.A. AND RÉMOND A. EEG Field Mapping.
*Electroenceph.clin.Neurophysiol., 1978, **45**, 417-421.*

RÉMOND A. Topological aspects of the organisation, processing and presentation of data. In: The analysis of central nervous system and cardiovascular data using computer methods (1964 symposium). Eds., Proctor L.D. and Adey W.R. Washington, NASA, 73-93.

RÉMOND A. AND TORRES F. A method of electrode placement with a view of topographical research. I. Basic concepts.
*Electroenceph.clin.Neurophysiol., 1964, **17**, 577-578.*

ROSE J.E. AND MOUNTCASTLE V.B. In: Handbook of Physiology. (Ed.)Magoun. Section 1, Neurophysiology, **1**, 387.

ROSENTHAL AND BIGELOW L.B. Quantitative brain measurement in chronic schizophrenia.
*Brit. J. Psychiat., 1972, **121**, 259-264.*

ROSSINI P.M., BABILONI F., BERNARDI G., CECCHI L., JOHNSON P.B., MALENTACCA A., STANZIONE P AND URBANO A. Abnormalities of short latency somatosensory evoked potentials in parkinsonian patients.
*Electroenceph.clin.Neurophysiol., 1989, **74**, 277-289*

SALAMY A. Commisural transmission: maturational changes in humans.
*Science, 1978, **200**, 1409-11.*

SEARS T.A. Action potentials evoked in digital nerves by stimulation of mechanoreceptors in the human finger.
*J.Physiol., **148**: 30P*

SHAGASS C., JOSIASSEN R.C., ROEINER R.A., STRAUMANIS J.J. AND SLEPNER S.M. Failure to replicate evoked potential observations suggesting corpus callosum dysfunction in schizophrenia.
Brit. J. Psychiat., 1983, ***142****, 471-476.*

SHAGASS C. AND SCHWARTZ M. Recovery functions of somatosensory peripheral nerve and cerebral evoked responses in man.
Electroenceph.clin.Neurophysiol., 1964, ***17****, 126.*

SHIBASAKI H., YAMASHITA Y. AND TSUJI S. Somatosensory evoked potentials. Diagnostic criteria and abnormalities in cerebral lesions.
*J.neurol.Sci., 1977,****34****, 427-439.*

SLIMP J.C., TAMAS L.B., STOLOV W.C., AND WYLER A.R. Somatosensory evoked potentials after removal of somatosensory cortex in man.
Electroenceph.clin.Neurophysiol., 1986, ***65****, 111-117.*

SPITZER A.R., COHEN L.G., FABRIKANT J AND HALLETT M. A method for determining optimal inerelectrode spacing for cerebral topographic mapping.
Electroenceph.clin.Neurophysiol., 1989, ***72****, 355-361.*

STEERS J.A. An introduction to the Study of Map Projections.
13th Edition. Univ. London Press, London, 1965.

STEJSKAL L., AND SOBOTA J. Somatosensory evoked potentials in patients with occlusions of cerebral arteries.
Electroenceph.clin.Neurophysiol., 1985, ***61****, 482-490.*

STEINMETZ H., FÜRST G., AND MEYER B-U. Craniocerebral topography within the international 10-20 system.
Electroenceph.clin.Neurophysiol., 1989, ***72****, 499-506*

STOHR P.E., GOLDRING S. Origin of somatosensory evoked scalp responses in man.
J. Neurosurg., 1969, ***31****, 117-127.*

SUNDERLAND S. AND BEDBROOK G.M. The cross sectional area of peripheral nerve trunks occupied by the fibres representing individual muscular and cutaneous branches.
*Brain, 1949, **72**, 613-624.*

SUTHERLING W.W., CRANDALL P.H., DARCEY T.M., BECKER D.P., LEVESQUE M.F., AND BARTH D.S. The magnetic and electric fields agree with intracranial localizations of somatosensory cortex.
*Neurology, 1988, **38**, 1705-1714.*

SUZUKI I. AND MAYANAGI Y. Intracranial recording of short latency somatosensory evoked potentials in man: identification of origin of each component.
*Electroenceph.clin.Neurophysiol., 1984, **59**, 286-296.*

SWADLOW H.A., GESCHWIND N. AND WAXMAN S.G. Commisural Transmission in Humans.
*Science, **264**, 530-531.*

SYNEK V.M. Somatosensory evoked potentials after stimulation of digital nerves in upper limbs: normative data.
*Electroenceph.clin.Neurophysiol., 1986, **65**,460-463.*

TAPIA M.C., COHEN L.G., AND STARR A. Selectivity of attenuation (i.e., gating) of somatosensory potentials during voluntary movement in humans.
*Electroenceph.clin.Neurophysiol., 1987, **68**, 226-230.*

THICKBROOM G.W., DAVIES H.D., CARROLL W.M. AND MASTAGLIA F.L. Averaging, spatio-temporal mapping and dipole modelling of focal epileptic spikes.
*Electroenceph.clin.Neurophysiol., 1986, **64**, 274-277.*

THICKBROOM G.W., MASTAGLIA F.L. AND CARROLL W.M. Spatio-temporal mapping of evoked cerebral activity.
*Electroenceph.clin.Neurophysiol., 1984, **59**, 425-431.*

THICKBROOM G.W., MASTAGLIA F.L. AND CARROLL W.M., AND DAVIES H.D.
Source Derivation: Application to topographic mapping of visual evoked potentials.
*Electroenceph.clin.Neurophysiol., 1984, **59**, 279-285.*

TRACEY D.J., ASANUMA C., JONES E.G. AND PORTER R. Thalamic relay to motor cortex: afferent pathways from brainstem, cerebellum and spinal cord in monkeys.
*J. Neurophysiol., 1980, **44**, 532-554.*

TRESS K.H., CAUDREY D.J. AND MEHTA B. Tactile-Evoked potentials in schizophrenia. Interhemispheric transfer and drug effects.
*Brit. J. Psychiat., 1983, **143**, 156-164.*

TSUJI S. AND MURAI Y. Scalp topography and distribution of cortical somatosensory evoked potentials to median nerve stimulation.
*Electroenceph.clin.Neurophysiol., 1986, **65**, 429-439.*

TSUJI S. AND MURAI Y., AND HASHIMOTO M. Frontal distribution of early somatosensory evoked potentials to median nerve stimulation.
*Electroenceph.clin.Neurophysiol., 1988, **71**, 273-279.*

TSUJI S. AND MURAI Y., AND KADOYA C. Topography of somatosensory evoked potentials to median nerve stimulation in patients with cerebral lesions.
*Electroenceph.clin.Neurophysiol., 1988, **71**, 280-288.*

UDDENBERG N. Functional organisation of long, second order afferents in the dorsal funiculus.
*Expl. Brain Res., 1968, **4**, 377-82.*

VALLBO Å.B., HAGBARTH K.-E., TOREBJÖRK H.E. AND WALLIN B.G. Somatosensory, Proprioceptive and Sympathetic Activity in Human Peripheral Nerves.
Physiological Reviews Vol 59, No.4, October 1979.

VAUGHAN H.G. The relationship of brain activity to scalp recording of event related potentials. In: E.Donchin and D.B. Lindsley (Eds.), Averaged Evoked Potentials: Methods, Results and Evaluation. NASA, SP-191, U.S. Govt. Printing Office, Washington, D.C., 1969, 45-94.

VEALE J.L., MARK R.F. AND REES S. Differential sensitivity of motor and sensory fibres in the human ulnar nerve.
*J. Neurol.Neurosurg.Psychiat., **36**, 75.*

WALTER W.G AND SHIPTON H.W. A new toposcopic display system.
*Electroenceph.clin.Neurophysiol., 1951, **1**, 195-204*

WIEDERHOLT W.C., MEYER-HARDTING E., BUDNICK B., AND MCKEOWN K.L.
Stimulating and recording methods used in obtaining short-latency somatosensory evoked potentials (SEP's) in patients with central and peripheral neurologic disorders.
*Ann. N.Y. Acad Sci., 1982, **388**, 349-357*

WILLIAMSON P.D., GOFF W.R. AND ALLISON T. Somatosensory evoked responses in patients with unilateral cerebral lesions.
*Electroenceph.clin.Neurophysiol., 1970, **28**, 566-575.*

WOOD C.C. Application of dipole localization methods to source identification of human evoked potentials.
*Ann. NY. Acad. Sci .,1982 ,**388**, 139-155*

WOOD C.C., COHEN D., CUFFIN B.N., YARITA M. AND ALLISON T. Electrical sources in human somatosensory cortex: identification by combined magnetic and potential recordings.
*Science, 1985, **227**, 1051-1053.*

WOOD C.C. Generators of Event Related Potentials.
In A Textbook of Clinical Neurophysiology. Ed., Halliday A.M.,
Butler S.R., and Paul R. John Wiley and Sons 1987.

WOOD C.C., SPENCER D.D., ALLISON T., MCCARTHY G., WILLIAMSON P.D. AND GOFF W.R.
Localization of human sensorimotor cortex during surgery by cortical surface recording of somatosensory evoked potentials.
*J. Neurosurg., 1988, **68**, 99-111.*

WOOLSEY C.N., WALKER A.E., ERIKSON T. Somatic afferent representation in the cerebral cortex of man.
*Proc. Tenth Neurological Congress, Paris, 1949, **2**, 70-71.*

YAMADA T., KAYAMORI, R., KIMURA J. AND VANGILDER J. Short latency somatosensory evoked potentials following median nerve stimulation in man.
*Electroenceph.clin.Neurophysiol., 1980, **48**, 367-376.*

YAMADA T., KAYAMORI R., KIMURA J. AND BECK D.O. Topography of somatosensory evoked potentials after stimulation of the median nerve.
*Electroenceph.clin.Neurophysiol., 1984, **59**, 29-43*

YAMADA T., KIMURA J. AND NITZ D.M. Short latency somatosensory evoked potentials following median nerve stimulation in man.
*Electroenceph.clin.Neurophysiol., 1980, **48**, 367-376.*

YAMADA T., SHIVAPOUR E., WILKINSON T., KIMURA J. Short and Long - latency evoked potentials in multiple sclerosis.
*Arch. Neurol., 1982, **39**, 88-94.*

ZEGERS DE BEYL D., DELBERGHE X., HERBAUT A.G. AND BRUNKO E. The somatosensory central conduction time: physiological considerations and normative data.
*Electroenceph.clin.Neurophysiol., 1988, **71**, 17-26*

LATENCY DATA FOR FRONTAL (F3/F4) COMPONENTS

	RIGHT LIMB			LEFT LIMB			T-TEST P VALUES	
Component	Mean (ms)/(S.D)	U.L.N.	Obs.	Mean (ms)/(S.D)	U.L.N.	Obs.	Paired/ (No. of pairs)	Unpaired
P14	14.41 (1.58)	18.36	30	13.91 (1.46)	17.56	27	**0.007 (26)**	0.228
N17	17.64 (1.72)	21.94	30	17.48 (1.71)	21.76	26	0.337 (25)	0.430
P20	21.04 (2.54)	27.39	29	20.35 (2.36)	26.25	25	0.396 (24)	0.312
N23	23.08 (2.14)	28.43	13	23.55 (2.25)	29.18	11	0.074 (07)	0.597
N30	29.72 (3.25)	37.85	29	29.71 (3.55)	38.59	25	0.942 (23)	0.998
P35	35.66 (3.29)	43.89	10	34.75 (1.87)	39.42	7	0.221 (05)	0.524
P42	41.42 (1.90)	46.17	13	44.09 (3.07)	51.76	12	0.040 (10)	0.023
N43	42.97 (4.55)	54.34	8	44.06 (4.19)	54.53	4	0.999 (03)	0.697

AMPLITUDE DATA FOR FRONTAL (F3/F4) COMPONENTS

	RIGHT LIMB			LEFT LIMB			T-TEST P VALUES	
Component	Mean (uV)/(S.D.)	U.L.N.	Obs.	Mean (uV)/(S.D.)	U.L.N.	Obs.	Paired/ (No. of pairs)	Unpaired
0-P14	1.61 (0.40)	2.61	30	1.48 (0.62)	3.03	27	**0.009 (26)**	**0.023**
P14-N17	1.15 (0.49)	2.38	30	1.33 (0.65)	2.96	26	0.054 (25)	0.253
N17-P20	1.07 (0.67)	2.75	29	1.07 (0.97)	3.5	25	0.889 (24)	0.974
P20-N23	1.58 (0.84)	3.68	13	1.44 (0.81)	3.47	11	0.934 (07)	0.682
N23-N30	1.59 (1.13)	4.42	13	0.97 (0.86)	3.12	11	0.375 (07)	0.147
P20-N30	2.50 (1.80)	7.00	28	2.67 (1.70)	6.92	25	0.589 (23)	0.719
N30-P35	2.33 (1.29)	5.56	10	3.02 (1.41)	6.54	10	0.350 (05)	0.316
P35-N43	1.53 (0.85)	3.65	8	3.03 (1.14)	5.88	5	0.656 (03)	0.020
N30-P42	3.12 (1.90)	7.87	13	3.29 (1.78)	7.74	11	0.519 (09)	0.831

INTERPEAK LATENCY DATA FOR FRONTAL (F3/F4) COMPONENTS

	RIGHT LIMB			LEFT LIMB			T-TEST P VALUES	
Component	Mean (ms)/(S.D)	U.L.N.	Obs.	Mean (ms)/(S.D)	U.L.N.	Obs.	Paired/ (No. of pairs)	Unpaired
ERBS-P14	4.21 (0.91)	6.49	20	3.93 (0.87)	6.11	17	0.391 (16)	0.35
P14-N17	3.36 (0.83)	5.44	30	3.43 (0.92)	5.73	26	0.466 (25)	0.781
N17-P20	3.22 (1.33)	6.55	29	3.02 (1.37)	6.45	25	0.660 (24)	0.581
N17-N23	5.43 (1.26)	8.58	13	6.47 (1.47)	10.15	11	0.027 (07)	0.071
N17-N30	11.93 (2.96)	19.33	29	12.38 (3.44)	20.98	25	0.899 (23)	0.609
N17-P35	17.06 (2.80)	24.06	10	16.71 (2.04)	21.81	7	0.363 (05)	0.784
N17-P42	24.53 (1.69)	28.75	13	27.55 (2.91)	34.82	12	0.029 (10)	**0.004**
N17-N43	24.17 (3.83)	33.74	8	25.50 (4.22)	36.05	4	0.917 (03)	0.594

TABLE A.1 FRONTAL COMPONENT DATA TABLE

S.D. = Standard Deviation U.L.N. = Upper Limits of Normality Obs. = Observations

Bold P-values indicate significance at the 1% level for comparison of Right versus Left limb data

INTERHEMISPHERE LATENCY DIFFERENCE FOR F3/F4 COMPONENTS

Component	Mean (ms)/(S.D)	U.L.N.	Obs.
RERB-LERB	0.23 (0.13)	0.49	21
RP14-LP14	0.41 (0.48)	1.61	26
RN17-LN17	0.68 (0.46)	1.83	25
RP20-LP20	1.08 (0.99)	3.56	24
RN23-LN23	0.44 (0.54)	1.79	7
RN30-LN30	1.59 (1.22)	4.64	23
RP34-LP34	1.10 (0.52)	2.40	5
RP42-LP42	3.39 (1.64)	7.49	10
RN43-LN43	2.16 (1.01)	4.68	3

INTERHEMISPHERE AMPLITUDE DIFFERENCE OF F3/F4 COMPONENTS

Component	Mean (uV)/(S.D.)	U.L.N.	Obs.
0-P14	0.49 (0.42)	1.54	26
P14-N17	0.43 (0.35)	1.31	25
N17-P20	0.44 (0.43)	1.52	24
P20-N23	1.13 (0.78)	3.08	6
N23-N30	1.28 (0.76)	3.18	6
P20-N30	0.87 (0.67)	2.55	26
N30-P34	0.77 (1.01)	3.29	5
N30-P42	1.01 (1.07)	3.68	9
P34-N43	0.67 (0.38)	1.62	3

TABLE A1.1 FRONTAL COMPONENT DATA TABLE (Right versus Left limb data)
S.D. = Standard Deviation U.L.N. = Upper Limits of Normality Obs. = Observations
Bold P-values indicate significance at the 5% level for comparison of Right versus Left limb data

LATENCY DATA FOR FRONTAL (F3/F4) COMPONENTS

	YOUNG GROUP			OLD GROUP			T-TEST
Component	Mean (ms)	S.D.	Obs.	Mean (ms)	S.D.	Obs.	P-Values
ERBS	9.91	0.45	11	10.85	1.47	8	0.060
P14	13.94	1.29	15	15.34	1.79	11	**0.029**
N17	17.17	1.48	15	18.68	2.01	11	**0.037**
P20	19.46	1.48	14	22.98	2.57	11	**0.000**
N23	22.71	1.50	11	26.38	2.65	2	**0.014**
N30	29.82	3.33	15	29.95	3.64	11	0.925
P35	28.75	-	1	36.42	2.36	9	-
P42	41.62	1.90	13	-	-	0	-
N43	34.00	-	1	44.25	2.97	7	-

AMPLITUDE DATA FOR FRONTAL (F3/F4) COMPONENTS

	YOUNG GROUP			OLD GROUP			T-TEST
Component	Mean (uV)	S.D.	Obs.	Mean (uV)	S.D.	Obs.	P-Values
0-P14	1.33	0.45	15	0.96	0.24	11	**0.021**
P14-N17	1.21	0.48	15	1.16	0.55	11	0.822
N17-P20	0.94	0.56	14	1.33	0.83	11	0.173
P20-N23	1.61	0.91	11	0.88	0.31	2	0.300
N23-N30	1.87	1.10	11	0.37	0.35	2	0.090
P20-N30	2.58	1.93	14	2.38	1.94	11	0.804
N30-P35	0.88	-	1	2.49	1.26	9	
P35-N43	0.86	-	1	1.63	0.87	7	
N30-P42	3.12	1.90	13	-	-	0	

INTERPEAK LATENCY DATA FOR FRONTAL (F3/F4) COMPONENTS

	YOUNG GROUP			OLD GROUP			T-TEST
Component	Mean (ms)	S.D.	Obs.	Mean (ms)	S.D.	Obs.	P-Values
ERBS-P14	3.98	1.09	9	4.59	0.76	8	0.204
P14-N17	3.23	0.62	15	3.34	1.07	11	0.743
N17-P20	2.24	0.84	14	4.31	1.11	11	**0.000**
N17-N23	5.21	1.00	13			2	-
N17-N30	12.65	3.02	15	11.28	3.12	11	0.268
N17-P35	12.50	-	1	17.57	2.43	9	-
N17-P42	24.53	1.69	13	-	-	0	-
N17-N43	17.75	-	1.00	25.08	3.05	7	-

TABLE A.2 FRONTAL COMPONENT DATA FOR YOUNG AND OLD AGE GROUPS (Right limb)

Young group = 17-30 years Old group = 60-86 years

S.D.= Standard Deviation Obs = Observations

Bold P-values indicate significance at the 5% level for comparison of young versus old age group data

INTERHEMISPHERE LATENCY DIFFERENCE FOR F3/F4 COMPONENTS

	YOUNG GROUP			OLD GROUP			T-TEST
Component	**Mean (ms)**	**S.D.**	**Obs.**	**Mean (ms)**	**S.D.**	**Obs.**	P-Values
RERB-LERB	0.14	0.08	11	0.26	0.15	7	0.133
RP14-LP14	0.17	0.08	11	0.22	0.11	6	0.364
RN17-LN17	0.19	0.27	13	0.78	0.58	9	**0.005**
RP20-LP20	0.70	0.49	12	0.68	0.40	9	0.860
RN23-LN23	0.44	0.54	7			1	-
RN30-LN30	1.71	1.26	12	1.72	1.33	8	0.991
RP35-LP35	-	-	0	1.10	0.52	5	-
RP42-LP42	2.39	1.64	10	-	-	0	-
RN43-LN43	-	-	0	2.17	1.01	3	-

INTERHEMISPHERE AMPLITUDE DIFFERENCE OF F3/F4 COMPS

	YOUNG GROUP			OLD GROUP			T-TEST
Component	**Mean (uV)**	**S.D.**	**Obs.**	**Mean (uV)**	**S.D.**	**Obs.**	P-Values
0-P14	0.42	0.33	13	0.59	0.54	9	0.359
P14-N17	0.32	0.30	12	0.63	0.39	9	0.054
N17-P20	0.33	0.27	12	0.69	0.62	8	0.089
P20-N23	1.13	0.78	7			1	
N23-N30	1.28	0.76	7			1	
P20-N30	0.83	0.65	12	0.82	0.76	11	0.974
N30-P35	-		0	0.77	1.01	5	
P35-N43	-		0	0.68	0.38	3	
N30-P42	1.01	1.07	9	-	-	0	

TABLE A2: FRONTAL COMPONENT DATA FOR YOUNG AND OLD AGE GROUPS

Young group = 17-30 years Old group = 60-86 years

S.D.= Standard Deviation Obs = Observations

Bold P-values indicate significance at the 5% level for comparison of young versus old age group data

LATENCY DATA FOR CENTRAL (C3/C4) COMPONENTS

	RIGHT LIMB			LEFT LIMB			T-TEST P VALUES	
Component	Mean (ms)/(S.D)	U.L.N.	Obs.	Mean (ms)/(S.D)	U.L.N.	Obs.	Paired/ (No. of pairs	Unpaired
P14	14.41 (1.58)	18.36	30	14.02 (1.55)	17.9	28	**0.000 (28)**	0.355
N19	18.80 (1.80)	23.3	30	18.71 (1.86)	23.36	29	0.797 (28)	0.859
P22	22.28 (2.67)	29.53	29	23.42 (2.45)	29.55	29	0.040 (27)	0.397
N24	23.08 (0.97)	25.51	6	25.40 (2.42)	31.45	6	0.205 (03)	0.058
P26	25.48 (1.34)	28.83	6	27.51 (3.18)	35.46	6	0.678 (03)	0.164
N31	31.66 (2.69)	38.39	30	31.71 (2.89)	38.94	29	0.604 (28)	0.943
P42	41.52 (2.88)	48.72	28	42.11 (3.75)	51.49	29	0.305 (27)	0.505

AMPLITUDE DATA FOR CENTRAL (C3/C4) COMPONENTS

	RIGHT LIMB			LEFT LIMB			T-TEST P VALUES	
Component	Mean (uV)/(S.D.)	U.L.N.	Obs.	Mean (uV)/(S.D.)	U.L.N.	Obs.	Paired/ (No. of pairs	Unpaired
0-P14	0.88 (0.42)	1.93	30	1.19 (0.37)	2.12	28	**0.003 (27)**	**0.004**
P14-N19	1.62 (0.63)	3.2	30	1.68 (0.91)	3.96	29	0.538 (28)	0.757
N19-P22	2.55 (2.20)	8.05	29	2.66 (1.60)	6.66	29	0.428 (27)	0.816
P22-N24	0.51 (0.31)	1.29	6	0.74 (0.51)	2.02	6	0.856 (03)	0.368
N24-P26	0.70 (0.35)	1.58	6	0.46 (0.26)	1.11	6	0.076 (03)	0.268
P26-N31	2.43 (2.13)	7.76	6	1.26 (0.15)	1.64	6	0.625 (03)	0.31
N31-P42	3.68 (2.14)	9.03	28	3.96 (2.08)	9.16	29	0.804 (27)	0.621
P22-N31	3.07 (2.50)	9.32	28	3.40 (2.69)	10.13	29	0.150 (27)	0.626

INTERPEAK LATENCY DIFFERENCE FOR CENTRAL (C3/C4) COMPONENTS

				LEFT LIMB			T-TEST P VALUES	
Component	Mean (ms)/(S.D)	U.L.N.	Obs.	Mean (ms)/(S.D)	U.L.N.	Obs.	Paired/(No. of pairs)	Unpaired
ERBS-P14	4.21 (0.92)	6.51	20	4.00 (0.90)	6.25	18	0.618 (17)	0.49
P14-N19	4.39 (0.89)	6.62	30	4.57 (0.93)	6.9	28	0.099 (27)	0.454
N19-P22	4.07 (1.82)	8.62	29	4.71 (1.77)	9.14	29	**0.026 (27)**	0.183
N19-N24	4.39 (0.53)	5.72	6	5.69 (1.25)	8.82	6	0.350 (03)	0.044
N19-P26	6.67 (0.94)	9.02	6	7.62 (1.89)	12.35	6	0.892 (03)	0.286
N19-N31	12.86 (1.93)	17.69	30	13.00 (2.65)	19.63	29	0.554 (28)	0.821
N19-P42	22.81 (2.93)	30.14	28	23.40 (3.99)	33.38	29	0.369 (27)	0.525

TABLE A3 CENTRAL COMPONENT DATA TABLE

S.D. = Standard Deviation U.L.N. = Upper Limits of Normality Obs. = Observations

Bold P-values indicate significance at the 5% level for comparison of Right versus Left limb data

INTERHEMISPHERE LATENCY DIFFERENCE FOR CENTRAL COMPONENTS

Component	Mean (ms)/(S.D)	U.L.N.	Obs.
RERB-LERB	0.23 (0.13)	0.56	21
RP14-LP14	0.35 (0.52)	1.65	27
RN19-LN19	0.50 (0.48)	1.7	28
RP22-LP22	1.14 (1.06)	3.79	27
RN24-LN24	0.75 (0.35)	1.63	3
RP26-LP26	0.23 (0.25)	0.86	3
RN31-LN31	1.27 (1.05)	3.9	28
RP42-LP42	1.63 (1.35)	5.01	27

INTERHEMISPHERE AMPLITUDE DIFFERENCE FOR CENTRAL COMPONENTS

Component	Mean (uV)/(S.D.)	U.L.N.	Obs.
0-P14	0.49 (0.31)	1.27	27
P14-N19	0.71 (0.49)	1.94	27
N19-P22	0.84 (0.88)	3.04	27
P22-N24	0.65 (0.21)	1.18	3
N24-P26	0.58 (0.10)	0.83	3
P26-N31	0.49 (0.32)	1.29	3
N31-P42	1.48 (1.50)	5.23	27
P22-N31	1.16 (0.86)	3.31	26

TABLE A3.1 CENTRAL COMPONENT DATA TABLE

S.D. = Standard Deviation U.L.N. = Upper Limits of Normality Obs. = Observations

Bold P-values indicate significance at the 5% level for comparison of Right versus Left limb data

LATENCY DATA FOR CENTRAL (C3/C4) COMPONENTS

	YOUNG GROUP			OLD GROUP			T-TEST
Component	Mean (ms)	S.D.	Obs.	Mean (ms)	S.D.	Obs.	P-Values
ERBS	9.91	0.45	11	10.85	1.47	8	0.060
P14	13.94	1.29	15	15.34	1.79	11	**0.029**
N19	18.06	1.34	15	20.00	1.96	11	**0.006**
P22	21.38	1.15	15	24.97	3.08	11	**0.000**
N24	23.07	1.08	5			0	
P26	25.15	1.43	5			0	
N31	30.83	2.03	15	32.85	3.37	11	0.070
P42	40.78	2.93	14	42.08	2.93	10	0.294

AMPLITUDE DATA FOR CENTRAL (C3/C4) COMPONENTS

	YOUNG GROUP			OLD GROUP			T-TEST
Component	Mean (uV)	S.D.	Obs.	Mean (uV)	S.D.	Obs.	P-Values
0-P14	0.99	0.46	15	0.78	0.35	11	0.222
P14-N19	1.61	0.74	15	1.61	0.53	11	0.973
N19-P22	2.32	1.31	15	3.01	3.23	11	0.457
P22-N24	0.55	0.33	5			0	
N24-P26	0.71	0.39	5			0	
P26-N31	2.83	2.42	5			0	
N31-P42	3.78	2.08	14	3.89	2.47	10	0.911
P22-N31	2.85	2.20	14	3.39	3.05	11	0.608

INTERPEAK LATENCY DIFFERENCE FOR CENTRAL (C3/C4) COMPONENTS

	YOUNG GROUP			OLD GROUP			T-TEST
Component	Mean (ms)	S.D.	Obs.	Mean (ms)	S.D.	Obs.	P-Values
ERBS-P14	3.98	1.09	9	4.59	0.76	8	0.204
P14-N19	4.12	0.76	15	4.66	1.04	11	0.136
N19-P22	3.32	1.00	15	5.10	2.03	11	**0.007**
N19-N24	4.39	0.59	5			0	
N19-P26	6.48	0.86	5			0	
N19-N31	12.77	2.08	15	12.85	1.95	11	0.927
N19-P42	22.70	3.12	14	22.31	2.41	10	0.745

TABLE A.4 CENTRAL COMPONENT DATA FOR YOUNG AND OLD AGE GROUPS

Young group = 17-30 years Old group = 60-86 years

S.D.= Standard Deviation Obs = Observations

Bold P-values indicate significance at the 5% level for comparison of young versus old age group data

INTERHEMISPHERE LATENCY DIFFERENCE FOR CENTRAL COMPONENTS

	YOUNG GROUP			OLD GROUP			T-TEST
Component	Mean (ms)	S.D.	Obs.	Mean (ms)	S.D.	Obs.	P-Values
RERB-LERB	0.14	0.08	11	0.26	0.15	7	0.133
RP14-LP14	0.19	0.27	13	0.73	0.57	10	**0.007**
RN19-LN19	0.54	0.48	13	0.55	0.56	11	0.988
RP22-LP22	0.82	0.76	13	1.36	0.83	11	0.110
RN24-LN24	0.75	0.35	2			0	
RP26-LP26	0.10	0.14	2			0	
RN31-LN31	1.23	0.87	13	1.05	0.92	11	0.614
RP42-LP42	1.64	0.98	13	1.82	1.91	10	0.773

INTERHEMISPHERE AMPLITUDE DIFFERENCE FOR CENTRAL COMPONENTS

	YOUNG GROUP			OLD GROUP			T-TEST
Component	Mean (uV)	S.D.	Obs.	Mean (uV)	S.D.	Obs.	P-Values
0-P14	0.56	0.30	13	0.42	0.29	10	0.277
P14-N19	0.83	0.56	12	0.73	0.45	11	0.650
N19-P22	0.82	0.58	13	0.92	1.25	11	0.789
P22-N24	0.65	0.21	2			0	
N24-P26	0.58	0.10	2			0	
P26-N31	0.32	0.15	2			0	
N31-P42	1.08	0.82	13	2.08	2.13	10	0.132
P22-N31	1.16	1.05	13	1.10	0.52	10	0.885

TABLE A4. CENTRAL COMPONENT DATA FOR YOUNG AND OLD AGE GROUPS

Young group = 17-30 years Old group = 60-86 years

S.D.= Standard Deviation Obs = Observations

Bold P-values indicate significance at the 5% level for comparison of young versus old age group data

LATENCY DATA FOR PARIETAL (P3/P4) COMPONENTS

	RIGHT LIMB			LEFT LIMB			T-TEST P VALUES	
Component	Mean (ms)/(S.D)	U.L.N.	Obs.	Mean (ms)/(S.D)	U.L.N.	Obs.	Paired/(No. of pairs)	Unpaired
P14	14.41 (1.58)	18.36	30	14.02 (1.55)	17.9	28	**0.010 (27)**	0.355
N20	19.81 (1.80)	24.31	30	19.63 (1.77)	24.06	29	0.129 (28)	0.703
P22	21.85 (1.50)	25.6	6	21.75 (1.32)	25.05	2	0.895 (02)	0.926
N25	24.96 (2.05)	30.09	6	25.88 (0.88)	28.08	2	0.410 (02)	0.585
P27	27.06 (3.56)	35.96	29	26.85 (3.01)	34.38	27	0.335 (27)	0.815
N33	32.79 (3.09)	40.52	27	33.74 (3.37)	42.17	26	0.114 (24)	0.291
P42	42.18 (3.76)	51.58	25	42.39 (3.48)	51.09	25	0.227 (22)	0.841

AMPLITUDE DATA FOR PARIETAL (P3/P4) COMPONENTS

	RIGHT LIMB			LEFT LIMB			T-TEST P VALUES	
Component	Mean (uV)/(S.D.)	U.L.N.	Obs.	Mean (uV)/(S.D.)	U.L.N.	Obs.	Paired/(No. of pairs)	Unpaired
0-P14	0.76 (0.45)	1.89	30	0.94 (0.40)	1.94	28	0.124 (24)	0.122
P14-N20	2.58 (1.06)	5.23	30	2.45 (1.25)	5.58	29	0.668 (28)	0.677
N20-P22	2.21 (1.61)	6.24	6	3.06 (1.34)	6.41	2	0.458 (02)	0.458
P22-N25	0.91 (0.94)	3.26	6	1.90 (0.90)	4.15	2	0.412 (02)	0.263
N25-P27	0.82 (0.57)	2.25	6	0.64 (0.13)	0.97	2	0.520 (02)	0.682
P27-N33	1.75 (1.94)	6.6	23	2.02 (1.88)	6.72	18	0.416 (18)	0.625
N33-P42	2.88 (1.80)	7.38	25	2.72 (1.69)	6.95	24	0.537 (22)	0.751
N20-P27	3.10 (2.11)	8.29	29	3.14 (2.00)	8.14	27	0.825 (27)	0.946

INTERPEAK LATENCY DIFFERENCE FOR PARIETAL (P3/P4) COMPS.

	RIGHT LIMB			LEFT LIMB			T-TEST P VALUES	
Component	Mean (ms)/(S.D)	U.L.N.	Obs.	Mean (ms)/(S.D)	U.L.N.	Obs.	Paired/(No. of pairs)	Unpaired
ERBS-P14	4.21 (0.92)	6.51	20	4.00 (0.90)	6.25	18	0.628 (17)	0.49
P14-N20	5.40 (0.83)	7.48	30	5.51 (0.75)	7.39	28	0.437 (27)	0.583
N20-P22	3.02 (1.14)	5.87	6	3.92 (1.16)	6.82	2	0.822 (02)	0.304
N20-N25	5.86 (2.17)	11.29	6	7.63 (0.88)	9.83	2	0.795 (02)	0.336
N20-P27	7.17 (3.10)	14.92	29	7.07 (2.54)	13.42	27	0.599 (27)	0.895
N20-N33	13.07 (2.92)	20.37	27	14.07 (3.08)	21.77	26	0.066 (24)	0.232
N20-P42	22.43 (3.60)	31.43	25	22.99 (3.35)	31.37	25	0.178 (22)	0.527

TABLE A.5 PARIETAL COMPONENT DATA TABLE

S.D. = Standard Deviation U.L.N. = Upper Limits of Normality Obs. = Observations

Bold P-values indicate significance at the 1% level for comparison of Right versus Left limb data

INTERHEMISPHERE LATENCY DIFFERENCE FOR PARIETAL COMPONENTS

Component	Mean (ms)/(S.D)	U.L.N.	Obs.
RERB-LERB	0.23 (0.13)	1.13	21
RP14-LP14	0.41 (0.47)	2.29	27
RN20-LN20	0.52 (0.39)	1.72	28
RP22-LP22	1.50 (0.66)	2.5	2
RN25-LN25	1.00 (1.06)	3.2	2
RP27-LP27	1.32 (1.46)	4.32	27
RN33-LN33	1.63 (1.57)	4.23	24
RP42-LP42	1.66 (1.00)	3.84	22

INTERHEMISPHERE AMPLITUDE DIFFERENCE FOR PARIETAL COMPONENTS

Component	Mean (uV)/(S.D.)	U.L.N.	Obs.
0-P14	0.45 (0.36)	1.35	27
P14-N20	0.85 (0.75)	2.73	28
N20-P22	0.54 (0.48)	1.74	2
P22-N25	0.37 (0.40)	1.39	2
N25-P27	0.67 (0.88)	2.87	2
P27-N33	1.12 (1.20)	4.12	18
N33-P42	1.18 (1.04)	3.78	22
N20-P27	1.16 (0.87)	3.34	27

TABLE A5.1 PARIETAL COMPONENT DATA TABLE

S.D. = Standard Deviation U.L.N. = Upper Limits of Normality Obs. = Observations

Bold P-values indicate significance at the 5% level for comparison of Right versus Left limb data

LATENCY DATA FOR PARIETAL (P3/P4) COMPONENTS

	YOUNG GROUP			OLD GROUP			T-TEST
Component	Mean (ms)	S.D.	Obs.	Mean (ms)	S.D.	Obs.	P-Values
ERBS	9.91	0.45	11	10.85	1.47	8	0.060
P14	13.94	1.29	15	15.34	1.79	11	**0.029**
N20	18.87	1.10	15	21.26	1.95	11	**0.001**
P22	21.71	1.90	3			1	
N25	25.60	2.62	3			1	0.224
P27	26.26	4.53	14	28.15	2.43	11	0.224
N33	32.29	3.80	13	33.31	2.42	10	0.470
P42	40.86	3.74	12	43.36	3.58	10	0.128

AMPLITUDE DATA FOR PARIETAL (P3/P4) COMPONENTS

	YOUNG GROUP			OLD GROUP			T-TEST
Component	Mean (uV)	S.D.	Obs.	Mean (uV)	S.D.	Obs.	P-Values
0-P14	0.75	0.56	15	0.82	0.36	11	0.742
P14-N20	2.56	0.80	15	2.77	1.41	11	0.630
N20-P22	2.83	1.59	3			1	
P22-N25	1.40	0.94	3			1	
N25-P27	0.98	0.75	3			1	
P27-N33	1.49	0.92	11	2.07	2.94	9	0.541
N33-P42	2.06	0.95	12	4.07	2.20	10	**0.009**
N20-P27	3.12	1.91	14	3.29	3.14	11	0.855

INTERPEAK LATENCY DIFFERENCE FOR PARIETAL (P3/P4) COMPS.

	YOUNG GROUP			OLD GROUP			T-TEST
Component	Mean (ms)	S.D.	Obs.	Mean (ms)	S.D.	Obs.	P-Values
ERBS-P14	3.98	1.09	9	4.59	0.76	8	0.204
P14-N20	4.93	0.73	15	5.93	0.74	11	**0.002**
N20-P22	3.23	1.37	3			1	
N20-N25	6.78	2.48	3			1	
N20-P27	7.30	4.37	14	6.89	1.30	11	0.771
N20-N33	13.44	3.62	13	12.30	1.97	10	0.378
N20-P42	22.05	3.58	12	22.35	3.50	10	0.846

TABLE A.6 PARIETAL COMPONENT DATA FOR YOUNG AND OLD AGE GROUPS

Young group = 17-30 years Old group = 60-86 years

S.D.= Standard Deviation Obs = Observations

Bold P-values indicate significance at the 5% level for comparison of young versus old age group data

INTERHEMISPHERE LATENCY DIFFERENCE FOR PARIETAL COMPS.

	YOUNG GROUP			OLD GROUP			T-TEST
Component	Mean (ms)	S.D.	Obs.	Mean (ms)	S.D.	Obs.	P-Values
RERB-LERB	0.17	0.08	11	0.26	0.15	7	0.133
RP14-LP14	0.19	0.27	13	0.73	0.57	10	**0.007**
RN20-LN20	0.43	0.31	13	0.66	0.45	11	0.158
RP22-LP22	1.50	0.66	2				
RN25-LN25	1.00	1.06	2				
RP27-LP27	1.77	2.02	12	0.95	0.66	11	0.213
RN33-LN33	2.30	2.06	11	1.04	0.70	10	0.081
RP42-LP42	1.84	1.20	10	1.53	0.83	9	0.532

INTERHEMISPHERE AMPLITUDE DIFFERENCE FOR PARIETAL COMPS.

	YOUNG GROUP			OLD GROUP			T-TEST
Component	Mean (uV)	S.D.	Obs.	Mean (uV)	S.D.	Obs.	P-Values
0-P14	0.54	0.33	13	0.39	0.44	10	0.347
P14-N20	0.87	0.56	13	0.96	1.00	11	0.781
N20-P22	0.30	0.33	2			0	
P22-N25	0.37	0.40	2			0	
N25-P27	0.67	0.88	2			0	
P27-N33	0.59	0.33	8	1.30	0.91	8	0.058
N33-P42	0.94	0.83	10	1.32	1.33	9	0.449
N20-P27	1.02	0.54	12	1.07	0.62	11	0.838

TABLE A6. PARIETAL COMPONENT DATA FOR YOUNG AND OLD AGE GROUPS

Young group = 17-30 years Old group = 60-86 years

S.D.= Standard Deviation Obs = Observations

Bold P-values indicate significance at the 5% level for comparison of young versus old age group data